



PB99-143331

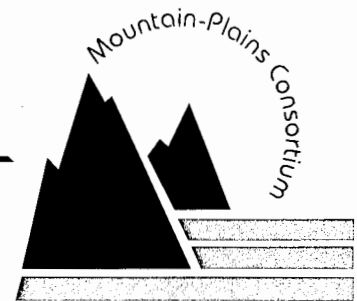
**A CENTER OF EXCELLENCE FOR  
RURAL AND INTERMODAL TRANSPORTATION**

**MPC REPORT NO. 99-99A**

**Cyclic Lateral Loading of a  
Model Pile Group in Clay Soil**

Joseph A. Caliendo  
Loren R. Anderson  
Mark A. Rawlings

February 1999



Colorado State University  
Fort Collins, Colorado

North Dakota State University  
Fargo, North Dakota

University of Wyoming  
Laramie, Wyoming

Utah State University  
Logan, Utah



# REPORT DOCUMENTATION PAGE

Form Approved  
OMB No. 0704-0188

Public reporting burden for this collection of information is estimated to average 1 hour per response, including the time for reviewing instructions, searching existing data sources, gathering and maintaining the data needed, and completing and reviewing the collection of information. Send comments regarding this burden estimate or any other aspect of this collection of information, including suggestions for reducing this burden, to Washington Headquarters Services, Directorate for Information Operations and Reports, 1215 Jefferson Davis Highway, Suite 1204, Arlington, VA 22202-4302, and to the Office of Management and Budget, Paperwork Reduction Project (0704-0188), Washington, DC 20503.

1. AGENCY USE ONLY (Leave blank)	2. REPORT DATE February 1999	3. REPORT TYPE AND DATES COVERED project technical	
4. TITLE AND SUBTITLE  Cyclic Lateral Loading of a Model Pile Group in Clay Soil		5. FUNDING NUMBERS	
6. AUTHOR(S)  Joseph A. Caliendo, Loren R. Anderson, Mark A. Rawlings Utah State University		8. PERFORMING ORGANIZATION REPORT NUMBER  MPC 99-99A	
7. PERFORMING ORGANIZATION NAME(S) AND ADDRESS(ES)  Mountain Plains Consortium North Dakota State University Fargo, ND		6. PERFORMING ORGANIZATION REPORT NUMBER	
9. SPONSORING/MONITORING AGENCY NAME(S) AND ADDRESS(ES)  University Transportation Centers Program U.S. Department of Transportation Washington, DC		10. SPONSORING/MONITORING AGENCY REPORT NUMBER	
11. SUPPLEMENTARY NOTES			
12a. DISTRIBUTION / AVAILABILITY STATEMENT		12b. DISTRIBUTION CODE	
13. ABSTRACT (Maximum 200 words)  Lateral loading on pile groups often controls the design of these foundation systems, but their behavior when subjected to lateral loading is extremely difficult to predict. To compensate for this, factors of safety are increased, thus increasing the overall cost of a project. The purpose of this research project was to design and build a model pile group according to similitude parameters and test it under cyclic lateral loading conditions to obtain data that will expand the knowledge on the behavior of pile groups when subjected to cyclic lateral loads.  Detailed descriptions are given regarding design and construction of the instrumented model piles, other instrumentation, and the data acquisition system. Step-by-step procedures are given for calibration of all instrumentation as well as for the testing setup and procedure. Great detail is used in covering these topics in the event that some of this effort must be duplicated in the future. Results covering four types of test output are explained and discussed, as are comparisons of the test output with predictions made using computer software.			
14. SUBJECT TERMS  cyclic lateral loading, pile groups, soil		15. NUMBER OF PAGES 371	16. PRICE CODE
17. SECURITY CLASSIFICATION OF REPORT	18. SECURITY CLASSIFICATION OF THIS PAGE	19. SECURITY CLASSIFICATION OF ABSTRACT	20. LIMITATION OF ABSTRACT  UL



*CYCLIC LATERAL LOADING OF A MODEL PILE GROUP IN CLAY SOIL*

*PHASE 2A*

Joseph A. Caliendo  
Loren R. Anderson  
Mark A. Rawlings

Utah State University  
Department of Civil and Environmental Engineering

PROTECTED UNDER INTERNATIONAL COPYRIGHT  
ALL RIGHTS RESERVED.  
NATIONAL TECHNICAL INFORMATION SERVICE  
U.S. DEPARTMENT OF COMMERCE

February 1999

## **Acknowledgments**

During the course of working on this thesis project, it has been my pleasure to interact with many people. Although at times the task at hand was difficult, these people were always friendly and willing to help out if possible. I need to express my thanks to them for what they have done.

I would like to start by thanking Dr. Loren R. Anderson for convincing me to get a master's degree in geotechnical engineering and for providing direction, encouragement, and unbounded enthusiasm along the way. My thanks also to the following people for help in many different ways: Becky, Carolyn, Marlo, Ken, Rene, Dr. Folkman, Dr. Fullmer, Dr. Halling, Dr. Haycock, Dr. Swenson, Dr. Watkins, Dr. Womack, and Steve Dapp. Thanks to Amy Jones for designing the data acquisition system. A special thanks to Clark Steed for taking on the LabVIEW programming when he already had too many other things happening. Clark was a true asset to the project. I believe that Robb E. S. Moss and I worked as a team on this project as few people could have. I am proud to call Robb a great friend and look forward to watching him become prominent in the geotech community because he is as good an engineer as he is a friend. Finally, I would like to express my gratitude to Dr. Joe Caliendo. His flexible style of leadership made working on this project enjoyable. His sincere concern for the personal well-being of his students is a trait that has endeared him to many, and I feel privileged to have been able to work with him and to be able to call him a dear friend. He always wanted me to address him this way, so, thanks a lot, Joe.

## **Disclaimer**

The contents of this report reflect the views of the authors, who are responsible for the facts and the accuracy of the information presented herein. This document is disseminated under the sponsorship of the Department of Transportation, University Transportation Centers Program, in the interest of information exchange. The U.S. Government assumes no liability for the contents or use thereof.

This report is part of an ongoing investigation on the response of individual piles and pile groups to various types of lateral loadings. This research has been undertaken on behalf of the Utah Department of Transportation and the Mountain Plains Consortium. Phase 1 of the study was completed in March 1996 and involved design and construction of a model test facility. A model pile was designed, instrumented, and laterally loaded under monotonic conditions.

This is the report for Phase 2A of the project. This report addresses the design, construction, calibration, and preliminary test results for a pile group subjected to cyclic lateral loading.

The report for Phase 2B of the project also has been completed. This report presents an in-depth analysis and design applications for pile groups subjected to the cyclic lateral loadings developed in the previous phase.

A much briefer executive summary of the two phases will be submitted as Phase 2C.





## ABSTRACT

Lateral loading on pile groups often controls the design of these foundation systems, but their behavior when subjected to lateral loading is extremely difficult to predict. To compensate for this, factors of safety are increased, thus increasing the overall cost of a project. The purpose of this research project was to design and build a model pile group according to similitude parameters and test it under cyclic lateral loading conditions to obtain data that will expand the knowledge on the behavior of pile groups when subjected to cyclic lateral loads.

Detailed descriptions are given regarding design and construction of the instrumented model piles, other instrumentation, and the data acquisition system. Step-by-step procedures are given for calibration of all instrumentation as well as for the testing setup and procedure. Great detail is used in covering these topics in the event that some of this effort must be duplicated in the future. Results covering four types of test output are explained and discussed, as are comparisons of the test output with predictions made using computer software.



## TABLE OF CONTENTS

INTRODUCTION .....	1
Background .....	1
Objectives .....	1
LITERATURE REVIEW .....	4
Full-Scale Tests .....	4
Brown .....	4
Roosevelt Bridge .....	6
Rollins .....	7
Model Tests .....	8
Background .....	8
McVay .....	9
Rao .....	10
PHYSICAL MODEL .....	12
Similitude .....	12
Analysis .....	12
Selection .....	13
Soil Test Vessel .....	14
Soil Container .....	14
Soil Placement and Consolidation .....	15
Soil Characteristics .....	15
Pretesting Modifications .....	17
Model Pile Construction .....	17
Background .....	17
Pile Preparation .....	17
Strain Gage Preparation .....	18
Strain Gage Mounting .....	20
Construction Completion Procedures .....	24
Instrumentation .....	27
Thermal Drift Compensation .....	27
Load Rod .....	27
Load Cells .....	29
Linear Variable Differential Transformers .....	31
DATA ACQUISITION SYSTEM .....	34
Background .....	34
Phase 1 System .....	34
System Origin .....	34
System Design .....	35
Requirements .....	35
Input Board Design and Function .....	35
Analog-to-Digital Conversion .....	37
System Construction .....	40
Input Board Assembly .....	40
Interface Bus Assembly .....	40
Box Construction .....	41

CALIBRATION .....	44
Calibration of the Model Piles .....	44
Background .....	44
Equipment .....	47
Input Board Connections .....	48
Calibration Setup and Procedure .....	50
Data Reduction and Analysis .....	57
Calibration of the Load Rod and Load Cells .....	59
Instrument Description .....	59
Input Board Connections .....	62
Calibration Apparatus, Setup, and Procedure .....	62
Data Reduction and Results .....	64
Calibration of the LVDTs .....	68
Equipment .....	68
Input Board Connections .....	68
Calibration Apparatus, Setup, and Procedure .....	69
Data Reduction and Results .....	71
PHYSICAL MODEL TESTING .....	74
Loading System .....	74
Background .....	74
Mount Design and Construction .....	75
Pressure System Design and Construction .....	79
Pressure System Testing .....	80
By-pass Cable Design .....	81
Loading System Control .....	81
Pile Installation .....	83
Preliminary Work .....	83
Pile Spacing Template .....	84
Pile Group Alignment .....	86
Pile Insertion .....	87
Testing .....	88
Hydraulic Cylinder Alignment .....	88
By-pass Cable Hookup .....	89
LVDT Mounting .....	89
Data Acquisition System Setup .....	89
Testing Procedure .....	90
Recalibration .....	95
RESULTS .....	98
Measured .....	98
Data Reduction .....	98
Load Distribution .....	99
Pile Group Moment Distribution .....	102
Individual Pile Moment Distribution .....	107
Load versus Deflection .....	110
Predicted .....	112
Background .....	112
Comparison .....	113

SUMMARY AND CONCLUSIONS .....	117
Discussion .....	117
Conclusions .....	119
REFERENCES .....	121
APPENDIX A: SOIL PROPERTIES .....	123
APPENDIX B: TEST RESULTS .....	133
APPENDIX C: STRAIN GAGE CALIBRATION .....	263
APPENDIX D: LabVIEW TESTING SOFTWARE CODE .....	363

1  
2  
3  
4  
5  
6  
7  
8  
9  
10  
11  
12  
13  
14  
15  
16  
17  
18  
19  
20  
21  
22  
23  
24  
25  
26  
27  
28  
29  
30  
31  
32  
33  
34  
35  
36  
37  
38  
39  
40  
41  
42  
43  
44  
45  
46  
47  
48  
49  
50  
51  
52  
53  
54  
55  
56  
57  
58  
59  
60  
61  
62  
63  
64  
65  
66  
67  
68  
69  
70  
71  
72  
73  
74  
75  
76  
77  
78  
79  
80  
81  
82  
83  
84  
85  
86  
87  
88  
89  
90  
91  
92  
93  
94  
95  
96  
97  
98  
99  
100

## LIST OF FIGURES

Figure 1	Soil Test Vessel .....	17
Figure 2	Pile Strain Gage Configuration .....	20
Figure 3	Strain Gage Mounting Tool .....	23
Figure 4	Pile Cap Assembly .....	27
Figure 5	Load Rod Strain Gage Details .....	29
Figure 6	Load Cell Details .....	31
Figure 7	LVDT Mounting Configuration .....	34
Figure 8	1/4 Wheatstone Bridge Configuration Used on Input Circuit Boards .....	37
Figure 9	Flow Sequence of Strain Measurements .....	39
Figure 10	Input Circuit Board Trace and Component Layout .....	40
Figure 11	Data Acquisition System Box Layout .....	43
Figure 12	Calibration Load Configuration .....	47
Figure 13	Pile Orienting Device .....	50
Figure 14	ZERO.VI Program Panel .....	52
Figure 15	GO-CAS.VI Program Panel .....	56
Figure 16	Calibration Output for a Defective Gage .....	61
Figure 17	Calibration Output for a Normal Gage .....	62
Figure 18	Calibration Output for Load Rod Gages Red and Black 1 .....	67
Figure 19	Calibration Output for Load Cell A .....	68
Figure 20	Calibration Output for the Blue LVDT .....	74
Figure 21	Loading System .....	78
Figure 22	Hydraulic Cylinder Mounting Frame .....	79
Figure 23	Pile Group Loading Assembly .....	83
Figure 24	Pile Group Installation Template .....	86
Figure 25	Pile Order in the Pile Group During Testing .....	93
Figure 26	ONE SHOT.VI Program Panel .....	95
Figure 27	Load Distribution for Cycle 1 at 450 lb. ....	101
Figure 28	Load Distribution for Cycle 5 at 400 lb. ....	102
Figure 29	Pile Group Moment Distribution for Cycle 1 at 450 lb. ....	105
Figure 30	Pile Group Moment Distribution for Cycle 25 at 350 lb. ....	106
Figure 31	Pile Group Moment Distribution for Cycle 50 at 150 lb. ....	107
Figure 32	Moment Distribution for Pile 6 at 450 lb. ....	109
Figure 33	Moment Distribution for Pile 4 at 450 lb. ....	110
Figure 34	Load versus Deflection .....	112
Figure 35	Maximum Bending Moment: Predicted versus Measured .....	115
Figure 36	Pile Group Deflection: Predicted versus Measured .....	116

1  
2  
3  
4  
5  
6  
7  
8  
9  
10  
11  
12  
13  
14  
15  
16  
17  
18  
19  
20  
21  
22  
23  
24  
25  
26  
27  
28  
29  
30  
31  
32  
33  
34  
35  
36  
37  
38  
39  
40  
41  
42  
43  
44  
45  
46  
47  
48  
49  
50  
51  
52  
53  
54  
55  
56  
57  
58  
59  
60  
61  
62  
63  
64  
65  
66  
67  
68  
69  
70  
71  
72  
73  
74  
75  
76  
77  
78  
79  
80  
81  
82  
83  
84  
85  
86  
87  
88  
89  
90  
91  
92  
93  
94  
95  
96  
97  
98  
99  
100



# CHAPTER 1

## INTRODUCTION

### Background

Lateral loading of piles, pile groups, and drilled shafts can be caused by earthquakes, scour, ship impact, and wind, and usually is the driving factor in the design of deep foundations in areas where these hazards might exist. Methods for predicting the capacity of a single pile subjected to lateral loads are quite reliable, and many full-scale pile tests have been conducted in the field to verify and refine the methods. Usually, however, piles are driven and connected in groups for which the single pile design methods are inadequate. Due to great expense, few full-scale lateral load tests have been conducted on pile groups to confirm design parameters and gather data on how pile proximity may affect the load-bearing capacity of the group. This lack of data and of confirmed design methods usually leads to overly conservative designs.

The expense of full-scale tests has given rise to other methods of testing pile groups. Scaled miniature piles have been tested in centrifuges where the effects of overburden can be simulated. Computer software employing finite element or finite difference methods is another tool used to analyze pile group design.

Florida Pier is a 3-D, nonlinear, finite element analysis program developed at the University of Florida under endorsement of the Federal Highway Administration for use in designing piles, pile groups, and drilled shafts subjected to lateral loads. Verification of this software through pile group lateral load tests will give greater confidence to people who currently use this software for pile group design and to those who might use it in the future. This project is part of an ongoing effort to validate the Florida Pier program through testing of model piles.

In Phase 1 of this project, the instrumentation configuration for model piles was developed and tested, and clay soil was consolidated in a vessel where the model piles were tested, and in which further testing could be done. Three model piles were made from 1.52 m (5.0 ft.) lengths of aluminum pipe. Twenty-eight foil strain gages were mounted in 14 diametrically opposed pairs spaced at regular intervals on the inside surface of the pipes. Two static lateral load tests were performed on one of the model piles after it had been calibrated. The loads were applied by hanging weights from a wire rope attached to the top of the pile. Data was gathered by a mechanical multiplexer that switched between all gage channels during sampling, after which the data were converted to digital output by a datalogger and stored in a personal computer. Bending moment and lateral pile displacement versus applied load data gathered during the tests was compared with predictions made using the Florida Pier and COM624P programs, the results of which were quite favorable.

### **Objectives**

Phase 2 built on the accomplishments of Phase 1, namely, the strain gage configuration of the model piles and the soil test vessel, and expanded the scope of the project to include a cyclic lateral load test on a model pile group. The results of this test were then compared to predictions made for group deflection and bending moment using Florida Pier.

The accomplishment of a number of tasks was required in moving from the statically-loaded single pile test of Phase 1 to the cyclically-loaded pile group test of Phase 2. They include the following:

1. Develop test hardware.
2. Design and construct a data acquisition system.
3. Calibrate all instrumentation.
4. Perform a pile group test.

5. Analyze data.

The model pile group tested consisted of five piles arranged in linear configuration and loaded on the group's long axis. Since only three piles had been made for Phase 1, and since they were used mainly as learning tools for instrumentation and calibration procedures, it was decided that six new piles should be constructed, thereby avoiding any compatibility problems between old and new piles. They were constructed based on the pattern set in Phase 1. If the project continues to progress in complexity, then a point might one day be reached where all piles could be implemented in a nine-pile group.

Linking piles together in a group necessitated design of a pile cap. It was decided that pinned connections would reduce the complexity of the whole project, and so a pinned pile cap/load rod was designed and fabricated to act, in conjunction with the piles, as a load cell between each pile while transferring the load through the group. Master load cells also were fabricated for measuring force delivered to the pile group.

Linear Variable Differential Transformers (LVDTs) were used to measure deflection at the pile cap elevation and at a distance of 76.2 mm (3.0 in.) above the pile cap. The higher deflection measurement was needed to continuously calculate the slope of the pile top. Hardware for mounting the LVDTs was specifically constructed for these purposes.

Cyclic loading of the pile group required a more sophisticated loading system than was used in Phase 1. On-hand hydraulic cylinders were central components in the new system, which used regulated air pressure to control load magnitude and a computer controlled solenoid valve to control cylinder actuation. Considerable effort went into developing this system.

The data acquisition system needed for Phase 2 far exceeded capabilities of the Phase 1 system. A new system was designed and constructed by Utah State University students specifically for this project. Emphasis was placed on allowing for a high number of instrumentation channels to be sampled

at a rate approaching 10 Hertz. LabVIEW™ software and an analog-to-digital converter circuit board, both products of National Instruments Inc., were key elements in the data acquisition system.

All instrumentation, from piles to the LVDTs, was calibrated using the new data acquisitions system. Calibration factors were calculated for all instruments by comparing measured stresses with theoretical stress values. These calibration factors were then used in post test data analysis.

The pile group test involved a great deal of effort to solve glitches in the loading and data acquisition systems. The testing was successful after ironing out the problems and developing a good test procedure.

MATLAB® software was used for the data reduction process. Output included moment distribution for individual piles and for the pile group, load distribution among the piles, and load versus deflection. This output was expressed in graphical form. Test results for load versus deflection and moment distribution were compared with predictions by Florida Pier as the final step in the project.

## CHAPTER II

### LITERATURE REVIEW

#### Full-Scale Tests

##### *Brown*

Most research dealing with lateral loading of piles has been done on single piles even though piles are most frequently used in groups. Until Dr. Dan Brown performed his full-scale cyclic lateral load test on a pile group, few well instrumented, carefully performed full-scale tests had been completed (Brown and Reese, 1985).

In Brown's 1985 full-scale test, nine closed-ended steel pipe piles, 273 mm (10.75 in.) in diameter, with 9.27 mm (0.365 in.) thick walls, were used. These piles had been driven to a depth of about 12.2 m (40 ft.) below grade in stiff overconsolidated clays that were kept saturated for his testing. The piles were installed in a 3 x 3 arrangement with a center-to-center spacing of three pile diameters. An instrumented single pile was tested and used as a reference to which the pile test data could be compared.

All nine of the piles were instrumented with strain gages that had been attached to pipes that were inserted in the piles and grouted in place. Four gages, in a full bridge configuration and spaced at 90° intervals, were mounted at eight locations starting 0.3 m (1 ft.) below the soil surface and extending downward at 0.3 m (1 ft.) intervals for 2.4 m (8 ft.). Three more levels of strain gages were located at depths of 2.9 m (9.5 ft.), 3.4 m (11.5 ft.), and 4.0 m (13 ft.).

Linear potentiometers were used to make deflection measurements at the point of loading and also 1.2 m (4 ft.) above the point of loading. From data collected at these different elevations, slope of the top of the pile was determined. Eighteen potentiometers were used to monitor the movement of the nine piles.

Power for all instrumentation was provided by a Kepco power supply. Two Hewlett-Packard 3497A Data Acquisition/Control units were used for analog-to-digital conversion and were controlled by a Hewlett-Packard 85 microprocessor. Estimated calibration factors were used in computing bending moments and experimentally determined calibration factors were used for the load cells and potentiometers. Reading of all 132 channels of instrumentation required 20 seconds.

Loading of the pile group was accomplished with a 305 mm (12.0 in.) bore diameter double acting hydraulic cylinder, pressurized by a hydraulic pump. A servo valve operated by a servo controller controlled hydraulic fluid flow. A closed loop system consisting of a digital function generator and a feedback linear potentiometer was used to provide the desired loading pattern. A load frame with moment-free hinged connections with integral load cells was used to transmit lateral loads to the pile group.

Testing was done under deflection controlled conditions. The first loading consisted of 100 cycles at a deflection near 2.5 mm (0.1 in.). Two hundred cycles were done at each of the four other deflection settings, which ranged up to approximately 53 mm (2.1 in.) for the fifth setting. The load on the pile group varied from a low of 120 kN (27 kip) at the end of the first set of cycles to a high of about 740 kN (167 kip) at the beginning of the last group of cycles.

Results of this testing showed that the piles in a group take less of a load per pile than does a single pile similarly loaded. The group piles deflect more than does a single pile at the equivalent load per pile, and the bending moment in the group piles is greater than the bending moment in a single pile subjected to the same average load per pile. After cycling, the difference between the group behavior and

the single pile behavior only slightly decreases. Trends from the loading showed that distribution of load through the group followed a front row to back row pattern, with the leading row taking more of the load. In the leading row, the center pile took more of the load, while the corner piles on the trailing row took more load than did the center pile on the trailing row.

### ***Roosevelt Bridge***

A large-scale test was conducted by Townsend et al. (1997) at the Roosevelt Bridge replacement at Stuart, Fla. The test group consisted of 16 760 mm (30 in.) prestressed concrete piles driven into sand to a depth of around 14 m (46 ft.) and subjected to lateral loads with a fixed head production pile group acting as the reaction. This test compared actual test data to predictions made for the lateral loading of the pile groups with the Florida Pier software package.

Ten of 16 piles in the test group were fully instrumented. Instrumentation was installed in the piles by inserting an instrumented 355 mm (14 in.) steel pipe into the center void of each pile and grouting it in place. The instrumented pipes had nine levels of strain gages, configured for measuring bending stresses only, attached to the outside surface and spaced every 914 mm (36 in.) below the mudline, except for the last gage, which was 1.83 m (72 in.) below the next to last gage level. Each level used four gages in a full bridge configuration. Slopes and deflections were measured at the top of the pile with slope inclinometers and potentiometers. Of the 16 piles in the reaction group, only six of them were instrumented and were used to gather data on bending as well as axial strains.

Ten load cells of 445 kN (100 kip) capacity were used on each of the instrumented piles in the test group, with an additional load cell on each of three other piles so that more information could be gathered. A 4.44 MN (1000 kip) load cell was used between the loading jack and the load frame of the test group.

The data acquisition system was a System 4000, provided by Measurements Group. Readings were taken every 15 seconds during the test, which lasted more than five hours. Each reading sampled 232 channels.

Thirteen load steps were made, nine going up in steps of about 556 kN (125 kip) each, and four going down. The maximum load was about 4.8 MN (1080 kip).

By comparing measured pile group response with predictions made using Florida Pier, it was found that Florida Pier modeled the load deflection response of both pile groups quite well, and did a good prediction even after pile cracking. It also was found that the leading and trailing rows of piles had similar load deflection curves and that the piles in the leading row took more load than did those on the trailing row. Florida Pier predictions for bending moment agreed well with measured moments in the piles. Maximum bending moment was higher for the lead piles than for the trailing piles in the test.

### ***Rollins***

Another full-scale lateral load test was conducted on a pile group at the Salt Lake International Airport by Rollins, Peterson, and Weaver (1996). The pile group was comprised of nine steel pipe piles arranged in a 3 x 3 configuration. The piles were 32.4 mm (1.275 in.) in diameter with 9.5 mm (0.375 in.) thick walls, and were filled with concrete. They were driven to a depth of 9.1 m (30 ft.) in a mixed soil strata consisting of clay, silt and sandy silt, and sand, and were spaced approximately three pile diameters apart. An isolated single pile was driven and tested for comparison with the results from the group tests.

Full details of instrumentation were not available, but strain gages and inclinometers were used for measuring bending moment and displacement of the piles. The piles were pin-connected to a loading frame for static load testing, and the load to each pile was measured through strain gage instrumented tie rods.



Lateral loading on the pile group was performed under four different conditions. The conditions were:

1. Static load applied with a 4.4 kN (1 kip) hydraulic jack on a single free-headed pile.
2. Static load applied with a 1.33 MN (300 kip) hydraulic jack with the piles in a free-headed condition.
3. Dynamic load applied with a 14.4 MN (3240 kip) Statnamic device with free-head piles at 180° to the static loading.
4. Dynamic load applied with a 14.4 MN (3240 kip) Statnamic device turned 90° to the static loading with the piles in a fixed-head condition.

Results from the testing showed that dynamic resistance is greater than static resistance for the group, and approaches the value found through the static loading of a single pile. The ratio of the average load carried by a pile in each row as compared with the load taken by a single pile showed that piles in the front row carried about 80 percent, the piles in the middle row carried about 50 percent, and the piles in the trailing row carried about 60 percent. Maximum bending moments for the dynamic loading were within about 15 percent of those measured in the static loading. Load distribution among the piles was similar for static and dynamic loading. Further analysis is being conducted on this pile group experiment.

## **Model Tests**

### ***Background***

To cut back on the expense of doing lateral pile group testing and to simplify the tests, pile groups have been modeled using dimensional analysis to scale down the piles and loads to much more manageable levels. Model tests involving sandy soils often are conducted in a centrifuge so that the effective stress associated with overburden can be simulated.

**McVay**

McVay et al. (1994) developed a device to drive model piles individually in a nine pile group and measure row contributions and group displacements, all while the centrifuge was moving.

McVay's centrifuge tests were used to study the effects of pile spacing and soil density on load distribution by row, as well as the lateral resistance of the group. A load cell mounted between each row of piles on the pile cap was used to measure the load distribution in the group. An LVDT was used to measure lateral deflection of the group.

Test results showed that the front row took more of the load than the other rows, with the middle row taking the next and the trailing row taking the least. Distribution was 41 percent, 32 percent, and 27 percent, respectively. Soil density also changes the amount of load taken by each row, with the lead pile taking more at higher densities and a near even distribution among the rows at lower densities. Results also showed that changing the spacing to five diameters caused the lateral load resistance to increase with a corresponding decrease in the effects one pile had on another due to proximity.

Further testing by McVay, Casper, and Shang (1995) on laterally loaded, 3 x 3 pile groups with 3-D and 5-D pile spacing was conducted and compared with results from a lateral load test on a single pile. Results showed that the shadowing effect is a function of soil density and pile spacing. In a dense soil, load distribution for a pile group with 3-D pile spacing was 45 percent, 32 percent, and 23 percent for the leading, middle, and trailing rows, respectively. In medium loose sands, distribution was 37 percent, 33 percent, and 30 percent for the leading to trailing rows. Pile group efficiency for lateral loading with a pile spacing of 3-D was approximately 0.74. For a pile group with 5-D spacing, the group efficiency was approximately 0.93 with load distribution being 36 or 35 percent for the leading row, 33 percent for the middle row, and 31 percent for the trailing row.

*Rao*

Instrumented model pile group tests were conducted in clay by Rao, Ramakrishna, and Raju (1996). Model piles 21.5 mm (0.85 in.) in diameter and 1,000 mm (3.3 ft.) long were instrumented with strain gages spaced 150 mm (5.9 in.) apart at seven locations along the length of the piles, and connected in six different group configurations of either two or three piles per group at various center to center spacings. The tests were conducted in a soil test tank with dimensions of 1.2 m (47.2 in.) x 0.8 m (31.5 in.) x 1.1 m (43.3 in.), where soil was placed around the piles. Loading was accomplished by placing weights on a hanger attached to the pile group by wire rope passed over a pulley. The applied load was measured by a load cell, and lateral displacement was measured with an LVDT. Strain gage data were acquired through an ORIONA (3530A) data logging system. LVDT and load cell measurements were collected using a frequency amplifier and computer data acquisition system. Tests were conducted on a single pile; a two-pile group in series with pile spacings of 3-D, 4-D, 5-D, and 6-D; a two-pile group in parallel with pile spacings of 3-D and 4-D; a three-pile group in series with 3-D and 4-D spacing; and three-pile group tests with spacing set at 3-D in triangular arrangements with either the apex or flat side leading.

From the tests conducted on the two-pile groups arranged in series at different spacings, it was shown that group capacity increased with increased spacing between the piles and that this capacity reached twice that of a single pile when the spacing was 6-D. Results from loading in the parallel configuration showed that larger capacities are possible than for a series arrangement for the same number of piles.

The results of tests conducted on three pile groups in the series, parallel, and triangular arrangements showed that the series arrangement carried the least load of all, with the triangular-apex side leading configuration taking the most load for a given deflection. Measured bending moment for

two- and three-pile groups arranged in the series configuration and with 4-D spacing was shown to be greater in the trailing piles than in the leading piles.

**CHAPTER III**  
**PHYSICAL MODEL**

**Similitude**

*Analysis*

In performing a dimensional analysis for the modeling in this project, there are seven fundamental variables that must be considered. Force (F) and length (L) are the only two basic dimensions contained in the fundamental variables as shown in Table 1. Subtracting the number of basic

**Table 1. Dimensional Analysis Variable Summary**

Fundamental variables	Basic dimensions
$\Delta$ - Pile deflection	L
P- Applied lateral load	F
D- Pile outside diameter	L
L- Pile length	L
EI- Pile stiffness	$FL^2$
C- Soil cohesion	$F/L^2$
H- Height of applied load	L

dimensions from the number of fundamental variables gives the number of Pi terms, which is five.

Deflection ( $\Delta$ ) is the non-repeating variable since it is the variable of interest and is a function of the four remaining Pi terms. This is shown by the relationship:

$$(\Delta/D) = f [ (PD^2/EI), (L/D), (H/D), (CD^4/EI) ]$$

By equating the model Pi terms with the prototype Pi terms (ie.  $(L/D)_m = (L/D)_p$  ..etc), the scale factors are established. Because Pi terms are dimensionless, they have no feel for size. Therefore, small-scale (model) tests are valid. An important factor to realize in modeling considerations is that the undrained shear strength of the soil is not a function of soil stress and therefore does not need to be scaled. This allows the test soil to be directly established as the prototype soil.

### *Selection*

Choosing a model pile diameter (D) fixes the length of the pile due to the Pi term L/D. This also fixes the height of the applied load (H) because it is linked through the Pi term H/D. Pile stiffness (EI) has not yet been set even though the pile diameter has been selected because the wall thickness, and thus the bending moment of inertia (I), has not been set. Reducing pile stiffness allows the model lateral load also to be reduced, thus making it easier to model the lateral load needed to simulate a full-scale load according to the Pi term  $PD^2/EI$ .

The modulus of elasticity (E) of the model pile also may be used to control pile stiffness (EI), and thus the modeled lateral load (P). A smaller model load may be used to simulate a given full-scale load if the modulus of elasticity of the model pile is reduced. Reducing the model pile stiffness will reduce the simulated lateral load, but it must be remembered that this also will increase the likelihood of damaging the model either through yielding the model material or by buckling the model pile.

A steel pipe pile 324 mm (12.75 in.) in diameter and with a 7.94 mm (0.313 in.) wall thickness, which commonly is specified by the Utah Department of Transportation (UDOT), was selected as the prototype pile. The model pile characteristics were then selected according to dimensional analysis based on the prototype pile. Schedule 40, 6061-T6 aluminum pipe conforming to ASTM B 241 with an outside diameter of 33.4 mm (1.315 in.) and a wall thickness of 3.38 mm (0.133 in.) was chosen as the model pile material. A summary of the characteristics as they relate to prototype pile are shown in Table 2. It

was necessary to select dimensions and characteristics that were consistent with the dimensional analysis while taking into consideration availabilities of possible model materials. The following relationships were established to relate the model and prototype functional parameters:

$$P_p = 98.6 \times P_m \quad \Delta_p = 9.7 \times \Delta_m$$

where P is the applied lateral load on the model and prototype and  $\Delta$  is the resulting deflection of the model and prototype. The relationships will not be used in the analysis in this project, but were included here for possible future reference.

**Table 2. Prototype and Model Characteristics**

Property	Prototype	Model
Material	Steel pile	Aluminum pipe
D	324mm (12.75 in.)	33.4 mm (1.315 in.)
E	200 MPa (29,000 ksi)	69 MPa (10,000 ksi)
L	11 m (36 ft.)	1.13m (3.71 ft.)
I	$1.163 \times 10^{-4} \text{ m}^4$ (279.3 in. <sup>4</sup> )	$3.635 \times 10^{-8} \text{ m}^4$ (0.0873 in. <sup>4</sup> )
P	88.9 kN (20,000 lb.)	903 N (203 lb.)
C	Same	Same

### Soil Test Vessel

#### *Soil Container*

A ribbed steel tank 3.05 m (10 ft.) long, 0.91 m (3 ft.) wide, and 1.22 m (4 ft.) deep was used to contain the clay soil used in lateral pile group tests. Plywood sideboards were added to the tank to increase the depth of the tank so that longer piles could be tested without introducing unwanted boundary

effects. The tank was lined with multiple sheets of heavy plastic to act as a barrier in retaining water, and a geocomposite was placed inside this liner to facilitate drainage during the consolidation process.

### ***Soil Placement and Consolidation***

The soil in the vessel was dredged from the gravel washing pond of a local contractor and was dumped into the tank in a slurry form. Obtaining soil in this form necessitated a consolidation period to bring the strength of the soil up to a point that would be typical for a saturated clay in the local environment. Consolidation was accomplished by mounting 10 hydraulic cylinders over the soil by means of five bolted yokes and pressurizing them to push steel plates against the soil. Figure 1 shows a schematic of the tank with the yokes in place. The consolidating pressure on the soil was maintained in increasing increments by a hydraulic accumulator with the final hydraulic pressure being 2.76 MPa (400 psi), which gave a simulated overburden stress of 80.2 kPa (1675 lb./ft<sup>2</sup>). The consolidation process took four and one-half months, after which the consolidation apparatus was disassembled and the soil was trimmed to a thickness of approximately 1.37 m (4.5 ft.). The soil was saturated during consolidation and was kept saturated for the duration of the time between consolidation and the lateral pile group tests.

### ***Soil Characteristics***

Atterberg limits tests were run on samples of the soil to determine its classification. It classed as a CL type soil. Torvane, pocket penetrometer, and hydrometer analyses also were run on the soil to further determine its characteristics. Multiple tests have been run on this soil to determine its postconsolidation properties using a mini-vane shear testing device. The earliest test was in January 1995 and the most recent test was in June 1996. The average undrained shear strength values have ranged from 28.8 kPa (4.12 psi) to 34.2 kPa (4.90 psi). The results of all soil properties tests can be seen in Appendix A.



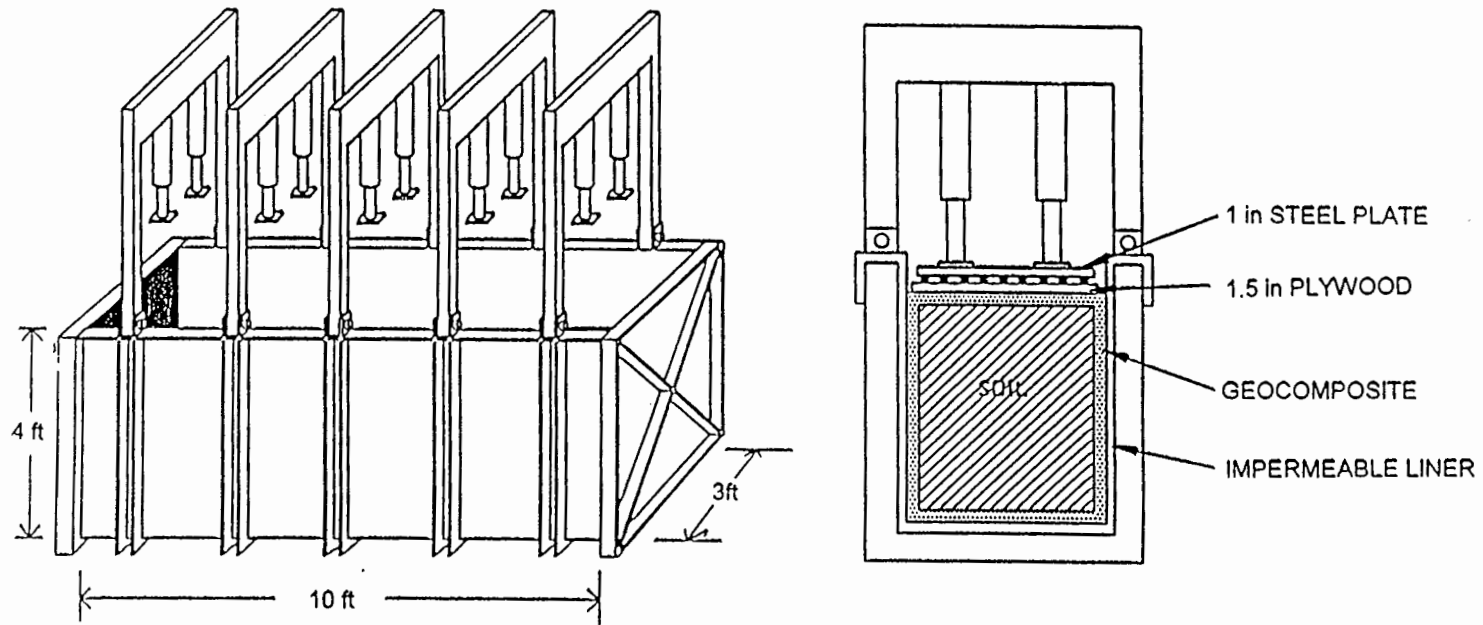


Figure 1. Soil test vessel.

### ***Pretesting Modifications***

The sideboards on the test vessel were cut down prior to the pile group tests to allow better access to the piles once inserted into the soil and also to allow the loading system to be mounted without any obstruction. This also permitted much easier viewing of the actual testing activities while allowing for enough freeboard to keep the soil saturated.

Two of the five consolidation yokes were left attached to the tank while the two hydraulic cylinders bolted to each of the yokes were removed. A large plank was bolted between the yokes to fix their relative spacing and to hold them motionless. This allowed the yokes to be used as a fixed reference to which displacement measuring instruments were later attached.

## **Model Pile Construction**

### ***Background***

For Phase 2, a substantial amount of new hardware was required. Due to the need to model a pile group, it was decided to construct six new piles that had been designed from the start as members of a group, and thus eliminate the possibility that differences between the new and old piles would introduce some compatibility problems. It also was decided that the piles should be arranged in a single row and be loaded on the linear axis of the row. This would provide the next step in complexity without introducing group effects from piles spaced laterally from each other. The new piles and the instrumentation necessary to measure loads and deflections during testing had to be designed and constructed.

### ***Pile Preparation***

The piles were made from 1 inch, Schedule 40, 6061-T6 aluminum pipe. The nominal inside diameter of this pipe is 26.645 mm (1.049 in.) with a wall thickness of 3.378 mm (0.133 in.). This pipe

was purchased in 6.1m (20 ft. ) lengths and cut to the proper length of 1.524m (5 ft.) for each pile by means of a disk type cutter.

To prepare the pipes for strain gage mounting, the inside surfaces were etched with dilute phosphoric acid to remove any manufacturing residue, grease, or scale. The etching process began by plugging one end of the pipe with a rubber stopper and then pouring about 50 ml of acid into the other. A steel wool-wrapped rod was then inserted into the pipe and spun by means of an electric drill to scrub the interior. The rod was moved in and out of the pipe several times while spinning at high speed until the whole interior surface had been thoroughly etched. The pipe was rinsed with water and the operation was repeated, except that the second time an ammonia water solution was used to neutralize any remaining acid. The pipe was again rinsed and then dried with air. At the conclusion of these operations, the inside of each pipe had a polished and clean finish.

When etching was completed, a pointed steel scribing tool was used to scratch straight reference lines about 6 inches long on the outside surface at the ends of the pipes. These reference lines would be used during the gage mounting procedure to assure that the gages were being positioned properly in the piles.

### ***Strain Gage Preparation***

Thin foil strain gages manufactured by Micro-Measurements of Raleigh, N.C., and of the type CEA-13-250UW-120 were chosen for the pile instrumentation. One hundred eighty gages were ordered along with the lead wire needed for connecting them and the epoxy for mounting them. As in the piles used in Phase 1, 28 gages were to be mounted on the inside surface of the pipes in diametrically opposed pairs spaced 95 mm (3.75 in.) apart, with the bottom most pair located 76 mm (3.0 in.) from the bottom end of the pipe, and with the upper most pair located 152 mm (6 in.) above the next closest pair. Figure 2 shows the spacing of strain gages in each pile.

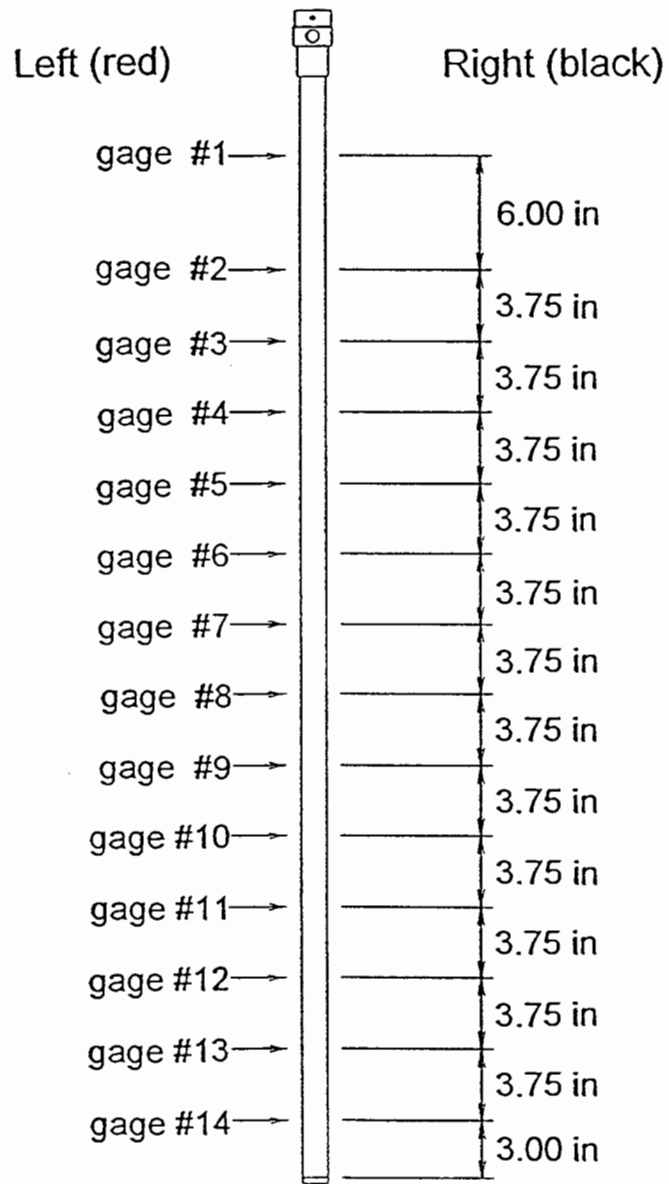


Figure 2. Pile strain gage configuration.

Before the gages could be mounted, the lead wire had to be attached. The lead wire for the gages was a three-strand, flat type wire with red-, white-, and black-colored insulation. The length of wire required to reach each gage location in the piles, with an additional 2.13 m (7.0 ft.) for connecting purposes, was calculated. The wire was then measured out and cut. This required use of 497.1 m (1631 ft.) of wire. Half the wire was stripped of its black strand, thus leaving the red and white strands together, and the other half of the wire was stripped of its red strand, leaving the black and white strands connected. This was done to keep track of which side of the piles the gages were on, the gages connected to the red and white wires going on one side of the pile, and the gages connected to the black and white wires going on the other. The ends of the lead wires were stripped of insulation and tinned in preparation for connection to the gages.

Connecting wires to the gages was a delicate process. First, the gage was positioned on a Teflon-covered mounting board where it was held in place with a small wire spring. Rosin core solder "buttons" were then melted onto the two strain gage connecting tabs. The wire leads were trimmed to fit the tabs and then positioned and taped to the mounting board surface. The gage was brought into position. The wires then were soldered onto the gage by pressing the wire leads against the solder buttons one at a time and holding them there with the tip of the soldering iron until the buttons and leads melted together. The connection points and any length of exposed wire were then waterproofed with an acrylic sealant, which was painted on with a brush. Later, the gages and lead wires were tested with a volt meter to check for any bad connections.

### ***Strain Gage Mounting***

All gage mounting activities took place in the CEE soils laboratory where all equipment could be left undisturbed for the work's duration. A mounting tool was specially designed and fabricated by the former CEE department technician for installing strain gages on the inside surface of the pipes. A pair of

gages is mounted by first inserting the tool into the pile by means of a two-piece telescoping handle. The outer handle holds the tool in the required location and has several sliding spacers on it to keep it centered in the pile. The inner tightening handle slides inside the outer handle and is rotated to actuate the screw and wedge assembly of the tool. As the screw is turned, the wedge forces the wings apart, which press the strain gages against the inside of the pipe and hold them there while the epoxy cures. Six of the tools were used so that all of the gages at a certain location in the piles could be quickly mounted with little confusion and possible mix up. Figure 3 is a diagram of the mounting tool.

In preparation for mounting, the gages first had to be affixed to each of the tools. This was done by slipping the tool into a small vise that held it in a horizontal position and allowed it free rotation. Teflon strips covered the rubber coated wings on the tools so that the gages would not be glued to the wings during mounting. Reference lines were drawn on these Teflon surfaces to aid in gage alignment. The gages were turned upside down and lined up on the reference lines with the lead wires pointed away from or out in front of the tool. Short strips of cellophane tape were used to tack the gages in place; a strip over the wires just where they met the gage, and another strip holding the tip of the gage down. Care was taken to cover only a small amount of the gage with tape so that the surface area of the gage available for gluing was as great as possible. Two gages were attached to each tool; a red gage on the one side, and a black on the other. The lead wires for both gages were then taped to a probe that protruded from the front of the tool. The purpose of the probe was to keep the wires from getting tangled while the gages were being slid into place inside the pile. When all six of the tools had been thus prepared, a single pile was clamped into a table-top vise with its scribed orientation line aligned with a reference line on the vise. The end of a slender rod was slid through the pile and attached to a string, which was then drawn through the pile as the rod was withdrawn. To the other end of this string, the lead wires for the strain gages to be installed in this pile were taped. The wires were then pulled through the pile until enough

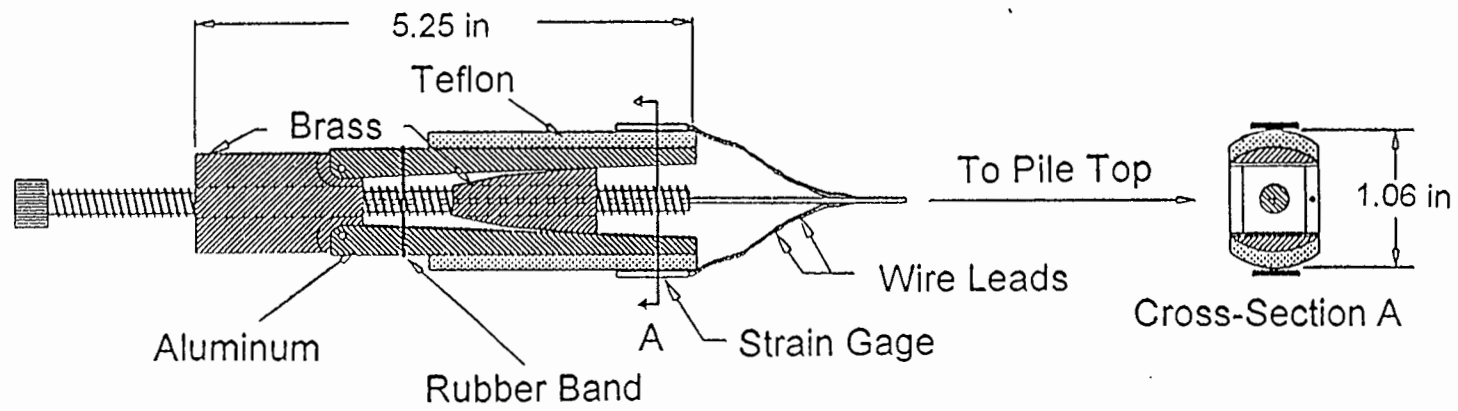


Figure 3. Strain gage mounting tool.

slack remained to permit movement of the tool to which they were attached. This mounting tool, with gages, was then positioned in the end of the telescoping insertion handle and lined up preparatory to the gluing and installation procedures.

Micro Measurements M-bond AE-10 two-part epoxy was used to glue the gages to the pile walls. Mixing the epoxy was begun by placing a glass slide and small wood spatula on a scale and zeroing the readout. Next, the spatula was used to dip 0.91 grams of resin from the bottle and place it on the slide. Three drops of hardener were put on the slide with the resin and the two were then thoroughly mixed. This prepared enough epoxy to mount 12 strain gages.

The spatula was used to smear epoxy onto the two gages prepared for insertion. The mounting tool was positioned in the end of the pile while the spacers on the handle were slid into place to keep the gages from touching the inside of the pipe and wiping off the epoxy. Slight tension was held on the lead wires as the tool was slid into the pile so that the wires would not get tangled. When the gages were in the proper position and oriented correctly as shown by markings on the insertion handle, the tightening handle was turned until the tool was securely in place. The handle was gently removed from the tool and withdrawn from the pile, leaving the mounting tool and gages in place to cure for six hours.

Butyl rubber had been affixed in the top end of the pile, and into this the lead wires were pushed to keep them out of the way of further gage mounting activities. An acrylic sealant was painted on the wires and butyl rubber to hold the wires firmly in place.

This pile was moved out of the way and the process was repeated for all six of the piles. It was important to clean the insertion handle with methyl alcohol after withdrawing it each time so that any smeared epoxy would not interfere with the mounting of subsequent gages.

The working time of the epoxy dictated that gages for all six piles had to be installed in less than 30 minutes. If this was not accomplished, a new batch of epoxy had to be mixed. Two people were required to make the gage installation procedure go smoothly. This procedure was used to mount all of



the gages at the 14 locations in each pile, starting with the top pair and finishing with the last pair, which was located 76.2 mm (3 in.) from the bottom.

After the six-hour curing time, the handle was pushed back into the pile until the mounting tool was engaged. The wedge actuating screw in the tool was then loosened and the wedge was forced forward from between the wings with a gentle tap to the end of the tightening handle. This allowed the wings to collapse. Gentle twisting action on the handle broke the wings loose from the gages, after which the tool was withdrawn from the pile. After the insertion tools had been removed from every pile, the strain gage circuit was checked for damage with a volt meter.

All 168 strain gages were successfully mounted without damage, but there were several anomalies noted during gage installation. One type of anomaly occurred three times, in which, upon removal of the insertion tool, one of the protective Teflon strips remained inside and attached to the wall of the pile. This was determined to be a minor problem which would not likely influence the strain reading from the affected gage. The other anomaly occurred only once and involved the Red 8 and Black 8 gages of Pile 1. During an attempt to remove the insertion tool, it was found that the gages had been mounted in a position rotated about 30 degrees off-axis from the rest of the gages. Nothing could be done to change this, but calibration factors for these gages would reflect their errant positioning.

### ***Construction Completion Procedures***

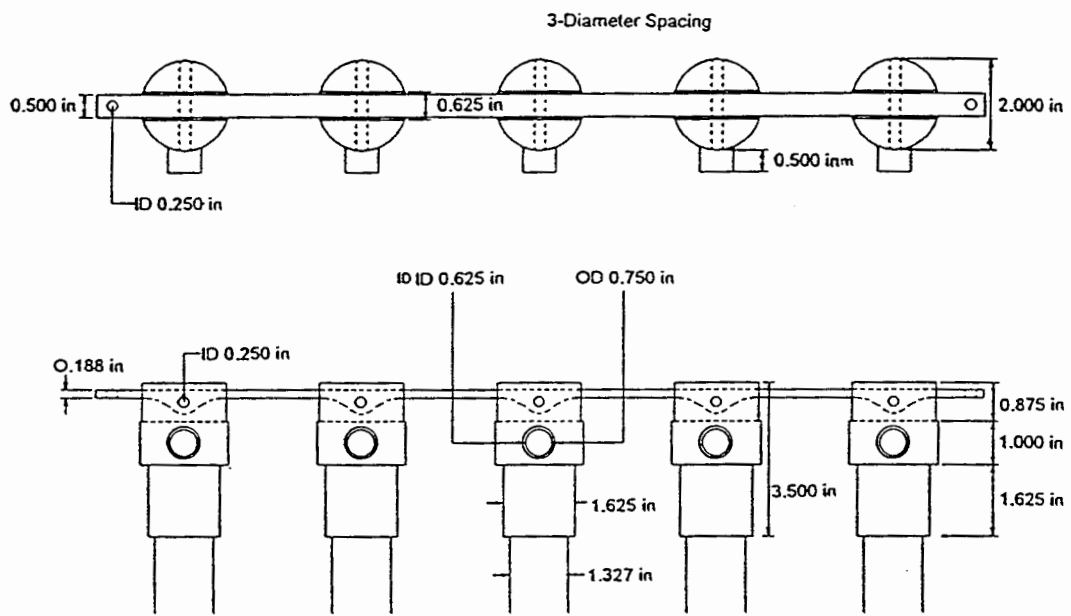
Plugs for sealing the bottom ends of the piles were machined from solid aluminum stock. The shoulders of the plugs were sized to match the outside diameter of the piles, while the necks of the plugs fit smoothly inside. The necks were grooved to accept an O-ring that would form a tight seal when installed. Installation of the plugs was accomplished by coating the O-rings with petroleum jelly and then inserting the plugs into the piles. As an extra barrier against moisture, a metal-to-metal epoxy was smeared into the gap between the bottoms of the piles and the shoulders of the plugs, after which the

plugs were pushed completely into the piles and held in place for several minutes until a primary bond could be made. Later, excess epoxy was trimmed from around the plugs.

Moisture in the piles was eliminated by purging them with nitrogen. This was done by threading a rubber hose down to the bottom of the pile and then slowly withdrawing it as nitrogen was pumped in. The nitrogen was first dried by running it through a crystal desiccant in an in-line container. A rubber stopper was then glued into the end of the pile and a seal of silicone glue was made on top of the stopper and around the wires.

Aluminum pile crowns for sealing the tops of the piles and with a provision for pinning the piles together in a linear group were designed and fabricated. Figure 4 shows the pile crowns as part of the pile cap assembly. Strain gage wires exit the crown through a side port. To assure a tight fit between crowns and piles, the inside diameter of the crowns were designed to be slightly smaller than the outside diameter of the piles. The crowns were installed by first threading all of the strain gage lead wires up through the bottom of the crown and then out through the port. Reference lines on the crowns were aligned with the lines that had earlier been scribed on the piles for the strain gage installation work. The crowns were then driven onto the piles with a heavy rubber mallet until seated.

The final step in the pile construction process was to shield lead wires from electromagnetic noise with stainless steel braided wire sheathing. Hose clamps were used to fasten sheathing to the wire ports on the pile crowns. A grounding wire was added by twisting it together with strands of the sheathing material. Enough lead wire was left exposed to allow easy connection to the data acquisition system.



Designed by Mark A. Rawlings

Figure 4. Pile cap assembly.

## **Instrumentation**

### ***Thermal Drift Compensation***

Since the strain gages in the piles would be electrically excited almost continuously, there was a chance that this could cause some heating of the gages and change their resistance, thus affecting voltage output. To monitor this possible thermal drift, one of the six piles was used as a control pile. It was sunk in the soil test vessel to the same depth as the other piles. Its gages also were electrically excited in the exact manner and at the same frequency as those in the other piles, but it was not subjected to loading in any way. By comparing its initial strain gage readings with its final ones, any amount of thermal drift was accounted for and applied to the measurements taken from the other piles.

### ***Load Rod***

One of the points of interest in this project is the amount of lateral load that is taken up by each pile in the group. A special rod was designed in conjunction with the pile crowns not only to connect the piles in their linear group at the correct spacing, but also to measure the load transferred to each. Strain gages affixed to necked down sections between each pile connection served to function as in-line load cells. Figure 5 shows the load rod strain gage configuration.

This load rod was fabricated from 0.5 inch square 6061-T6 aluminum rod stock. The spacing of three pile diameters was set by drilling 6.35 mm (0.25 in.) holes for the pins at the proper distance intervals. Holes, 6.35 mm (0.25 in.) in diameter, for connecting the pile group to the loading mechanism also were drilled in each end. The material between the pin joints was machined down to a thickness of 4.763 mm (0.188 in.) so that strains within the range of the type CEA-13-250UW-120 strain gages to be used would be experienced.

To prepare the load rod for gage mounting, all necessary surfaces were sanded to remove any flaws or scratches left over from machining. Dilute phosphoric acid was used to etch these surfaces,

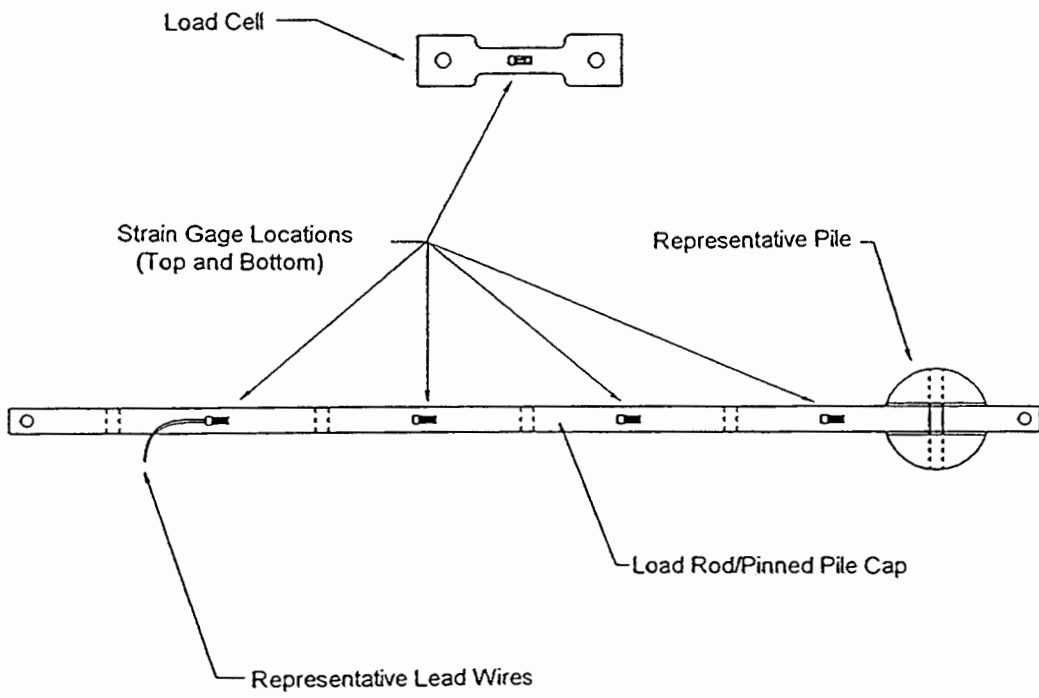


Figure 5. Load rod strain gage details.

which were then rinsed with water. Neutralizing was accomplished by rinsing with ammonia water. The rod was rinsed again with water and blown dry with air. The strain gages were wired and waterproofed in the same manner as those used in the piles. Four gages were first mounted to the top of the rod at the points half way between the pile pin connections. This was done by mixing a measured amount of epoxy and spreading it on each gage. The gages were placed in position on the rod and covered with small pieces of Teflon to prevent anything other than the gages from getting glued to the rod. Rubber-padded metal tabs were then placed over the gages, and spring clamps were applied to supply the holding pressure. After the requisite six-hour curing time, the other four gages were applied to the bottom of the load rod directly opposite those on the top. Butyl rubber strips then were attached to the load rod directly over and completely covering each gage to protect them from any damage. Strips of aluminum tape were wrapped around the four gage sections of the load rod, covering the gages at each location. An acrylic sealant was then painted on all of the tape seams to encapsulate the gages in waterproof environments.

Stainless steel true size pins were used to connect the load rod to the piles. Due to the precise size of these pins, very little relative movement between the load rod and the piles was possible.

### ***Load Cells***

Two load cells were used to measure the forces exerted on the pile group during lateral load testing, by incorporating them in the linkage between the load applying hydraulic cylinders and the pile group. Figure 6 shows the basic outline of the load cells. Aluminum 6061 T-6 strap stock 4.763 mm (0.188 in.) thick was first machined to a width of 25.4 mm (1.0 in.) and a length of 101.6 mm (4.0 in.). Connecting holes 7.938 mm (0.313 in.) in diameter were drilled in each end, and a gauge section 31.75 mm (1.25 in.) long and 12.70 mm (0.50 in.) wide was machined in the central section of each load cell. Two CEA-13-250UW-120 strain gages were mounted to this gauge section, one on each side of the cell, using the same procedure as was used for attaching strain gages to the load rod.

Aluminum 6061 T-6 Strap  
0.188 inches thick

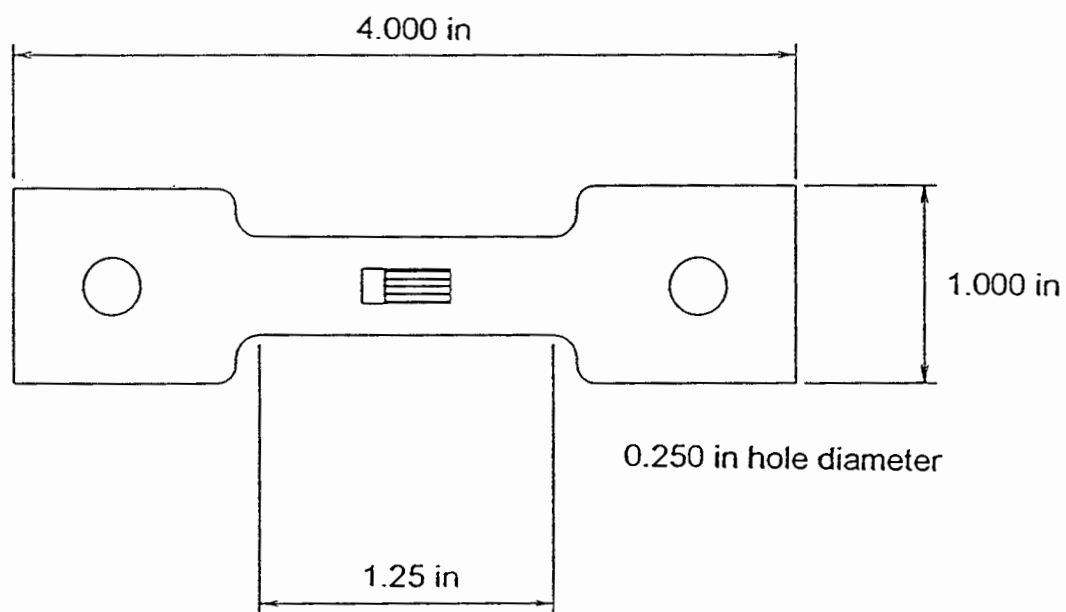


Figure 6. Load cell details.

### ***Linear Variable Differential Transformers***

Measurement of the pile group displacement during testing was accomplished by using two Linear Variable Differential Transformers (LVDTs). Using two LVDTs not only allowed for measuring deflection of the pile group, but by comparing the deflections in two places, the slope of the piles could be determined. The LVDTs were purchased from RDP Electrosense Inc. of Pottstown, Penn. Since the LVDTs both were type LDC 3000C, they were identical in appearance and nearly identical in functioning characteristics. Pieces of blue and red tape were affixed to the LVDTs so they easily could be distinguished from each other. The LVDT marked with red tape was used in Phase 1 of this project. Its specification sheet gave its linear range at  $\pm 75$  mm (3.0 in.) with a sensitivity of 29.91 mV/mm (0.76 V/in.) and a linearity of 0.12 percent. The second LVDT was purchased for this phase of the project because it was necessary to have two LVDTs with the capability to measure large deflections. According to the specification sheet sent with this LVDT, it had a linear range of  $\pm 75$  mm (2.9527 in.), a sensitivity of 30.23 mV/mm (0.768 V/in.), and a linearity of 0.10 percent. Blue tape was used to mark this LVDT.

Ball and socket fittings were screwed into the stationary ends and onto the sliding ends of the LVDTs. The fittings permitted a slight amount of angular movement at each end without causing binding or bending in either the LVDTs or the testing equipment and they were the means of mounting the LVDTs to the pile group.

It was necessary to use two LVDTs during testing to record deflections that were used as boundary conditions in the data reduction process. One was mounted at the pinned load rod/pile crown connection elevation to measure group deflection, and the other was mounted 76.2 mm (3.0 in.) above the load application axis to record a second set of deflection data that was used in calculating the angle of rotation of the piles.



To connect the LVDT at the load rod-pile cap elevation, a 25.4 mm (1.0 in.), 10-24 flat head machine screw was glued onto the end of the stainless steel pin used to connect the load rod to the end pile in the group. The ball and socket end fitting on the LVDT slider was slid over the machine screw and held in place with wing nuts, which could be used to adjust the horizontal position of the LVDT.

Modifications had to be made to the pile crown on the end pile in the group in order to allow the second LVDT to be mounted in the elevated position necessary for calculating pile head slope. Figure 7 shows the mounting configuration of the LVDTs. The first step in the modification process was to drill a hole vertically down into the solid part of the pile crown, far enough away from the pin connection to not interfere with the pin. This hole was then tapped with a 10-24 thread. The head was cut off a 101.4 mm (4.0 in.) 10-24 machine screw, which was then screwed down into the hole. A nut was then screwed all the way down onto the machine screw until it tightened up against the top of the pile crown. This secured the machine screw and kept it from coming out or wiggling. The ball and socket fitting on the slider end of the LVDT was then slid down over the machine screw and held in position with wing nuts, which also were used to vertically align the LVDT.

A bracket was made from a piece of steel strap material 3.2 mm x 63.5 mm x 203.2 mm (0.125 in. x 2.5 in. x 8 in.) to which the nonmoving ends of the LVDTs were mounted by means of two 50.8 mm (2.0 in.) 10-24 machine screws. Holes were drilled in the steel strap at 12.7 mm (0.5 in.) intervals to allow the LVDTs to be spaced as conditions required. The machine screws were inserted through the holes and tightened down with nuts. Two wing nuts were used on these to allow horizontal LVDT adjustment and to fix LVDT position once they were aligned.

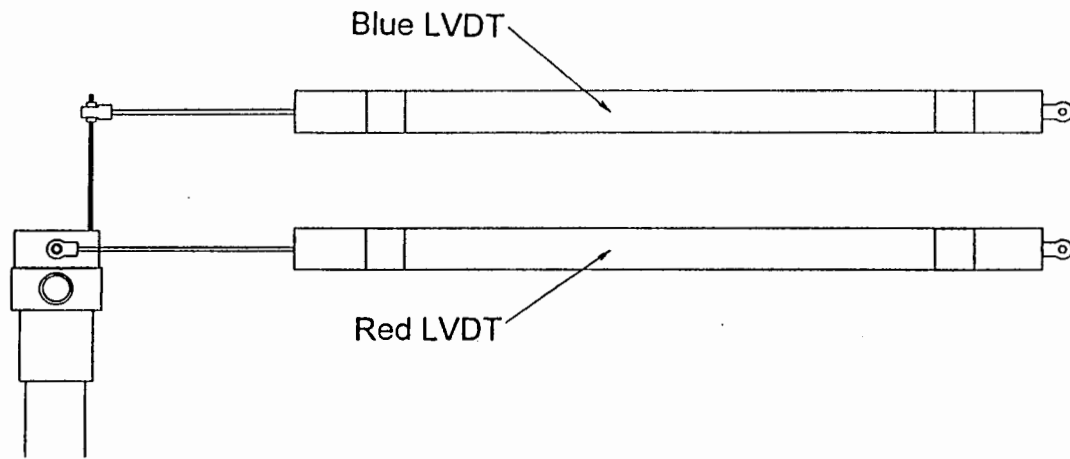


Figure 7. LVDT mounting configuration.

## CHAPTER IV

### DATA ACQUISITION SYSTEM

#### Background

##### *Phase 1 System*

The data acquisition system for Phase 1 of this project consisted of a Campbell Scientific AM416 mechanical relay multiplexer to switch between the 28 strain gage channels of the single pile being tested, a Campbell Scientific 21X data logger to collect the strain gage voltages and convert them to digital data, and an IBM compatible 386 computer to program the data logger and to store test data. This system worked well for single pile testing, but with the necessity to collect data from six piles at a much higher sampling rate, a completely new system was needed for this phase of the project.

##### *System Origin*

A considerable effort was put toward finding an adequate system that could be purchased off the shelf. Any system capable of reading so many strain gage channels at an approximate required rate of 10 Hertz was much more costly than the project budget allowed. An effort also was made to buy into a system being purchased by the Civil Engineering Structures Division, but again system requirements could not be met with the funds available. These findings led to the idea of designing and building a data acquisition system. The Electrical Engineering Department at USU was contacted to determine feasibility of such a venture. An undergraduate student volunteered to take on the task, with faculty assistance, of designing the data acquisition system, which also could be used as a senior design project.

## System Design

### *Requirements*

System specifications called for designing a system that could sample 256 channels at a rate of 10 Hertz, and interface with a personal computer where the testing could be monitored and the data stored in a user-friendly format. The specification for 256 channels was made so that future pile group tests might be expanded to include nine piles with 28 strain gages each with several extra channels for other instruments.

The system designed was based around a commercial analog-to-digital (A/D) circuit board manufactured by National Instruments, which interfaced with the piles through custom designed printed circuit boards. National Instruments LabVIEW™ software programs were written to control the data acquisition processes.

### *Input Board Design and Function*

The basic unit of the data acquisition system is the Wheatstone bridge circuit. Printed input circuit boards were designed to accommodate quarter-Wheatstone bridge circuits for every strain gage. Figure 8 shows a Wheatstone bridge as configured on the input circuit boards. One side of the bridge is made up of one 160-ohm resistor and the 120-ohm strain gage. The other side of the bridge contains a 160-ohm resistor, a 100-ohm resistor, and a 25-turn potentiometer that was included in the circuit to provide a means of balancing the two sides of the bridge to compensate for variance in the resistance of the resistors. The values of the resistors were chosen to minimize induced noise.

Analog multiplexing was used to allow use of a single A/D converter. Voltage readings from each side of the bridge were routed to a separate multiplexer (mux) allowing simultaneous passing to a differential operational amplifier (op amp). The differential op amp receives small voltages from the dual muxes, which correspond to voltages on each side of the Wheatstone bridge, and takes the difference

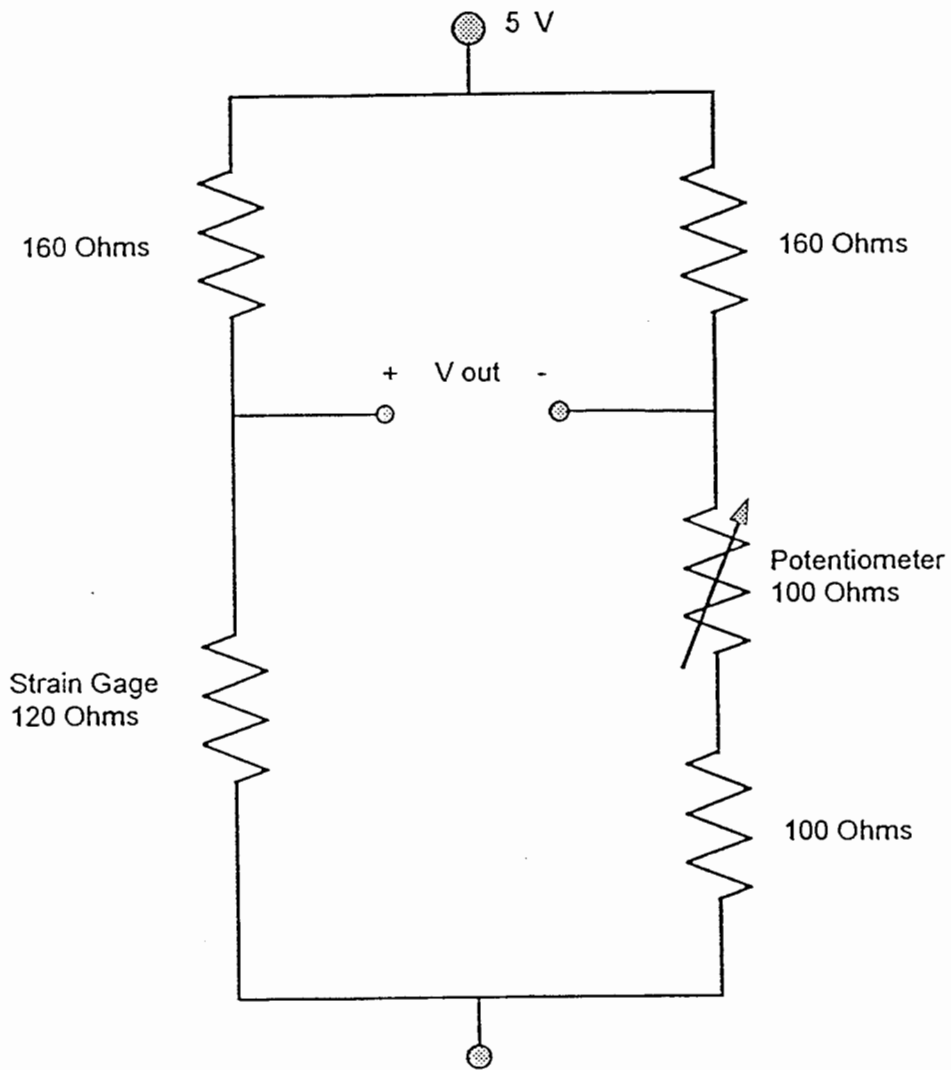


Figure 8. 1/4 Wheatstone bridge configuration used on input circuit boards.

between them, multiplies the difference by desired gain, and provides a single output. The signal is then sent to a low pass filter with a cutoff frequency of 230 Hertz and a settling time of around 6 milliseconds. Figure 9 shows the flow sequence of a strain measurement. An attempt was made to filter out noise signals at lower frequencies, particularly in the 60 Hertz range, but the settling time would have been too great to allow the system to operate at the desired sampling rate of 10 Hertz. The speed of the filter drove the design of the system in order to run at the desired rate of 10 Hertz, all sampling for 16 lines in parallel had to be collected in 6.25 milliseconds. After filtering, only 0.25 milliseconds remained for all other settling and switching functions. All readings get sent to the A/D converter after filtering.

Sixteen Wheatstone bridges were placed on a single input circuit board along with the two muxes, the op amp, and the low pass filter. The whole data acquisition system has a maximum capacity of 16 of the input boards. Figure 10 shows the input boards' design with bridge circuit traces and silk screened component locators.

### ***Analog-to-Digital Conversion***

The A/D converter board purchased for this project was manufactured by National Instruments and was of the type PC-LPM-16, and was plugged into an IBM compatible personal computer. The PC-LPM-16 had 16 single-ended analog and eight digital input lines, along with digital output lines that were used to control muxes on each of the input boards. Each of the 16 single-ended analog input lines was dedicated to one input board and was connected by means of a printed interface bus circuit board with card edge connectors for the input boards and a ribbon cable that ran from the interface bus to the PC-LPM-16 board. LabVIEW software is a graphical programming language from National Instruments and interfaces automatically with the PC-LPM-16 A/D converter board and was used to control all functions of the data acquisition system.

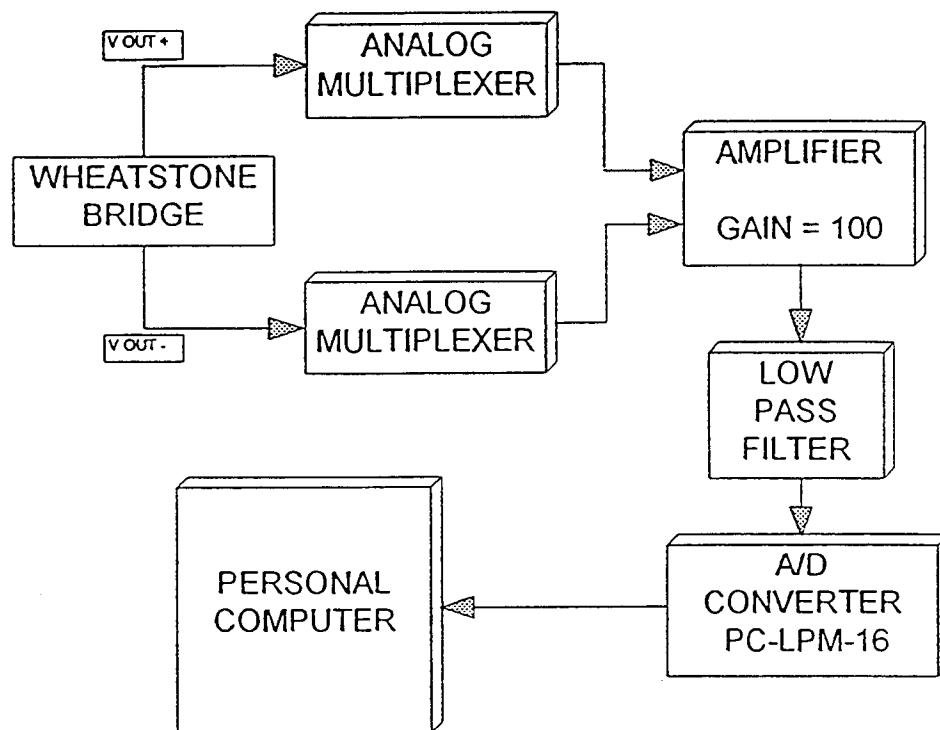


Figure 9. Flow sequence of strain measurements.

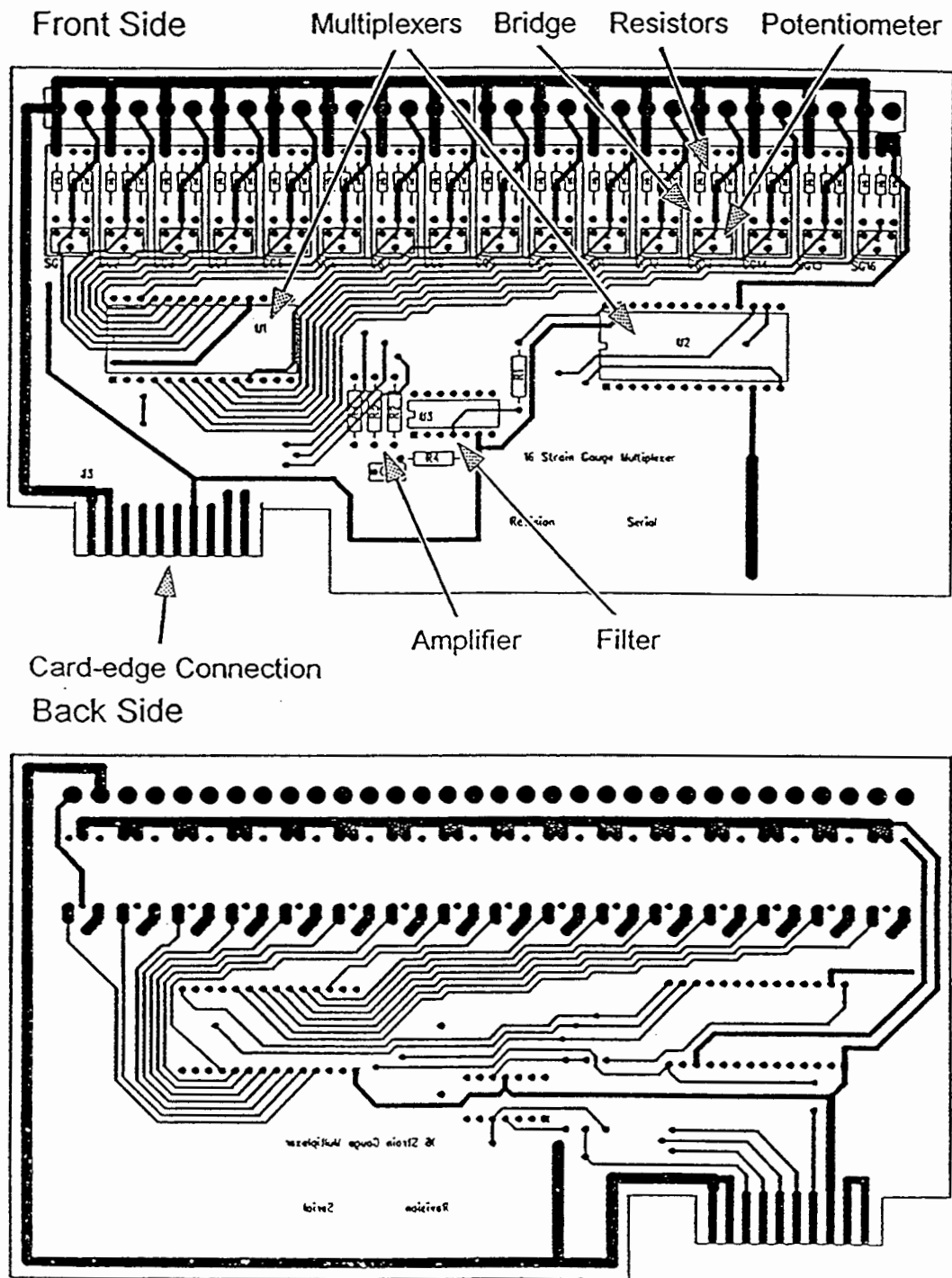


Figure 10. Input circuit board trace and component layout.



Power for exciting the strain gages was provided by a Sola model SLS-05-120-1 linear, open frame, DC power supply. It is capable of providing 12 amps of current at +5 volts. A smaller Sola model SLS-05-030-1 power supply was used to power the analog multiplexers with a possible 3 amps of current at -5 volts.

## **System Construction**

### ***Input Board Assembly***

Once the design of the input circuit boards was completed, the blueprints were sent to Quick Turn Circuits in Salt Lake City, Utah, where the circuit boards were actually fabricated in a matter of days. All connection holes were predrilled and all component positions were labeled with silk screening.

Each of the 16 input boards was built up with the following: 48 resistors of two types for the Wheatstone bridges, 16 potentiometers, two 16-port screw-type terminal blocks for the strain gage wire connections, two 28-pin analog multiplexer sockets, one 14-pin amplifier chip socket, four amplifier resistors, one capacitor for the low pass filter, and one filter resistor. The multiplexer and amplifier chips then were pressed into their respective sockets, with the only requirement being that they were installed with a small detent in each chip facing to the left side of the input board.

### ***Interface Bus Assembly***

The interface bus also was fabricated by Quick Turn Circuits and was assembled next. The components soldered to the interface bus included 16 20-contact card edge connectors for connecting to the input boards, one 50-pin socket-to-socket connector for the ribbon cable connection to the PC-LPM-16 A/D board, one four-position screw type connection terminal block for power supply hook up, and one 20-pin socket for the signal buffer chip, which amplifies control signals coming from the computer. To assure that the card edge connectors would not be damaged or get pulled off by the repeated plugging

in and unplugging of the input boards, holes were drilled through the interface bus to match holes predrilled in the connectors. Machine screws were inserted through the holes and fastened on the other side with nuts. After installing the signal buffer chip, the interface bus assembly was complete.

### ***Box Construction***

All of the components had to be housed, therefore a decision was made to bring all components external to the personal computer together in one box, including input boards, interface bus, power supplies, fuses, and all components necessary to control the pile group loading system. This would allow for easier management of all of the testing systems. Figure 11 shows the layout of the data acquisition system box.

The box was constructed of 4.8 mm (0.2 in.) thick plywood and is 476 mm (18.75 in.) long, 422 mm (16.6 in.) wide, and 178 mm (7.0 in.) high. The inside surface of one of the long sides was slotted with 16 3 mm (0.13 in.) slots spaced at 20.3 mm (0.8 in.) intervals to be used as guides for holding the input boards when plugged into the interface bus. A cooling fan was added to the box to provide the 0.57 m<sup>3</sup>/min (20 ft<sup>3</sup>/min) of convective cooling air required by the large power supply. A circular hole was cut in one of the short sides to accommodate the fan. Two slots were cut in the wall opposite the fan. Through one of the slots the ribbon cable passes in going from the interface bus to the A/D board in the computer. The second slot was positioned so cooling air could be drawn into the box and pass across the heat-sink resistors on the underside of the large power supply. Other holes were drilled in the box for power cords, one for bringing in power and the other for sending power to the pile group loading system. The component positions were laid out and holes were drilled for mounting bolts, after which the box was painted inside and out. Brass bushings were used as standoffs for the power supplies, interface bus, and the loading system switching relays and logic circuit.

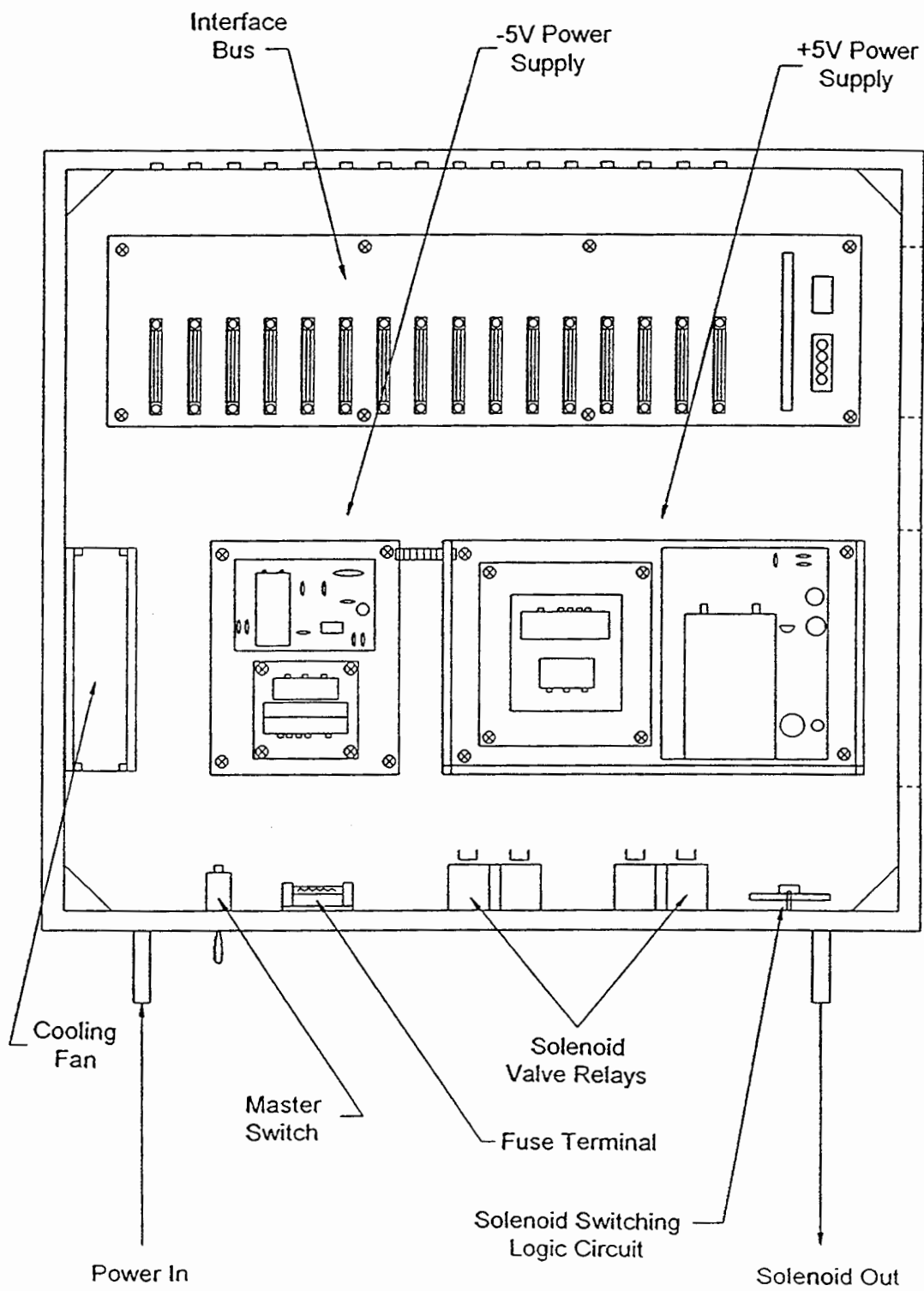


Figure 11. Data acquisition system box layout.

The loading system logic circuit and relays were wired so they could be controlled by the A/D board in the computer and the LabVIEW software. Wires for power and signal passing were soldered to the proper pins for these functions on the interface bus underside where the 50-pin socket connector pins protruded.

Once all of the other components had been mounted, a wiring scheme had to be established and all of the wiring done. Fourteen-gauge wire was used so there would be as little chance as possible of power being dissipated by the wires. Wiring connections were either soldered joints or forked-end connectors fastened in place with screws. Heat shrink tubing was used in an attempt to cover as many exposed and potentially hazardous connections as possible. The power supplies were grounded with wires connecting them to the ground wire from the supply cord. For grounding the piles, a short bolt with enough nuts to fasten each of the grounding wires from the piles was attached to the frame of the large power supply. Finally, all of the wires were connected to either hot, neutral, or ground wires with wire nuts and then tied in place with zip ties.

A two-piece lid for the box was constructed of plywood and fitted with handles for easier removal. Cabinet door hardware was installed to hold the lid in place. The lid was made in two pieces so that the inside of the box could be accessed easily without having to disturb wire bundles coming in from the piles, which are trapped between the lid sections to keep them from being jostled when the lid is in place. It is important to keep the lid on the box as much as possible when running the full system so that cooling air will be drawn across the large power supply through the air vent. Otherwise, it might overheat because air does not circulate through the box properly. If only one- or two-piles are hooked up it is not as important to keep the lid on as the large power supply does not heat up as much.

## CHAPTER V

### CALIBRATION

#### Calibration of the Model Piles

##### *Background*

Since the strain gages were mounted on the inside surface of the piles and placement could not be absolutely controlled, some minor mounting errors probably were made. These errors could be misplacement of the gages on either side of the planned gage position, misalignment of the gages so they were not perfectly straight with respect to the axis of the pile, or they could have been mounted in a rotated position, as in the case of the Red 8 and Black 8 gages in Pile 1, which were rotated about 30 degrees from the position of the rest of the gages.

All of the construction flaws have the potential of inducing errors in the strain data when the piles are loaded because the gages will be strained differently than expected. To overcome the unknowns, it was necessary to calibrate every strain gage in each pile under controlled conditions so that a correction factor could be determined and implemented when the piles were used in an actual lateral loading test.

To avoid damaging piles during a lateral load test, the piles were loaded to a maximum of 65 percent of the yield strength of the 6061-T6 aluminum pipe from which they were made. Calibration was done to 70 percent of the yield strength so that an envelope could be established in which reaction of the piles to loading would be documented. Seventy percent of the aluminum's yield strength was equal to a stress of 180.9 MPa (25900 lb/in.<sup>2</sup>) in the piles, and a corresponding allowable moment of 388.6 N-m (3440 lb-in.) using the equation:  $M=(\sigma)(I)/c$ , with  $I=3.635 \times 10^{-8} \text{ m}^4$  (0.08734 in<sup>4</sup>), and  $c=0.0167 \text{ m}$  (0.6576 in.).

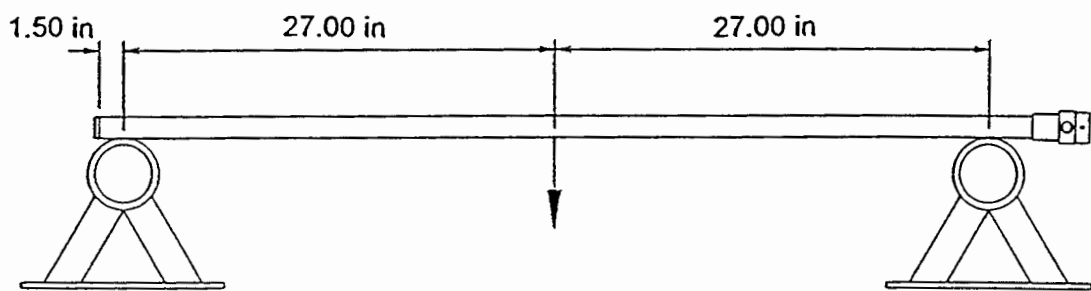
Calibration was accomplished by placing the piles horizontally on supports and loading them as simple beams using two loading configurations, subjecting the gages to tension and compression by turning the pile 180 degrees after the first set of loadings was completed and repeating with the other side up, thus reversing the stress state. Figure 12 shows the two calibration configurations. The first configuration used a concentrated load centered between the supports. This set-up provided a different moment value for each strain gage location at each load increment according to the equation:  $M=Px/2$ , where P is the load and x is the distance from the support to the strain gage.

The second configuration used two equal concentrated loads symmetrically spaced with respect to the supports. Loading in this manner gave different moment values for the gages between the supports and the loads according to the beam equation:  $M=P_x$ , again with P as the load magnitude and with x as the distance from the support to the strain gage. Between the symmetrically spaced loads, the moment would be a constant value as given by the equation:  $M=Pa$ , where a is the distance from the support to the position of the load.

Using the two calibration configurations gave not only more data points with which to compute a calibration factor, but also allowed diagnosis to be done in the event that a strain gage was giving output much different than expected, based on theoretical calculations. If a strain gage was out of position on either side of its assumed location, it consistently would give moment values much different than expected. These values could be compared with theoretical moment values and the gage's actual location could be determined. This new location would then be used for all testing involving that pile.

The magnitude of the maximum possible calibration load, while staying under the moment limit of 388.6 N-m (3440 lb-in.), was determined by the number of weights available for calibration, the length of piles, and location of the strain gages with respect to the placement of the supports and

### Single Load



### Double Load

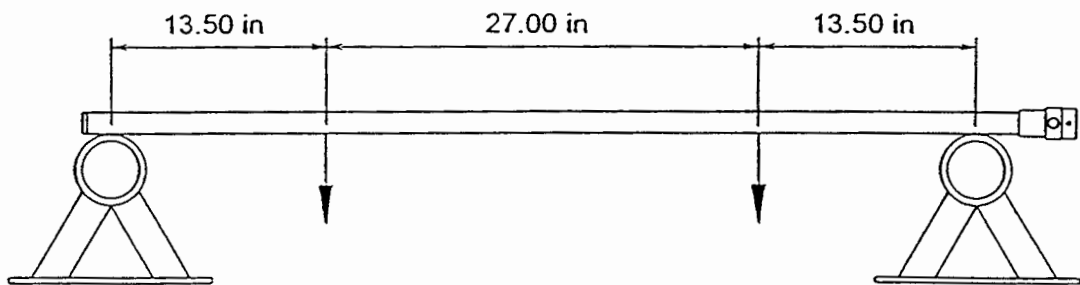


Figure 12. Calibration load configuration.

loads. Based on the number of calibration weights available, it was decided to let the maximum load be 1112 N (250 lb.). Since the maximum moment (M) was 388.6 N-m (3440 lb-in.), and with the maximum load (P) set at 1112 N (250 lb.), the distance between the supports and spacing of the symmetric loads was determined by equating the beam equations:  $M=PL/4$  for the centrally placed single load where L is the distance between the supports, and  $M=Pa$  for the symmetrically placed double loads, where a is the distance from the support to the load. The result was  $L/4=a$ . Using this equation, and the locations of the strain gages, distance between the supports was determined and positions of the loads were fixed. Care was taken to keep the gages at least 19 mm (0.75 in.) away from supports and loads so that Saint Venant's effects would not be read by the gages.

### ***Equipment***

Calibration equipment consisted of frames to support the piles, calibration weights and the means to hang them from the piles, a pile alignment or orientation device, and the data acquisition system and computer.

Heavy steel A-frames were used to support the piles during calibration. Because of the height of the stacked calibration weights, the A-frames had to be set on lengths of 2x4 boards to elevate piles so the weights cleared the floor at all times during calibration.

The 48 weights used for calibration were slotted, steel plates used in the USU soils lab for consolidation tests. Prior to calibration, the mass of each of the weights was checked on a scale. To have pairs of matched weights for use in the double load configuration, regular masking tape was used to add a small amount of mass to certain weights to raise them to equal the mass of other weights. The mass of each of the weights ranged from 4.000 kg (8.818 lb) to 4.945 kg (10.902 lb).

Weights were set on two hangers borrowed from the USU soils lab's consolidation equipment. Short lengths of one-eighth inch stainless steel wire rope were cut and bound into loops with wire rope



clips, trapping short lengths of long link chain cut to the proper length and slid onto the piles. The hangers were hung from these to give clearance between the stacked weights and the pile.

During calibration, a pile must be positioned with the strain gages oriented parallel to the axis of loading so they experience only tension or compression without any bending. To facilitate proper orienting of the pile, a device was specially designed and constructed. It is shown in Figure 13. This device was a small oak board 15 inches long that had been machined straight and sized to fit snugly into the pile crown slot, where it could be pinned by means of a hole drilled in one end. A small mirror, which was cut to fit the device was glued to the other end. Proper pile orientation was accomplished by sighting across the string from a plumb bob suspended from an eye bolt in the board and aligning it with reference lines drawn on the centerline of the board. The pile could be considered properly oriented when the lines and a single image of the string were aligned.

### ***Input Board Connections***

To facilitate the data reduction process and to lower the overall complexity of the pile-to-data acquisition system hookup because the number of strain gages per pile did not directly correlate to the number of channels on an input board, the piles were allotted two input boards each. One input board was dedicated to the red gages, all which are on one side of the pile, and one input board was dedicated to the black gages, on the other side of the pile. The boards were then referred to as the red and black boards accordingly. This left two channels unused on each board.

All input boards were hooked up in the same manner, with wires from gage number one clamped into the terminal block at channel number one and finishing with wires from gage number 14 clamped into the terminal block at channel number 14. Due to the small diameter of the strain gage lead wires, some of the connections were loose. When this problem was encountered, an extra amount of

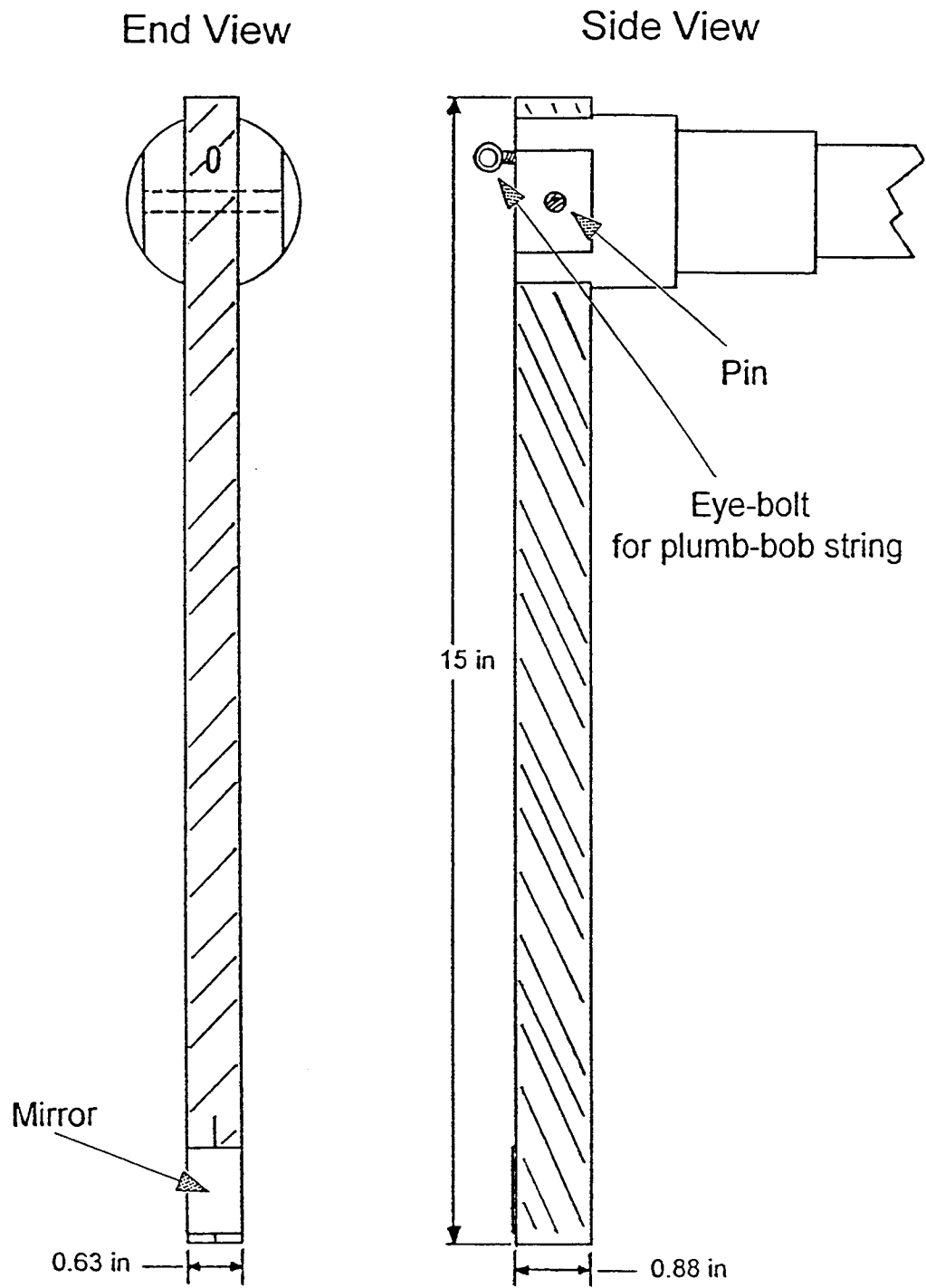


Figure 13. Pile orienting device.

solder was melted onto the wire lead, thus increasing the diameter of the wire and improving connection.

### ***Calibration Setup and Procedure***

The calibration setup and procedure was the same for all piles, so only a detailed description of the steps taken to calibrate Pile 1 will be given. Any variances and anomalies peculiar to other piles will be noted at the appropriate place.

Once the pile was properly hooked up to the red and black input boards, the Wheatstone bridges for each gage had to be balanced. The pile was placed on the loading supports during this procedure. This was only for convenience as pile position was not critical.

Due to the close spacing of the card edge connectors on the interface bus, there was no room for accessing the potentiometers on the red board if the black board was also plugged in; therefore work could be done only on one board at a time. For Pile 1, the red board was plugged into slot 1 on the interface bus. The data acquisition box was turned on and the bridge zeroing program, ZERO.VI, was called up on the computer. This program was written by specifically for balancing the strain gage Wheatstone bridges using LabVIEW software. Figure 14 shows the ZERO.VI program control panel. A real-time display of bridge voltage output was the main feature on the control panel of this program. There also was a user input display for entering the number of the input board to be read, as well as a user input display for selecting the strain gage channel that was to be balanced. To balance the first bridge on red board, Pile 1, the board designator and the strain gage designator were set at zero because this program starts all counting from zero instead of one, and thus all boards and gages must be designated by the number one less than their respective positions. With all settings properly made, the program was started.

BALANCING THE BRIDGES

Current S.G. #

▲ 9 ▼

Device #

▲ 1.00 ▼

Voltage

Board #

10

1.7261

Digital Port #

0

Figure 14. ZERO.VI program panel.

In the first attempt to balance a bridge, a hardware malfunction was discovered that persisted throughout the calibration process for every pile and has yet to be rectified. The problem was that when first starting the system, the voltage readout for not only the gage that was being balanced, but for all gages on that board went immediately to -2.5 volts and remained stuck there no matter how much the potentiometer for that bridge was turned. It was found by trial and error, that by unplugging the board or by leaving the board unplugged while turning on the system and then plugging it in, this problem could be sidestepped and bridge balancing could proceed.

After unplugging and replugging the input board, the voltage readout began to bounce around, thus showing that the bridge could be balanced. Balancing the bridge was done by turning the screw in the potentiometer whichever direction caused the readout to approach zero. The sensitivity of the 25 turn potentiometers was such that when nearing zero, just applying pressure to the screw could cause the readout to overshoot the goal. A soft touch was necessary when getting close to zero. It was not possible to balance the bridge at a perfect zero reading, but since an initial reading of all gages would be made before pile calibration as a reference, a perfectly balanced bridge was not necessary. Nevertheless, it was desirable to get as close to zero as possible so there would be no danger of going out of the voltage range of the straining gage during calibration. When a satisfactory voltage reading was attained, the program was turned off, the next strain gage bridge was selected, the program was restarted, and the process repeated until all the bridges on the red board for Pile 1 were satisfactorily balanced. The black board then was plugged in to slot two in the interface bus. At this point it also was found that plugging in another circuit board could cause the voltage readouts on a previously inserted board to jump to the value of -2.5 volts and stick. Again, trial and error showed that by unplugging and replugging the already balanced board, normal voltage readings could be regained and that previously balanced bridges were not seriously affected. The proper changes were made to the ZERO.VI panel by setting the board designator at 1 and the bridge designator at 0. This numbering scheme was confusing

at times. Perhaps it can be changed in the future by reprogramming. With input designators properly set, the program was restarted and all of the bridges were balanced following the procedure used for the red board. With all of the bridges for Pile 1 balanced, the pile was ready for calibration.

To assure proper pile positioning and load placement during calibration, stripes were marked on the piles at the correct locations. Supports were situated the proper distance apart and aligned parallel to each other. The load hanging loops were slid onto the pile and the pile was positioned on supports according to the support markings and seated there with chunks of butyl rubber, which allowed enough movement for fine positioning of the pile yet held it in place when set. Every pile calibration started with the pile turned right side up. The special pile orienting device described earlier was then inserted into the pile crown slot and pinned there. A plumb bob was hung from the eye bolt in the device and the pile was twisted until the string lined up with the centering lines on the device and with its own reflection in the mirror at the end of the device. The butyl rubber then held the pile in the correct position when the pile was pushed firmly into it. This finished calibration preparations for the pile.

To prepare the computer, the calibration program GO-CAS.VI was first called up. This program also was programmed with LabVIEW software specifically for calibration purposes. GO-CAS.VI collected data from the red and black boards and stored it in separate files, which were named by means of file designators on the program control panel. Figure 15 shows the Go-CAS.VI program control panel with the associated setting designators. Since pile calibration started with the pile laying on its right side and with the single central loading configuration, the file names selected for the red and black output files were chosen as Pile1RRS and Pile1BRS, respectively, meaning Pile 1, Red gages, Right side up, Single load, and Pile 1, Black gages, Right side up, Single load. Other designators on the front panel used for instructing the computer which boards to look for and read were set at 0 and 1 for the first two positions on the interface bus. Two other user input designators told the computer

how many of the channels on each board were to be read. These were set at fourteen, which would leave the fifteenth and sixteenth channels unscanned.

When all of the inputs were made, the program was started by clicking the run button on the row of icon buttons on the program control panel. This caused a virtual light on the panel to flicker, which meant that the program was ready. After checking the vertical alignment of the pile, and holding the load hanging loops up off the pile so that no load would be registered, a baseline reading was taken by clicking the GO button on the control panel. Twenty readings of each strain gage were taken after which the GO button clicked off. This took about 10 seconds during which time the virtual light froze. It then resumed flickering when the readings were finished, thus signaling that the reading phase was complete. The load hanging loop was positioned at the center load position and the weight hanger and the first load plate were hung in place. Care was taken after this and all load plates were placed on the hanger to stop the load from swinging and bouncing. The first load reading was taken by clicking the GO button and so on until the maximum load of 1115.5 N (250.8 lb) was reached in 24 load increments. Further readings were made as each of the load plates was taken off going from the maximum load back down to and finishing with another baseline reading. This gave a total of 49 load steps with 20 readings taken by each strain gage at each step. After the concluding zero load reading, the program was stopped by clicking the STOP button. To assure that no load steps were missed or no double readings were taken at the same load increment, the output files were checked to see if they contained 980 lines of data.

Preparation for the double load configuration test was begun by renaming the output file for the red board to Pile1RRD for Pile 1, Red gages, Right side up, Double load and by renaming the output file for the black board to Pile1BRD for Pile 1, Black gages, Right side up, Double load. If this was not done, the new data would be amended to the files previously mentioned. No other changes were necessary on the calibration program control panel. The pile was readied by positioning the load

Calibration Program Settings


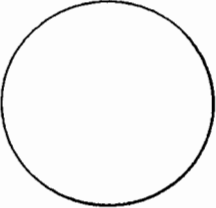

<b>Device Number</b> ▲ 1.00 ▼	<b>Dout Port</b> 0	<b>High Limit</b> ▲ 2.50 ▼	<b>Red Board</b> 4	<b>Ready</b> 
<b>Output File Red</b> D:\pile3rrs	<b>Digital Port Width</b> ▲ 8.00 ▼	<b>Low Limit</b> ▲ -2.50 ▼	<b>Black Board</b> 5	<b>Go</b> 
<b>Output File Black</b> D:\pile3brs	<b>Number of Strain Gauges Per PCB</b> ▲ 16.00 ▼			<b>Stop</b> 

Figure 15. GO-CAS.VI program panel.



hanging loops on the correct marks at 13.5 inches away from each support. The pile alignment was checked for verticality and the program was restarted. A baseline reading was taken while the load loops were held in the air. Then the hangers and the first load plates were put on and the first load reading was taken. The loading order and procedure was exactly the same as with the single load, and the load plates were paired so that no discrepancy in the loading existed. At the test's conclusion, data files were checked for 980 lines of data corresponding to the 49 readings.

During the double load test, it was noticed that the pile tended to rotate out of its proper orientation as the total load increased. This was probably due to the wire rope load loops gripping the pile on one side more than the other, thus turning it slightly. By carefully watching for this problem, it was prevented from causing difficulty during the remainder of this test. Afterward, short pieces of wood were cut and sized to fit between the pile orientation device and the legs of the support, which would hold the pile in the correct position during subsequent tests without continual monitoring.

Calibration continued by turning the pile 180 degrees and repositioning it in the proper place and in the correct orientation. The double load configuration was used first with the left side of the pile turned up. New file names were chosen to reflect this.

Calibration of Pile 1 was completed with the single load test after which the calibration program was stopped and all data files were checked for the proper volume of data. If for some reason a data file had greater than 980 lines of data, the file could be scanned manually to find the redundant set or sets of 20 lines of data, which could then be deleted. It was quite easy to find this extra data because the voltage readings changed so much from load to load. If it was found that output files contained less than 980 lines of data, the whole test in that position and configuration had to be repeated to get full calibration data.

### *Data Reduction and Analysis*

Completed calibration data files were given the suffix .prm when downloaded to a floppy disk so they could be imported into a Quattro Pro spreadsheet for data analysis. The file Pile1RRS.prm was imported into Quattro Pro and was used for development of the calibration figures. Since 20 readings of each strain gage were taken at every load increment, they had to be averaged before anything could be done to the data. The next step was to subtract the voltage value at the baseline reading from the rest of the voltage readings. Next, strain was calculated by multiplying the voltages by the constant  $3.87046 \times 10^{-3}$ , which comes from the Wheatstone bridge strain equation,  $\epsilon = V_0(R_2 + R_3)^2 / V_s S R_2 R_3 \times$  (amplification value), where  $V_0$  is the voltage difference,  $R_2$  is the resistance of the resistors in the bridge (160 Ohms),  $R_3$  is the resistance of the strain gage (120 Ohms),  $V_s$  is the magnitude of the supply voltage (5 volts),  $S$  is the strain gage factor (2.11), and the amplification value is 100. Stresses at each location and load were obtained by multiplying strain values by the modulus of elasticity for aluminum ( $E=68,950$  MPa or  $E=10,000,000$  psi). The theoretical stresses for each load increment at each strain gage location were calculated using beam theory for a simply supported beam loaded with a single concentrated load at a distance halfway between the supports. This completed the data reduction process for the file Pile1RRS and was the most difficult step of the data reduction procedure. Thereafter, this page of the spreadsheet was just copied to other pages where raw data from the seven remaining data files could be imported and the computations could be performed automatically.

After importing and processing all data for the eight Pile 1 calibration files, stress results from each file were copied onto two new pages in the spreadsheet according to the strain gage type, red or black. This was done so that results of the four different loading configurations could be used in a regression analysis of theoretical versus measured stresses for each strain gage. The regression analysis gave a factor with which the measured stresses could be corrected with multiplication to match theoretical stresses. This value then became the calibration factor for each strain gage. To complete the

calibration of Pile 1, a graph was made of all the measured stresses plotted against the theoretical stresses for each strain gage.

Once this first pile calibration spreadsheet was completed, data reduction for the rest of the piles was easily accomplished by copying and renaming the whole calibration spreadsheet, importing data into the appropriate places, and changing relevant names and titles on output graphs to reflect results of the computations. It was necessary to do the regression analyses one by one because this was not an automatic operation that could be copied from file to file.

Results of the calibration of Pile 1 showed that the Red 8 and Black 8 gages inadvertently had been mounted backward so that the red gage was on the black side of the pile and vice versa. This also was the case with Pile 3 gages Red 6 and Black 6 and Pile 4 gages Red 3, Black 3, Red 5, and Black 5. This problem was easily rectified in all cases by simply switching wires for the gages from one board to the other. All the gages in Pile 6 were reading the opposite of what was expected, so it was determined that the pile crown must have been installed backward. It must be remembered when Pile 6 is used that this is the case and the input boards installed accordingly, or all output data will be reversed.

Calibration also revealed that several gages, their connections, or lead wires were defective. These gages were Pile 1, Black 11, Pile 2, Red 2, and Pile 3, Red 1. These gages gave random output data, shown on their calibration graphs. Figure 16 shows the random output from a defective gage. The Black 14 gage in Pile 2 had a short circuit before calibration was started and was not even hooked up to its input board for calibration.

Several trends were noticed when comparing calibration graphs from all of the piles. One of these was how the gages near the pile's center measured stresses closer to theoretical than the gages at the ends of the piles. This was probably because the gages in the pile's center were subjected to a much larger range of stresses by the nature of the loading configurations than were the end gages. It also was

noticed that in general, one side of the pile had higher calibration factors than the other side. Red or black, it did not matter, but it was a fairly consistent phenomenon.

The overall performance of the gages was quite good, with the average calibration factor being 1.126, meaning that theoretical stresses were on the average 1.126 times greater than the measured stresses. Most of the calibration factors were off by less than 20 percent of the theoretical value, with one gage off by only 0.03 percent. Figure 17 shows the typical calibration output from a functioning strain gage. The four gages at the ends of the piles had an average calibration factor of 1.28. This could probably be improved if the piles were calibrated in an additional configuration where the piles were loaded as a cantilever beam. This would be especially important for the top end of the pile, since that is where the loading takes place under testing conditions. For comparison sake, Pile 1 was recalibrated to see how much change in calibration factor might occur from its initial calibration. None of the calibration factors from the second trial agreed exactly with those from the first trial, but the average difference for all gages was only 0.525 percent. This concluded the pile calibration.

### **Calibration of the Load Rod and Load Cells**

#### ***Instrument Description***

The load rod was designed and fabricated from 6061-T6 aluminum so that it could not only transfer the load to all the piles in the group, but it also would act as four load cells to measure loads that were transferred to each pile. The load cells were fabricated from 6061-T6 aluminum so that the same strain gages that were used in the piles and load rod could be used.

The load rod was designed to allow maximum pile head movement with a minimum of interference, but this resulted in the axis through which the load rod pins would act being below the centroidal axis of the aluminum strap material between the pin connections. Bending stresses could then be induced from the moment created by loading along the unaligned axes. Therefore, it was

# Pile 3 Red Gage 1

Calibration Factor=

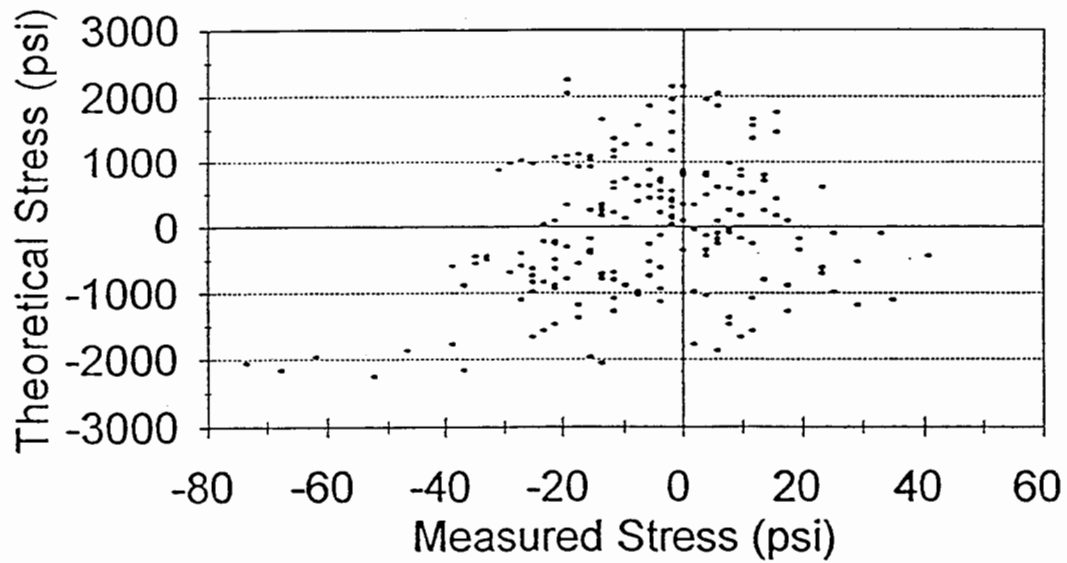


Figure 16. Calibration output for a defective gage.

# Pile 3 Black Gage 8

Calibration Factor=1.000371

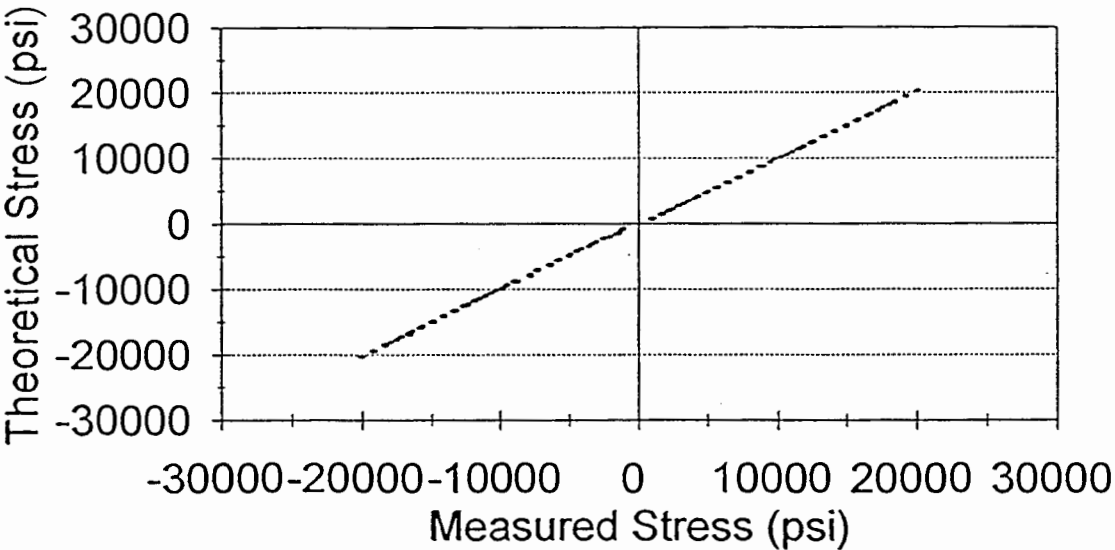


Figure 17. Calibration output for a normal gage.

essential that all the gages on the load rod be functioning so that bending stresses could be eliminated from total stresses by averaging output readings from gages on opposite sides of the load rod.

As in the piles, the eight strain gages on the load rod and the two strain gages on each of the load cells had to be calibrated before being used in a pile group test to account for possible alignment errors and mounting defects.

### ***Input Board Connections***

Connecting the load rod and load cell strain gages to the input board was done starting with Red gage number 1 as designated on the load rod. Its wires were clamped into the terminal block at channel number one. Black gage 1 was then clamped into the terminal block at channel number two and so on until all gages were thus connected with the last gage, Black gage 4, clamped into channel number eight.

The red and black gages from load cell A were connected to the circuit board at channels nine and 10, respectively, with the red and black gages from load cell B going into channels 11 and 12.

Although the absolute order probably does not matter, to assure consistency, improve data acquisition speed, and reduce software complexity, the input board dedicated to the load rod and load cells was plugged into the interface bus at slot number 13, where it was during the pile group lateral load tests.

### ***Calibration Apparatus, Setup, and Procedure***

Upon completion of the hookup, it was necessary to balance the Wheatstone bridges in each strain gage channel. The LabVIEW program ZERO.VI was called up on the computer, and the proper input board number was entered to tell the computer where to look for the gages to be balanced. The program was started and each of the 12 bridges were balanced individually by turning the screw on the

bridge's potentiometer until the readout was as close as possible to zero. This required turning the screw through about eight complete revolutions before the readout started to change from its initial reading, which was always -2.5 volts. Once the readout started to change, it continued to change rapidly with only slight pressure to the potentiometer screw. All bridges were rechecked and readjusted as necessary before calibration was begun.

The apparatus necessary for calibration included the data acquisition system, a C- clamp from which everything would be suspended, chains of various lengths, clevises for connecting the components, S hooks and lengths of rope for hanging the weights, and the calibration weights themselves.

The load rod and load cells were calibrated using the same procedure and so only the procedure for calibrating the load rod will be explained in detail. Any step specific or peculiar to the load cell calibration will be highlighted at the proper time.

Calibration was done in the basement of the USU engineering building where the necessary apparatus could be suspended from a floor joist I-beam of the first floor. A C-clamp was fastened to the flange of the I-beam and a three-foot length of long link chain was hung from the clamp to allow for convenient vertical positioning of the load rod and the calibration weights. The load rod was connected to the chain by means of a specially ordered stainless steel twisted clevis with a threaded pin. The dimensions of the clevis were such that it barely fit over the end of the load rod. The threaded pin fit through the hole in the end of the load rod so that little relative movement was allowed. Another clevis of the same type was pinned in the other end of the load rod, and a 22-inch length of chain was hung from it. Calibration weights were then suspended from this chain by means of S-hooks put into the individual chain links, with two-foot pieces of rope connecting the weights to the S-hooks. Fifteen weights were borrowed from the Utah Water Research Laboratory for the calibration. Fourteen of the weights weighed 222.4 N (50 lb.) each and one weighed 111.2 N (25 lb.).



The calibration procedure was begun by calling up the LabVIEW calibration program, GO-CAS.VI, naming the output files, and adjusting the settings so the proper interface bus slots and the correct number of strain gages were read. For the load rod calibration, the number of strain gages to be read was set at eight, since the load cells could not be calibrated at that same time. This allowed the program to run faster and also eliminated extraneous data that would be collected from the load cells. Later in the calibration of the load cells, the number of strain gages to be read would be increased to pick up the load cell channels, but the eight channels of extraneous data collected from the load rod strain gages would have to be discarded in the data reduction process. With all of the settings initialized, the program was begun.

The load rod was calibrated using load increments of 111.2 N (25 lb.), beginning with a zero-load baseline reading, increasing to a maximum of 3225 N (725 lb.), and then decreasing to a final zero-load reading. This was accomplished by hanging the 111.2 N (25 lb.) weight from the chain attached to the load rod, taking a reading, removing this load and putting on a 222.4 N (50 lb.) weight, and taking a reading. The 111.2 N (25 lb.) weight was again hung from the load rod and a reading was taken. It was removed and another 222.4 N (50 lb.) weight was added and a reading taken. This procedure produced 59 data points with which to calculate a calibration factor for each gage pair on the load rod. The initial and final zero load readings on all eight of the load rod strain gages were compared at the end to determine if any yielding of the rod had occurred. Output file names were changed when the load cells were calibrated, but the procedure was the same in all cases.

### ***Data Reduction and Results***

Before downloading the load rod and load cell calibration data files, the .prn suffix was added to their file names so they could be imported into the calibration spreadsheet. They were then copied to a backup disk for protection.

The load rod data file was imported directly into the calibration spreadsheet, but as was mentioned earlier, the load cell data files had to be imported into an intermediate spreadsheet where data from the load rod the load cell not being calibrated was deleted. Once this was done, the load cell files were imported to the calibration spreadsheet.

When properly imported, the 20 voltage values taken at each load increment for each strain gage were averaged automatically. The initial baseline reading for each gage served as the basis from which all other readings were referenced. Differences between the voltage at the baseline reading and the voltages at each of the loadings were calculated. Using the strain equation cited above and the voltage differences, the strain induced by each load was calculated. Stress at each load increment was calculated by multiplying the strain value by the modulus of elasticity for aluminum. All of the calculations could have been accomplished in a single step, but by using this method intermediate results could be examined and printed out, and errors could be more easily found. At this point in the data reduction, affects of the bending stresses on the calibration output could be readily seen. Gages opposite each other on the load rod showed stress levels that were vastly different. When these opposing gage stresses were averaged, the bending stresses were eliminated according to theory, and the resultant stress was compared to the theoretical normal stress by a regression analysis to determine a calibration factor for each gage pair. Although there should not have been any bending stress in the load cells, their measured stresses also were averaged before doing the regression analysis.

In all cases, the averaged, measured stresses turned out to be quite close to theoretical stresses for the many loadings, with calibration factors close to 1 and output data plots showing straight lines indicating linear measurements. Figures 18 and 19 show calibration output for a pair of strain gages on the load rod and a load cell. The results of these calibrations show that the load rod and load cells can be used with confidence in the capacities for which they were designed.

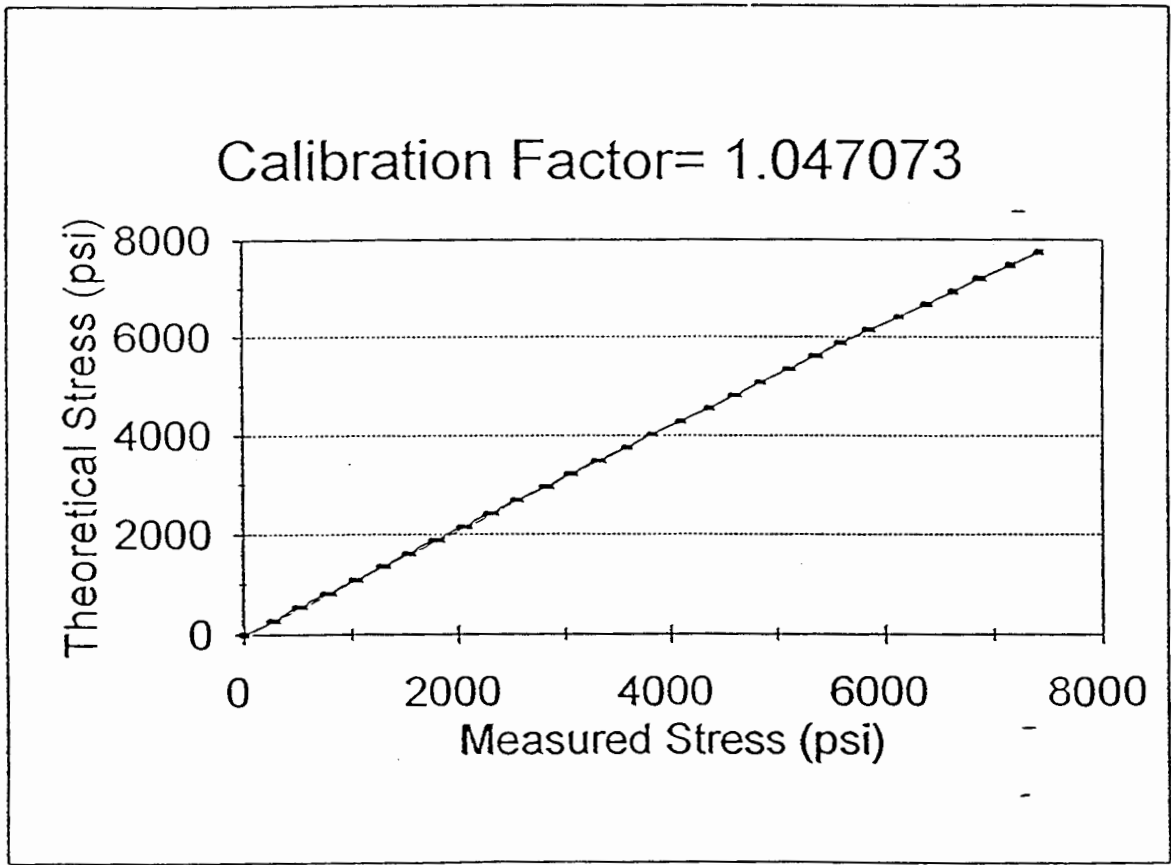


Figure 18. Calibration output for load rod gages Red and Black 1.

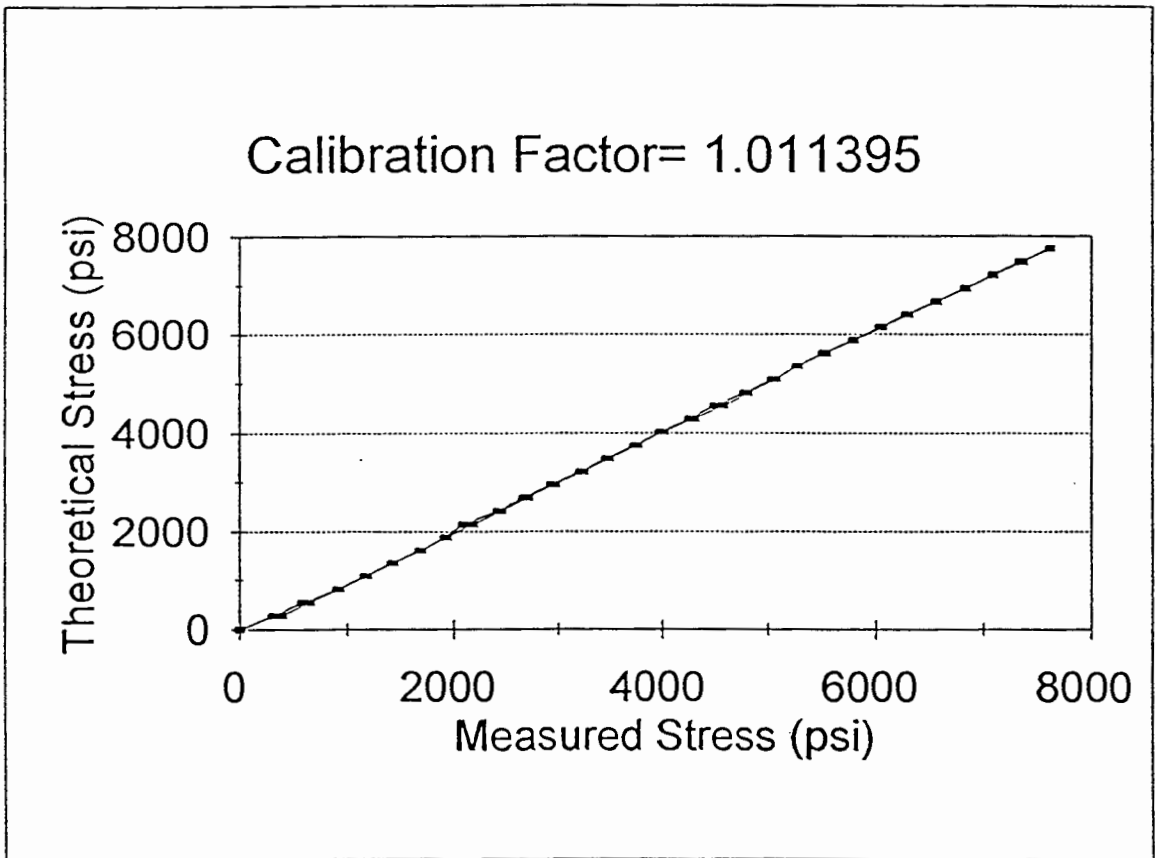


Figure 19. Calibration output for load cell A.

## Calibration of the LVDTs

### *Equipment*

Two LVDTs used were purchased from RDP Electrosense Inc. of Pottstown, Penn., and are of the type LDC 3000C. They were identical in appearance and so were distinguished by marking them with red and blue tape. They will hereafter be referred to as the blue or red LVDT. The LVDTs have a linear range of three inches on either side of the zero point with a linearity of 0.12 percent. They were calibrated at the factory and have a sensitivity of 0.76 volts/inch for the red LVDT and 0.768 volts/inch for the blue.

### *Input Board Connections*

The LVDTs arrived from the manufacturer with seven colored wires extending from their connecting cables. An accompanying wiring diagram showed the connection details for the proper hookup. The LVDTs had the capability of being powered by a 12- volt power supply, so it was decided to modify one of the input boards so the power could be supplied to the LVDTs while taking advantage of the multiplexing, filtering, and amplifying capabilities already built into the circuit board. Channels 15 and 16 on board number 16 were chosen as hookup points for the LVDTs so that if, at a future time, expansion of the strain gage monitoring capabilities of the system is desired, the LVDT monitoring capabilities could be retained without encountering undue difficulties.

Before the actual hookup, the LVDTs were tested with a digital volt meter to measure voltage at the extremes of slider position. Limits of the linear range were found to occur at just over  $\pm 3$  inches of travel with corresponding voltage outputs of  $\pm 2.35$  volts.

A voltage dividing circuit was used for connecting LVDTs to the data acquisition system, and because a standard strain gage circuit board was used, the output signal gain had to be reduced by a factor of 100, since it would have to be processed through the board's amplifier, which would amplify

it by a factor of 100 and thus bring it back to its original magnitude. Power was supplied by a jumper wire from the power input trace of the interface bus. All LVDT wires were hooked up as specified by the LVDT connection details sheet with soldered connections.

After connecting the LVDTs, it was found that when the sliders were moved to points where the output reached approximately  $\pm 2$  volts, a sudden jump in output occurred to  $\pm 2.5$  volts where it remained constant no matter how much movement was made with the slider, until the slider was returned to positions where the output was approximately  $\pm 1.8$  volts, after which the output returned to normal. The cause of this problem is unknown, but to avoid it, sensitivity of the LVDTs was reduced so that at the extremes of slider travel, the output would never go beyond  $\pm 1.75$  volts.

To accomplish this, 270-ohm resistors were added in parallel to the 100-ohm grounding resistors in the voltage divider circuit. This procedure limited voltage output to  $\pm 1.75$  volts and succeeded in eliminating the problem, but since this also changed the sensitivity of the LVDTs, it was necessary to recalibrate the LVDTs to determine their new sensitivities.

### ***Calibration Apparatus, Setup, and Procedure***

The calibration apparatus included a dial gauge with a mounting bracket, a C-clamp, and a 24-inch ruler. The dial gauge used was an ELE International brand, model LC 10, graduated to read 0.001 inch movement over a two-inch span. The mounting bracket fastened to the dial gauge with a thumb screw and allowed for fixing the position of the dial gauge to a table top with the C-clamp. The ruler was taped to the table top and used as a coarse reference for placement of the dial gauge during the calibration process.

The program, GO-CAS.VI, was used for calibration. The Red Board and Black Board settings were initialized at 14 and 15 and the number of channels to be read was set at 16 so that the whole board would get read, and thus pick up the LVDT data from the last two channels on the board. A

random name was given to the Output File Red file designator for the fourteenth board, since no data would be collected from that slot and would therefore be less confusing when locating data files in the computer directory. For the data recorded from the fifteenth board, a name corresponding to the LVDT being calibrated was used and sent through the Output File Black file designator. When the blue LVDT was calibrated, the file name BLUELVDT was used, and for the red LVDT, the file name was REDLVDT.

Before calibration, the total travel distance of each LVDT slider was measured with a measuring tape. This distance was necessary for planning the calibration process and for data reduction.

To begin the calibration procedure, the LVDT was positioned parallel to the reference ruler with the stationary end butted against a rigid stop. It was then taped to the table to prevent movement. The slider of the LVDT was pushed in completely and the dial gauge was positioned so that its plunger touched and was aligned with the end fitting on the LVDT slider. The dial gauge was then clamped in place with the C-clamp once it had been properly oriented to give the dial a reading of zero. After final alignment checks were made, the calibration program, GO-CAS.VI, was brought up on the computer and all of the settings were checked and the program was started. A reading was taken with the LVDT slider completely pushed in and the dial gauge reading 0. The LVDT slider was then extended 0.1 inches as measured by the dial gauge and held in place by hand while another reading was taken. The slider was moved another 0.1 inches and a reading was taken. This procedure was followed until the slider had been extended the full two-inch travel of the dial gauge plunger, and resulted in the taking of 21 readings. At this point, the calibration program was stopped while the dial gauge was moved. The initial position of the dial gauge, with respect to the ruler taped to the table, was recorded, and then the dial gauge was moved approximately 1-7/8 inches farther away from the LVDT and reclamped to the table. The dial gauge was not moved a full 2-inch distance from the LVDT so that some data overlap would be assured and thus preserve the continuity of the calibration data. After alignment between the

dial gauge and the LVDT was corrected and the dial gauge reading was zeroed, the calibration program was restarted and another set of 21 readings was taken over the two-inch travel distance of the dial gauge.

This same procedure was followed for a third group of readings, after which the dial gauge was repositioned so that the next set of data would be taken with the LVDT slider starting at its fully extended position and moving back in. This was done to read from the known boundary of the full extension of the LVDT slider and thus the limits of LVDT voltage output could be correlated to the known distance of travel. The procedure used in collecting this set of data was the same used for the other three sets, with the only difference being that the 21 data points were reversed in order from the rest of the data because of the different direction of slider travel. The four sets of data resulting from this calibration covered the full range of LVDT slider travel with enough overlap to guarantee that no portion escaped calibration.

### ***Data Reduction and Results***

As with all calibration data, the LVDT data files were given the .prn suffix when downloaded to a floppy disk so they could be imported directly into a Quattro Pro spreadsheet. The LVDT calibration data as gathered by the acquisition, system contained 16 columns of numbers corresponding to the 16 channels that had to be read to include the 15th and 16th channels to which the LVDTs were connected.

The raw data first were imported into an intermediate spreadsheet where the 15 columns of extraneous data were deleted. The remaining data were then copied into the calibration spreadsheet where the 20 values from each reading were averaged. Once the averages were obtained, groups of data from the four separate calibration steps could be recognized by looking for overlapping numbers or for the numbers gathered at the extremes of LVDT slider travel. The 21 readings from the fourth



calibration step were located easily because of their reverse order caused by readings taken as the slider was moved into the LVDT and not out as with the other three steps. These values were manually reversed so that all of the data would be consistent. Graphs of voltage versus extended distance were made using the data and total possible travel distance, as measured before the calibration was begun. From these graphs, the linear range of the LVDTs was readily determined, as was extent of the linear range, which remained at six inches as given by the manufacturer's specifications. Figure 20 shows the calibration output for the blue LVDT.

The sensitivity of each LVDT was determined next. Four groups of readings were separated and the difference in voltage between each data point in each group was calculated. By using the graphs of voltage versus extended distance, the voltage differences corresponding to the readings that fell in the nonlinear regions were thrown out and the average of all of the remaining values was figured. The resulting sensitivities were calculated as 0.5196 volts/inch for the blue LVDT and 0.5195 volts/inch for the red LVDT where their respective sensitivities had been 0.768 volts/inch and 0.76 volts/inch when received from the manufacturer.

The close agreement between the two recalibrated sensitivities is a verification of the process used to change the sensitivities to a range compatible with the data acquisition system and lends confidence to the overall calibration procedure.

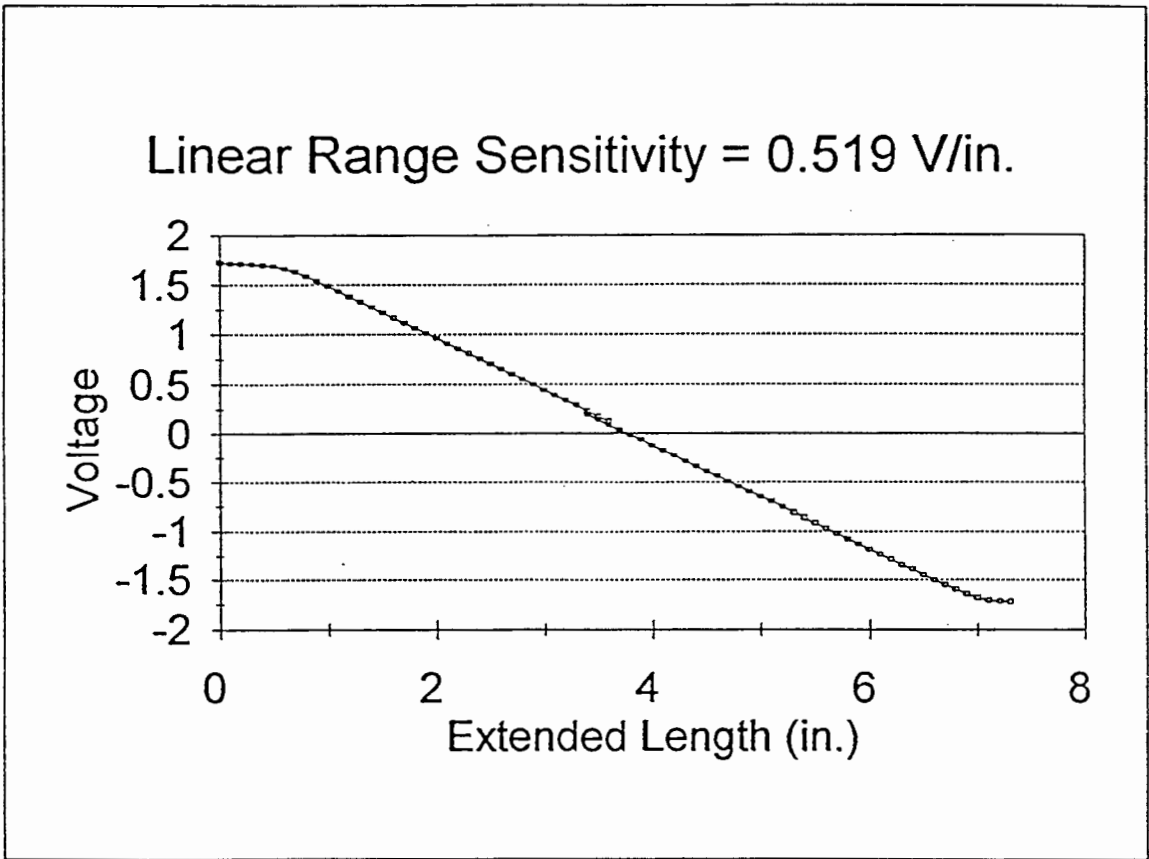


Figure 20. Calibration output for the blue LVDT.

## CHAPTER VI

### PHYSICAL MODEL TESTING

#### Loading System

##### *Background*

In Phase 1 of this research, a pile was loaded laterally in a static fashion by hanging weights from a cable that was attached near the top of the pile and run over a pulley. Increasing the load was done by stacking more weights on the hanger at the end of the cable. When the direction of loading had to be reversed, the weights were unstacked, the pulley apparatus was disassembled and then reassembled on the opposite side of the soil test vessel, and the weights were restacked as the testing procedure required.

This loading system was simple and worked well for the static load tests. For Phase 2, the initial ideas for laterally loading a pile group were based on Phase 1's system. Several other concepts were proposed for the loading system, and when financial needs were considered, it was decided to use as much on-hand equipment as possible. The hydraulic cylinders used for soil consolidation were not being used for anything at the time, but there was no means of using them to provide the lateral force for testing the piles. Since they were available, it was decided that an effort should be made to see if they could be used and once the decision was made to use the hydraulic cylinders for loading, design work began on how to mount the cylinders on the soil test vessel and how to power, operate, and control them.

### ***Mount Design and Construction***

The cylinders were mounted in a horizontal position on frames that were constructed to hold them in this manner and be sturdy enough to allow a large range of loads. The cylinders were mounted pointing toward the center of the soil test vessel. They loaded the pile group by pulling it back and forth as each of the cylinder rams was retracted in turn.

The hydraulic cylinders, as previously stated, were used to consolidate the test soil. All 10 of the cylinders were manufactured by Atlas Hydraulics and have a 101.6 mm (4.0 in.) bore diameter, a 50.8 mm (2.0 in.) ram diameter, and a 305 mm (12.0 in.) stroke. Two cylinders paired for the consolidation process were selected for the pile group testing. Changes had to be made to the plumbing of the two hydraulic fluid port fittings so that the cylinders would function as required. A male hydraulic hose quick-connect fitting was screwed into the retraction port on the cylinder to permit pressurized fluid to enter. An elbow with a short length of hydraulic hose was screwed into the extension port to allow free drainage of any fluid that might leak past the piston seals during testing. The foot plate at the end of each ram was drilled and fitted with a large U-bolt to which linkage for pulling on the pile group would be attached. Test runs on the cylinders could not be made until a pressurizing system was designed and assembled, but the cylinders were cleaned up and painted in preparation. U-frames used for mounting the pulley in the loading system from Phase 1 were the basic members of the new load frames on which the hydraulic cylinders were mounted. The U-frames were made from 76.2 mm (3 in.) steel channel, sized and welded to fit around the ends of the soil test vessel and bolt to end ribs of the tank. Two identical frames already were available, so two more of the frames were fabricated by USU Technical Services. Square structural tubing 89 mm x 89 mm (3.5 in. x 3.5 in.) with 6.35 mm (0.25 in.) thick walls was cut into four 1.22 m (4 ft.) lengths. Then they were welded to the U-frames at the corner positions so that two identical load frames were built up consisting of two of the lengths of structural tubing mated with two of the U-frames. The load frames were bolted to the soil

test vessel with grade 8 bolts. Once in place, the frames were rigid. Figure 21 shows the loading system with the load frames in place.

Measurements were made of the hydraulic cylinder base plates so that mounting frames could be fabricated, which would allow the cylinders to be mounted on the load frames. Steel channel 76.2 mm x 38.1 mm (3.0 in. x 1.5 in.) was cut into four lengths, each 0.965 m (38 in.) long, to span the width of the load frames. These channel lengths were slotted with six 17.5 mm (0.688 in.) wide slots of two different lengths oriented perpendicular and parallel to the axis of the channel to allow for vertical and horizontal adjustment of the cylinders when aligning them with the pile group before testing. Steel strap was welded to the ends of the channels to bind them together at the proper distance to match the bolt holes in the base plates of the cylinders. Grade 8 bolts were purchased for mounting cylinders to the mounting frames and for bolting the mounting frames to the load frames. Figure 22 shows a view of a mounting frame.

With the load frames in place, placement of the mounting frames and hydraulic cylinders with respect to the top of the pile group was laid out by measuring from the top of the soil to a string that had been strung between the load frames. This string was leveled at the proper elevation, measurements were made and markings placed at the proper locations on the load frames where the bolt holes for mounting the frames were to be drilled. A portable 12.7 mm (0.5 in.) electromagnetic drill press was used to drill the holes for the 15.9 mm (0.625 in.) diameter bolts. A C-clamp was used to bolster the electromagnetic base on the drill press, which allowed it to be attached to the frames in a horizontal position for drilling. The drill bit used for cutting holes was long enough to drill through both sides of the box beam without having to reposition the drill press. Grade 8 bolts were purchased for bolting the hydraulic cylinders to the mounting frames and the mounting frames to the load frames.

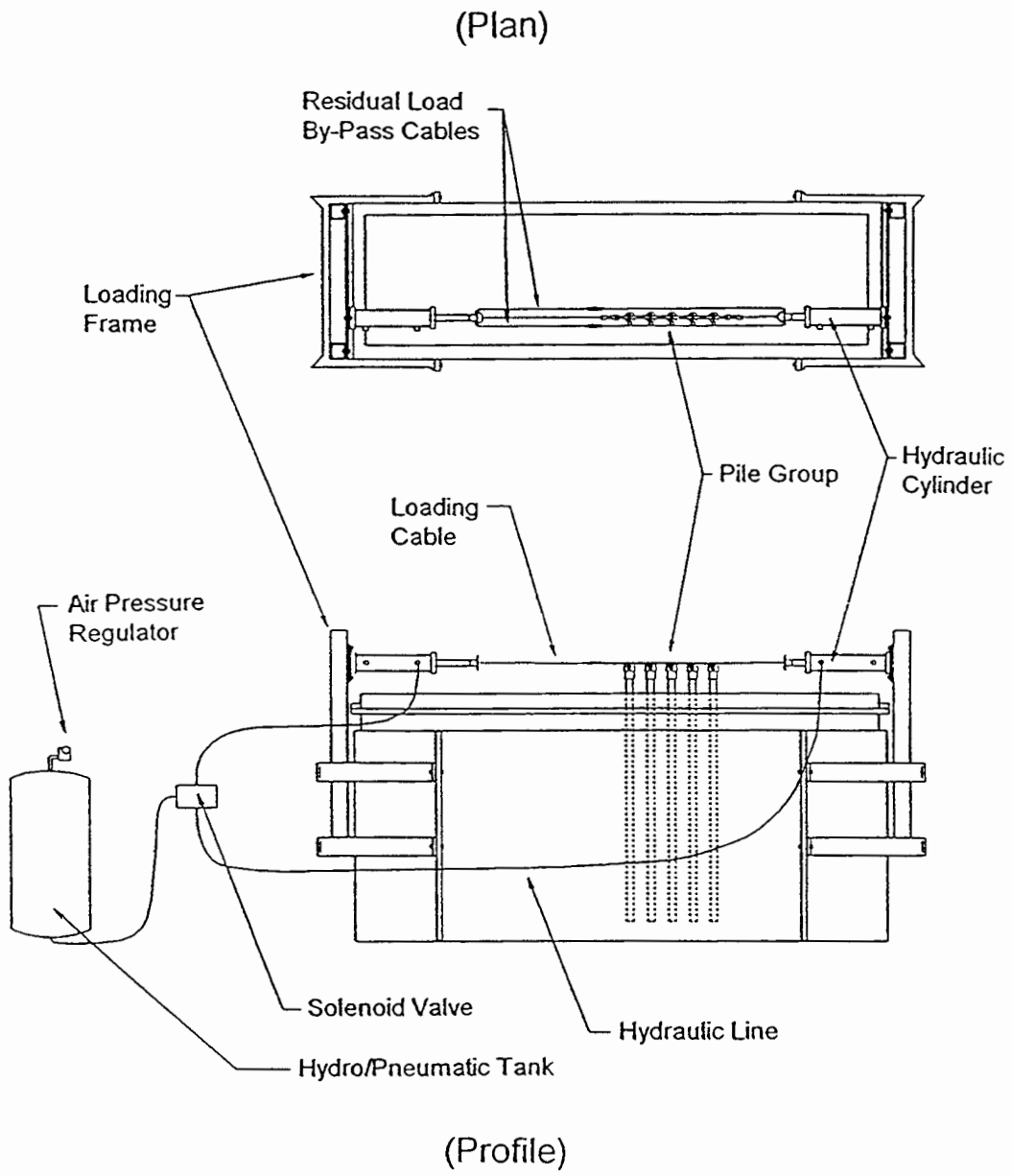


Figure 21. Loading system.

3.0 in x 1.5 in Channel Section  
0.688 in Slot Width

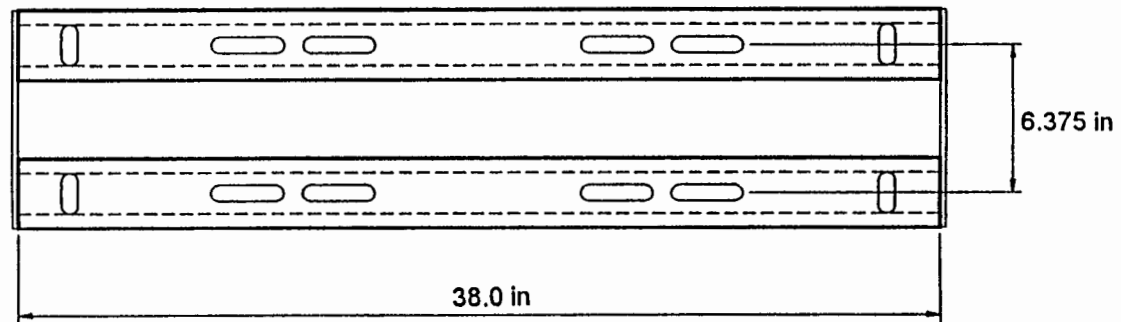


Figure 22. Hydraulic cylinder mounting frame.

### ***Pressure System Design and Construction***

Initially, hydraulic power for the cylinders was to be provided by the electric motor/hydraulic pump system used for consolidating the test soil, but calculations showed that a pressure change of only 36.5 kPa (5.3 p.s.i.) would produce a load change of 222 N (50 lb.), and a pressure of only 439 kPa (64 p.s.i.) would produce the target load of 2.67 kN (600 lb.). Controlling the pump at such low pressures and holding the pressure change steps to the desired 36.5 kPa (5.3 p.s.i.) would have been difficult, so it was decided that compressed air be used to provide hydraulic power to the loading system. A compressor provided compressed air to a tank holding hydraulic fluid which was connected to the cylinders by hoses. The pressure in the tank was controlled by an air pressure regulator mounted on the tank. Directional flow control was provided by a hydraulic control valve. Refer to Figure 21 for a diagram of the loading system.

A 0.113 m<sup>3</sup> (30 gal.) upright steel tank that was pressure rated to 1.38 MPa (200 p.s.i.) was purchased to hold the hydraulic fluid. A port in the bottom of the tank was fitted with a brass elbow to which the outlet hose for the pressurized fluid was attached. Galvanized pipe fittings were assembled and screwed into two 19 mm (0.75 in.) ports in the tank, one in the top of the tank to which the air pressure regulator was mounted and served as an air inlet, and the other on the side of the tank near the top to serve as a filler spout for the hydraulic fluid. A 6.35 mm (0.25 in.) port in the top of the tank was fitted with a galvanized nipple to which a ball valve was attached. This valve served as the pressure release valve so that pressure in the tank could be blown down quickly. All other tank ports were sealed with screw-in plugs.

The air pressure regulator had a flow capacity of 0.03 m<sup>3</sup>/s (65 c.f.m.) and a maximum pressure rating of 2.07 MPa (300 p.s.i.) and was fitted with a pressure gauge that read from 34.5 kPa to 1034 kPa (5-150 p.s.i.). A male-end quick disconnect hose coupling was screwed into the regulator so the air supply hose could be attached easily.



For control of the hydraulic fluid flow, a D03 size, 120-volt AC solenoid operated directional control valve manufactured by Waterman Hydraulics was purchased. This valve had a three-position, blocked center, spring-centered spool with a flow capacity of  $6.3 \times 10^{-4} \text{ m}^3/\text{s}$  (10 g.p.m.) and a maximum operating pressure of 34.5 MPa (5000 p.s.i.). The solenoids in the valve were tested by wiring up a simple electrical circuit and listening for the tell-tale click as each solenoid was energized.

Flow of oil to and from various ports in the bottom of the solenoid valve was facilitated by a side ported subplate that was ordered with the valve. This subplate was bolted to the valve and permitted mounting of the valve to a steel channel section base plate, and also was the means by which four hydraulic hoses were connected to the valve. One hose supplied pressurized fluid to the valve, and one hose served as an exhaust oil dump. The two other hoses transported the pressurized oil, as directed by the valve, to the two hydraulic cylinders. All of the components had to be assembled after either being purchased or fabricated.

### ***Pressure System Testing***

Once the loading system was assembled, it was tested in the CEE shop. The two hydraulic cylinders were hung from an A-frame by their U-bolts and the hoses were attached. Air pressure was supplied by hooking the air pressure regulator to the shop's air system. Pressure to the tank was slowly increased to determine the pressure required to make the cylinders start to move. The solenoid valve repeatedly was switched to send oil to each of the cylinders. Each cylinder lifted itself as the ram was retracted, but one of the cylinders would not extend when manually pulled, and the plumbing had to be switched and fluid sent to the other port to extend it. Another test determined the amount of force needed to extend the ram. This test showed that extension resistance in one of the cylinders was much greater than the other. Several different cylinders were tested until a pair of cylinders with similar working characteristics was found.

### ***By-pass Cable Design***

Upon seeing the results of the cylinder tests and seeing that the force needed to extend the cylinder rams was not negligible, an idea was proposed that the cylinders be linked so that the force needed to overcome the residual extension resistance of the rams by-passed the pile group and thus allow the pile group to be loaded only with the load intended for causing displacement. It was decided to link the cylinder foot plates with wire rope, then that they be tensioned and adjusted with turn buckles. Four brackets were cut from steel strap and drilled with two holes each for the needed connections. Two were then bolted to the back of each foot plate. The residual load by-pass cables were attached to the brackets. Figure 23 shows the residual load by-pass cables. Another benefit of using the by-pass cables was that forces in the load cells, on either end of the pile group, did not have to be compared, therefore the residual cylinder resistance could be subtracted and provide the net load on the pile group.

### ***Loading System Control***

LabVIEW Software, coupled with the PC-LPM-16 A/D converter board, has the capability of acquiring data and sending analog signals. This ability was used to control the loading system. The solenoid valve was AC powered, and was switched externally using switching with relays that were controlled by LabVIEW.

Two solid-state switching relays, manufactured by Teledyne Inc., were mounted in the data acquisition box, wired to the fuse box, and powered by the 120 Volt AC supply cord. A relay-controlling logic circuit was wired between the A/D output line that was wired to the interface bus ribbon cable connector and the relays. This logic circuit was designed to prevent power from being sent to both solenoids on the valve at the same time, and thus prevent damage to the valve.

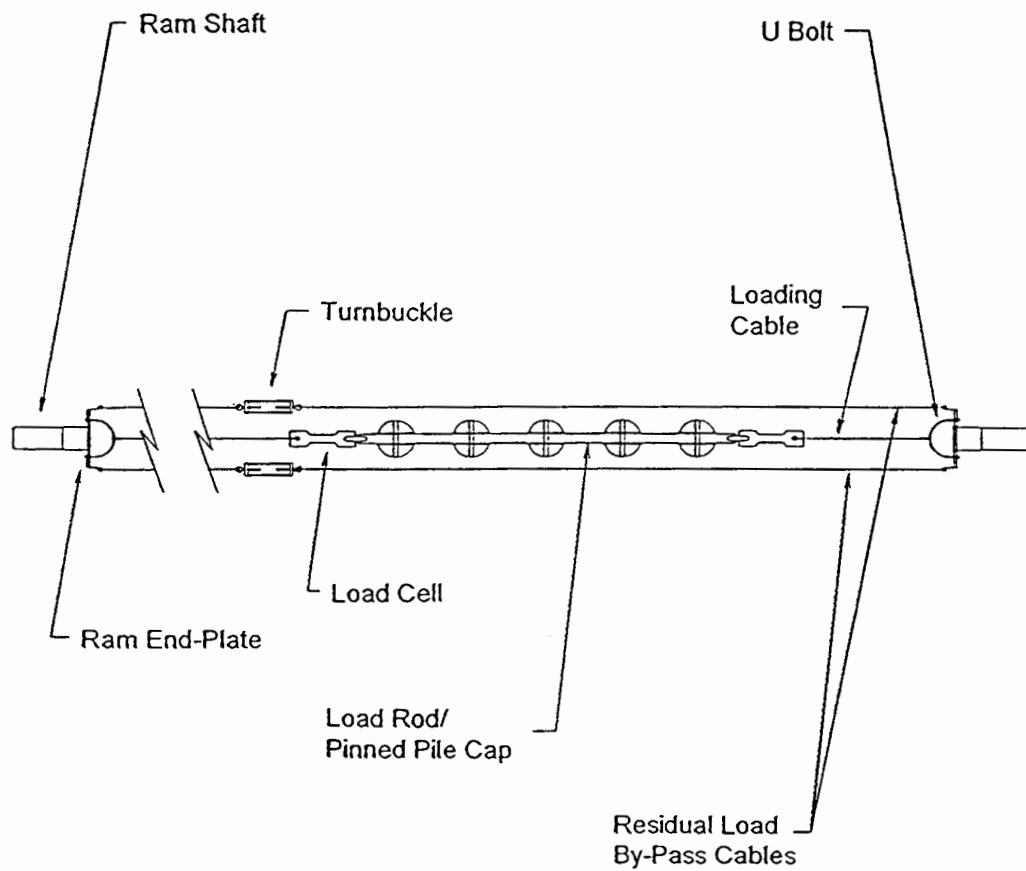


Figure 23. Pile group loading assembly.

Power was delivered from the relays to the valve by a three-wire extension cord wired in a hot/hot/neutral configuration, rather than the standard hot/neutral/ground configuration. One wire from each of the solenoids was connected with the neutral lead. The other wires were each connected to a hot lead. This wiring scheme was used so that a single cord could be used to send power from the relays to the solenoids.

The cord leading to the solenoid valve was fitted with a plug with blades horizontally oriented rather than the normal vertical, and this plug mated with a socket of the same type coming from the data acquisition box. This allowed the solenoid valve to be detached from the data acquisition box as needed and also prevented the solenoid valve from being plugged in to a standard outlet so that it would not be damaged due to its wiring configuration.

This switching system was tested by replacing the solenoid valve with small red and green lights that were wired the same as the solenoid valve and turned on when the relays were triggered by LabVIEW.

## **Pile Installation**

### ***Preliminary Work***

One of the concerns for continued testing of model piles was how many tests could be done in the soil that had already been consolidated in the soil test vessel. In Phase 1, a single pile test was conducted in each end of the test vessel, with the pile located approximately 0.46 m (18 in.) from the end wall and centered between the side walls. Soil properties tests also were performed around the sites, thus disturbing soil in the ends of the vessel enough to prevent any further testing from being done.

A plot of soil in the vessel with a cushion of undisturbed soil of five pile diameters in every direction from the pile group would be large enough to conduct a group test without introducing any

change in soil properties due to prior disturbance or boundary effects. Using this five pile diameter (5D) cushion as a guideline, it was determined that there was enough undisturbed soil to conduct four pile group tests. This information was necessary for planning where to install the pile group and how to set up the loading system.

### *Pile Spacing Template*

Driving the pile group into the soil could have been done by either pushing them in connected as a group or inserting them individually and then pinning them together on the load rod. Because of the extremely tight fit between the load rod, pins, and piles, it was decided to pin the pile group together and drive it into the soil rather than push the piles separately and then try to pin them together.

To keep the piles aligned in 3D spacing during driving, two templates were made, through which the pile group was driven, while the proper spacing was maintained. Figure 24 shows the template design. Plywood was cut into four sections 230 mm (9 in.) wide and 610 mm (24 in.) long. The pieces were bound with wood screws in a stack, four boards high, so that the edges matched. The pile locations were marked on the top board, after which holes 34.9 mm (1.375 in.) in diameter were bored through the whole stack at the five locations. The boards were then split through the middle of the holes with a saw so that two identical pieces were made from each of the original boards. Two of the paired boards were used for templates, while the other two were stored for future use.

Two 2 x 6 planks, long enough to span the distance between the two yokes still attached to the soil test vessel, were split down the middle and used as mounts for the templates. After again laying out the four possible pile test locations on soil using the spacing template already mentioned, measurements were taken to determine the position where the piles should be placed with respect to the test vessel walls and the two yokes. The measurements were used to locate the pile spacing templates on the split planks, where they were fastened, so that when the planks were clamped to the yokes, the

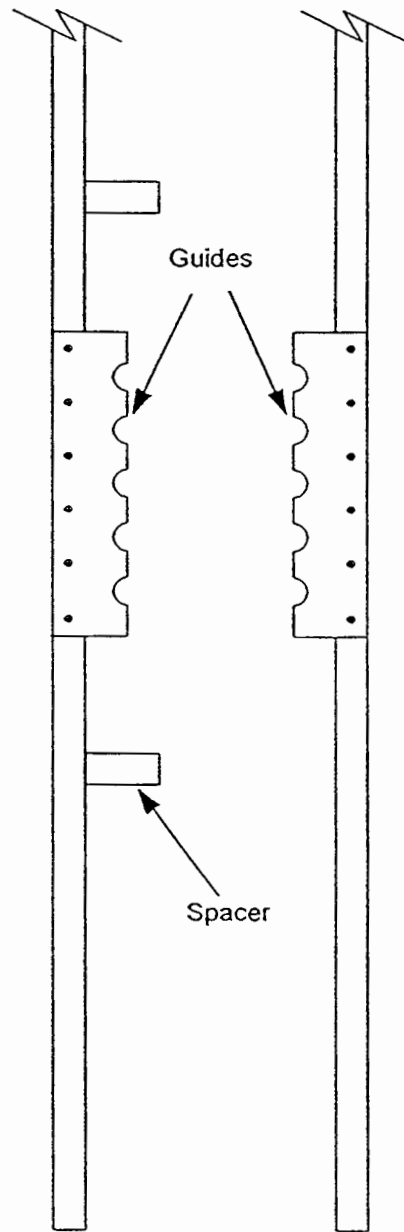


Figure 24. Pile group installation template.

templates would be in the proper position for driving piles. Two blocks of wood were screwed on to one of the spacing template planks to act as spacers for clamping the template halves together, after which the templates were matched together with C-clamps.

### ***Pile Group Alignment***

The cylinder mounting frames were bolted to load frames and a string was strung through the bolt holes of one mount frame, across the soil and through the matching bolt holes on the other mount frame. When pulled tight, this string showed the axis for proper pile group alignment.

One of the spacing templates was clamped to the underside of the two yokes with C-clamps in a position roughly close to where the piles should be placed. A plumb bob string-guide was slipped into one of the end template holes, the plumb bob was suspended from the guide, and then lowered until it hung just above the string. The spacing template end nearest the plumb bob was moved until the plumb bob was centered over the string and then clamped in place. Next, the plumb bob was moved to the opposite end of the template and lowered until an alignment check could be made, after which the nearest end of the driving template was moved to center the plumb bob over the string. This procedure was repeated many times until the plumb bob could be lowered from either end of the spacing template and deflect the string downward with its pointed tip. The C-clamps were securely tightened to conclude the alignment procedure for the lower template. The other template was aligned in the same manner after it had been clamped on top of the yokes. To be considered satisfactorily aligned, the plumb bob had to be lowered from the upper template through the lower template in rapid succession several times without touching the lower template at all, and then rest its tip on the alignment string. Template alignment took several hours, but was crucial to guaranteeing pile group spacing and alignment.

### ***Pile Insertion***

With the templates set up for pile group placement, the piles and the load rod were pinned together in a prechosen order so as to place the piles with the highest number of reliable strain gages on the outside of the group, and the piles with a lesser number of reliable gages in the interior spots. Pile 4 was positioned as the lead pile on the left with Pile 2 next in line. Pile 1 was placed in the center with Pile 5 in the second position from the right. Pile 6 was the lead pile on the right. Since Pile 3 had two unreliable gages in the two uppermost positions, which are important for good boundary condition data, it was relegated to the role of thermal drift monitor.

The pile group was lifted up and slid down into the templates until the pile toes rested on the soil surface. Due to the soil resistance, the pile group had to be jacked into the soil with the ceiling of the Water Lab acting as the reaction member. A scissors-type automobile jack with a 230 mm (9 in.) travel distance was used to push the piles into the soil. Two redwood blocks 510 mm (20 in.) in length had been drilled to a shallow depth with large diameter bit in three equally spaced locations along the length of the blocks to accept 25.4 mm (1.0 in.) diameter ball bearing to make a one-directional moment-free joint. Then, if jack alignment was not true, the piles would not be pushed out of proper alignment during driving. One of the blocks was placed on top of the five pile caps while the ball bearing, second block, and jack were positioned on this block, after which jacking commenced. A torpedo level was used to help keep the piles level as they were forced into the soil. Each time the jack was fully extended and then compressed, a block of wood had to be inserted under the jack to take up space so that the pile group could be pushed farther into the soil.

When the piles were pushed in far enough that the uppermost spacing template interfered with movement, the clamps holding its ends were loosened and the template was removed. The lower spacing template was removed when the pile group reached that level as well. Pile driving ceased when the piles had been pushed 1.295 m (51 in.) into the soil. This left the top of the pile group 279 mm



(11.0 in.) above the top of the soil at the load rod elevation. The pile caps were checked for level and the piles were checked for plumb during the entire process. Some cracking of the soil occurred during driving, but measurements with a hand held ruler showed that the cracks were only superficial.

Pile 3, the thermal drift monitoring pile, was pushed by hand into the soil in the end of the vessel where it would not disturb soil that could be used for further group testing.

## **Testing**

### ***Hydraulic Cylinder Alignment***

With the pile group installed in the soil, further preparations for testing could be made, first of which was mounting the hydraulic cylinders to the soil test vessel. Actual bolting of the cylinders to the previously installed mounting frames was straight-forward. As stated earlier, grade 8 bolts were used for this attachment along with doubled-up high strength washers to help transfer the pulling force to a larger area of the web of the mounting frame channel sections. Other washers were placed between the cylinder base plates and the mounting frames to act as shims to level the cylinders, which was checked with a torpedo level. Getting the cylinders aligned longitudinally with the pile group was a much more difficult task. First a reference was needed, which could be aligned with the pile group and then used to align the cylinders. A 6.1 m (20 ft.) length of angle iron served as the reference. It was laid on the lower channel of the mounting frames and then aligned with the pile group by measuring the distance from its flat edge to each end of the pile group load rod. Adjustments were made in small increments until there was no perceptible difference in the distances from each end of the load rod to the angle iron. It was then firmly clamped to the mounting frames. The slots in the mounting frames allowed cylinders to be adjusted up and down and side to side. By measuring from the reference angle iron to two different spots on the cylinder bodies, the cylinders were moved and shimmed until alignment requirements were met.

### ***By-pass Cable Hookup***

Once the hydraulic cylinders were aligned, they could be hooked to the pile group and to each other with the by-pass cables. Since the pile group was not centered between the cylinders, different linkage arrangements were needed on each end of the pile group to hook them to the cylinders. On the end nearest to a cylinder, a quick link was connected to the twisted clevis in the end of the load rod. The load cell was hooked onto the quick link on one end and to a turnbuckle on the other end. The turnbuckle was bolted to the foot plate on the end of the ram. A similar arrangement was used for the other side, except that a piece of steel strap 25 mm (1.0 in.) wide and 508 mm (20 in.) long was connected to the load cell by a quick link. The other end of the strap was hooked to a turnbuckle, which was connected to the ram foot plate with a quick link. These linkage assemblies were designed for versatility and ease of adjustment, which proved quite beneficial during testing.

### ***LVDT Mounting***

A wide flange, thin section aluminum T-beam was aligned with the pile group and clamped to the underside of the soil vessel yokes. To this T-beam the LVDT mounting bracket was clamped, and then the LVDTs were hung in place between the pile group and the mounting bracket. They were leveled and aligned by adjusting the wing nuts on the pile group and the bracket.

### ***Data Acquisition System Setup***

Having accomplished installation, assembly, and alignment of the piles and other instruments, the input boards for all of them were plugged into the data acquisition box. Since the problem of voltage saturation still occurred when turning on the system, all boards were plugged in while the system was running. Pile input boards were inserted so the piles were arranged in the group, with boards from the thermal drift monitoring pile next in line, and finally, input boards from the load rod

and load cells, and the LVDTs. With all input boards in place and taking readings, the large power supply heated up quickly and a warm-up time was needed to bring the data acquisition system into a stable equilibrium. The system was quite thermally sensitive, and opening the box could change the readouts on many of the strain gages, so the system was left running all the time.

### *Testing Procedure*

Three different testing strategies were tried in an attempt to find a method that produced the most consistent, meaningful output. Time-controlled cycling of the pile group was used in the first attempt to perform a lateral load test. The cycle rate was 0.1 Hertz, during which time the testing program sampled and averaged three readings of all of the instruments right before the loading direction changed, thus picking up the interval of maximum load. Testing was halted after three 100-cycle test iterations at loads of 222.4 N (50 lb.), 444.8 N (100 lb.), and 667.2 N (150 lb.), because frictional differences between the two hydraulic cylinders caused quicker ram movement in one direction than in the other, and thus unequal and inconsistent loading of the pile group.

This unequal loading was highly undesirable, so the testing method and software were changed to a closed-loop configuration to allow cycling to be controlled by reading the load on the load cells and switching the solenoid valve when the target load was reached. The testing program was modified so that it continuously sampled all of the gages at a rate of three readings every five seconds. When the triggering load was reached, the last three samples taken were averaged and stored.

Since the test soil already had been disturbed by the previous test iterations, testing resumed at the load of 667.2 N (150 lb.), and continued in 222.4 N (50 lb.) increments of 100 cycles each until it was halted after 28 cycles at 1779.3 N (400 lb.) because the soil had deformed so much that the LVDTs were in danger of being damaged due to the excessive travel of the tops of the piles. This great amount of soil deformation was unexpected but the testing was deemed successful. Post test analysis of test

data revealed that a small programming error had caused the baseline conditions data to be written repeatedly to the output file instead of the data gathered at the end of each half cycle, and so this test data was useless. During this initial testing, the load exerted by hydraulic cylinders was changed by adjusting the air pressure in the tank with the air pressure regulator. Hitting the target load proved to be quite difficult.

These initial tests proved to be valuable learning experiences, and out of them evolved a new approach to conducting testing. The lateral force on the pile group would be increased to a maximum of 1779.3 N (400 lb.) while continuously sampling all gages at the fastest rate possible so the desired data would be captured as the load passed through the targeted loads. All soil deformation would be unique to each cycle, and would not reflect accumulated disturbance of lower loadings seen in the other tests.

The piles were pulled from the spot where the earlier tests were conducted and reinstalled in a new location in the soil test vessel with the piles positioned in the group as shown in Figure 25. A new testing program, named One Shot.VI, was written for the new test procedure. It incorporated many features that made testing much easier. This program automatically named the output data files according to the cycle number and whether the pile group was being pulled to the right or the left. The load that was delivered to the pile group, as well as group displacement and pile-top angle as measured by the LVDTs, was displayed in real time on the computer monitor. All operations of the hydraulic system were controlled through signals sent to the solenoid valve. Streamlining of the program also allowed for faster data acquisition rate. A sample of some of the LabVIEW code used in this program is contained in Appendix B.

The procedure for conducting testing consisted of repeating the same basic steps many times to collect and store the data in half-cycle blocks, determined by whether the pile group was being pulled to the right or the left. To run a half-cycle test, the testing program One Shot.VI was called up on the

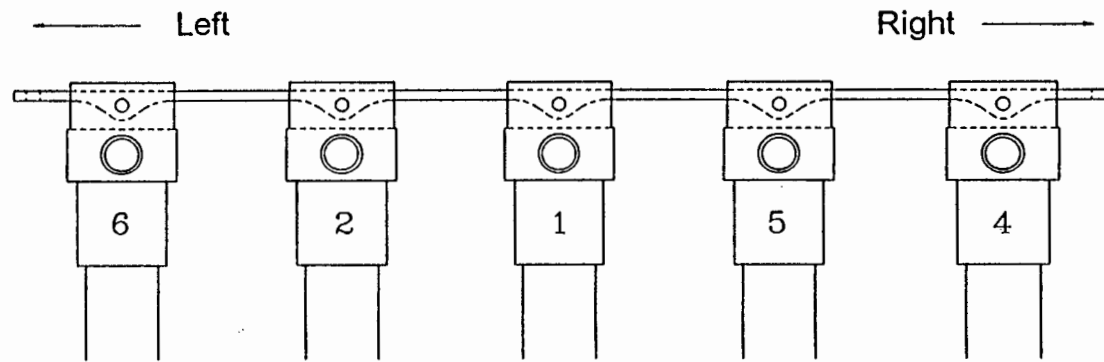


Figure 25. Pile order in the pile group during testing.

computer and a baseline reading of all instruments was made. The program would not allow testing to begin without this initial reading. When this was accomplished, data acquisition was started by clicking the start button. Figure 26 shows the program control panel for One ShotVI. This started data acquisition and opened the solenoid valve. The air pressure regulator on the tank was slowly opened allowing the hydraulic fluid to be pressurized. As the cylinder being pressurized pulled on the pile group, the load, as monitored by the active load cell, was called out to help the person opening the regulator maintain a constant rate. The linkage on the inactive load cell was kept loose so that it would not register any load other than the weight of the linkage. As the load continued to rise, the pile group could be seen to deflect, and pile top displacement and angle were displayed on the computer. When the air pressure in the tank rose high enough to produce the desired 1779.3 N (400 lb.) load in the active load cell, the computer switched the solenoid valve, thus causing the hitherto unpressurized cylinder to pull the pile group in the opposite direction until the load on the active load cell fell below a given threshold, usually 89 N (20 lb.), at which point the solenoid valve was closed and data acquisition stopped. The pressure in the tank was released and the air regulator was reset in preparation for the next half-cycle.

Testing proceeded smoothly overall, except for the power going out for about three minutes throughout the whole city. Only the data being collected in one half-cycle were lost, but to resume testing without overwriting the existing data files, the program had to be modified. Testing was terminated after 50 full cycles because the soil had deformed to the point where the pile top movement threatened to damage the LVDTs. Nearly 53 megabytes of data were gathered during this test. The data acquisition rate was four samples from every channel per second. Continuously sampling all instrumentation at this rate produced data for 200 to 300 loads in each half-cycle. The data were checked for any readily noticeable problems and then saved on a set of six floppy disks. This concluded the testing phase of this project.

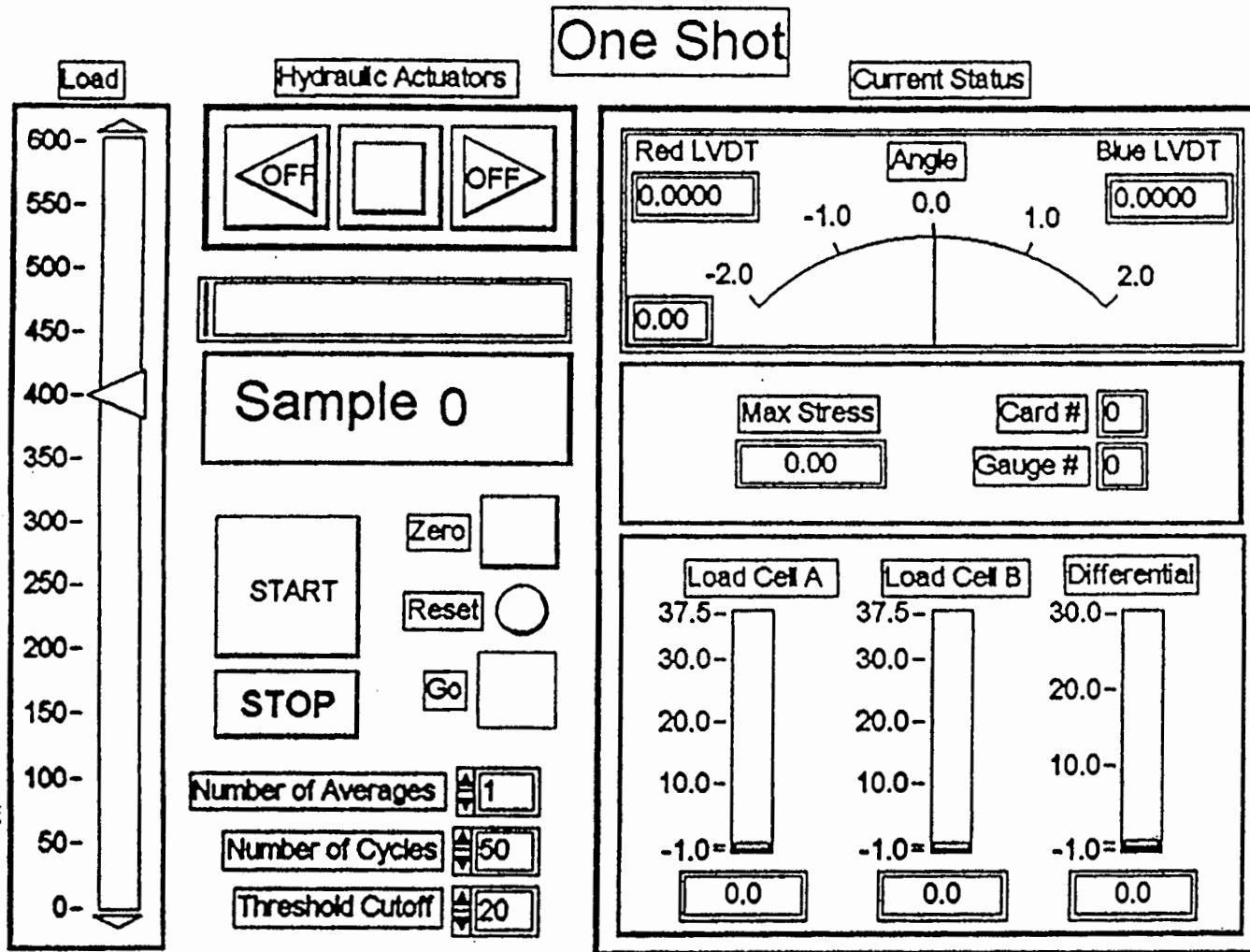


Figure 26. ONE SHOT. VI program panel.

### ***Recalibration***

During the course of the testing and during the preliminary work to debug the system hardware and software, it was noticed that some of the strain gage readings seemed to be lower than expected, even when they were corrected by the calibration factors, so it was decided to recalibrate all of the instrumentation at the end of testing with everything configured as it was during the final test and under the same conditions. The piles were unplugged, pulled from the soil and cleaned off, and then reconnected to the data acquisition system.

Although the same procedure was followed for this calibration as was used in the initial calibration, a new calibration program was used that simplified and speeded up this somewhat tedious task. The new program, named Calibrate.VI, averaged 20 voltage readings for every gage at every load and converted them to stress values. The capabilities of LabVIEW were demonstrated during testing and instilled confidence in its ability to generate reliable calibration output without having to convert the voltage to stress in a spreadsheet. The LabVIEW output was imported into a Quattro Pro spreadsheet for regression analysis and graphical conversion. The calibration output for every strain gage in Pile 1, Pile 2, Pile 3, Pile 4, Pile 5, and Pile 6 can be viewed in Figures C-1 through C-6, respectively. Calibration output for the load rod is found in Figure C-7. Load cell calibration output is contained in Figure C-8, and LVDT calibration results are found in Figure C-9.

The wisdom of doing a second calibration was verified by the new calibration factors, which all came out to be roughly 20 to 25 percent greater than the initial factors. This was most likely because in the initial calibration work, only the input boards connected to the pile being calibrated were installed in the data acquisition system at the time of calibration, and so power demands and electrical noise conditions were much different than those experienced during testing. As stated earlier, the system heated up quite a lot when the full complement of instrumentation was being sampled, and the effects of this temperature difference also might have contributed to the discrepancy in the calibration factors.



The effects of allowing the system to come to equilibrium can be seen in the calibration output from Pile 4 when compared with the calibration output of the other piles. Pile 4 was calibrated first, and as is evidenced by the slightly erratic calibration output, the data acquisition system had not quite settled down to its best operating noise level. Pile 2 was calibrated second, and the output from all of its strain gages is consistent, showing that the system equilibrium had been reached.



## CHAPTER VII

### RESULTS

#### Measured

##### *Data Reduction*

Nearly 53 megabytes of data were collected during the test. MATLAB<sup>®</sup> software version 4.2b by The Mathworks Inc. was used for the data reduction. MATLAB is a powerful software package that executes FORTRAN-type commands to perform mathematical operations on raw data and to generate desired output.

After recalibrating the piles, load rod, and load cells, new calibration factors for the load cells were used to calculate the magnitudes of all of the loads in cycles 1, 5, 10, 25, and 50, which were the cycles chosen for analysis. It was found that the actual maximum load delivered to the pile group in each cycle was consistently near 2135 N (480 lb.). Based on this finding, the data starting at 667 N (150 lb.) and at every 222 N (50 lb.) increment thereafter, up to 2000 N (450 lb.), in the cycles mentioned above, were selected for analysis. The load at 667 N (150 lb.) was chosen as the minimum because at lower loads, the data acquisition system noise levels caused inconsistent output.

Four categories of output were produced from the test output:

1. load distribution
2. pile group moment distribution
3. individual pile moment distribution
4. load versus deflection

Separate output was produced for the half-cycle in which the pile group was pulled to the left and for the half-cycle in which the group was pulled to the right. All figures, except for those showing

load versus deflection, reflect this output format and if unlabelled, the curves on the left half of plots are for the left half-cycle and vice versa. The piles were not organized in the pile group in numerical order. Because of hardware defects, either in the piles themselves or in the data acquisition input boards, a number of strain gages did not function properly. The piles were ordered in the group according to their apparent reliability. That is why the group order was Pile 6, Pile 2, Pile 1, Pile 5, Pile 4, going from left to right. Referring to Figure 25 during this discussion will be helpful in keeping straight the pile order used in testing.

### ***Load Distribution***

Some readily expected and also unusual output was produced from the strain gages mounted on the load rod, which measured the loads taken up by each pile in the group. Overall, results from the left loading and right loading show few similarities other than the fact that for almost all of the load increments in most of the cycles, the lead pile takes more of the load than any of the other piles. In cycle 1-Left, the lead pile (#6) takes more of the load for all load increments up to 2000 N (450 lb.), but the two trailing piles (#5, #4) take more load than the other two (#2, #1) as shown in Figure 27. Cycle 1-Right does not show a trend of this nature and all of the piles except the lead pile (#4) seem to assume the load fairly evenly.

In cycle 5 in both directions, the load distributions are similar to what was seen in cycle 1. The lead pile again takes more of the load than the other pile, with random distributions of load spread among the four other piles. In cycle 5-Right, as the load passes through the 1780 N (400 lb.) and 2000 N (450 lb.) increments, a very nice stair step distribution is shown. See Figure 28.

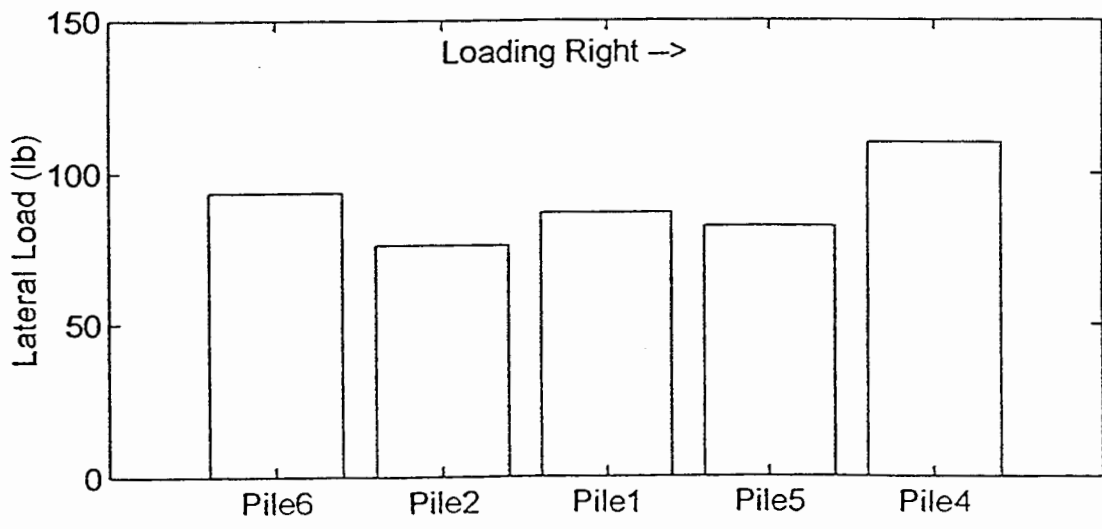
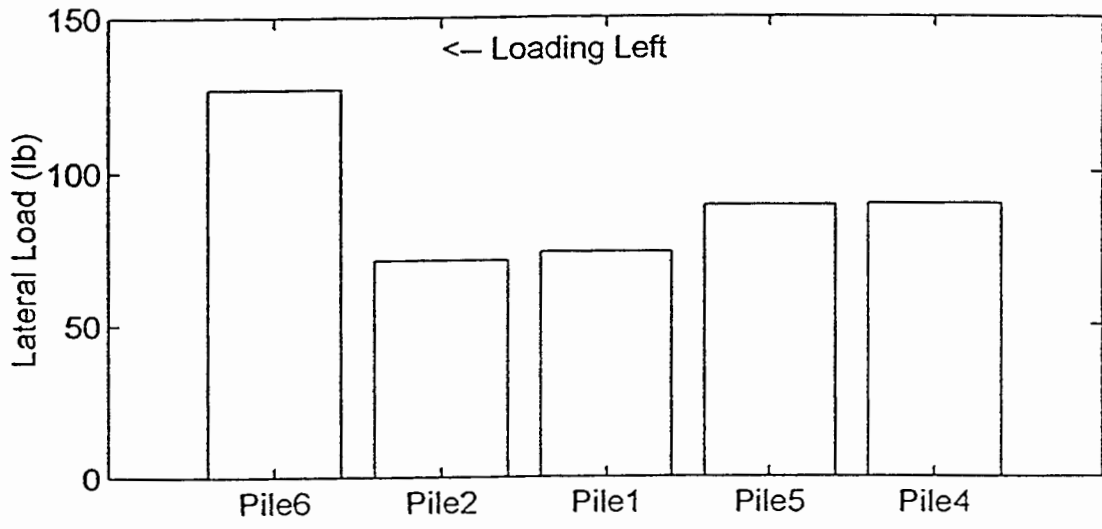


Figure 27. Load distribution for cycle 1 at 450 lb.

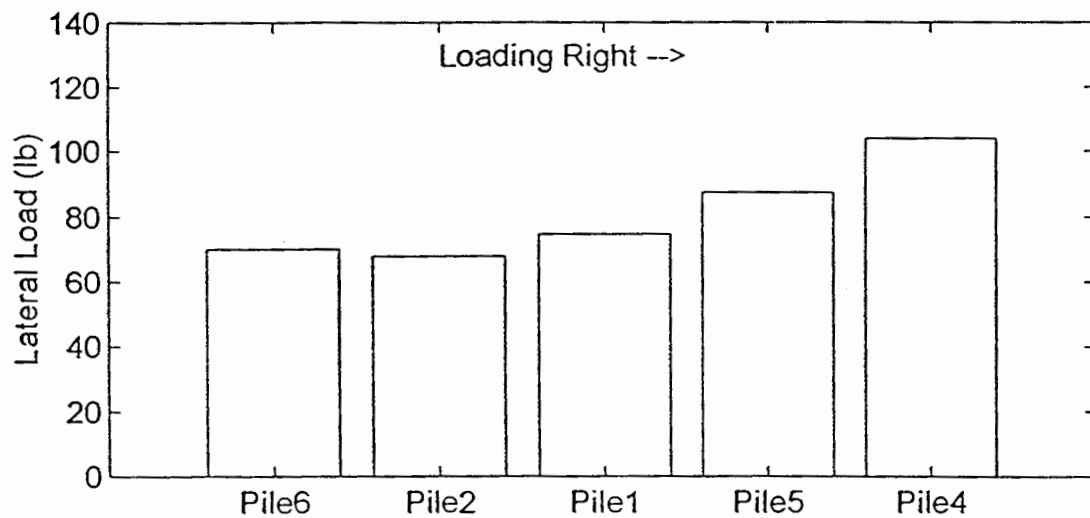
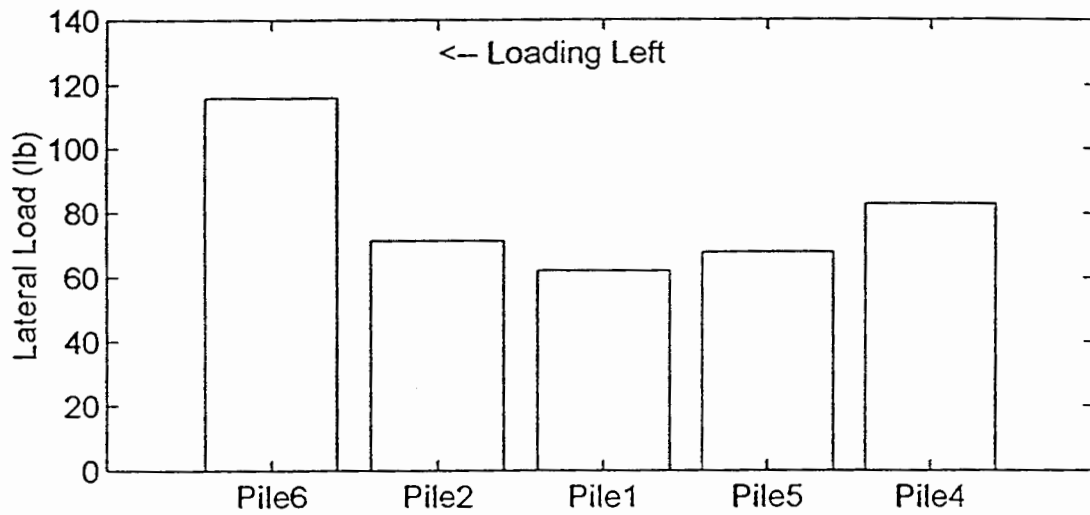


Figure 28. Load distribution for cycle 5 at 400 lb.

Cycle 10-Right shows probably the most consistent load distribution pattern for any of the cycles analyzed. The lead pile (#4) takes more of the load, with the second pile (#5) fairly consistently taking the next highest amount and then followed generally in turn by the fourth (#2), the third (#1), and then the trailing pile (#6). Cycle 10-Left shows only the lead pile (#4) taking the most load.

As the load increases to 1334 N (300 lb.) in both directions for cycle 25, the load is distributed evenly through the whole group, and not until the 1557 N (350 lb.) load increment does the lead pile in each direction again start to take more of the load than the other piles. Perhaps this is due to the displacement of soil from around the piles to the point where resistance to movement in the lower load regions is equal for all piles, until the lead pile again encounters undisturbed soil at the higher loads.

In cycle 50, it can clearly be seen up through the 1557 N (350 lb.) load increment that the trailing piles take more of the load than do the other piles. The leading pile (#6) in cycle 50-Left takes the least load of all of them until the 1780 N (400 lb.) load increment is reached, when it resumes and takes more load up through the last load step. The same phenomenon can be seen for the lead pile (#4) in cycle 50-Right.

Other than the consistent demonstration that the lead piles take more of the load than the other piles, except when much movement occurs where they may take the least load of all, no strong trend can be seen. It appears that piles other than the lead pile take about the same load with no real trend in hierarchy. Complete load distribution output can be found in Figures B-1 through B-5.

### ***Pile Group Moment Distribution***

Unlike the output for load distribution, strong trends are easily seen in the group moment distribution output plots. The plots all show closely grouped moment curves for all the piles. The shape of the curves is similar for the left and right half-cycles. Usually, the moment curves for the lead pile in

each loading direction stand out slightly from those of the other piles because the lead piles take more of the total load than do the other piles. This can be seen in Figure 29.

All through cycle 1, it can be seen that the piles are acting as “long” piles with points of counter-flexure starting at a depth of around 560 mm (22 in.) at a load of 667 N (150 lb.) and moving downward, until at a load of 2000 N (450 lb.), the points of counter-flexure are at a depth of about 760 mm (30 in.). A second point of counter-flexure can be seen in each pile in all load increments up to 1557 N (350 lb.), after which only one point can be seen.

Output for cycle 5 shows that only one point of counter-flexure exists in each pile, even at the lowest load increment. The points of counter-flexure are at approximately the same depth, 760 mm (30 in.), as they were for the 2000 N (450 lb.) load in cycle 1. As in cycle 1, the points of counter-flexure move down the piles, ending at a depth of about 890 mm (35 in.) at the highest load. Even though the points of counter-flexure move down the piles as the load increases, the depths at which the maximum moments occur remain fairly constant through the whole cycle.

In cycle 10, the output plots are much the same as from cycle 5. The points of counter-flexure move down the piles as the load increases, and the depth at which the maximum moment occurs is a little deeper than in cycle 5.

At a load of 1557 N (350 lb.) in cycle 25, the points of counter-flexure disappear altogether, and a moment of 0 is registered at the lowest strain gages in the piles, as seen in Figure 30. This demonstrates that the piles have become “short” piles. The points of counter-flexure occur in the loads lower than this in this cycle, but remain unseen in the loads higher than this. The depth at which the maximum moment occurs is again lower than in the previous cycles.

Cycle 50 shows some interesting results. At the load of 667 N (150 lb.), the bending moment output for the lead piles in each half-cycle is distinctly lower than that of the other piles as shown in Figure 31. This correlates well with the load distribution data for this same cycle and load. There also



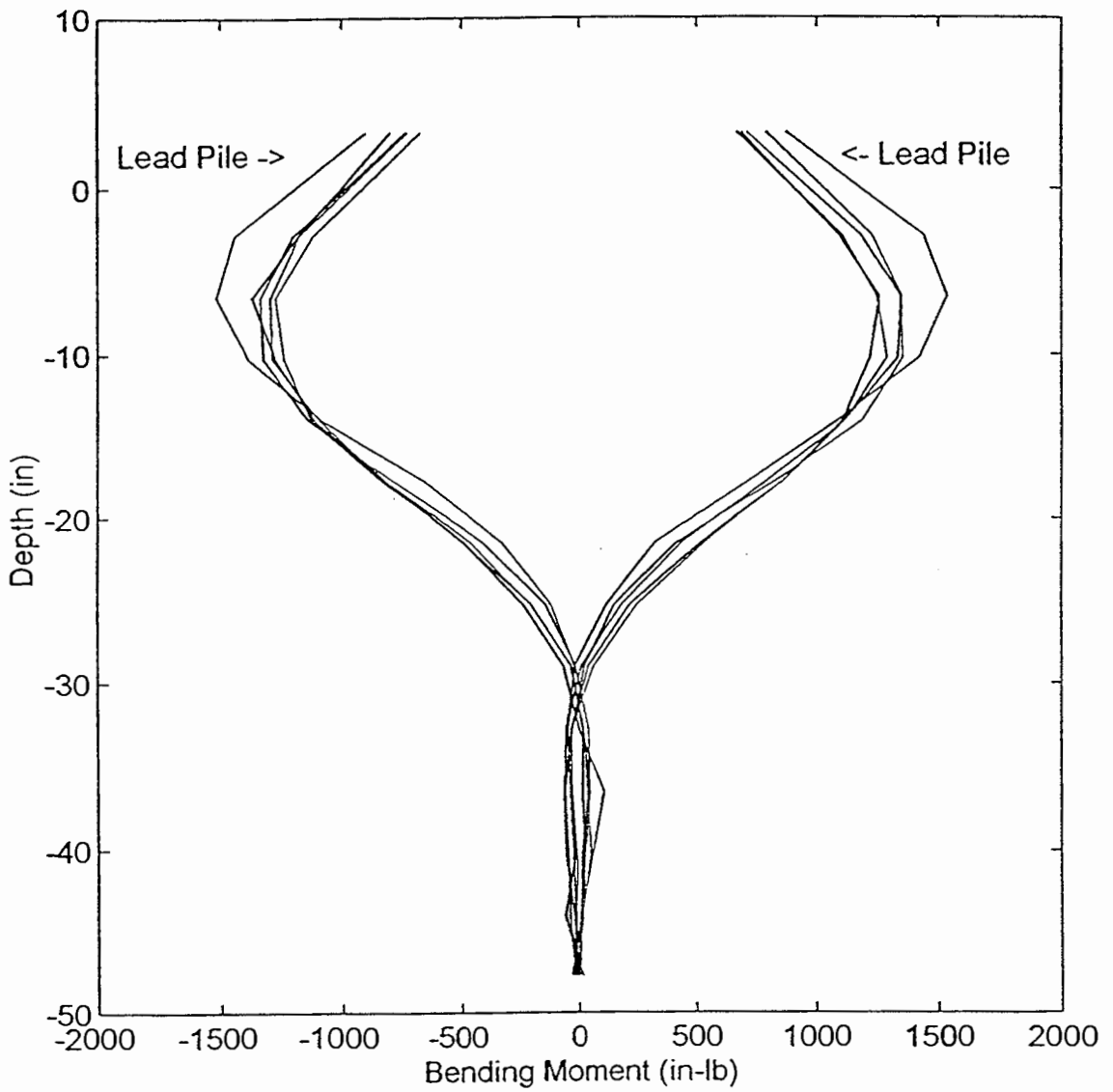


Figure 29. Pile group moment distribution for cycle 1 at 450 lb.

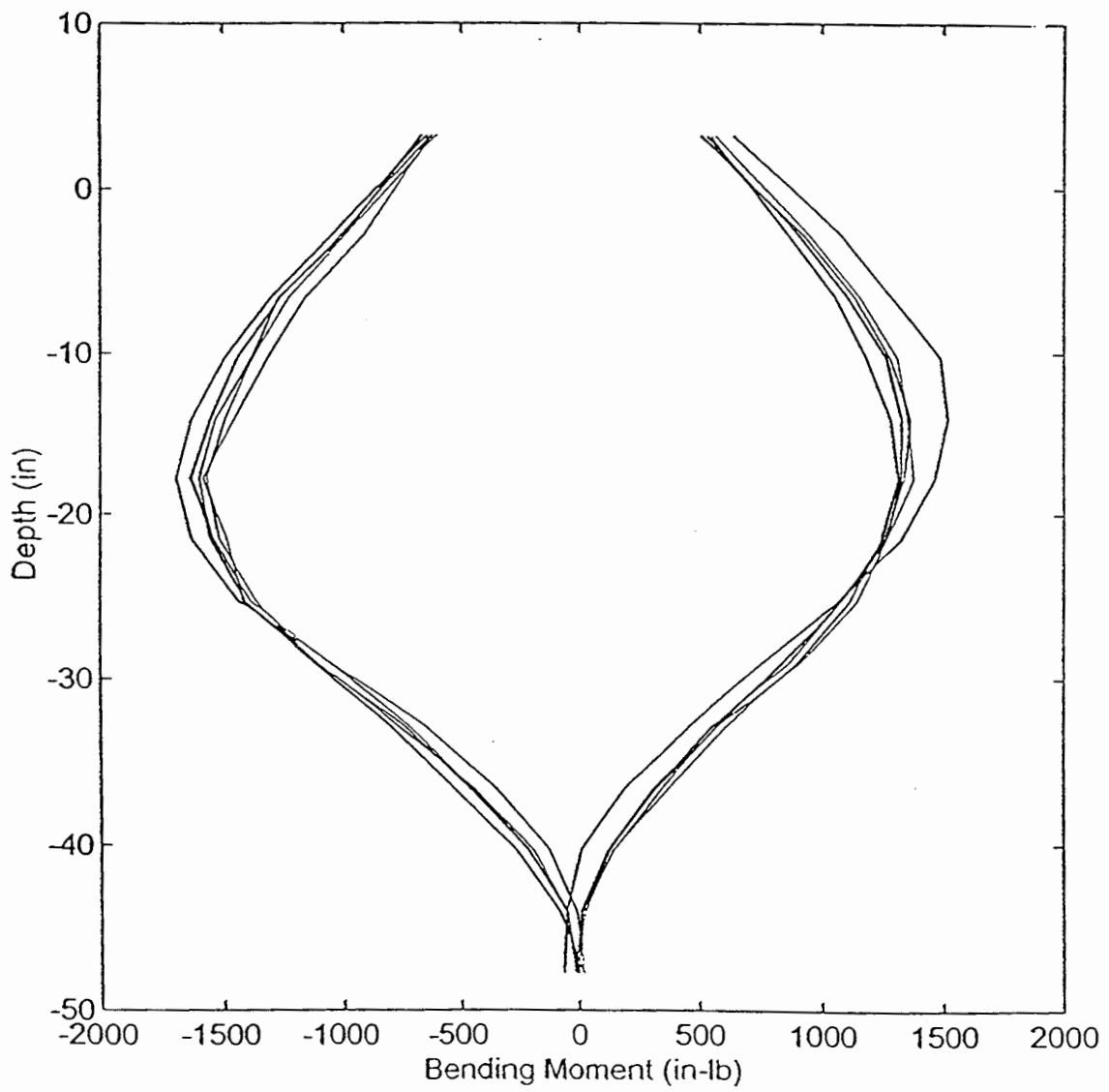


Figure 30. Pile group moment distribution for cycle 25 cycle 25 at 350 lb.

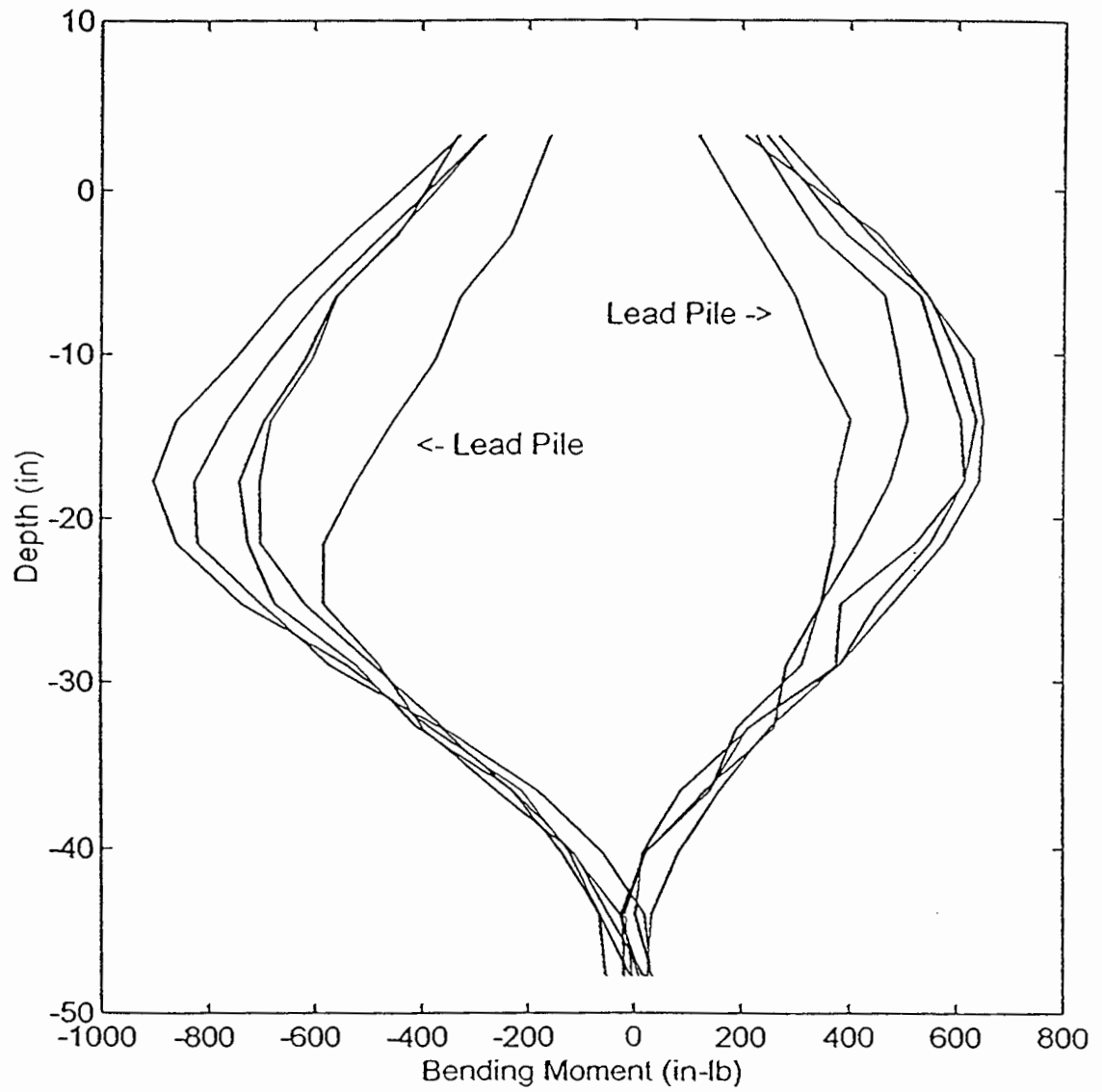


Figure 31. Pile group moment distribution for cycle 50 at 150 lb.

are no counter-flexure points at this or any other load in this cycle. Unlike the situation discussed for cycle 25 at the 1557 N (350 lb.) load, where the moment is 0 at the bottom of the piles, moment readings occur at all depths through this whole cycle. Because of this, it can be reasoned that even though the piles act as short piles, the bottoms of the piles are still fixed; otherwise, there would be no reaction to cause the bending that is registered at the pile tips.

By examining the data as a whole, several other trends can be seen. One trend that cannot be readily explained is the often occurring mismatched magnitudes of bending moment from the left and right half-cycles. While on some plots the moment data matches up well, on other plots the moment data in one half-cycle is larger than in the other half, with the trend showing larger moments for the left half-cycle. Soil inhomogeneity is a possible reason but not an absolute explanation. It was interesting to note that from cycle to cycle, the depth at which the maximum moment occurs increases, but remains relatively constant as the load increases in each cycle, while the depth at which counter-flexure occurs increases during the cycle. For complete group moment distribution output, refer to Figures B-6 through B-16.

### ***Individual Pile Moment Distribution***

Moment distribution output from the individual piles at each load increment and for all cycles creates an interesting plot, and some good comparisons can be made. At each of the seven load increments, the output for each pile for all five cycles can be examined for trends and similarities.

The plots of the lead piles, Pile 6 when loading was to the left, and Pile 4 when loading was to the right, have symmetric curves for all loads and cycles as seen in Figures 32 and 33. The magnitudes of the moment data do not match as well as the curve shapes, but the effects of acting as a leading pile and as a trailing pile are evident. When a pile is leading, the maximum moment in each cycle occurs at a shallower location than it does in the same cycle when trailing. At the lowest loads, 667 N (150 lb.)

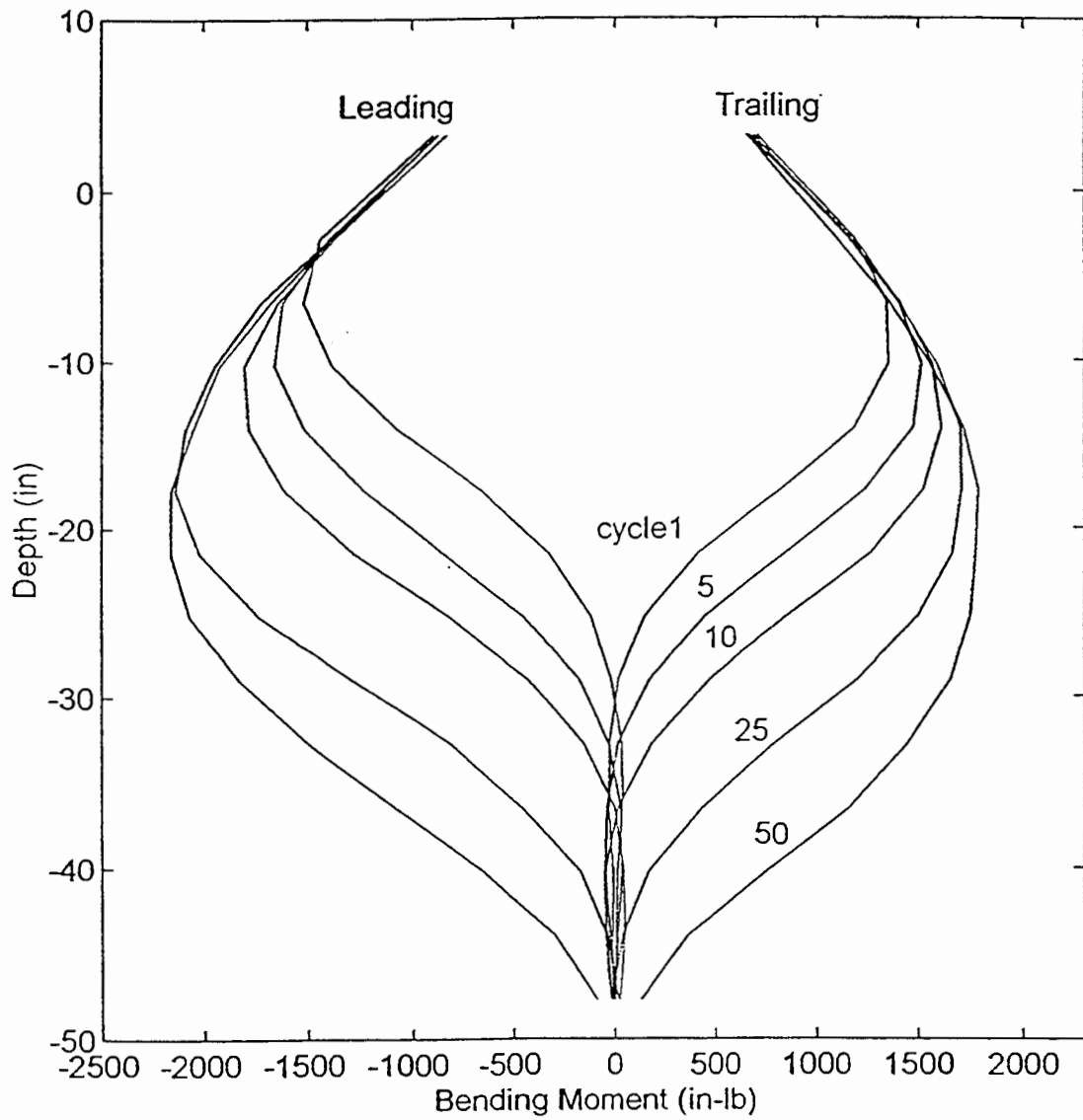


Figure 32. Moment distribution for Pile 6 at 450 lb.

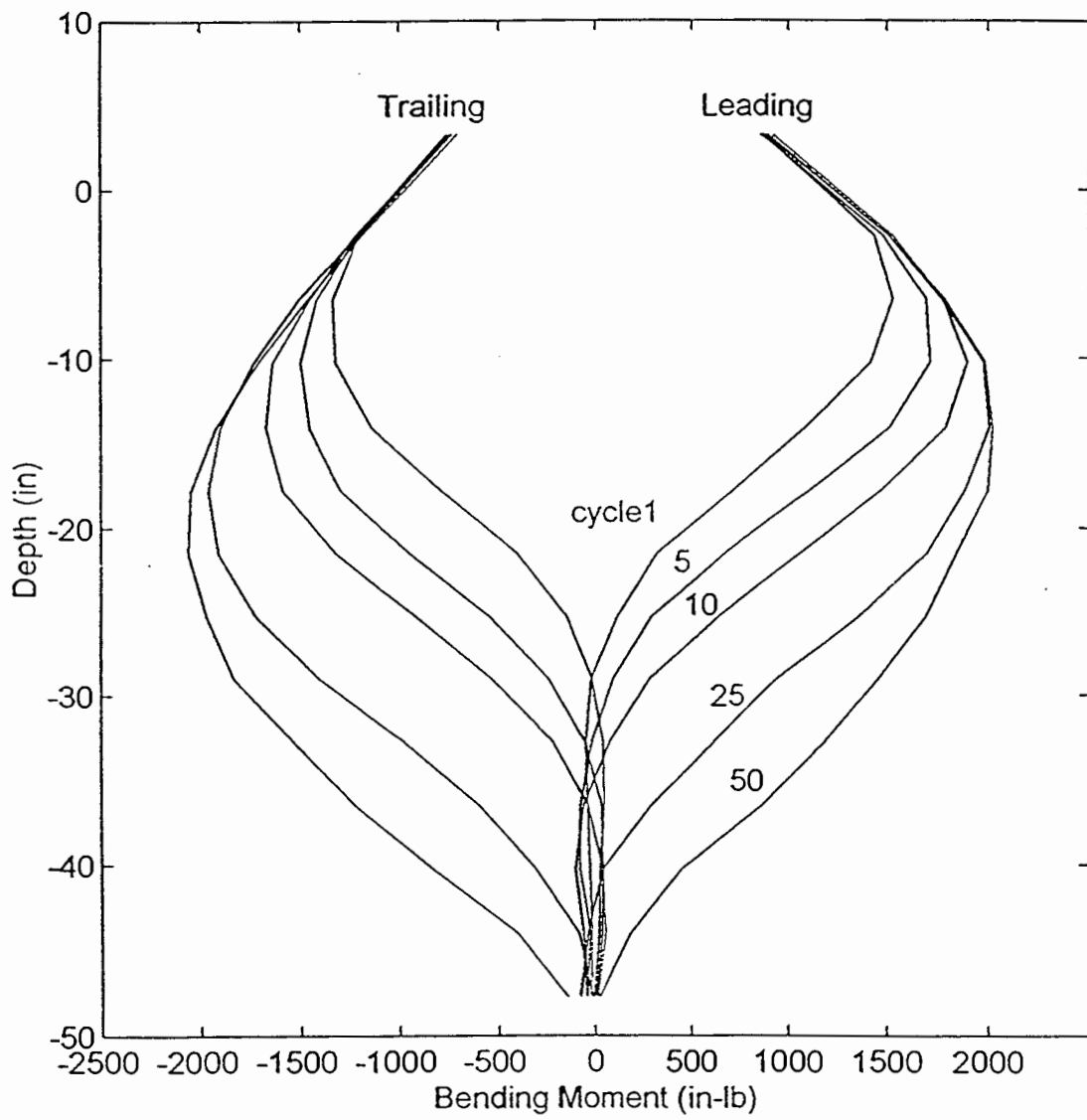


Figure 33. Moment distribution for Pile 4 at 450 lb.

and 890 N (200 lb.), in cycle 50, it can be seen that more bending moment occurred when the piles were acting as trailing piles than when they were acting as leading piles. This correlates well with the load distribution output already discussed.

The output from the inner piles (#2,#5) shows some interesting trends. For the early cycles, the moment in each of these piles is almost exactly the same regardless of loading direction. As the number of cycles increases and at lower loads, each of the piles has a greater moment when acting as a trailing pile than when acting as a leading pile. For example, when loading was to the left in cycle 50 at 1112 N (250 lb.), Pile 5 had more moment than Pile 2, and when loading was to the right in this same cycle at this same load, Pile 2 had more moment than Pile 5. This trend continued until the load approached its maximum value, at which each pile took almost the same amount of the load, whether leading or trailing.

The moment curve shapes for the middle pile (#1) are more symmetric than any of the other piles, but the magnitudes at the maximum values do not agree for left and right loading. As stated in the last section, this phenomenon has yet to be explained. Complete test output for individual pile moment distribution is contained in Figure D-1.

### ***Load versus Deflection***

The load versus deflection output was straight forward. As load magnitude increased in each of the five cycles, the deflection increased in a linear fashion. If the deflection at each load increment is compared from cycle to cycle, the deflection does not increase in a linear fashion. For example, deflection of the pile top at the maximum load of 2000 N (450 lb.) at cycle 10 was not 10 times greater than it was in cycle 1 at this same load. This can be seen in Figure 34.

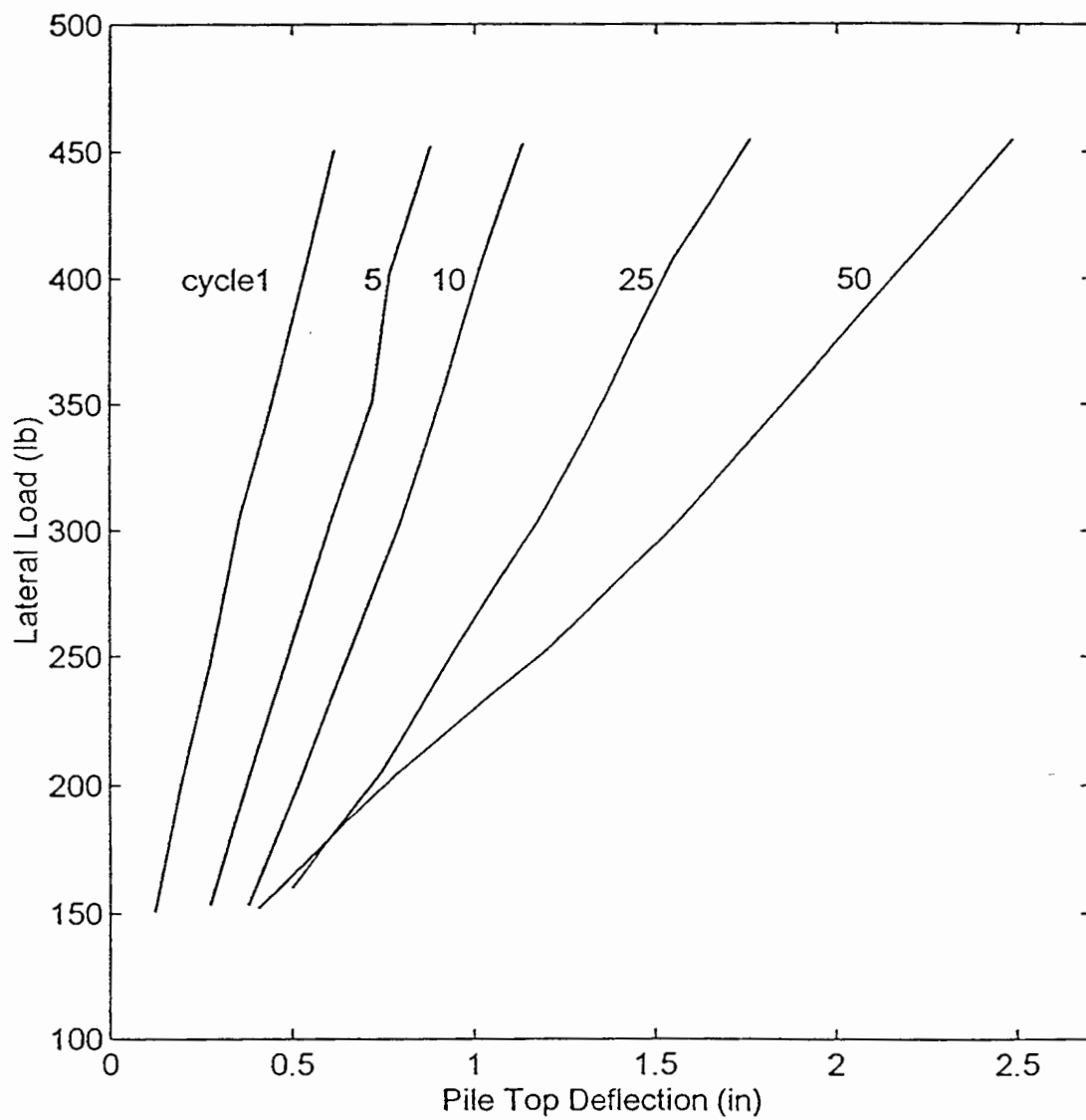


Figure 34. Load versus deflection.



The load versus deflection curve for cycle 50 showed a lesser deflection at a load of 667 N (150 lb.) than the deflection at this load for cycle 25. This can be explained by the conditions during testing. In the latter cycles of the test, when the target load was reached, the pile group was pulled back in the direction opposite the one in which it was being loaded, to unload it. It was pulled back until the load on the active load cell dropped below the cutoff threshold, whereupon the hydraulic cylinders stopped moving. Since the pile group had been pulled so far to one side, soil resistance continued to hold the pile group in a displaced position, and after the cutoff threshold was reached, the piles moved back slightly in the direction in which they had just been loaded. This produced a starting point for the next half-cycle that was slightly displaced in the direction opposite to the one in which the next loading would occur. For complete load versus deflection output, refer to Figure B-16.

## **Predicted**

### ***Background***

Florida Pier is a 3-D, nonlinear, finite element analysis program developed at the University of Florida for designing piles, pile groups, and drilled shafts. Predictions were made using this software and the properties of the model pile group and of the test soil, to validate the Florida Pier program through a comparison with the testing results. Florida Pier is capable of modeling the conditions under which the testing occurred, so no scaling of the test output was necessary for making the comparison. Predictions also were made using the COM624P software by following the pile group method outlined by the Federal Highway Administration (U.S. Department of Transportation, 1996). This prediction also was made for a linear, five-pile group, laterally loaded in a cyclic fashion 50 times, using the soil properties of the test soil. Predicted bending moment output from each of the computer programs only applied to the lead pile in the group. Pile head deflection was modeled for pinned pile connections and

the output reflects the displacement at the cap level, 280 mm (11 in.) above the top of the soil, where the load was applied.

### ***Comparison***

In cycle 50 at a load of 2000 N (450 lb.), the bending moment on the lead piles reached an average maximum of 237 N-m (2100 in-lb.) in the test. Florida Pier predicted a value of about 180 N-m (1600 in-lb.) and COM624P predicted a value of 264 N-m (2340 in-lb.). Figure 35 shows the results of the predictions compared with the actual test results. Measured response was bracketed on both sides by the predictions with the COM624P prediction being the closer of the two. The measured response was quite linear, whereas both of the predictions had curved lines.

For pile group top displacement, Florida Pier predicted 32 mm (1.25 in.) of deflection, COM624P predicted 29 mm (1.12 in.) of deflection, and testing ceased at 62.2 mm (2.45 in.) of deflection. The predictions were far under the measured displacement after 50 cycles. Figure 36 shows the deflection predictions and test results.

As a matter of interest, the measured results for the lead piles from cycle 1 also were compared with predictions. Maximum measured bending moment reached just under 170 N-m (1500 in-lb.), and was quite close to the prediction made using Florida Pier. Displacement measured 15.7 mm (0.62 in.), and was close to the prediction made by COM624P up to the 1334 N (300 lb.) load increment.

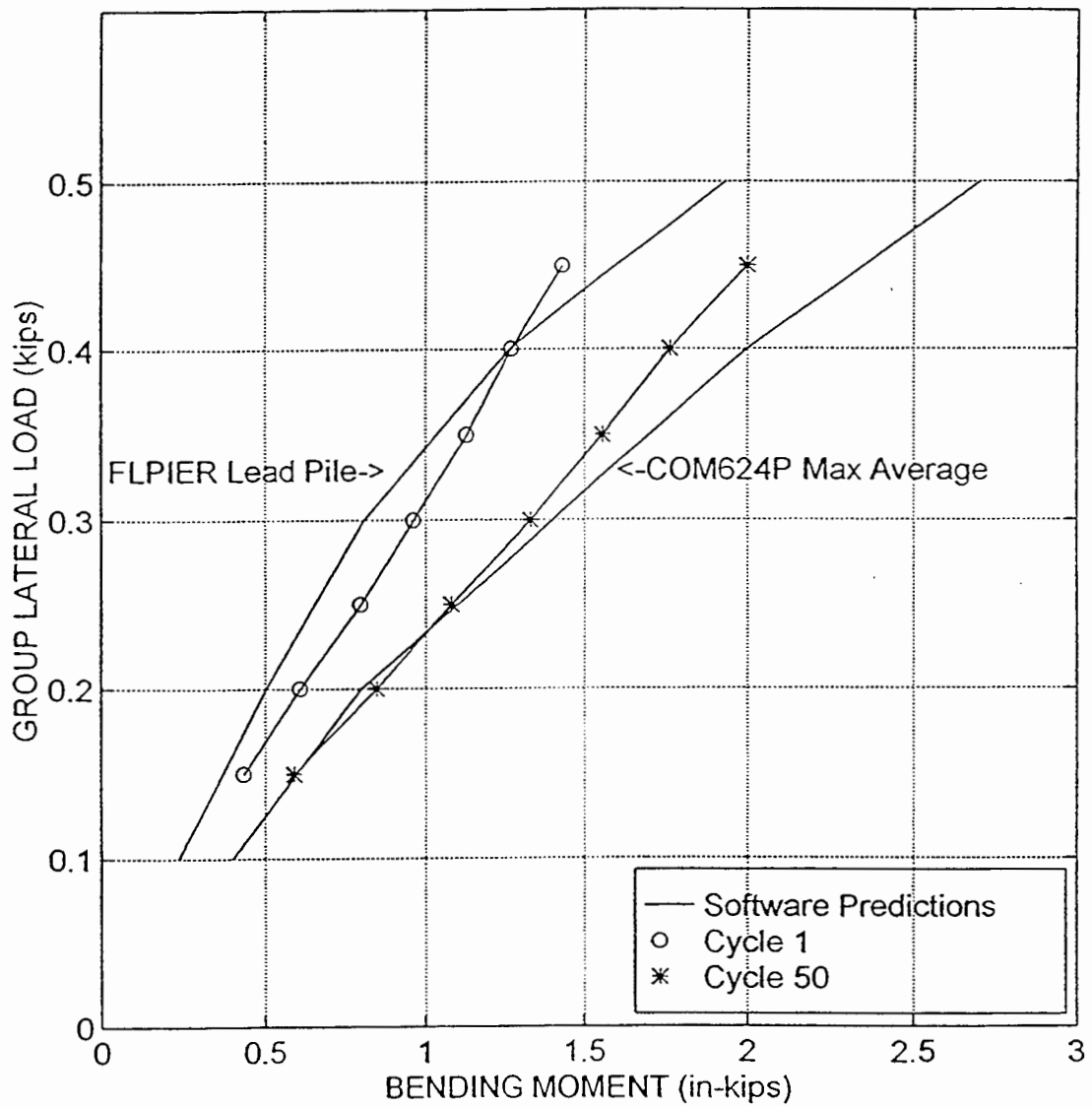


Figure 35. Maximum bending moment: predicted versus measured.

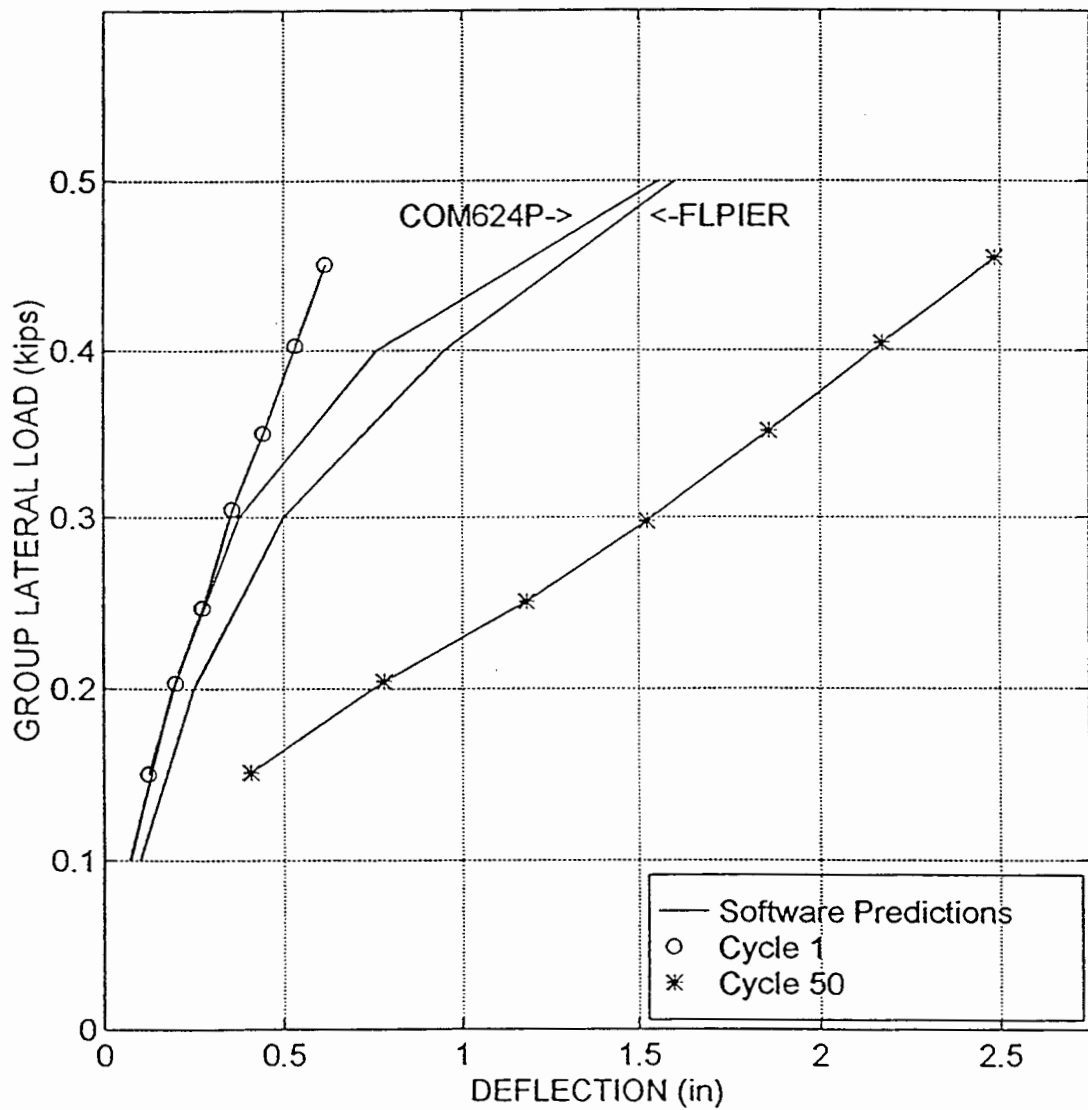


Figure 36. Pile group deflection: predicted versus measured.

## CHAPTER VIII

### SUMMARY AND CONCLUSIONS

#### Discussion

Five tasks were planned to complete this phase of the ongoing research in laterally loaded piles.

These tasks were:

1. Develop test hardware.
2. Design and construct a data acquisition system.
3. Calibrate all instrumentation.
4. Perform a pile group test.
5. Analyze data.

All of the tasks were accomplished with results being as good or better than planned. The model piles with their designed features, such as the pinned pile crown/load rod arrangement, can be adapted for further pile group testing. Changing spacing between the piles, for example, can be accomplished simply by fabricating a new load rod with smaller or greater distances between the pin holes.

The load distribution output obtained from the load rod was not conclusive. This probably was due to some degree to electronic noise in the data acquisition system. If the levels of strain in the load rod were increased, either by testing at higher lateral loads, or by fabricating a new load rod with thinner inter-pile gage sections, the system noise would have a much smaller influence on the strain gage output. If a new load rod were to be fabricated for further testing, it should be constructed in such a way that the axis on which the connecting pins act should be on the same plane as the centroidal axis of the inter-pile gage sections so that no bending stress is introduced during loading, thus keeping the total stress on the load rod at a lower level.

The data acquisition system proved to be capable of the design requirement in most aspects. Sampling at the rate of 4 Hertz was adequate for testing done in this project. With the capability to expand to 256 input channels, the system should function well for future testing. Several problems still exist with the system, such as the voltage saturation problem when the system is turned on. Hopefully a solution will be found, but this problem can be worked around for the time being. LabVIEW software for testing is a powerful tool and proved invaluable for making the data acquisition system work and in controlling the loading system.

The loading system worked quite well once operating procedures were figured out. The unequal loading by the hydraulic cylinders was overcome by monitoring the load cells. Perhaps this approach will work for all future applications. Further refinement could be made in this area for smoother operation. The load by-pass cables and the other linkage elements proved to be very versatile and were a necessity to make pile group loading possible while preventing possible damage to the pile group or other instruments. The LVDT hookup apparatus also proved to be quite versatile and functional.

Calibration procedures and software evolved during this project to the point where it is not a tedious task to calibrate any of the instrumentation. LabVIEW software and the calibration spreadsheet make data reduction simple, with regression analysis the only manual step in the process.

After 50 full cycles of testing, the testing procedure was refined to make this task fairly simple. Many obstacles were overcome, including a power outage, in getting the testing completed. The quality and quantity of data gathered demonstrate the abilities of all systems and show that if desired, the response of any pile, at any location along its length, at any load, and in any cycle can be determined. Group response also can be studied at the same time.

MATLAB software proved to be a valuable tool in the data reduction work. Once basic steps were learned, data analysis and output preparation were quickly accomplished.

## Conclusions

Test output clearly showed that the lead pile takes more of the lateral load than the other piles, except after many cycles and at lower loads, where the trailing pile takes more of the load. As load levels increase, the lead pile again takes more load than the other piles. There was no clear trend showing how the other piles take up the remaining load. A statistical analysis of the load distribution data could yield more information in this area.

Bending moment data showed some definite trends. As the number of cycles increased, the point along the pile at which the maximum moment occurs moved down the pile. This result was expected. Another trend showed that for a single cycle, the depth at which the maximum moment occurred remained quite constant as the load increased. It also appeared that the inner piles had close to the same bending moment in both loading directions at higher loads. At lower loading levels, more moment occurs in the inner piles when they are trailing than when they are leading.

The comparison of test output with predictions made by Florida Pier and COM624P did not clearly show a correlation in either bending moment or pile top deflection.

Since the piles were sized using dimensionless Pi terms, results from this research can be applied to any full-scale pile foundation. The results are valid for predicting performance of prototype piles.





## REFERENCES

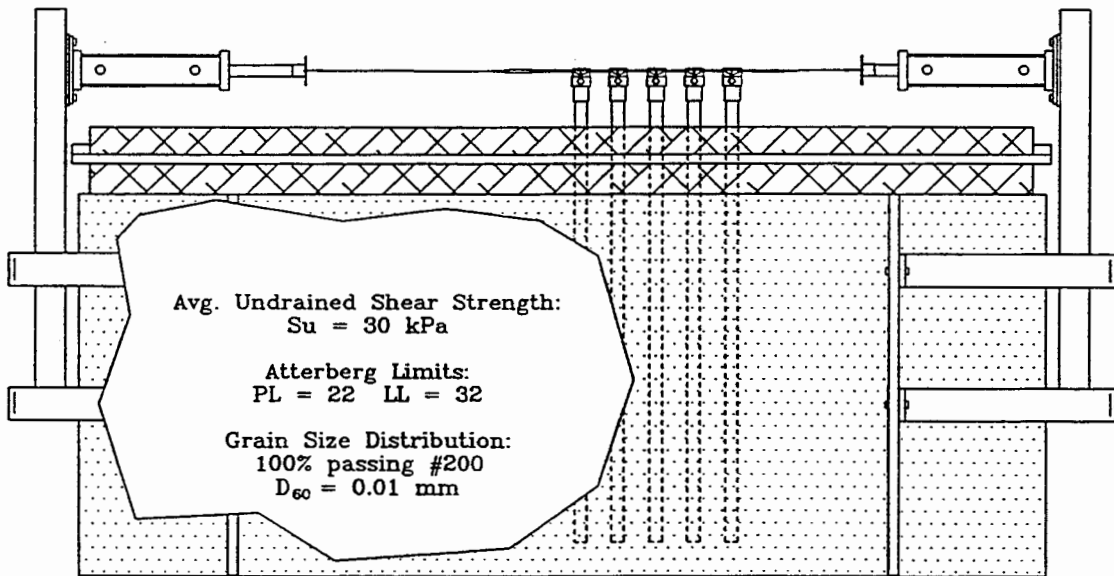
- Brown, D. A. and L. A. Reese, 1985. Behavior of a large-scale pile group subjected to cyclic lateral loading. Minerals Management Service, U.S. Department of Interior, Department of Research, FHWA, U.S. Army Engineer Waterways Experiment Station. Report no. GR 85-12. 399 p.
- McVay, M., D. Bloomquist, D. Vanderline, and J. Clausen. 1994. Centrifuge modeling of laterally loaded pile groups in sands. *Geotechnical Testing Journal*, GTJODJ17 (2):129-137.
- McVay, M., R. Casper, and T. Shang. 1995. Lateral response of three-row groups in loose to dense sands at 3D and 5D pile spacing. *Journal of Geotechnical Engineering* 121(5):436-441.
- Rao, S., V. Ramakrishna, and G. Raju. 1996. Behavior of pile-supported dolphins in marine clay under lateral loading. *Journal of Geotechnical Engineering* 122(8):607-612.
- Rollins, K., K. Peterson, and T. Weaver. 1996. Full-scale pile group lateral load testing in soft clay. *National Center for Earthquake Engineering Research Bulletin*, 10(4):9-11.
- Townsend, F., M. McVay, P. Ruesta, and L. Hoyt. 1997. Prediction and evaluation of a laterally loaded pile group at Roosevelt Bridge. Florida DOT Final Report. State Project No. 99700-3508-119. 381 p.
- U.S. Department of Transportation. 1996. Design and construction of driven pile foundations. FHWA DTFH61-93-C-0015. 822 p.



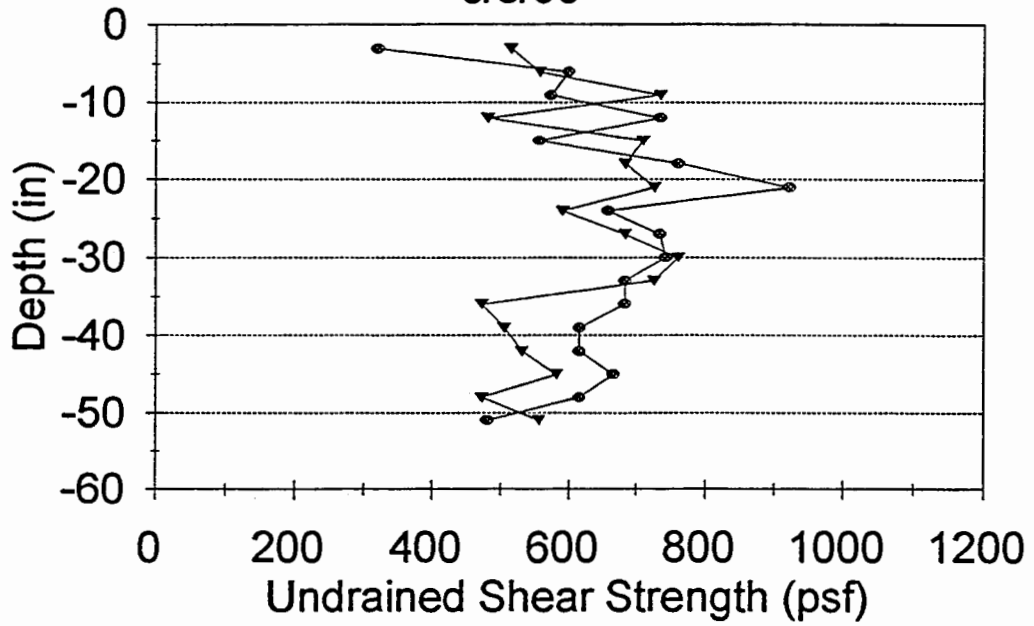
**APPENDIX A: SOIL PROPERTIES**



Figure A1. Soil properties (next 6 plots).



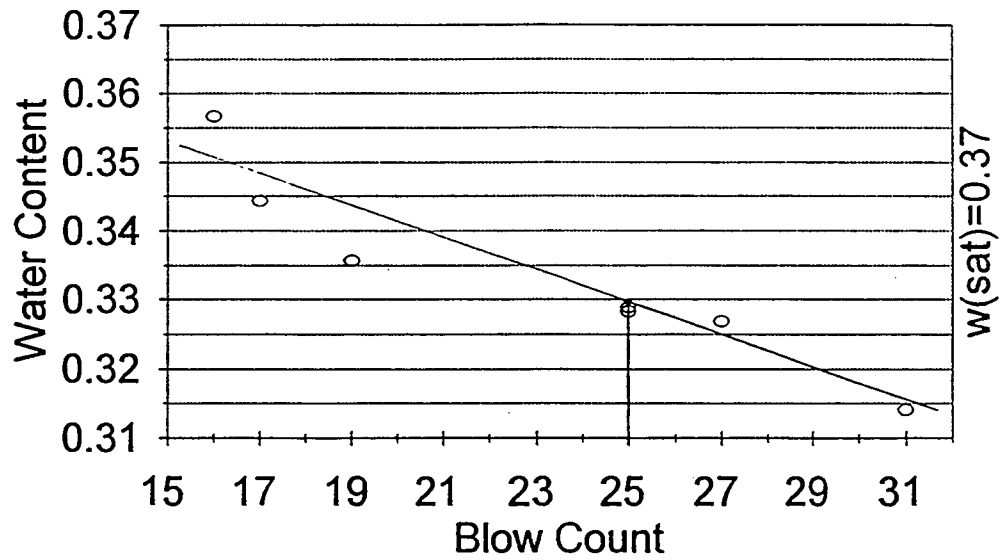
### Shear Strength Profile 6/5/96



← West End   ← East End

# Clay for Model Lateral Load Tests

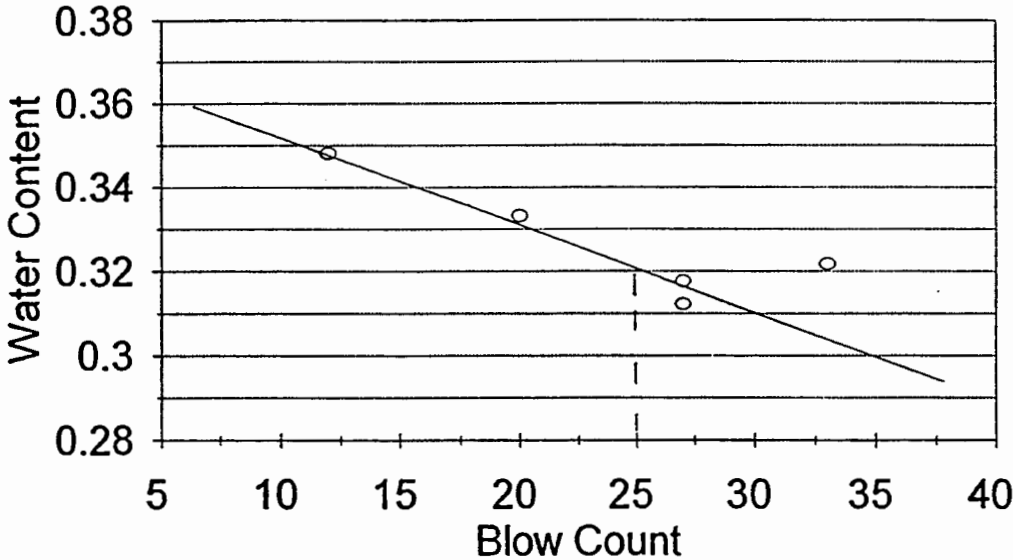
PL=20 (June 6, 1996)



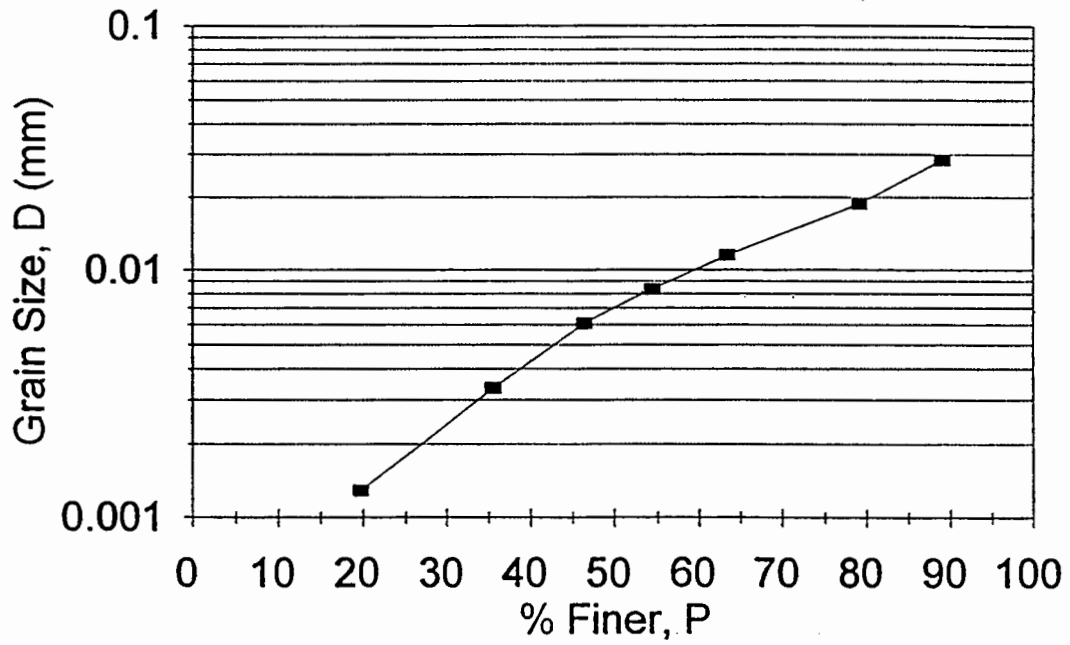


# Clay for Model Lateral Load Tests

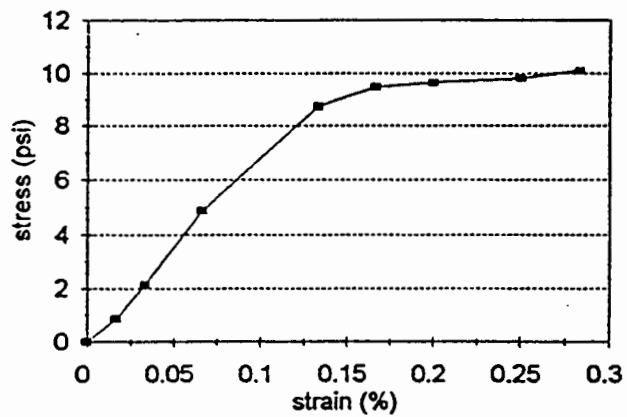
PL=24 (July 18, 1996)



### Hydrometer Analysis 10/18/96



deformation (in)	load (dial)	strain (%)	area (in <sup>2</sup> )	load (lbs)	stress (psi)
0.000	0.0	0.0000	1.53938	0	0
0.050	15.5	0.0167	1.565472	1.356199	0.86632
0.100	39.0	0.0333	1.592462	3.412372	2.142827
0.200	92.0	0.0667	1.649336	8.049698	4.880569
0.400	177.0	0.1333	1.776208	15.48692	8.71909
0.500	200.0	0.1667	1.847256	17.49934	9.473153
0.600	212.0	<b>0.2000</b>	1.924226	18.5493	<b>9.639881</b>
0.750	230.0	0.2500	2.052507	20.12425	9.804714
0.850	248.0	0.2833	2.147973	21.69919	10.10217



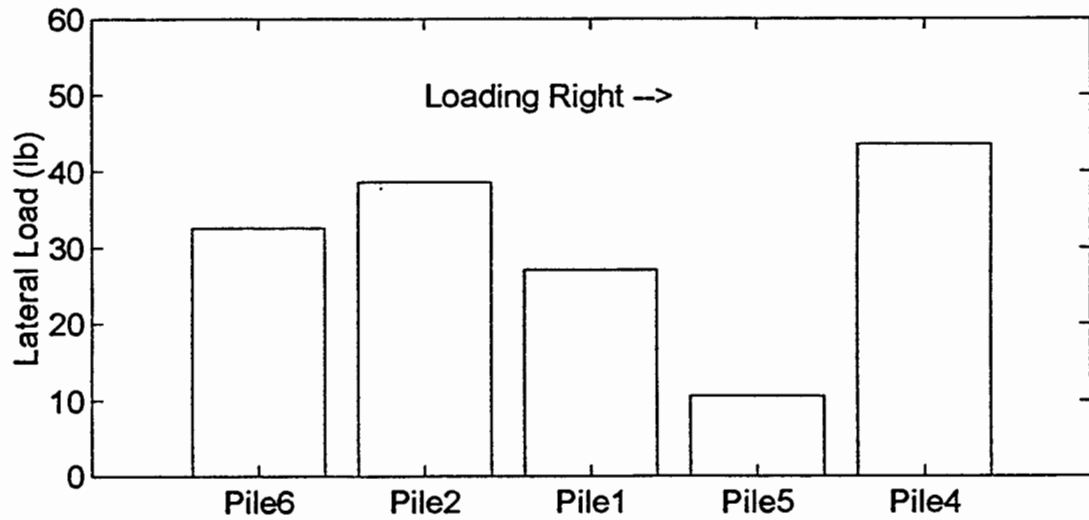
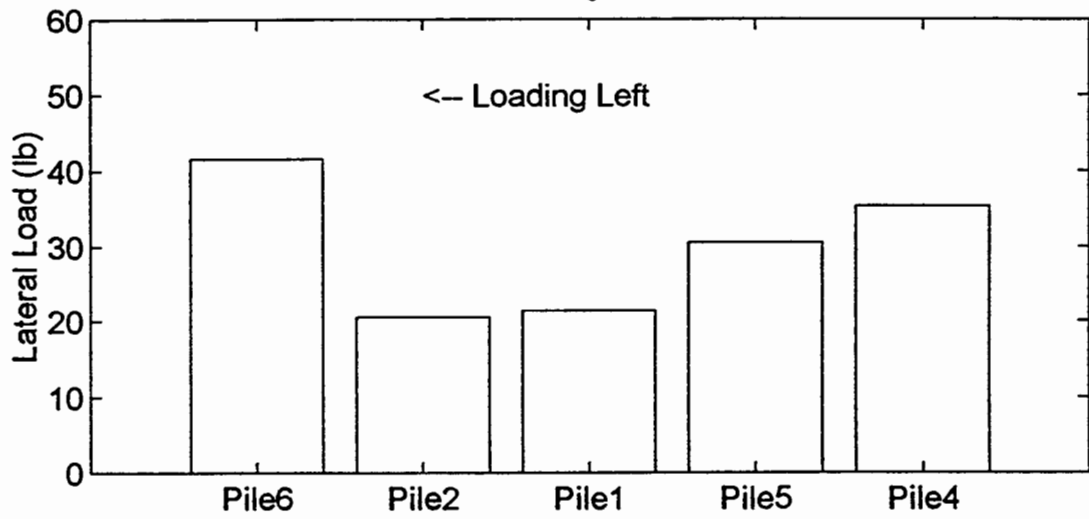


**APPENDIX B: TEST RESULTS**



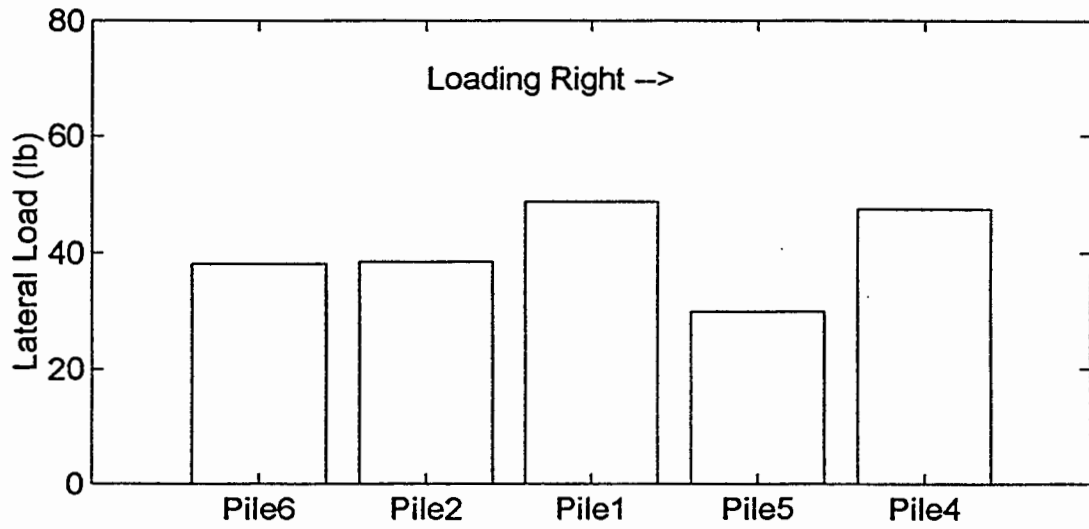
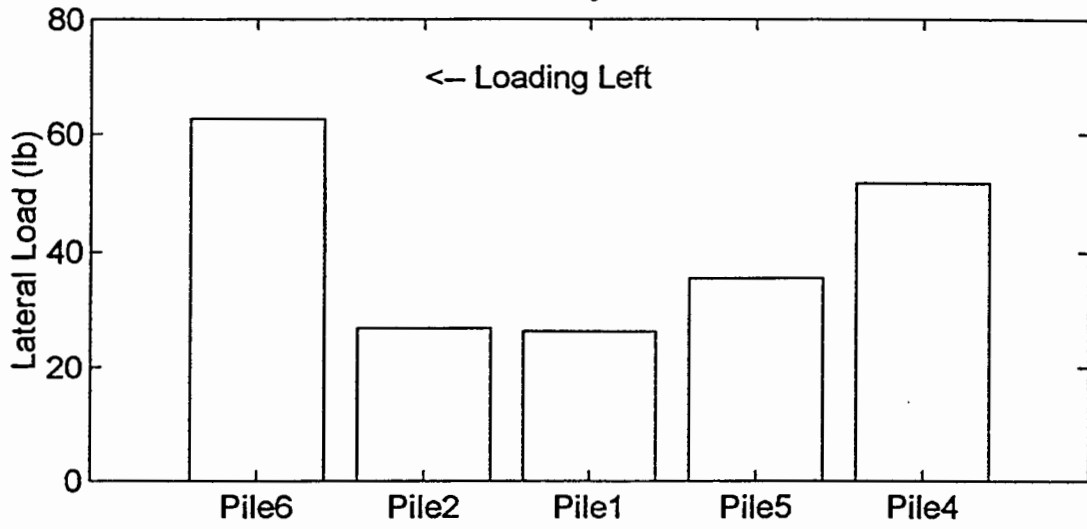
Figure B1. Load distribution @ cycle 1 (next 7 plots).

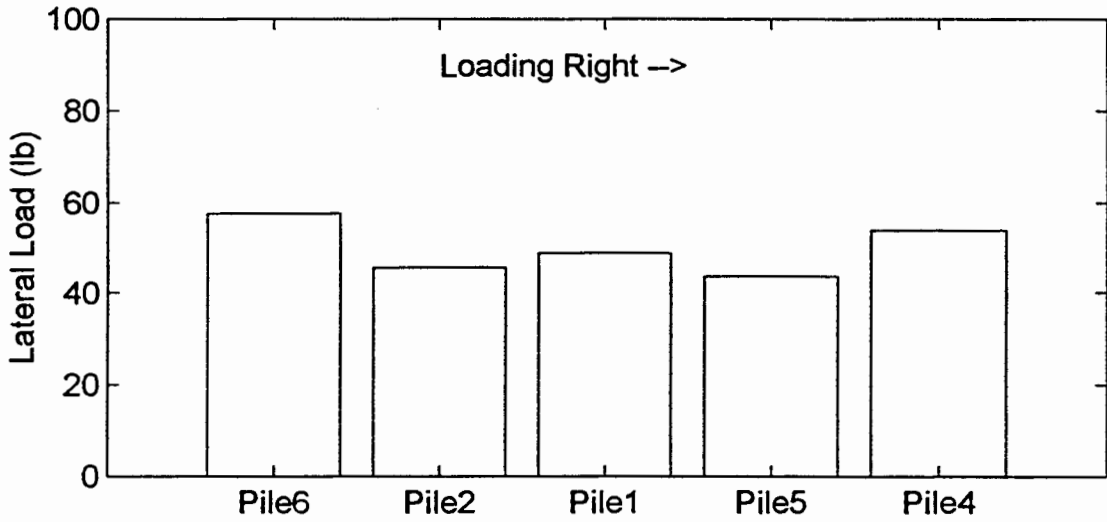
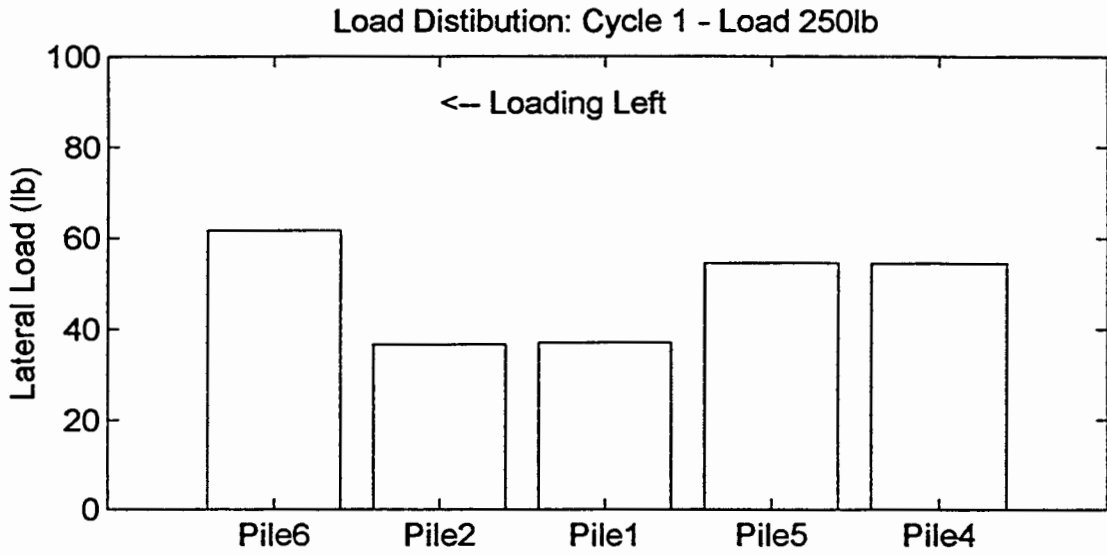
Load Distribution: Cycle 1 - Load 150lb



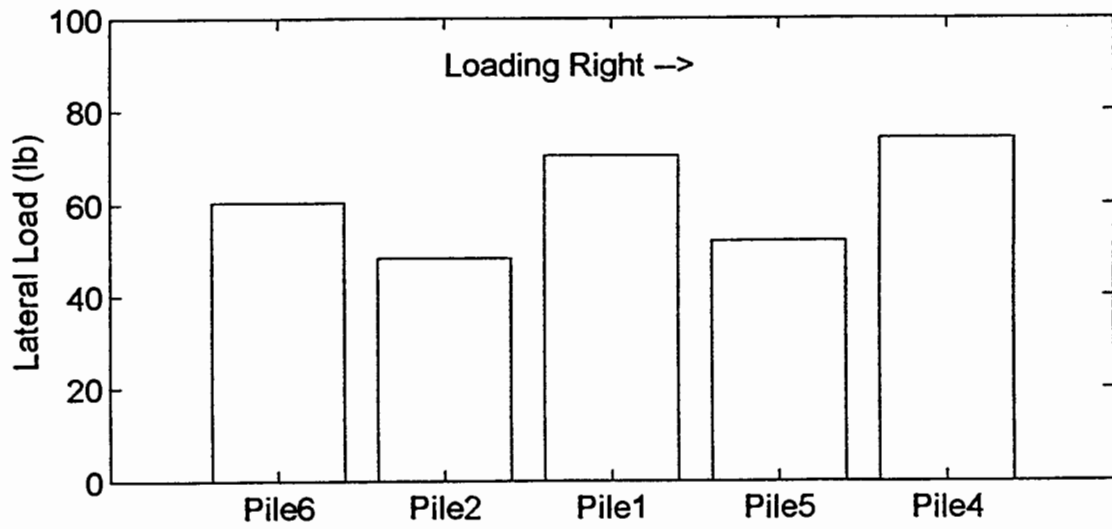
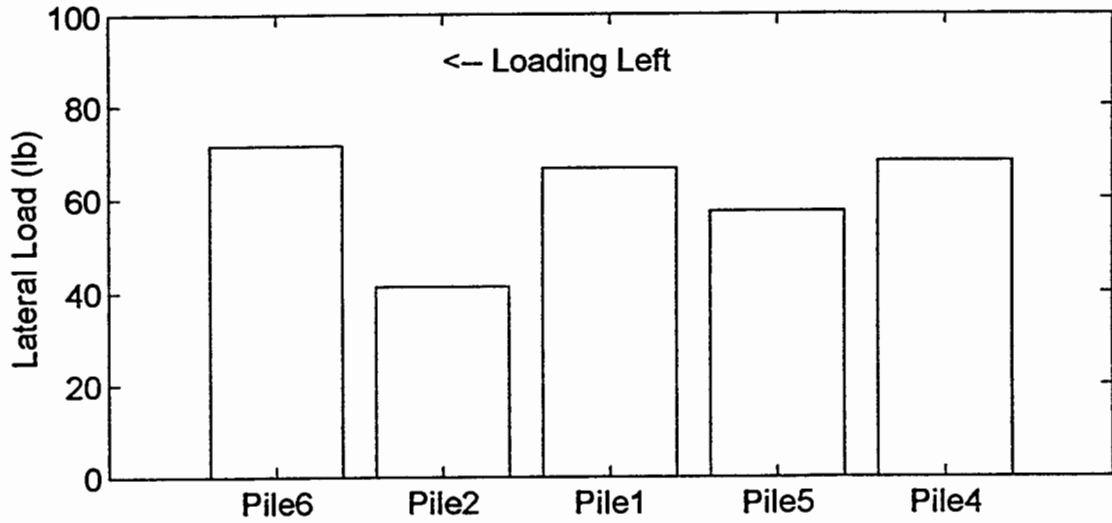


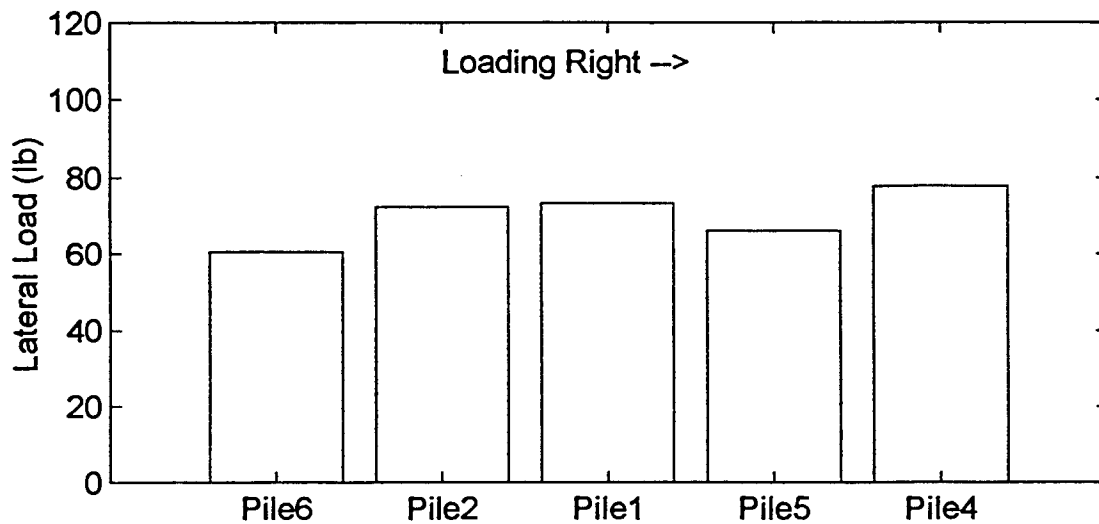
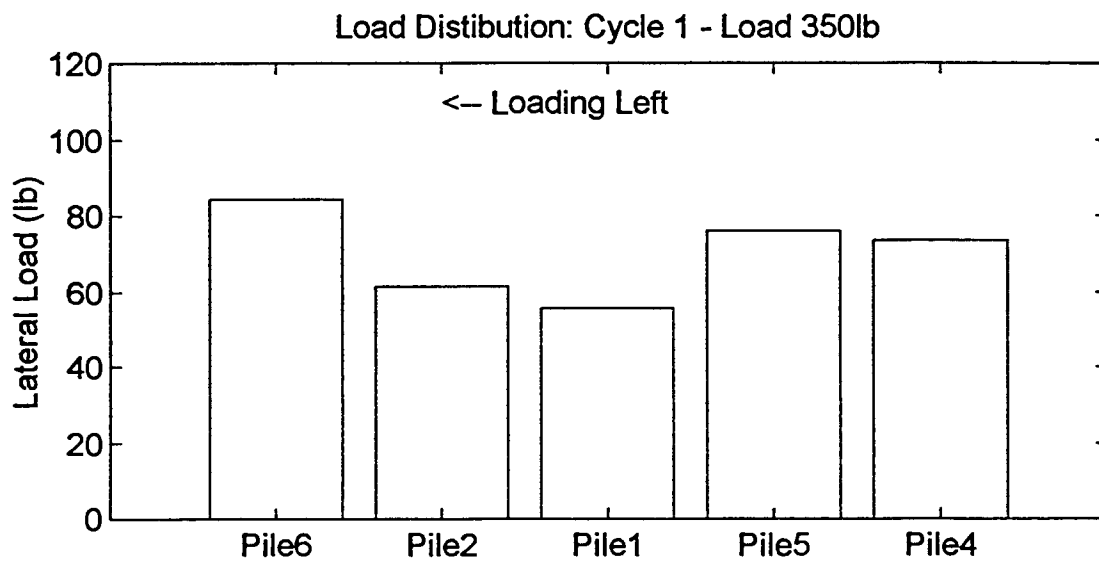
Load Distribution: Cycle 1 - Load 200lb



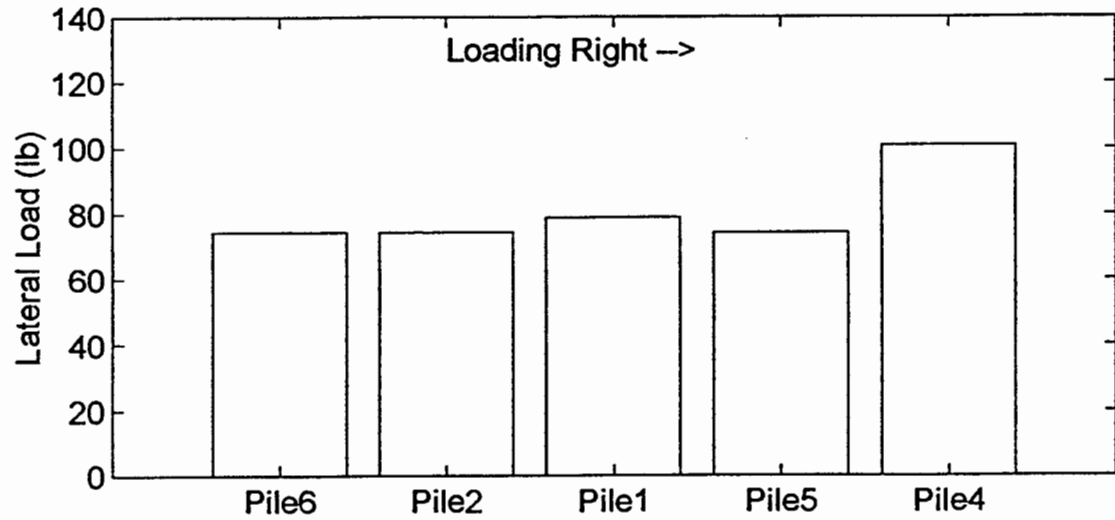
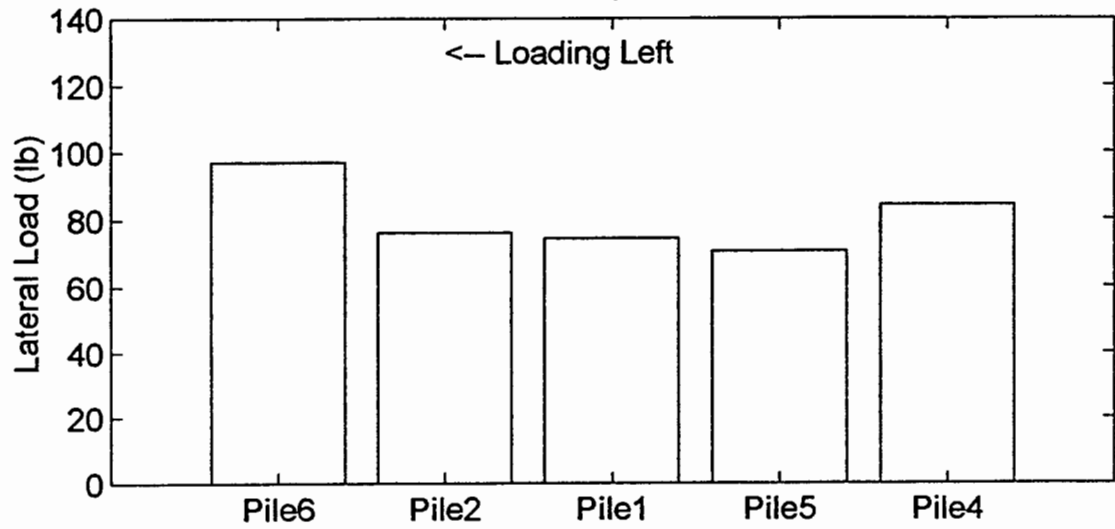


Load Distribution: Cycle 1 - Load 300lb





Load Distribution: Cycle 1 - Load 400lb



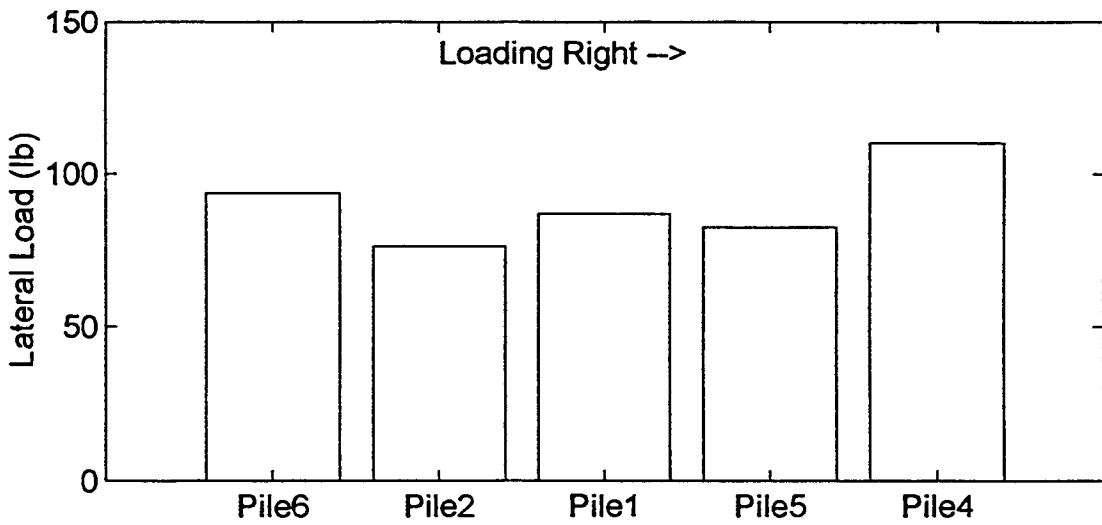
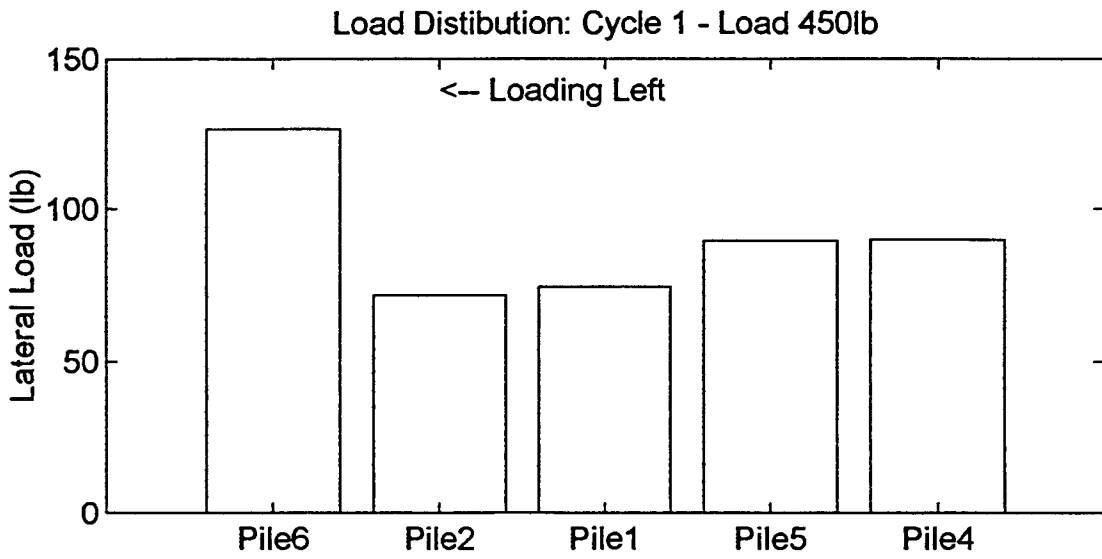
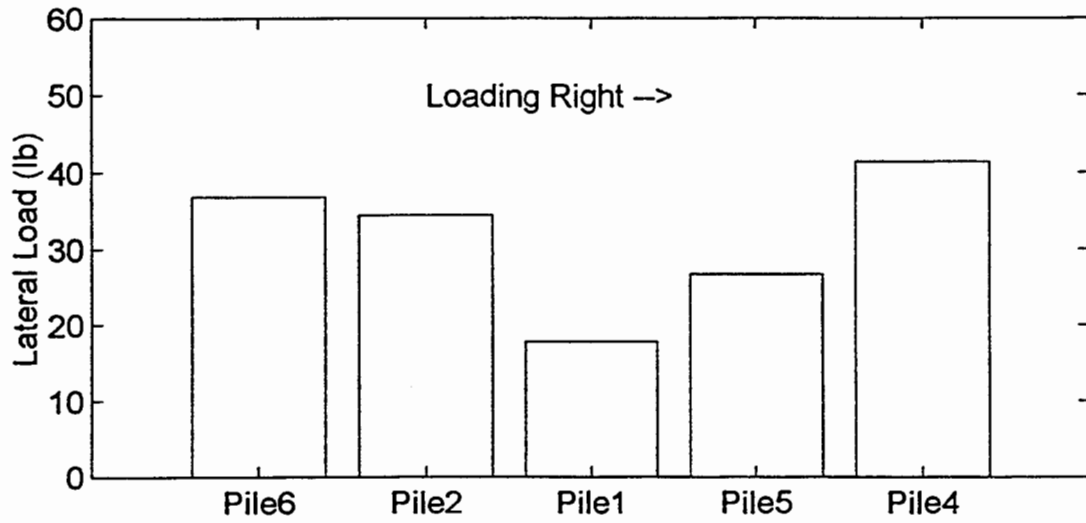
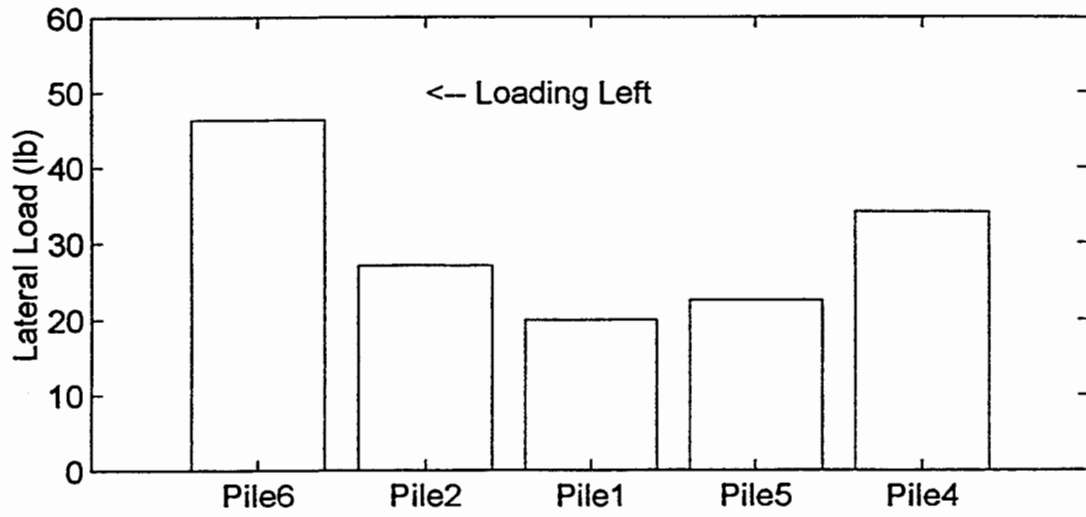


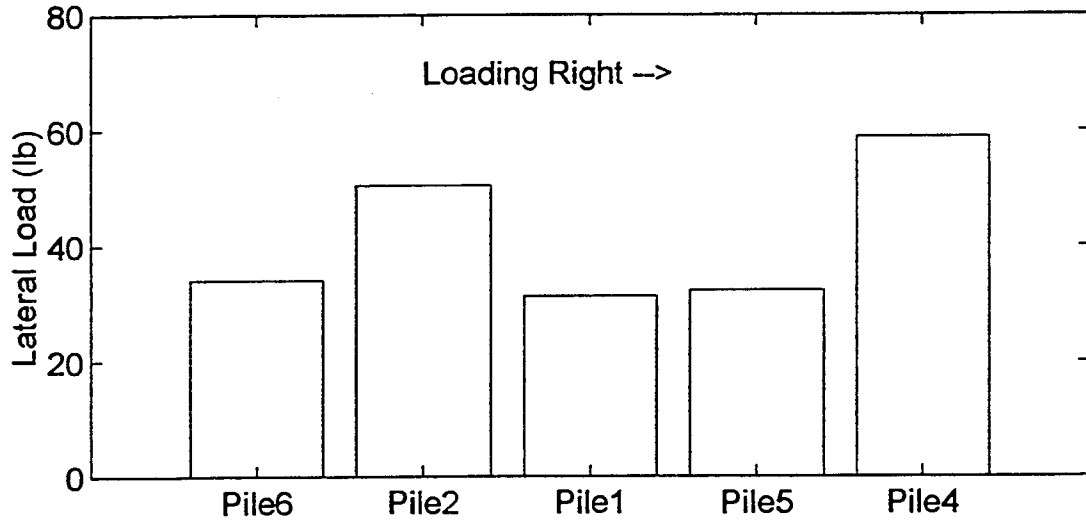
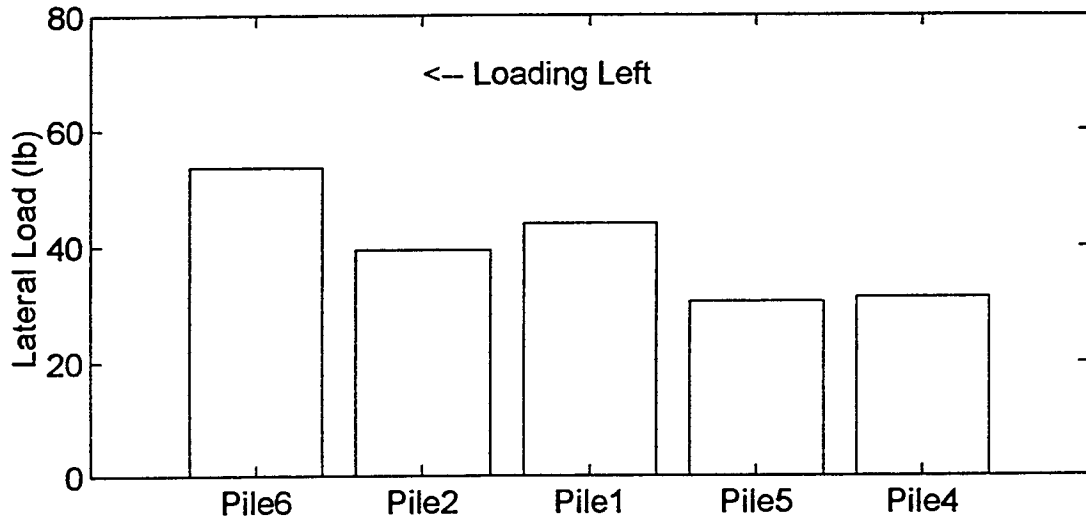
Figure B2. Load distribution @ cycle 5 (next 7 plots).

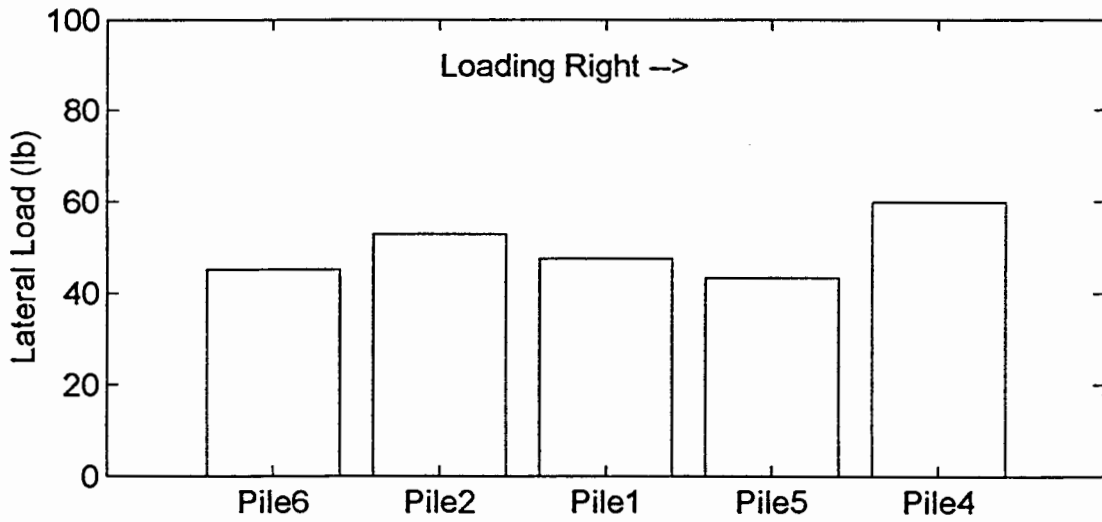
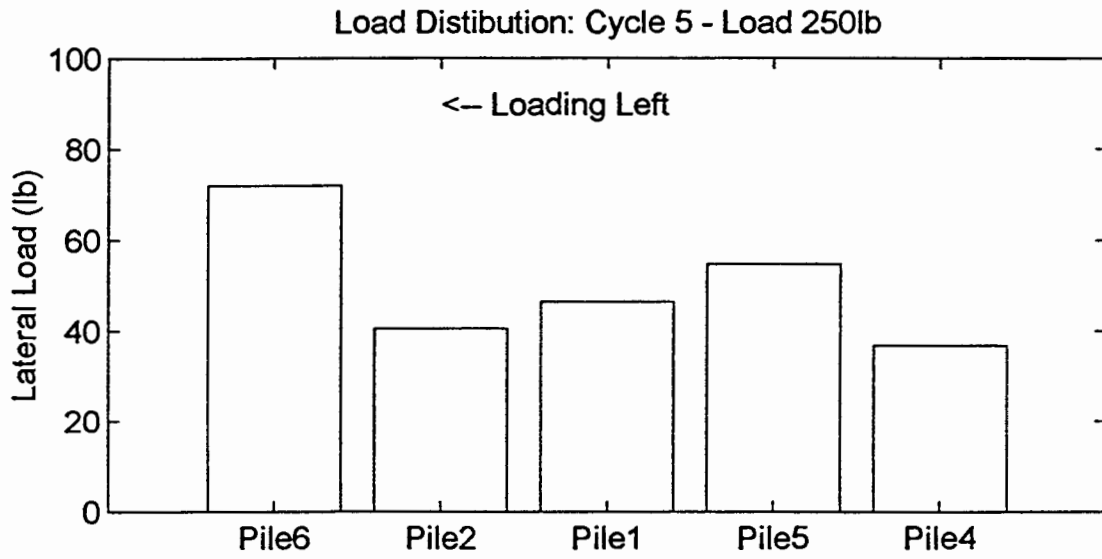
Load Distribution: Cycle 5 - Load 150lb



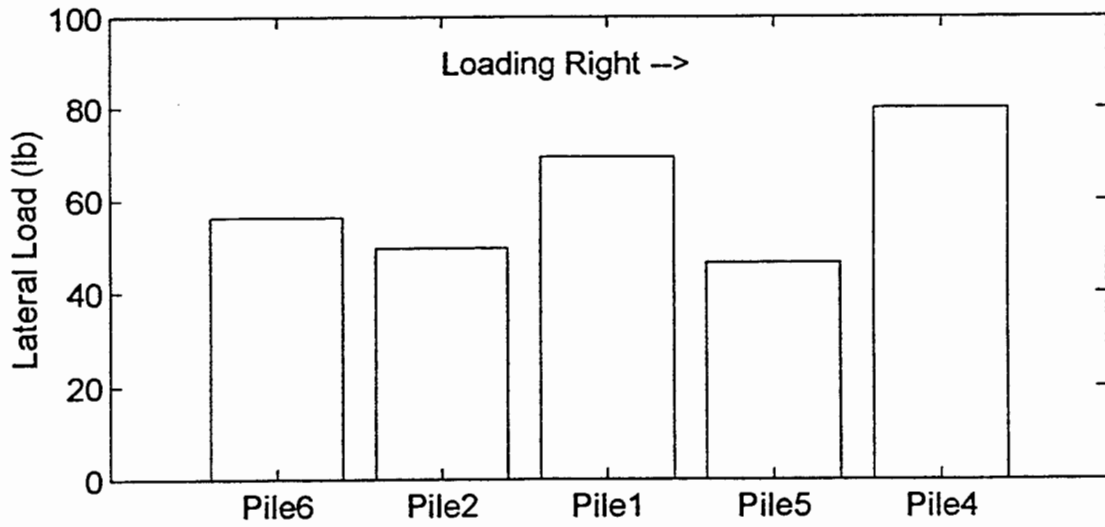
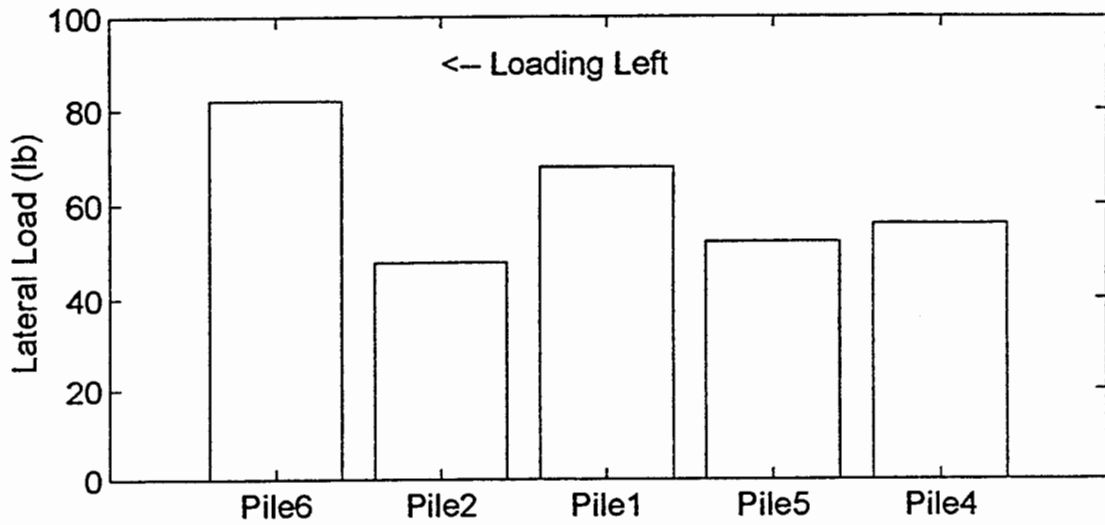


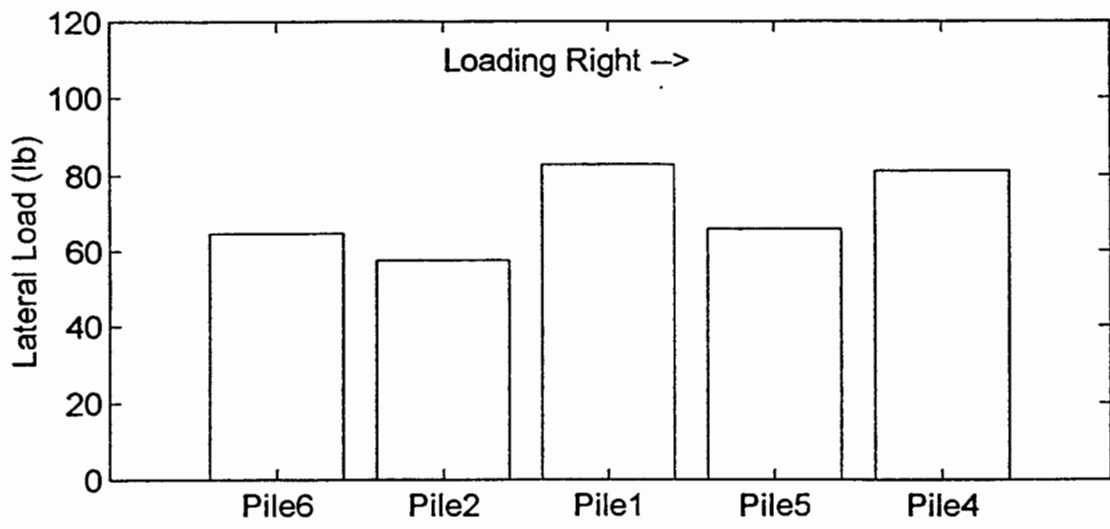
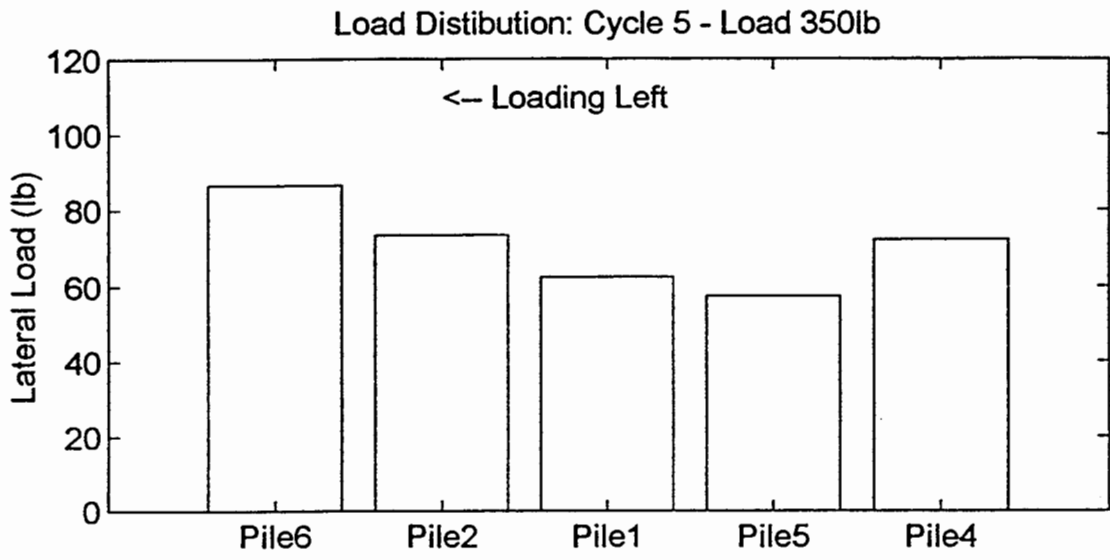
Load Distribution: Cycle 5 - Load 200lb



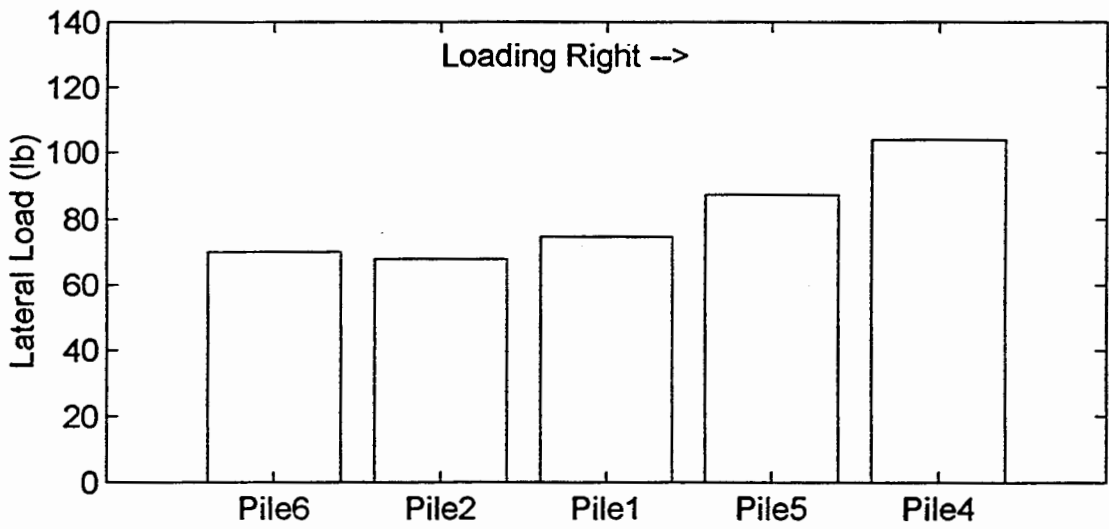
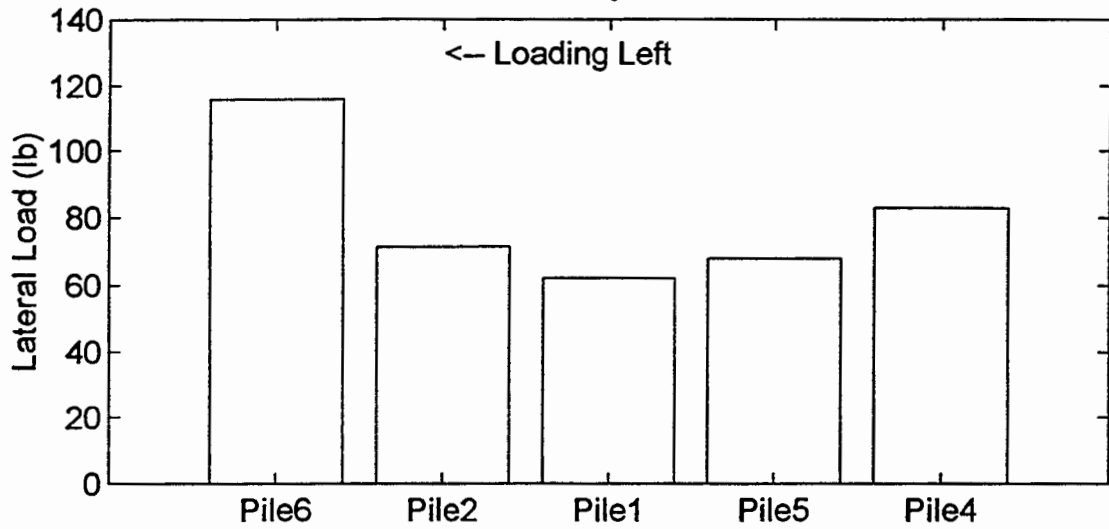


Load Distribution: Cycle 5 - Load 300lb





Load Distribution: Cycle 5 - Load 400lb



Load Distribution: Cycle 5 - Load 450lb

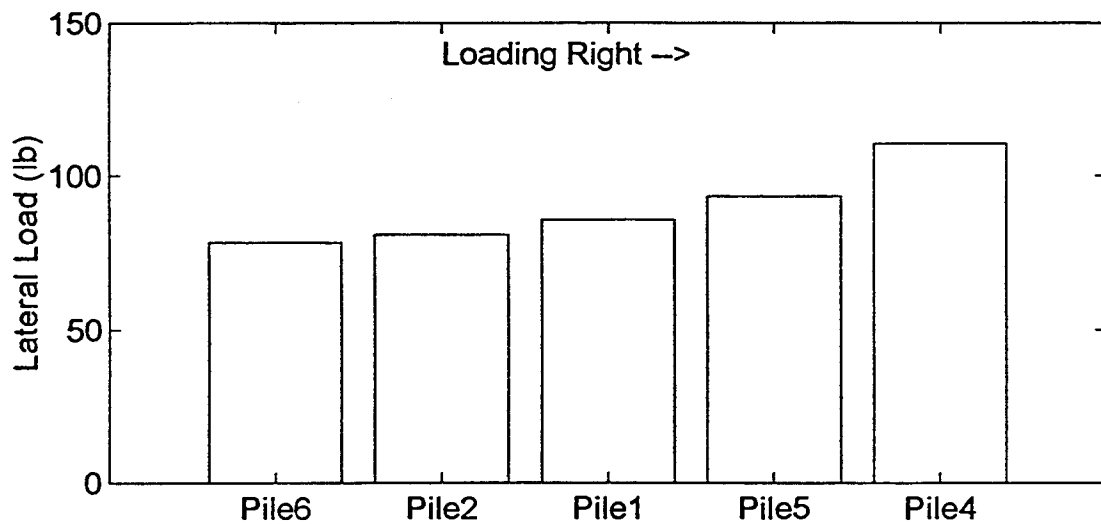
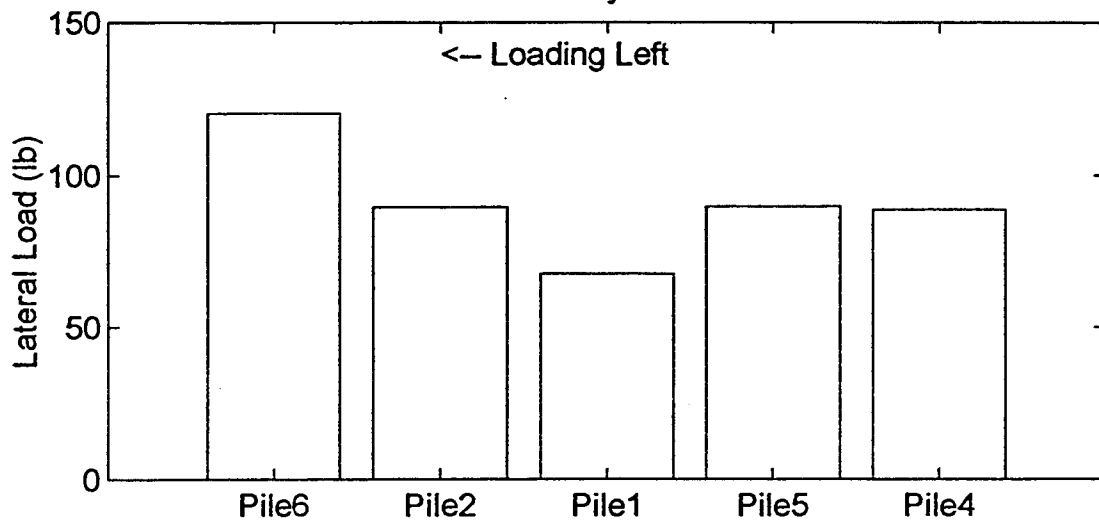
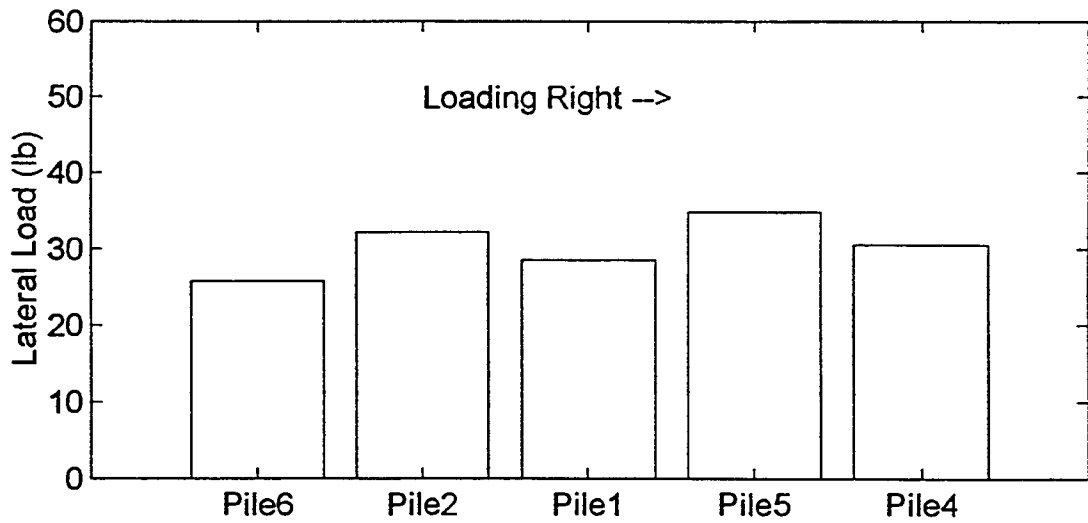
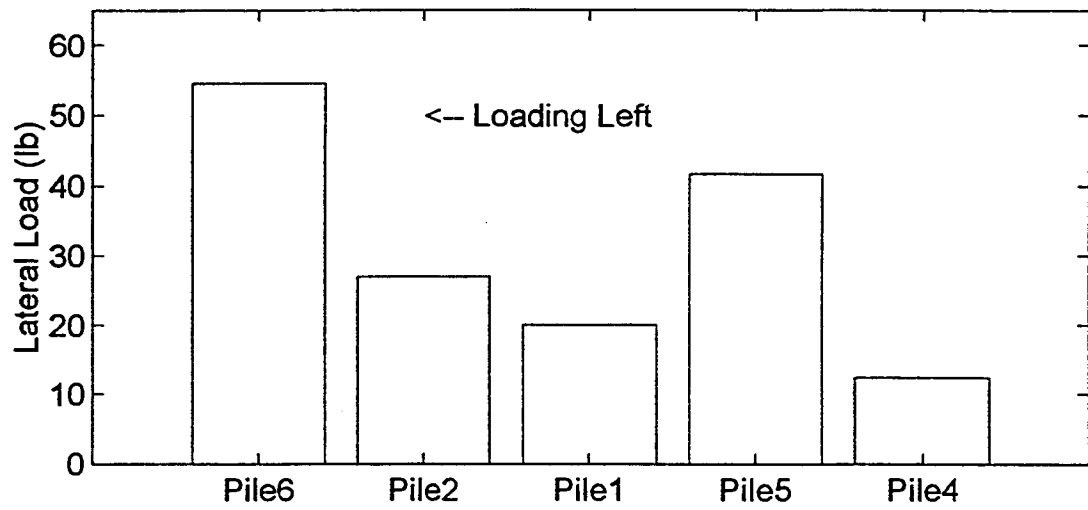


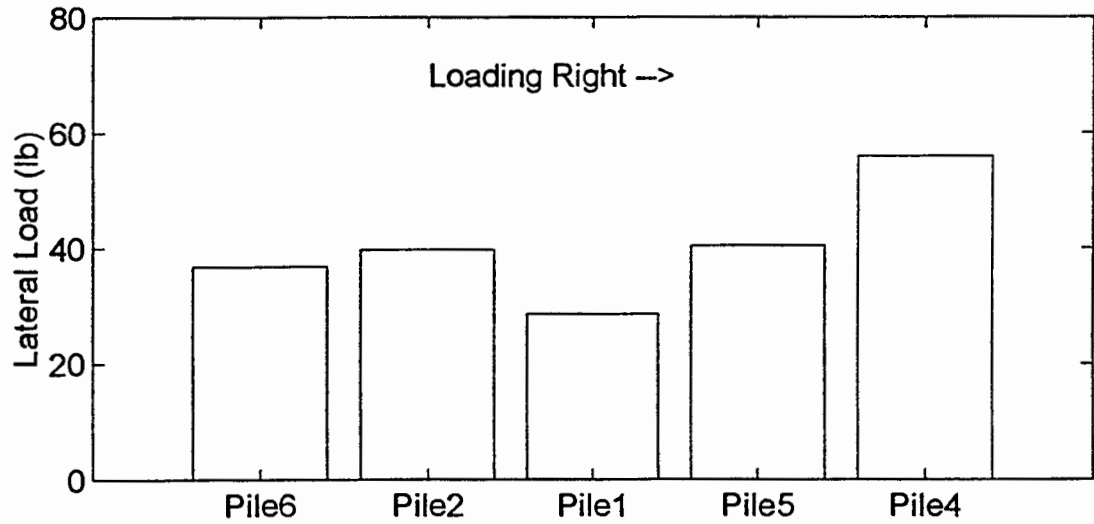
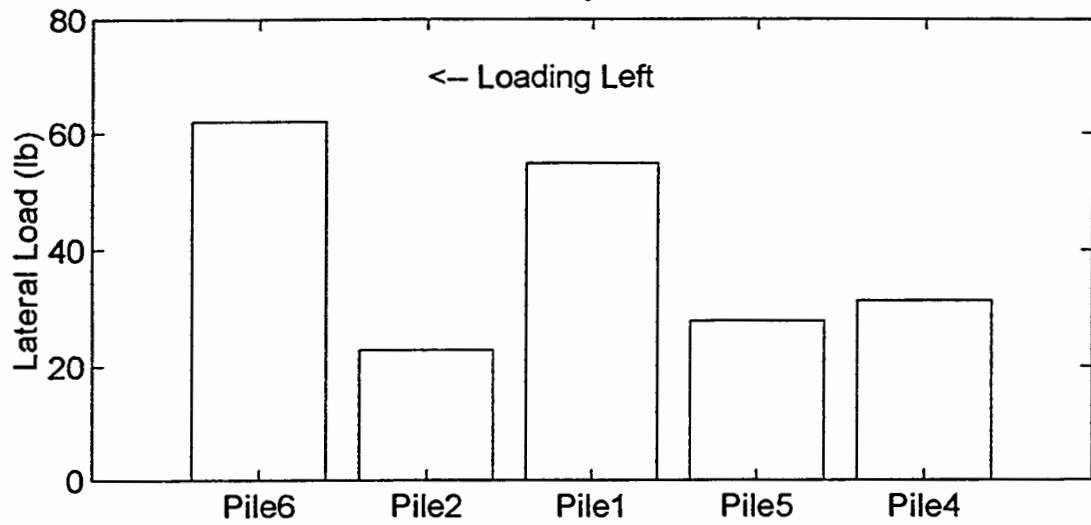
Figure B3. Load distribution @ cycle 10 (next 7 plots).

Load Distribution: Cycle 10 - Load 150lb

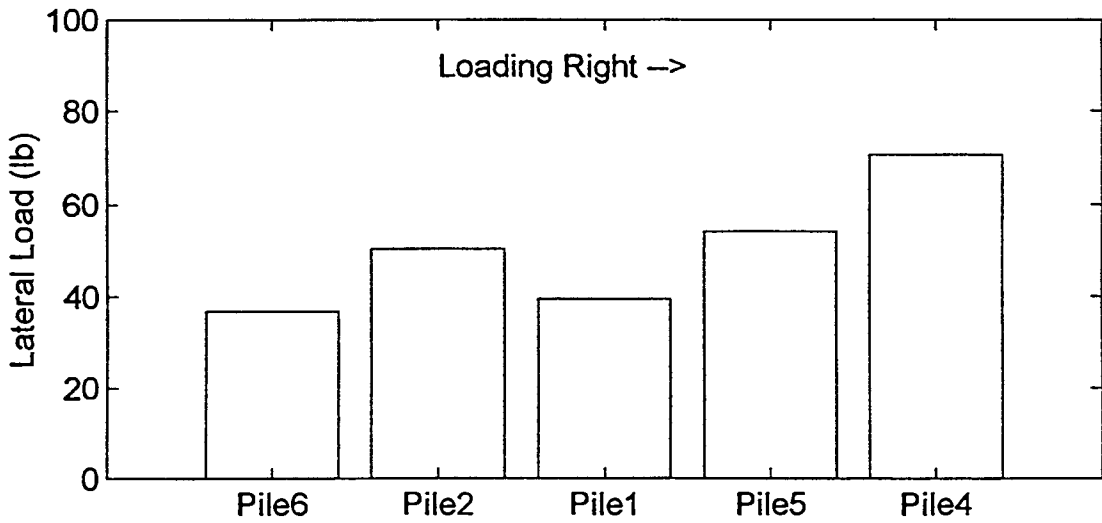
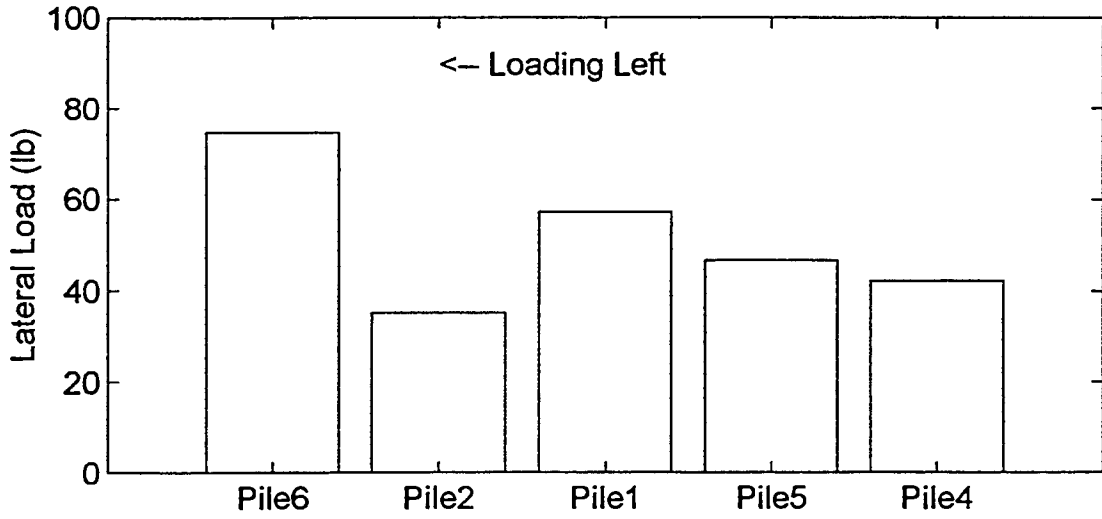




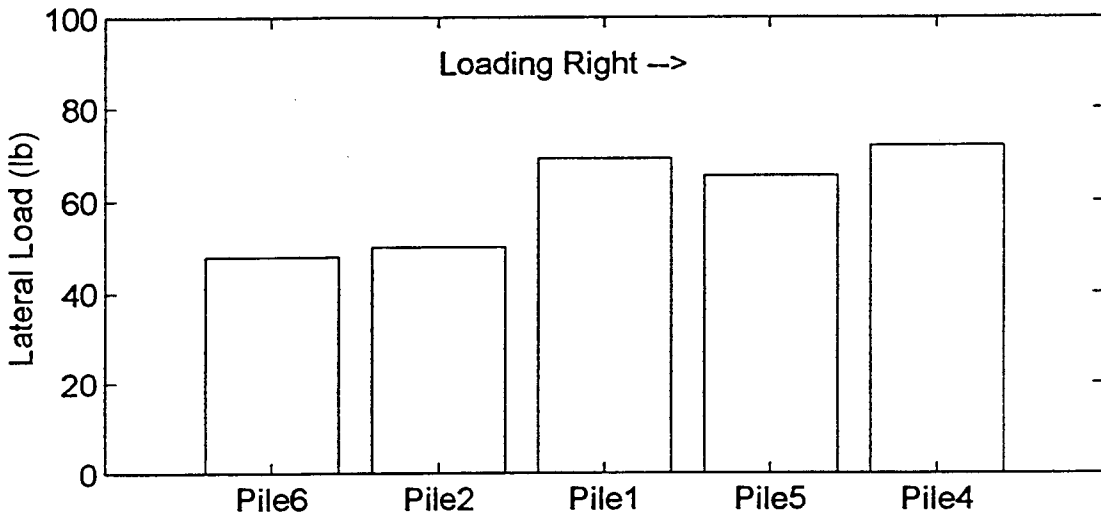
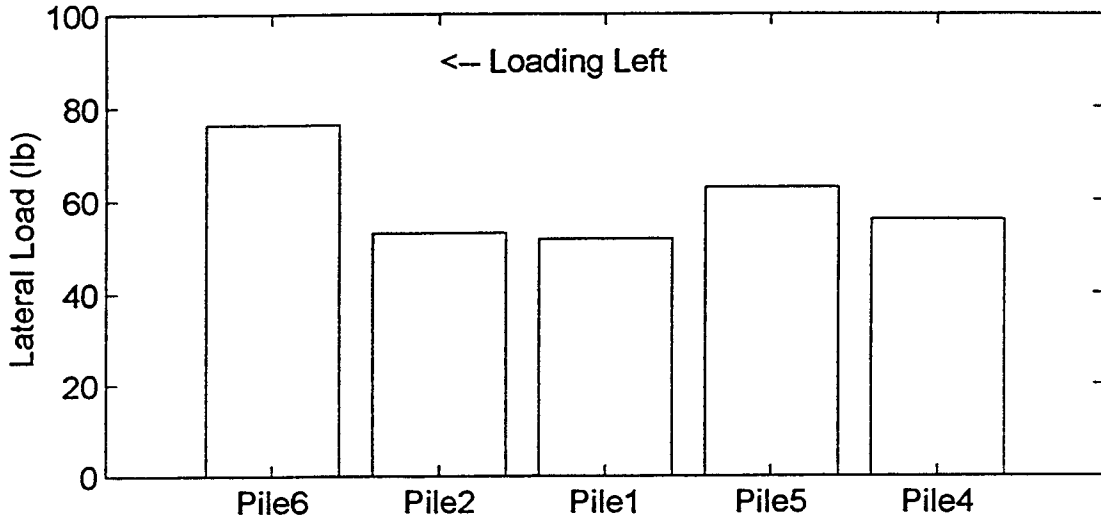
Load Distribution: Cycle 10 - Load 200lb

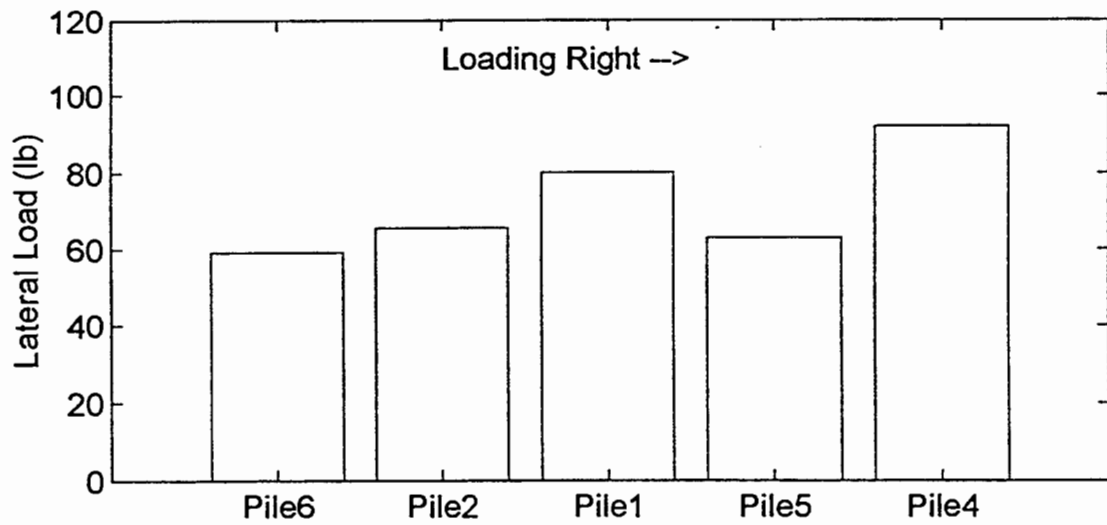
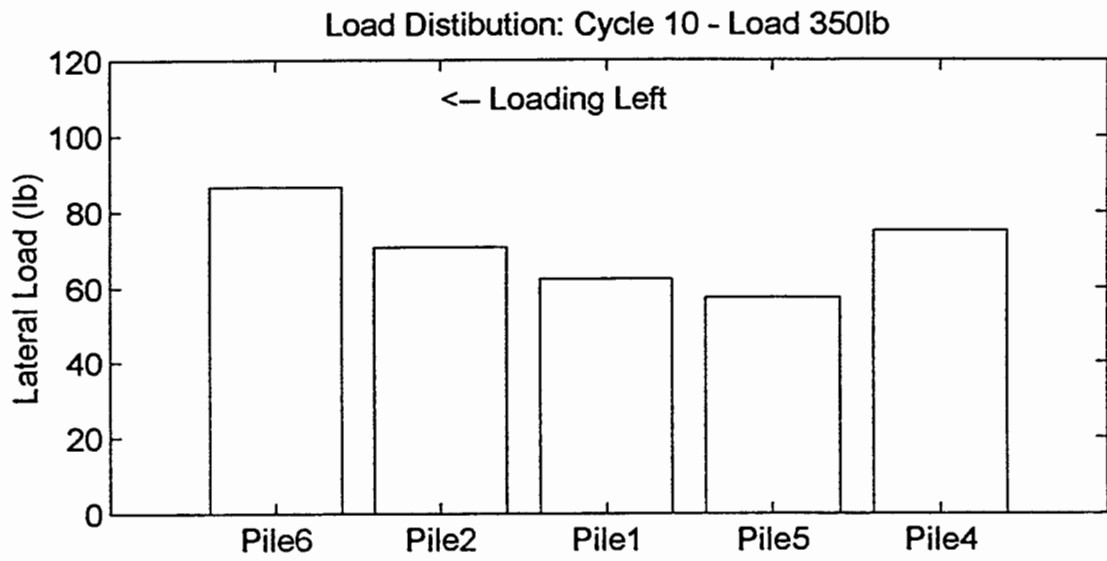


Load Distribution: Cycle 10 - Load 250lb

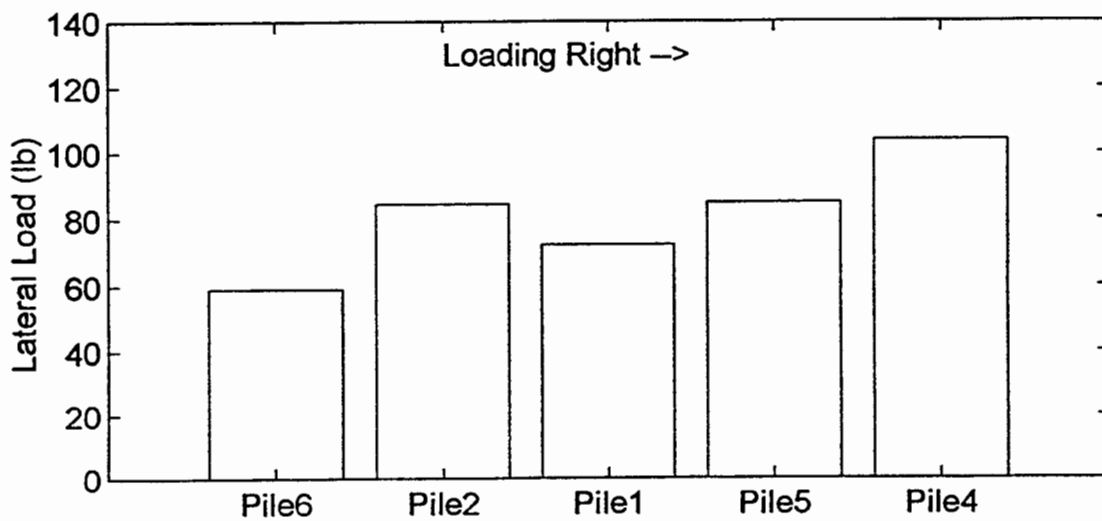
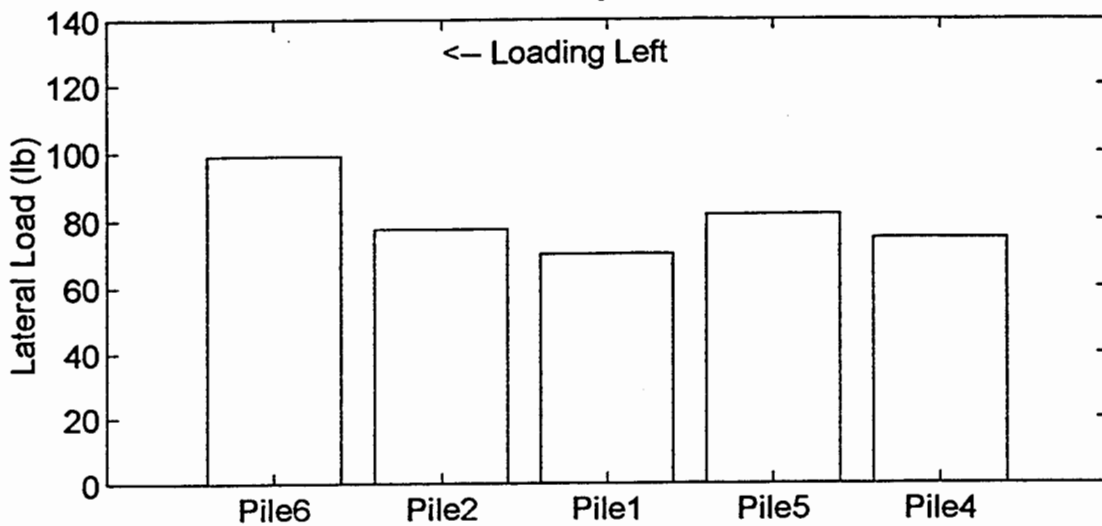


Load Distribution: Cycle 10 - Load 300lb





Load Distribution: Cycle 10 - Load 400lb



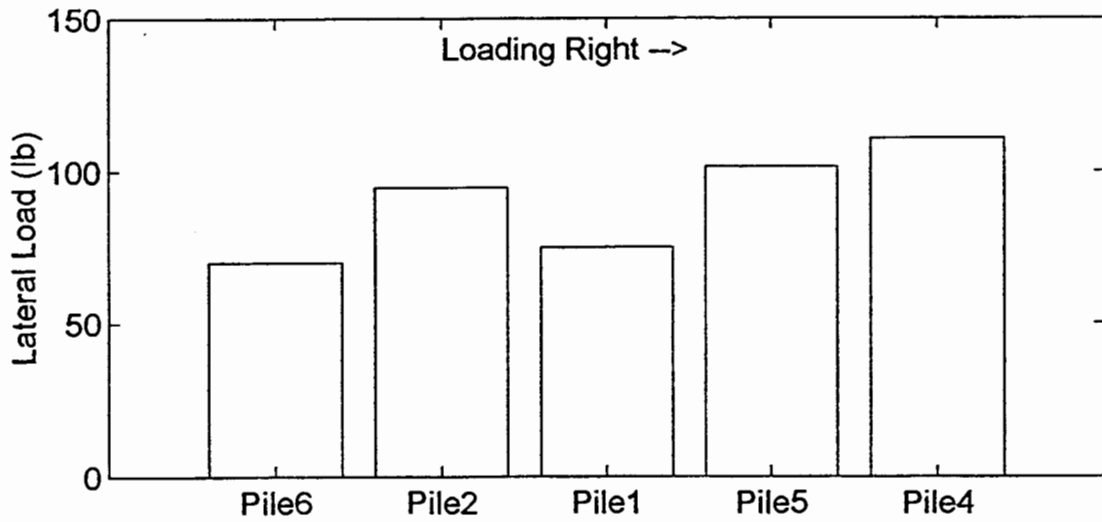
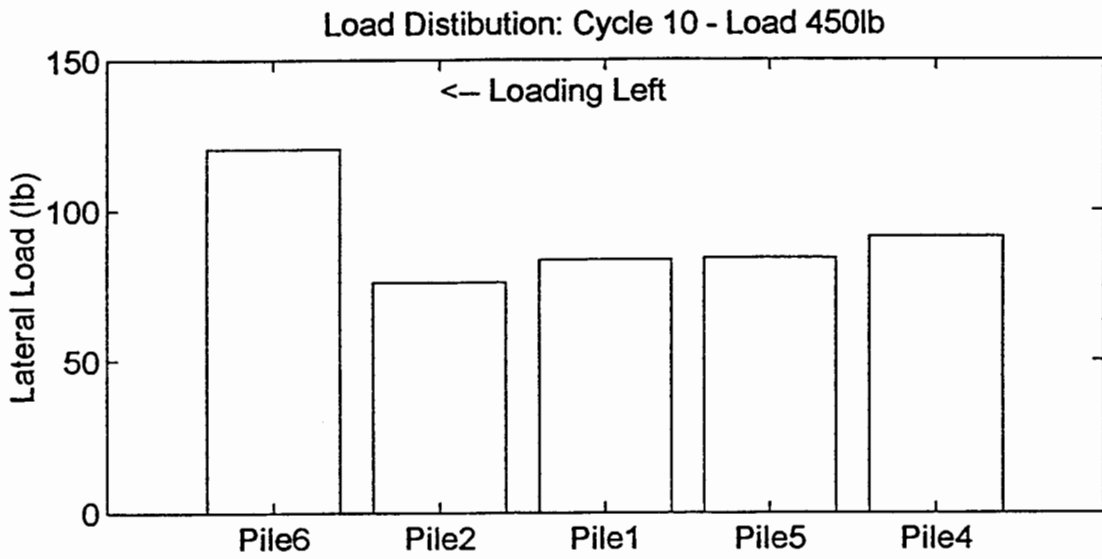
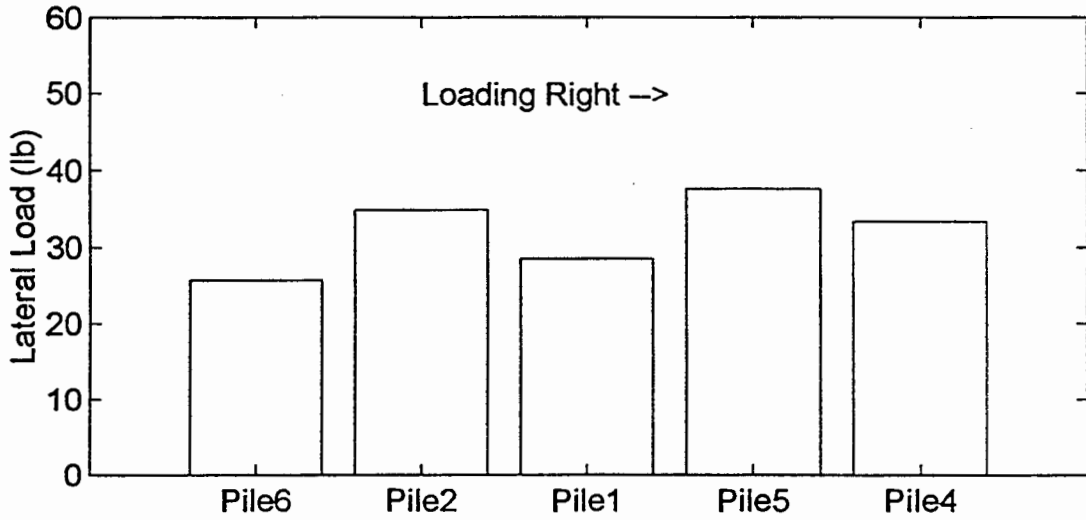
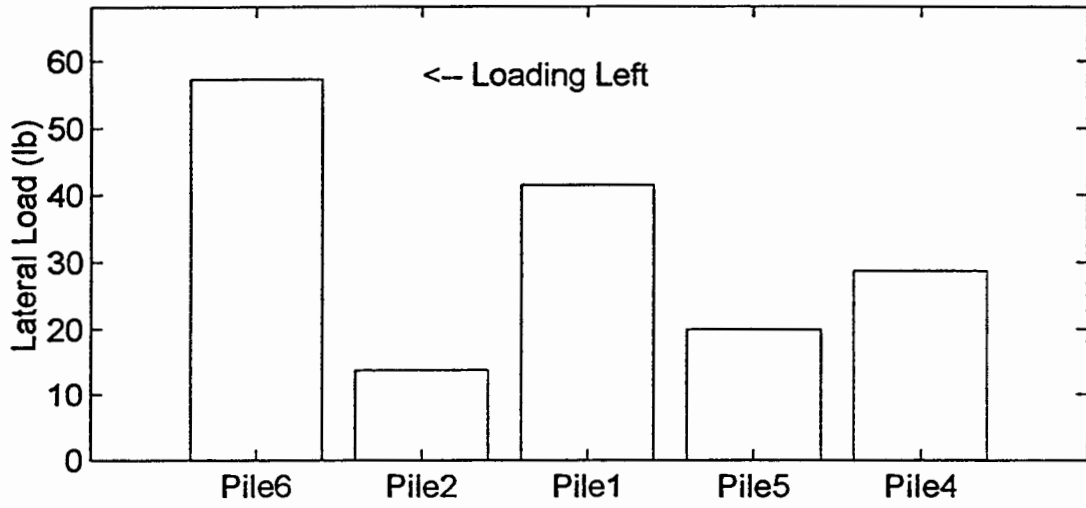


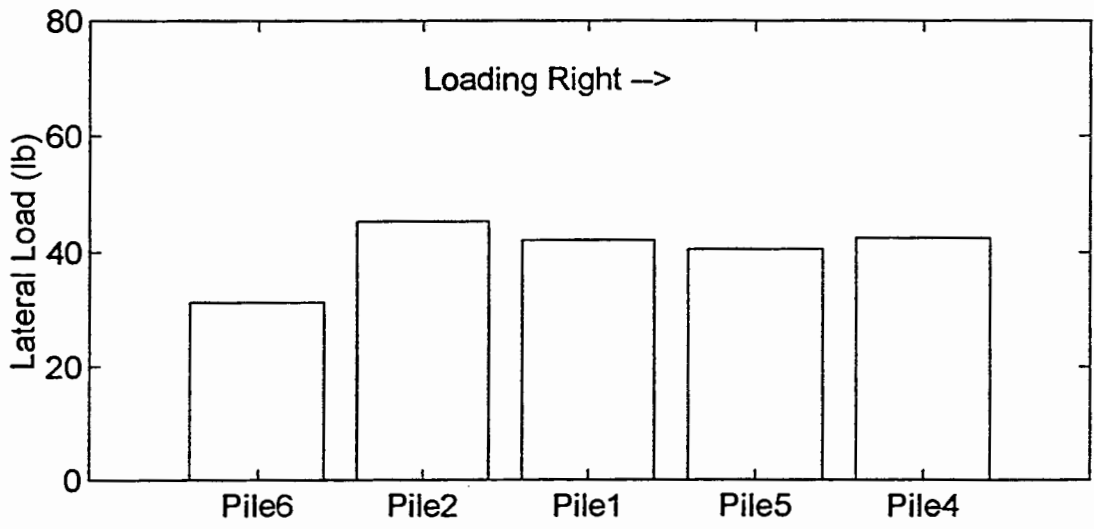
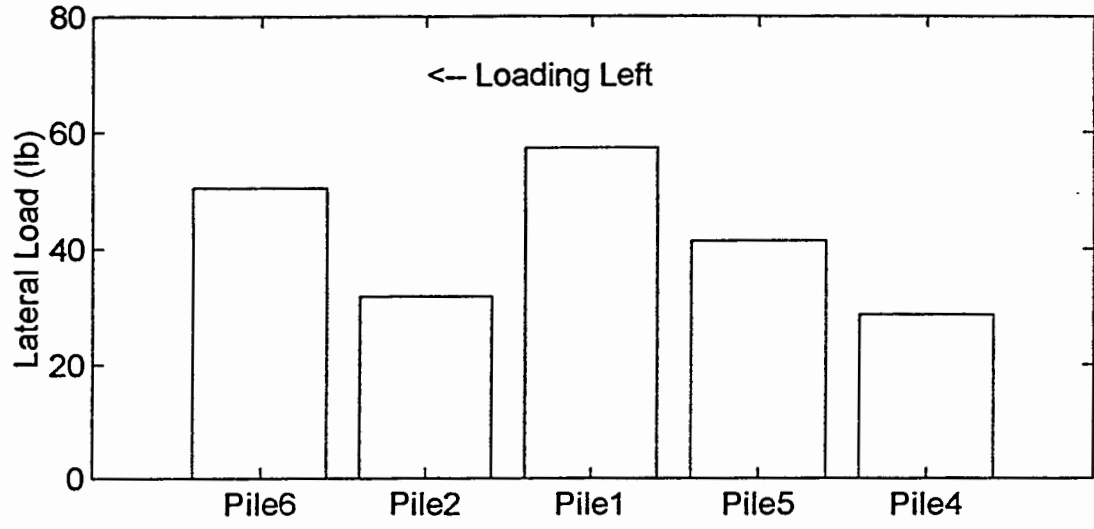
Figure B4. Load distribution @ cycle 25 (next 7 plots).

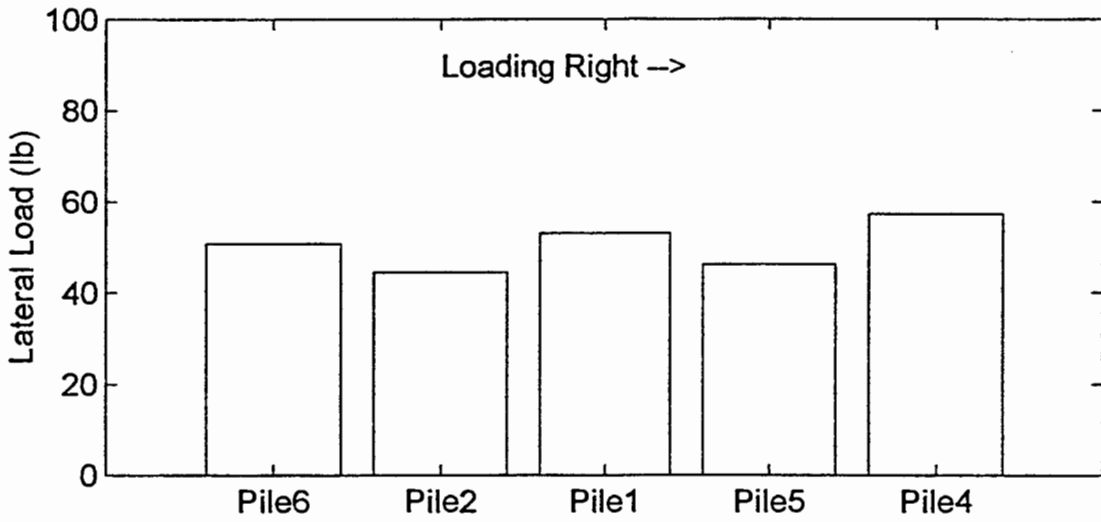
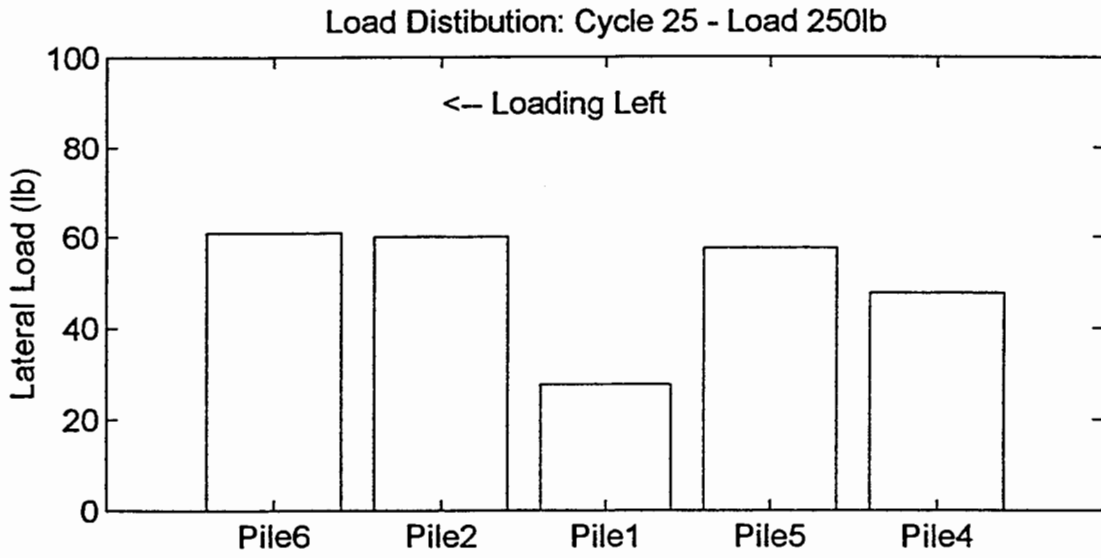
Load Distribution: Cycle 25 - Load 150lb



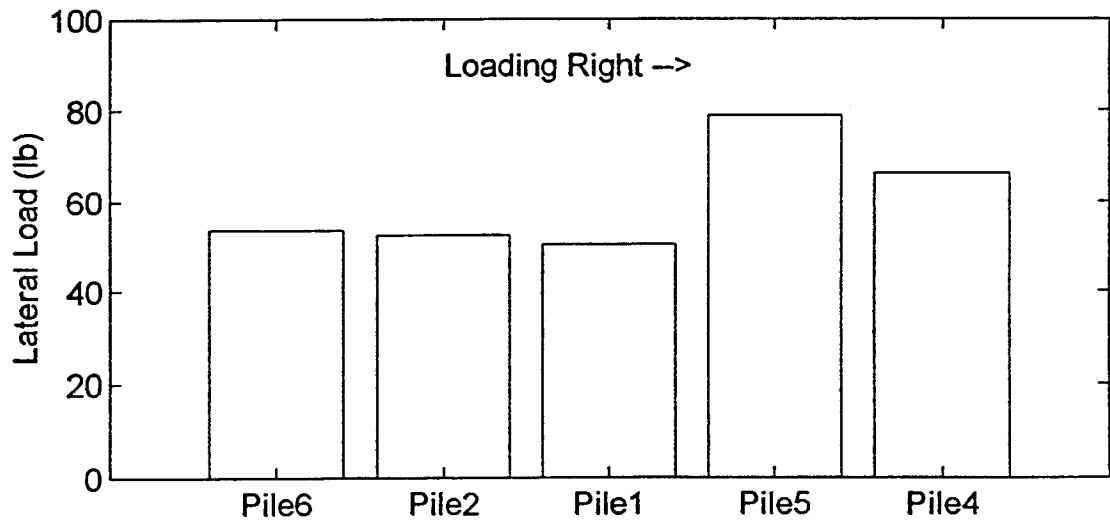
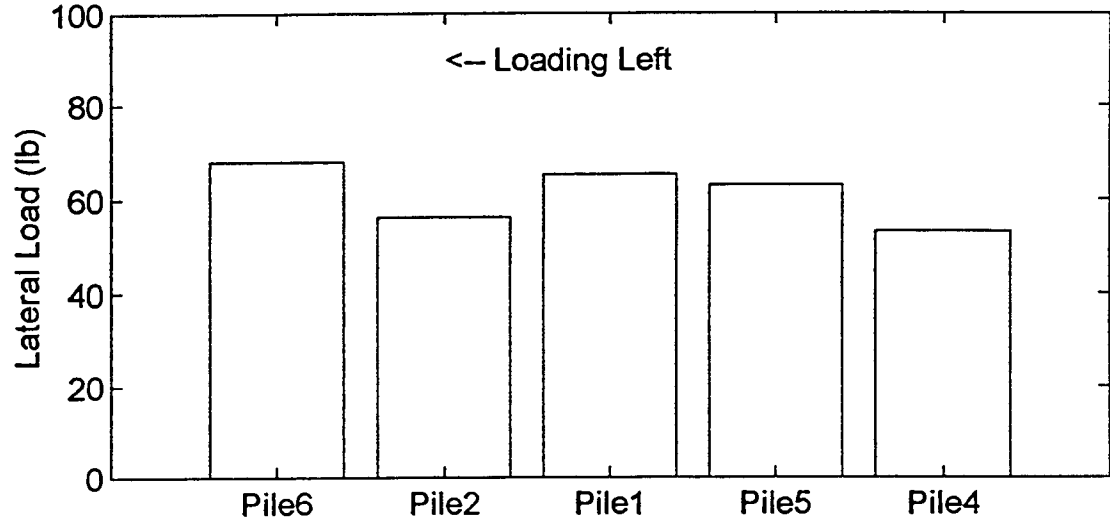


Load Distribution: Cycle 25 - Load 200lb

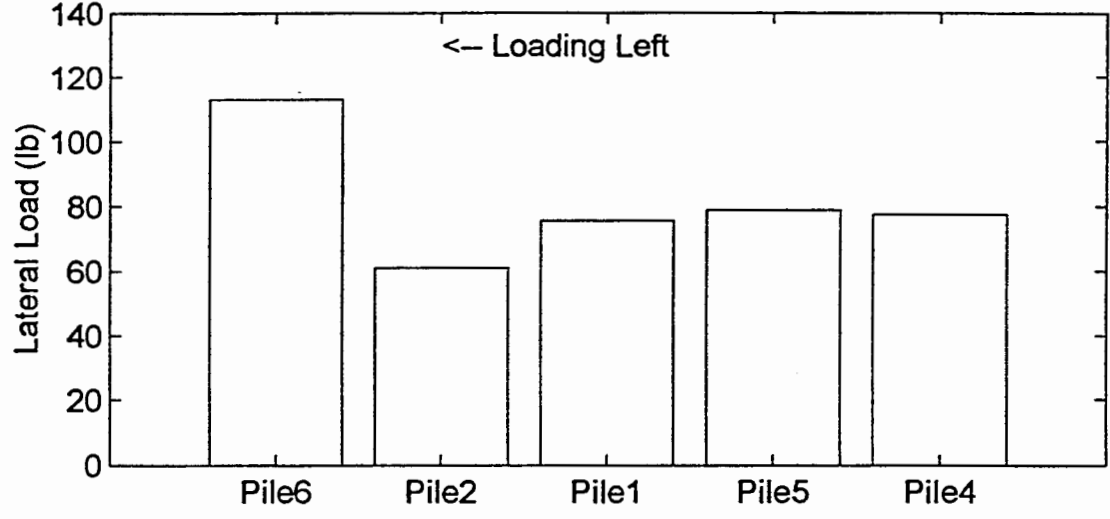




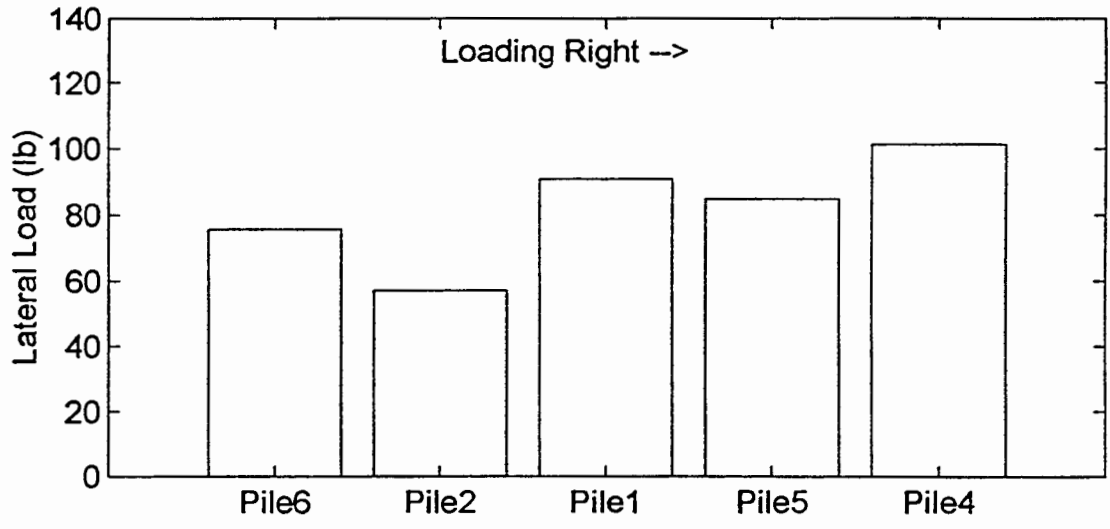
Load Distribution: Cycle 25 - Load 300lb



Load Distribution: Cycle 25 - Load 400lb



Loading Right -->



Load Distribution: Cycle 25 - Load 450lb

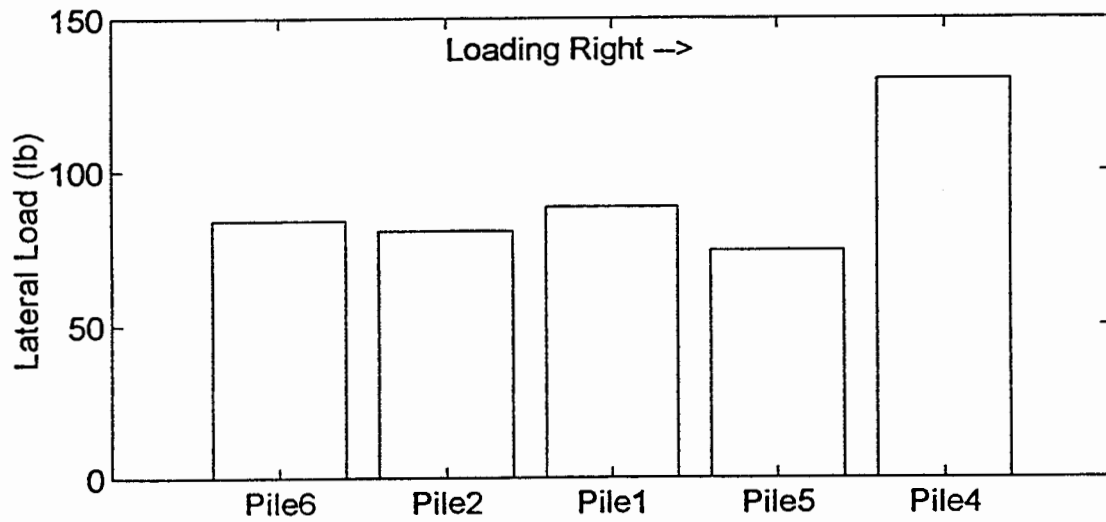
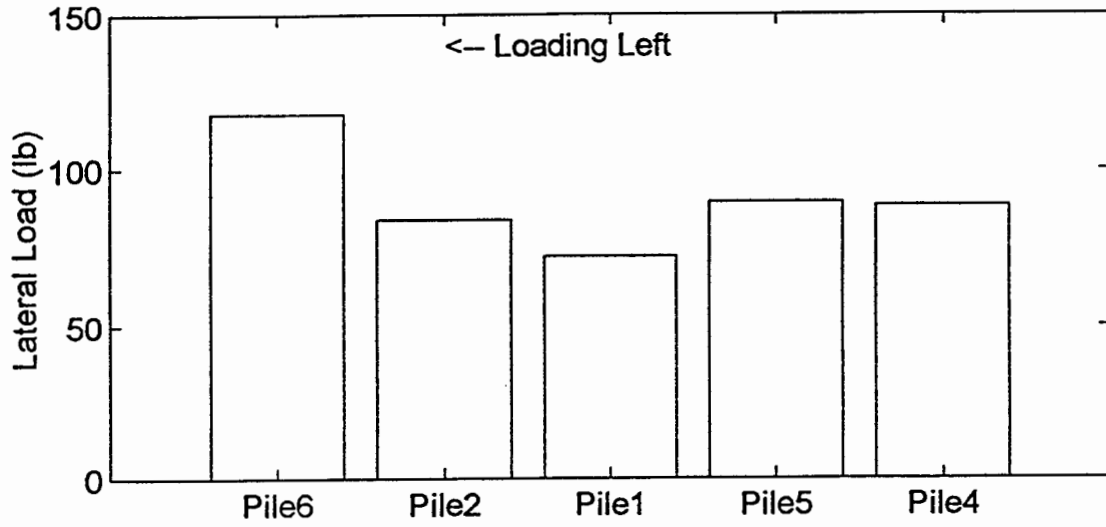
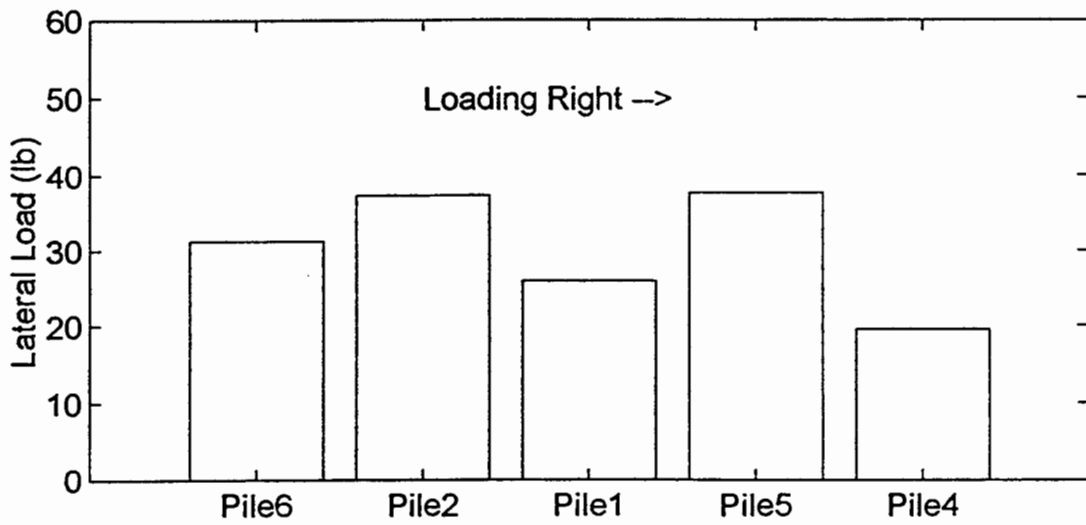
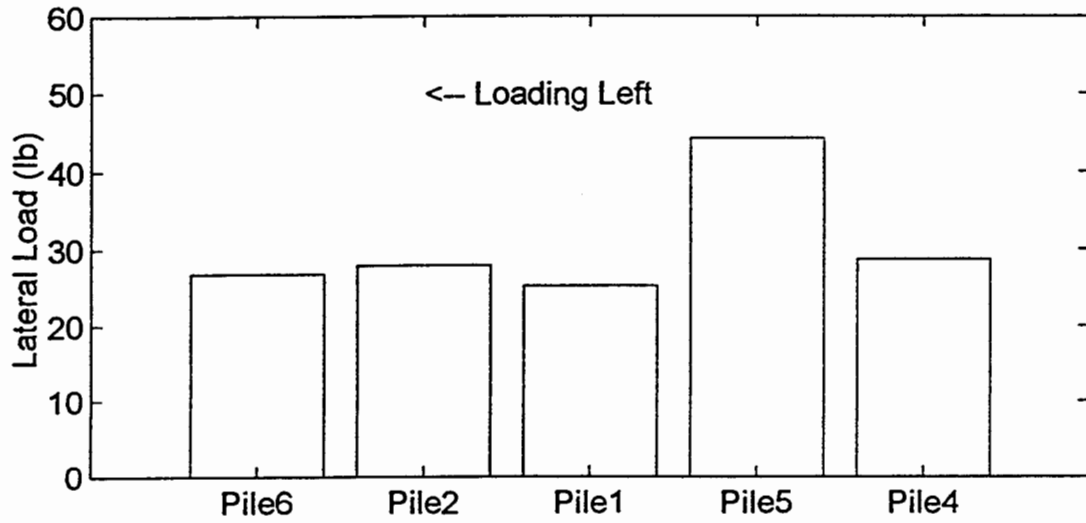
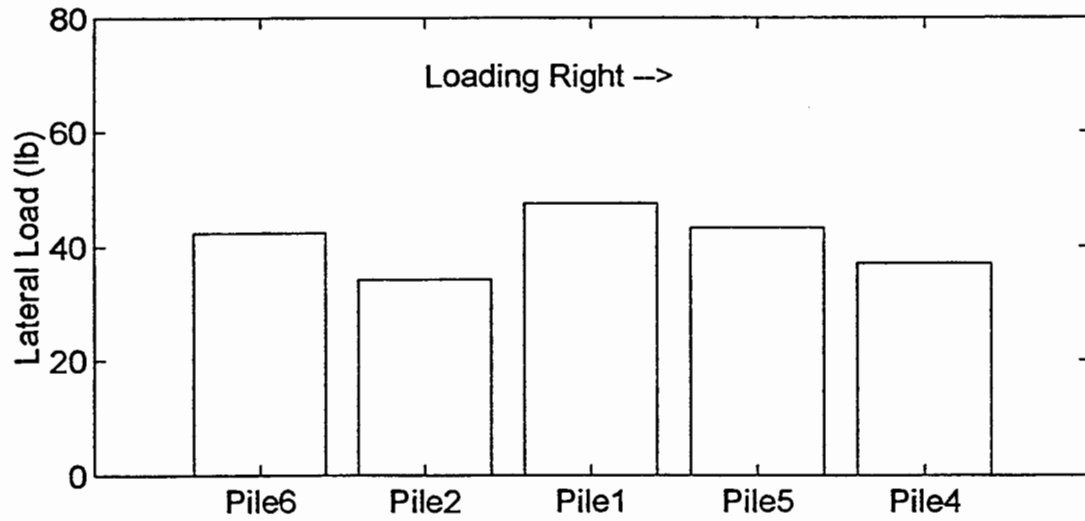
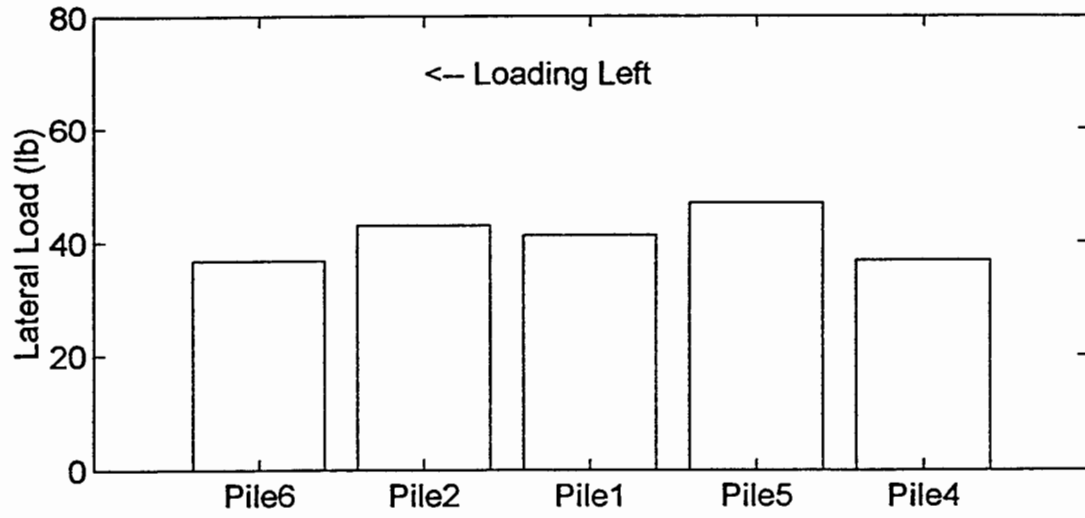


Figure B5. Load distribution @ cycle 50 (next 7 plots).

Load Distribution: Cycle 50 - LOAD 150lb

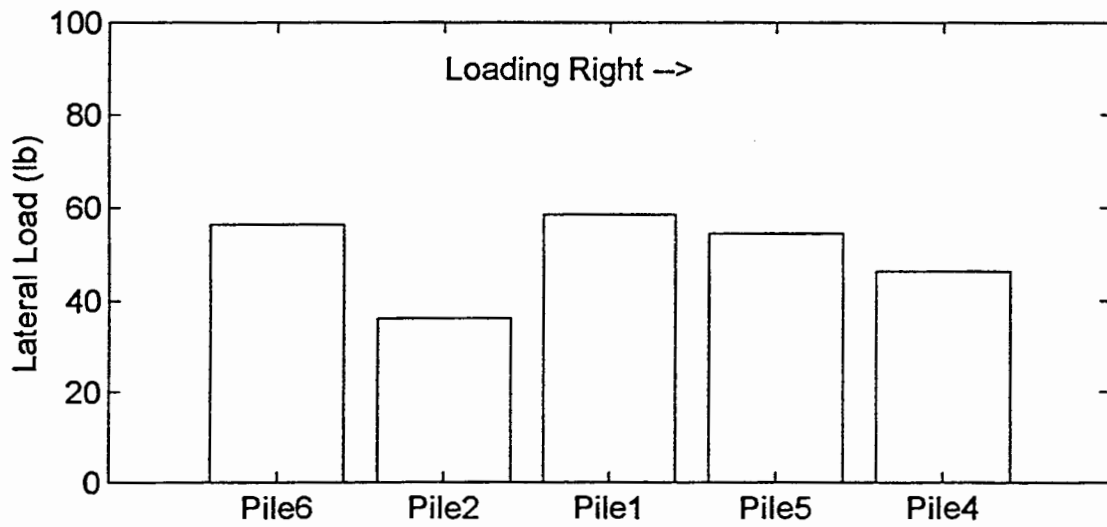
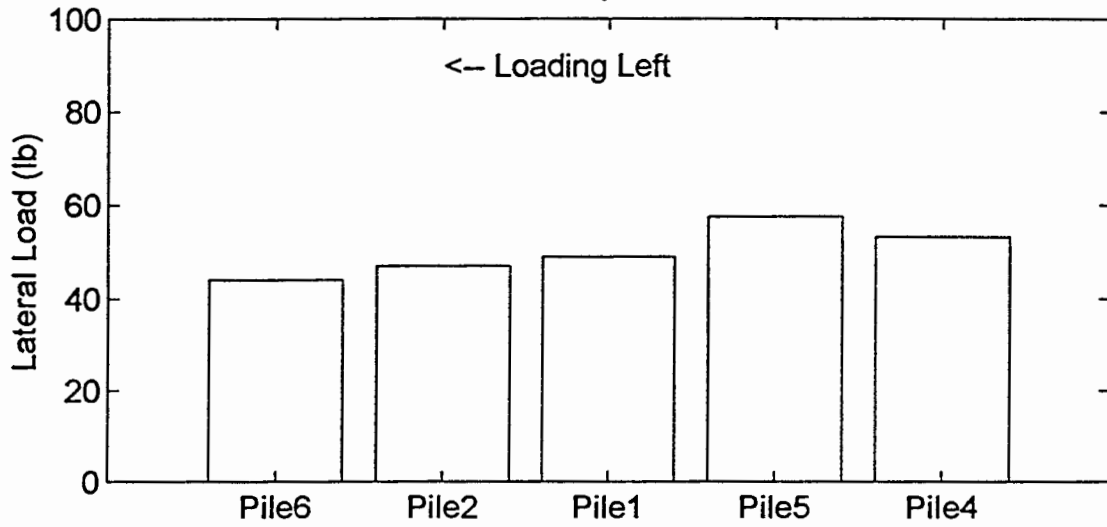


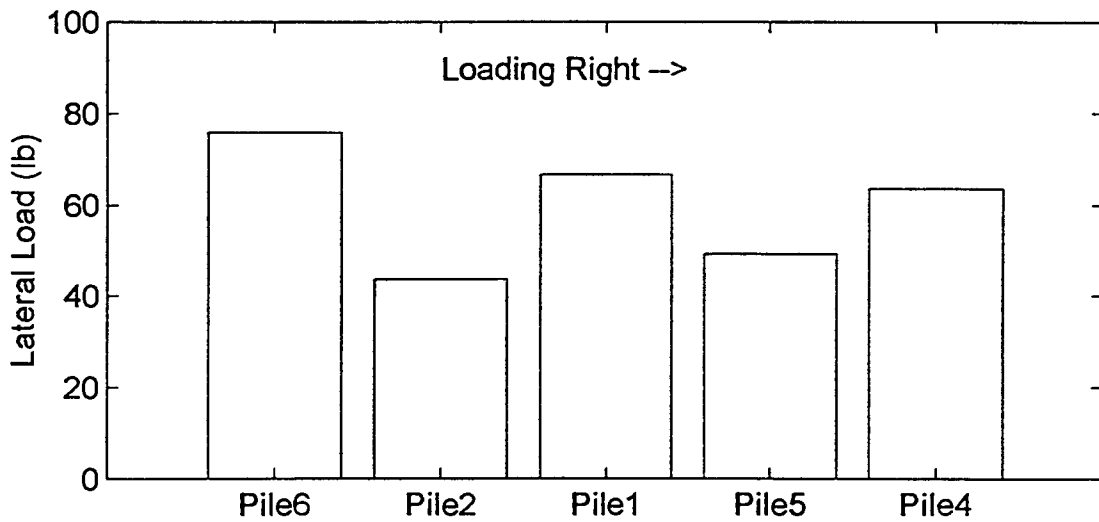
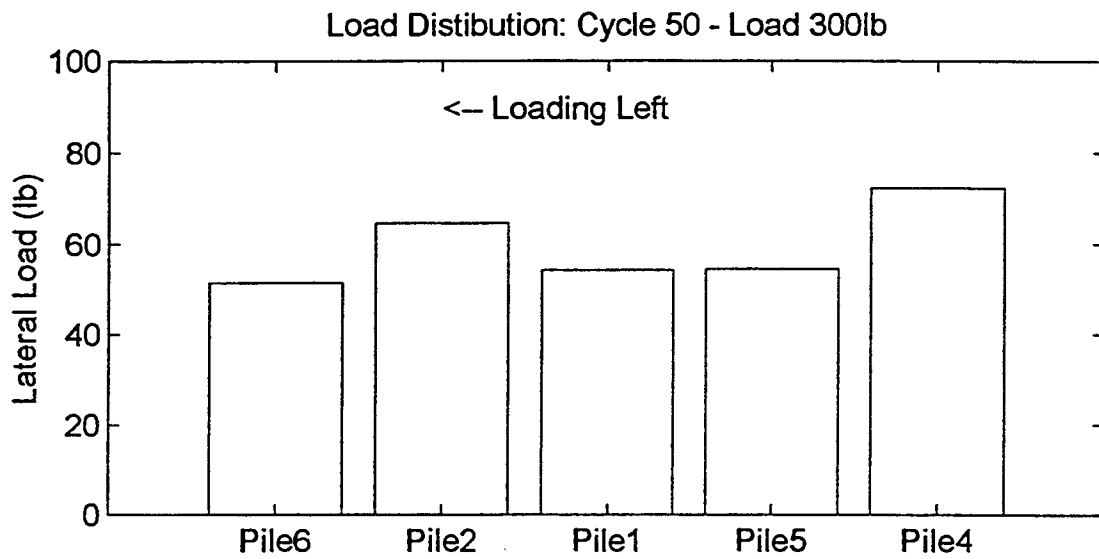
Load Distribution: Cycle 50 - Load 200lb



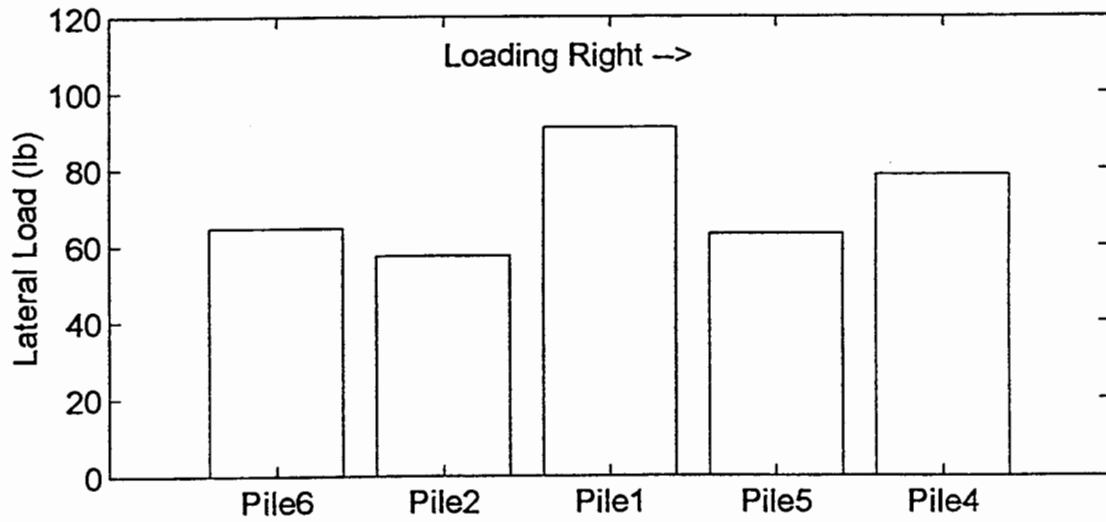
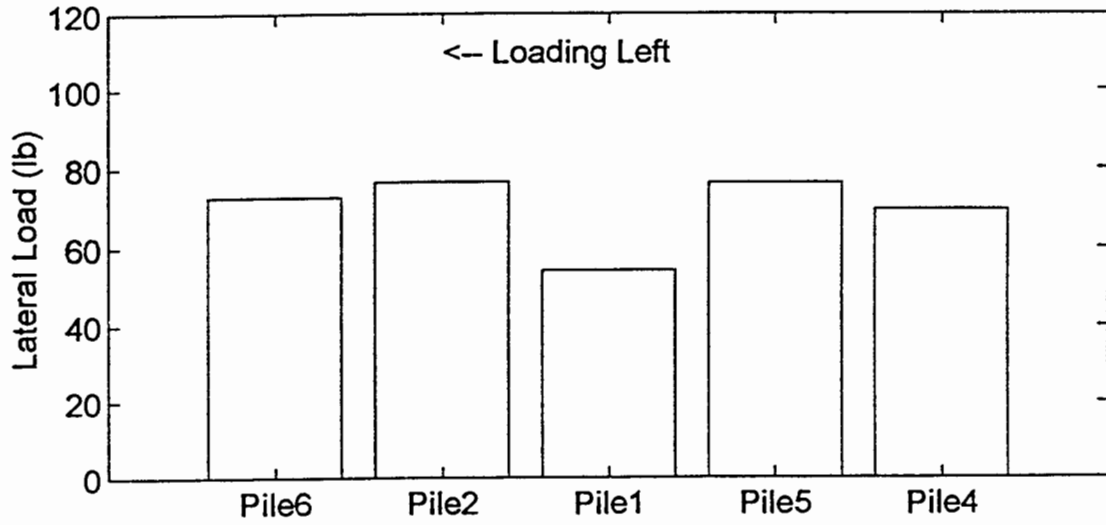


Load Distribution: Cycle 50 - Load 250lb

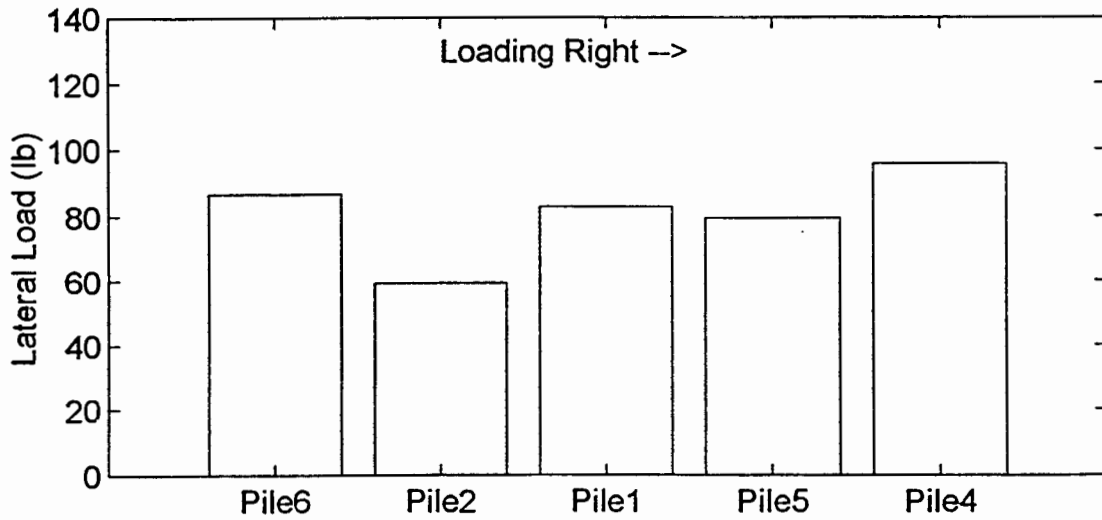
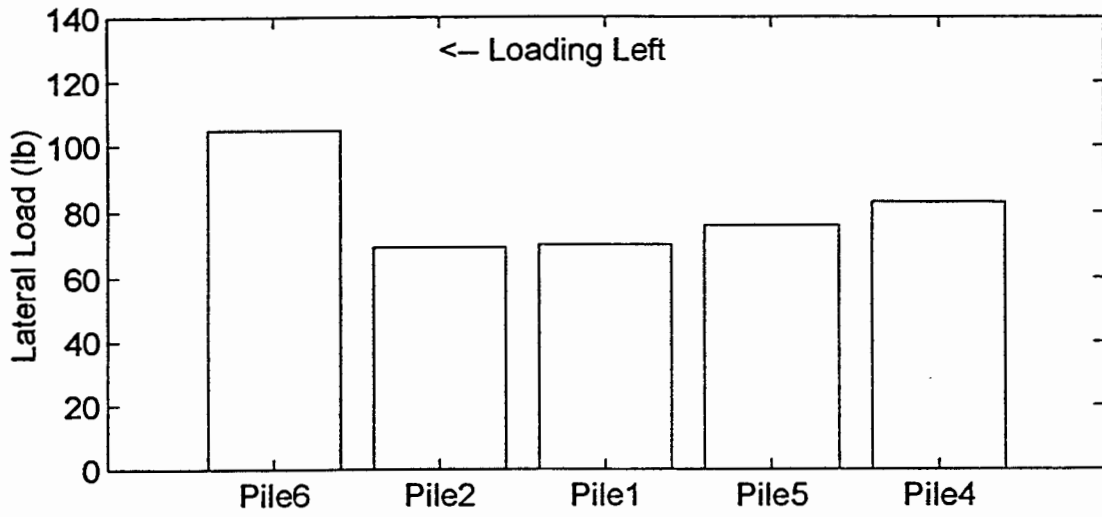




Load Distribution: Cycle 50 - Load 350lb



Load Distribution: Cycle 50 - Load 400lb



Load Distribution: Cycle 50 - LOAD 450lb

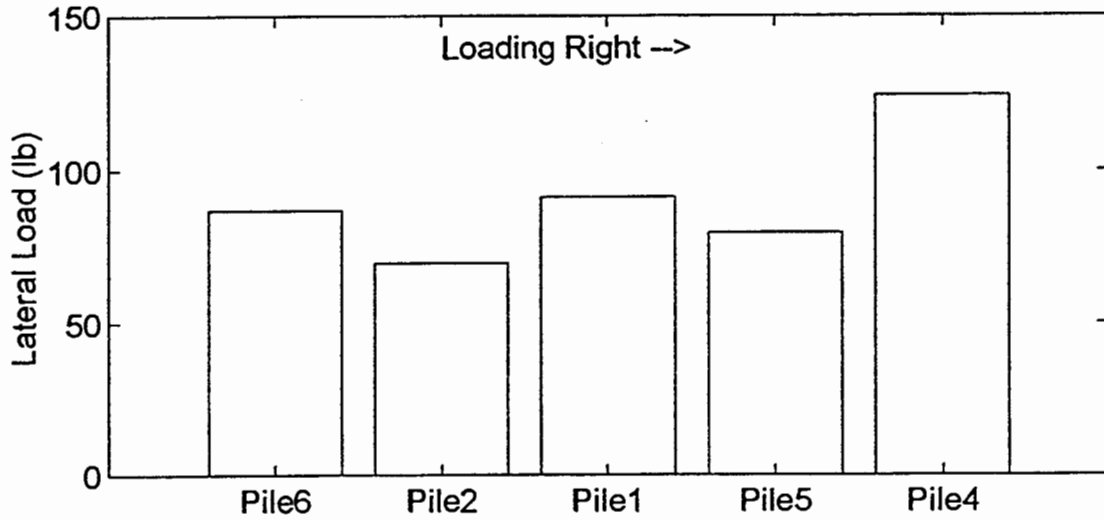
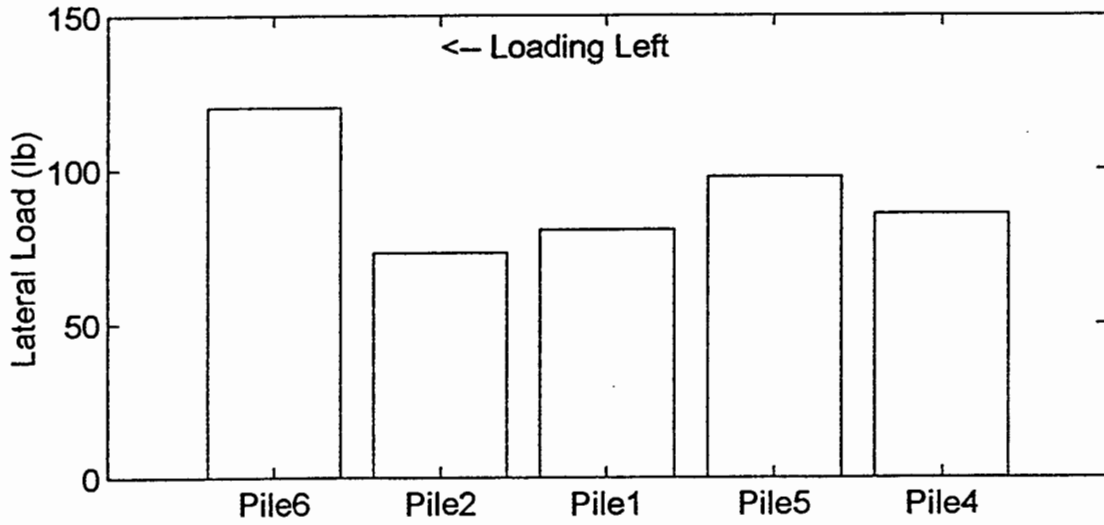
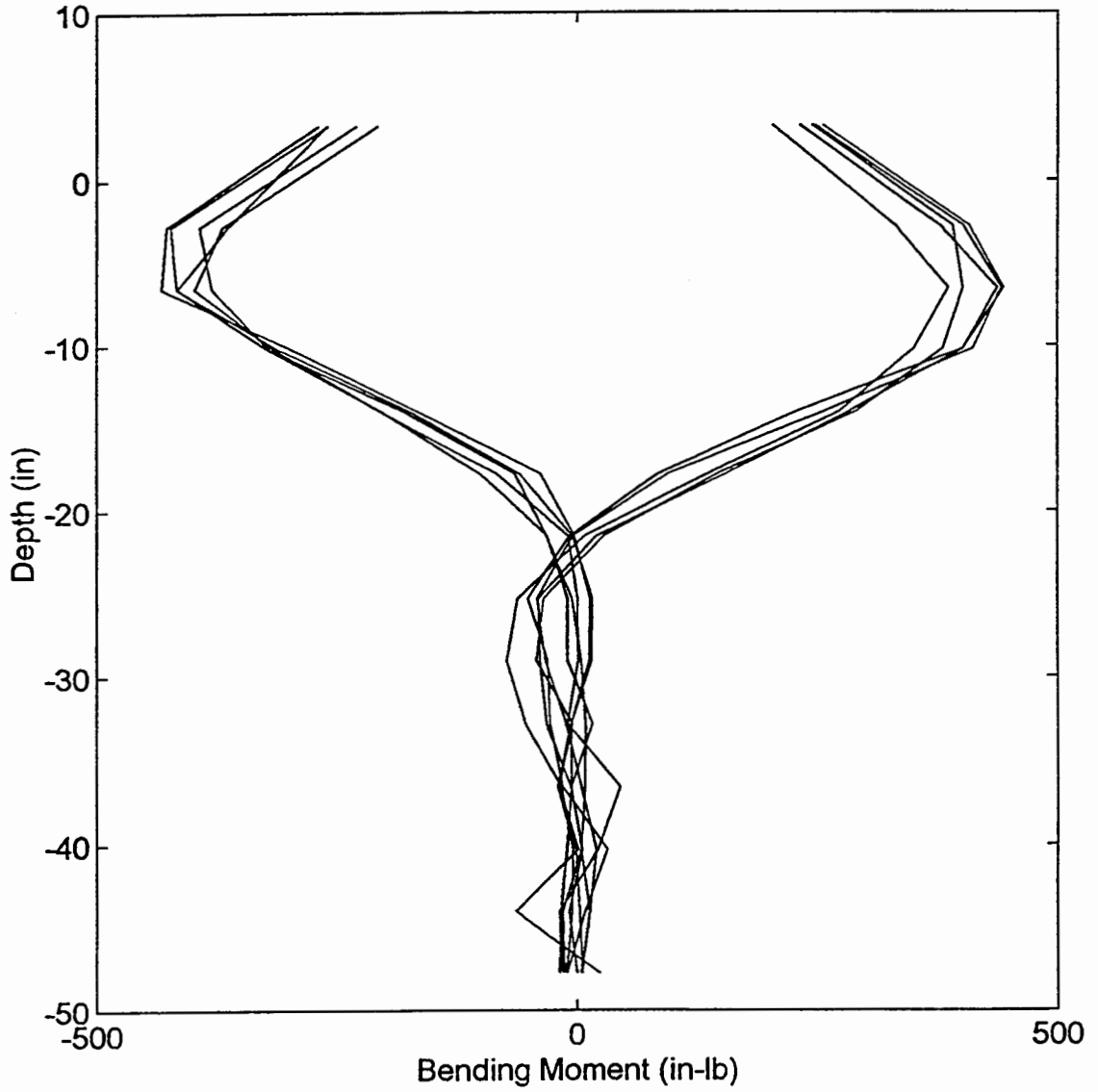
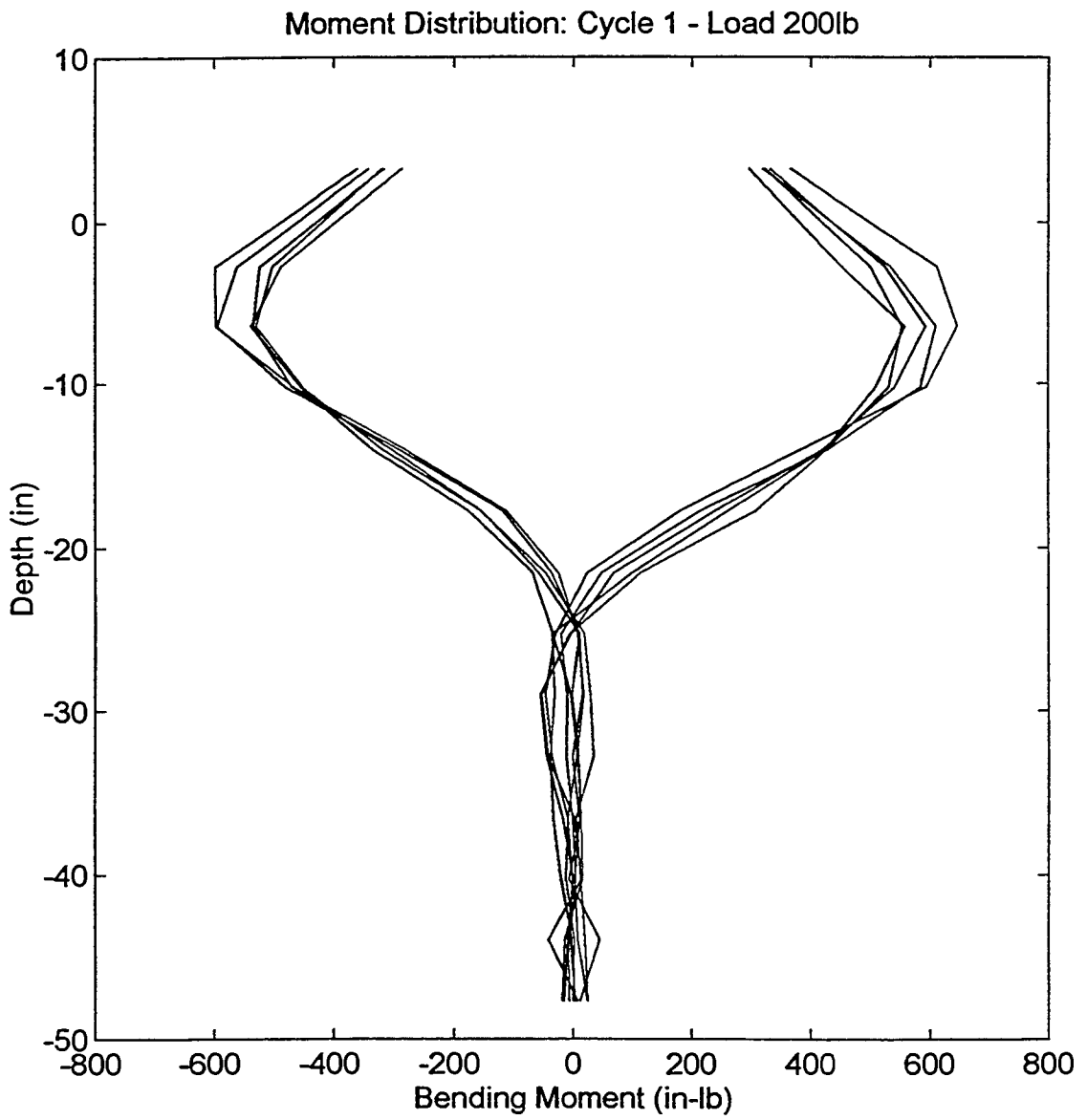


Figure B6. Moment distribution @ cycle 1 (next 7 plots).

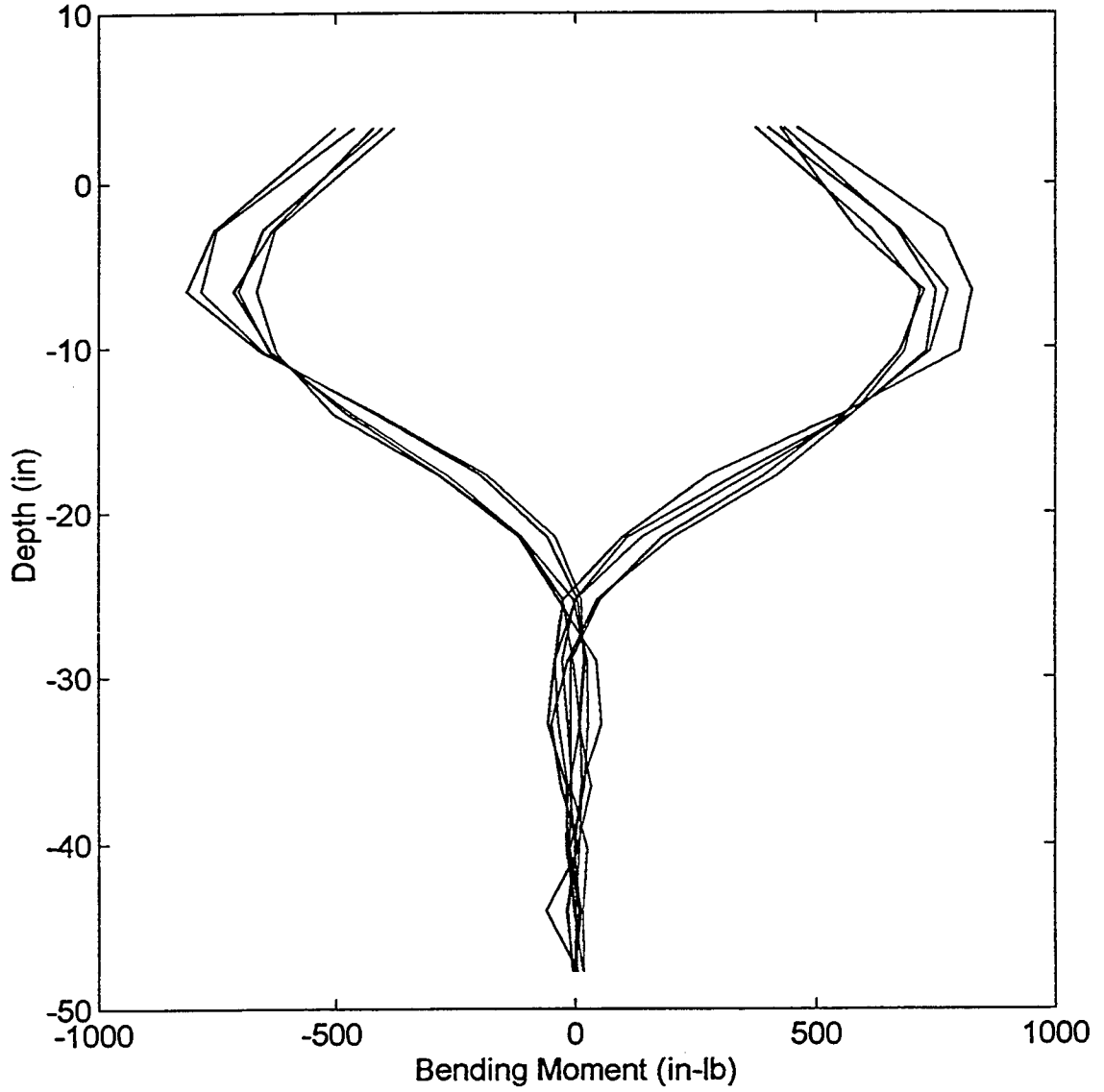
Moment Distribution: Cycle 1 - Load 150lb

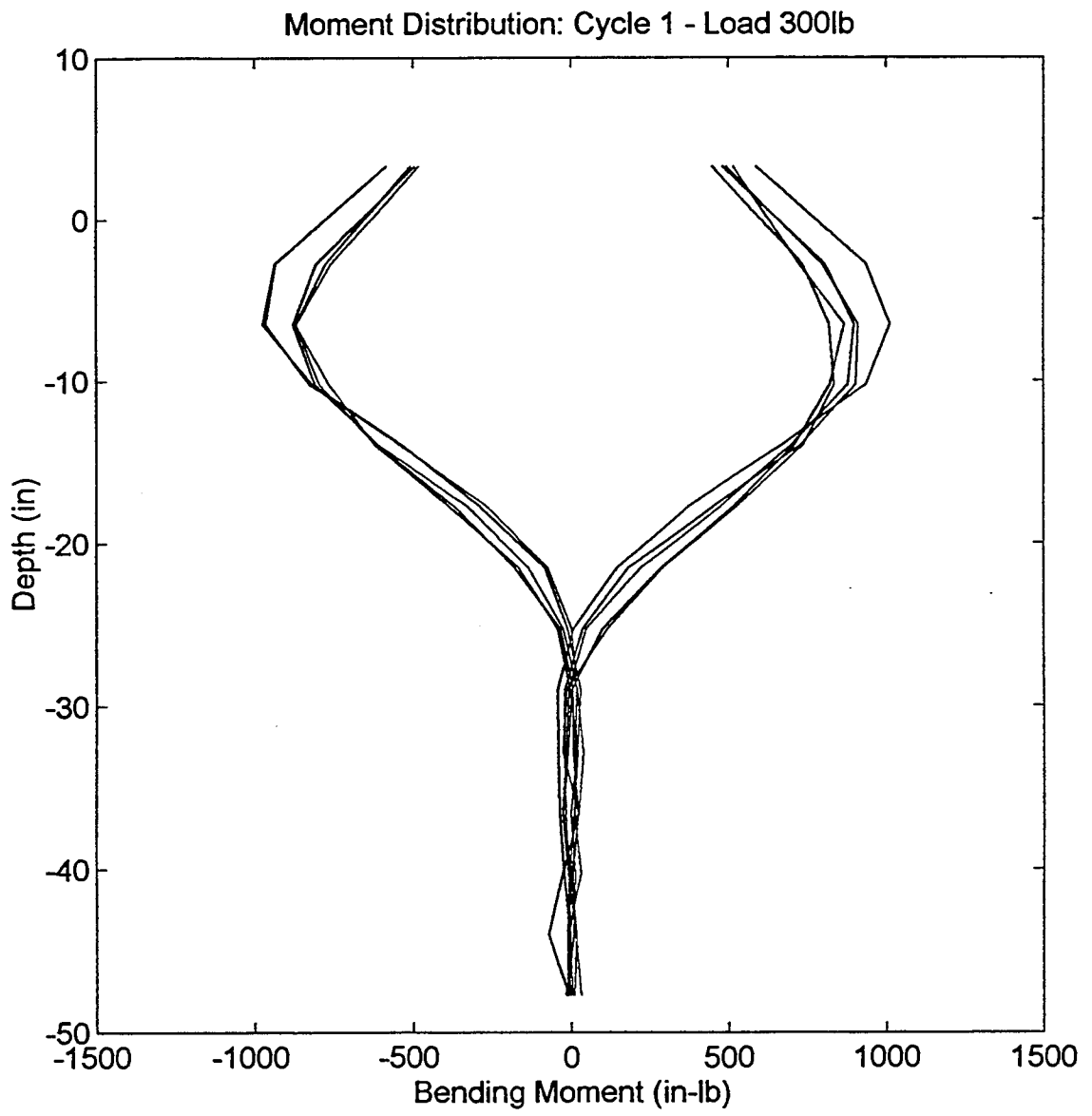






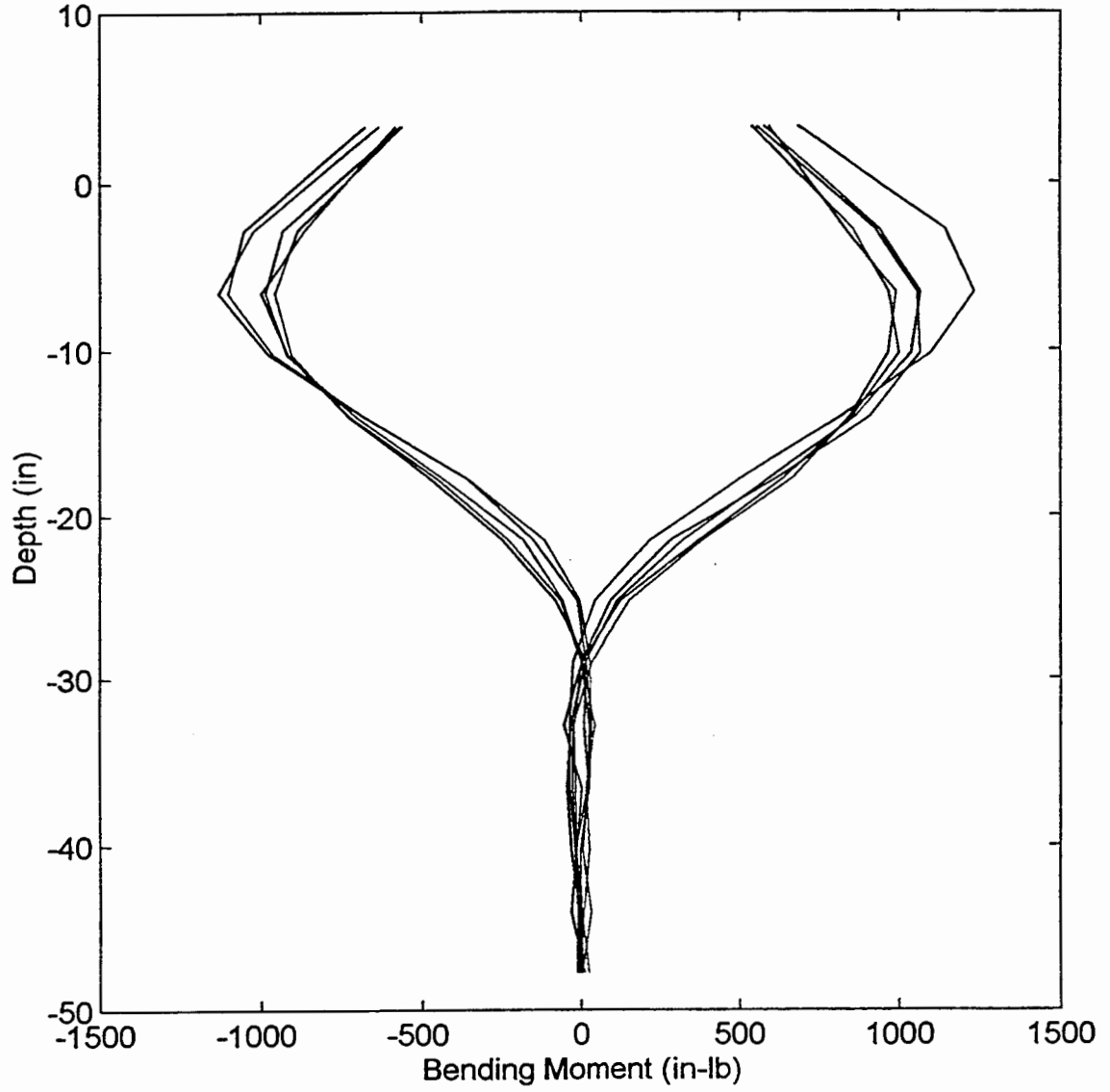
Moment Distribution: Cycle 1 - Load 250lb

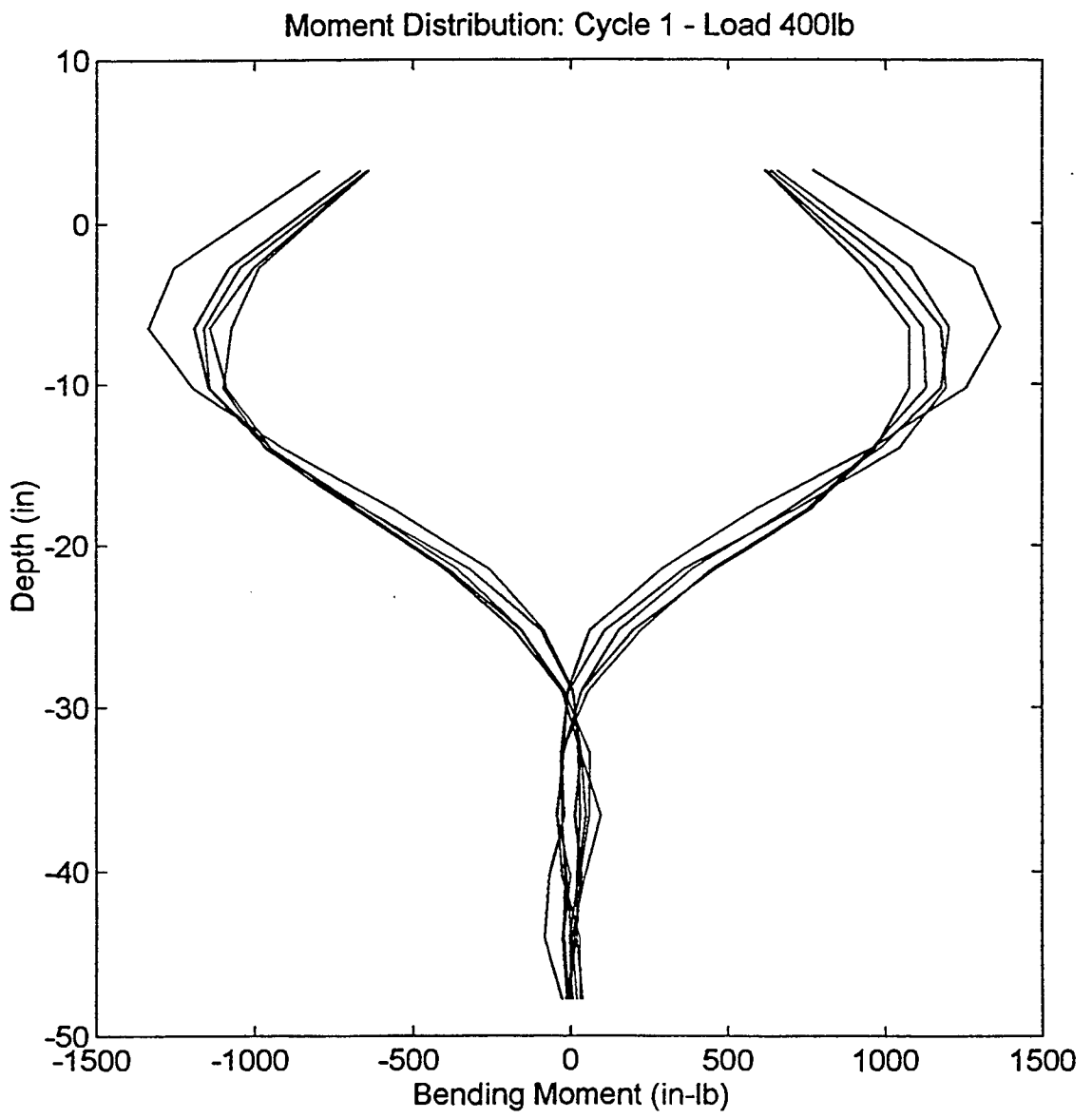






Moment Distribution: Cycle 1 - Load 350lb





Moment Distribution: Cycle 1 - Load 450lb

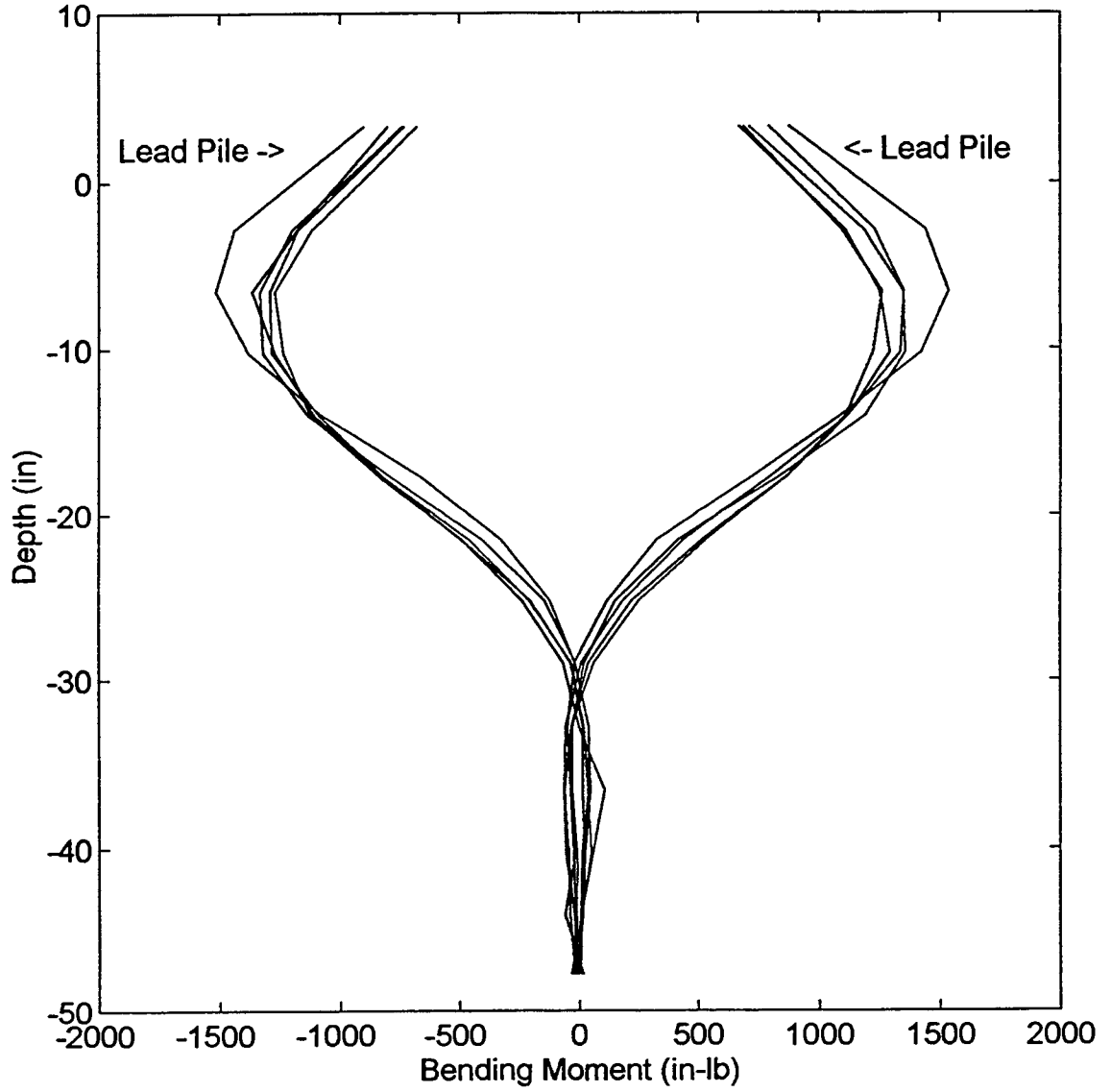
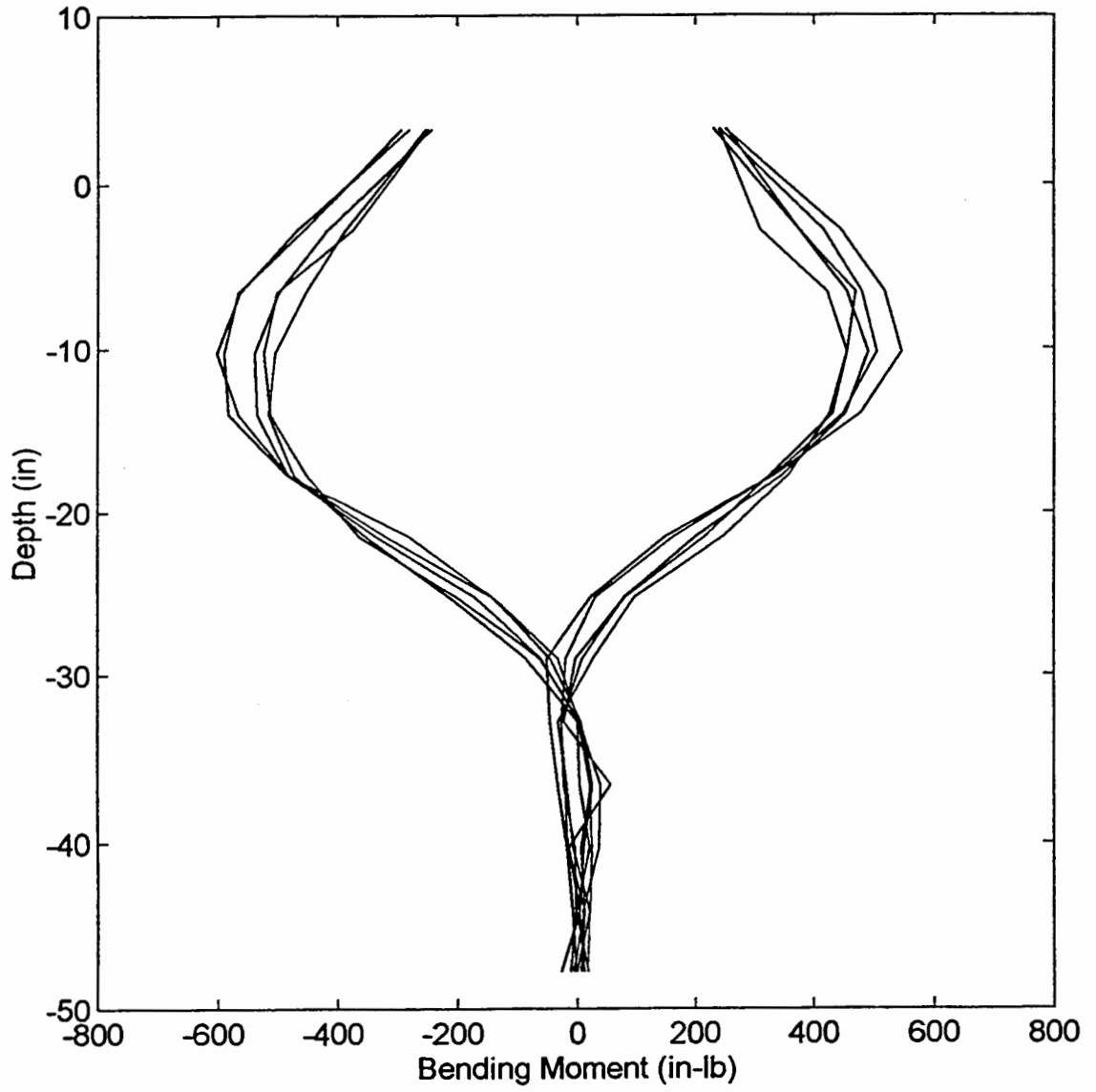
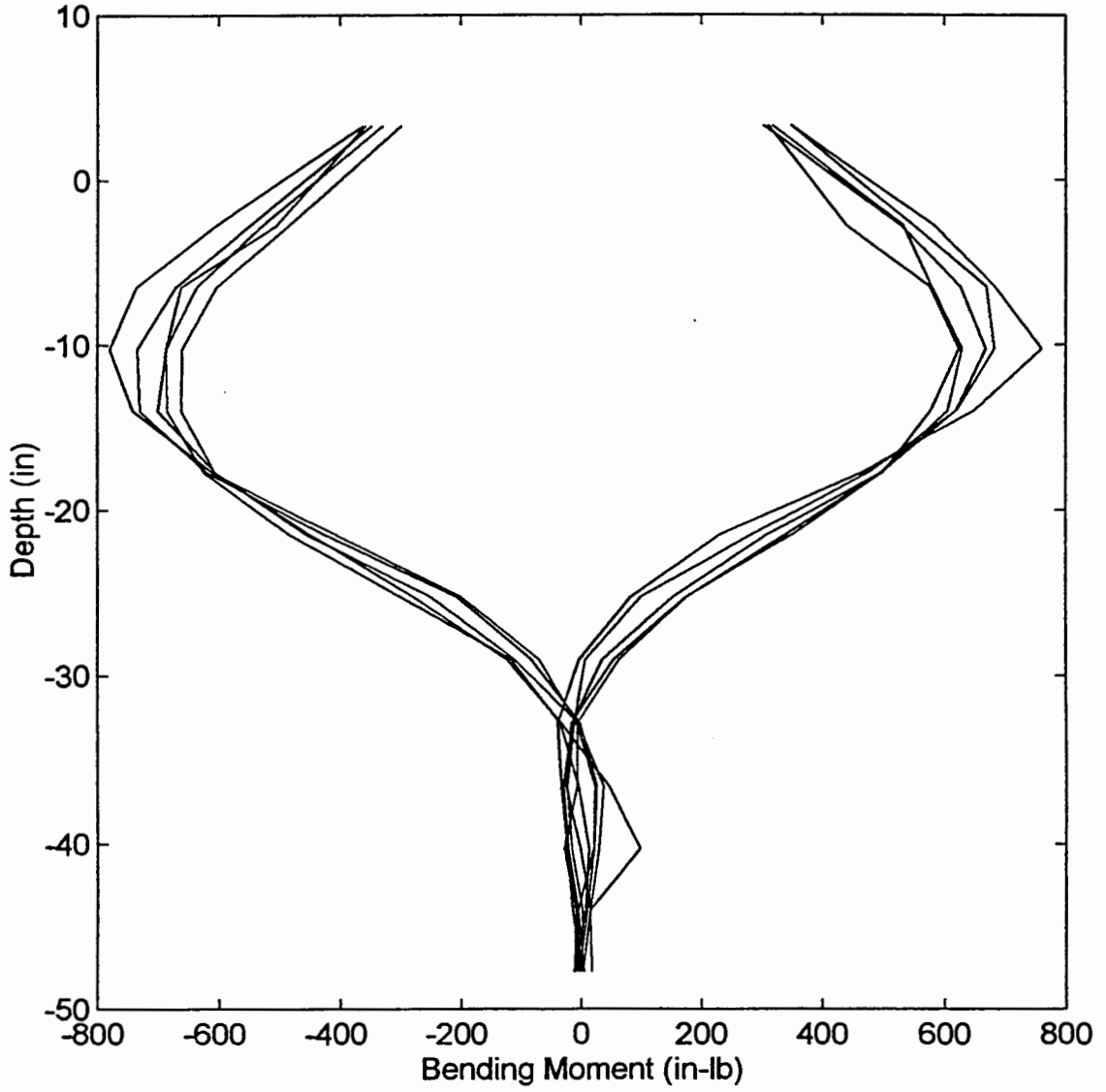


Figure B7. Moment distribution @ cycle 5 (next 7 plots).

Moment Distribution: Cycle 5 - Load 150lb

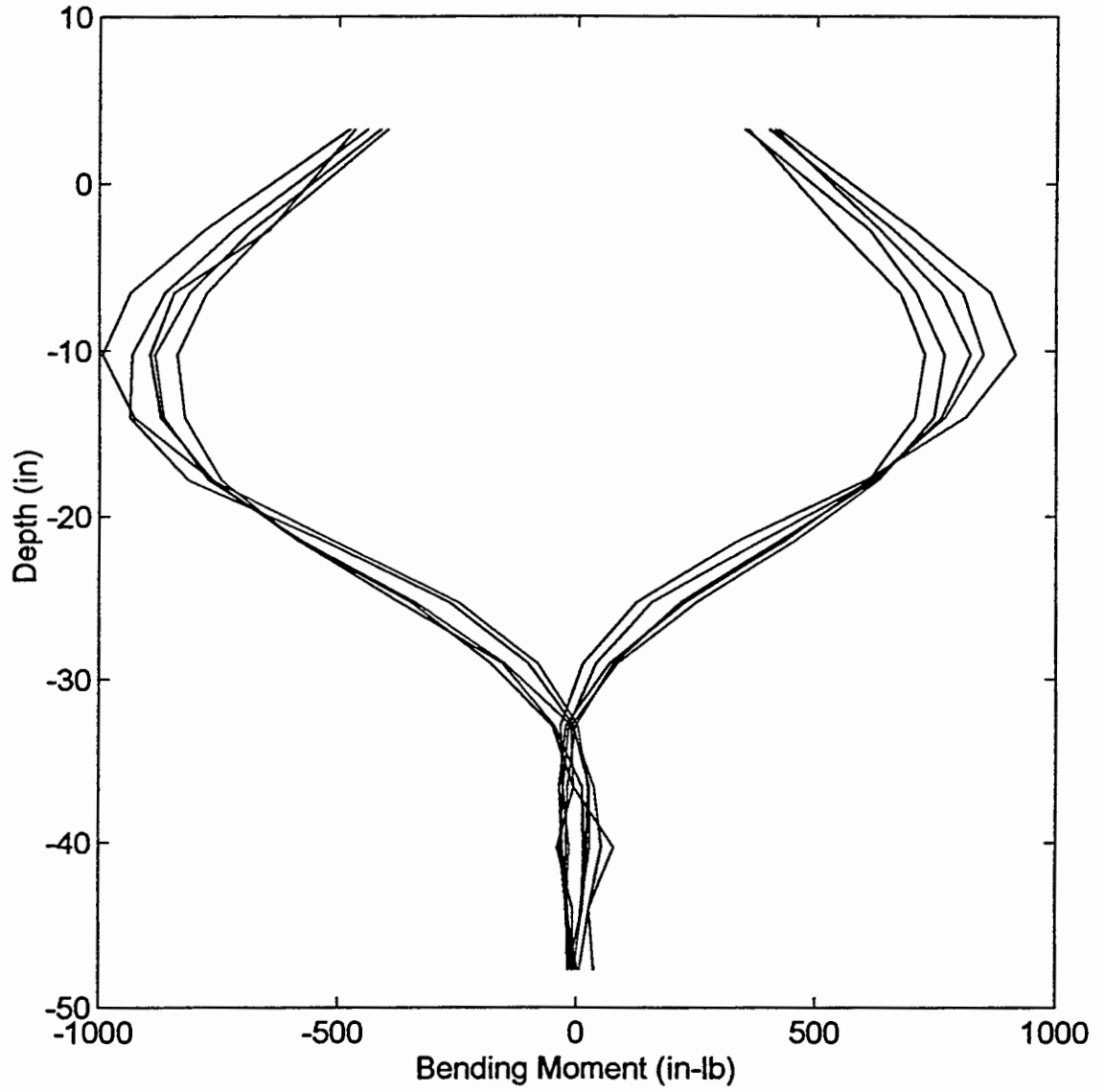


Moment Distribution: Cycle 5 - Load 200lb



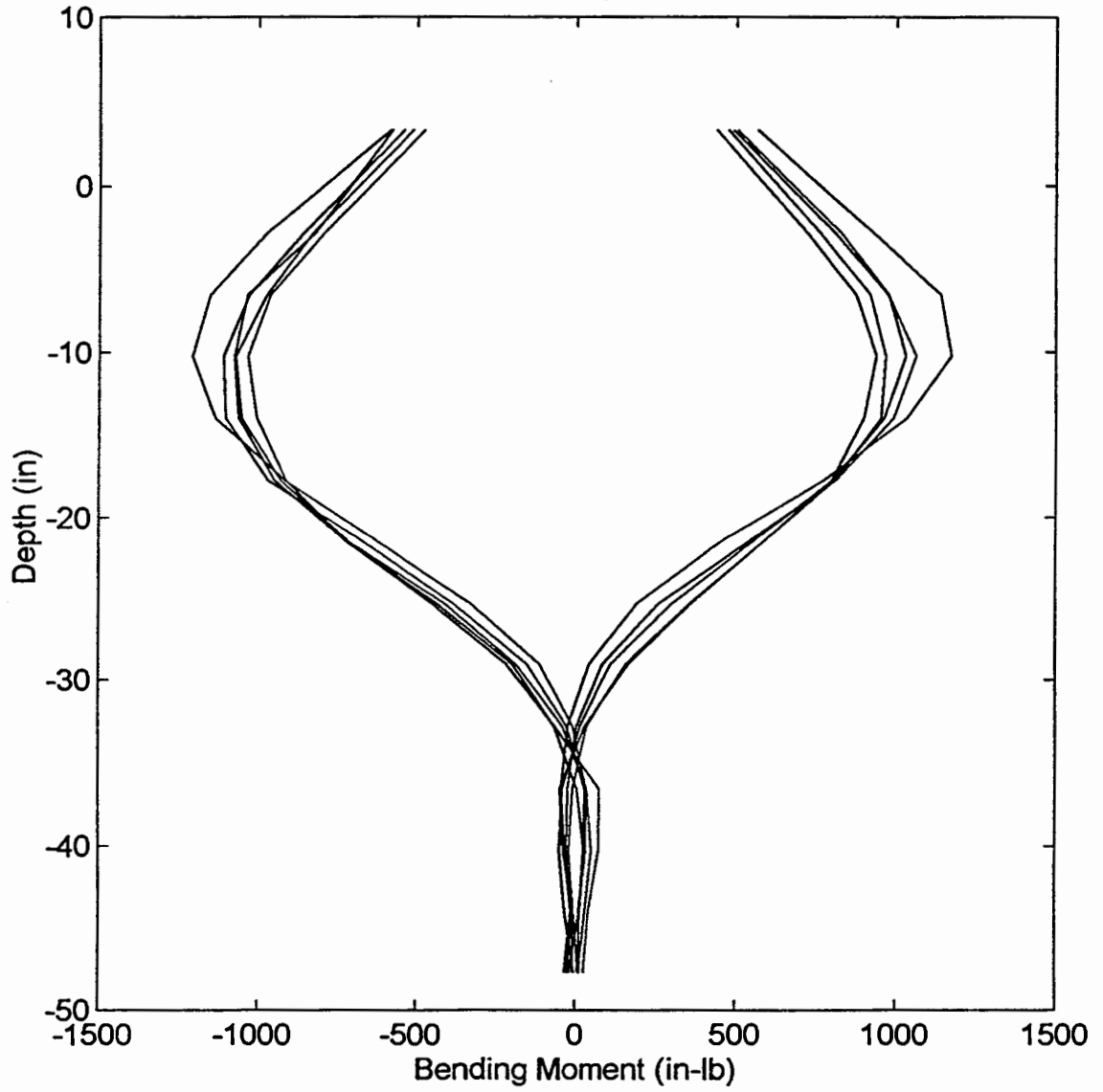


Moment Distribution: Cycle 5 - Load 250lb

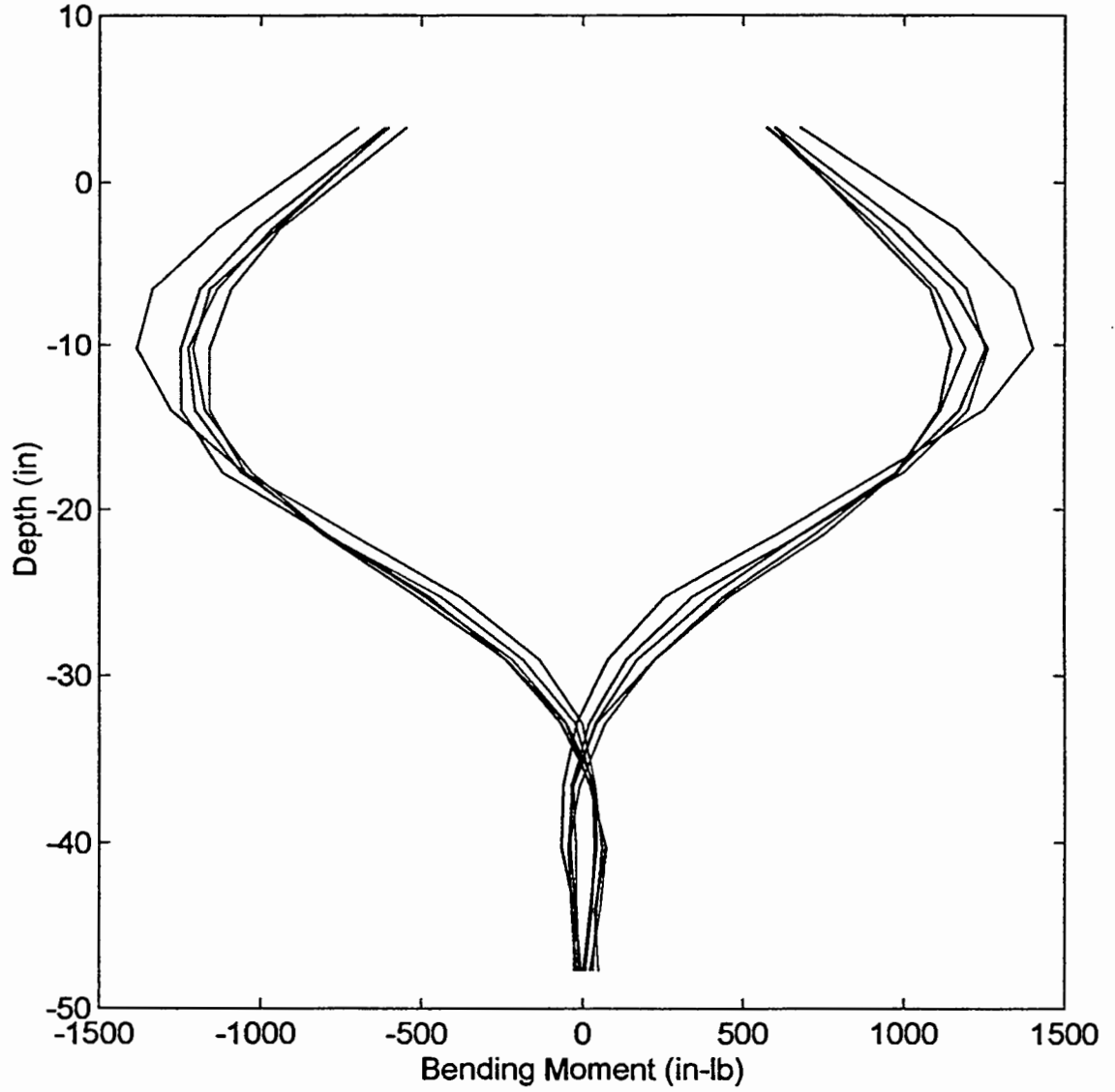




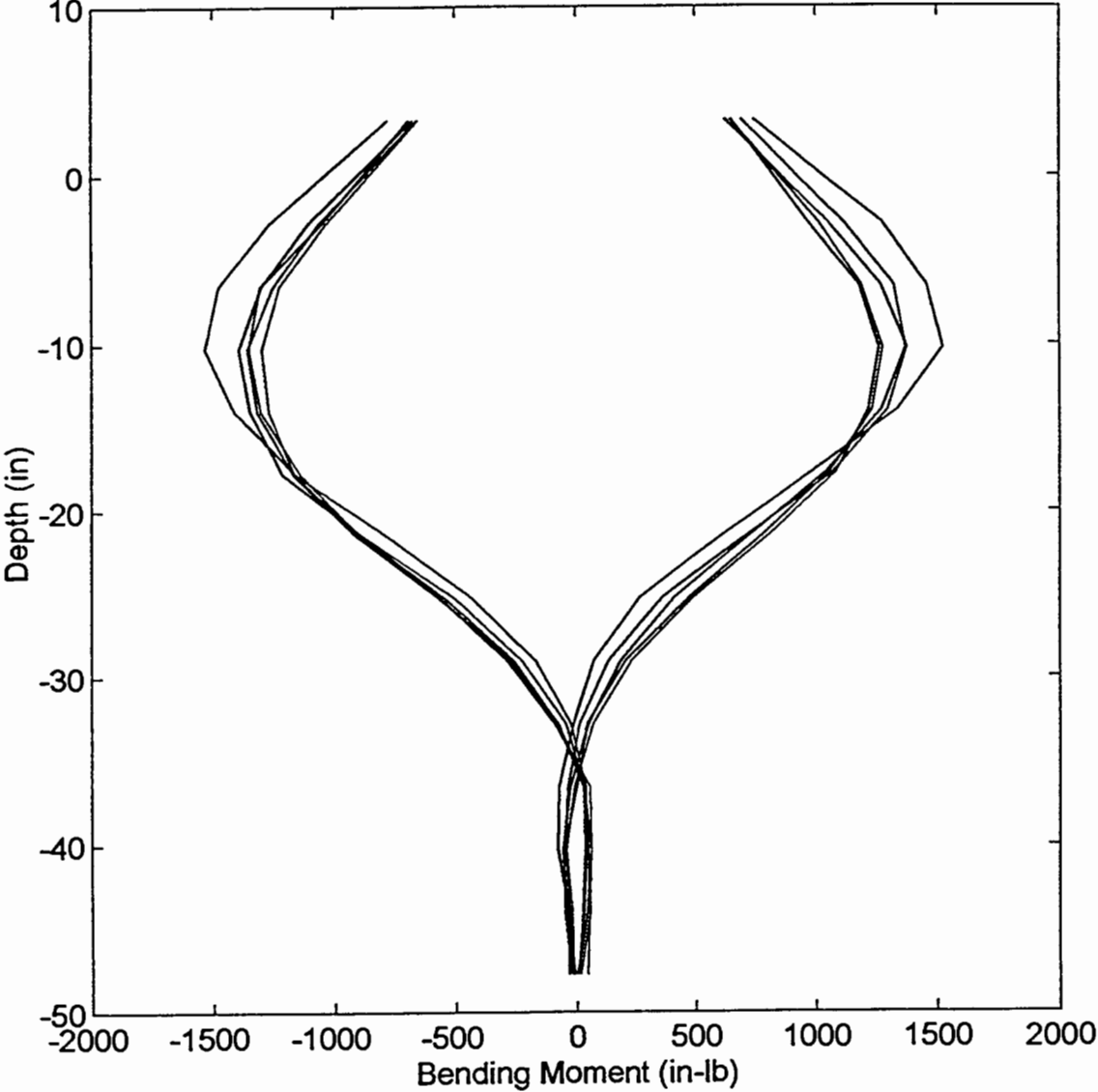
Moment Distribution: Cycle 5 - Load 300lb



Moment Distribution: Cycle 5 - Load 350lb



Moment Distribution: Cycle 5 - Load 400lb



Moment Distribution: Cycle 5 - Load 450lb

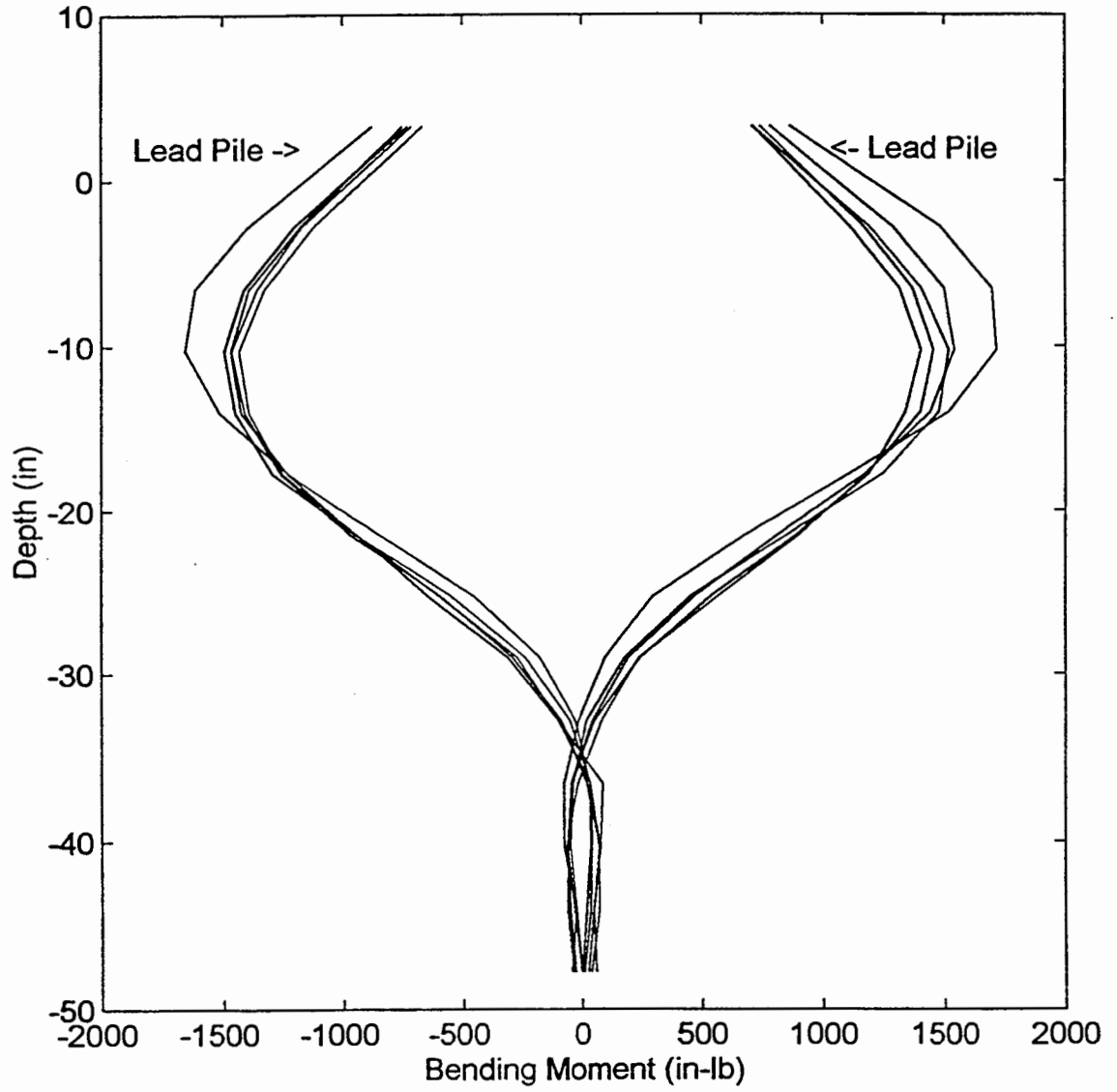
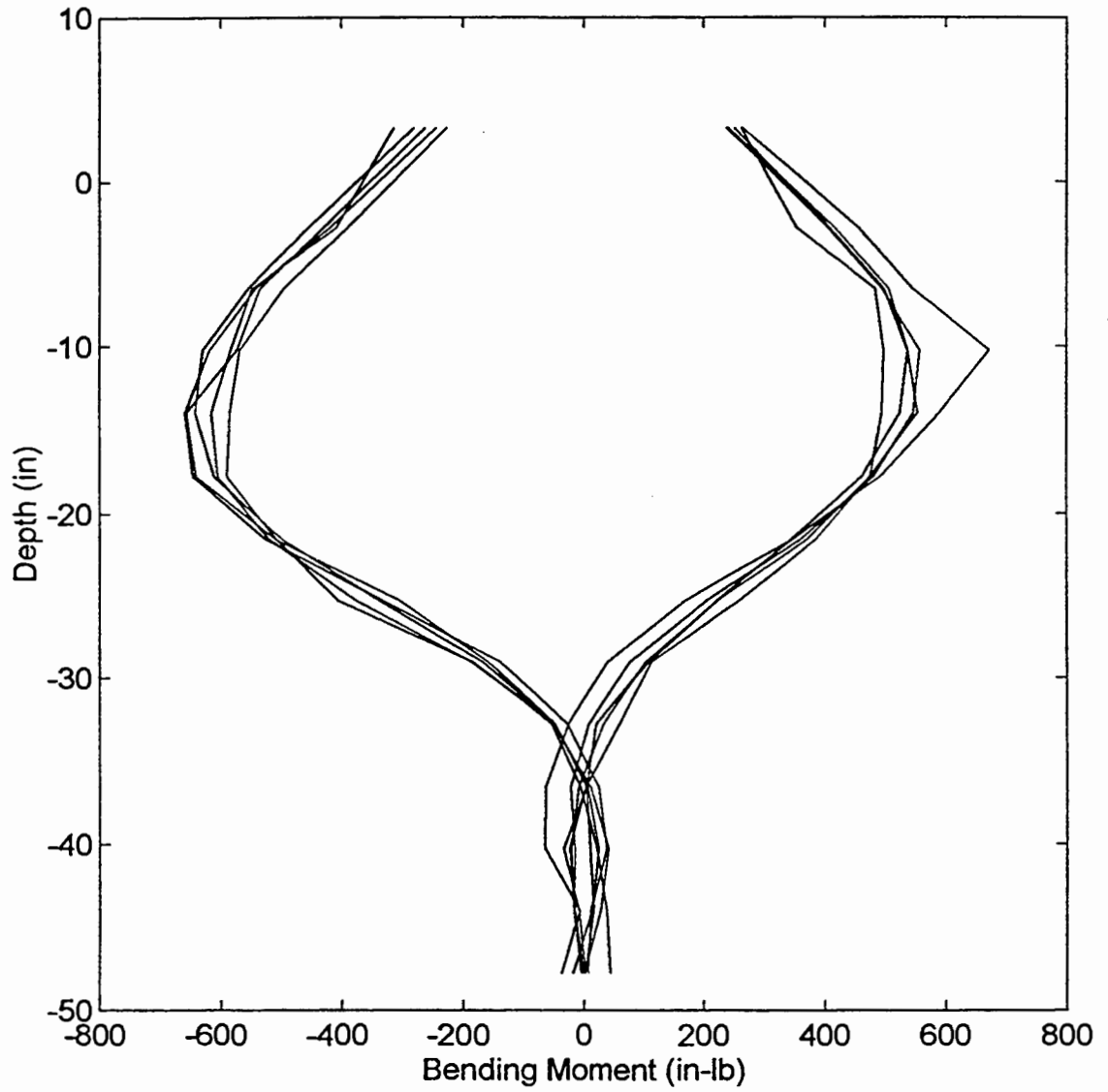


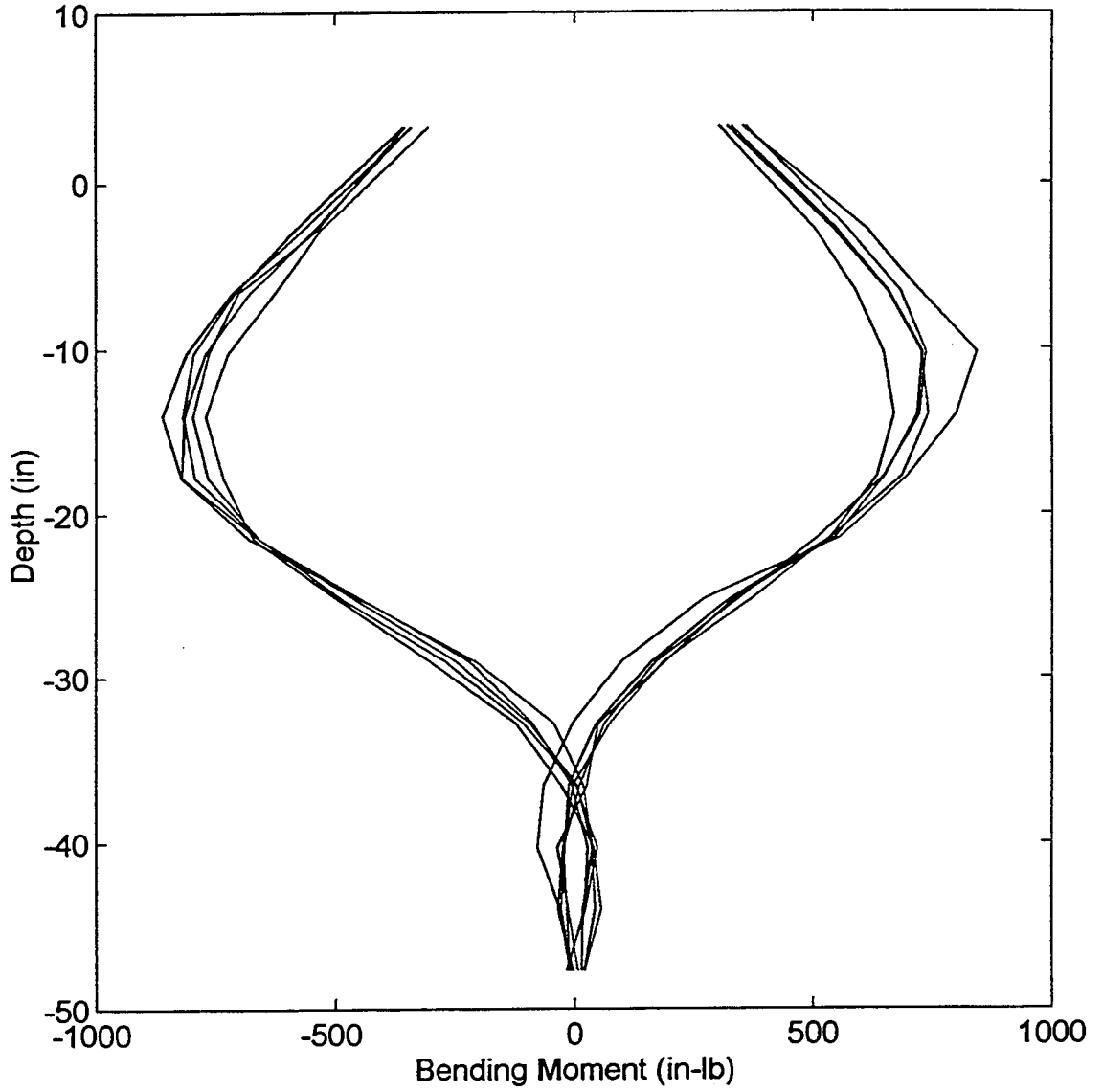
Figure B8. Moment distribution @ cycle 10 (next 7 plots).

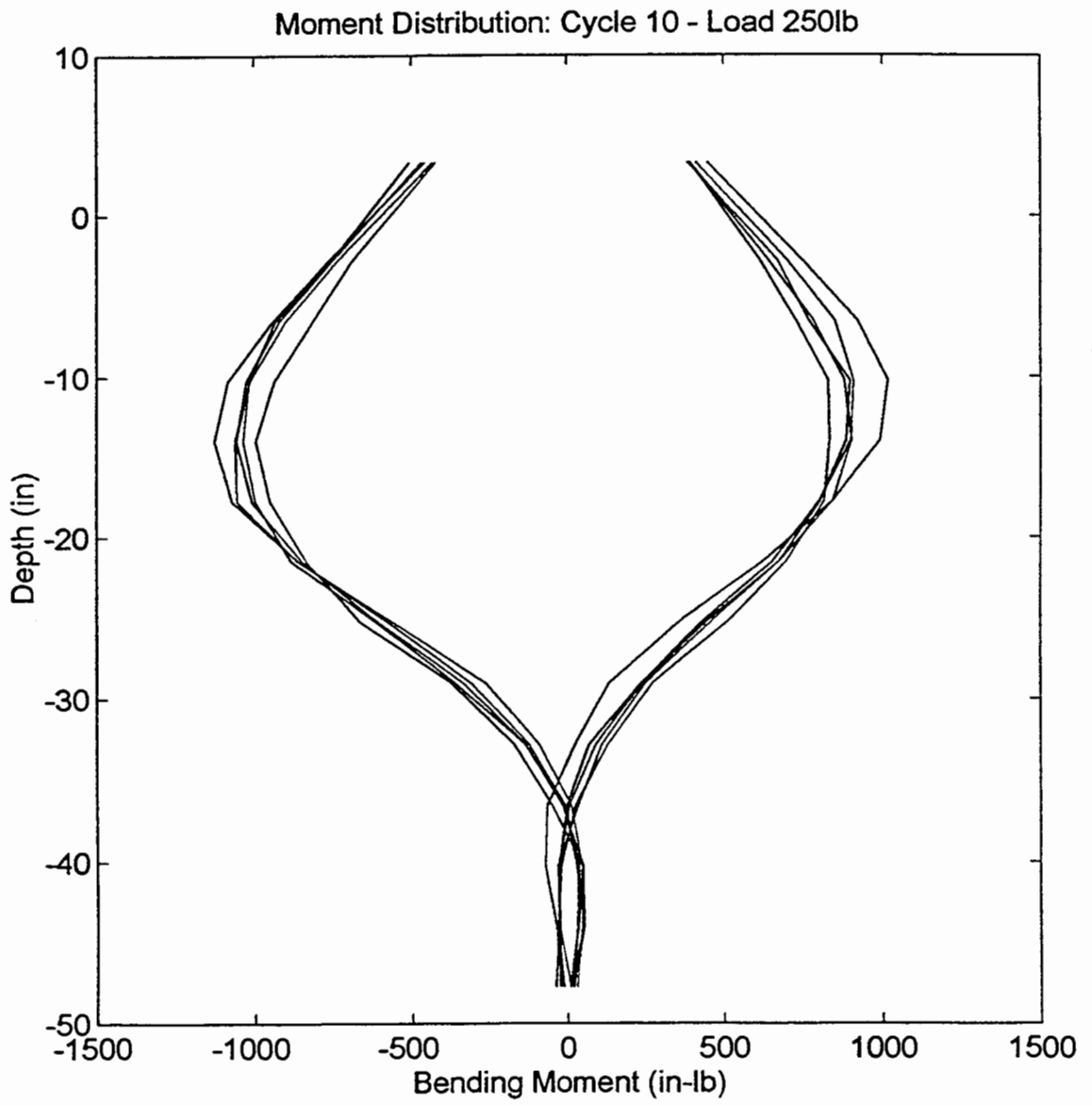
Moment Distribution: Cycle 10 - Load 150lb



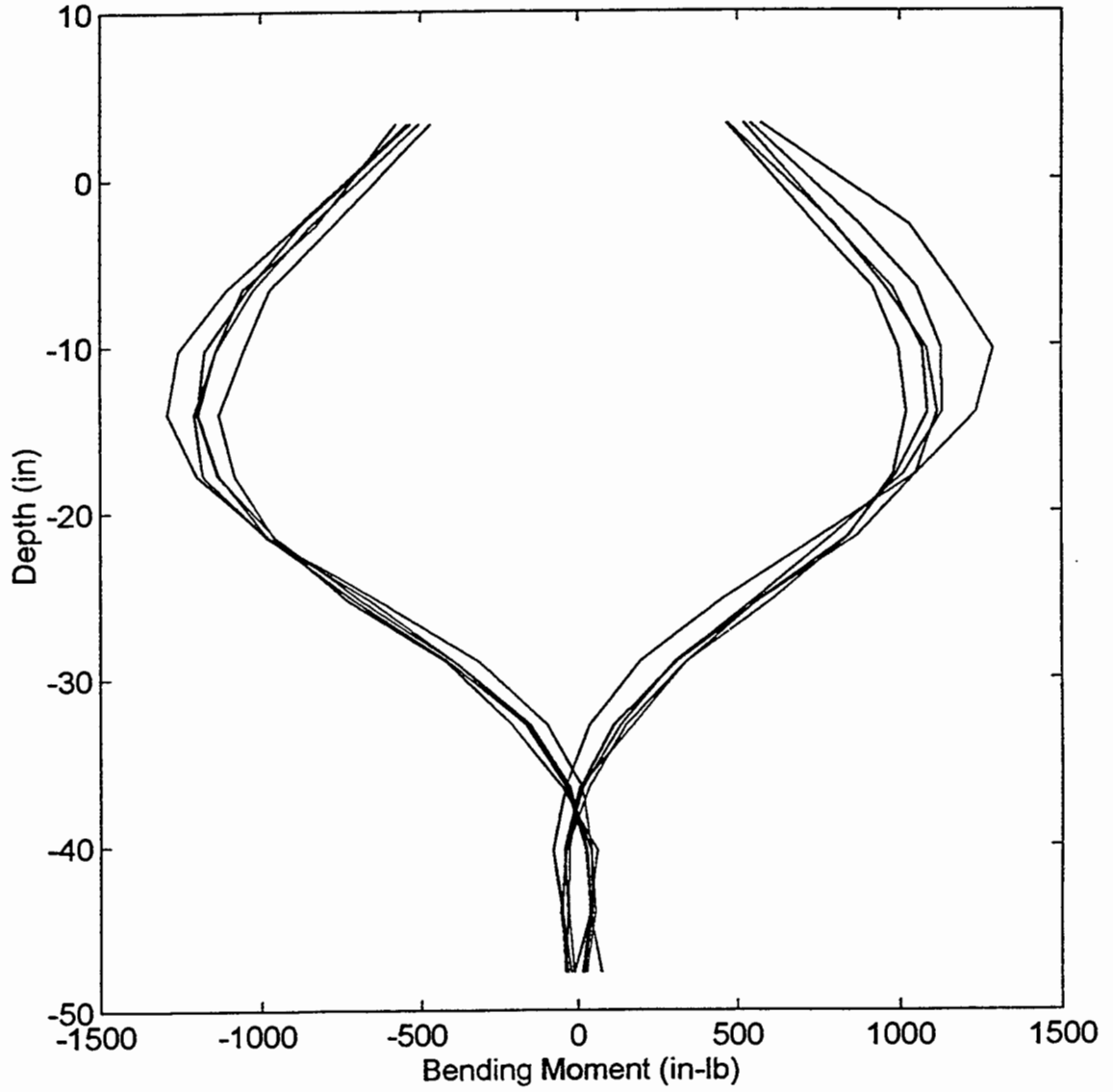


Moment Distribution: Cycle 10 - Load 200lb

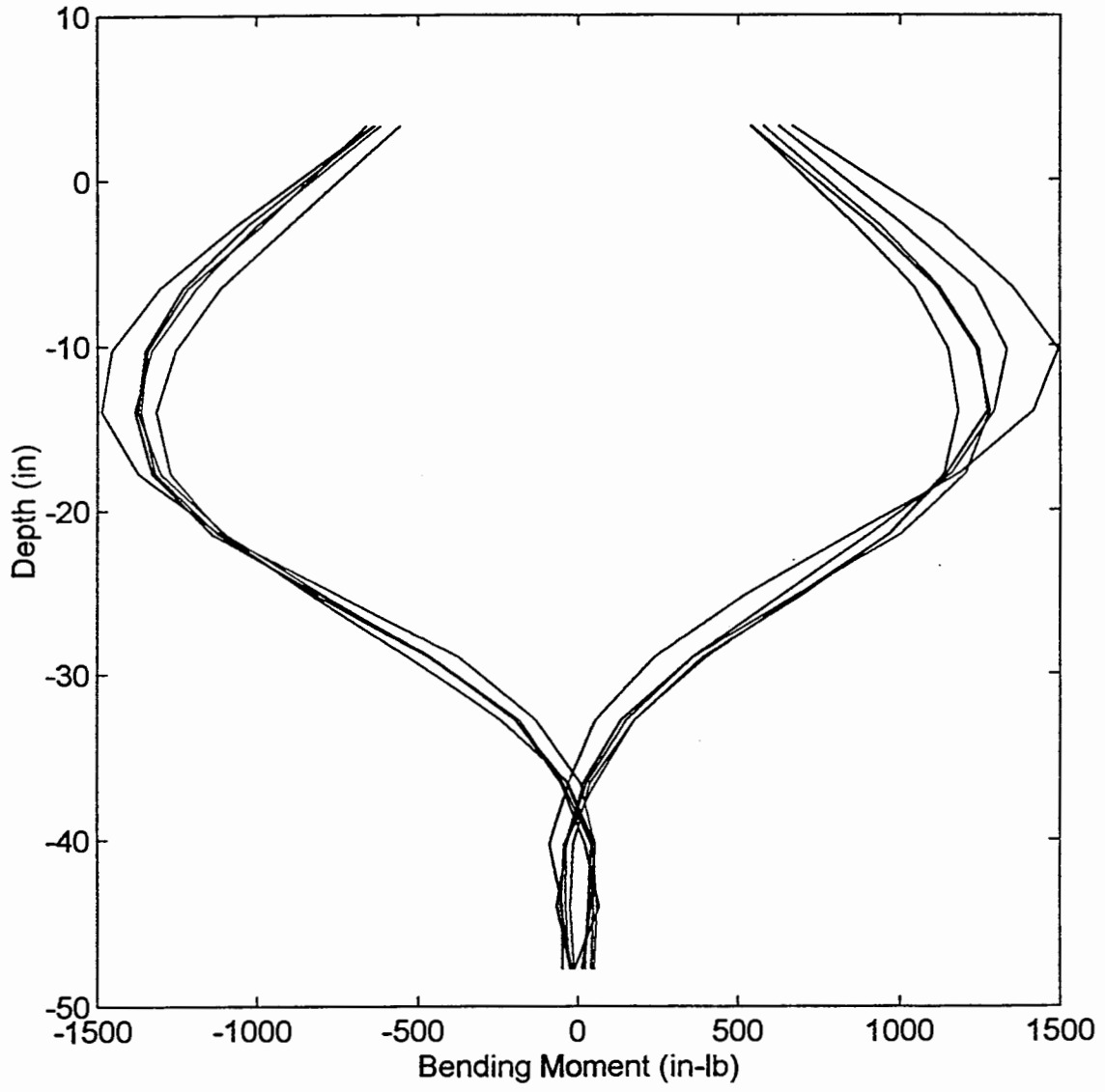




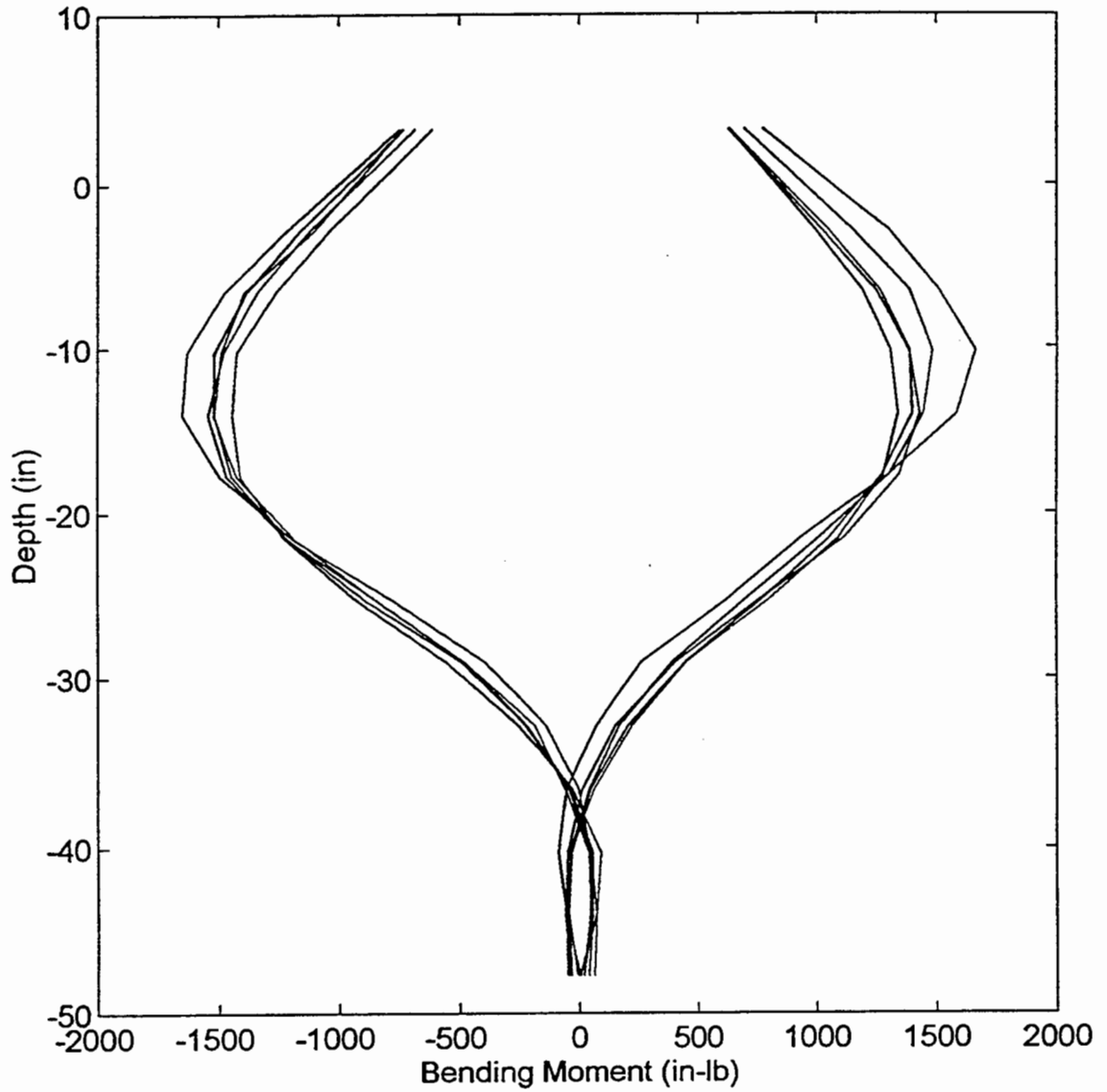
Cycle 10 - Load 300lb



Moment Distribution: Cycle 10 - Load 350lb



Moment Distribution: Cycle 10 - Load 400lb



Moment Distribution: Cycle 10 - Load 450lb

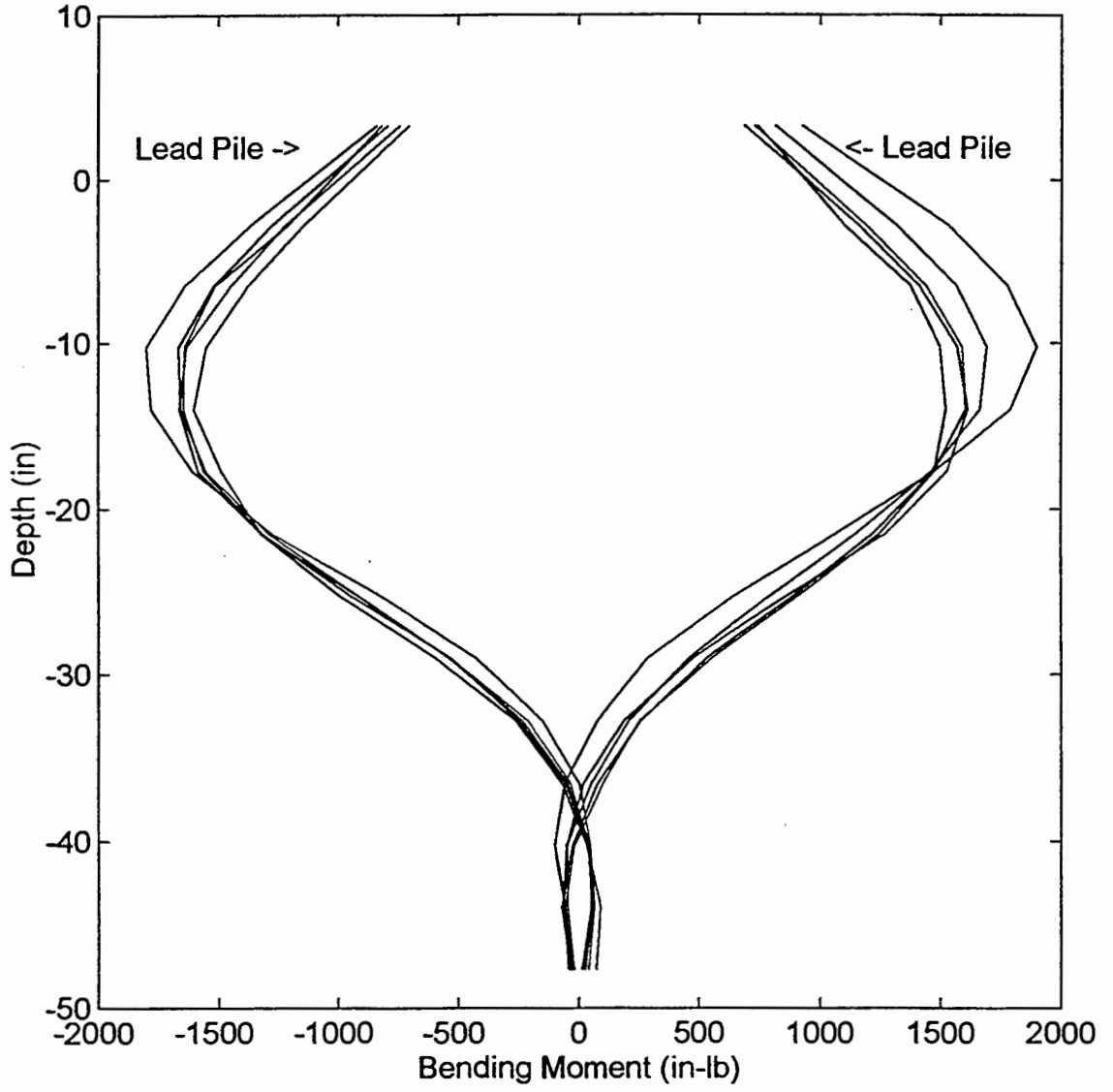
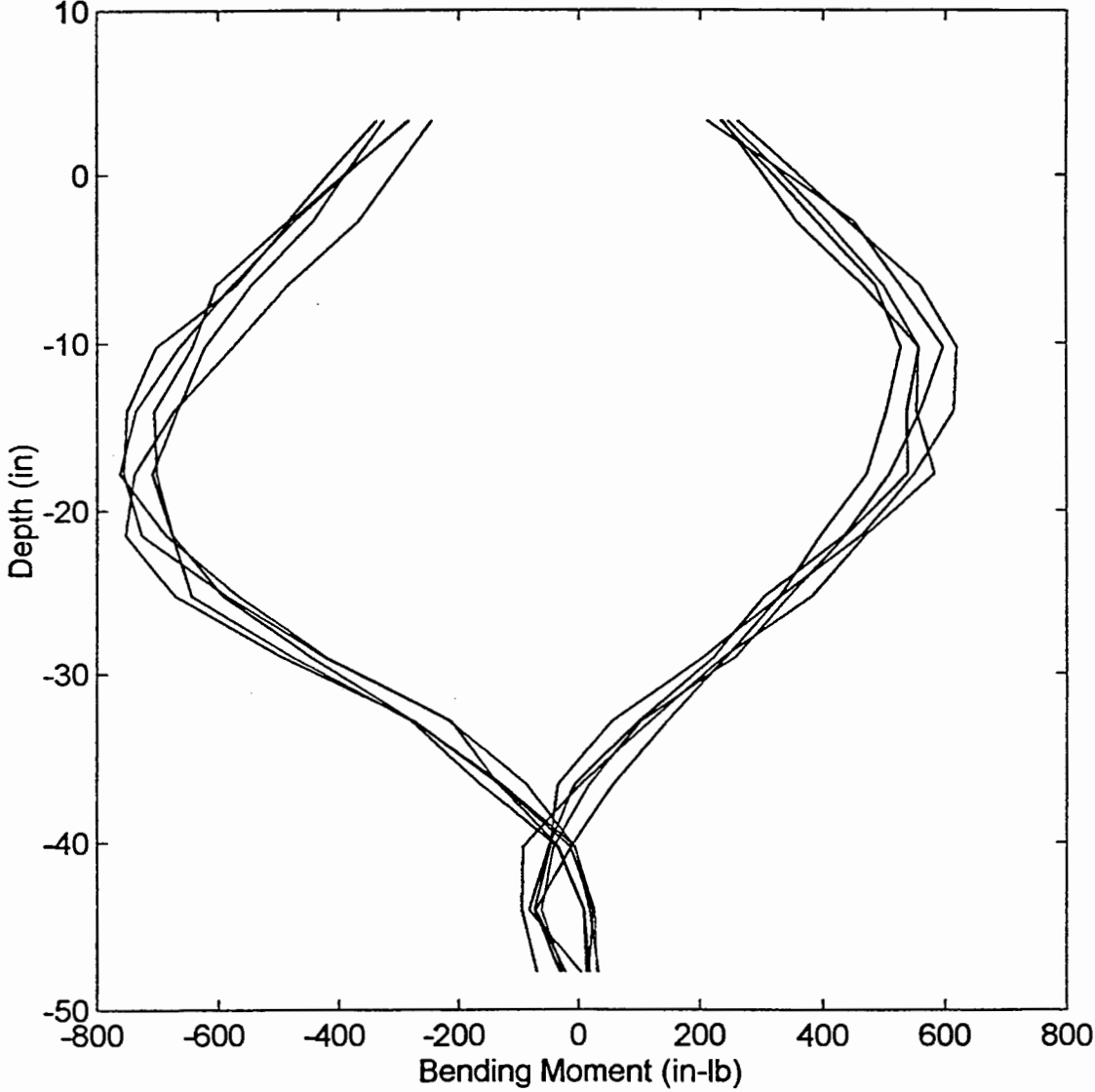


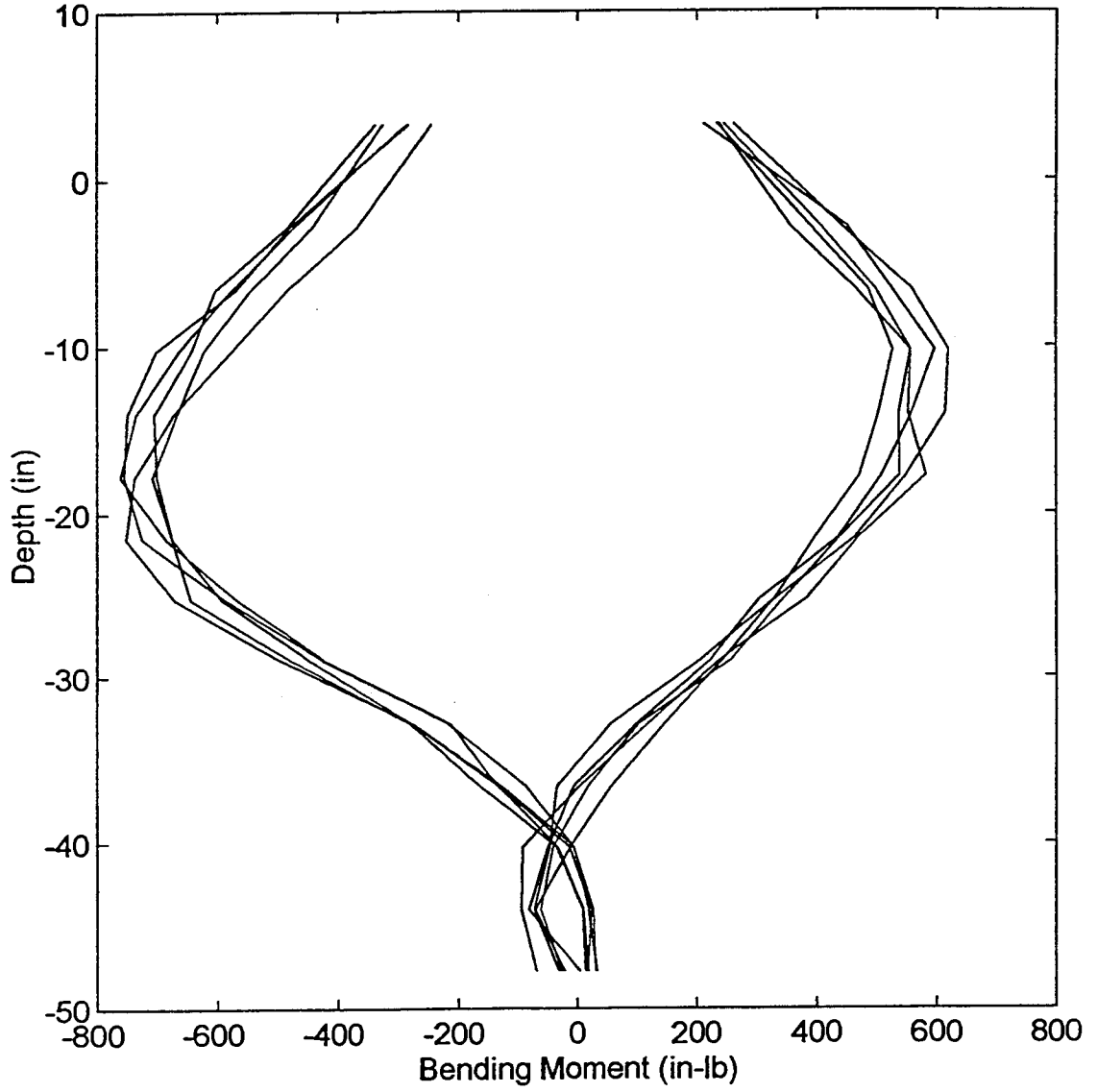
Figure B9. Moment distribution @ cycle 25 (next 7 plots).

Moment Distribution: Cycle 25 - Load 150lb

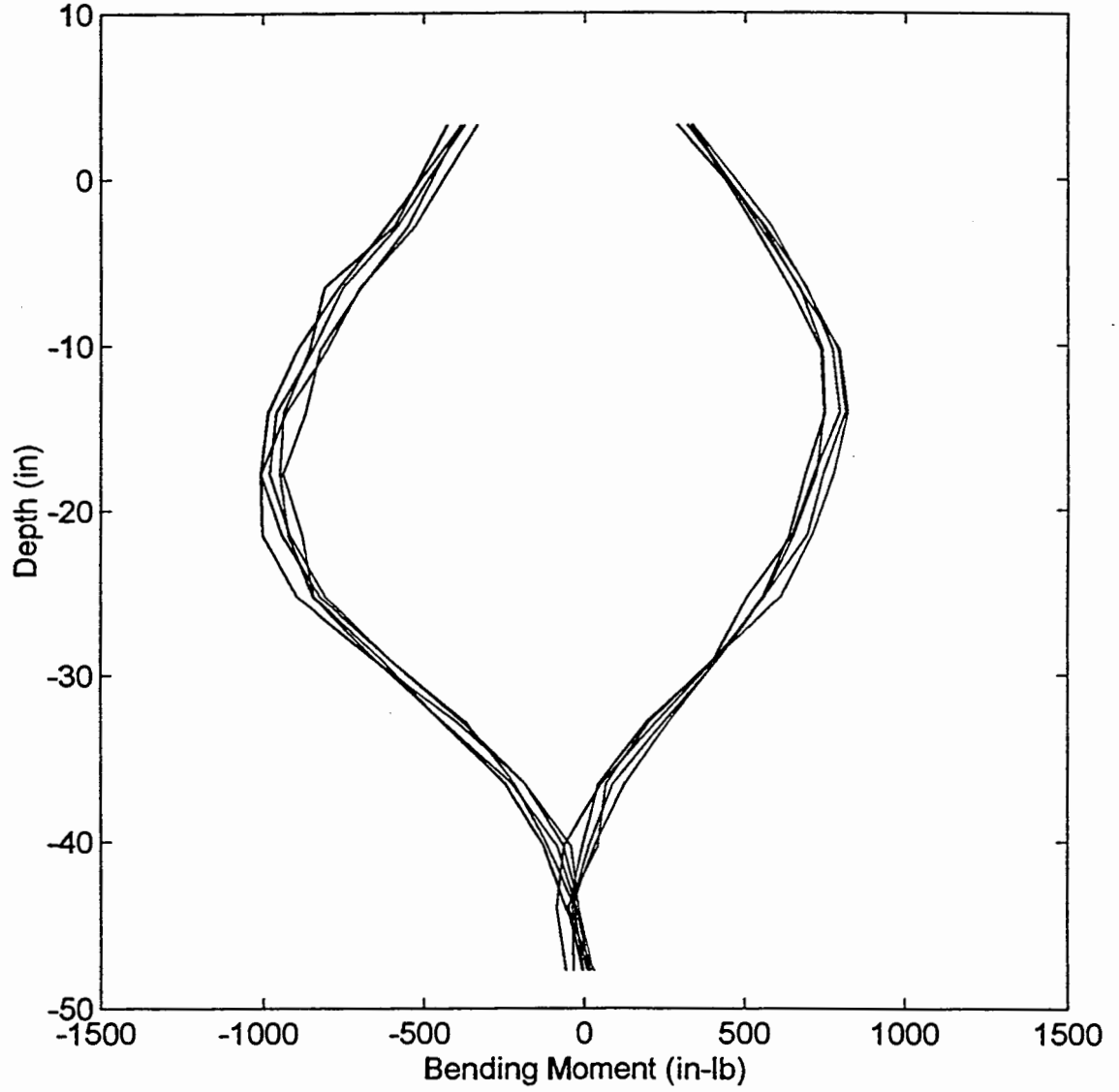




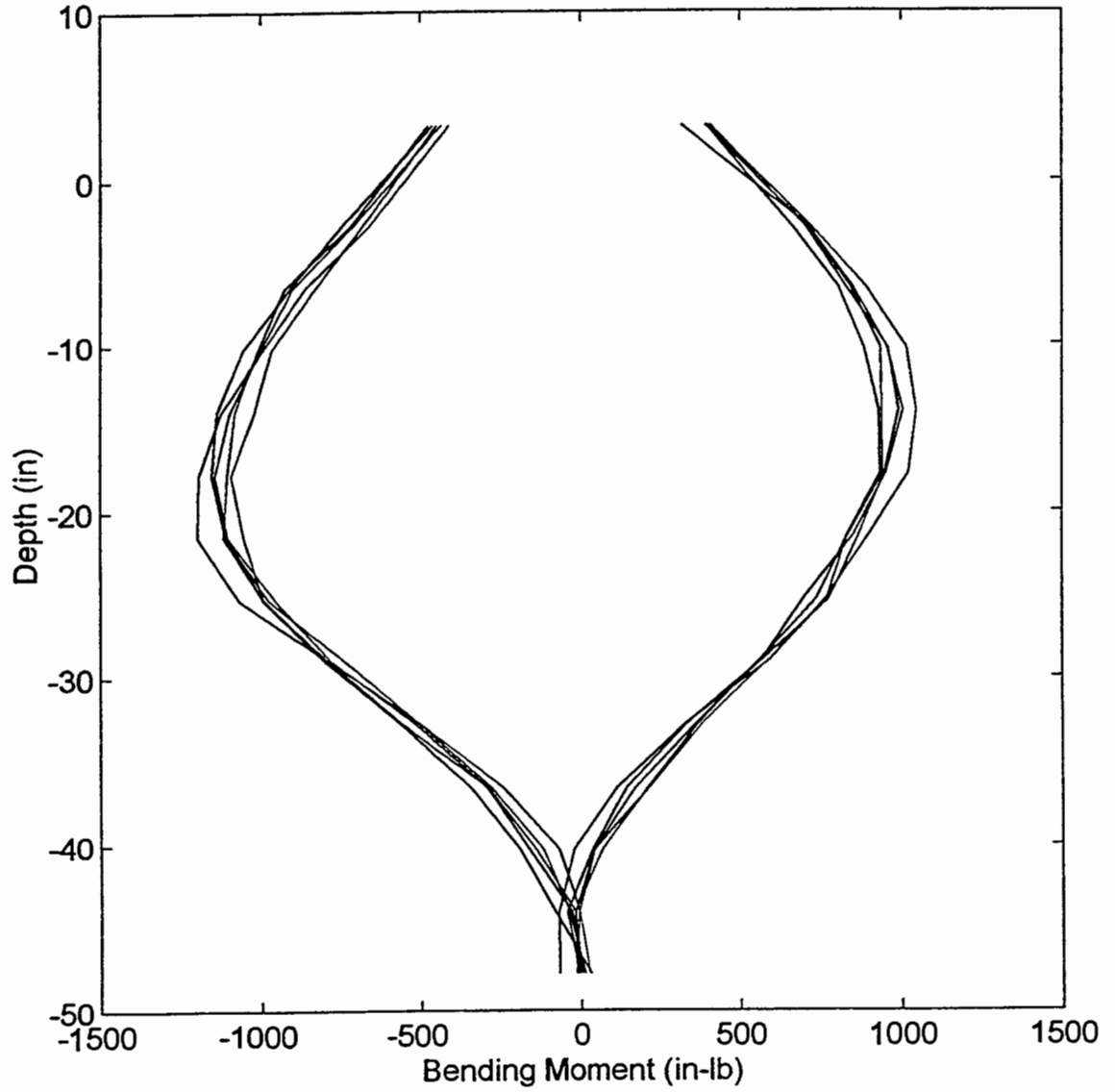
Moment Distribution: Cycle 25 - Load 150lb



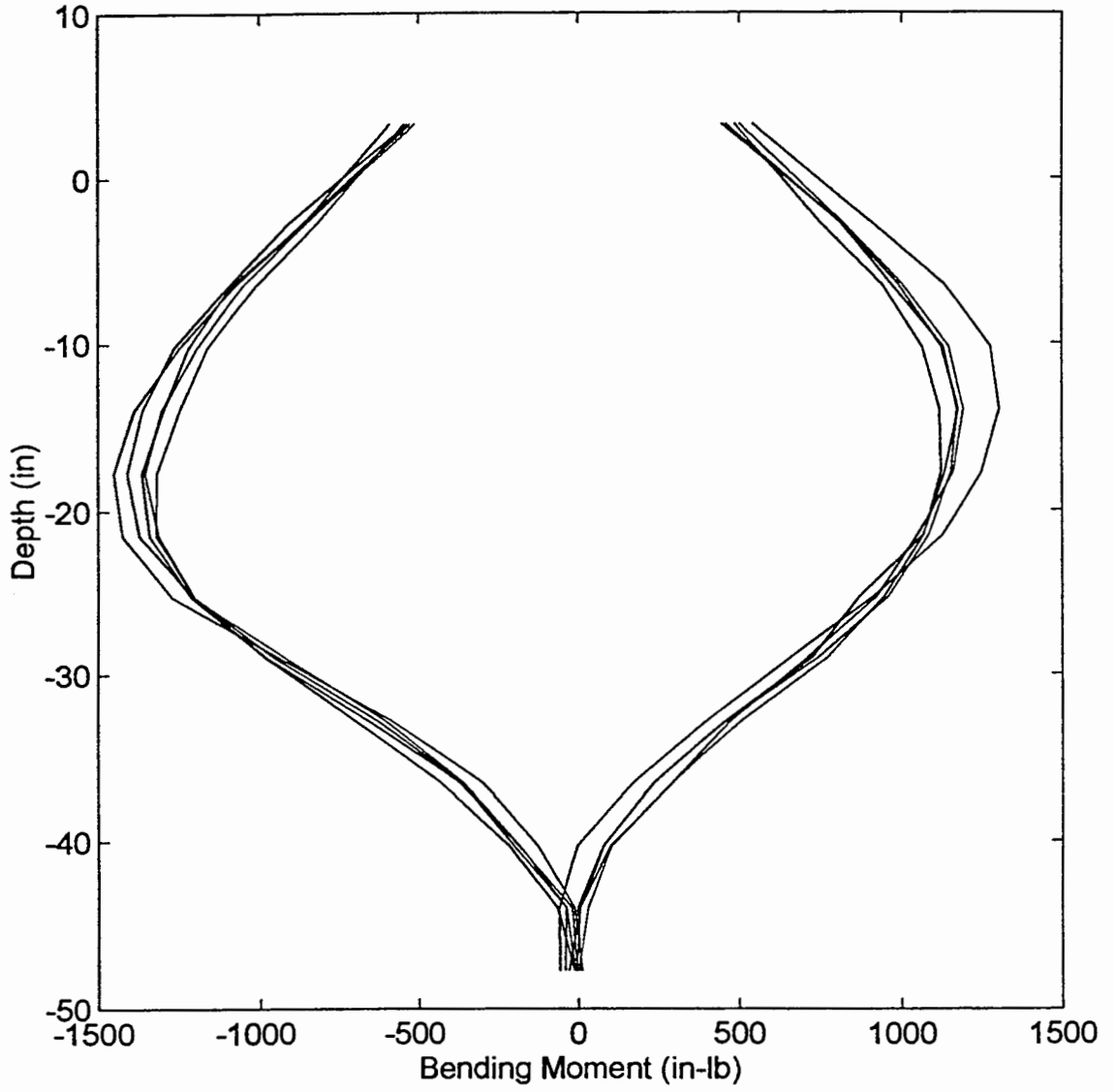
Moment Distribution: Cycle 25 - Load 200lb



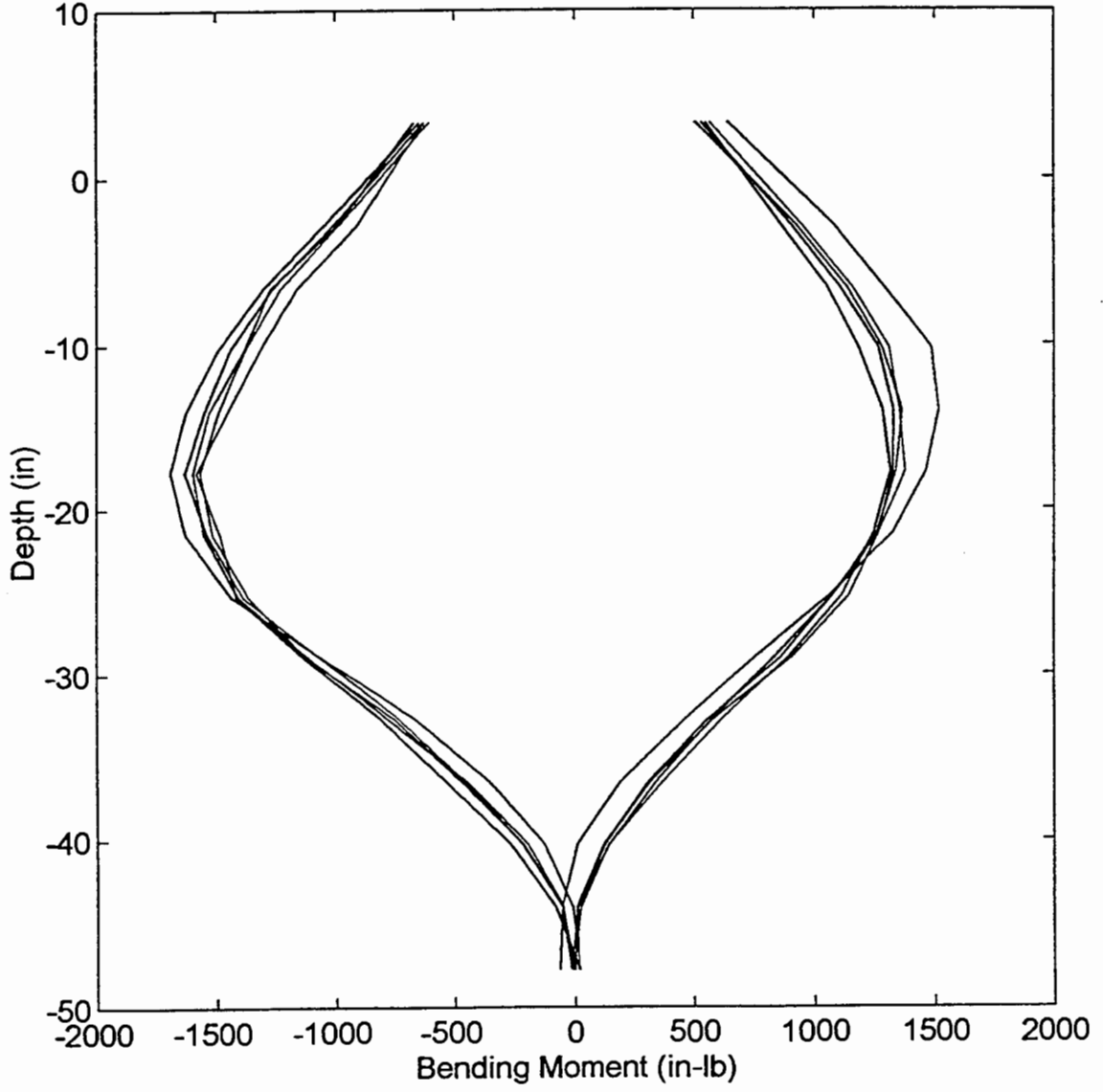
Moment Distribution: Cycle 25 - Load 250lb



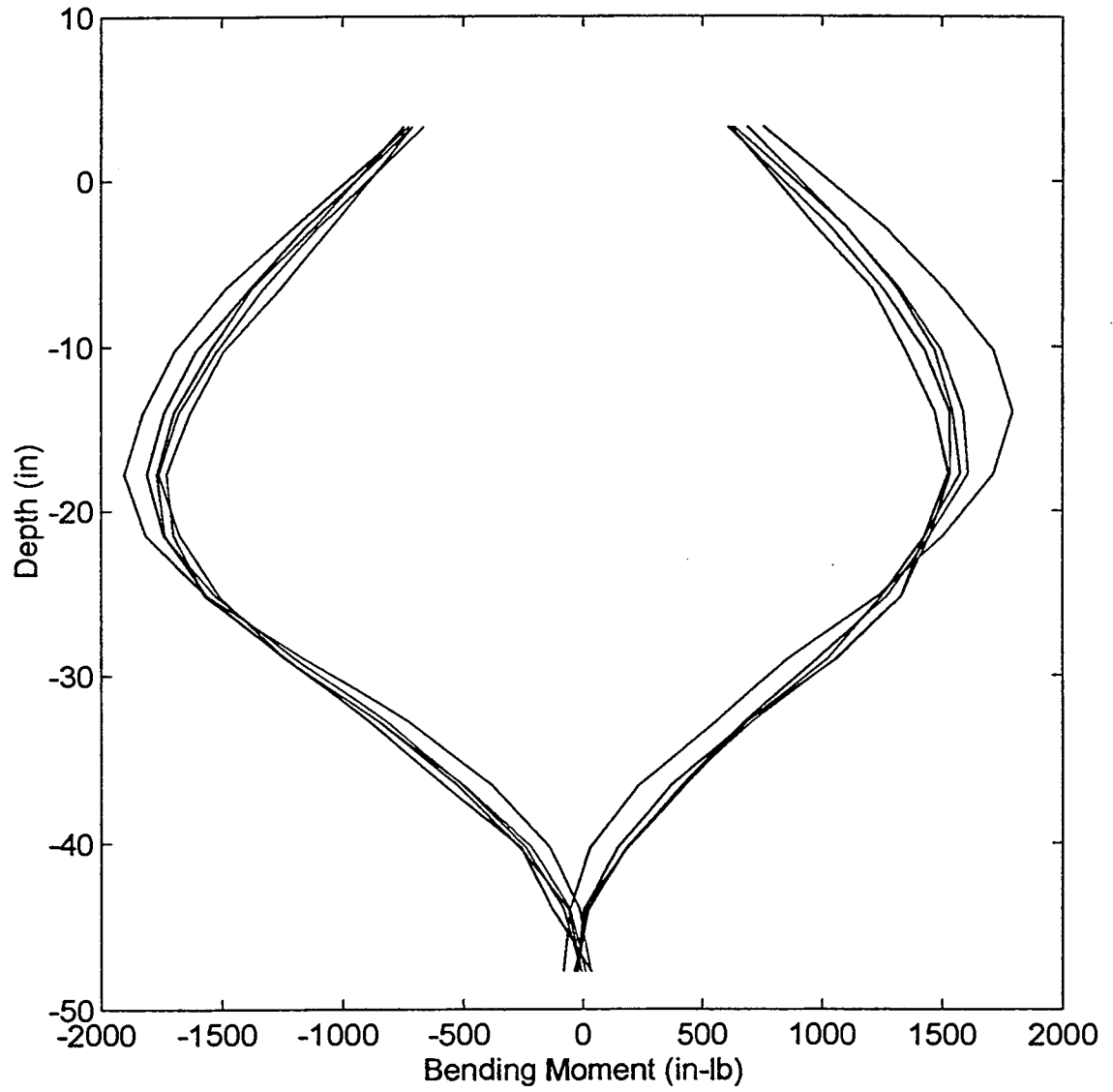
Moment Distribution: Cycle 25 - Load 300lb



Moment Distribution: Cycle 25 - Load 350lb



Moment Distribution: Cycle 25 - Load 400lb



Moment Distribution: Cycle 25 - Load 450lb

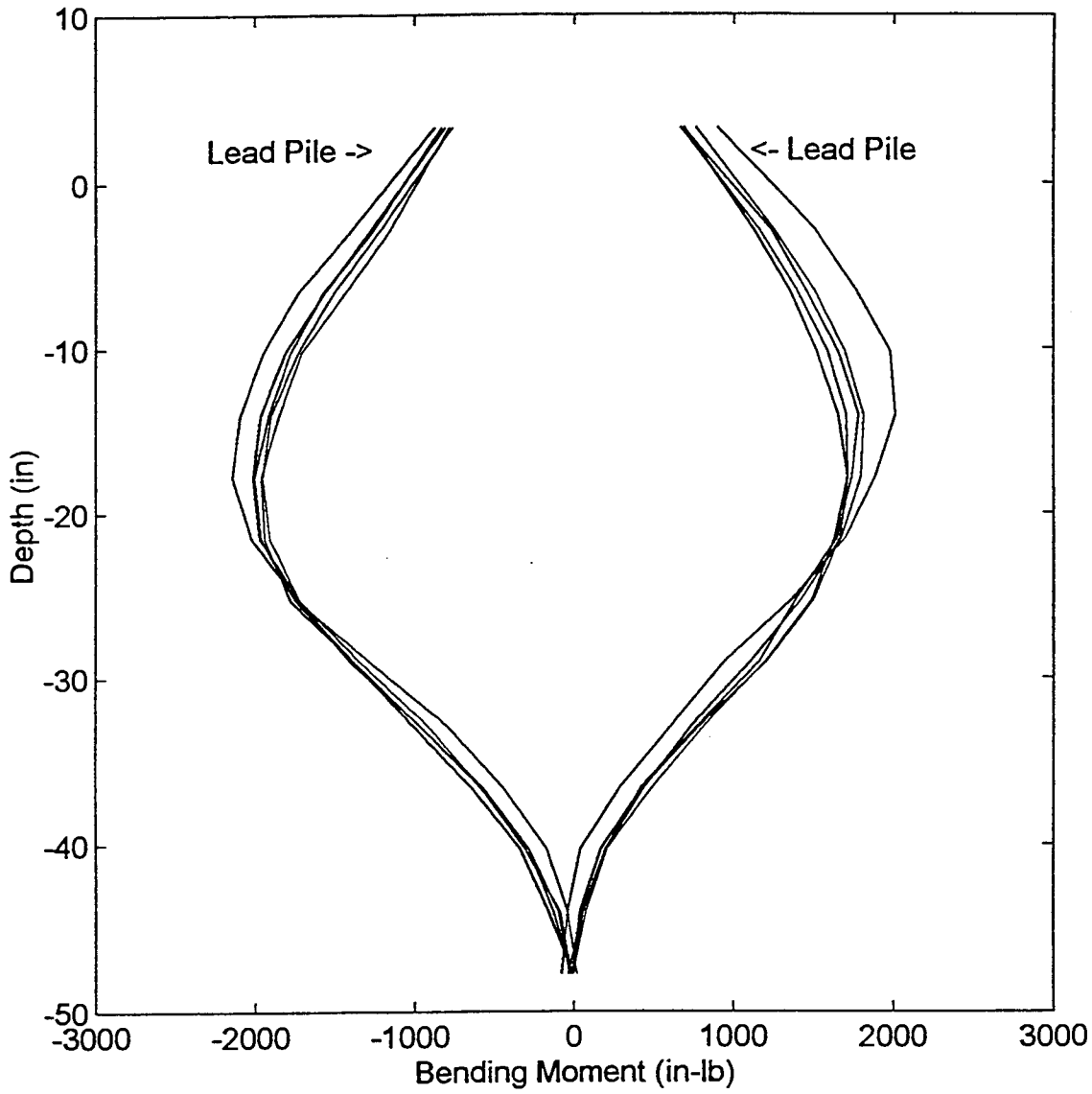
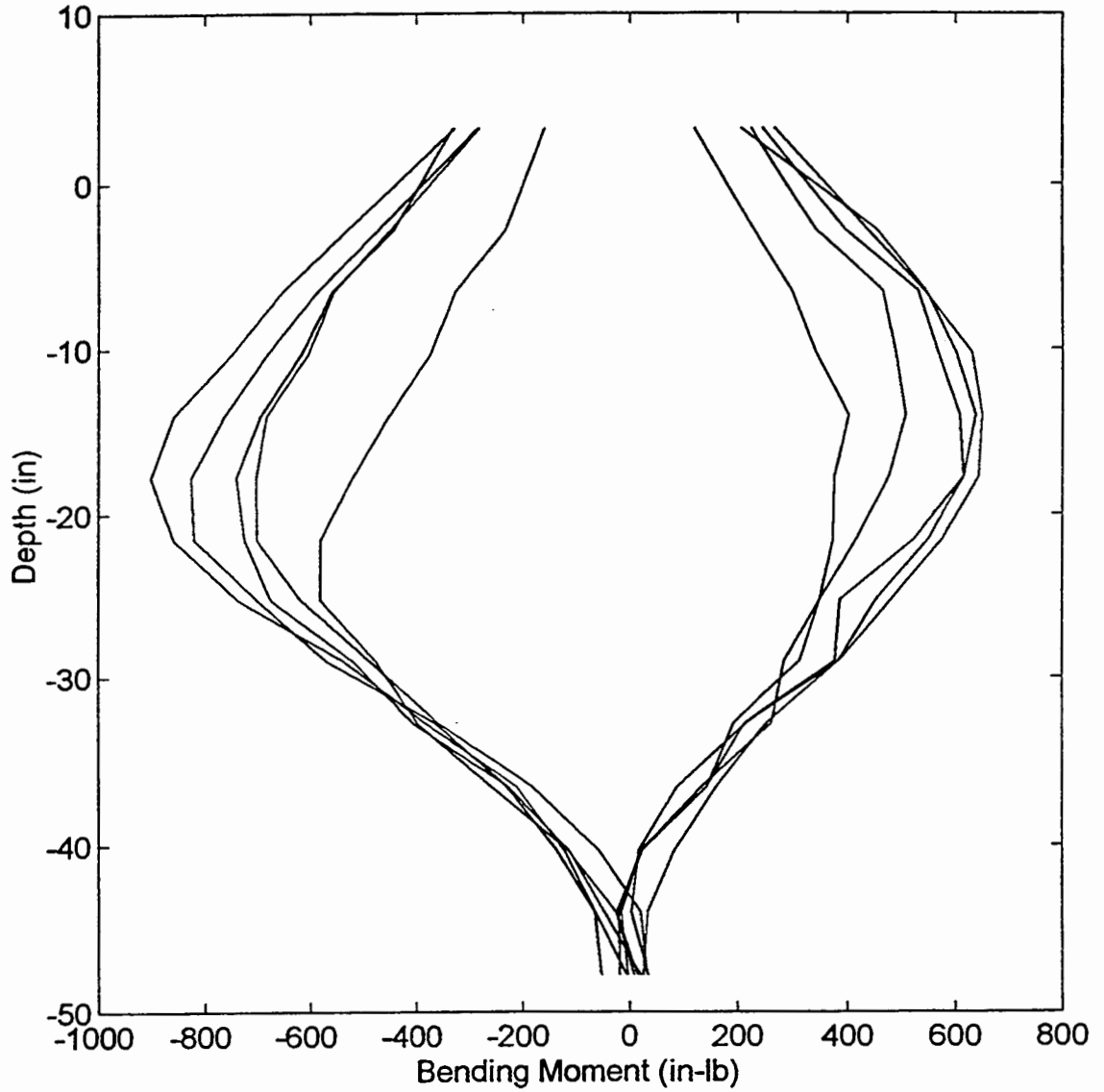
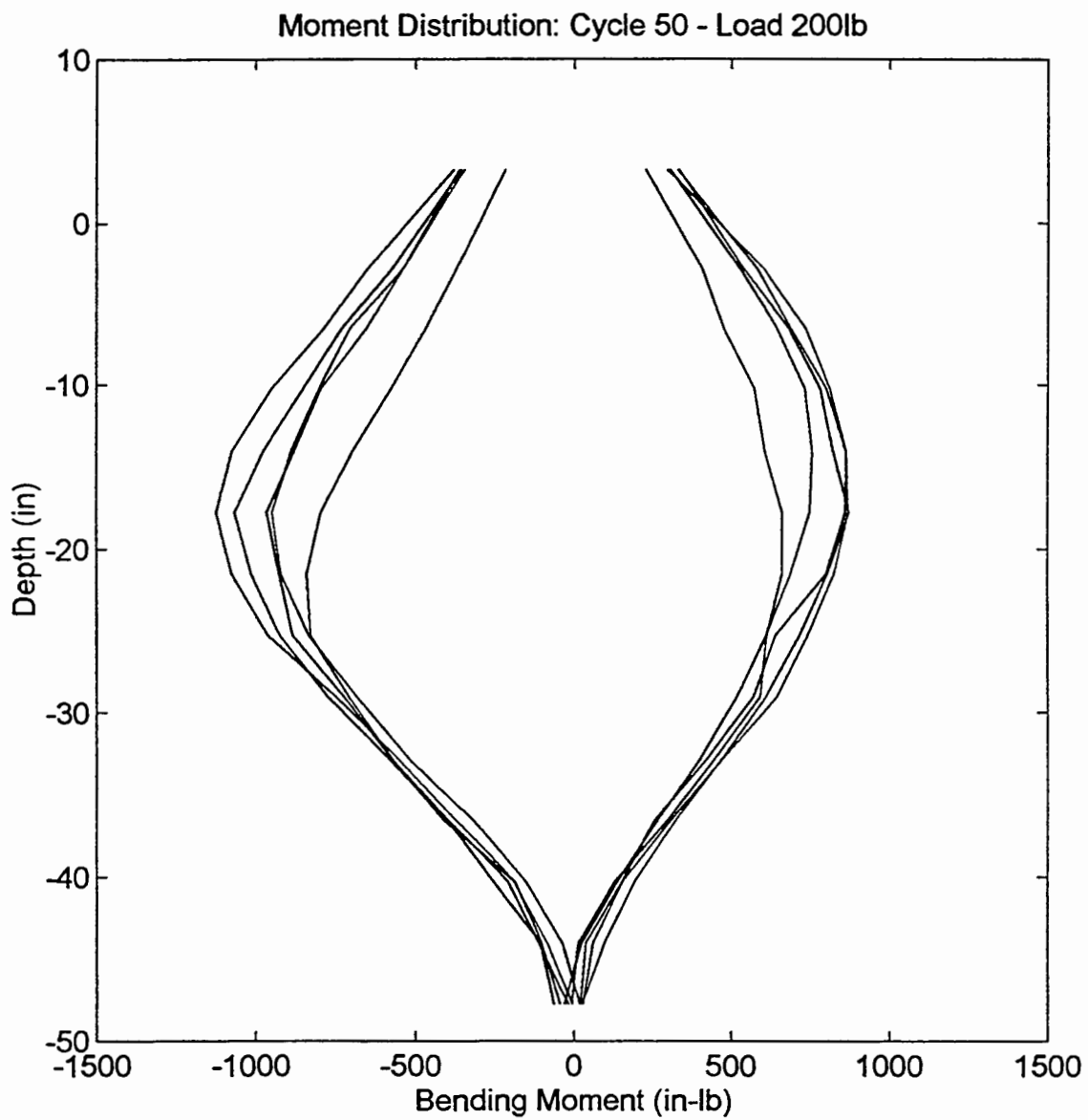


Figure B10. Moment distribution @ cycle 50 (next 7 plots).

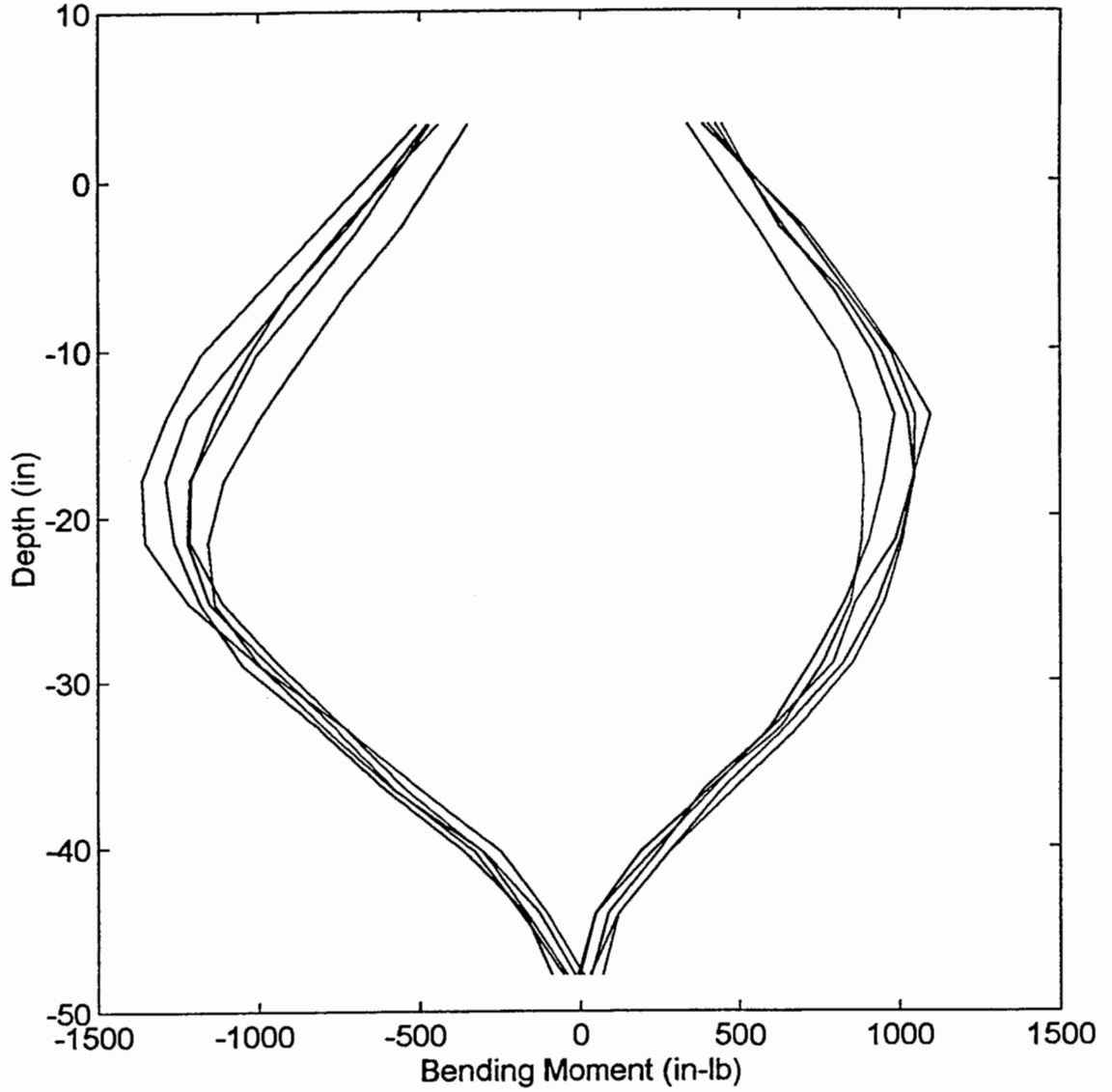


Moment Distribution: Cycle 50 - Load 150lb

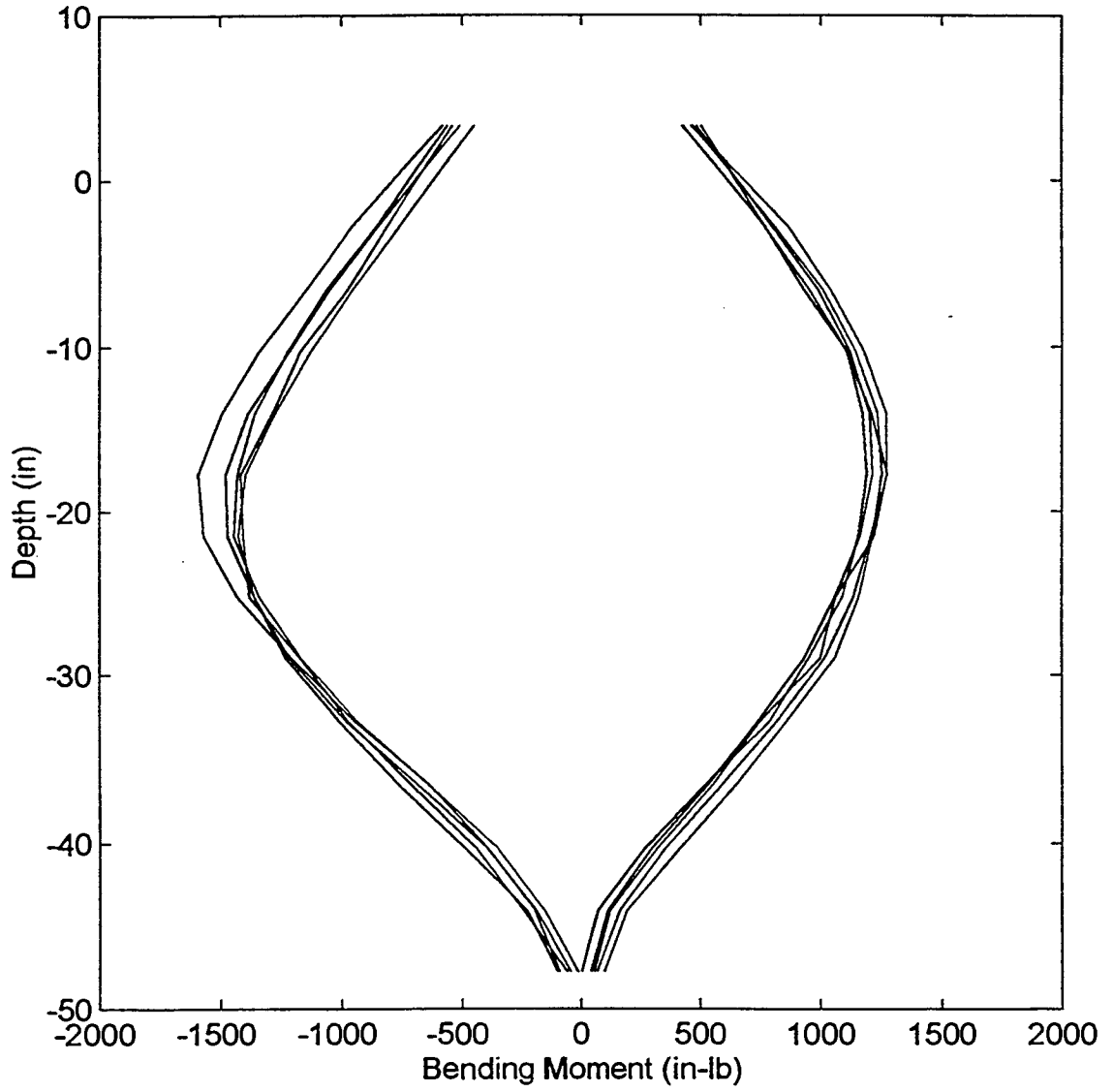




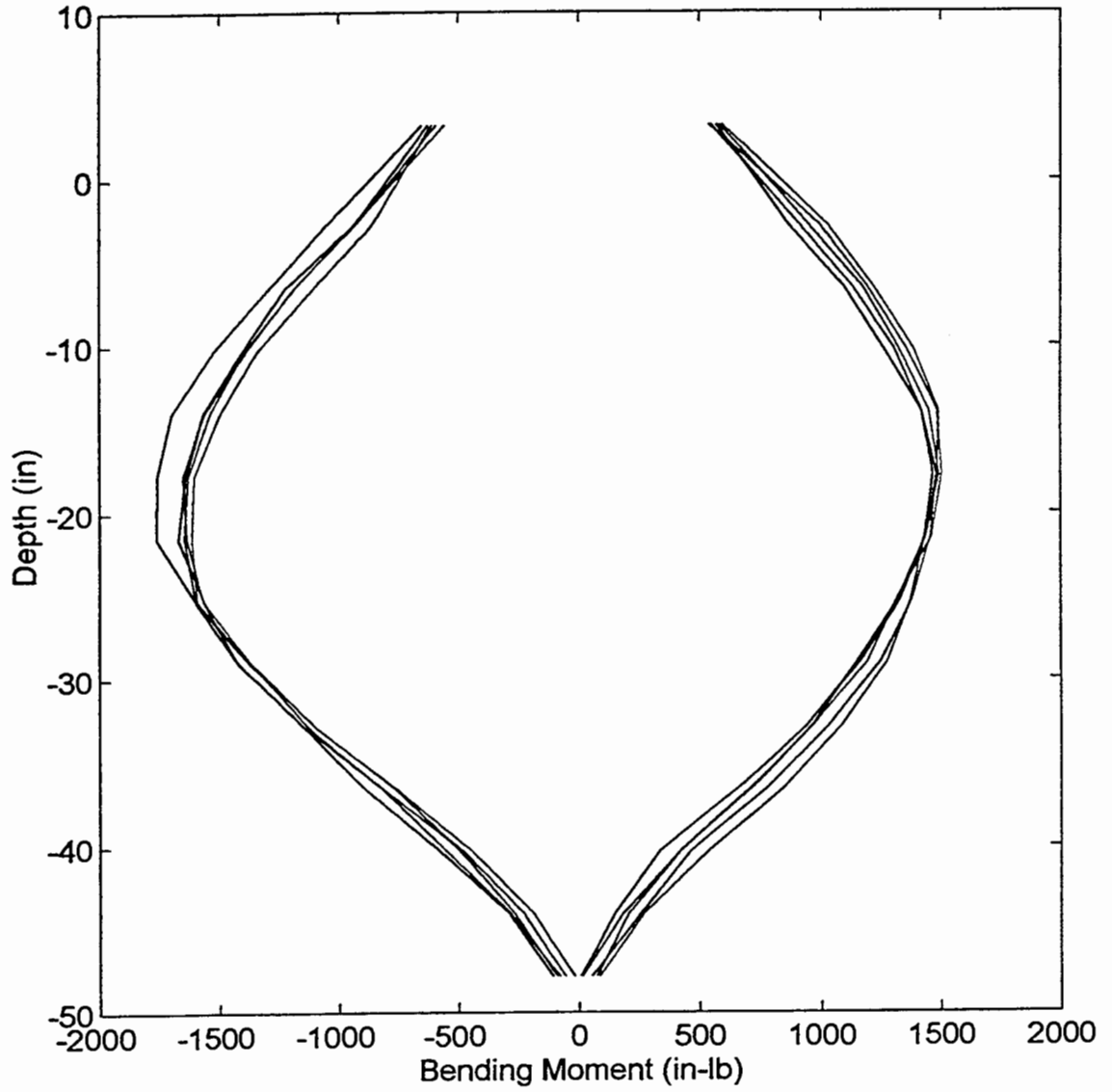
Moment Distribution: Cycle 50 - Load 250lb



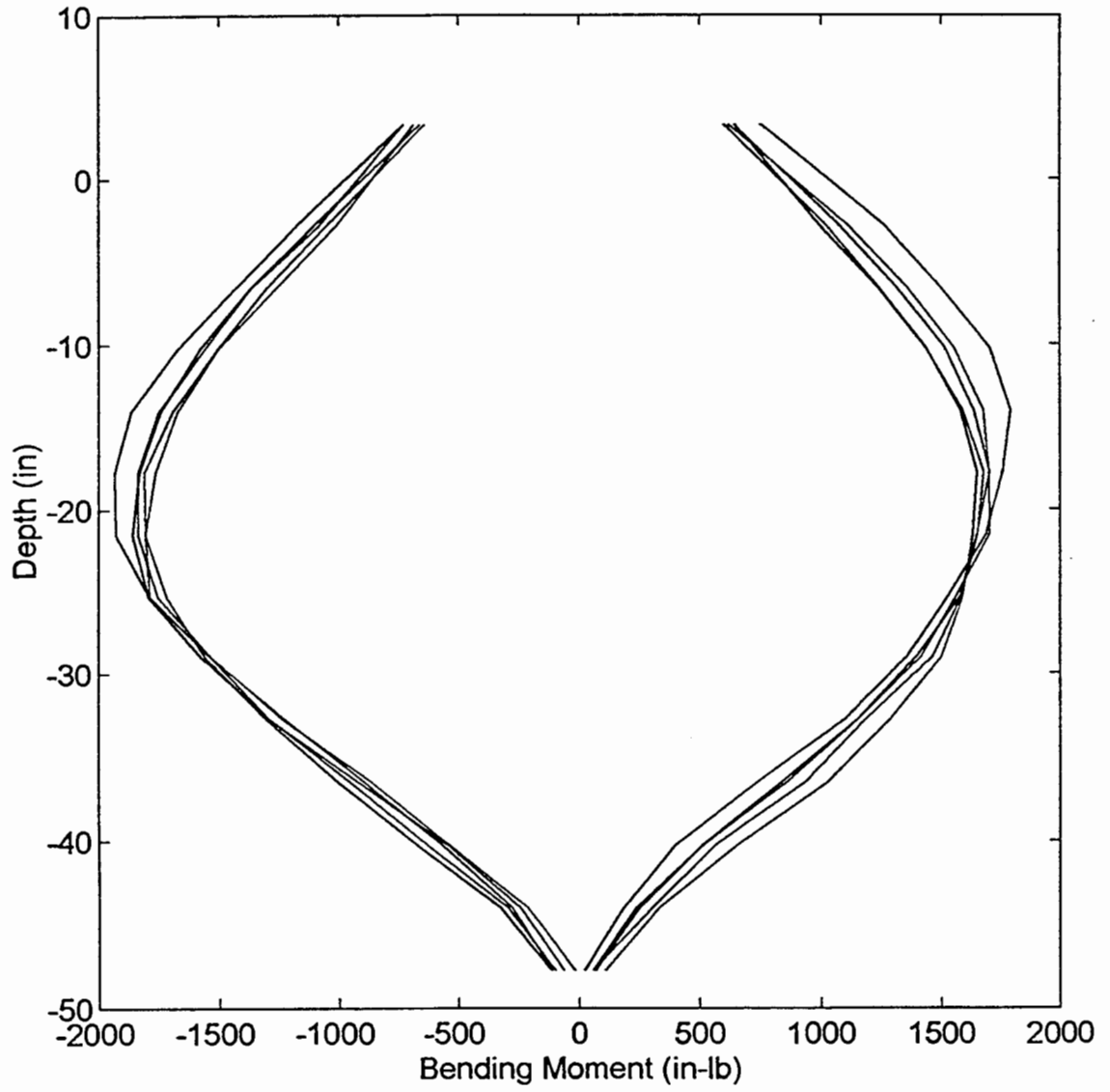
Moment Distribution: Cycle 50 - Load 300lb



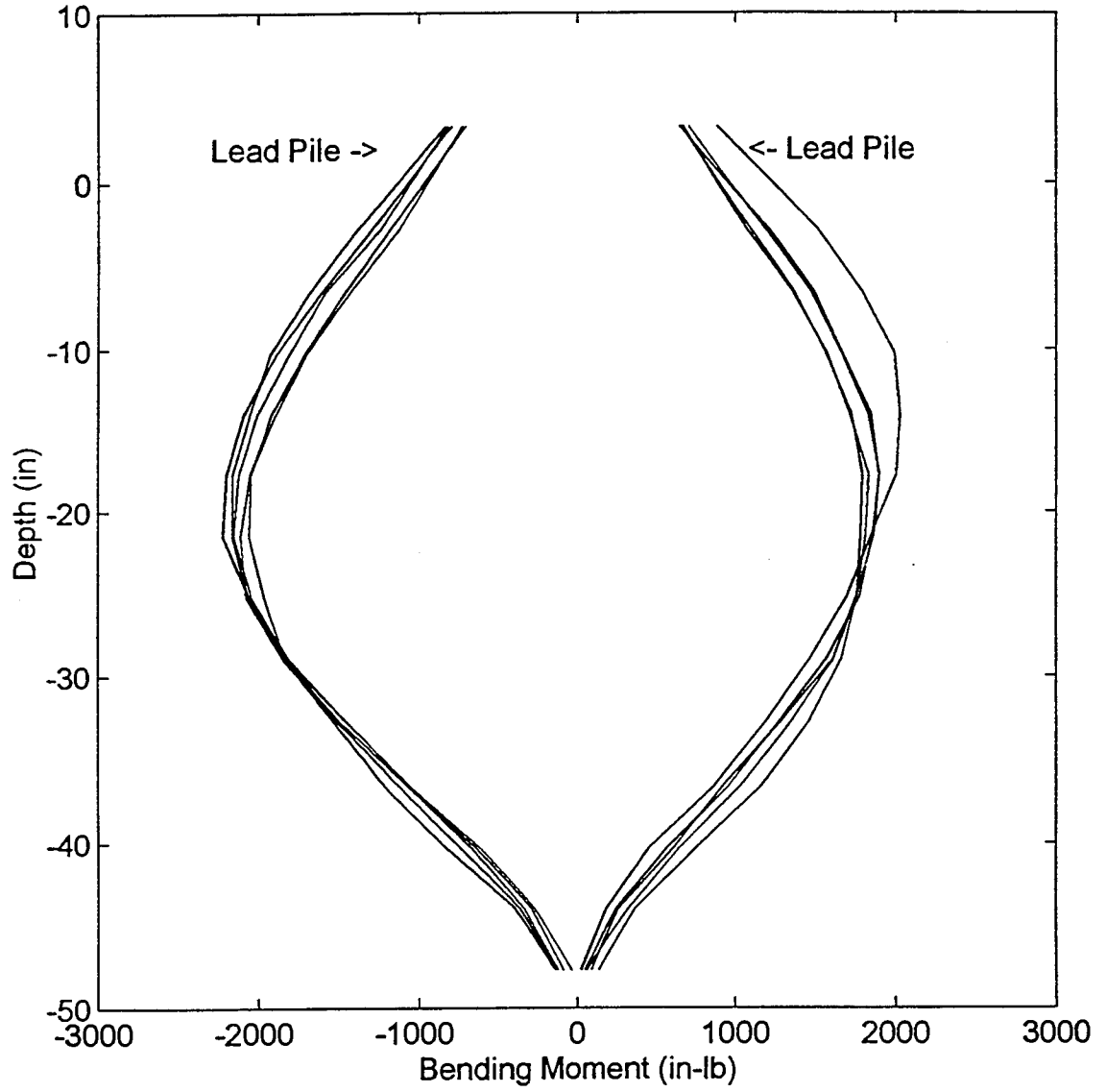
Moment Distribution: Cycle 50 - Load 350lb



Moment Distribution: Cycle 50 - Load 400lb



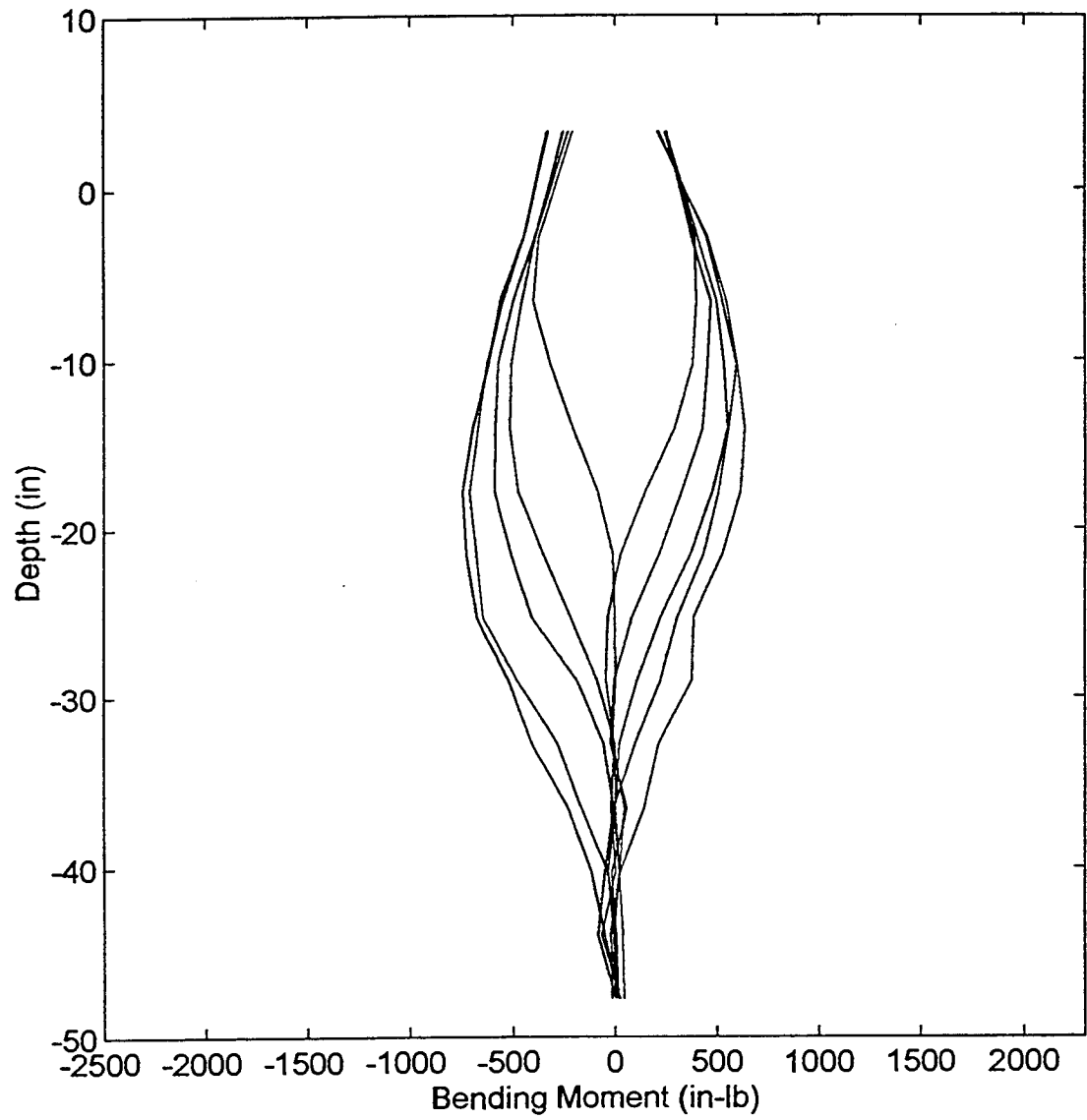
Moment Distribution: Cycle 50 - Load 450lb



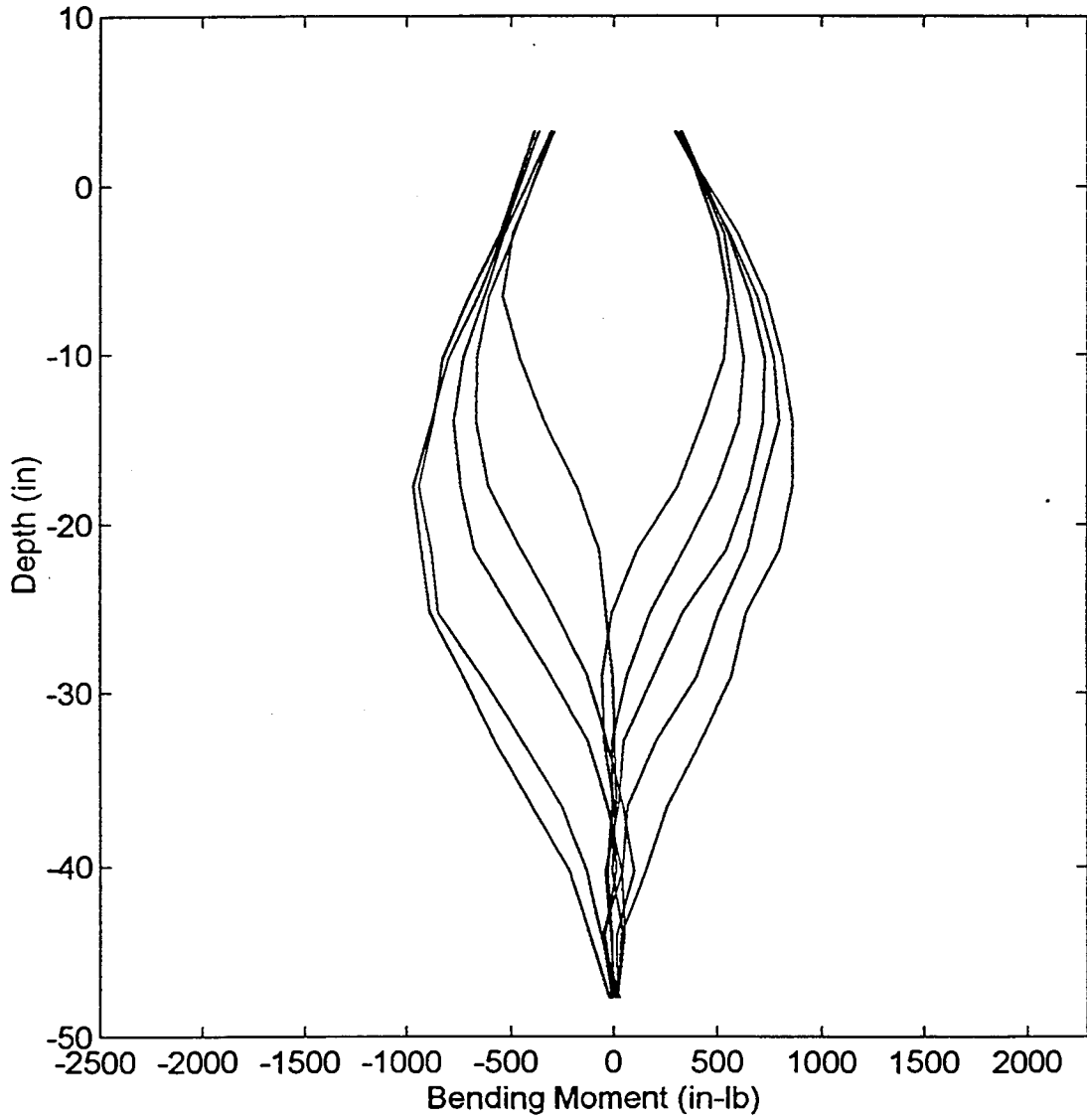
B11. Moment distribution: Middle Pile-#1 (next 7 Plots).



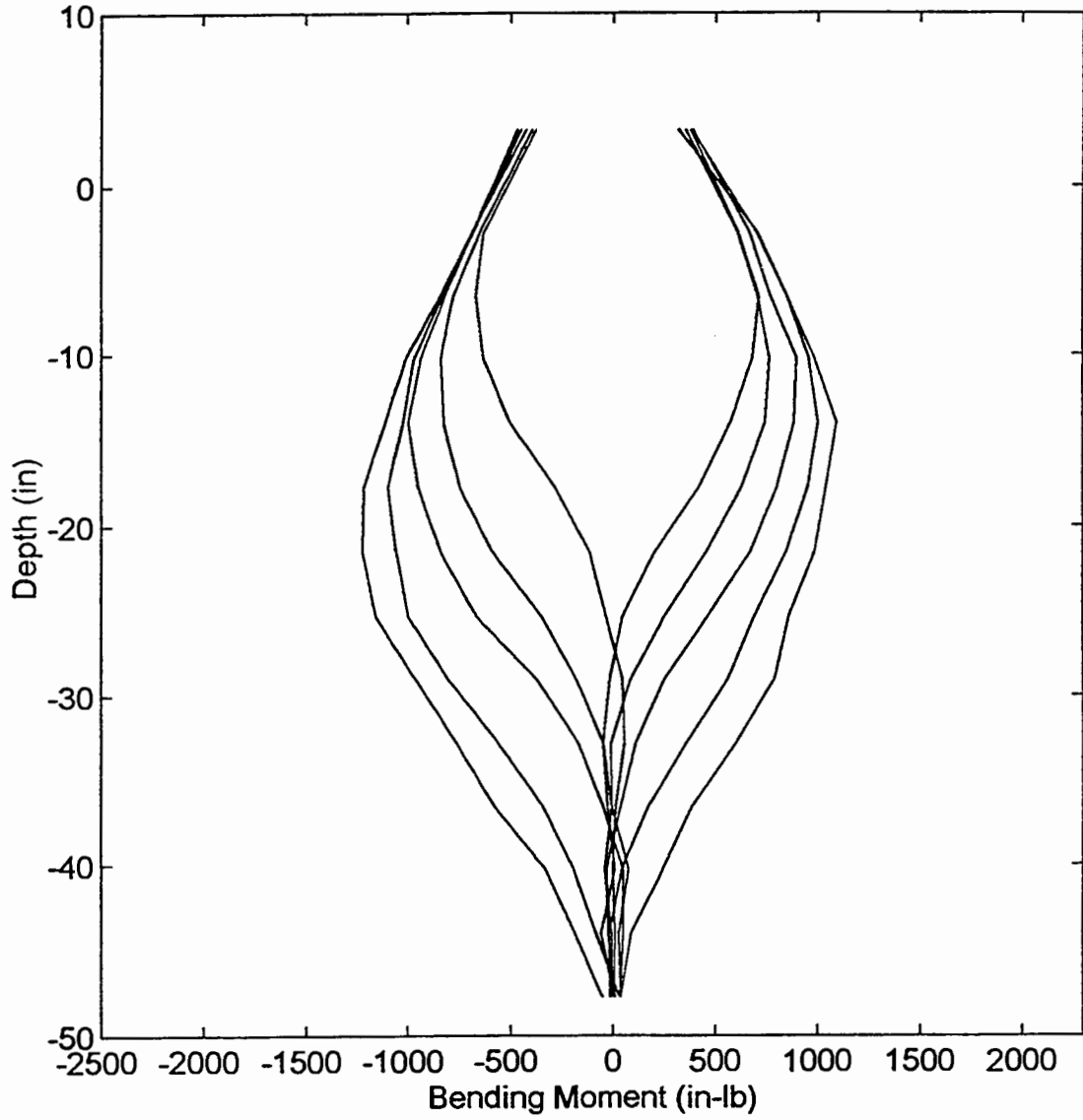
Moment Distribution: Middle Pile (#1) - Load 150lb



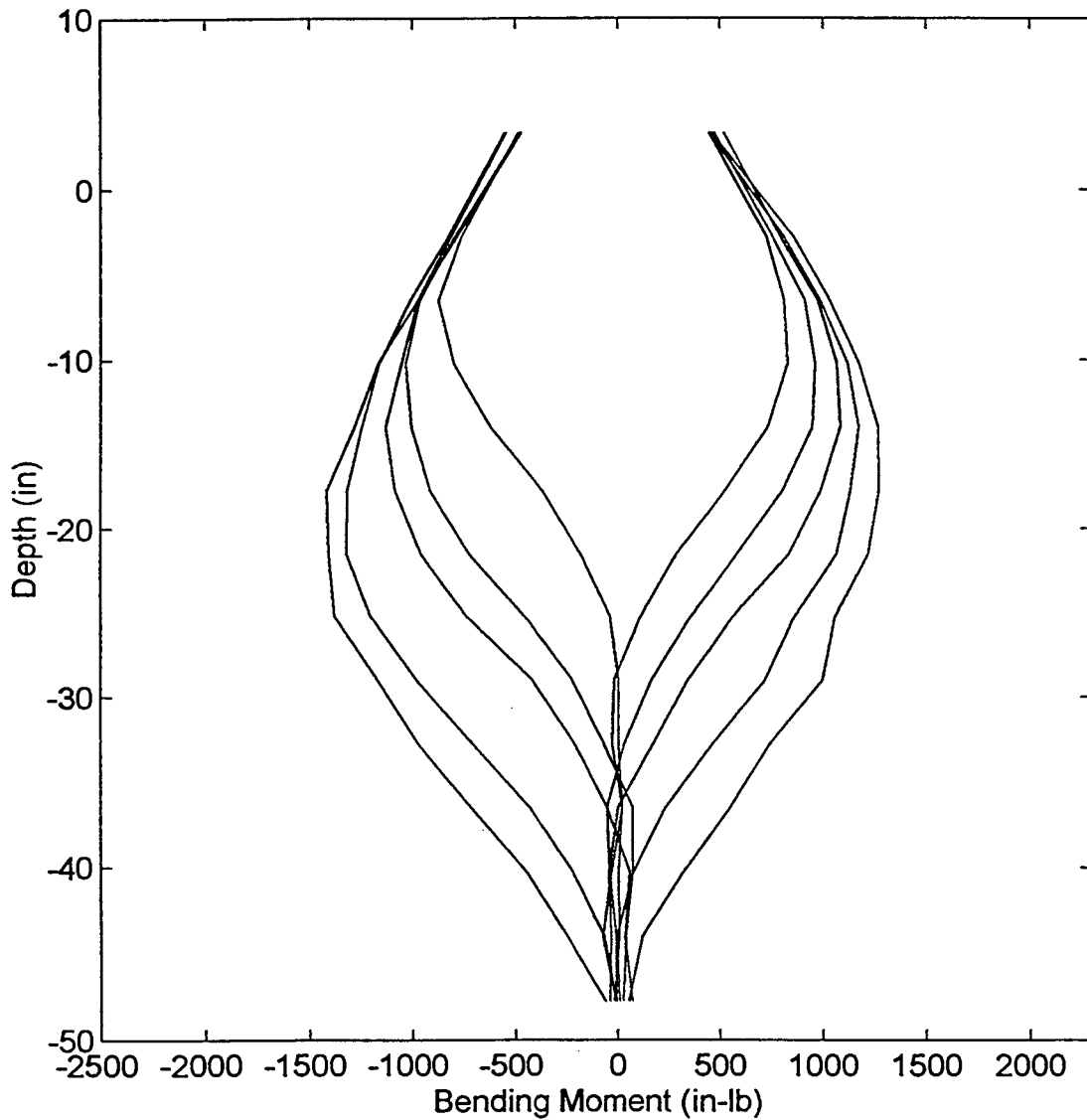
Moment Distribution: Middle Pile (#1) - Load 200lb



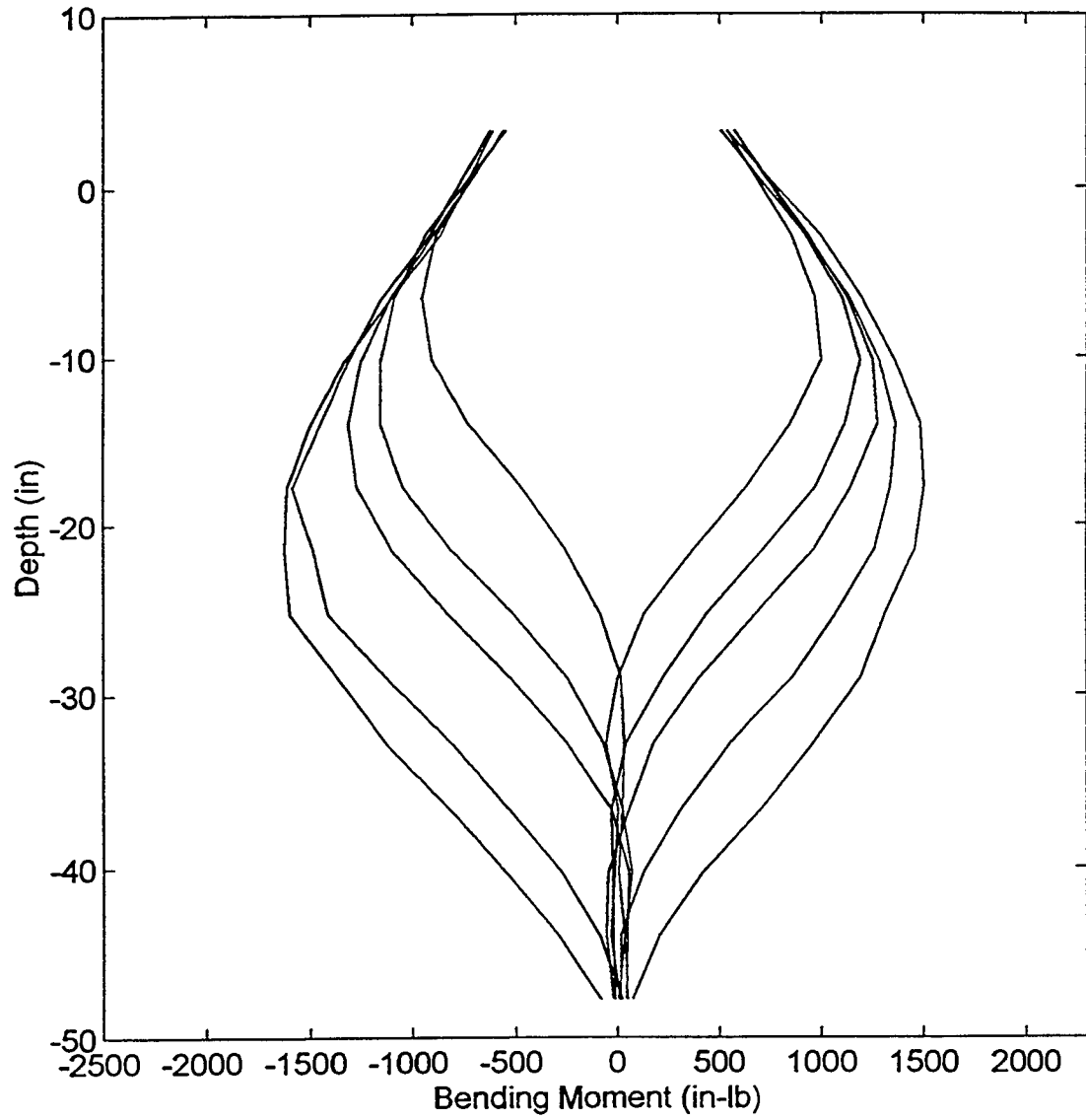
Middle Pile (#1) - Load 250lb



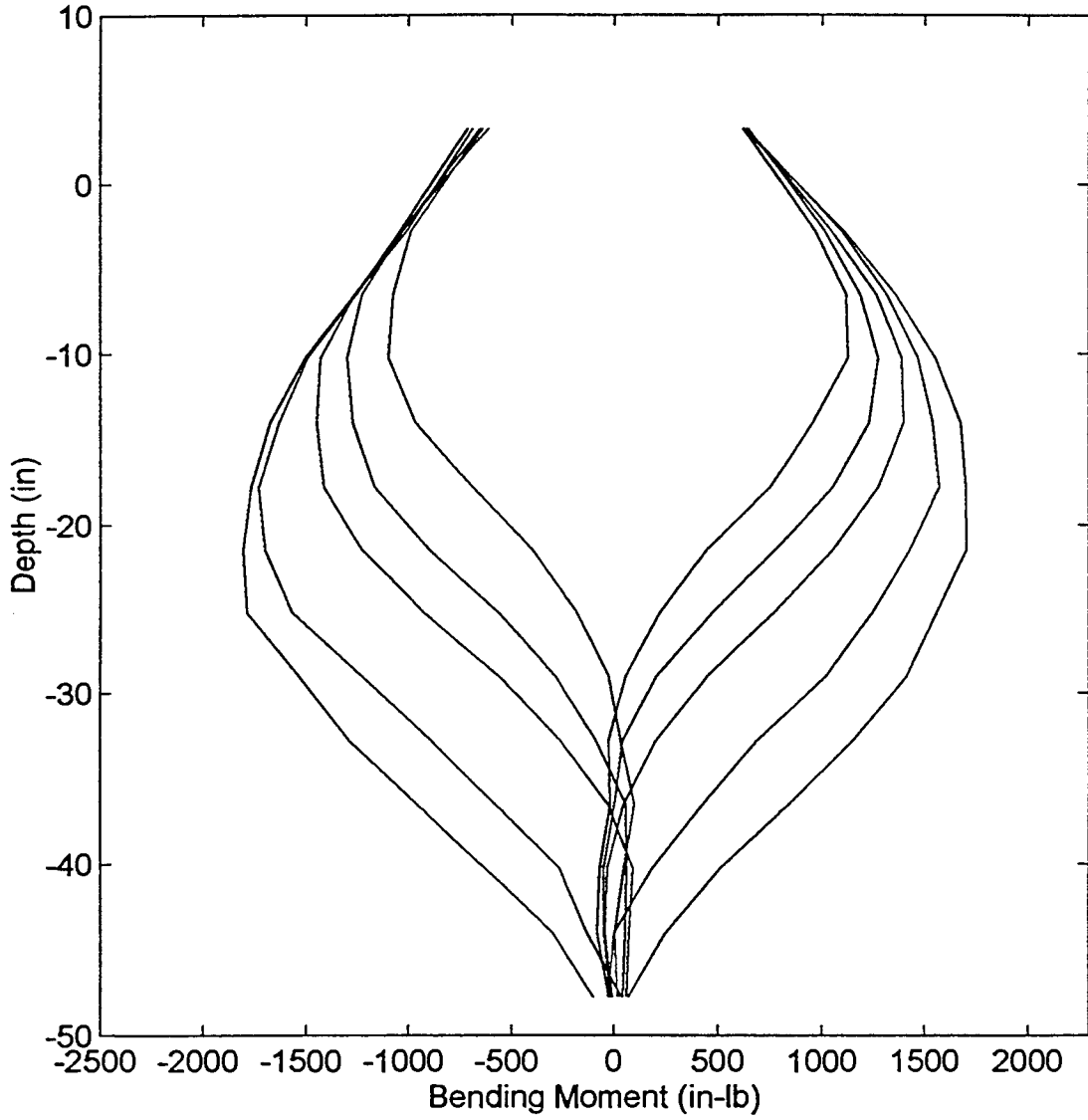
Moment Distribution: Middle Pile (#1) - Load 300lb



Moment Distribution: Middle Pile (#1) - Load 350lb



Moment Distribution: Middle Pile (#1) - Load 400lb



Moment Distribution: Middle Pile (#1) - Load 450lb

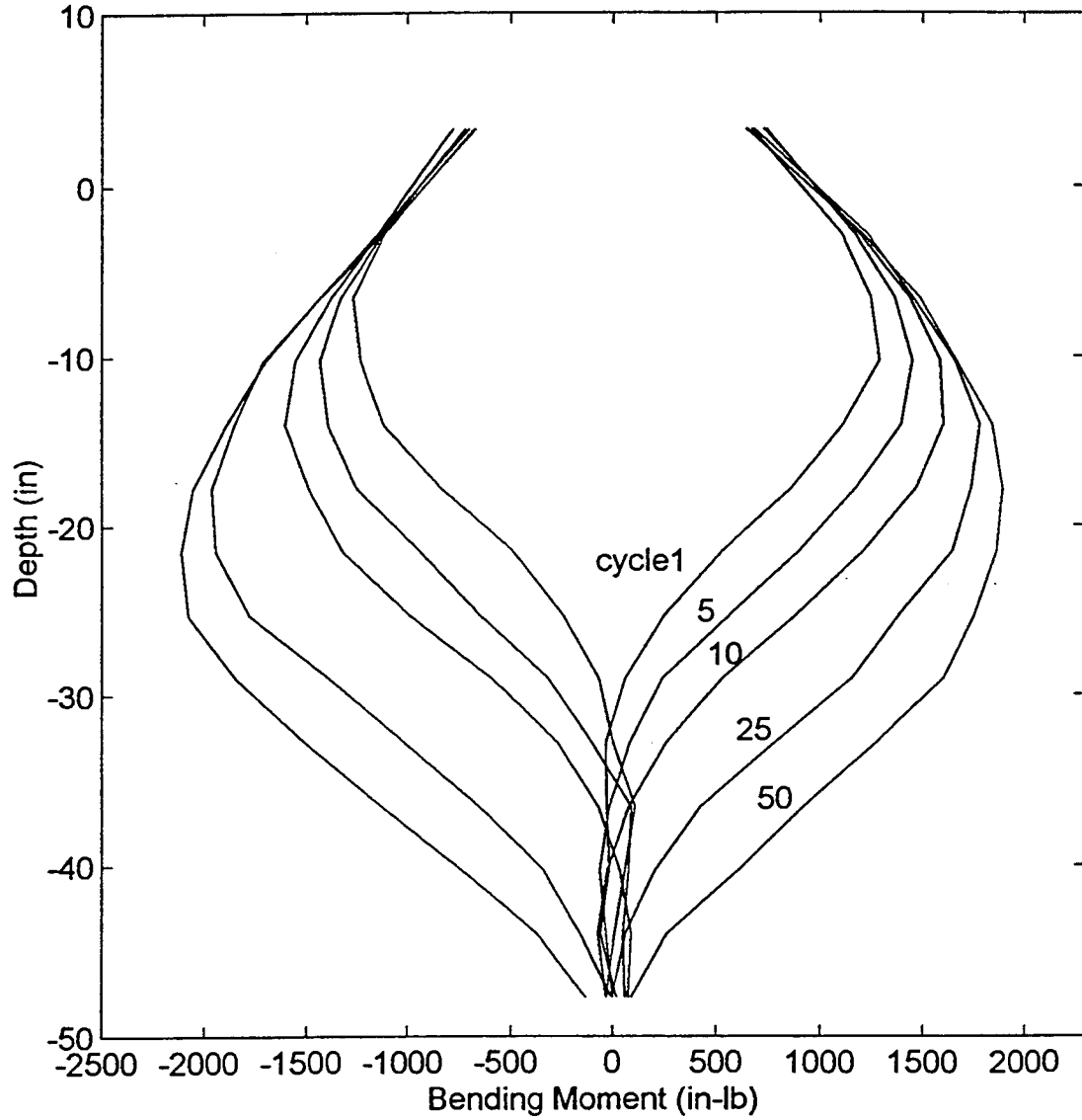
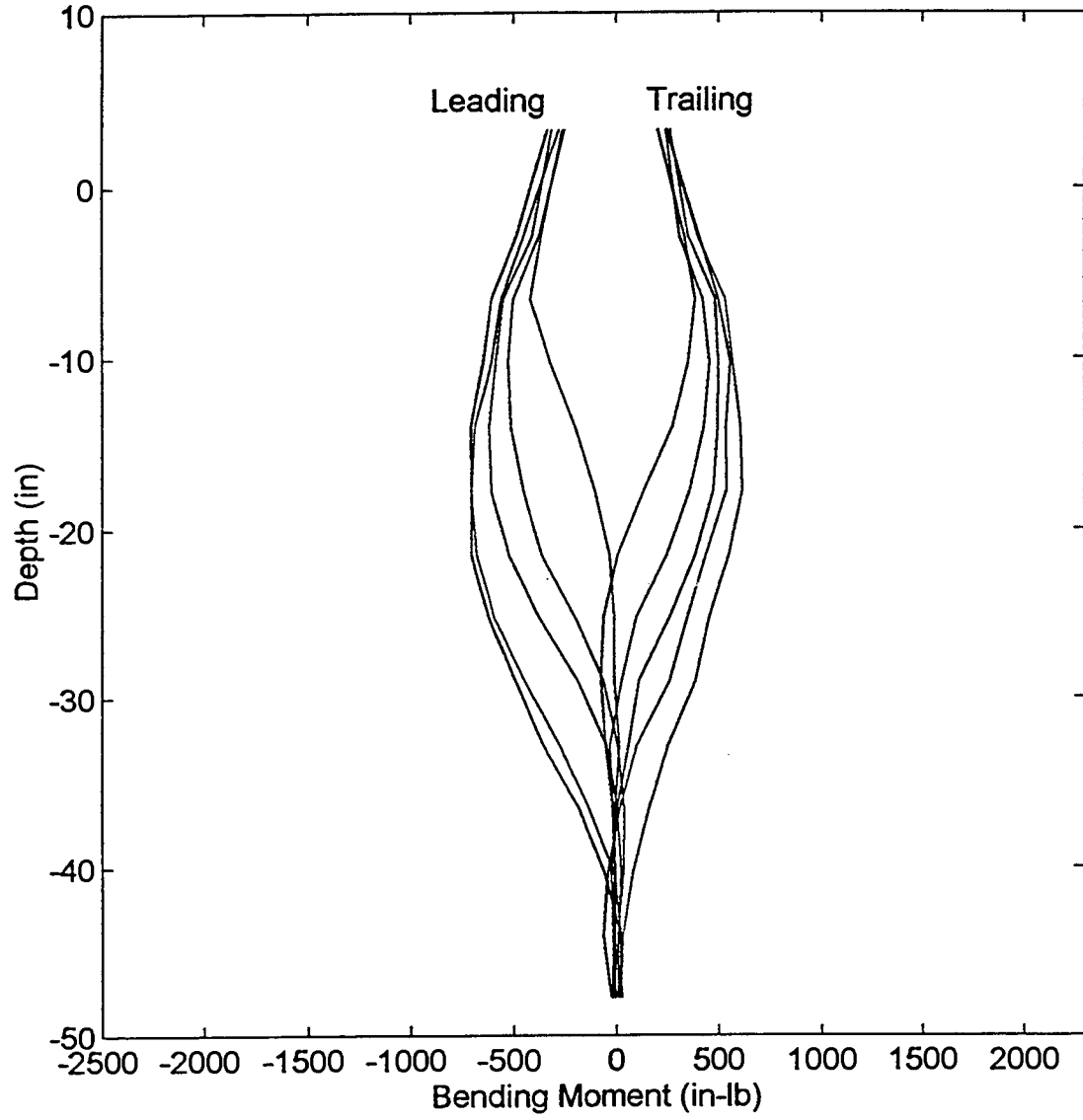


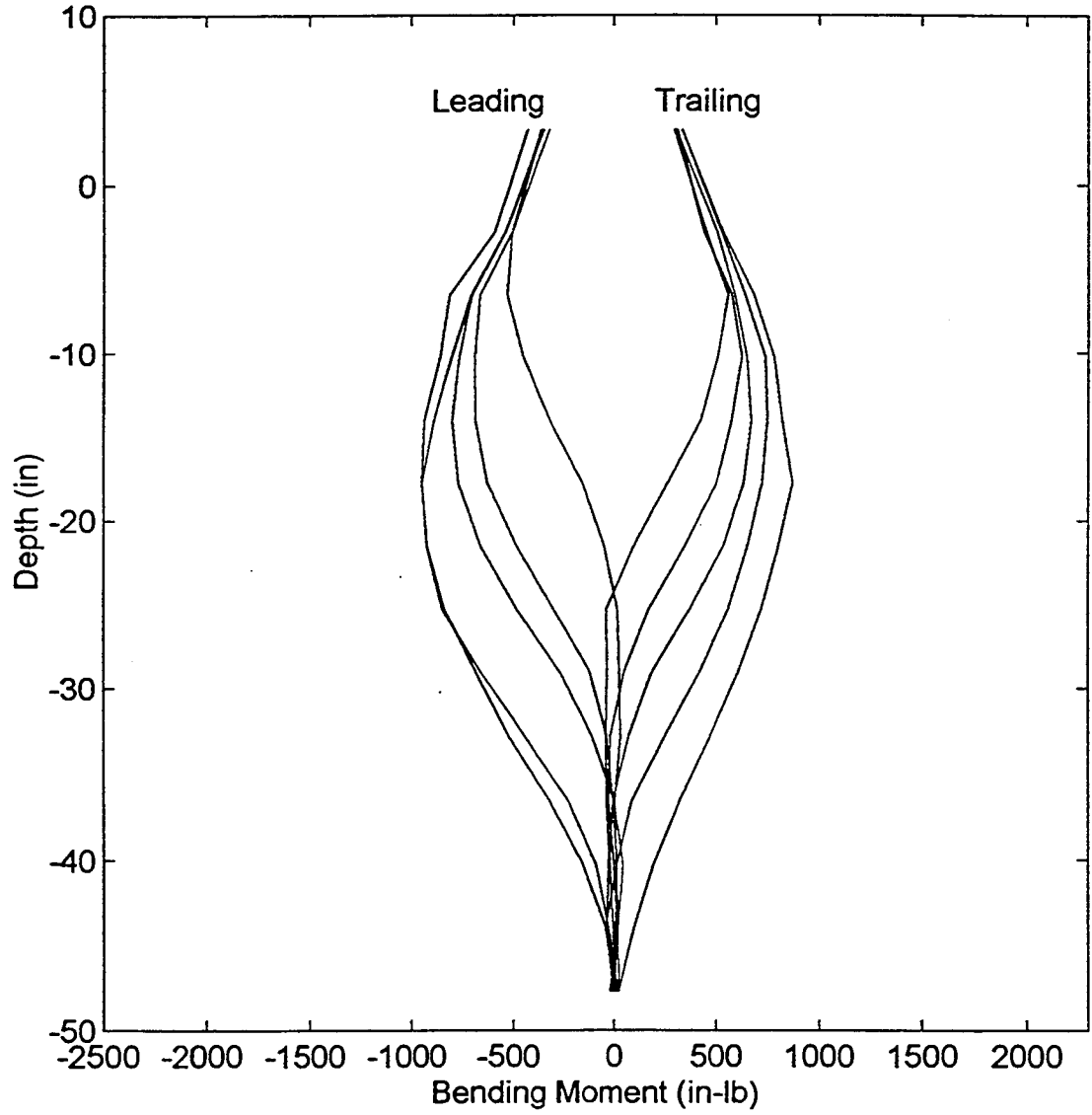
Figure B12. Moment distribution: Second Pile-#2 (next 7 plots).



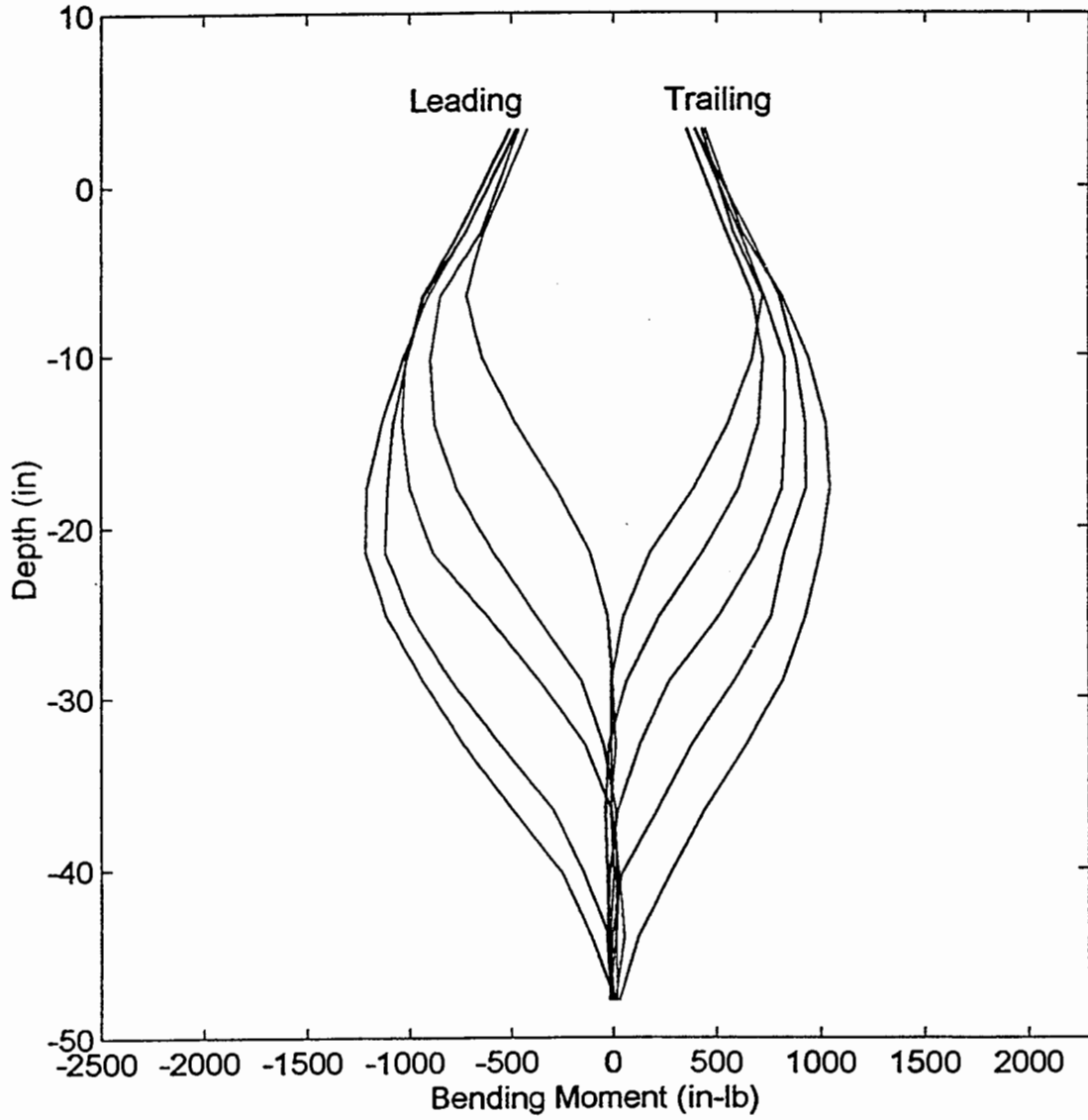
Moment Distribution: Second Pile Left (#2) - Load 150lb



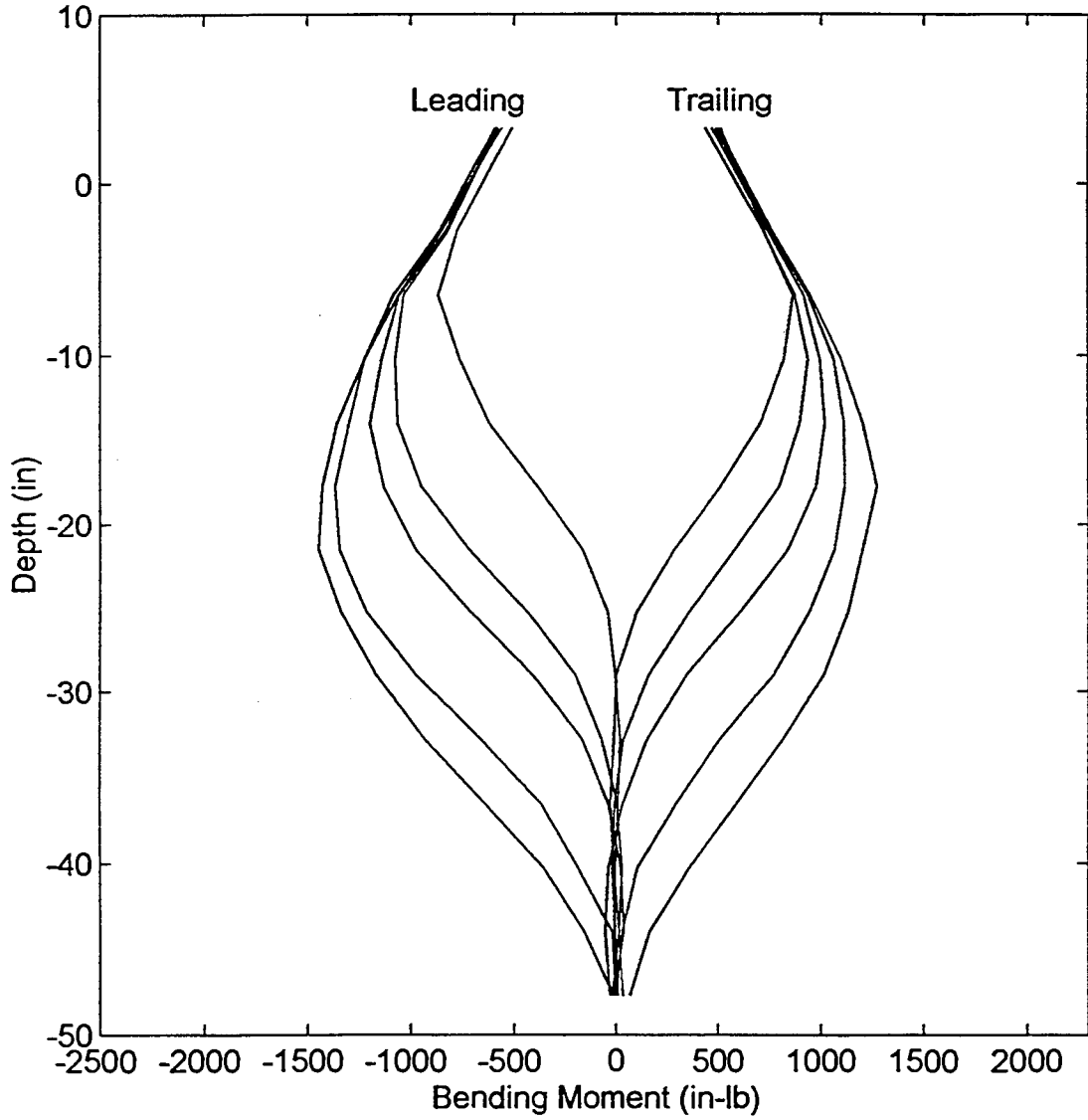
Moment Distribution: Second Pile Left (#2) - Load 200lb



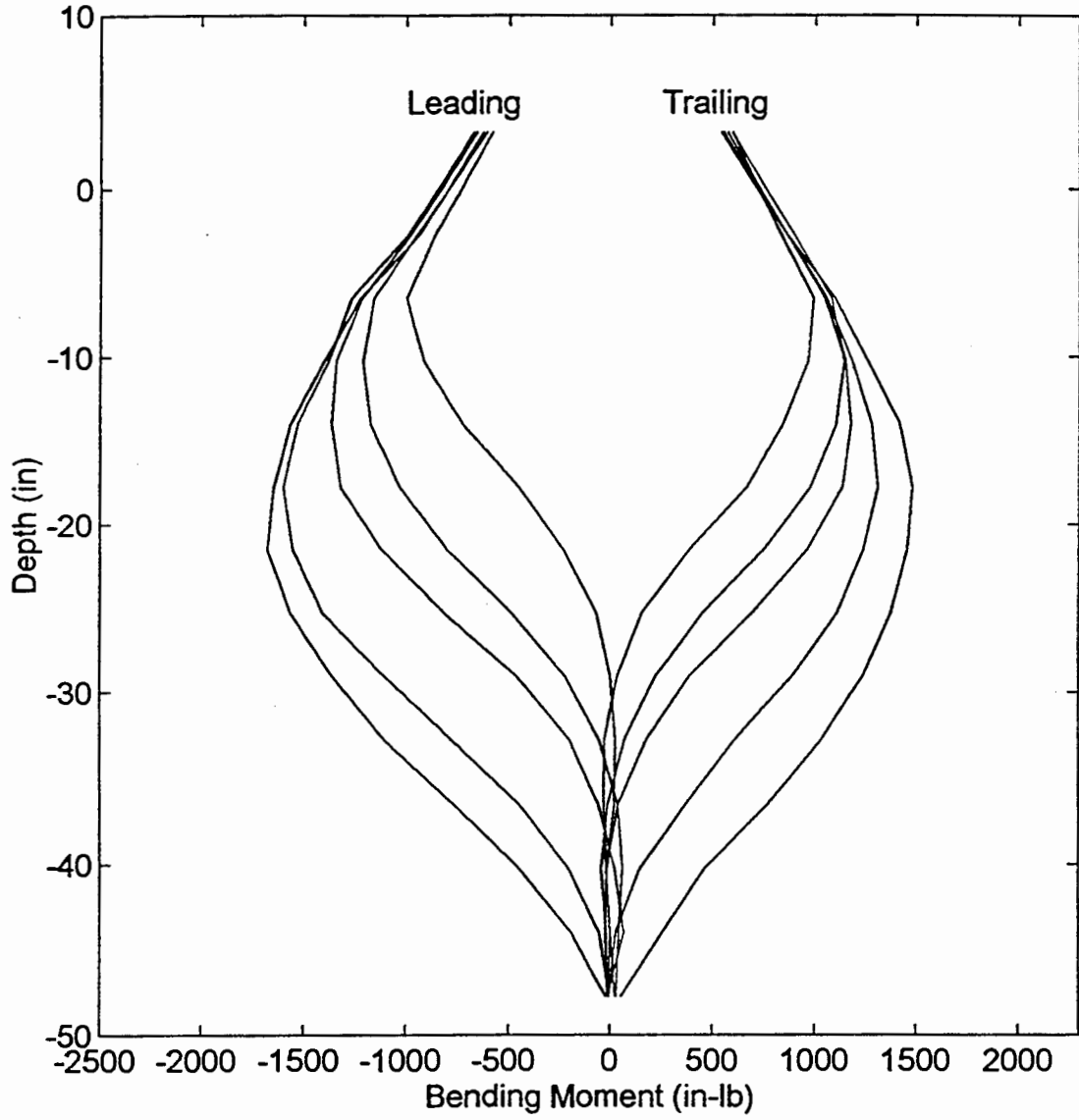
Moment Distribution: Second Pile Left (#2) - Load 250lb



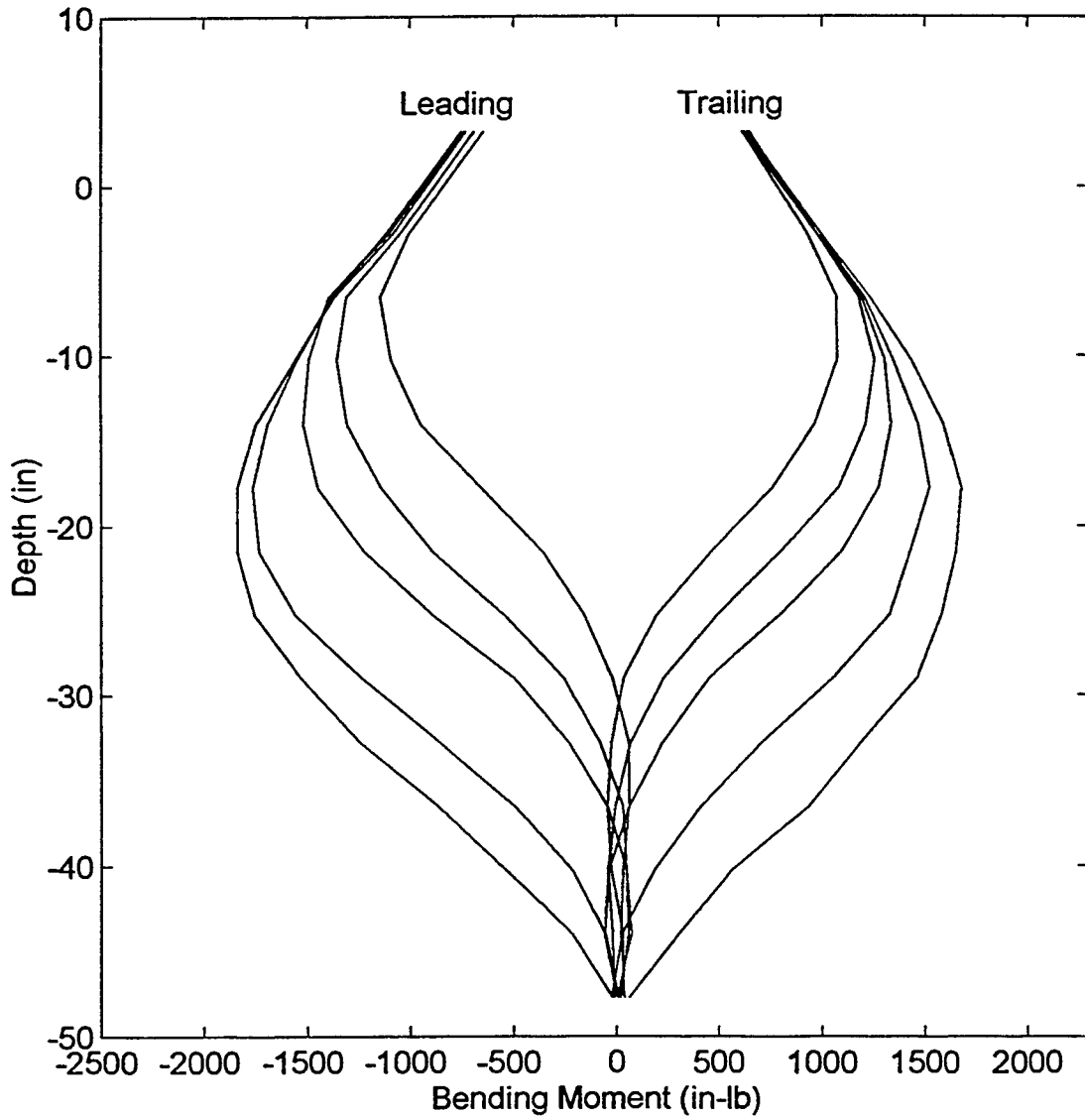
Moment Distribution: Second Pile Left (#2) - Load 300lb



Moment Distribution: Second Pile Left (#2) - Load 350lb



Moment Distribution: Second Pile Left (#2) - Load 400lb



Moment Distribution: Second Pile Left (#2) - Load 450lb

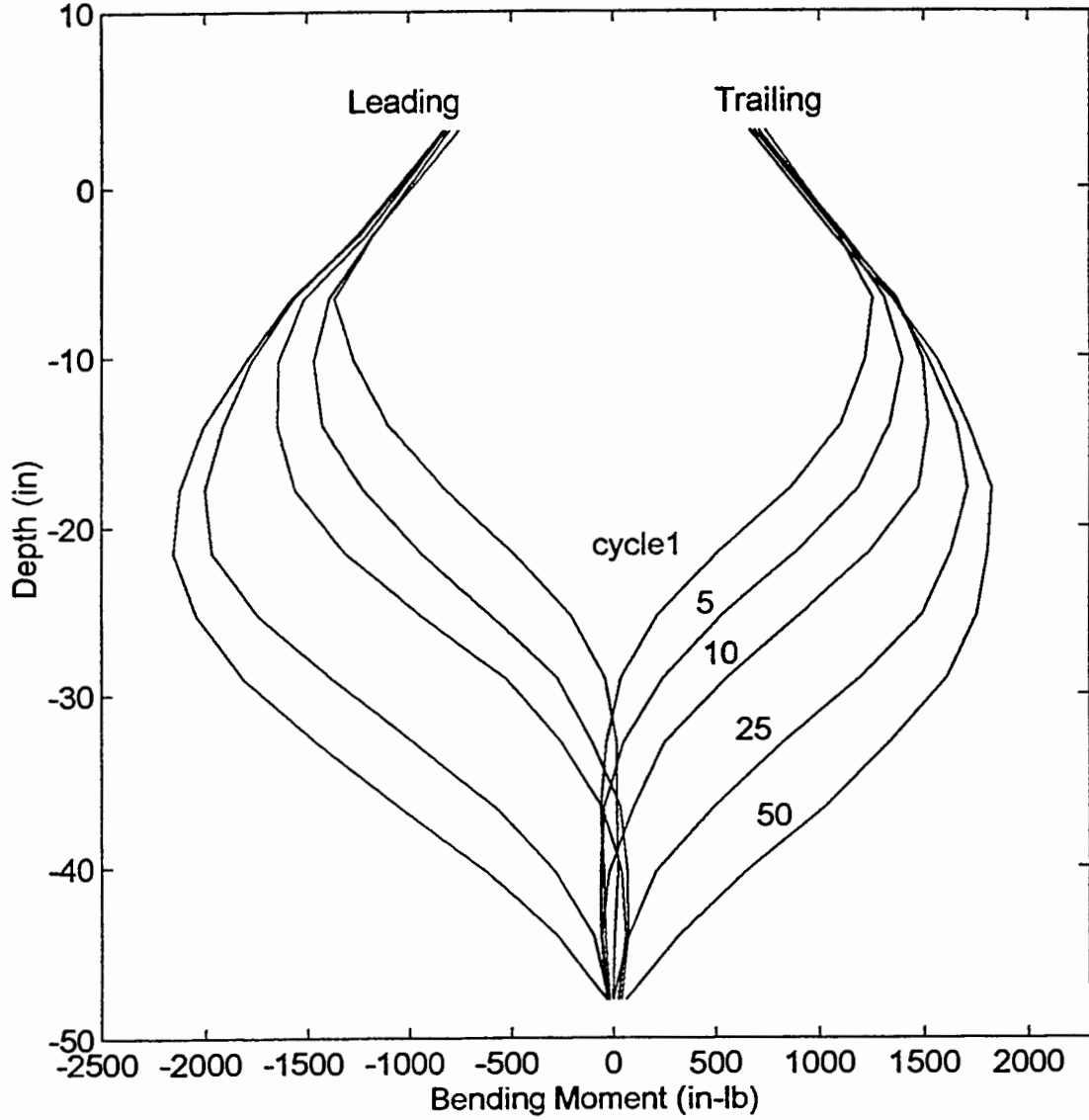
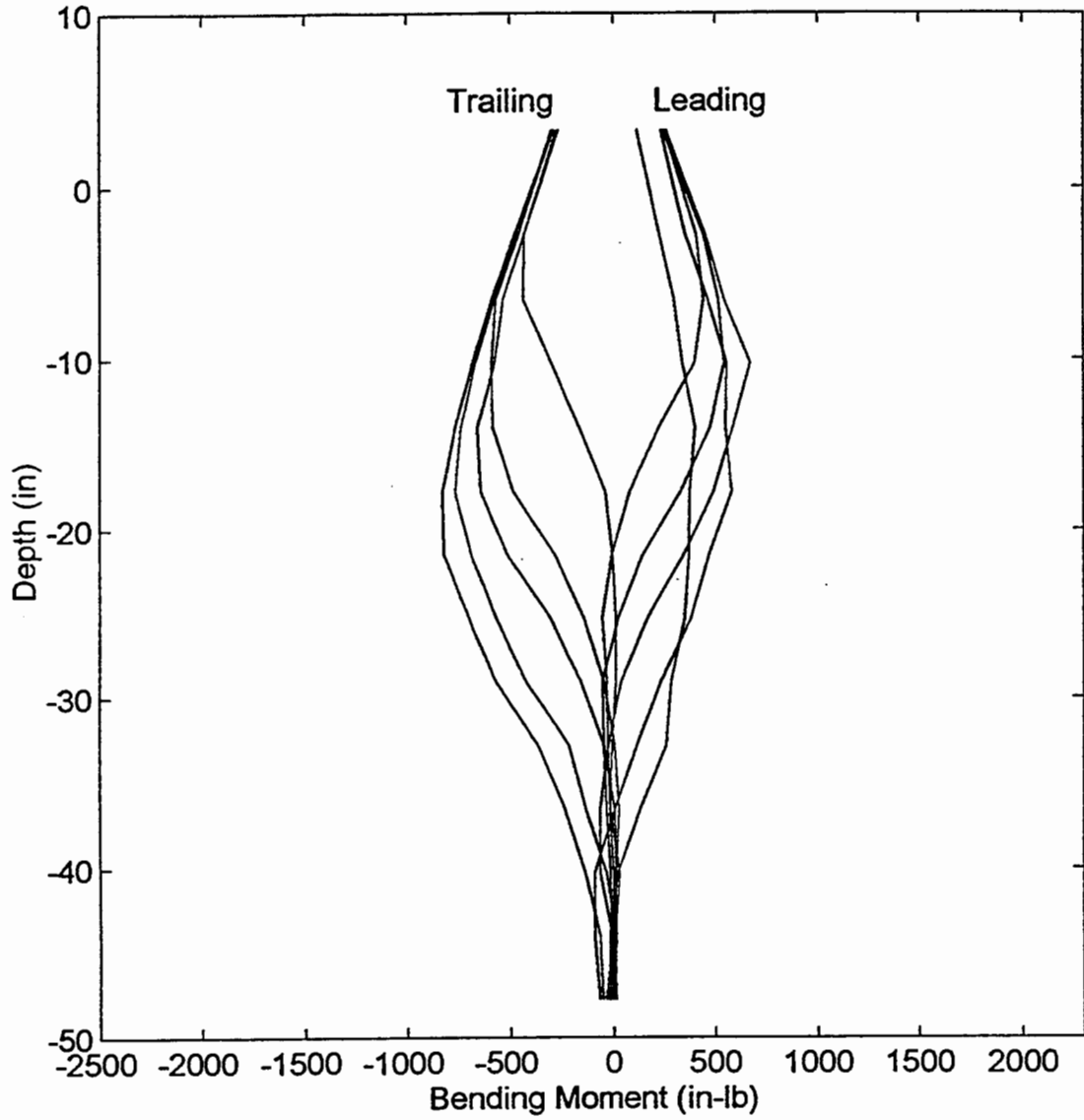


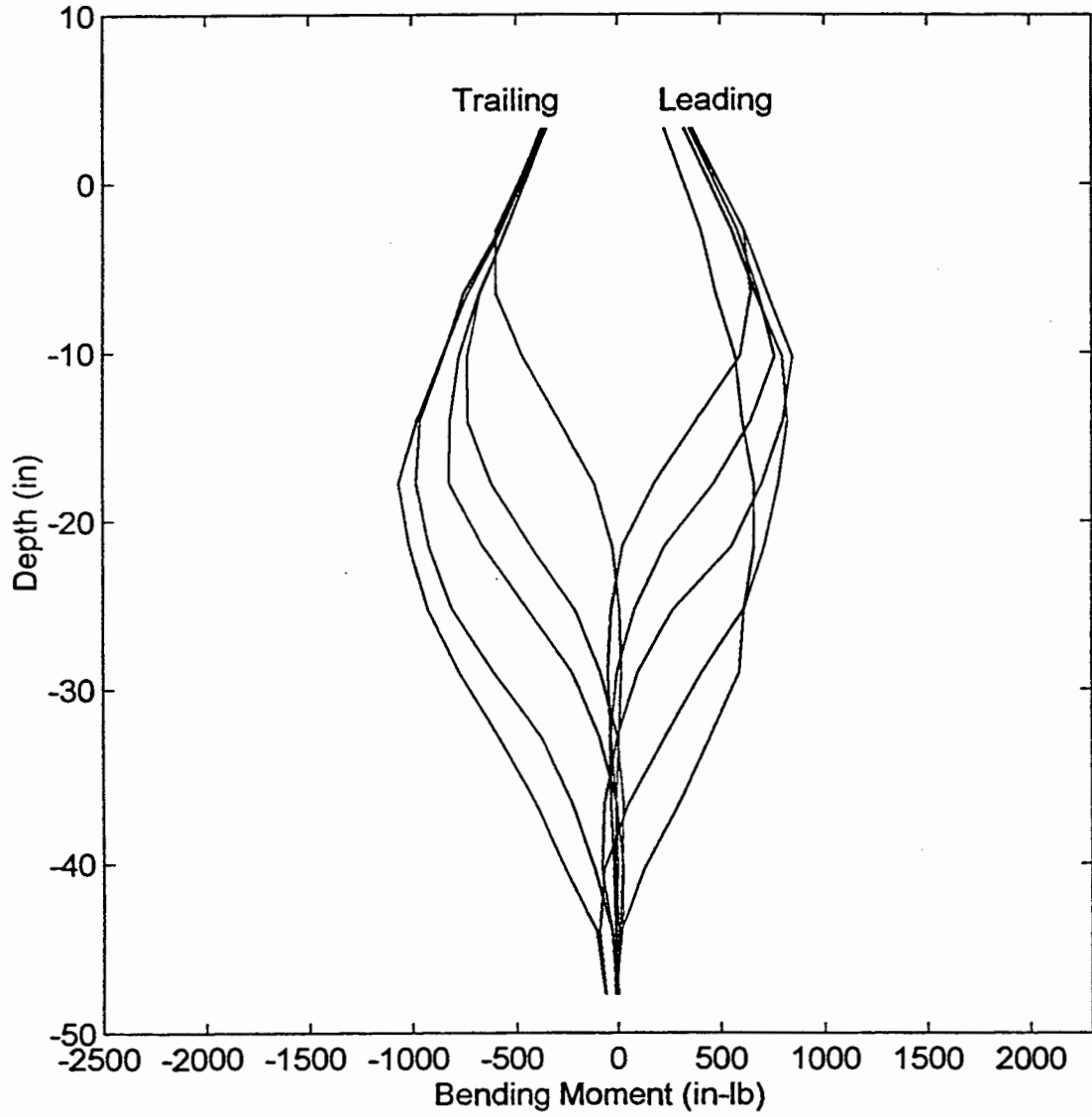
Figure B13. Moment distribution: End Pile-#4 (next 7 plots).



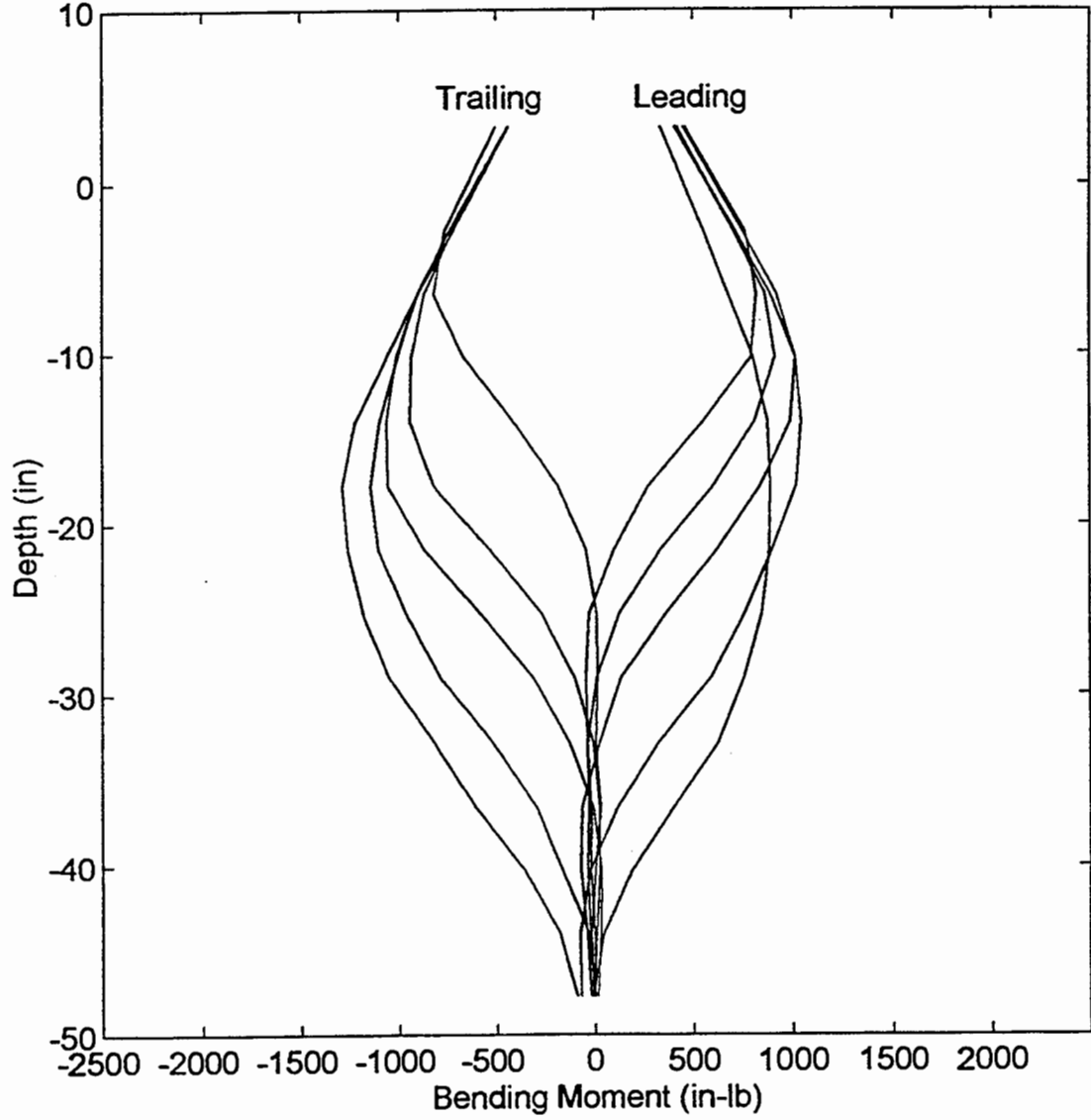
Moment Distribution: End Pile (#4) - Load 150lb



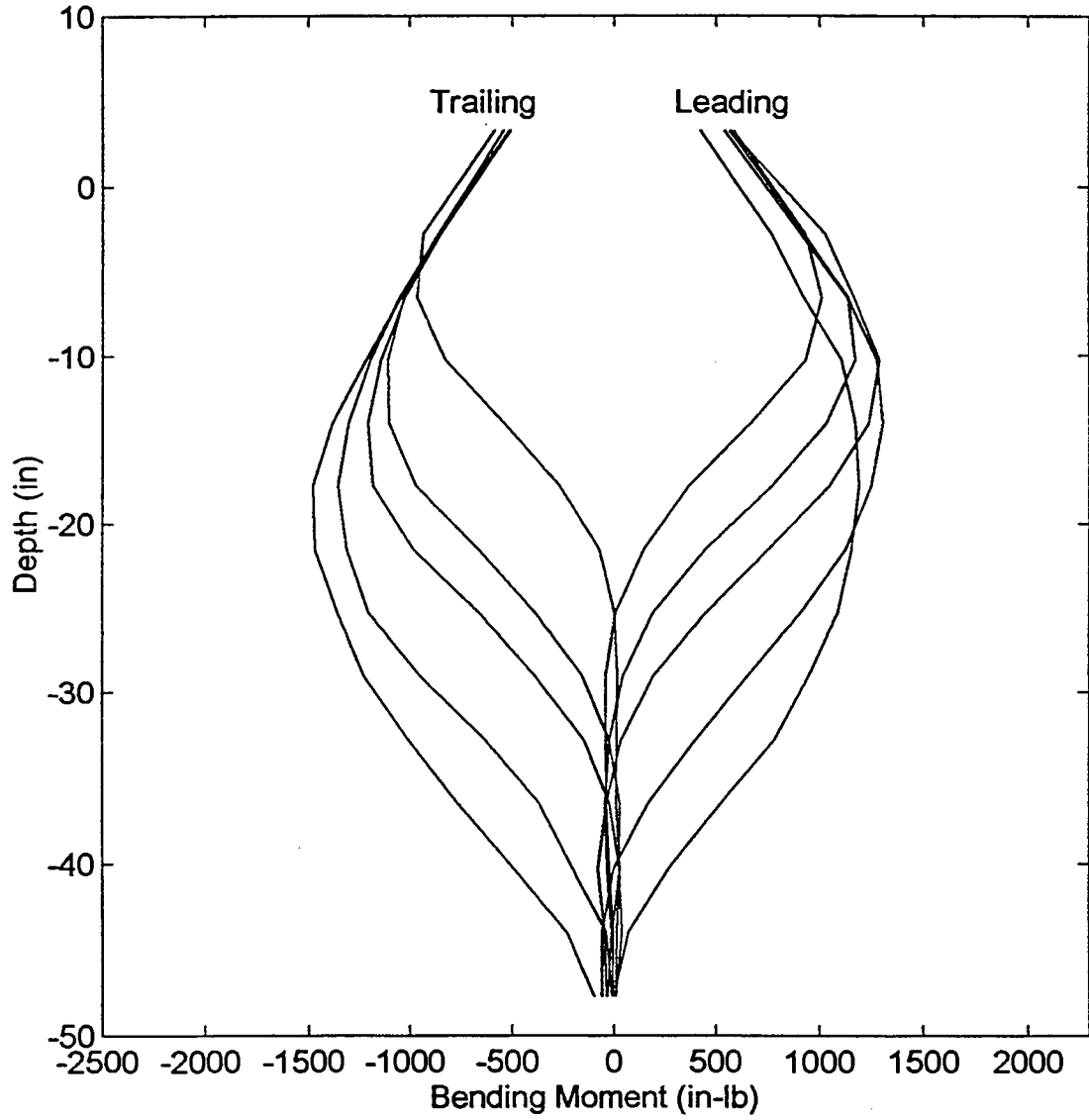
Moment Distribution: End Pile (#4) - Load 200lb



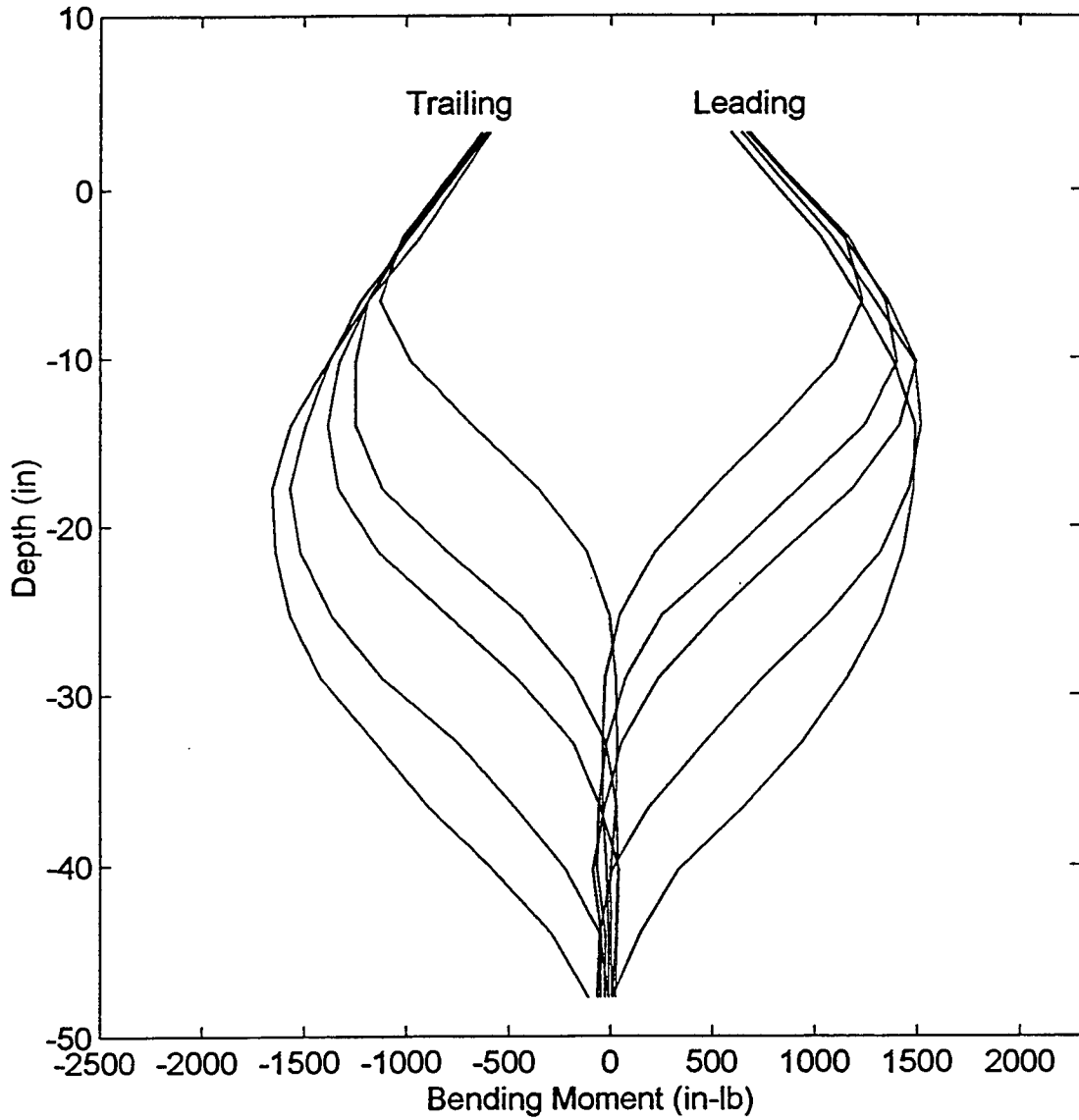
Moment Distribution: End Pile (#4) - Load 250lb



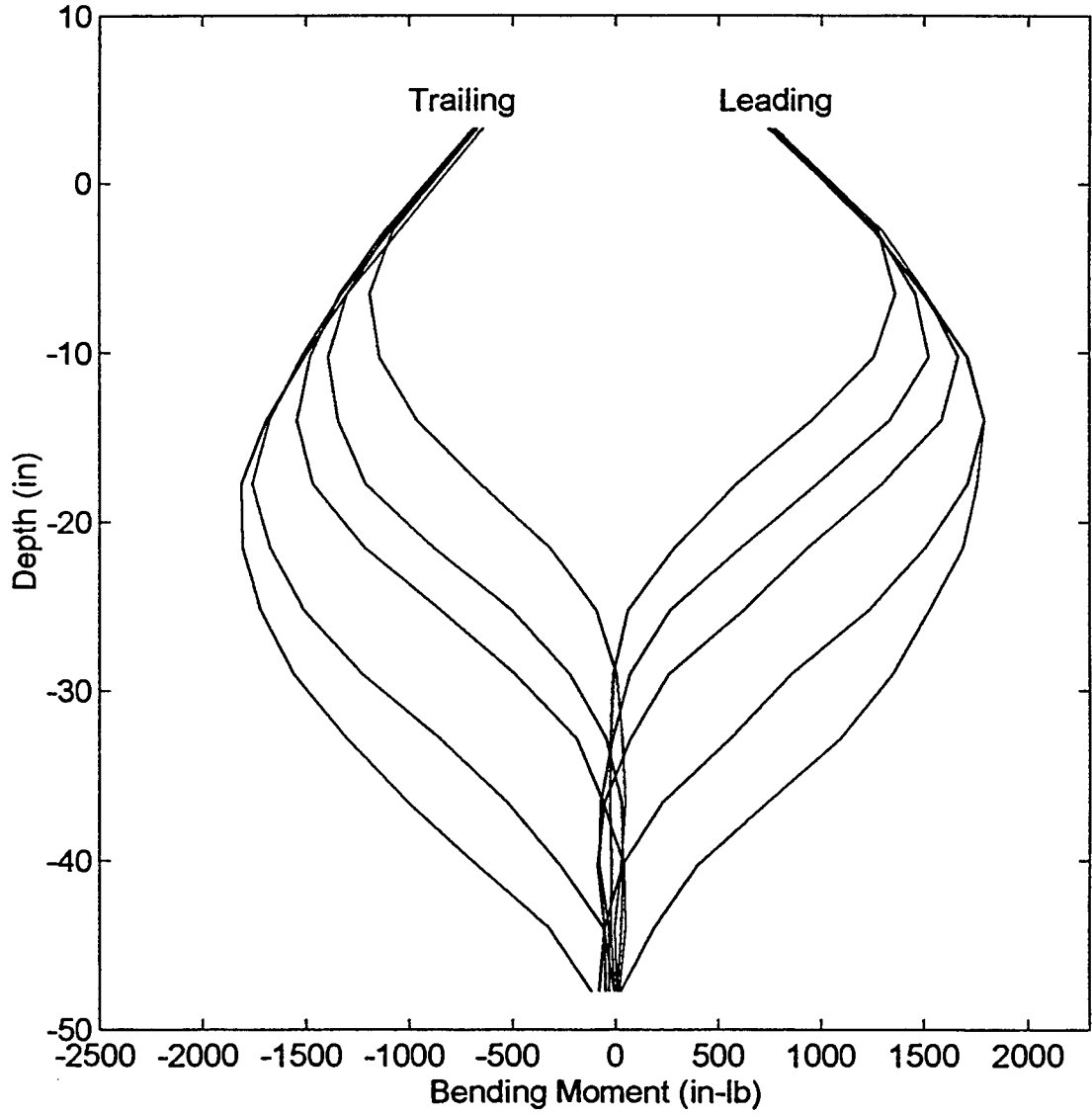
Moment Distribution: End Pile (#4) - Load 300lb



Moment Distribution: End Pile (#4) - Load 350lb



Moment Distribution: End Pile (#4) - Load 400lb



Moment Distribution: End Pile (#4) - Load 450lb

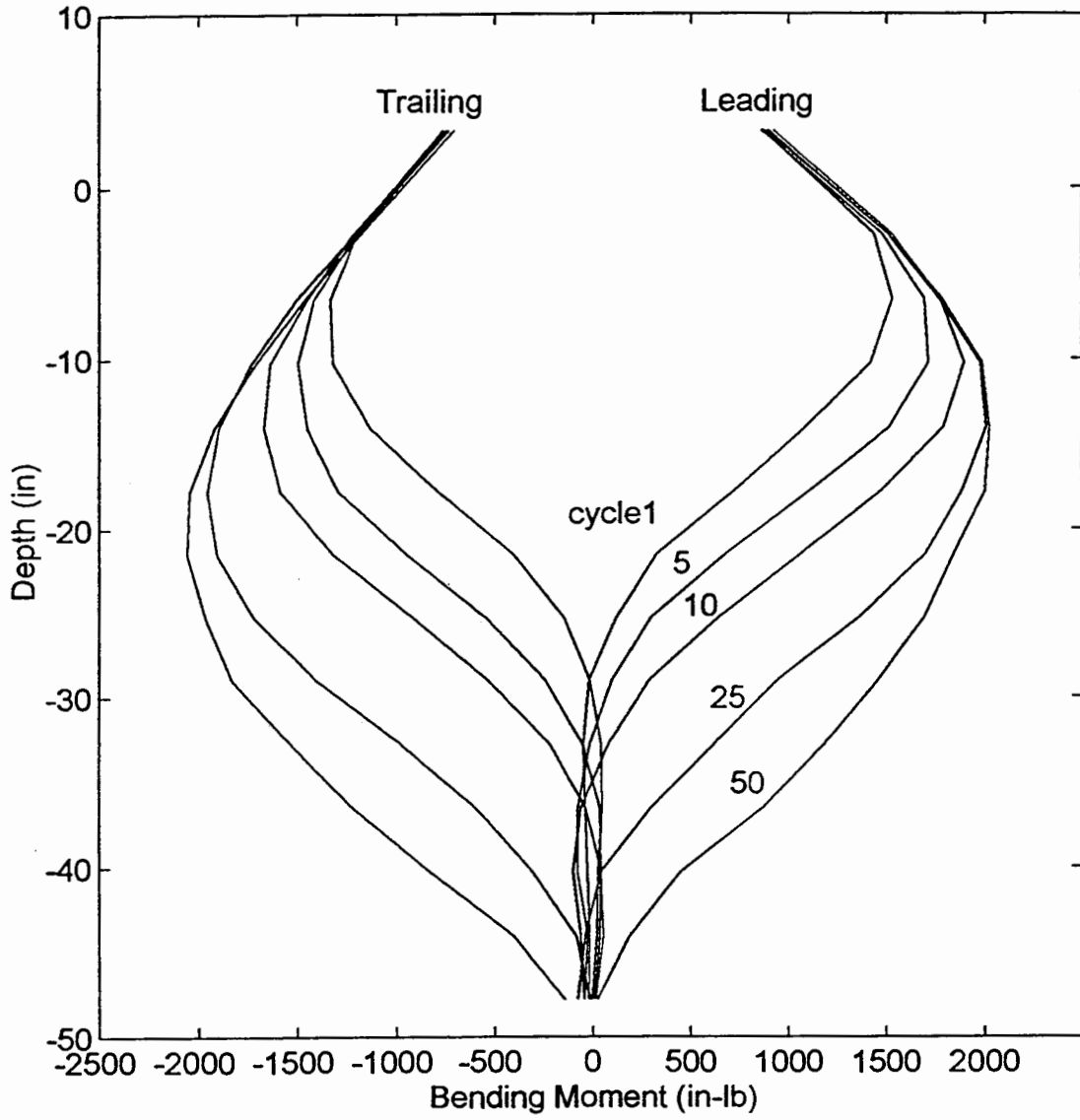
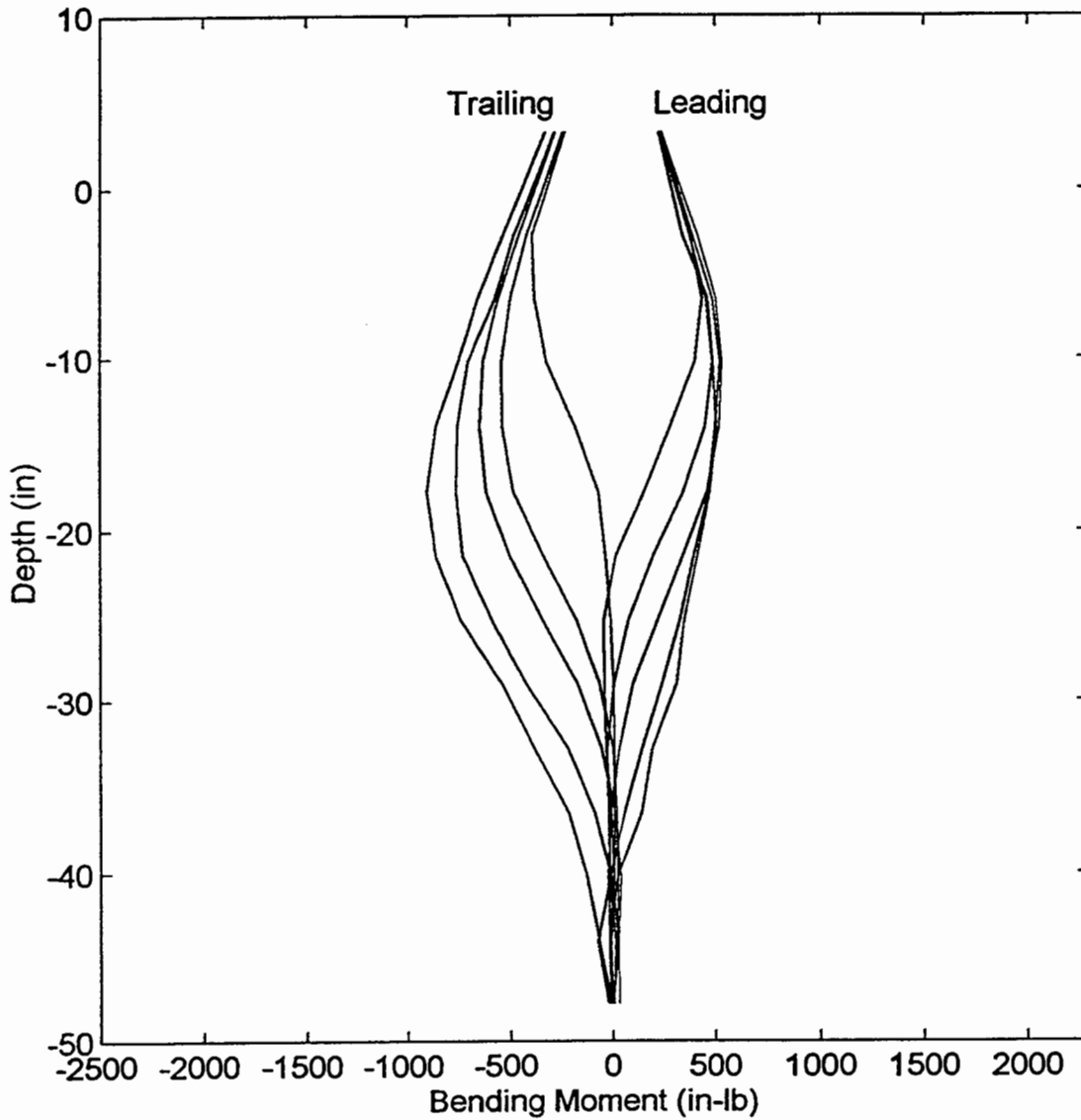


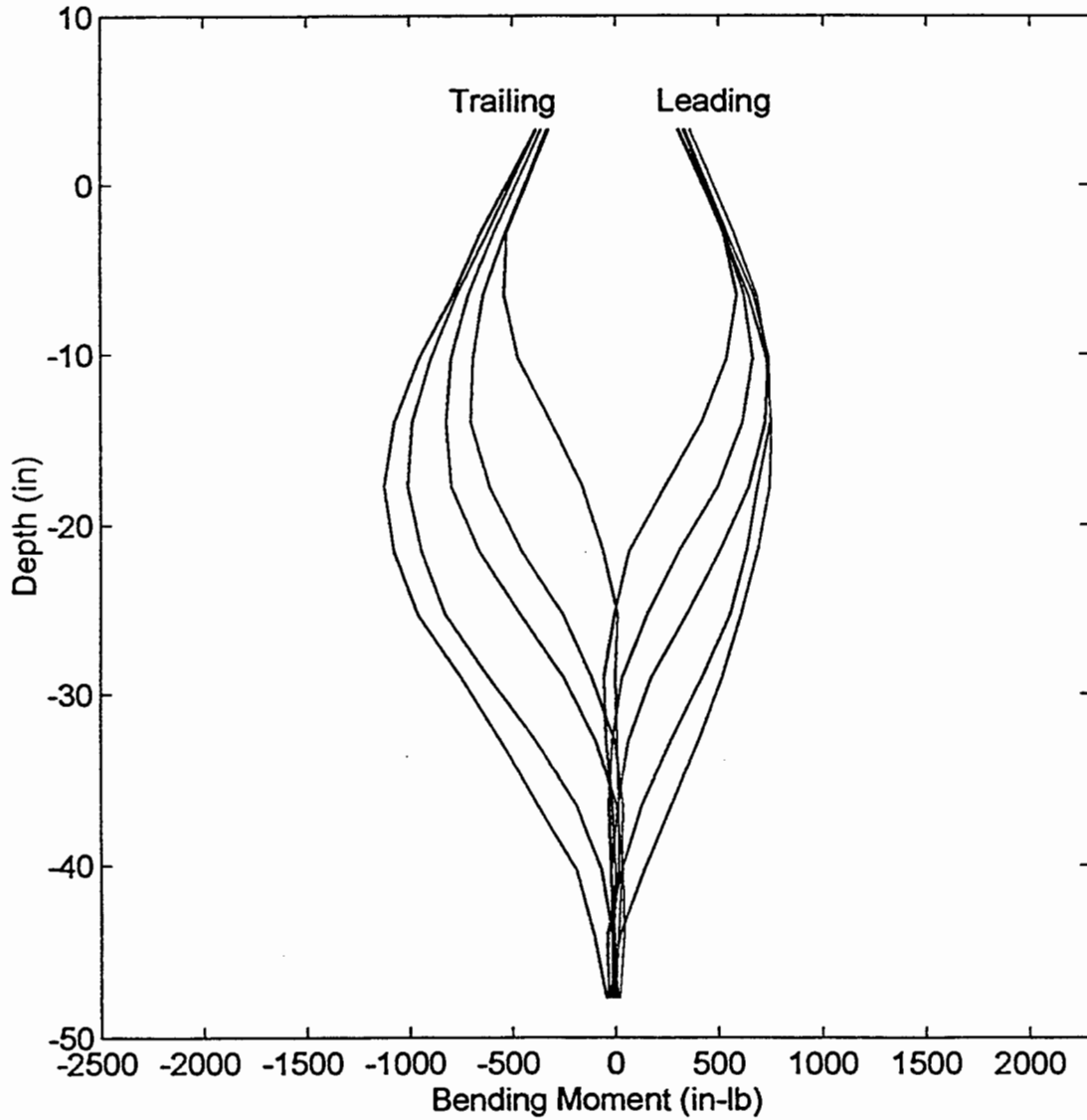
Figure B14. Moment distribution: Second Pile-#5 (next 7 plots).



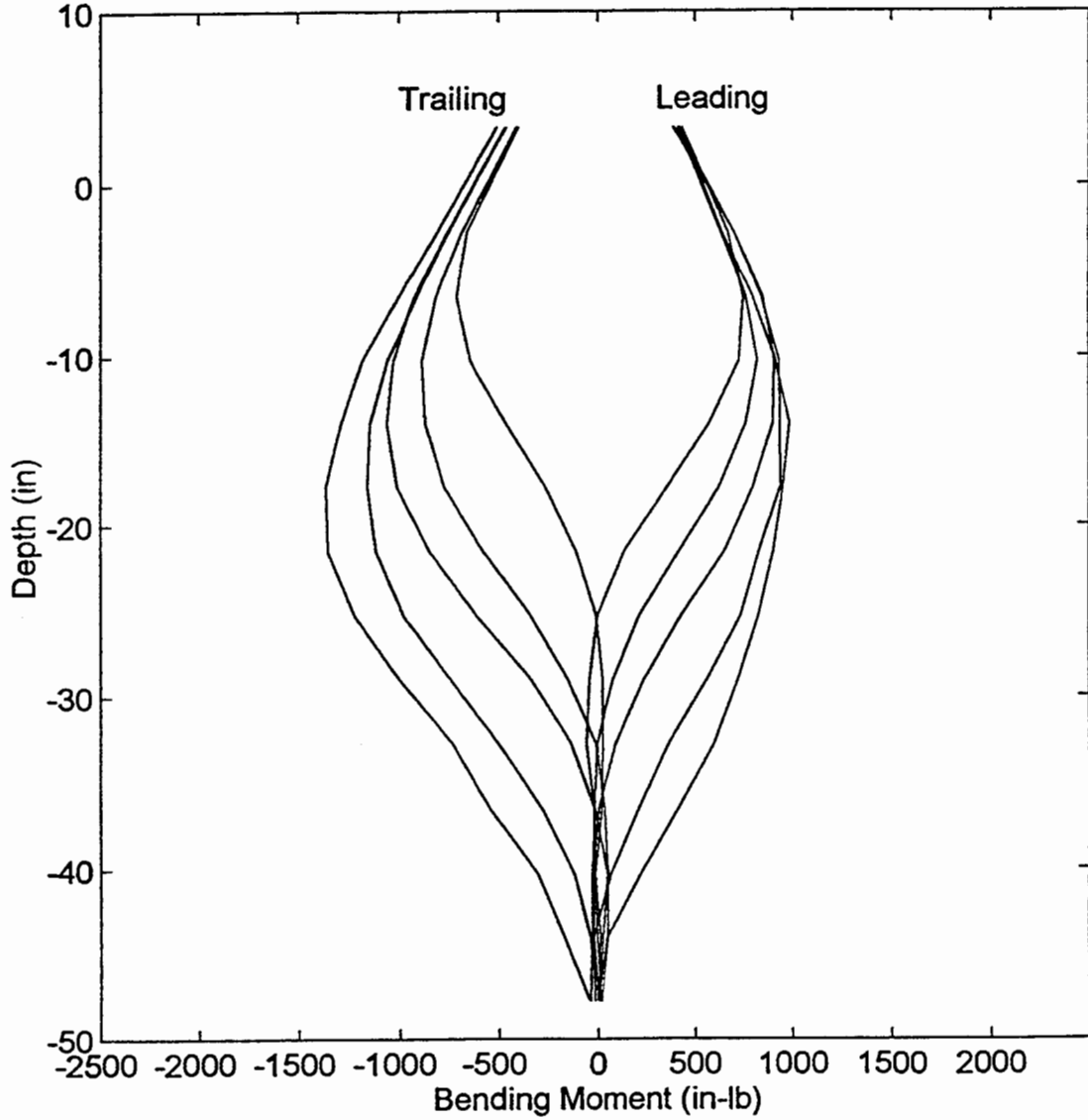
Moment Distribution: Second Pile Right (#5) - Load 150lb



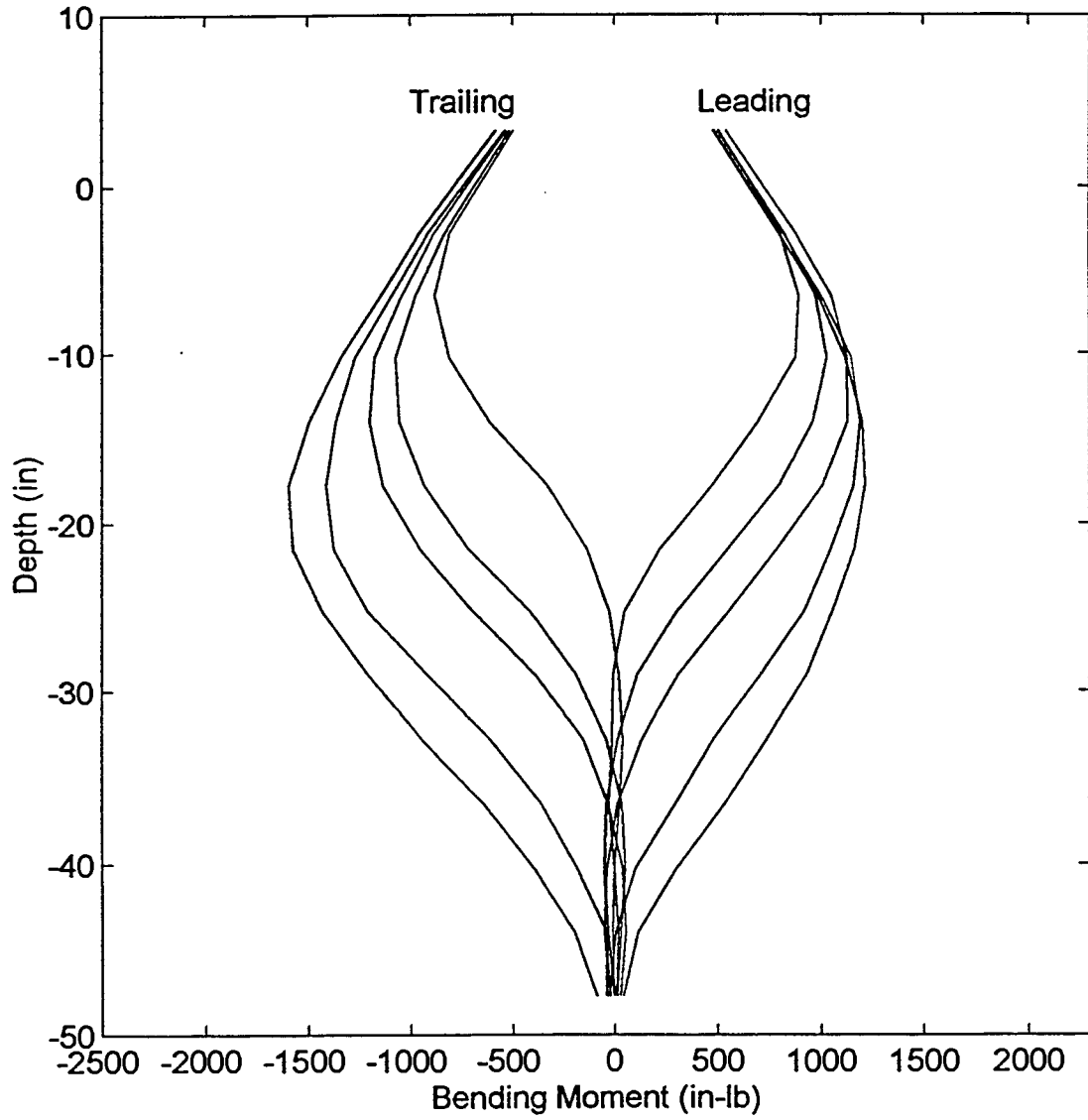
Moment Distribution: Second Pile Right (#5) - Load 200lb



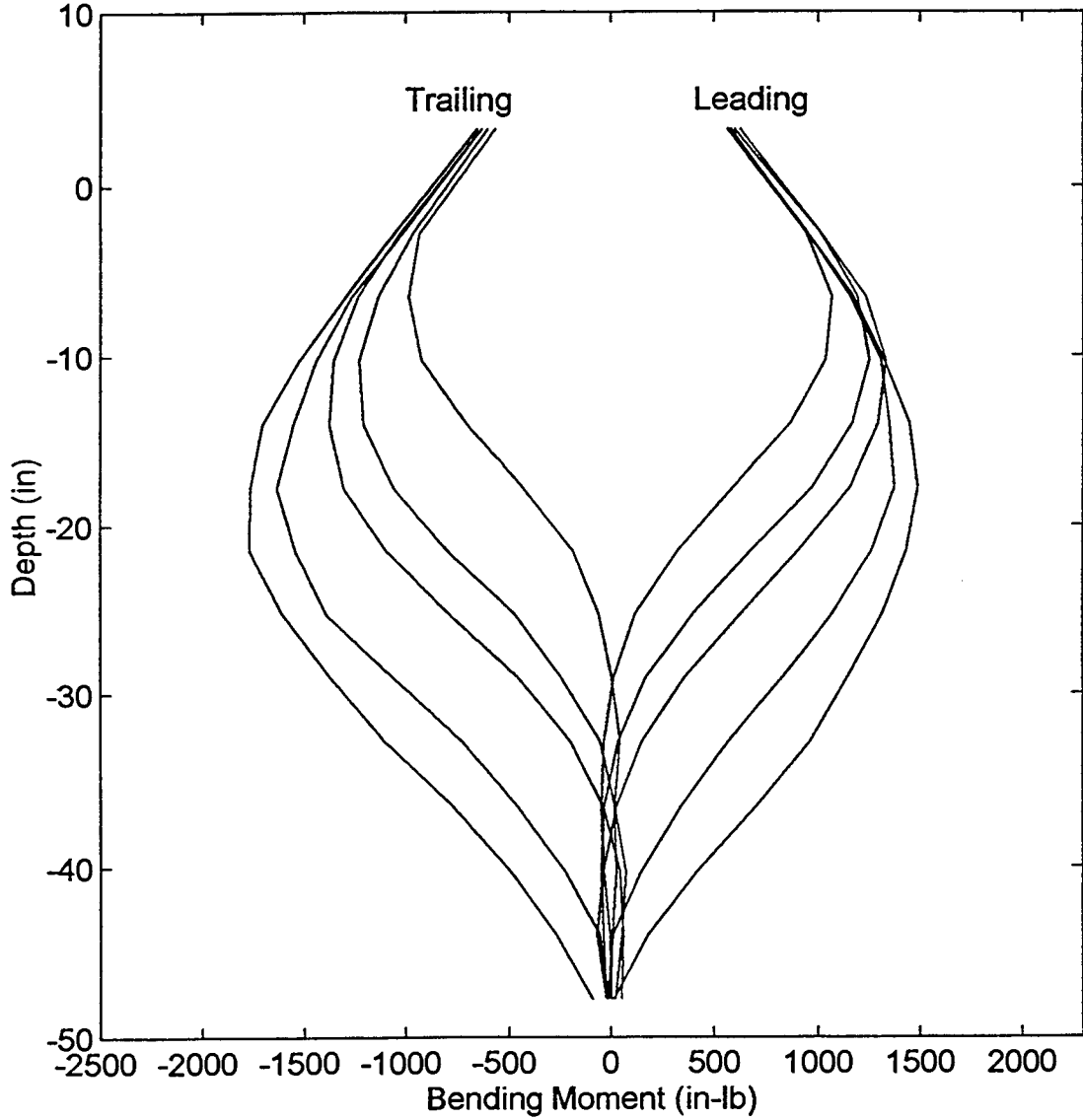
Moment Distribution: Second Pile Right (#5) - Load 250lb



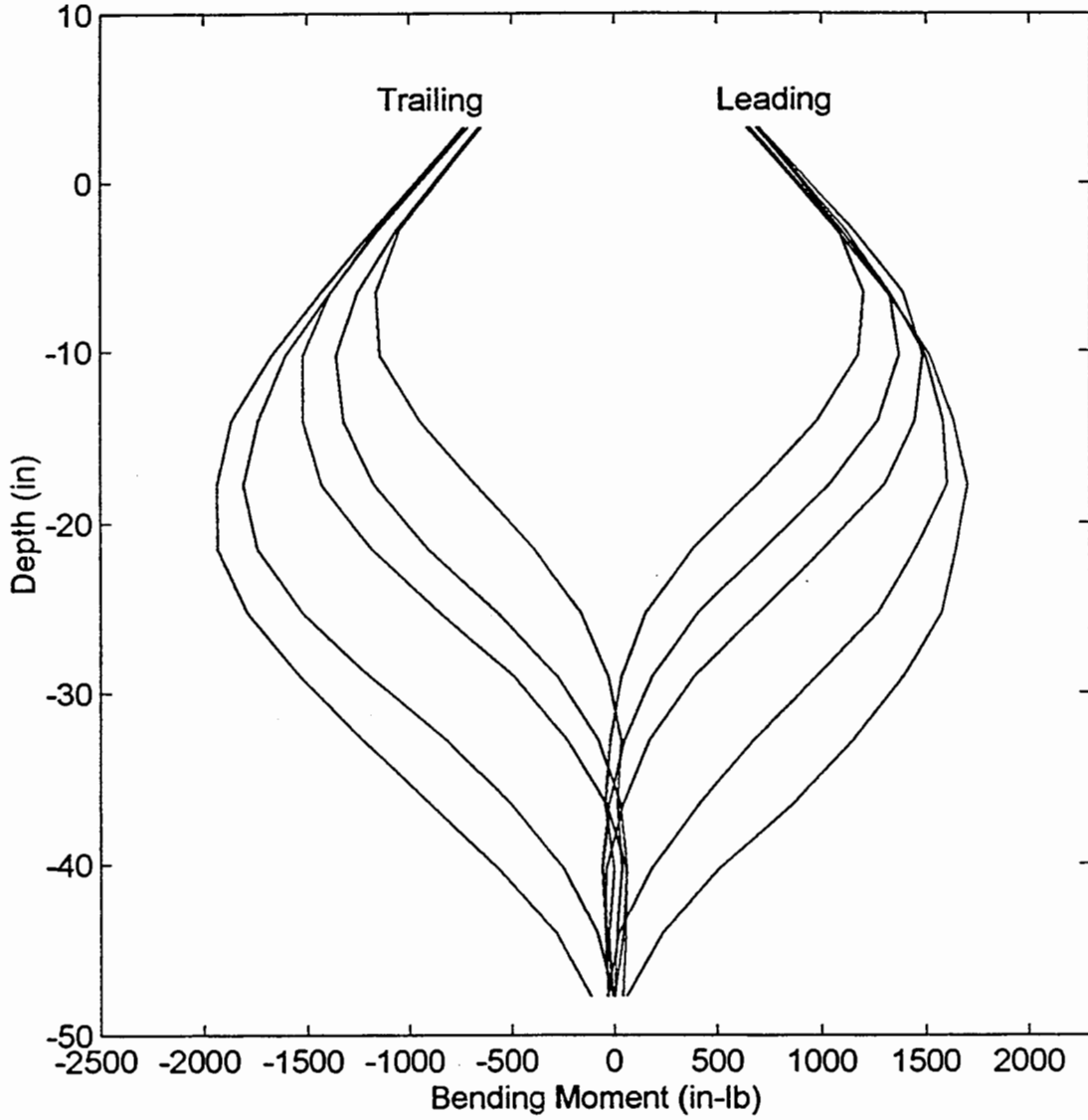
Moment Distribution: Second Pile Right (#5) - Load 300lb



Moment Distribution: Second Pile Right (#5) - Load 350lb



Moment Distribution: Second Pile Right (#5) - Load 400lb



Moment Distribution: Second Pile Right (#5) - Load 450lb

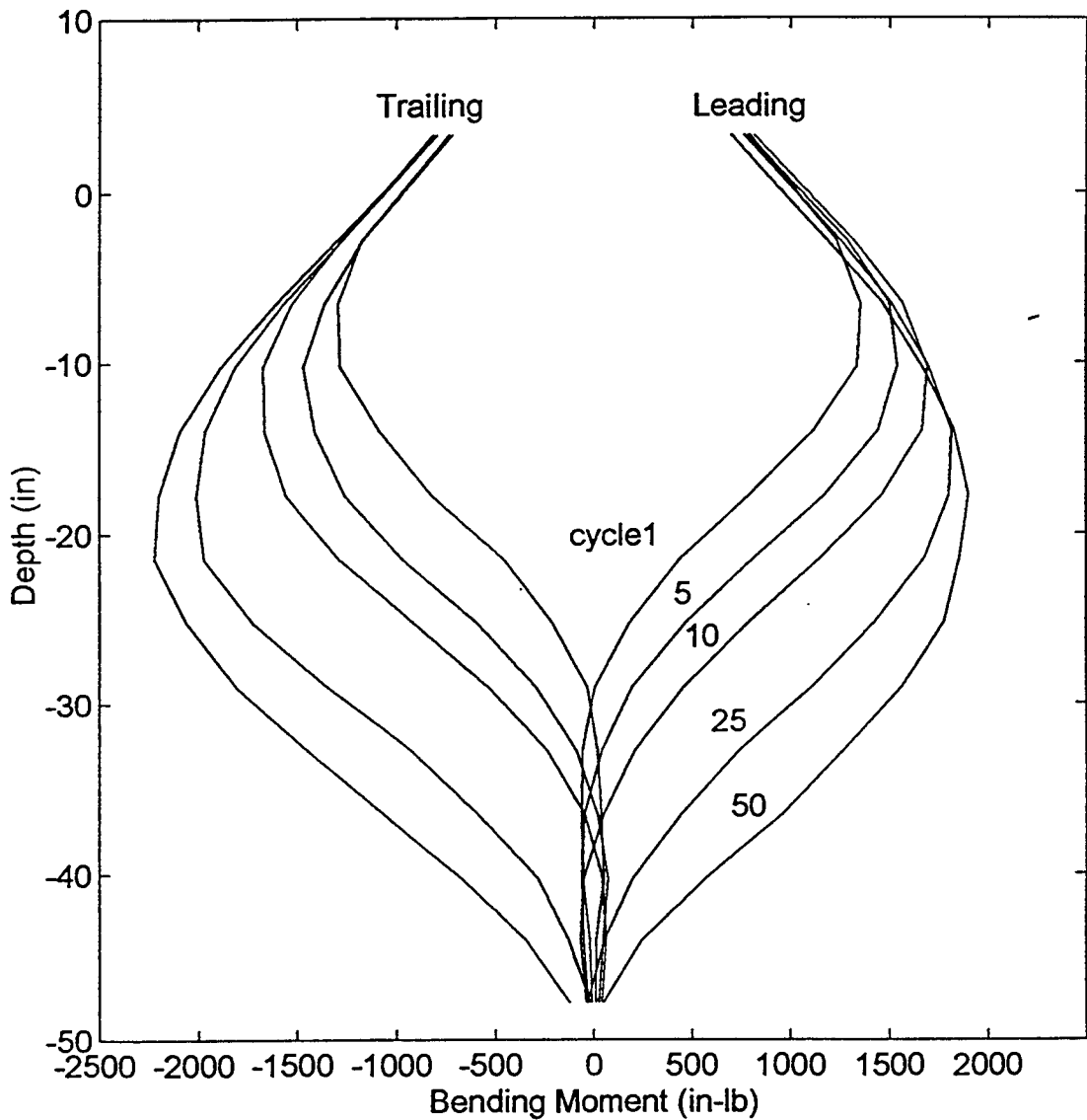
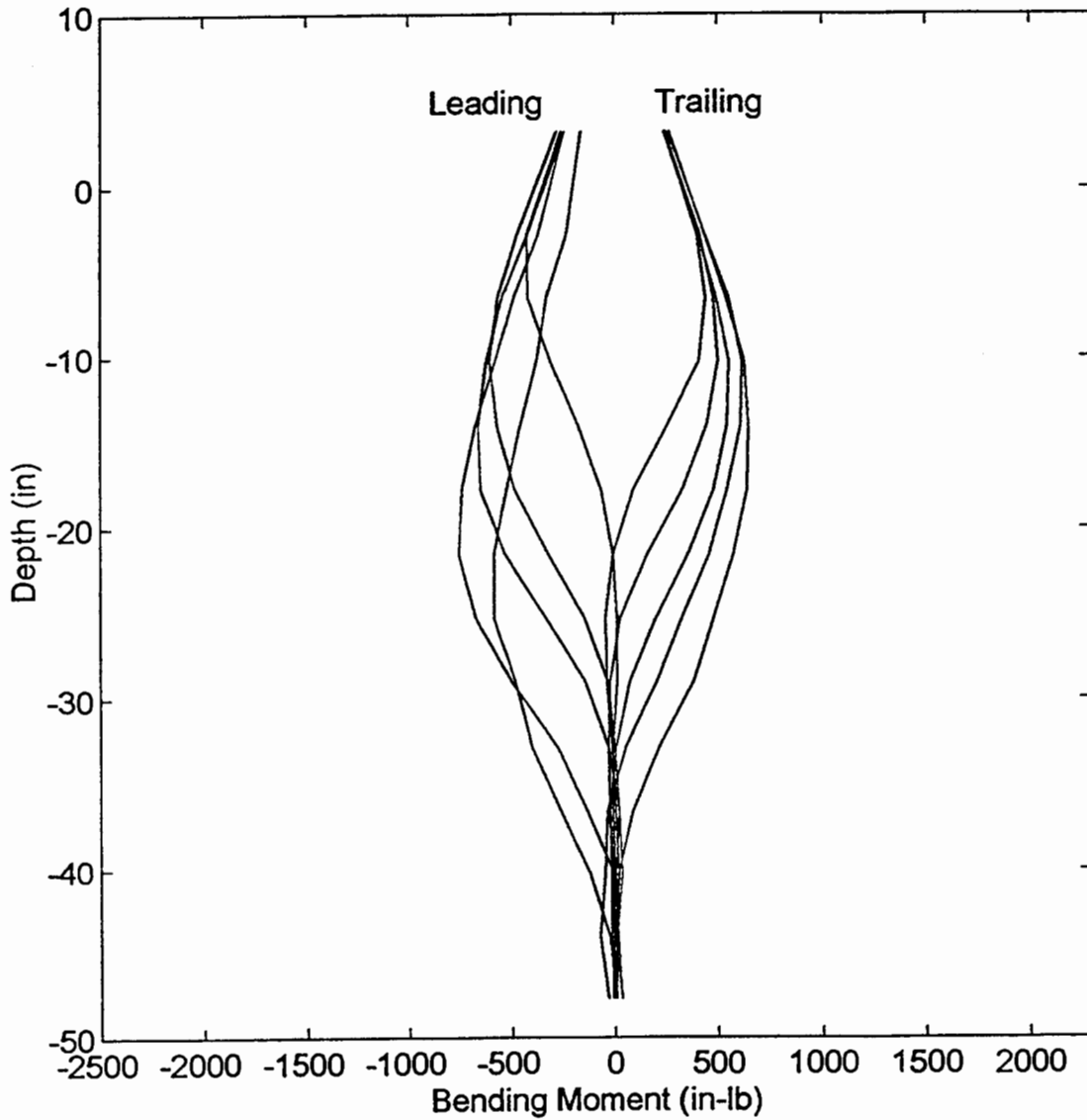


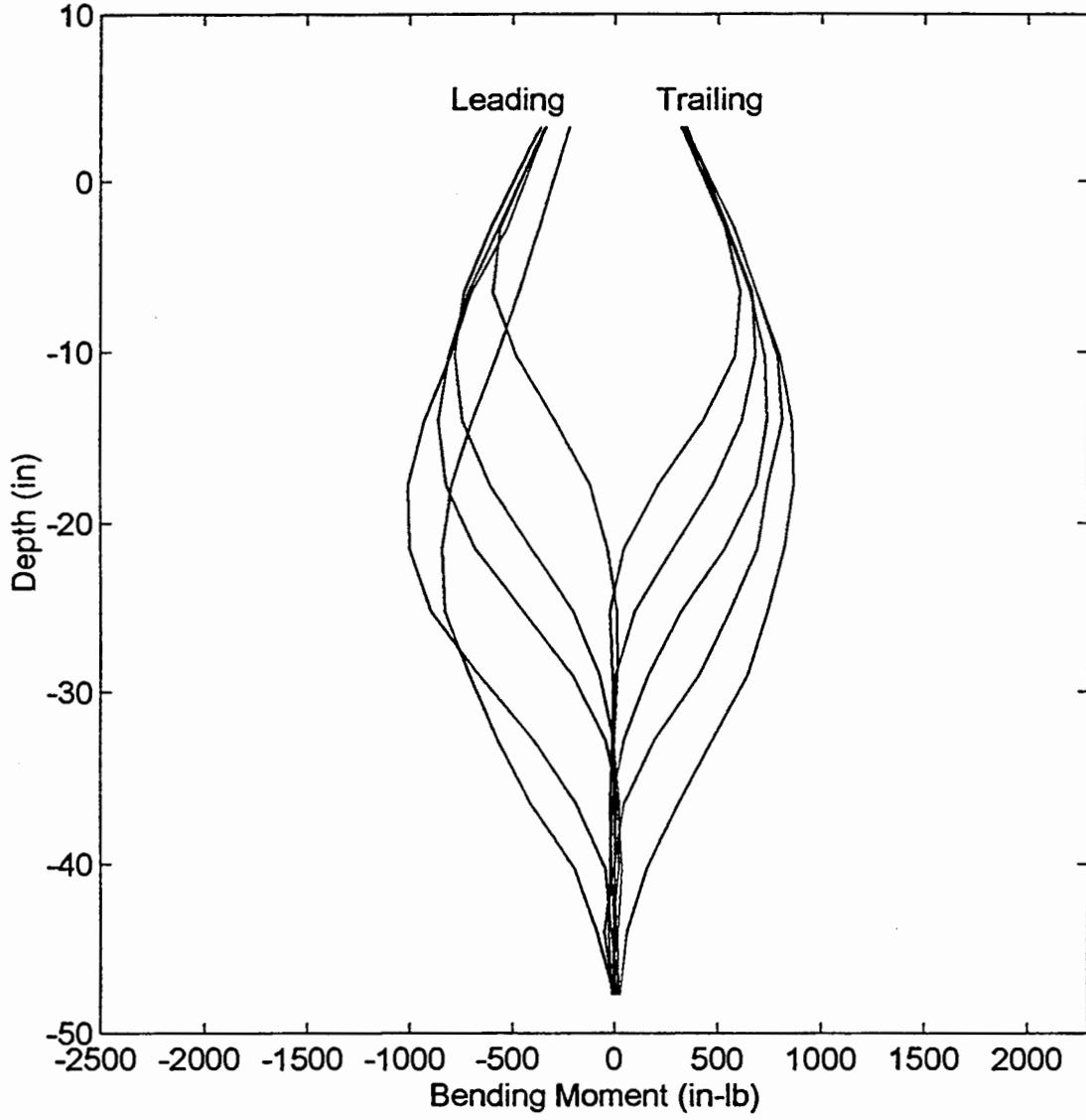
Figure B15. Moment distribution: End Pile-#6 (next 7 pages).



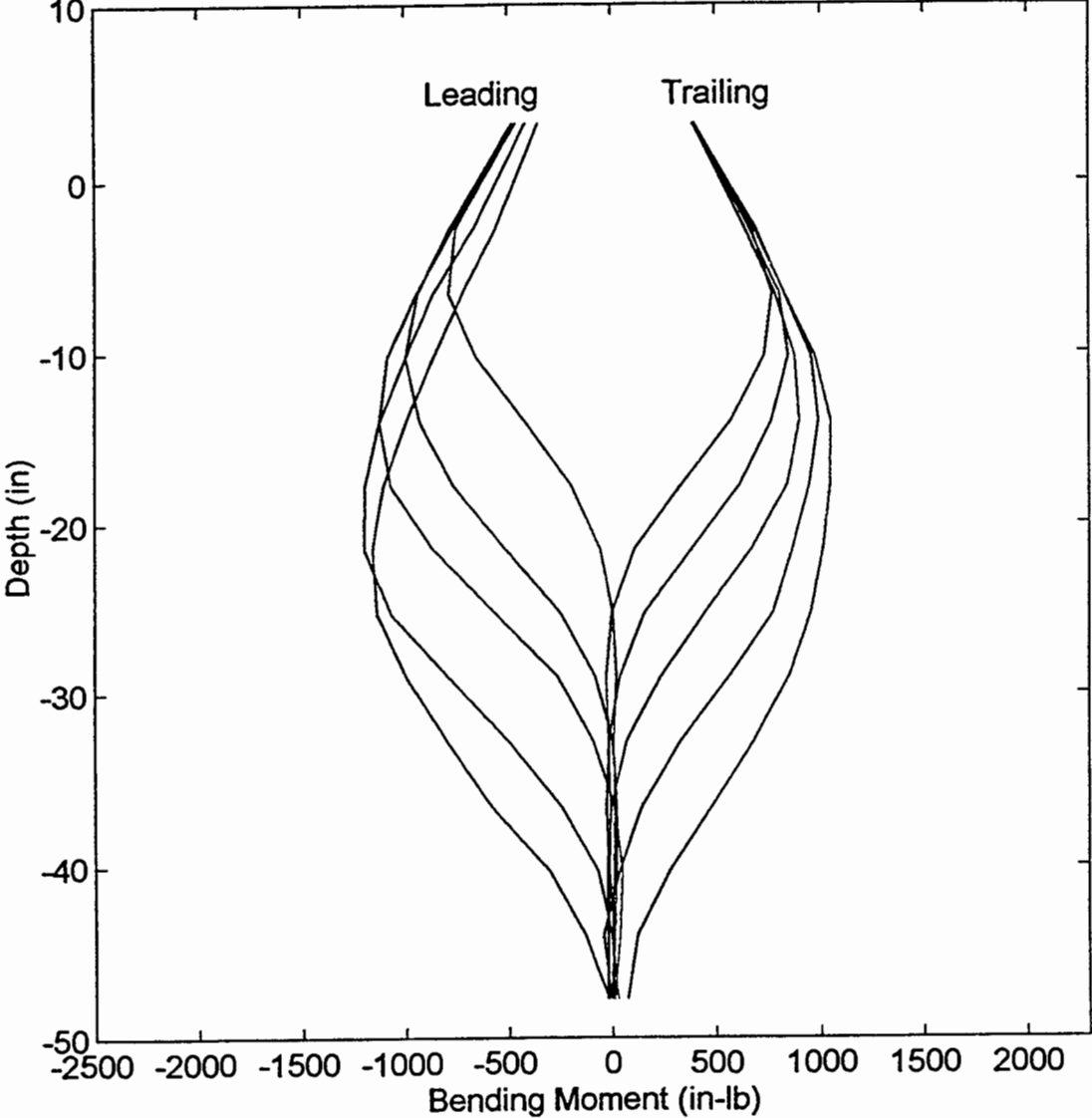
Moment Distribution: End Pile (#6) - Load 150lb



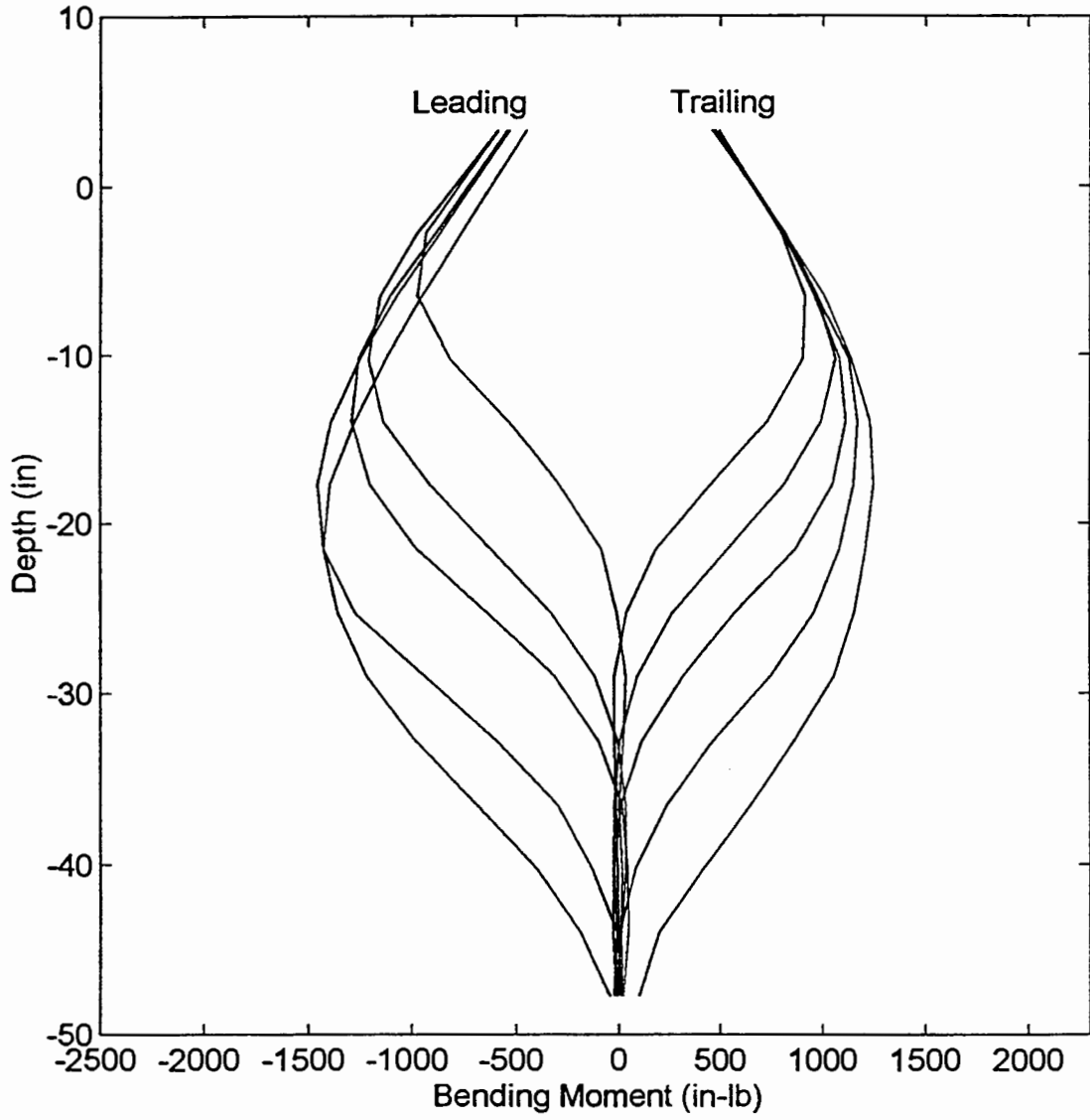
Moment Distribution: End Pile (#6) - Load 200lb



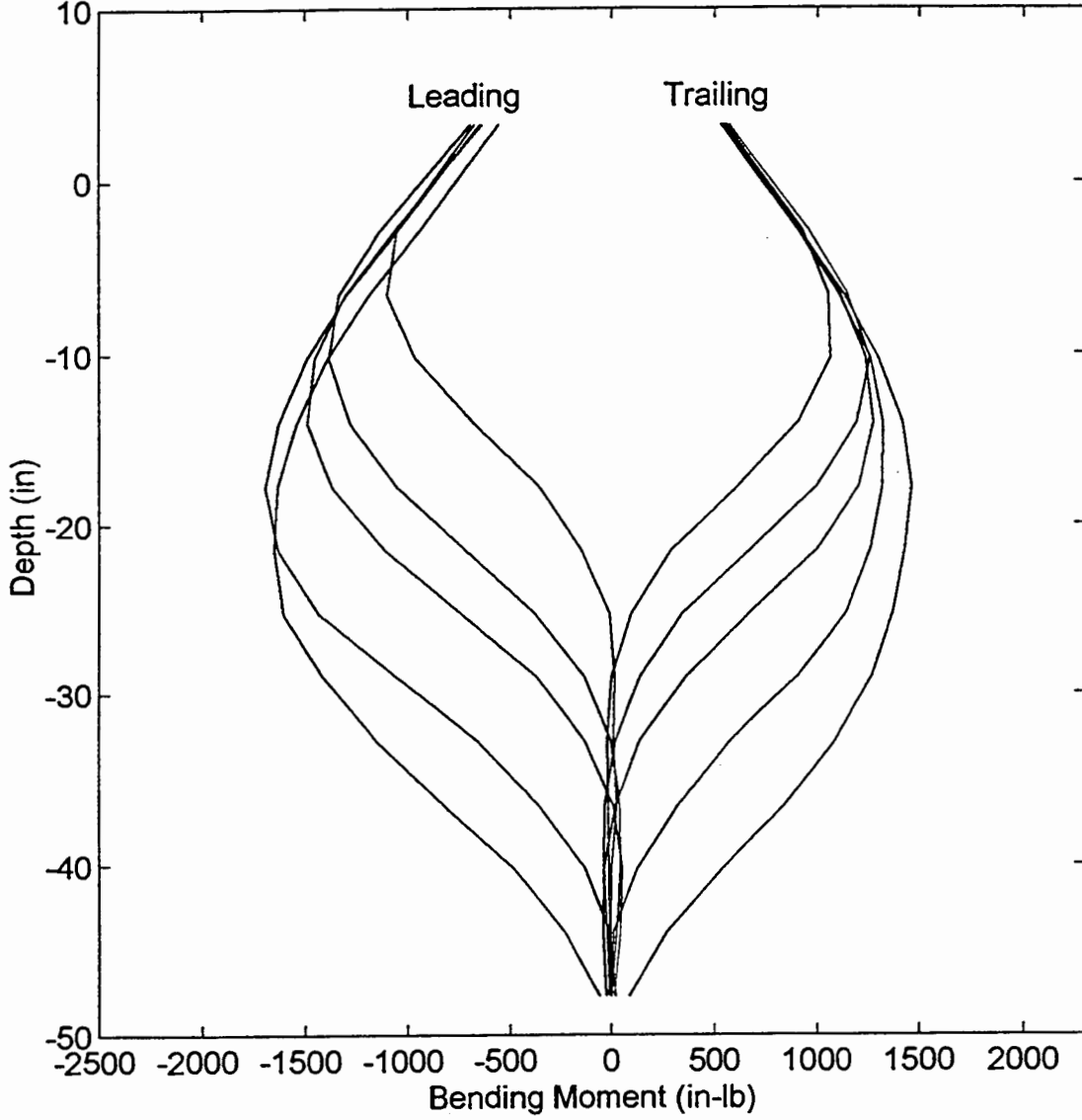
Moment Distribution: End Pile (#6) - Load 250lb



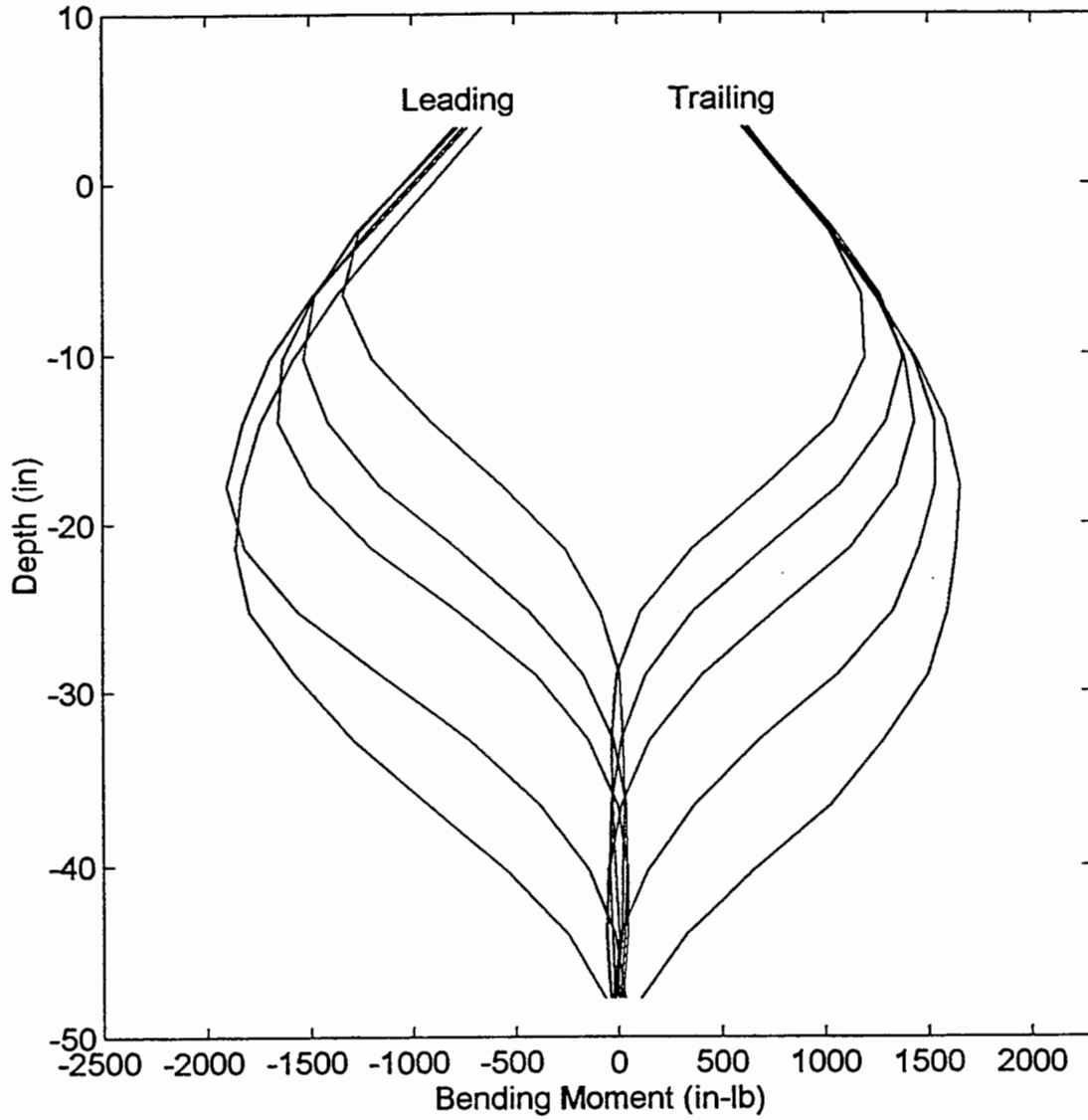
Moment Distribution: End Pile (#6) - Load 300lb



Moment Distribution: End Pile (#6) - Load 350lb



Moment Distribution: End Pile (#6) - Load 400lb



Moment Distribution: End Pile (#6) - Load 450lb

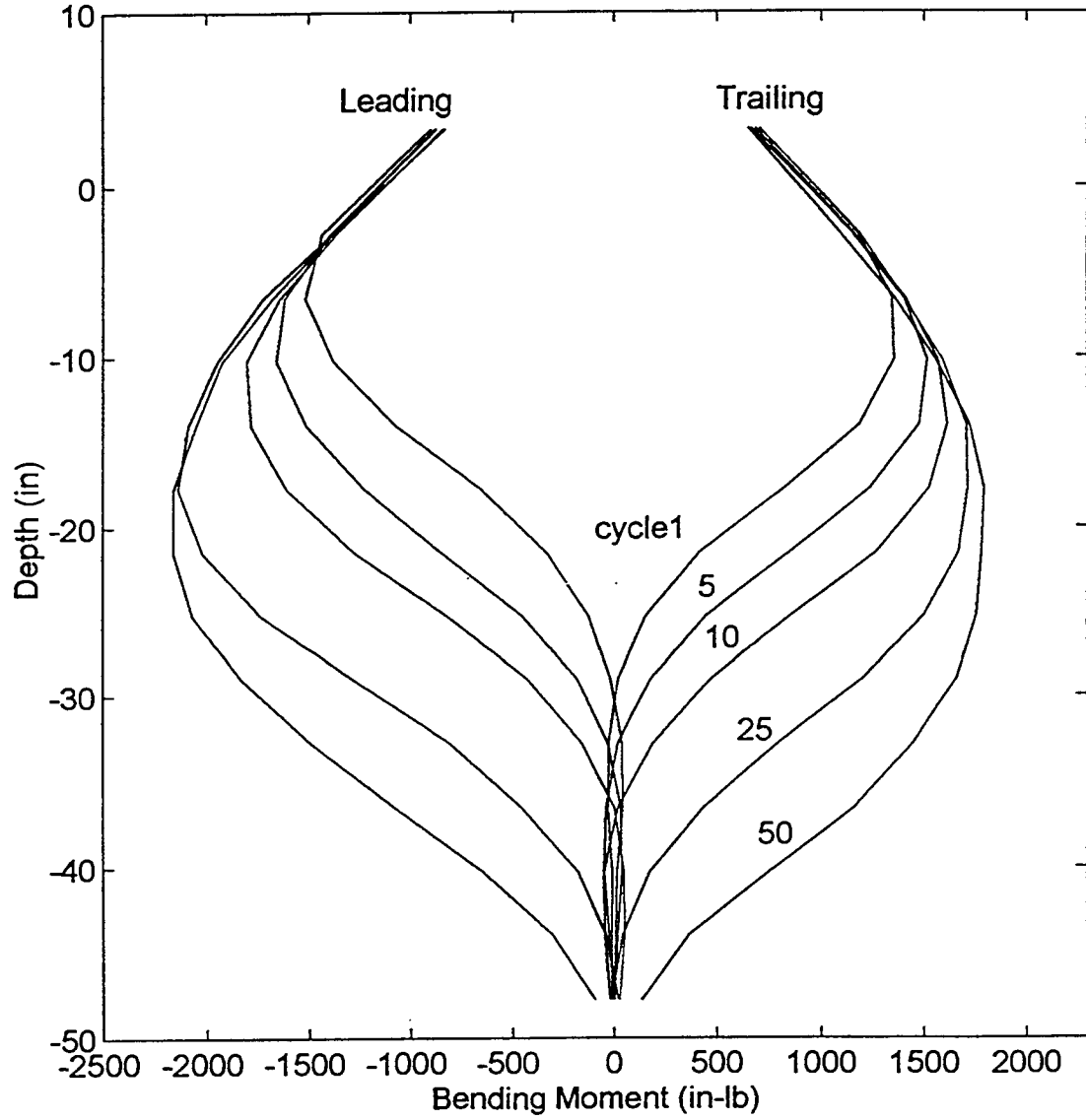
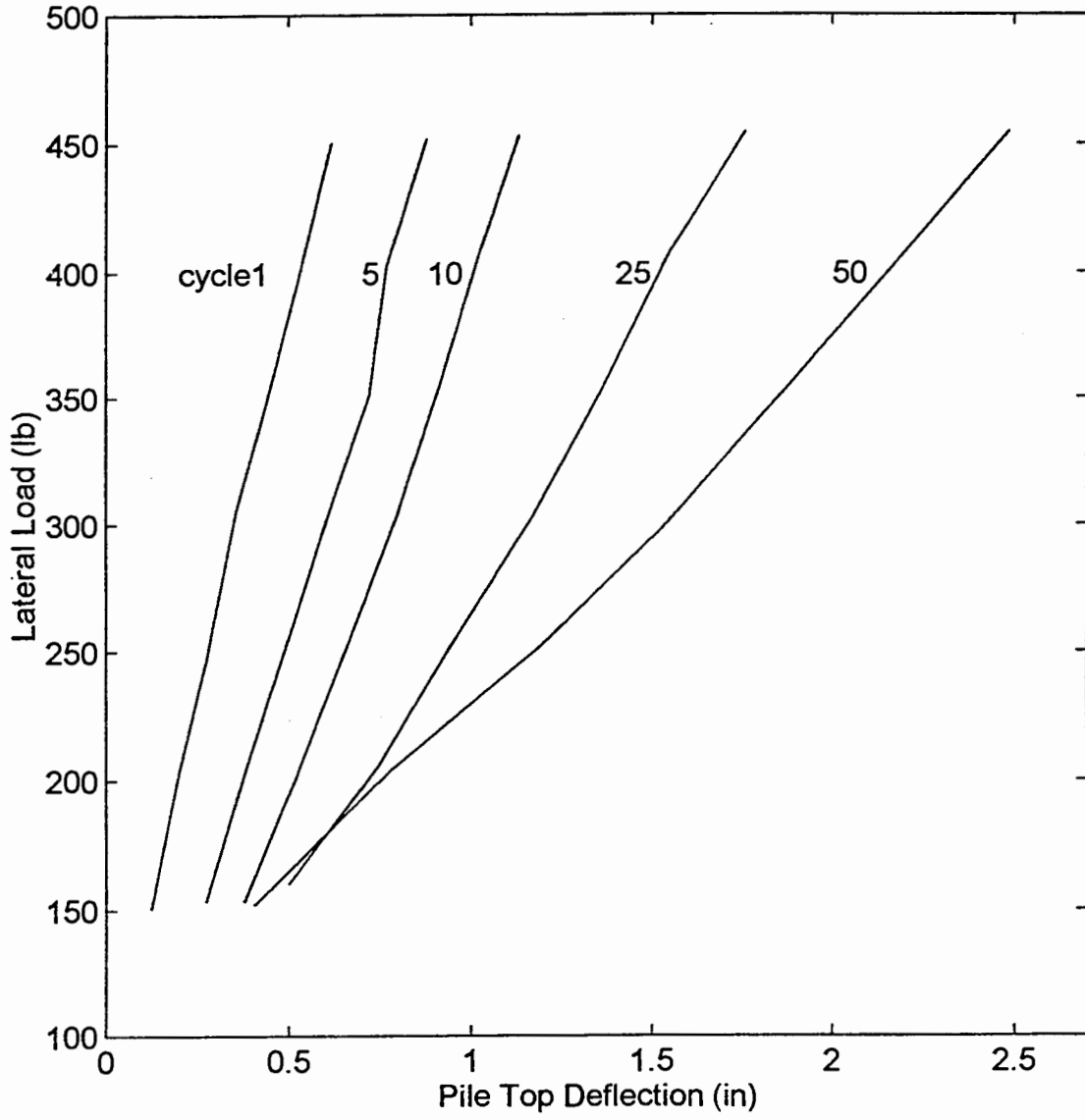


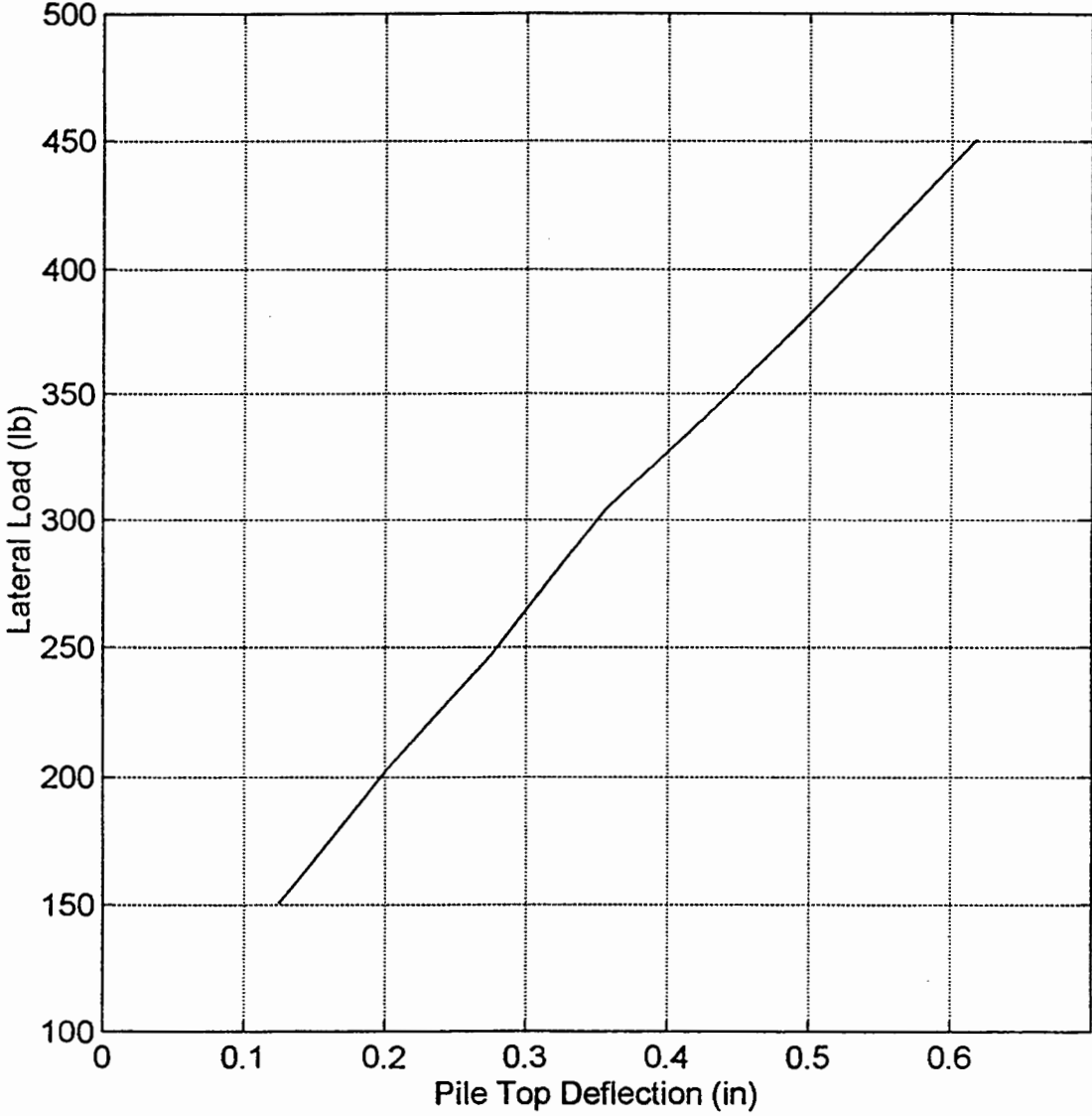
Figure B16. Load vs. deflection (next 6 plots).



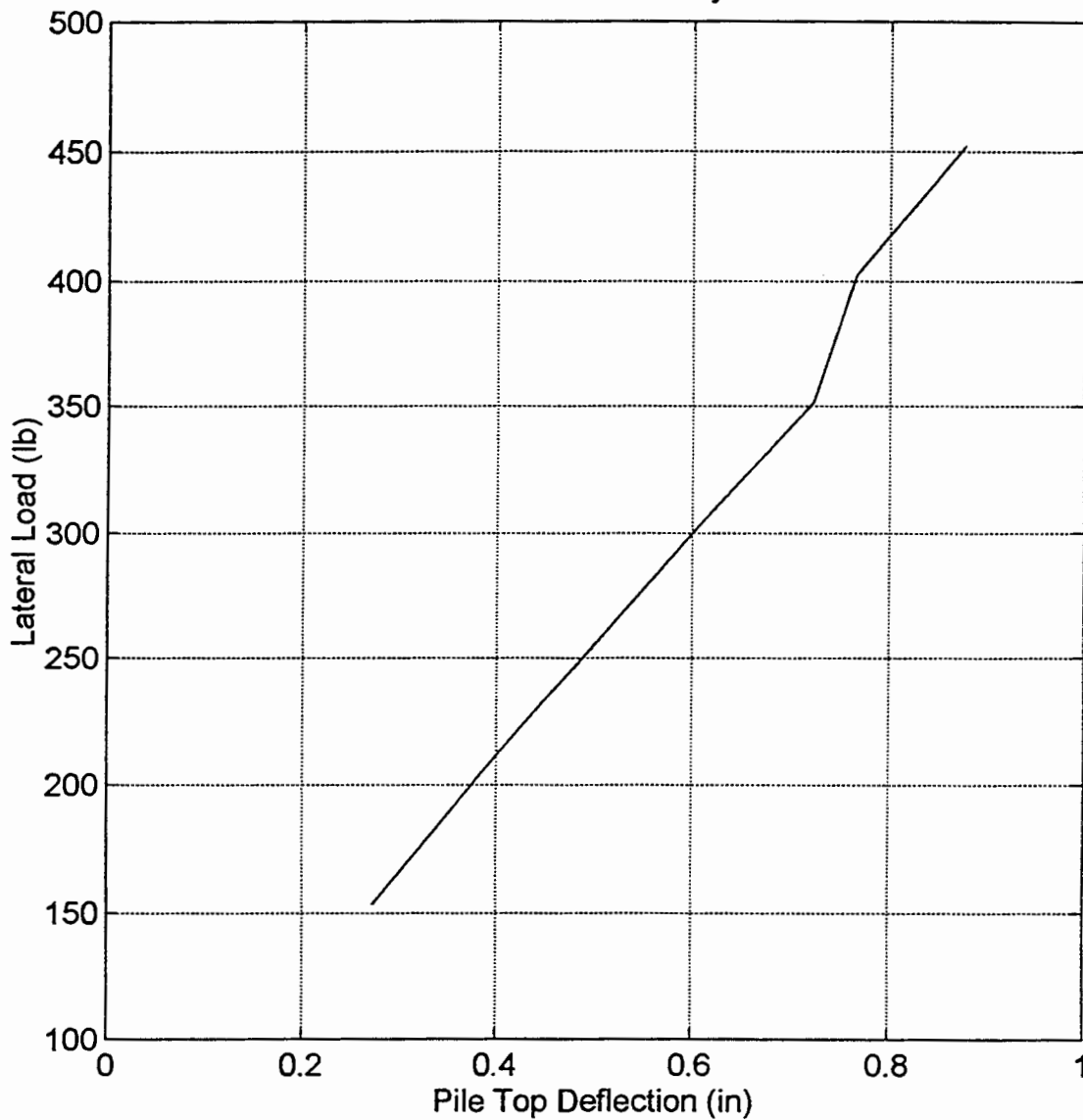
Load vs. Deflection



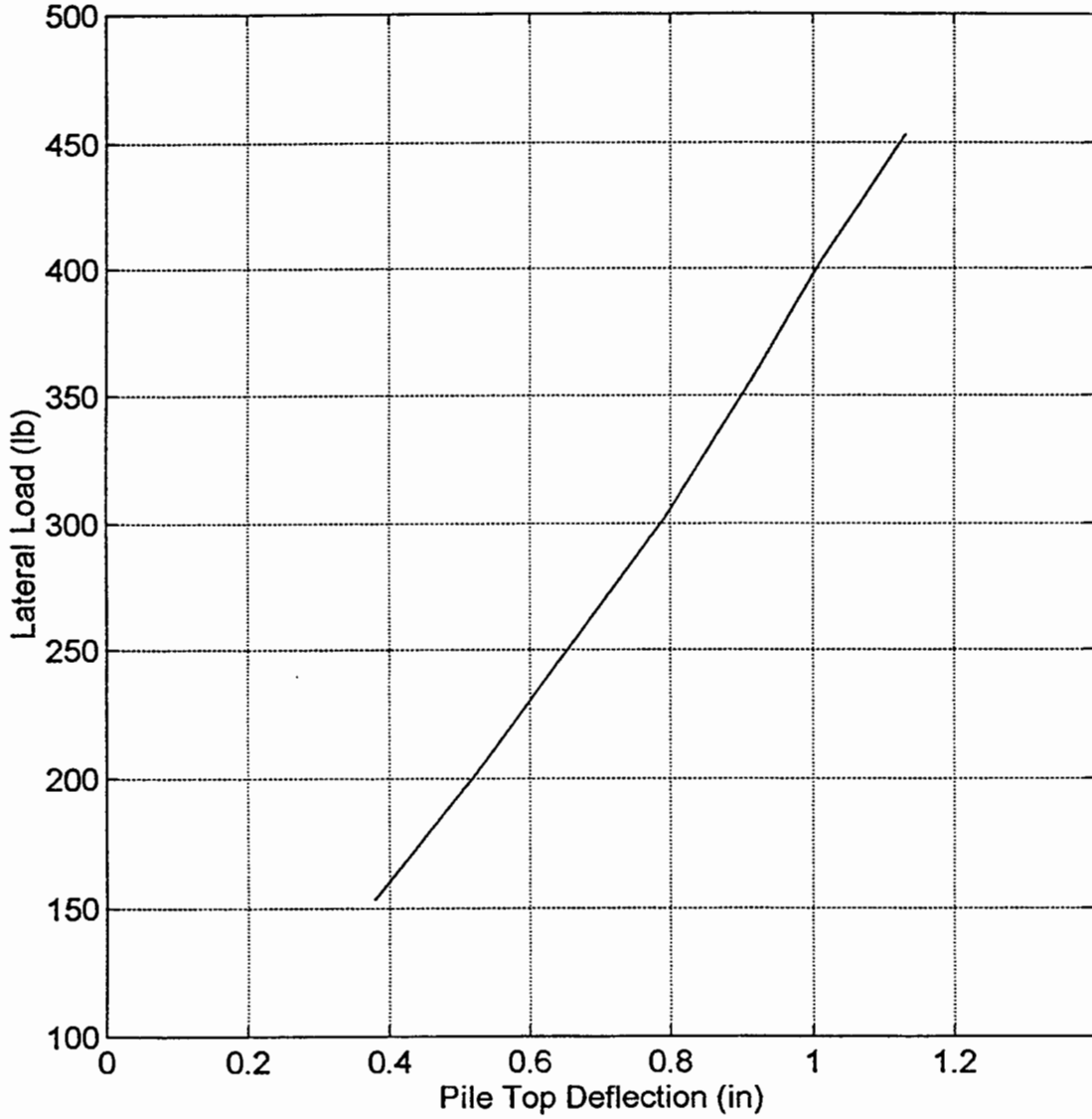
Load vs. Deflection: Cycle 1



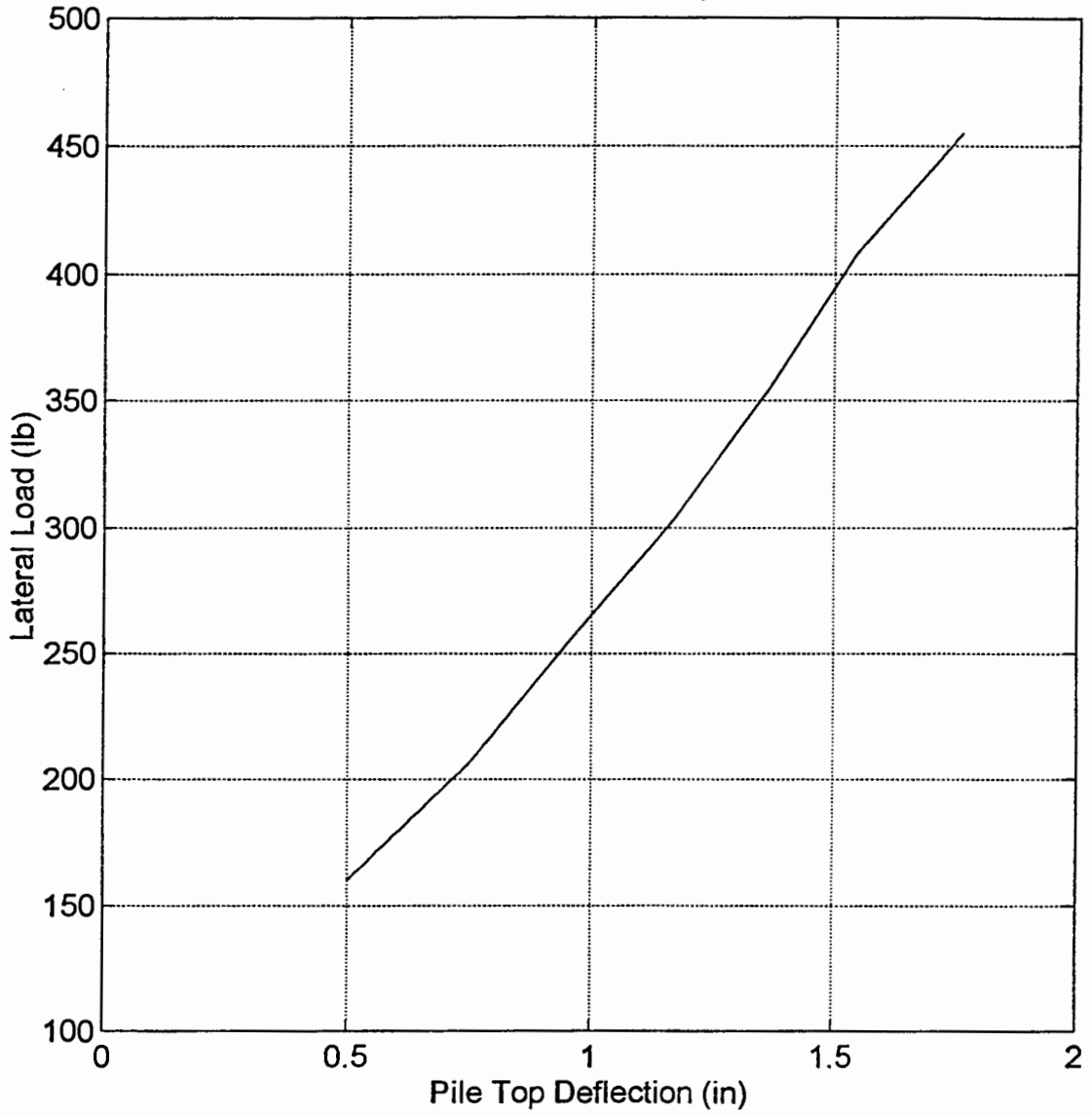
Load vs. Deflection: Cycle 5



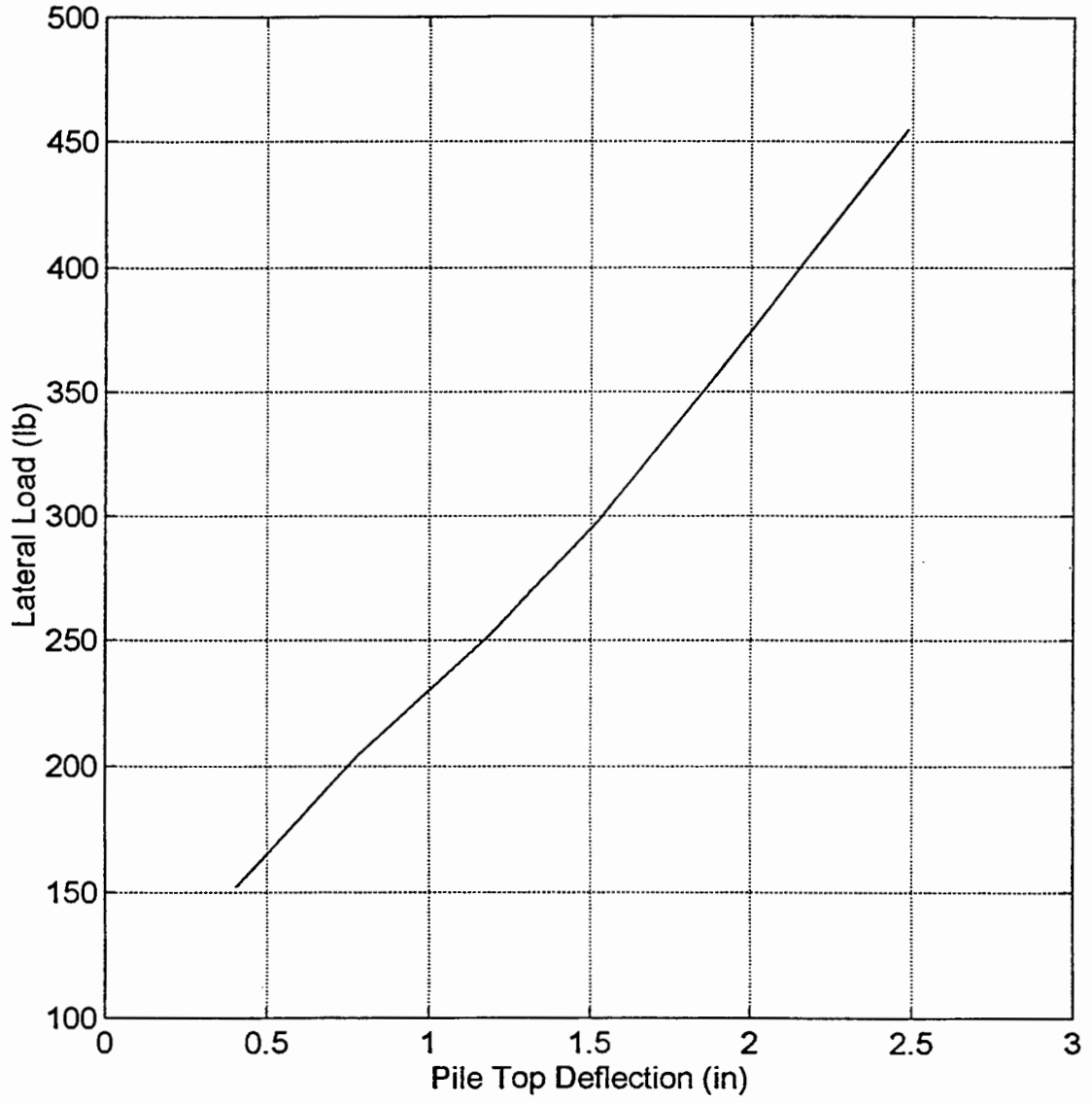
Load vs. Deflection: Cycle 10



Load vs. Deflection: Cycle 25



Load vs. Deflection: Cycle 50





**APPENDIX C: STRAIN GAGE CALIBRATION**

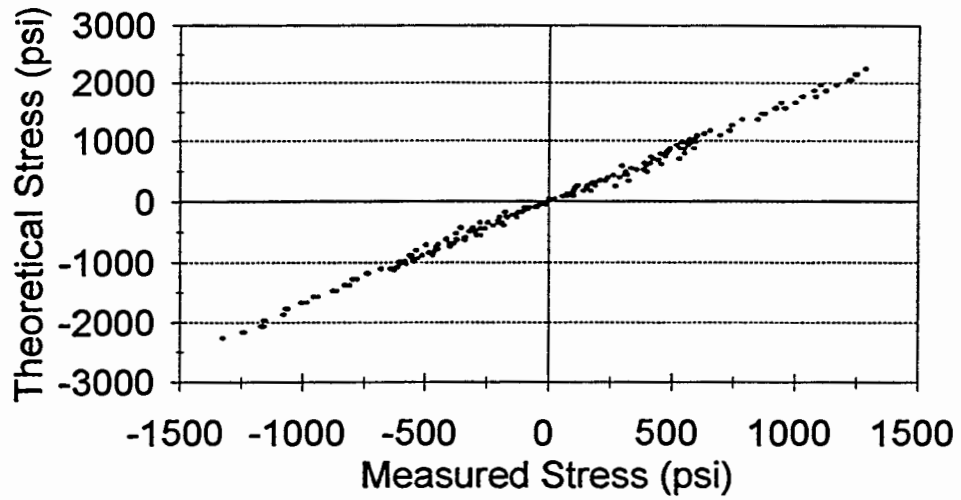




Figure C1. Pile 1 calibration (next 14 plots).

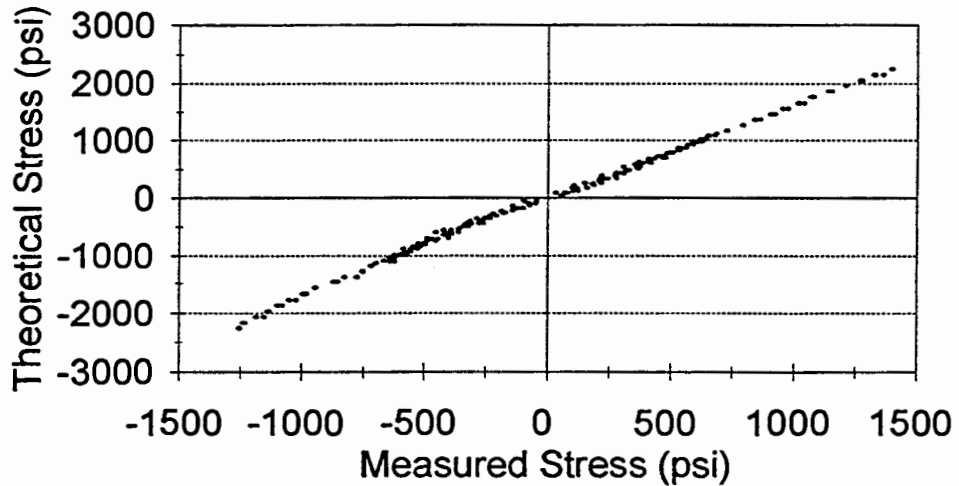
### Pile 1 Red Gage 1

Calibration Factor=1.688715



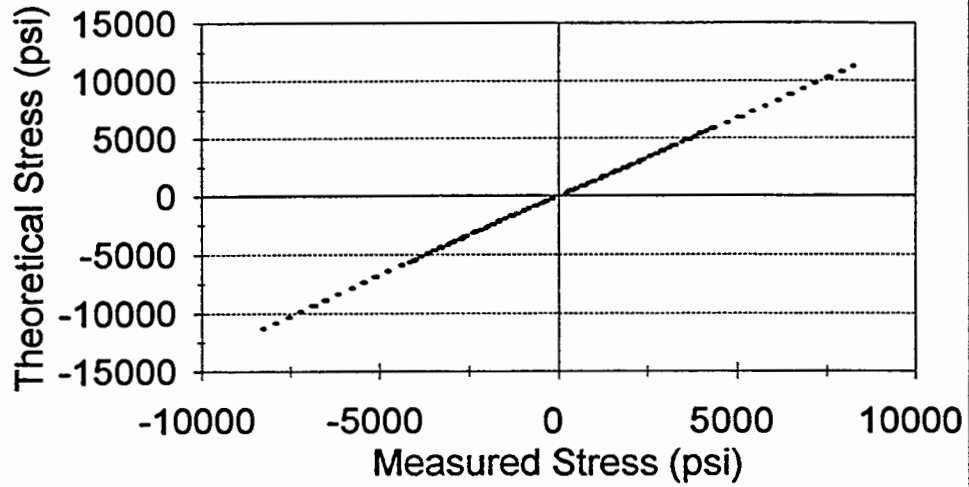
### Pile 1 Black Gage 1

Calibration Factor=1.641947



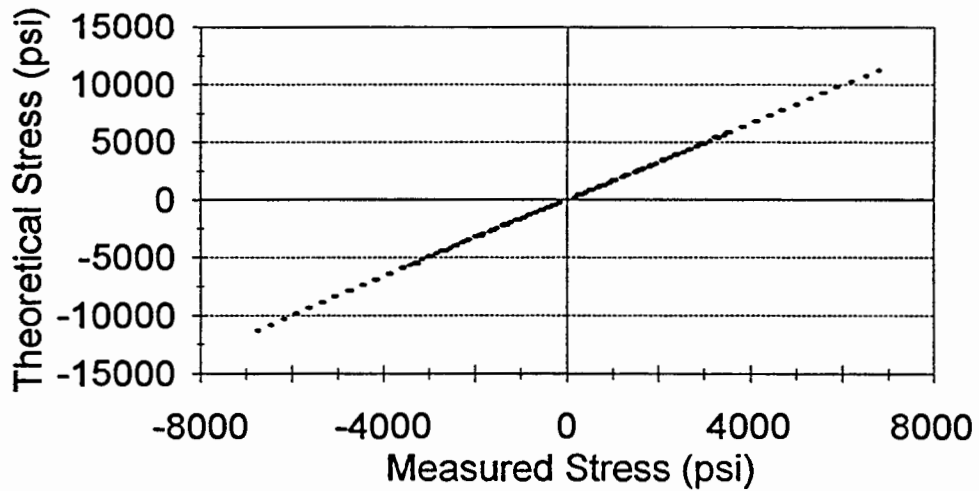
## Pile 1 Red Gage 2

Calibration Factor=1.355413



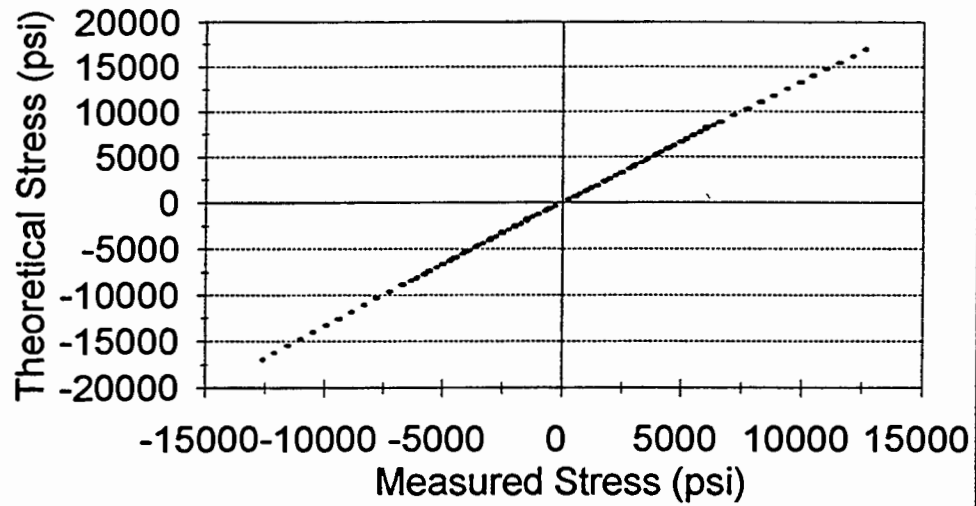
## Pile 1 Black Gage 2

Calibration Factor=1.659661



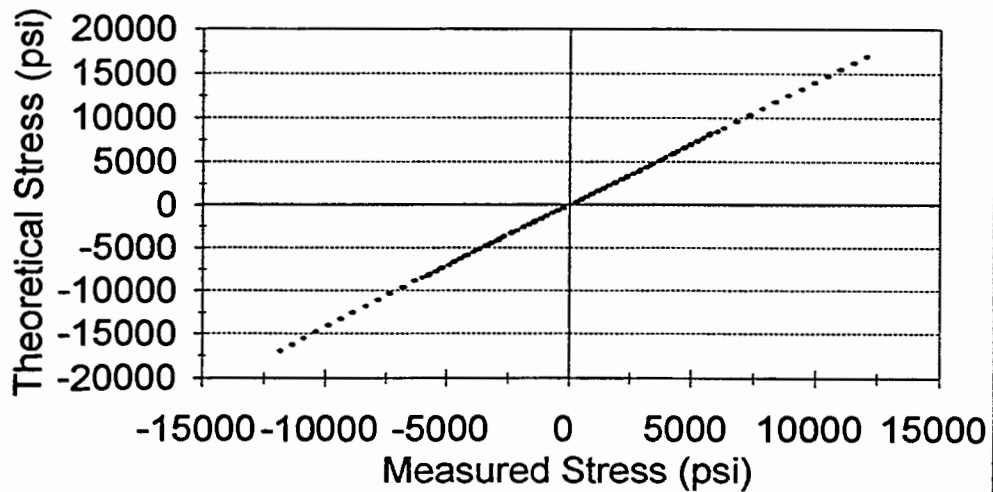
### Pile 1 Red Gage 3

Calibration Factor=1.336919



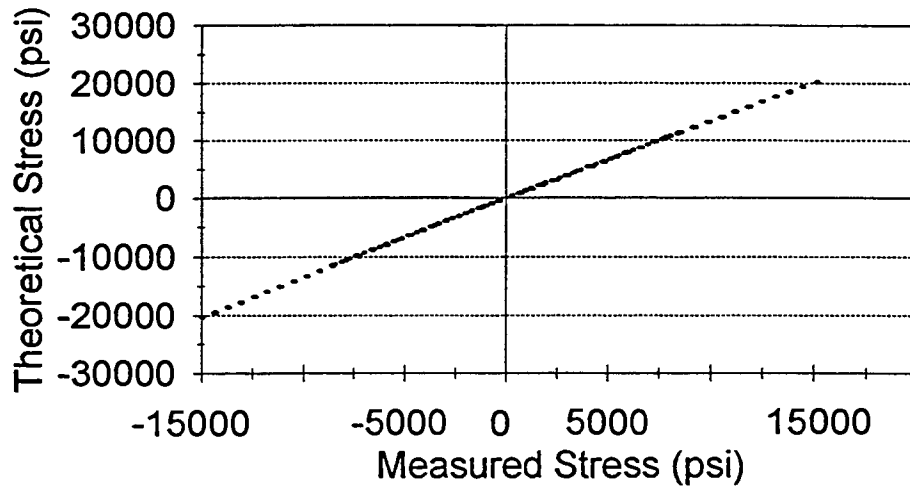
### Pile 1 Black Gage 3

Calibration Factor=1.4122



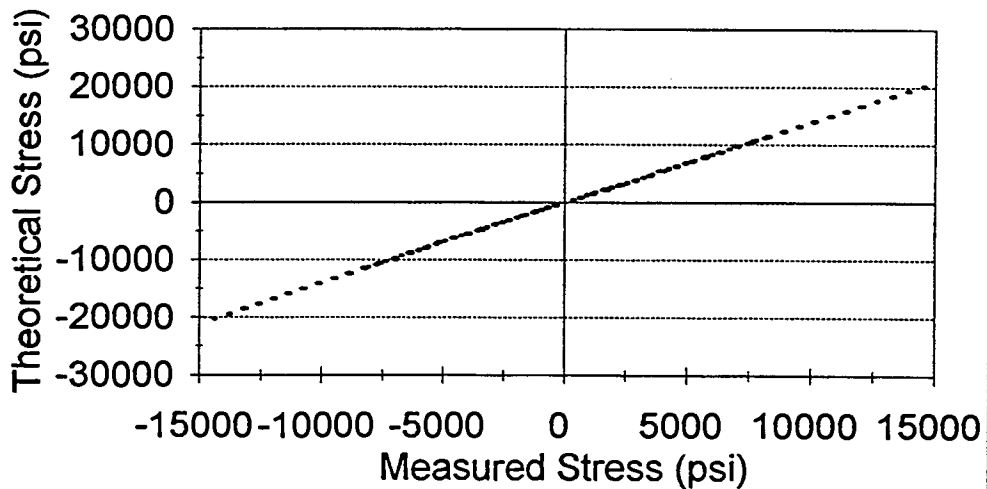
### Pile 1 Red Gage 4

Calibration Factor=1.345627



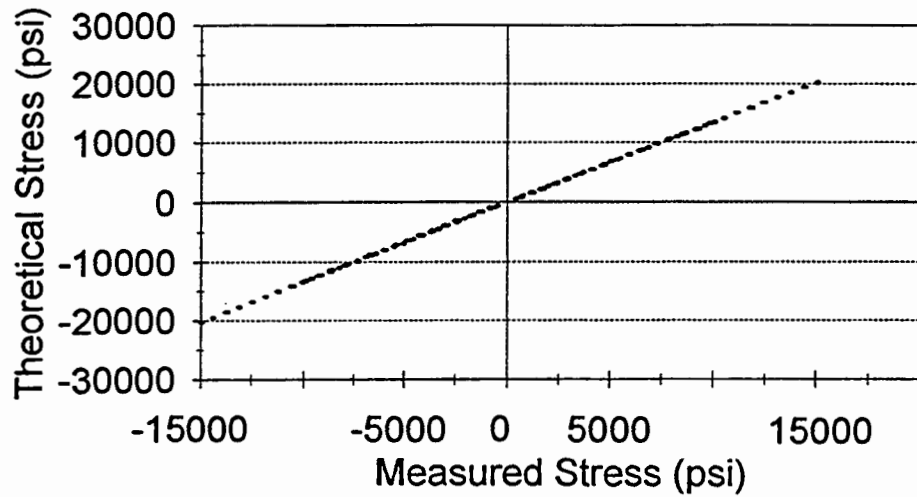
### Pile 1 Black Gage 4

Calibration Factor=1.397454



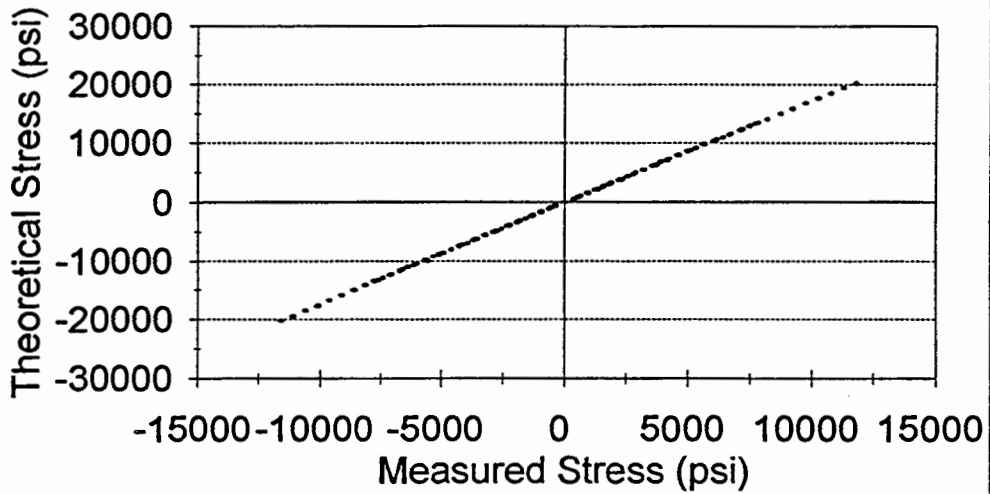
### Pile 1 Red Gage 5

Calibration Factor=1.34572



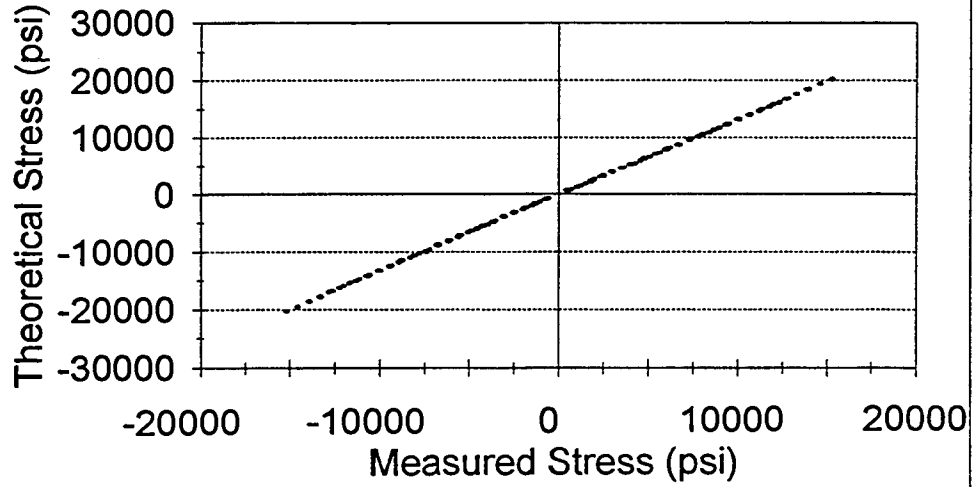
### Pile 1 Black Gage 5

Calibration Factor=1.735096



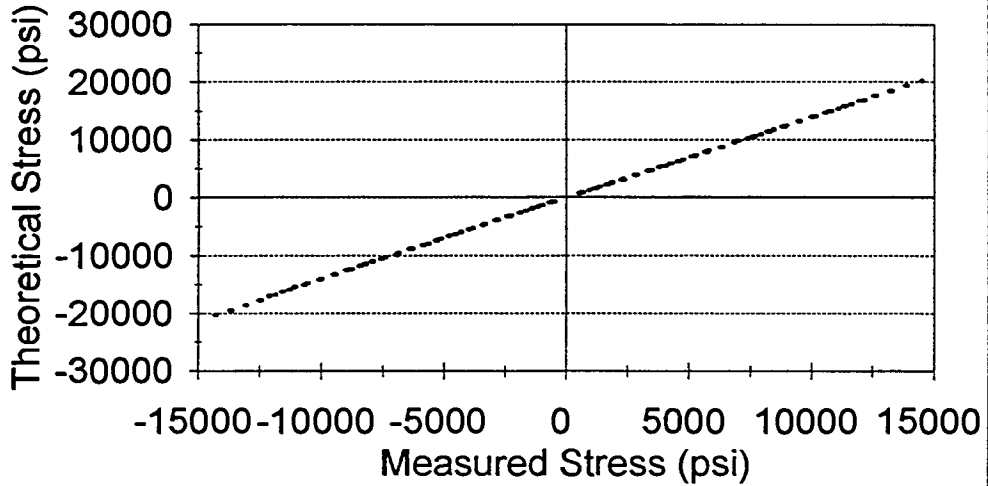
# Pile 1 Red Gage 6

Calibration Factor=1.323879



# Pile 1 Black Gage 6

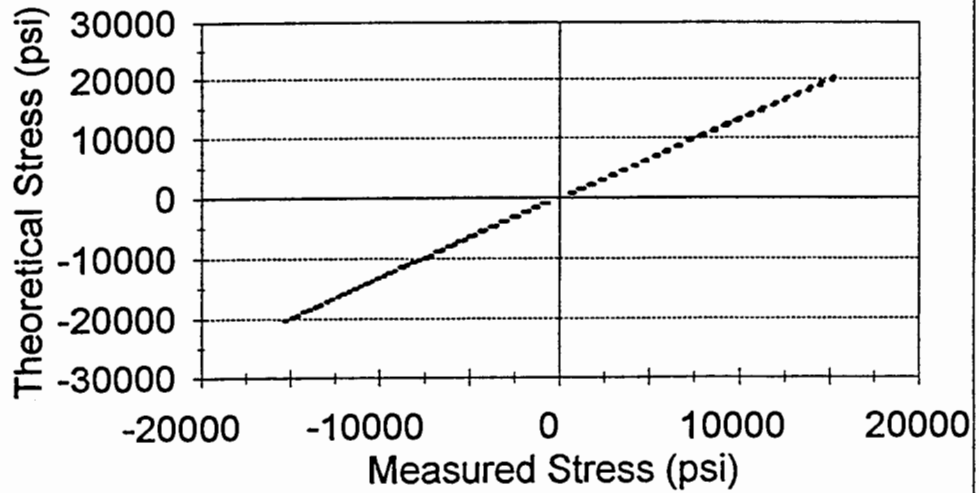
Calibration Factor=1.40233





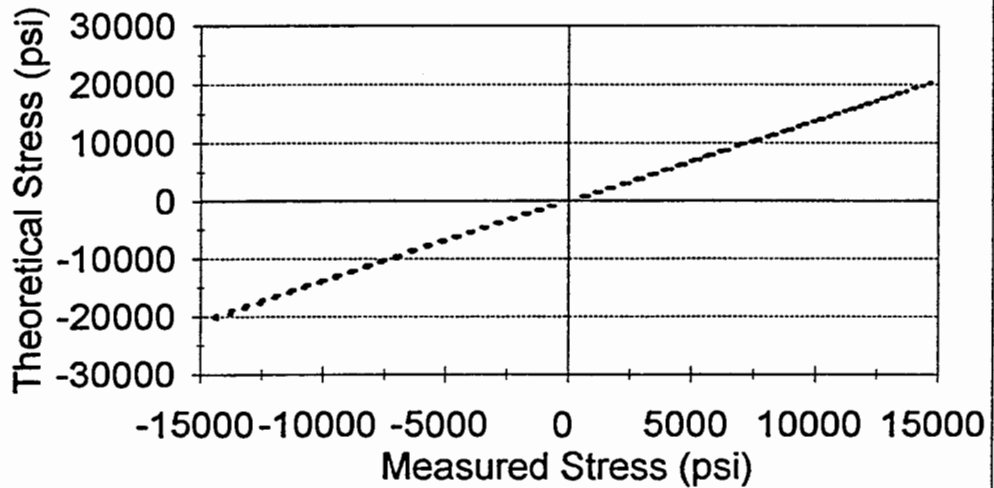
### Pile 1 Red Gage 7

Calibration Factor=1.320227



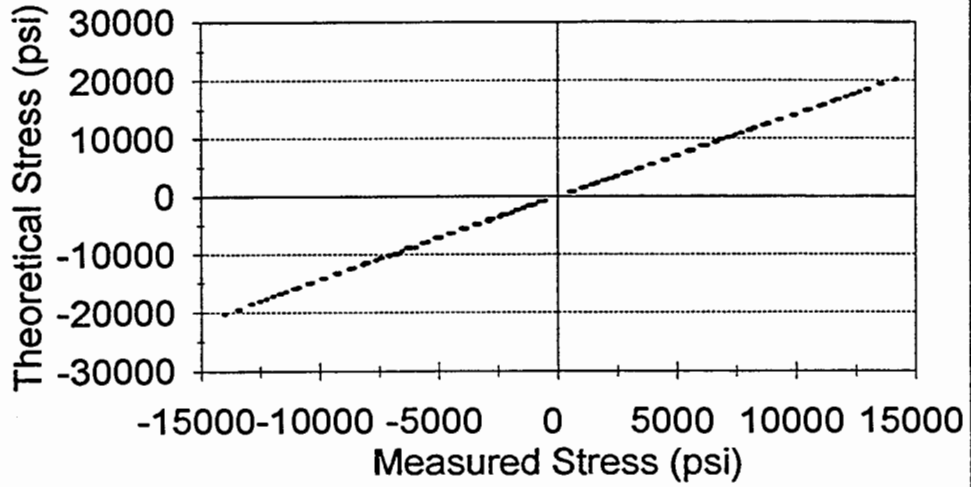
### Pile 1 Black Gage 7

Calibration Factor=1.384852



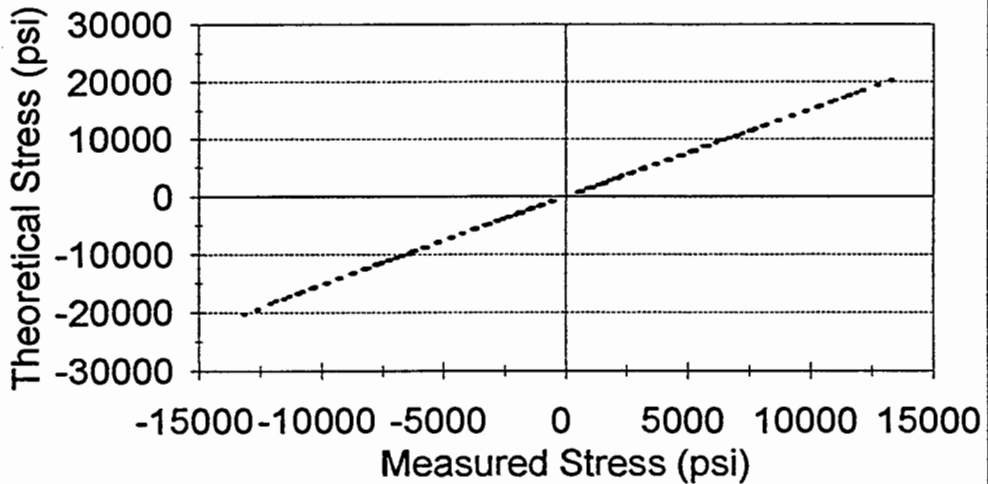
### Pile 1 Red Gage 8

Calibration Factor=1.434439



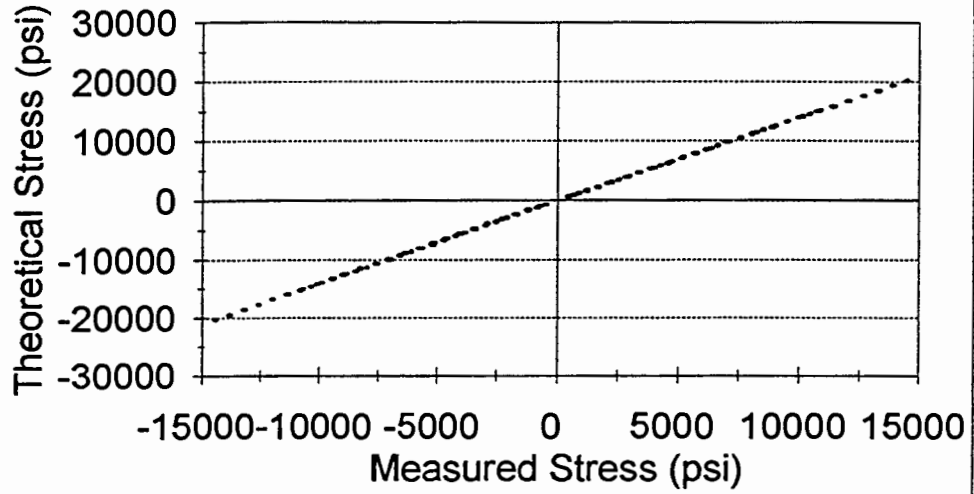
### Pile 1 Black Gage 8

Calibration Factor=1.529399



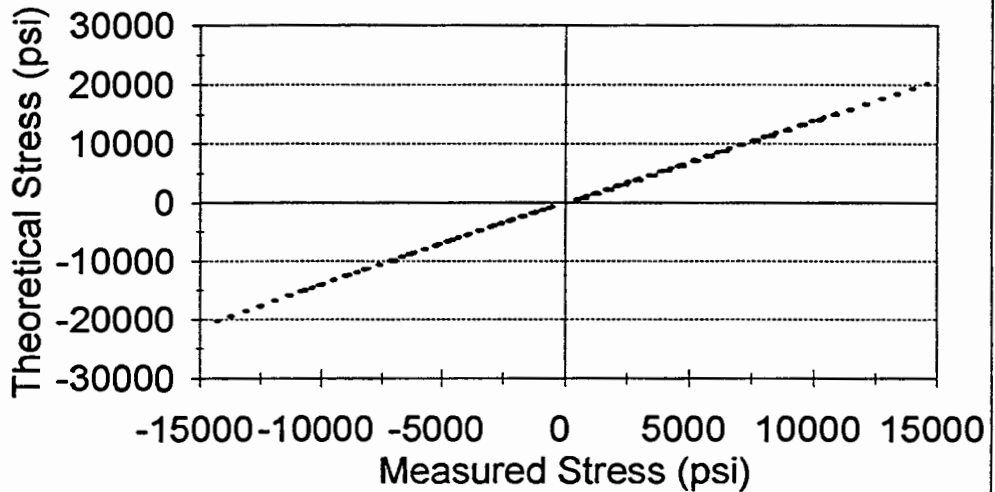
### Pile 1 Red Gage 9

Calibration Factor=1.401955



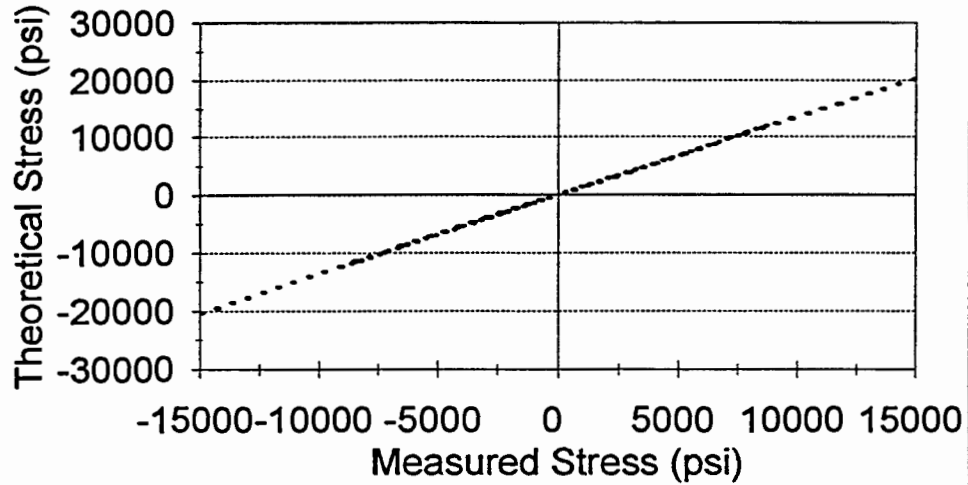
### Pile 1 Black Gage 9

Calibration Factor=1.398476



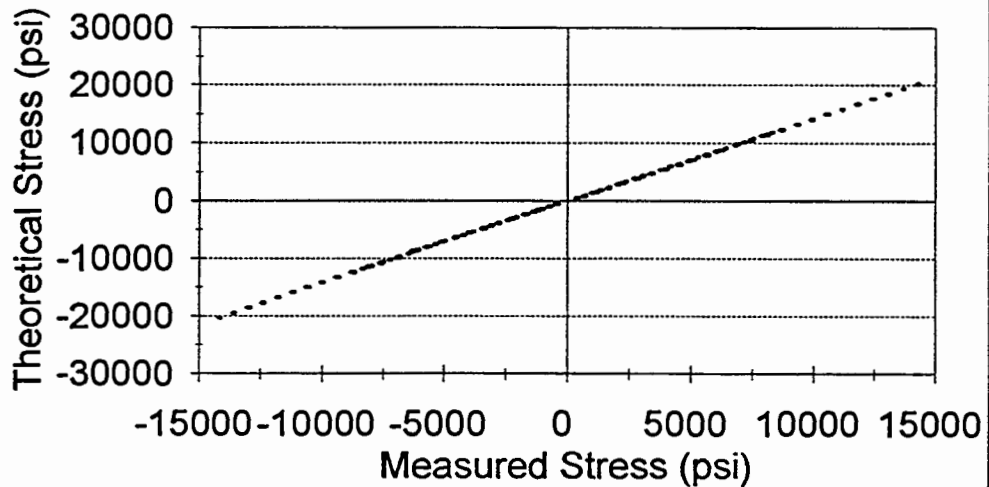
### Pile 1 Red Gage 10

Calibration Factor=1.363312



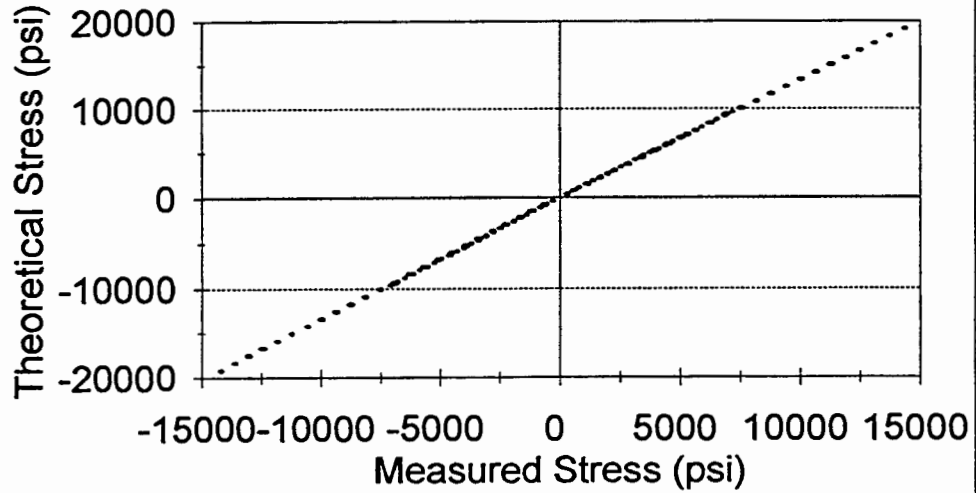
### Pile 1 Black Gage 10

Calibration Factor=1.42491



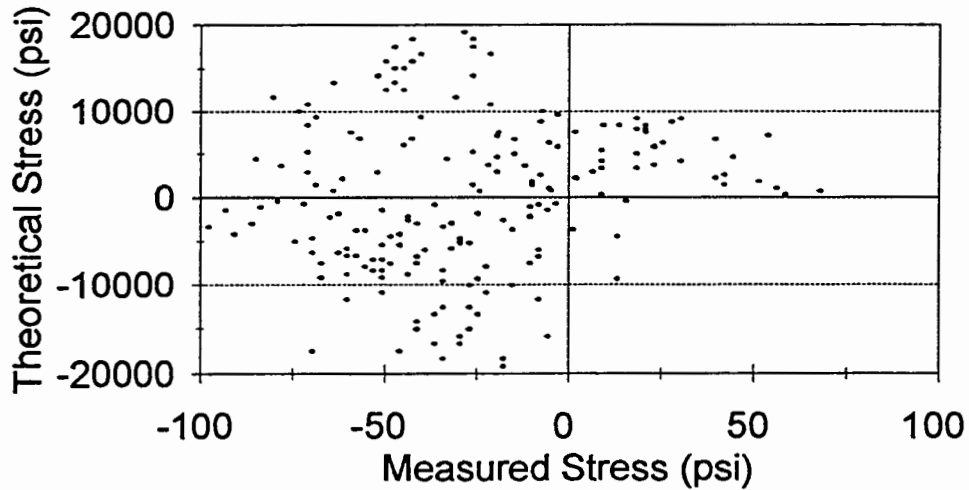
### Pile 1 Red Gage 11

Calibration Factor=1.338958



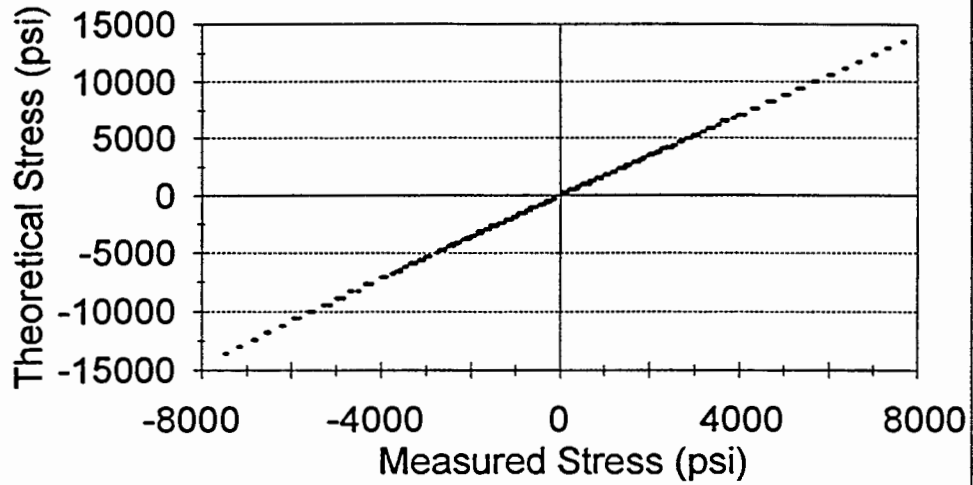
### Pile 1 Black Gage 11

Defective Gage



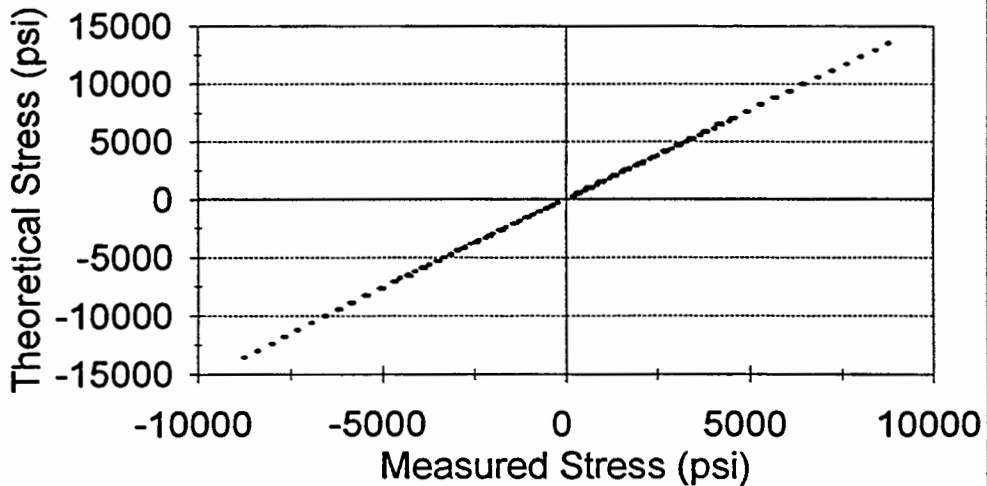
### Pile 1 Red Gage 12

Calibration Factor=1.780704



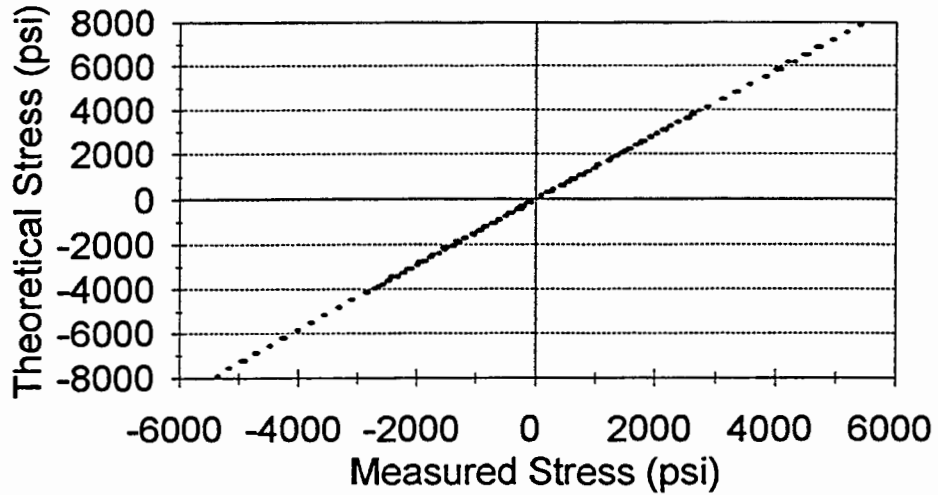
### Pile 1 Black Gage 12

Calibration Factor=1.53509



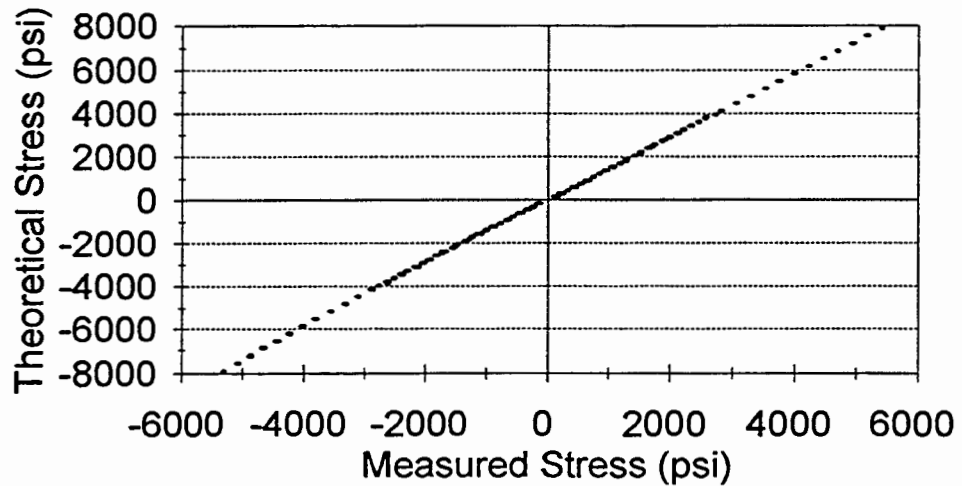
### Pile 1 Red Gage 13

Calibration Factor=1.453792



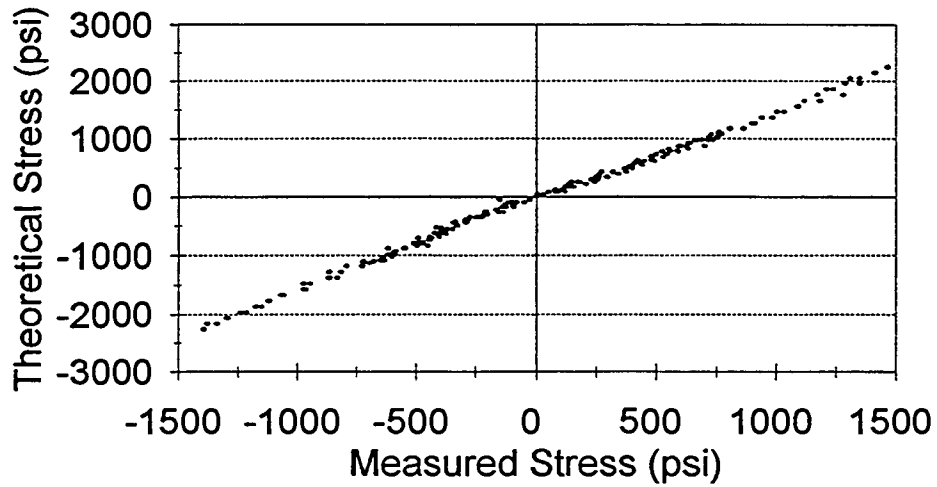
### Pile 1 Black Gage 13

Calibration Factor=1.459325



### Pile 1 Red Gage 14

Calibration Factor=1.512776



### Pile 1 Black Gage 14

Calibration Factor=1.902158

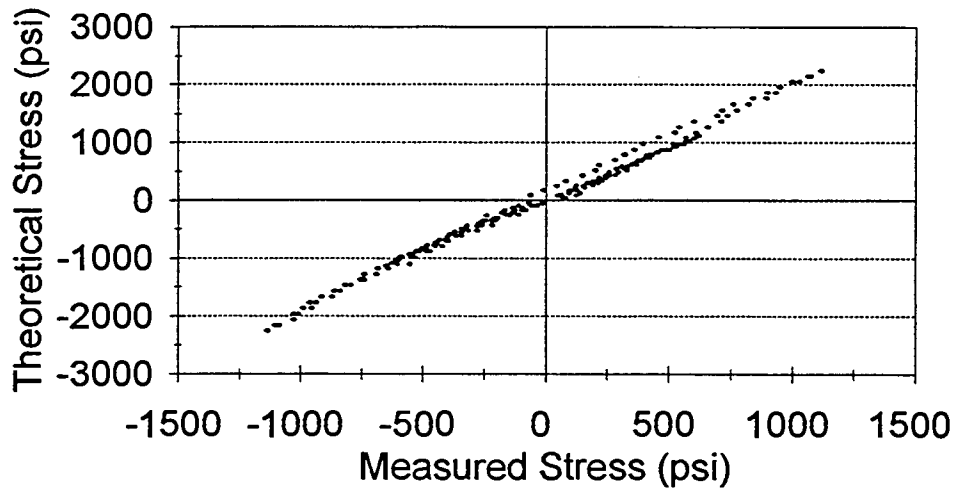
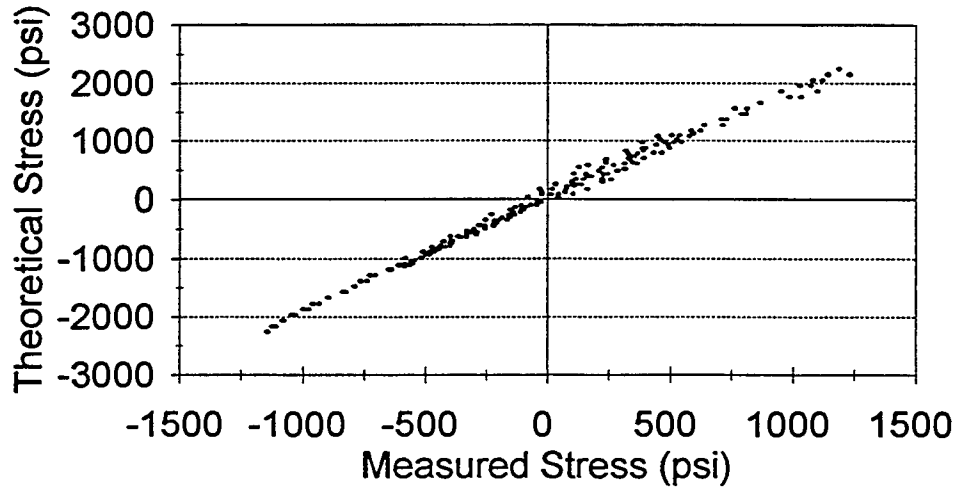




Figure C2. Pile 2 calibration (next 14 plots).

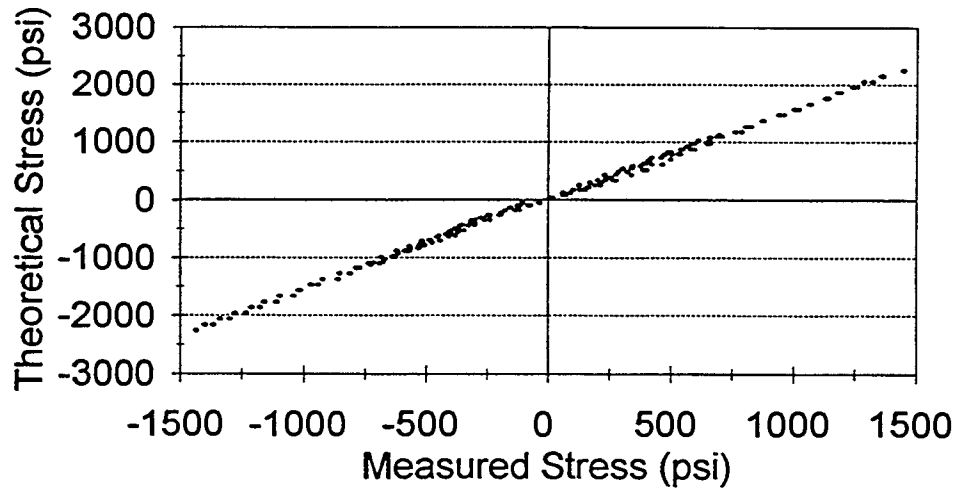
## Pile 2 Red Gage 1

Calibration Factor=1.885923

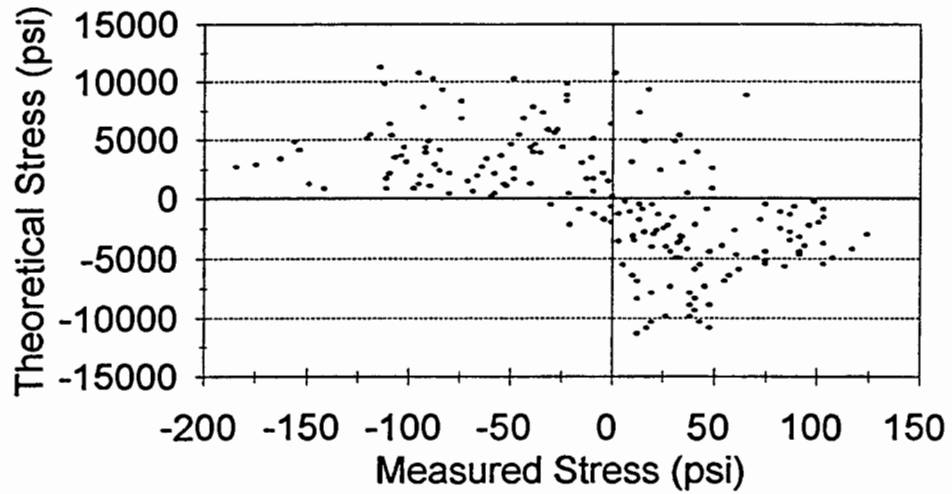


## Pile 2 Black Gage 1

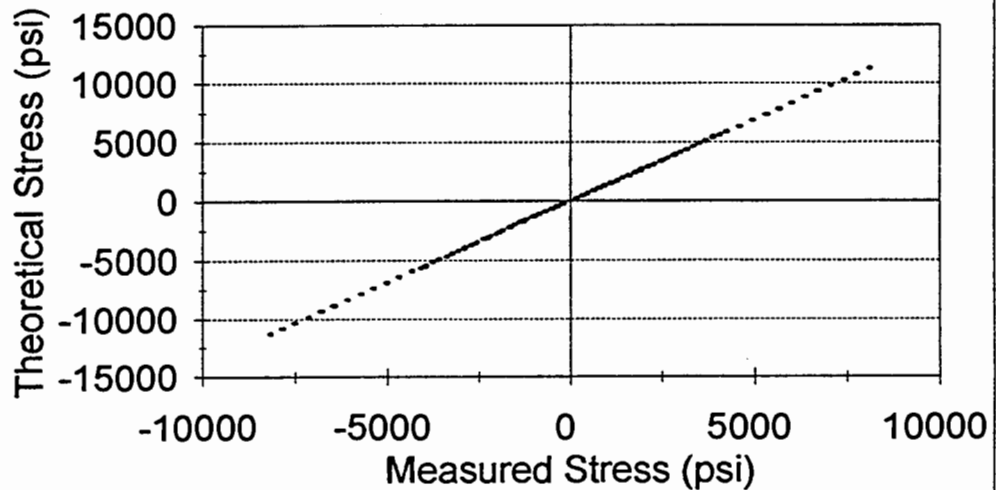
Calibration Factor=1.548181



### Pile 2 Red Gage 2 Defective Gage

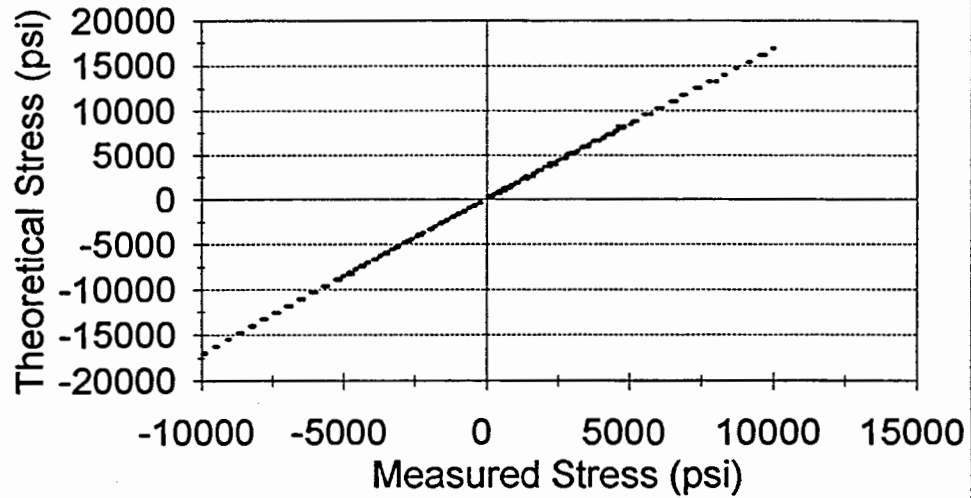


### Pile 2 Black Gage 2 Calibration Factor=1.380112



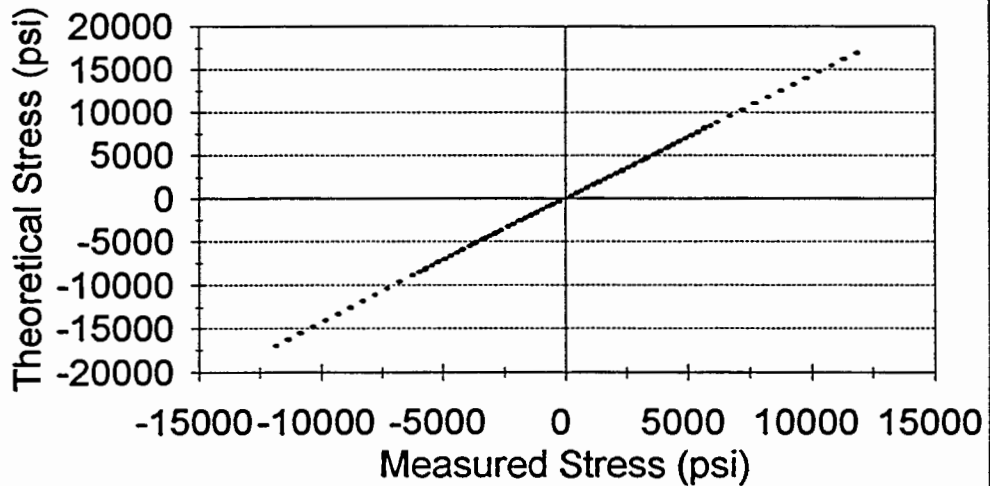
### Pile 2 Red Gage 3

Calibration Factor=1.701942



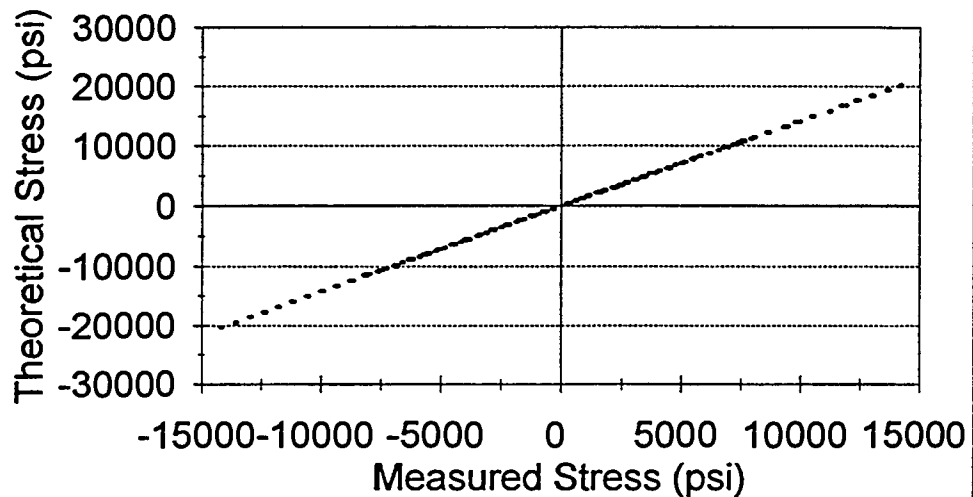
### Pile 2 Black Gage 3

Calibration Factor=1.42655



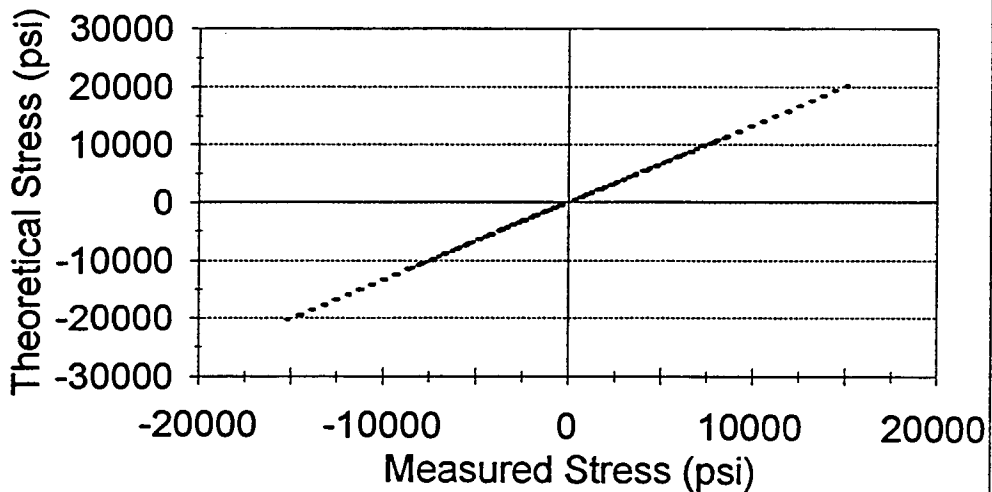
### Pile 2 Red Gage 4

Calibration Factor=1.436071



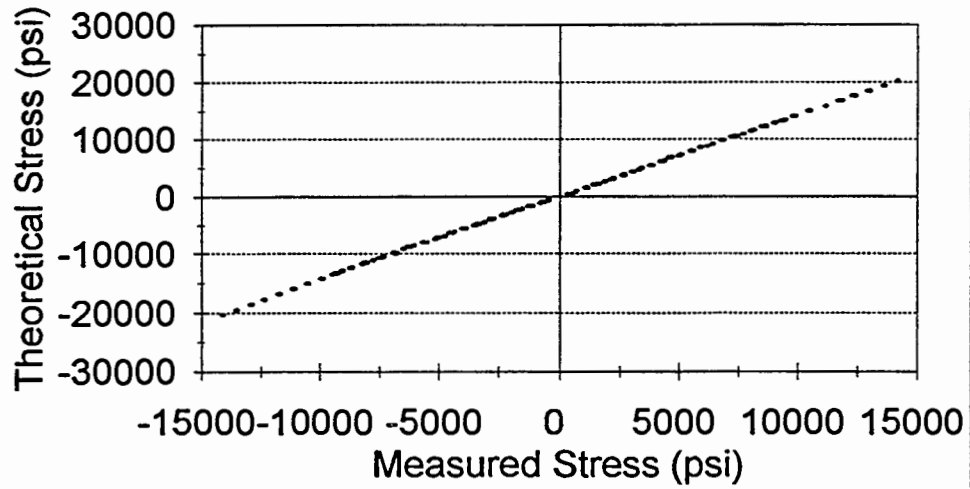
### Pile 2 Black Gage 4

Calibration Factor=1.340539



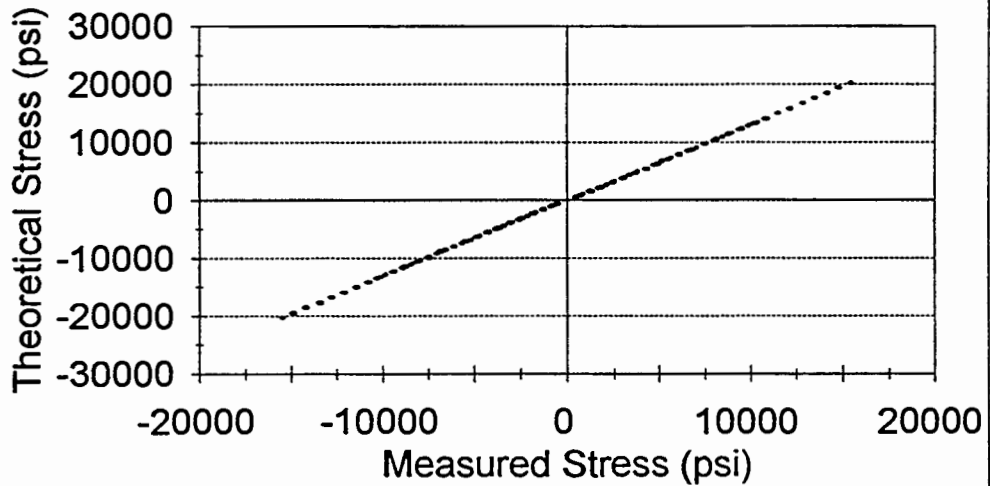
## Pile 2 Red Gage 5

Calibration Factor=1.431615



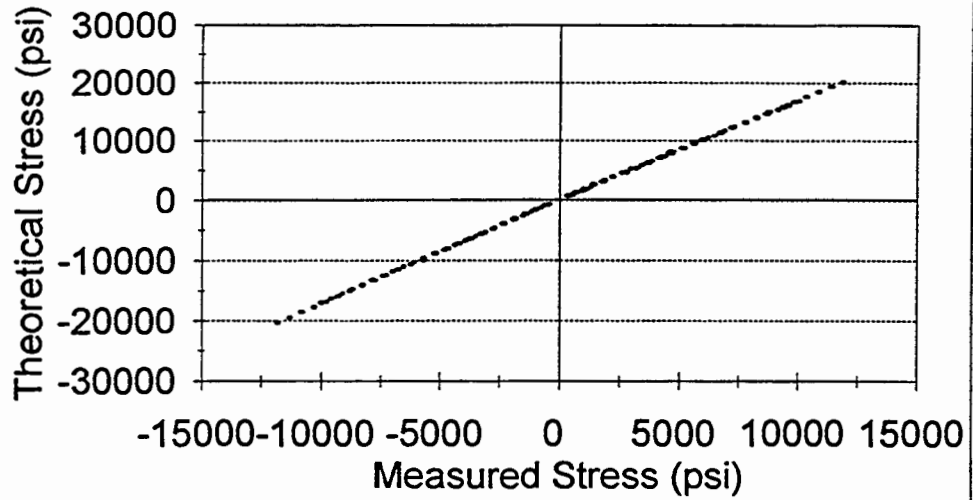
## Pile 2 Black Gage 5

Calibration Factor=1.309019



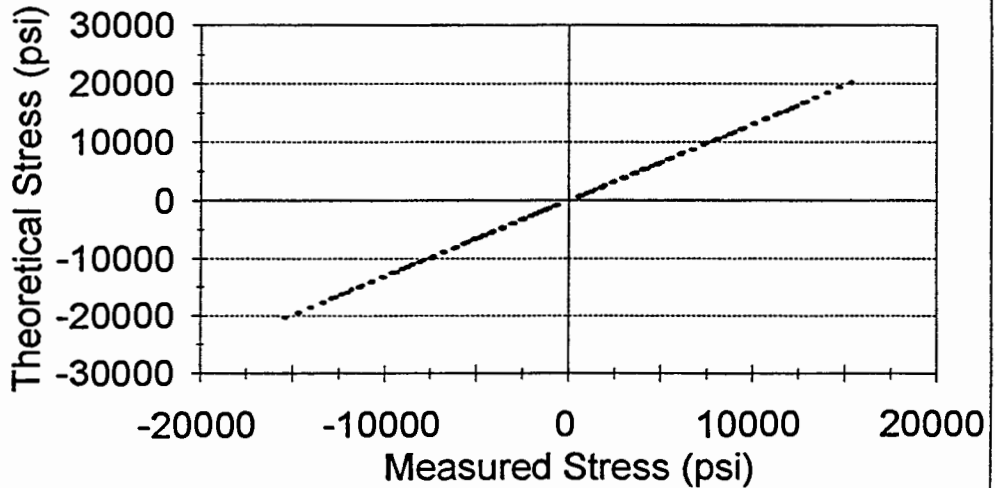
### Pile 2 Red Gage 6

Calibration Factor=1.707355



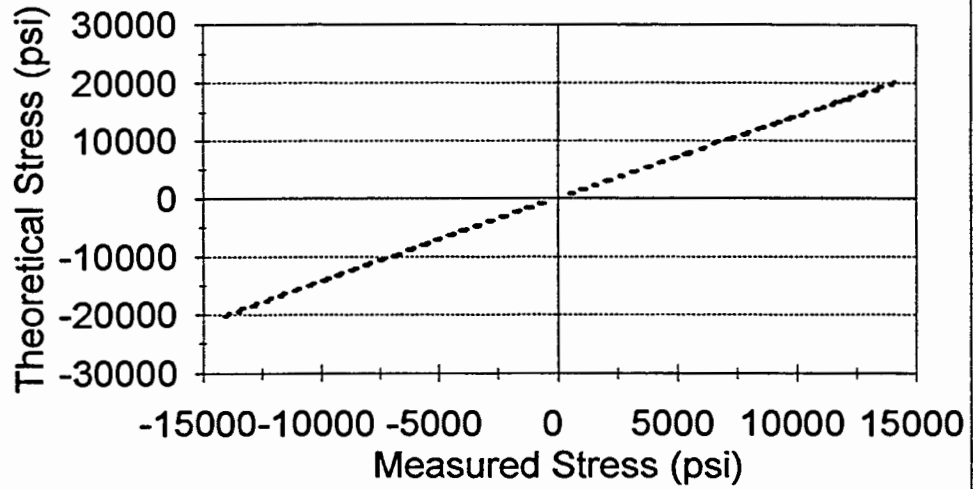
### Pile 2 Black Gage 6

Calibration Factor=1.315351



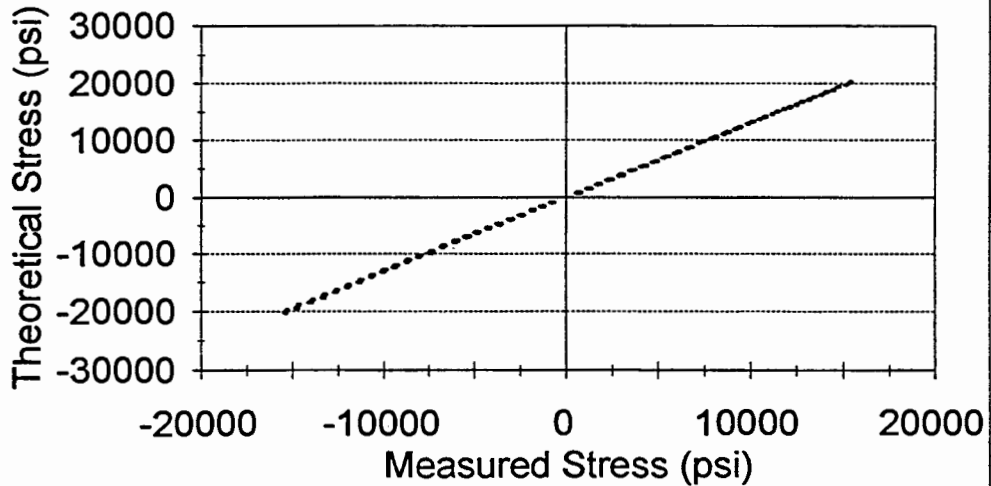
### Pile 2 Red Gage 7

Calibration Factor=1.429349



### Pile 2 Black Gage 7

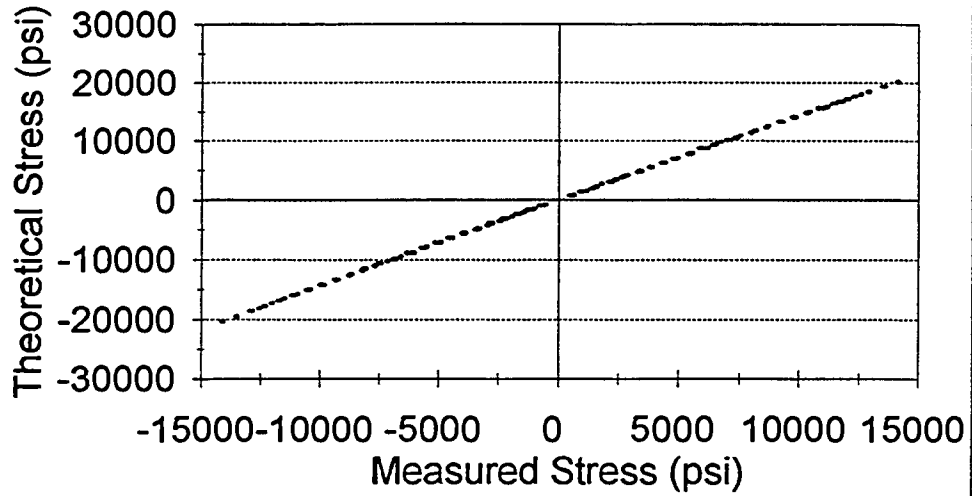
Calibration Factor=1.310399





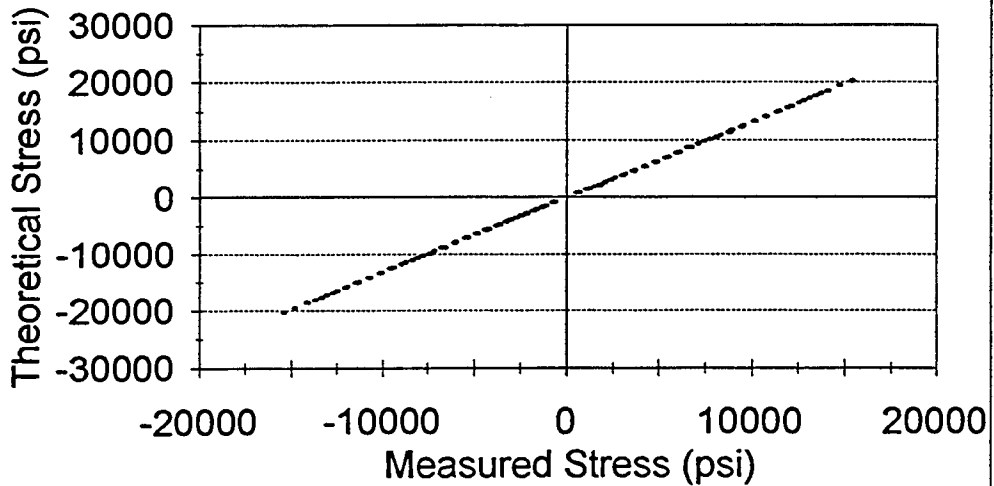
## Pile 2 Red Gage 8

Calibration Factor=1.437146



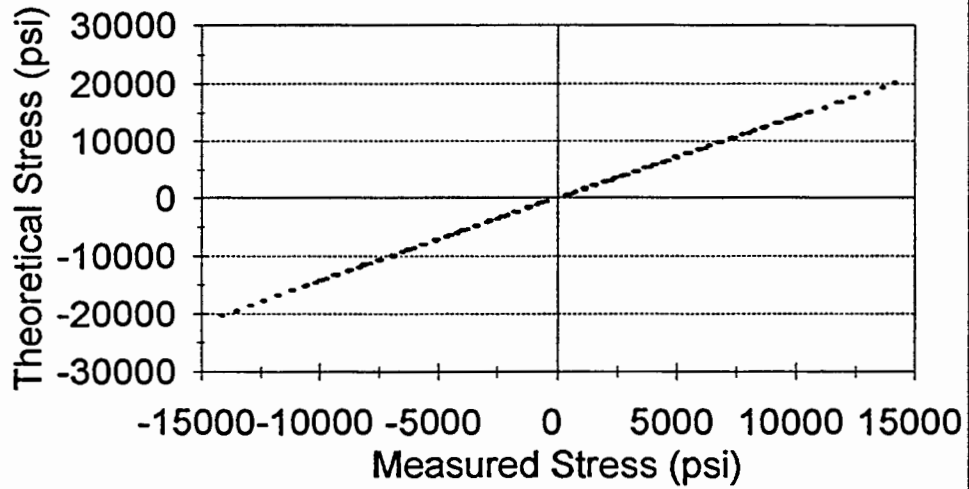
## Pile 2 Black Gage 8

Calibration Factor=1.318516



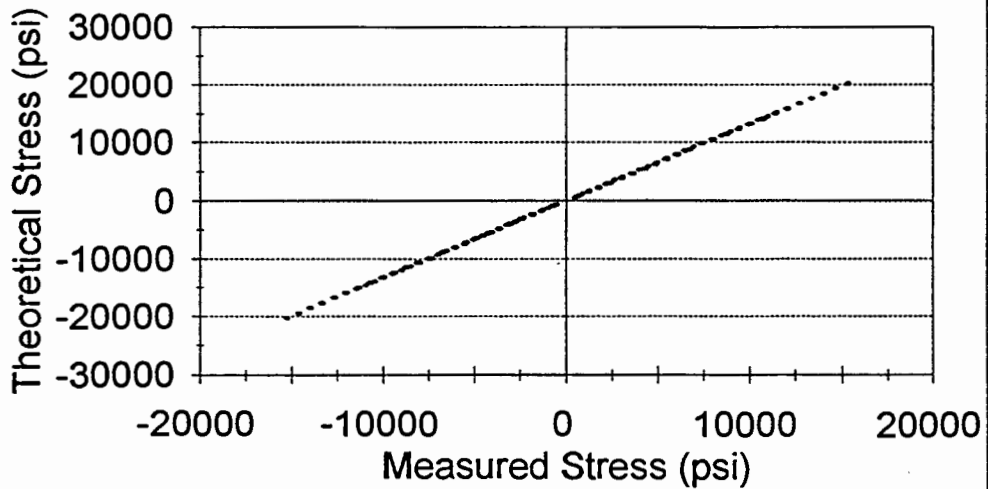
## Pile 2 Red Gage 9

Calibration Factor=1.432497



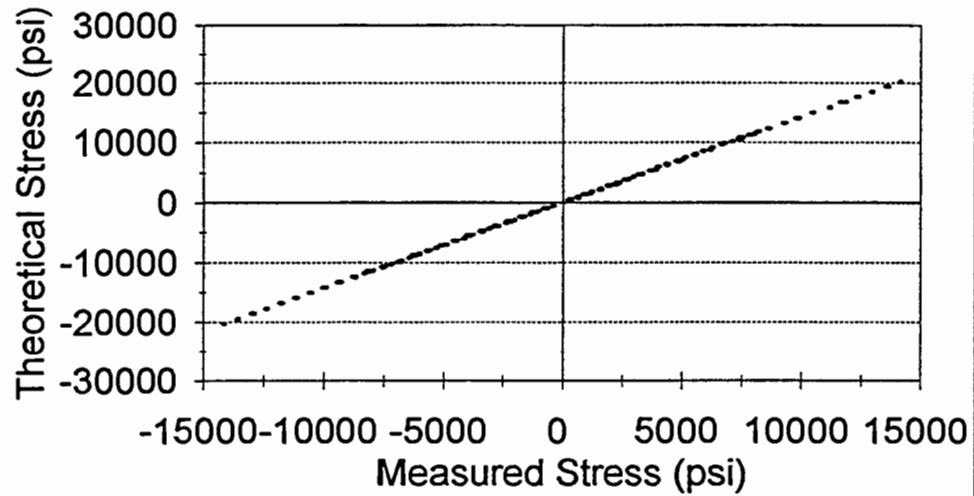
## Pile 2 Black Gage 9

Calibration Factor=1.325436



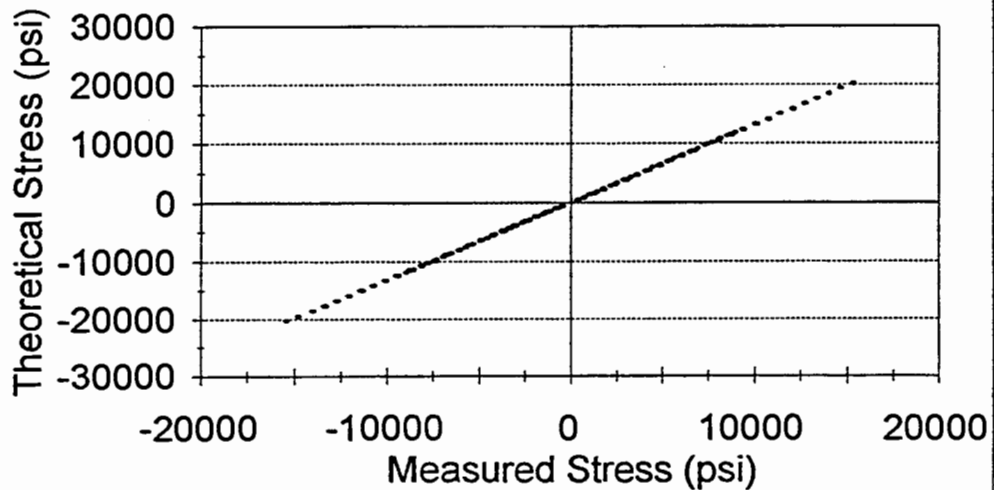
## Pile 2 Red Gage 10

Calibration Factor=1.432111

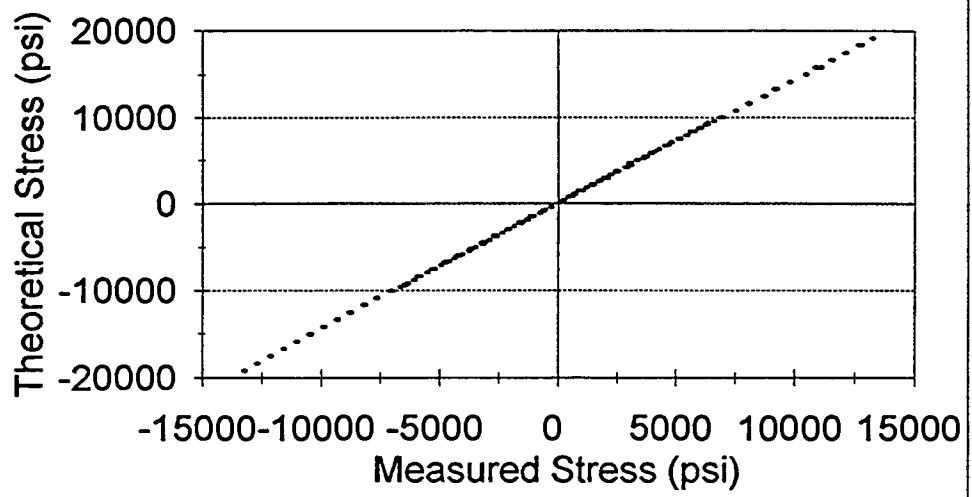


## Pile 2 Black Gage 10

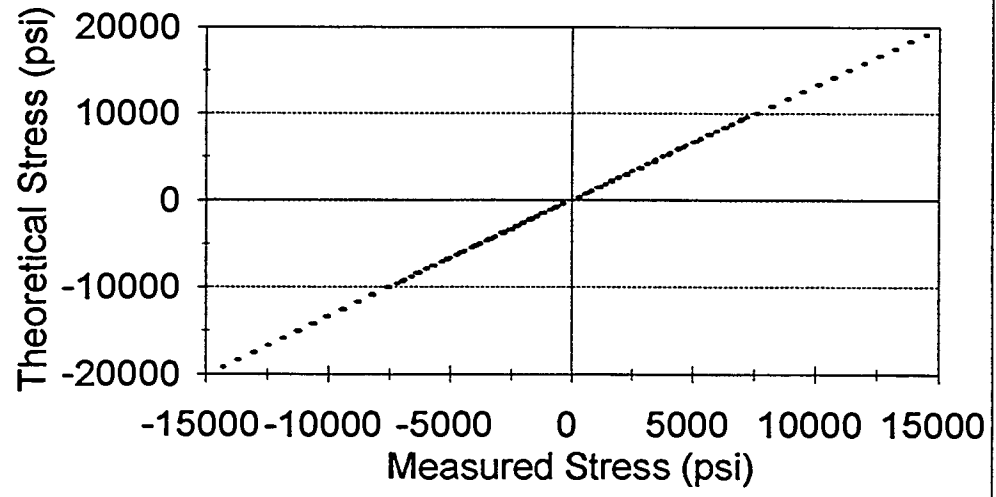
Calibration Factor=1.321356



**Pile 2 Red Gage 11**  
Calibration Factor=1.443233

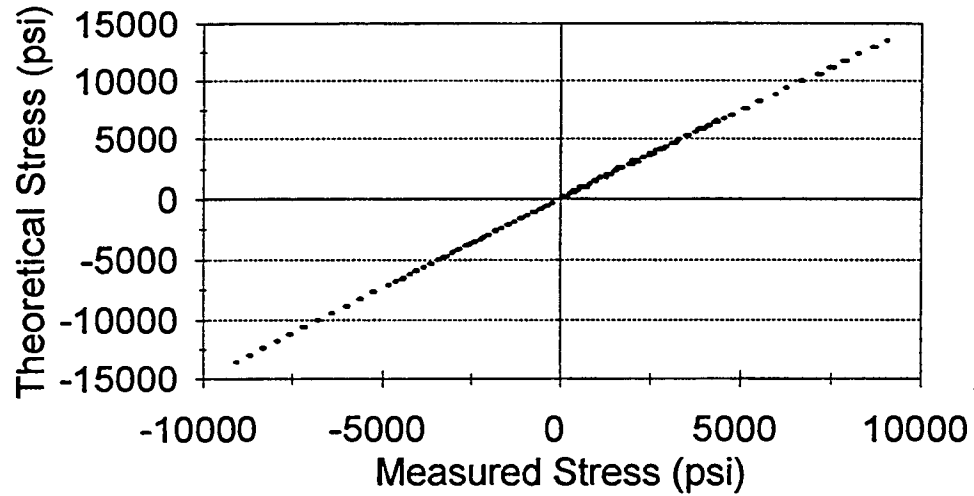


**Pile 2 Black Gage 11**  
Calibration Factor=1.329698



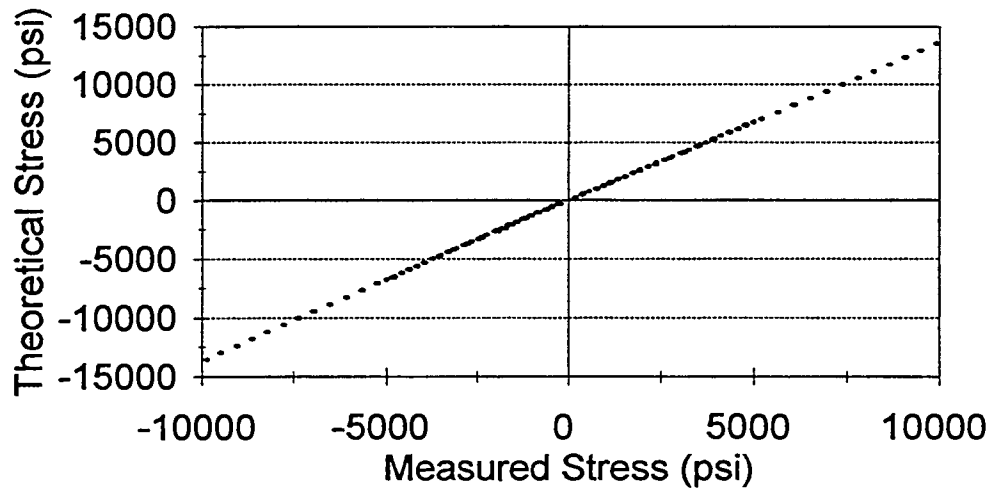
## Pile 2 Red Gage 12

Calibration Factor=1.487817



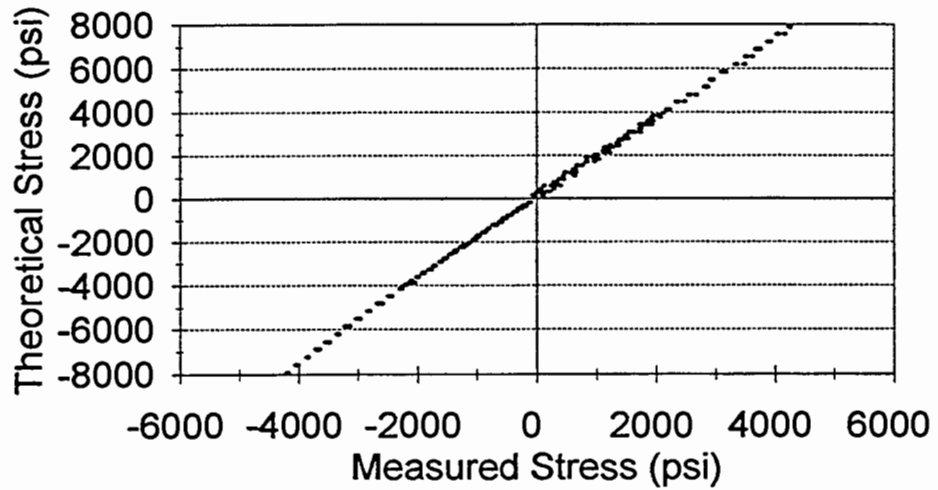
## Pile 2 Black Gage 12

Calibration Factor=1.358868



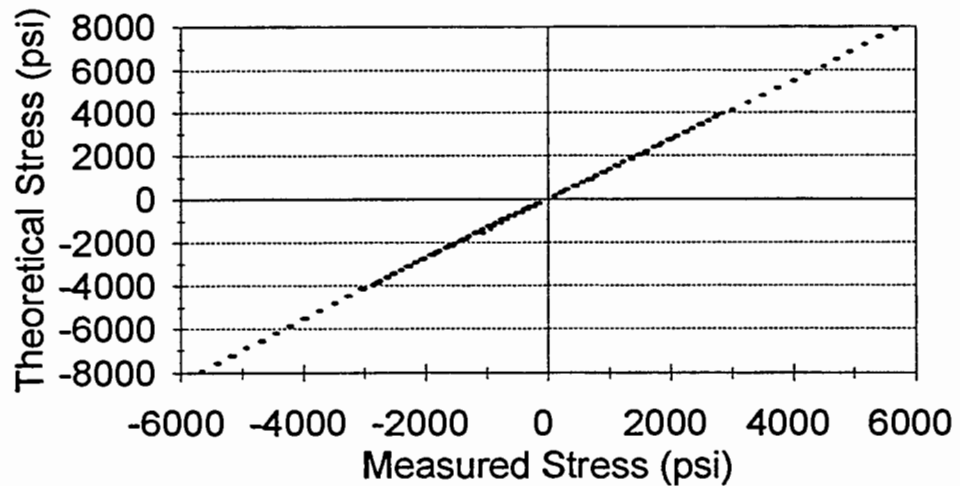
### Pile 2 Red Gage 13

Calibration Factor=1.849786



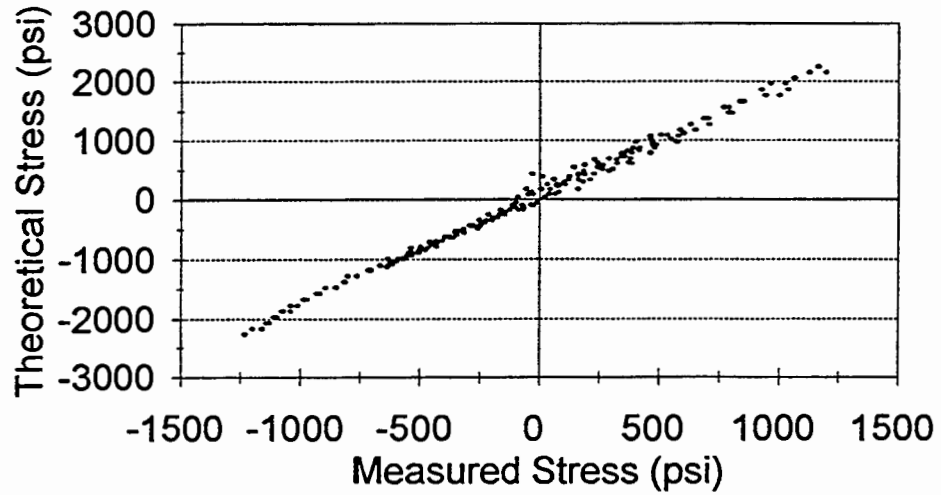
### Pile 2 Black Gage 13

Calibration Factor=1.381962



### Pile 2 Red Gage 14

Calibration Factor=1.819006



### Pile 2 Black Gage 14

Defective Gage

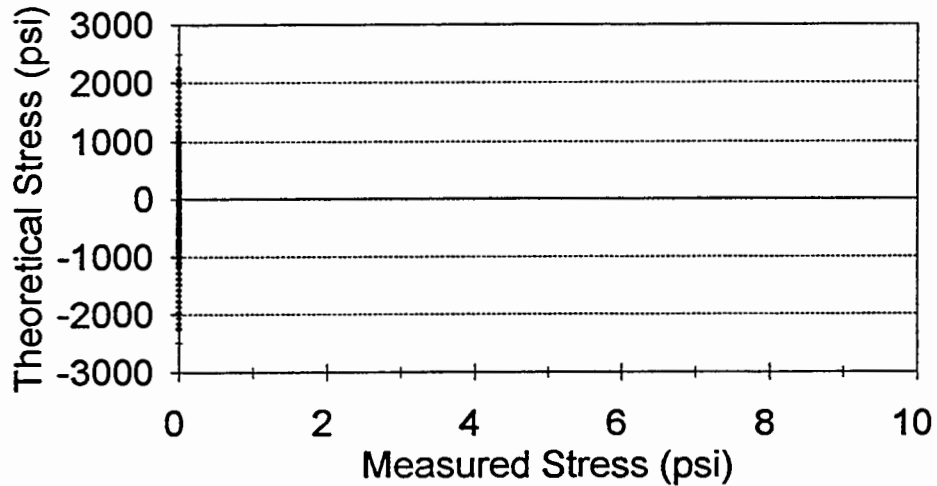
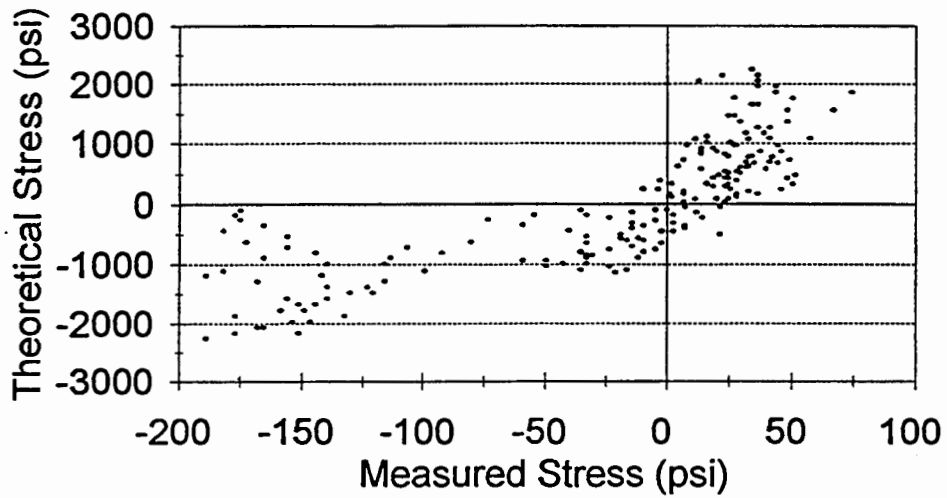


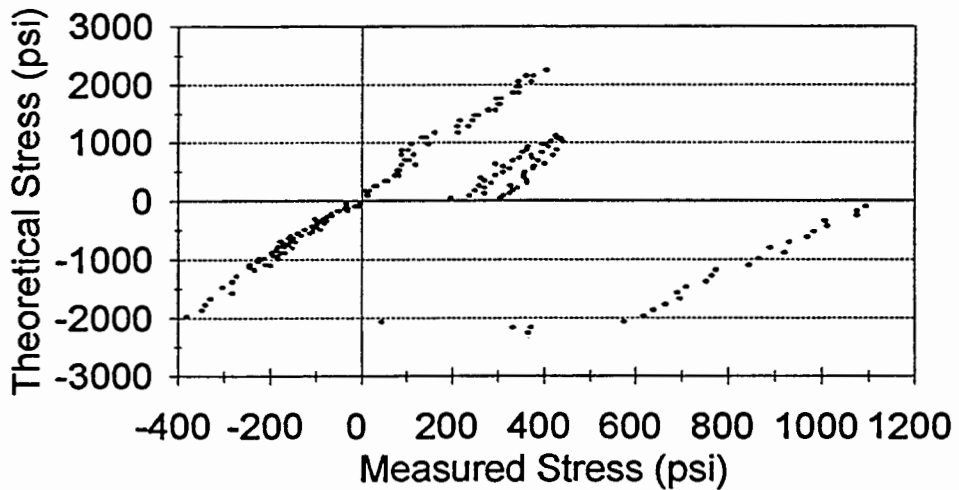
Figure C3. Pile 3 calibration (next 14 plots).



### Pile 3 Red Gage 1 Defective Gage

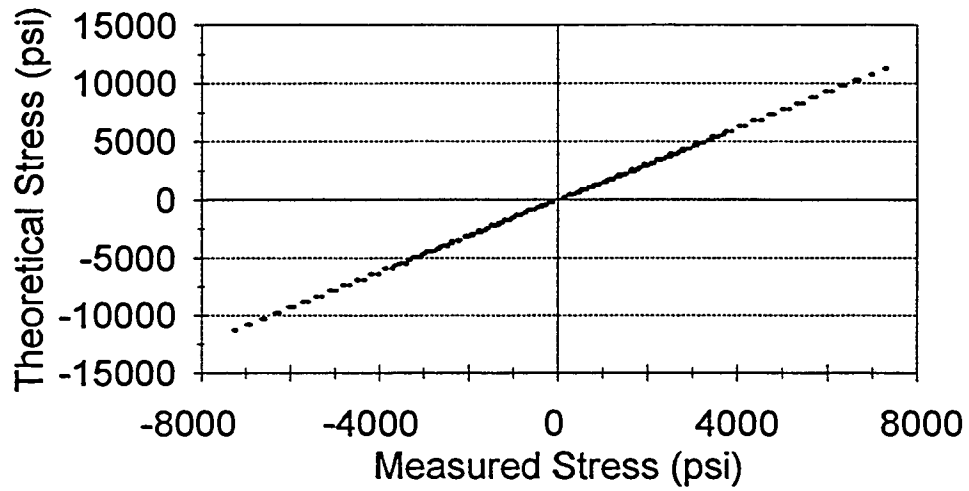


### Pile 3 Black Gage 1 Defective Gage



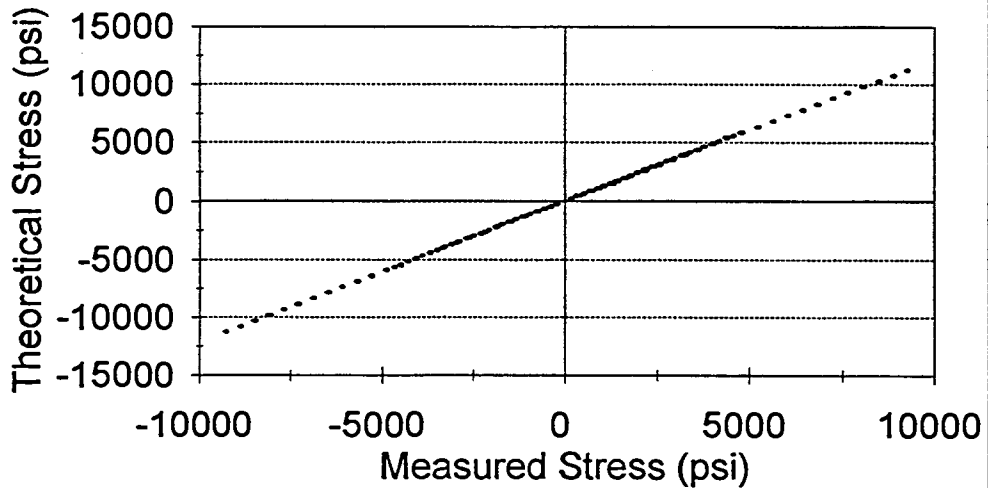
### Pile 3 Red Gage 2

Calibration Factor=1.549544



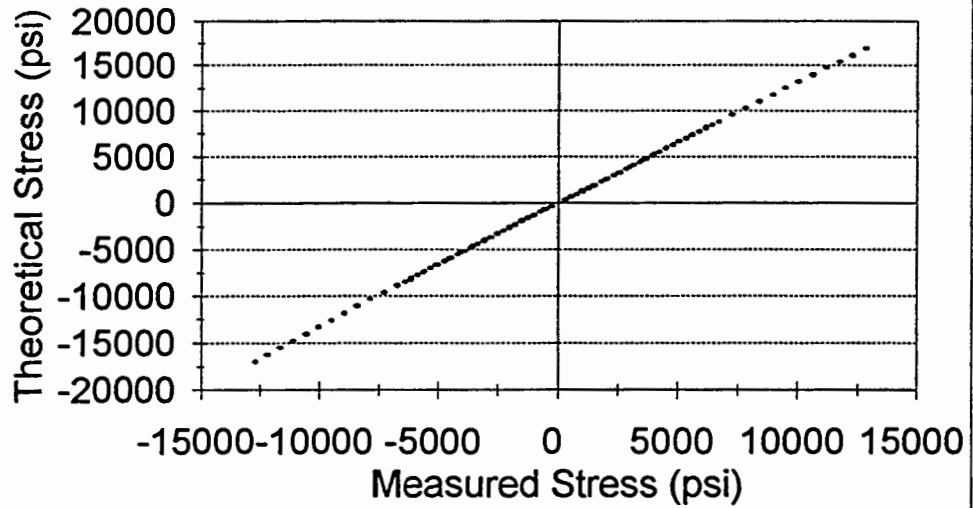
### Pile 3 Black Gage 2

Calibration Factor=1.216912



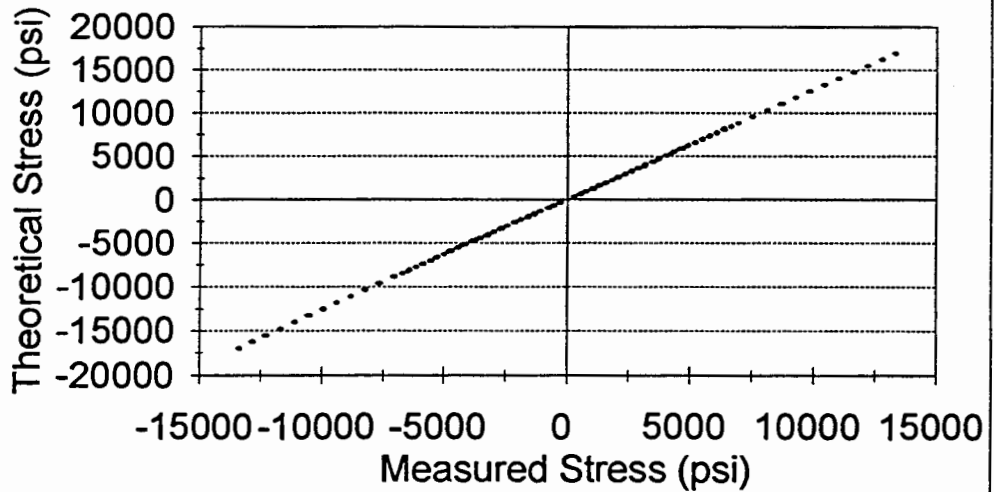
### Pile 3 Red Gage 3

Calibration Factor=1.319578

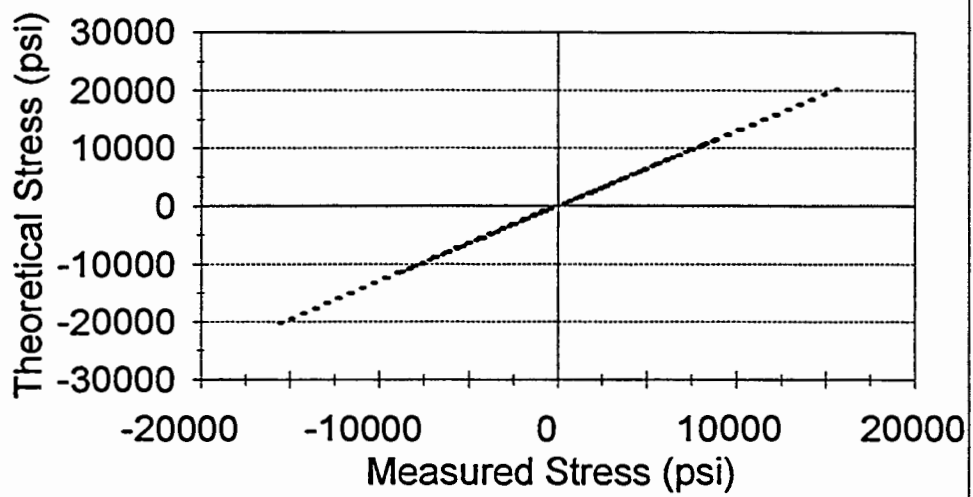


### Pile 3 Black Gage 3

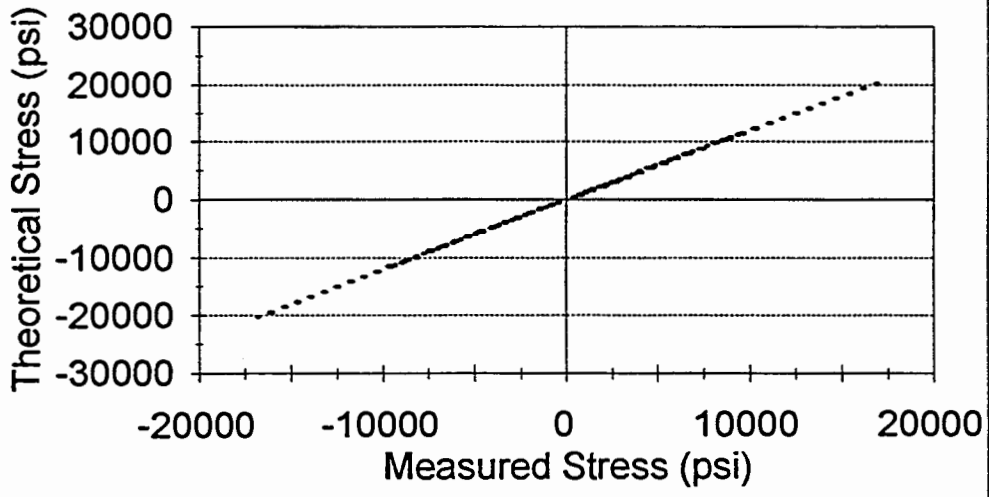
Calibration Factor=1.265008



**Pile 3 Red Gage 4**  
Calibration Factor=1.298574

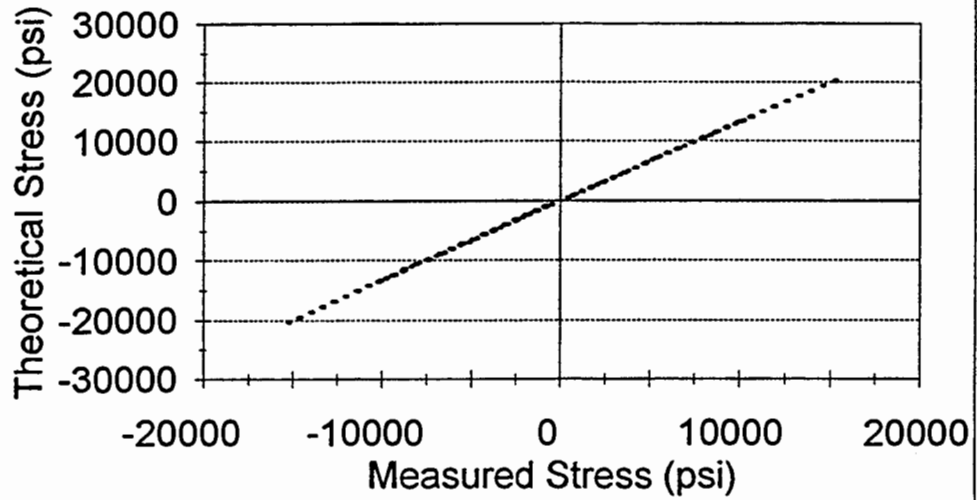


**Pile 3 Black Gage 4**  
Calibration Factor=1.203908



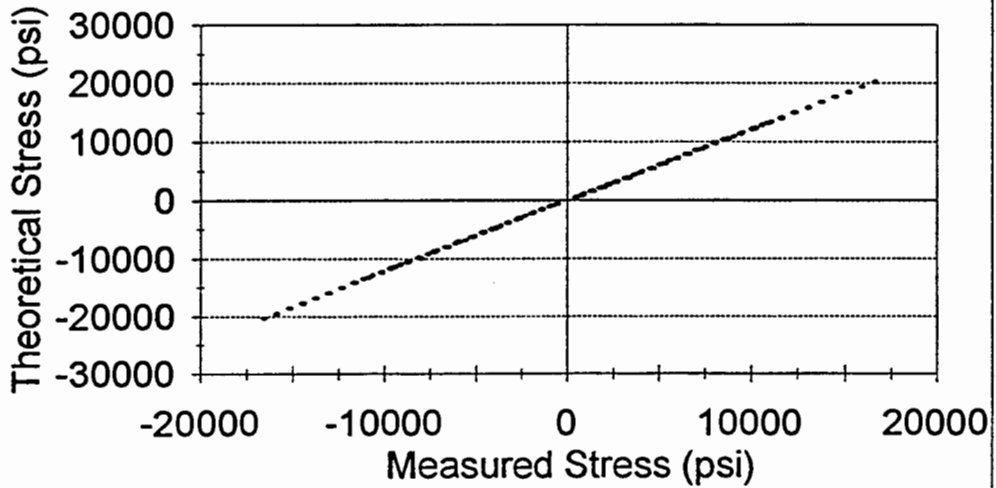
### Pile 3 Red Gage 5

Calibration Factor=1.326144



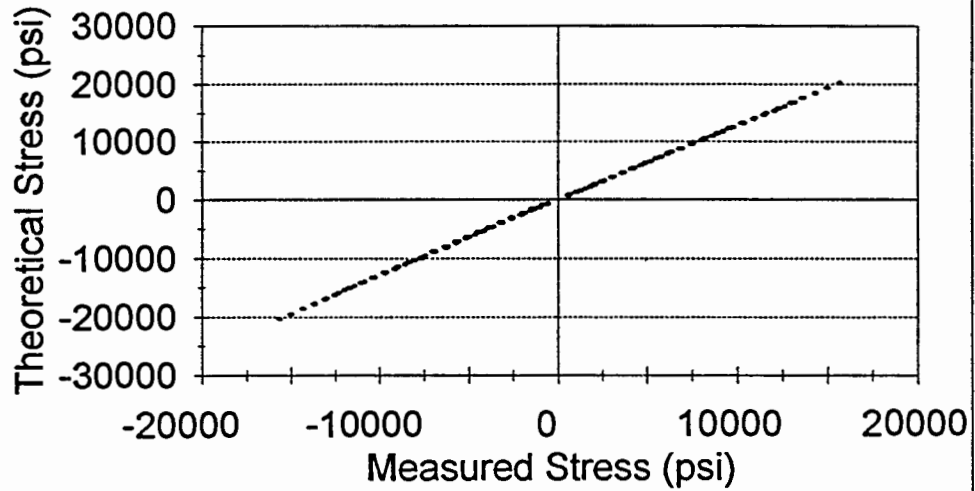
### Pile 3 Black Gage 5

Calibration Factor=1.218816



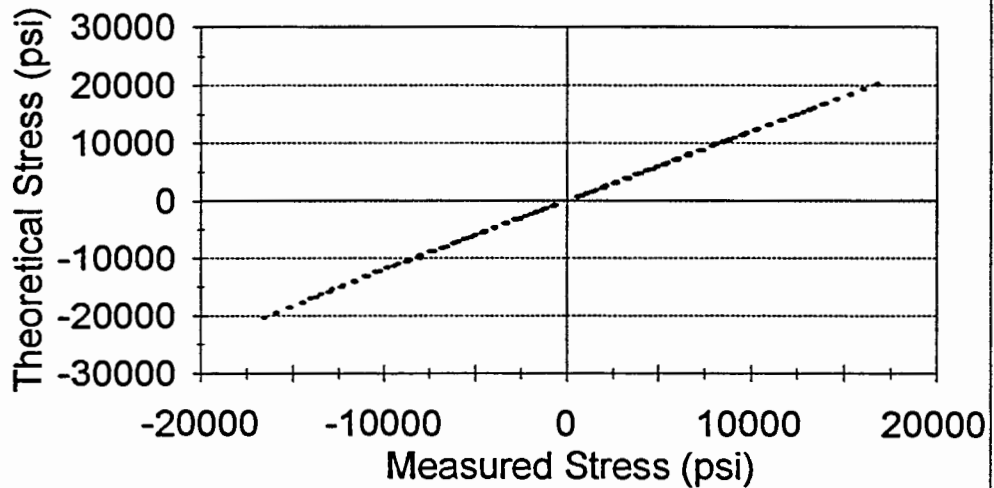
### Pile 3 Red Gage 6

Calibration Factor=1.287826



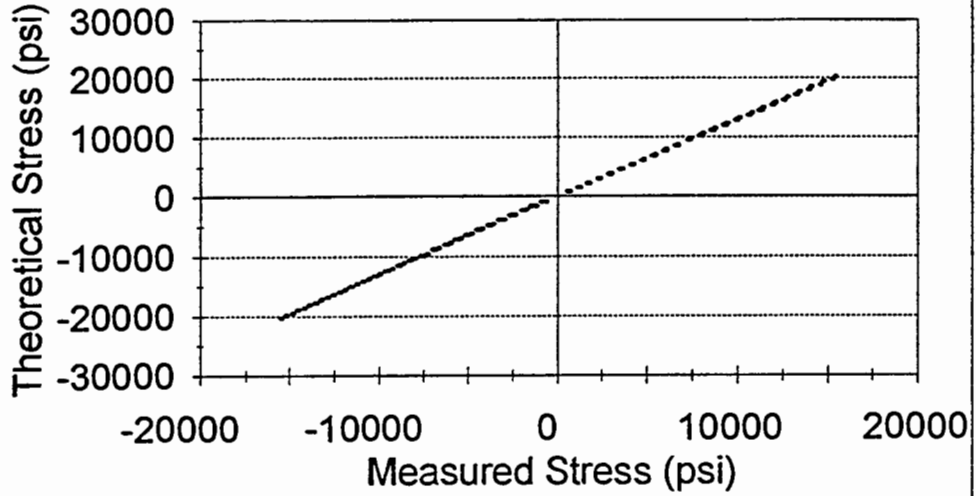
### Pile 3 Black Gage 6

Calibration Factor=1.210826



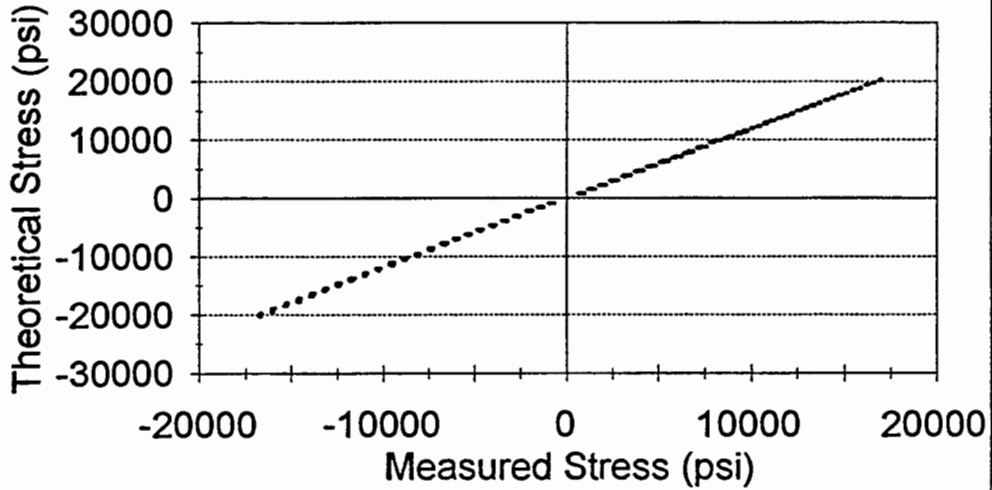
### Pile 3 Red Gage 7

Calibration Factor=1.302568

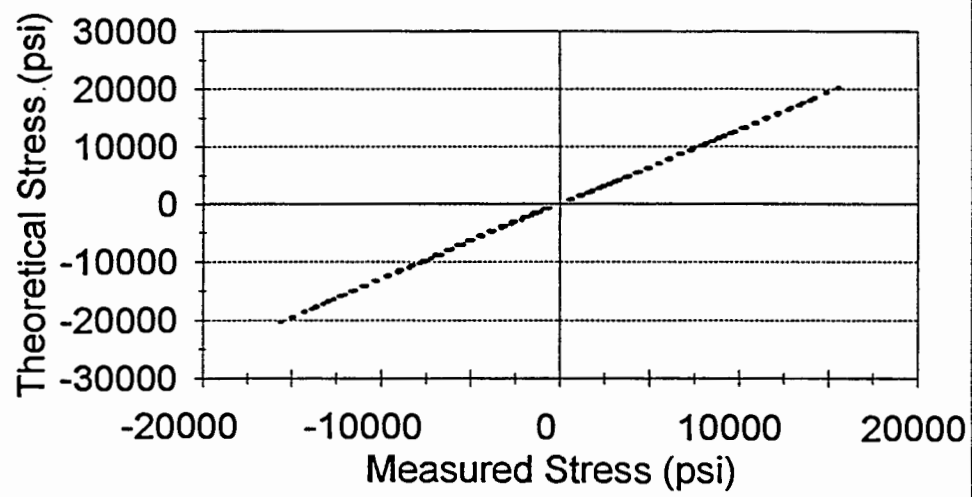


### Pile 3 Black Gage 7

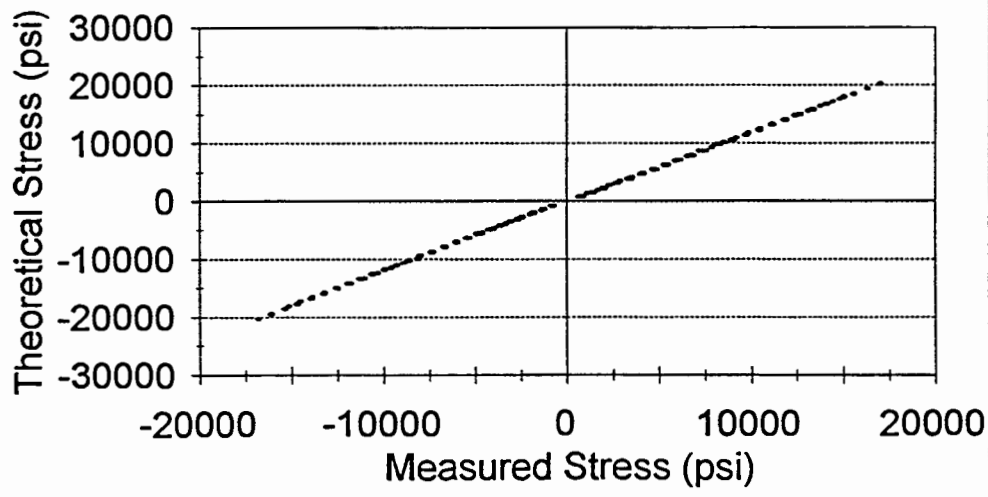
Calibration Factor=1.194451



**Pile 3 Red Gage 8**  
Calibration Factor=1.297134



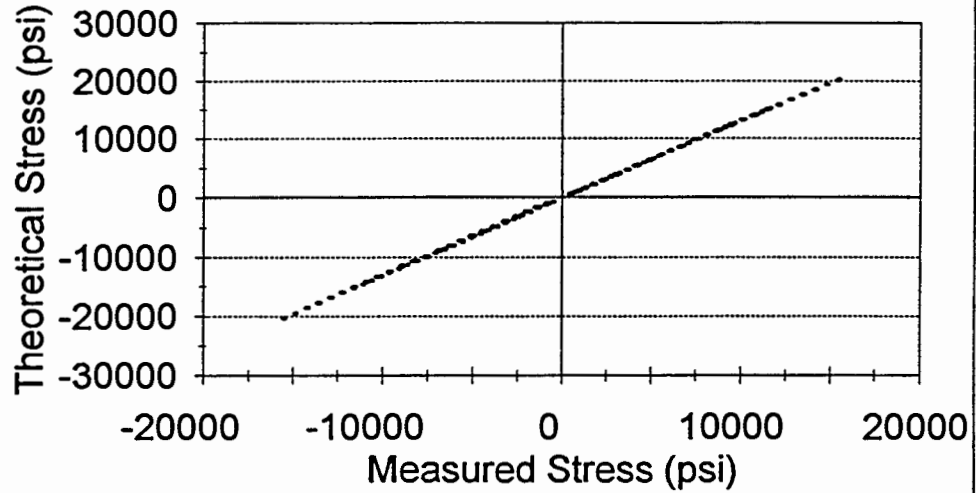
**Pile 3 Black Gage 8**  
Calibration Factor=1.194959





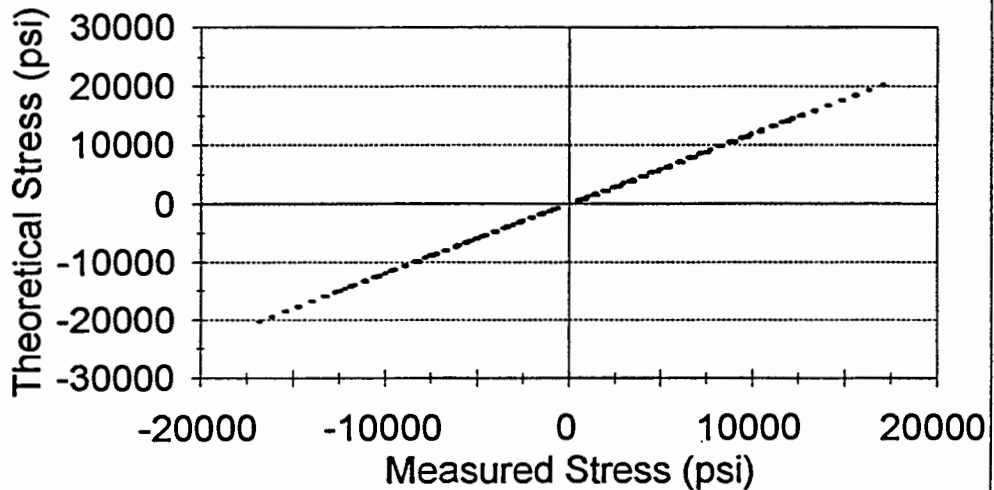
### Pile 3 Red Gage 9

Calibration Factor=1.308108



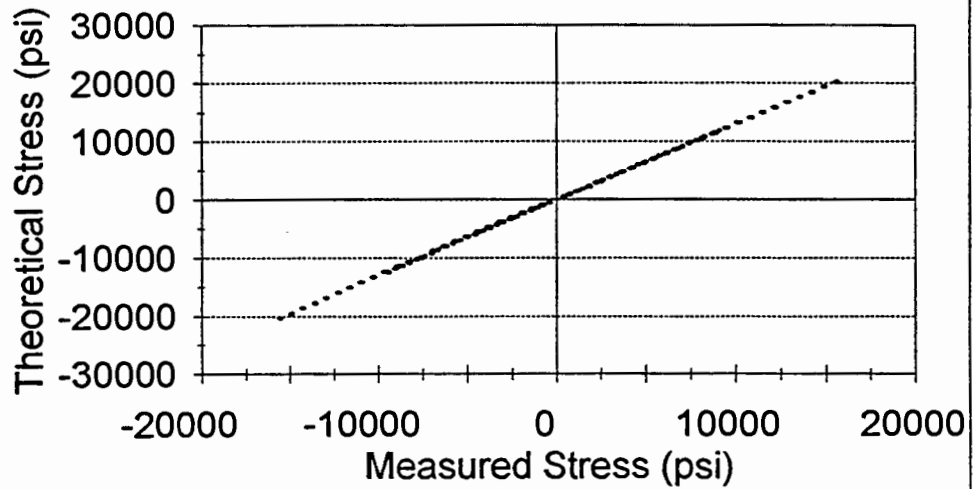
### Pile 3 Black Gage 9

Calibration Factor=1.1943



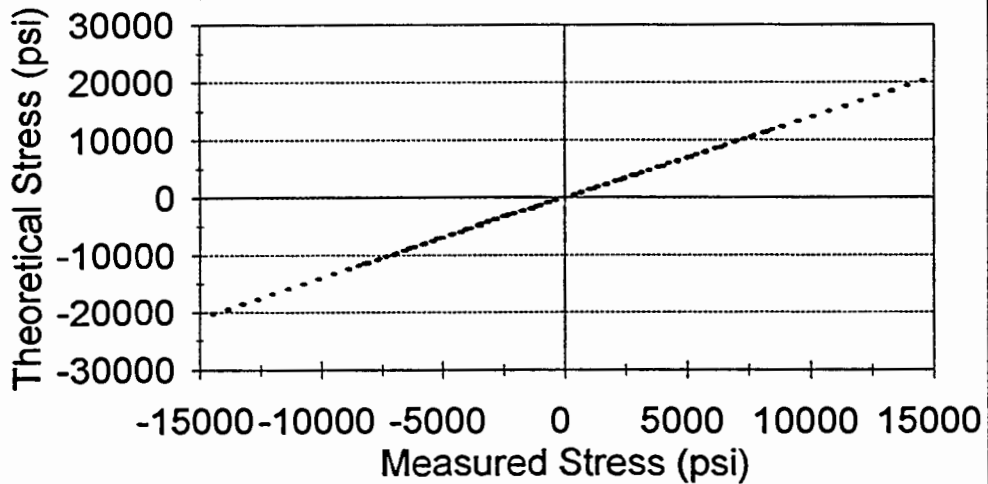
### Pile 3 Red Gage 10

Calibration Factor=1.301789



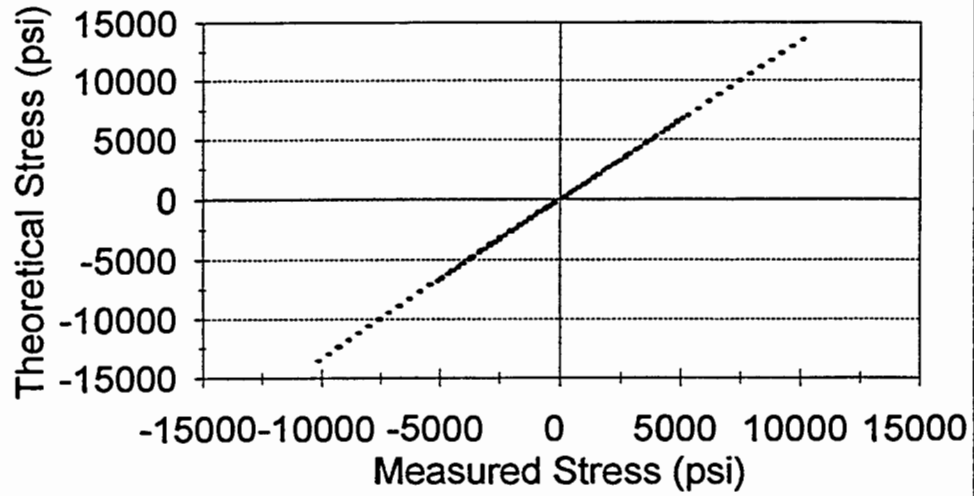
### Pile 3 Black Gage 10

Calibration Factor=1.398623



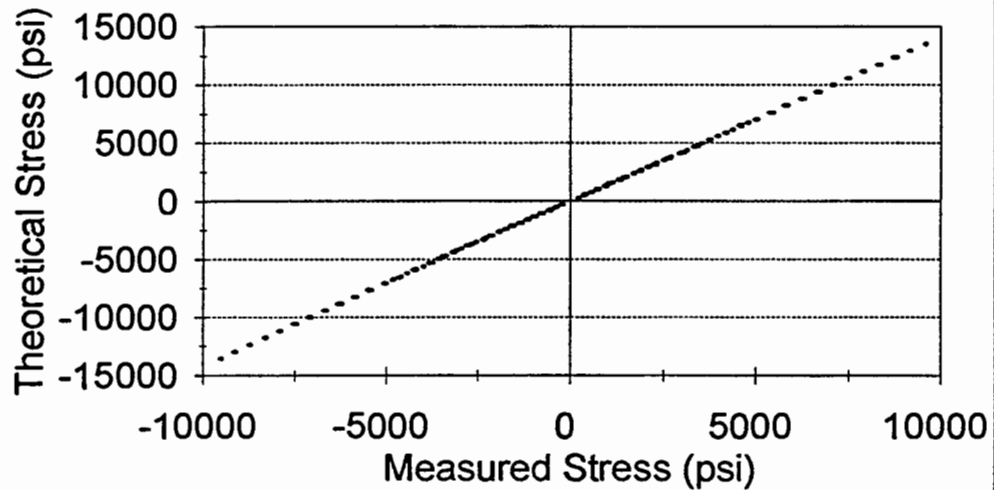
### Pile 3 Red Gage 12

Calibration Factor=1.331283



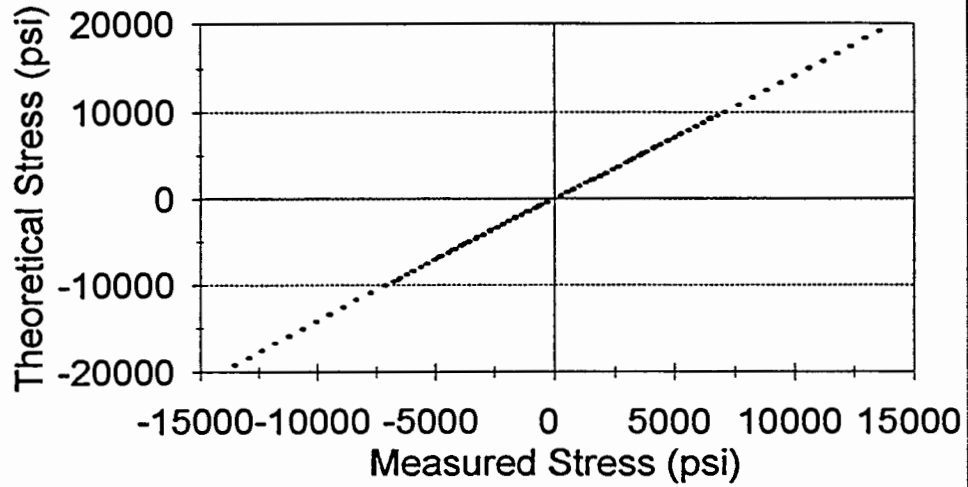
### Pile 3 Black Gage 12

Calibration Factor=1.412325



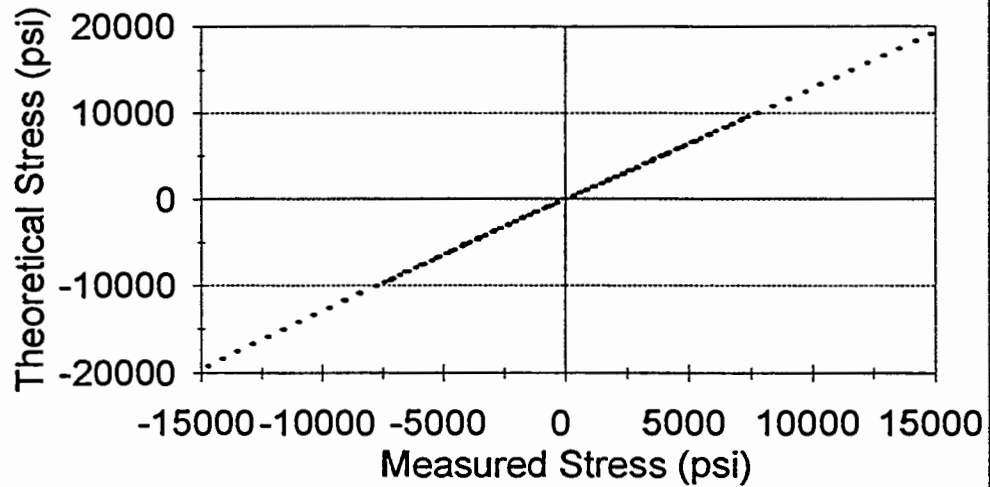
### Pile 3 Red Gage 11

Calibration Factor=1.414312



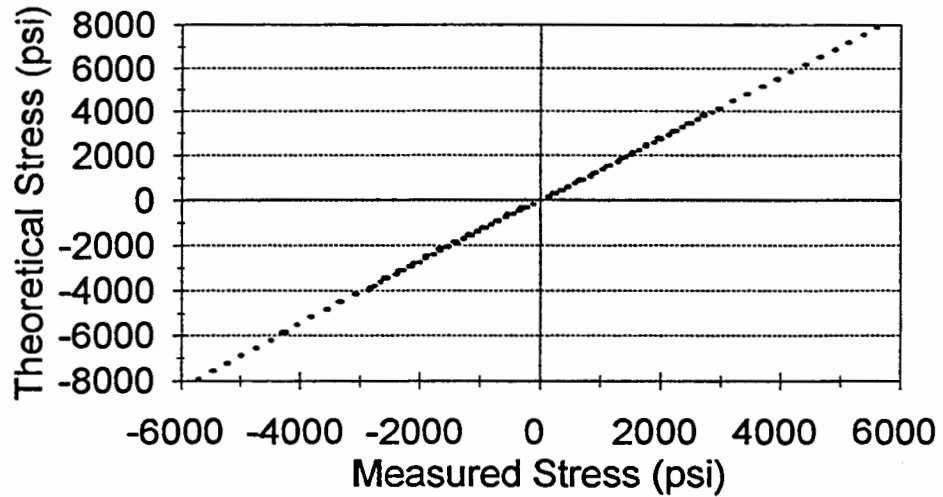
### Pile 3 Black Gage 11

Calibration Factor=1.293776



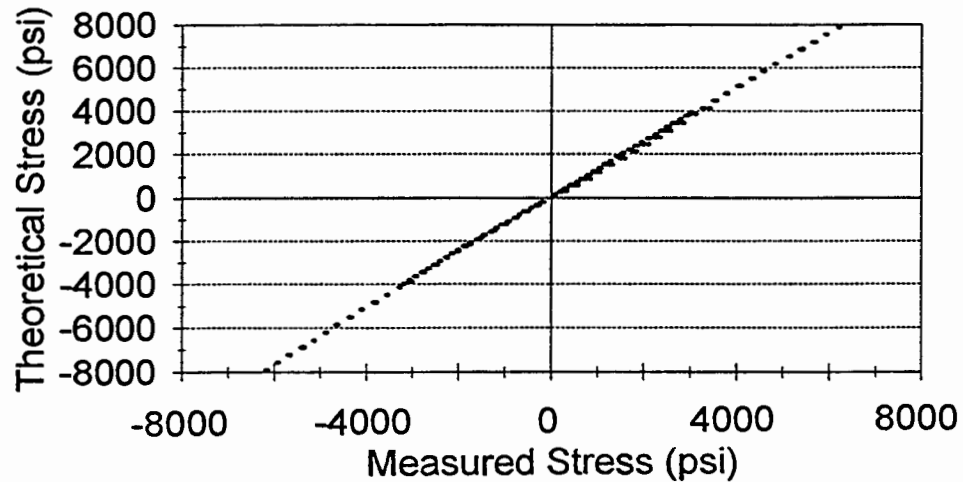
### Pile 3 Red Gage 13

Calibration Factor=1.379867



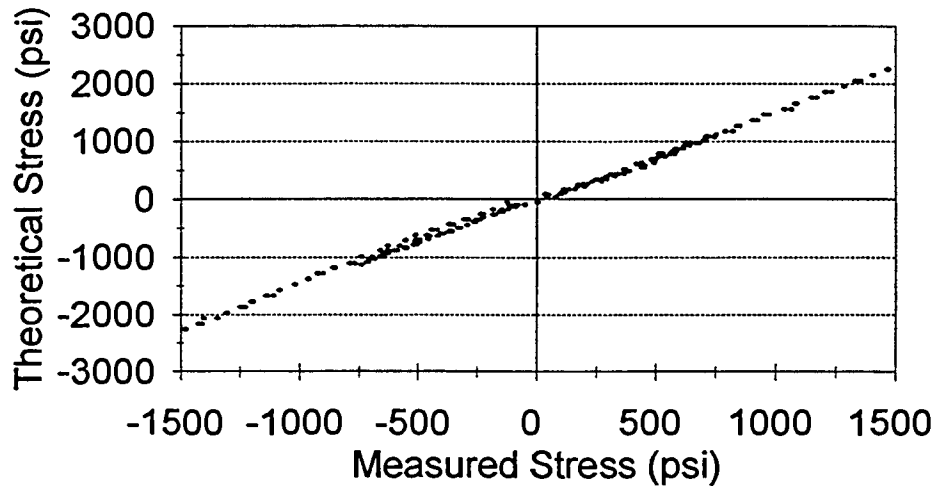
### Pile 3 Black Gage 13

Calibration Factor=1.265274



### Pile 3 Red Gage 14

Calibration Factor=1.478234



### Pile 3 Black Gage 14

Calibration Factor=1.374964

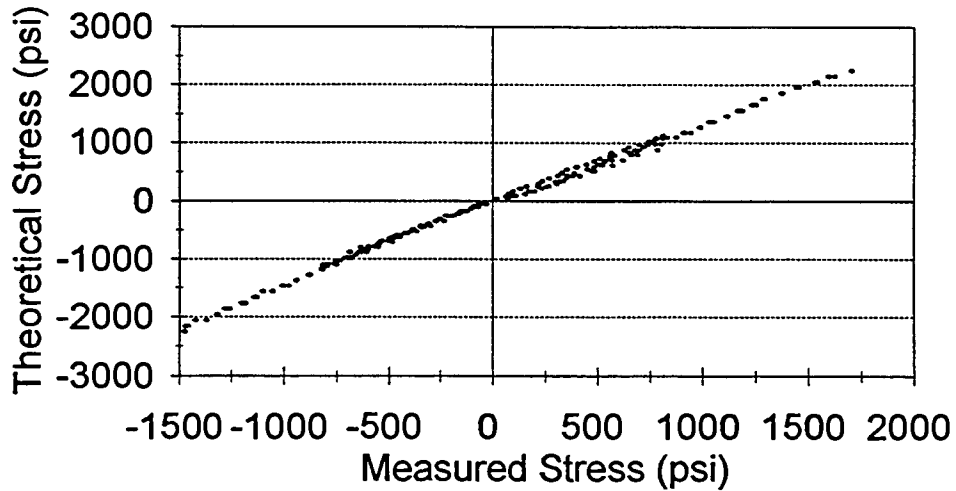
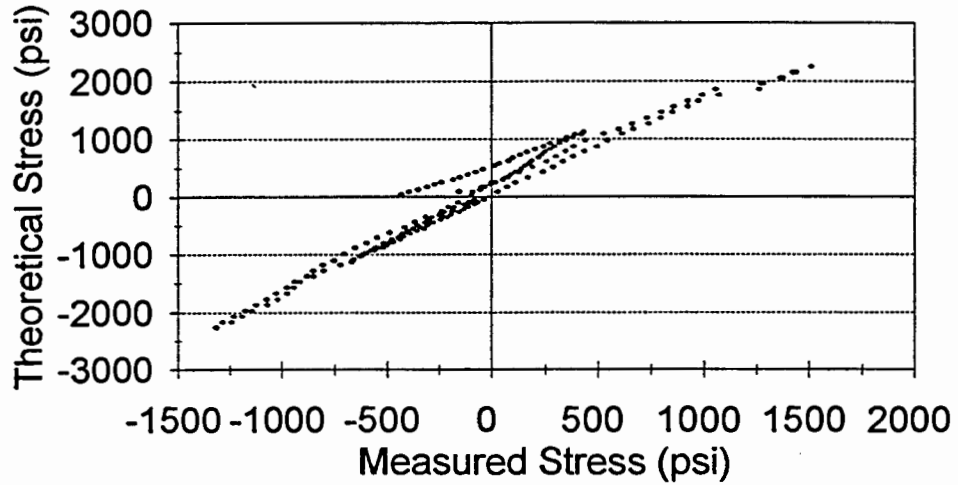


Figure C4. Pile 4 calibration (next 14 plots).

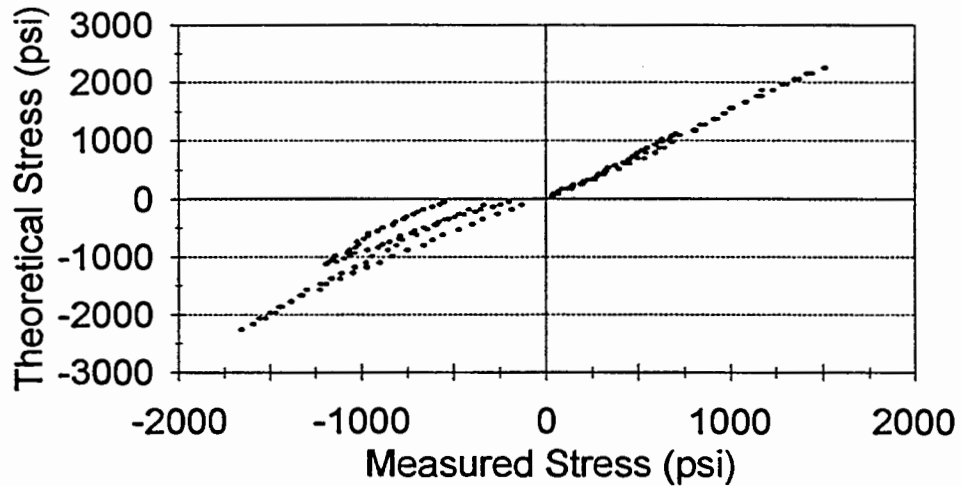
### Pile 4 Red Gage 1

Calibration Factor=1.645359



### Pile 4 Black Gage 1

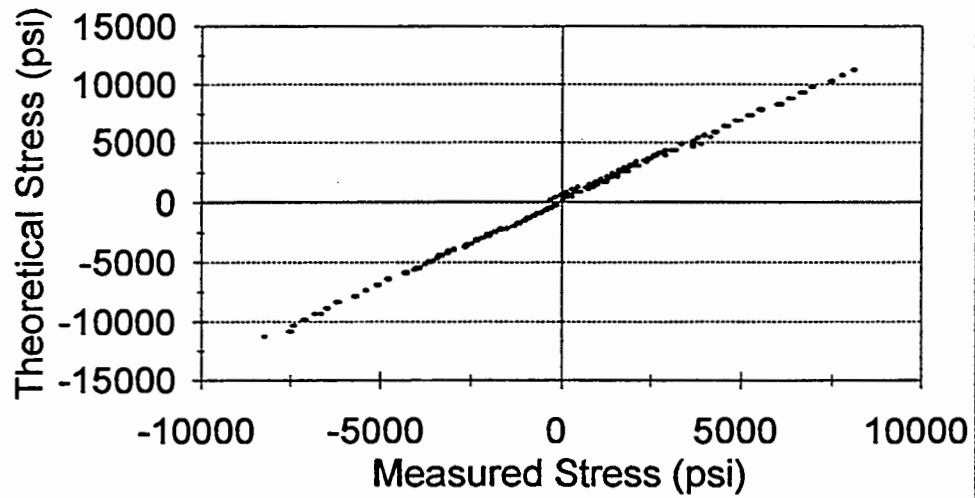
Calibration Factor=1.203739





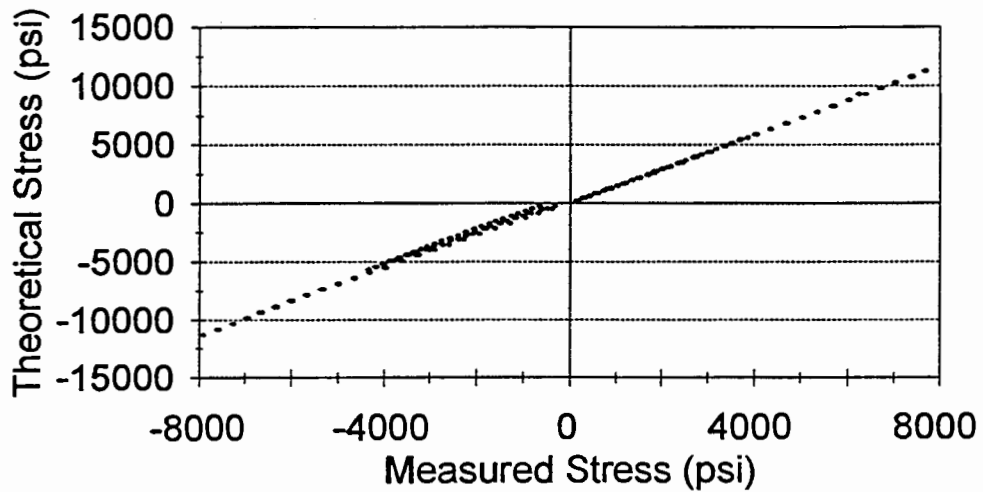
## Pile 4 Red Gage 2

Calibration Factor=1.389296



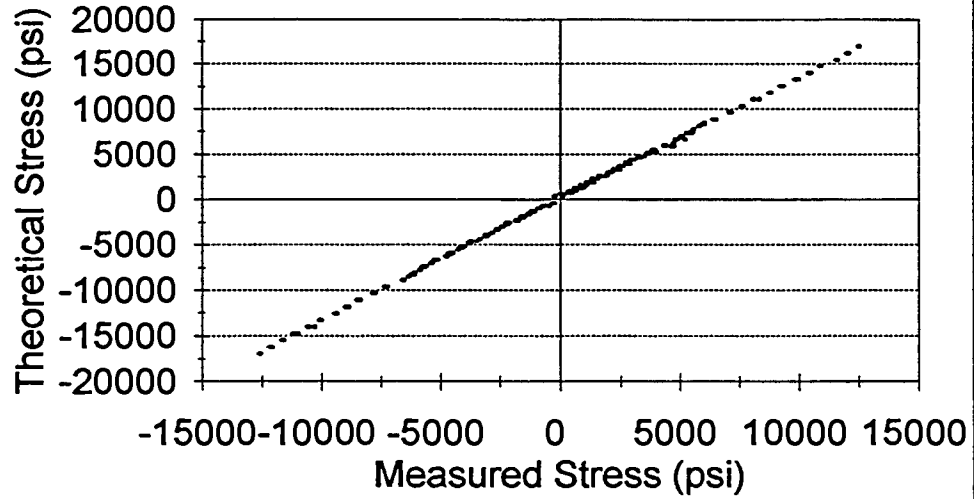
## Pile 4 Black Gage 2

Calibration Factor=1.406007



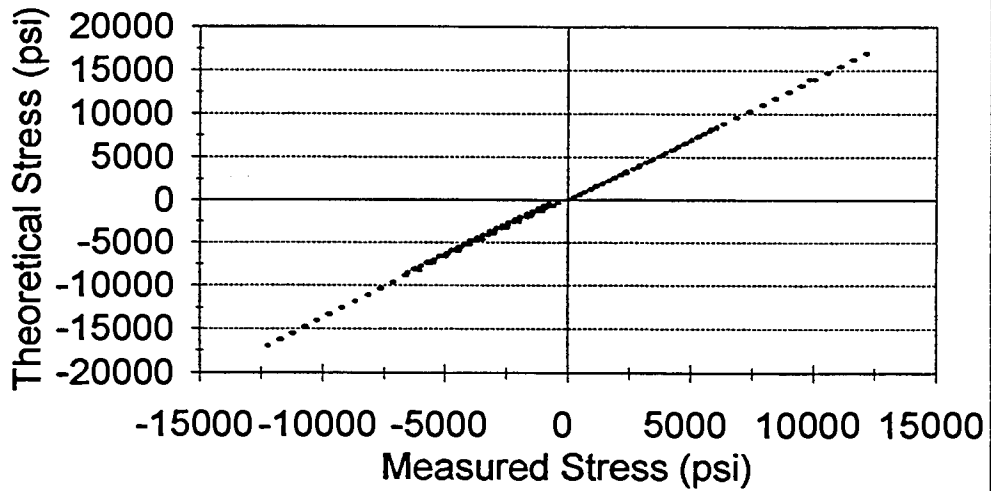
### Pile 4 Red Gage 3

Calibration Factor=1.337074



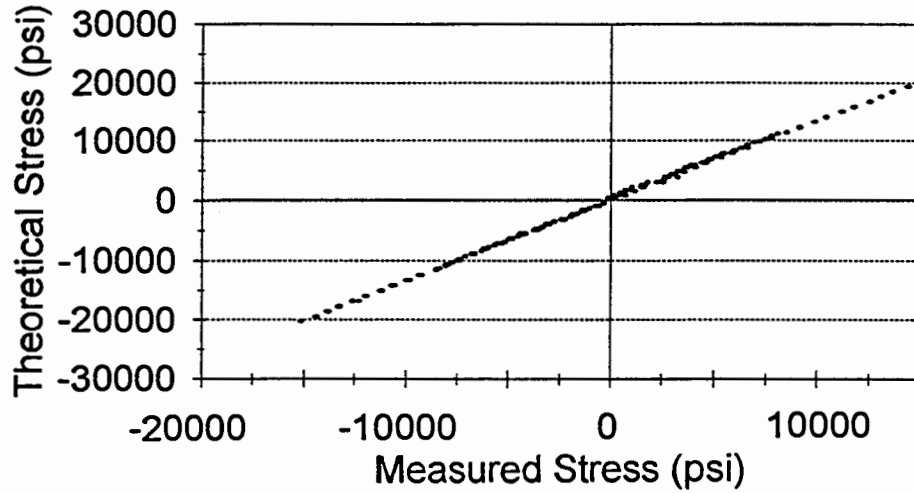
### Pile 4 Black Gage 3

Calibration Factor=1.366595



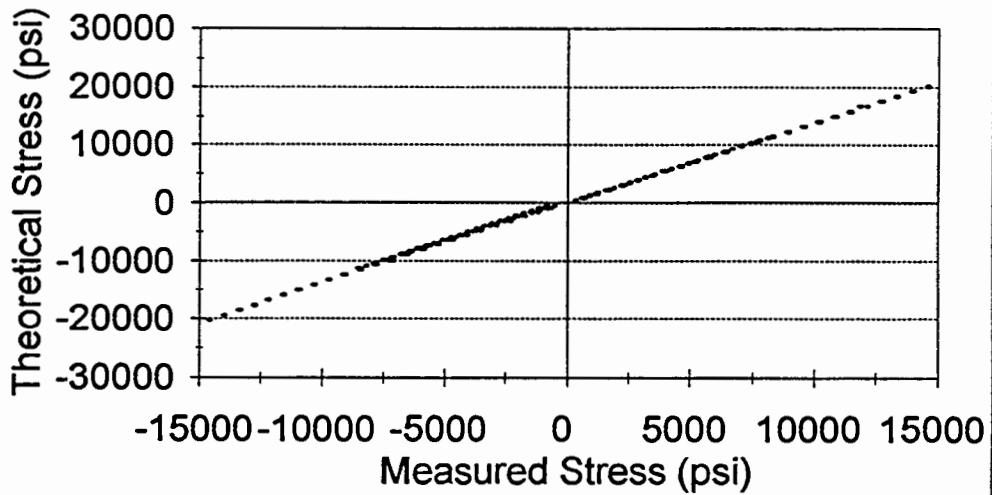
### Pile 4 Red Gage 4

Calibration Factor=1.351371



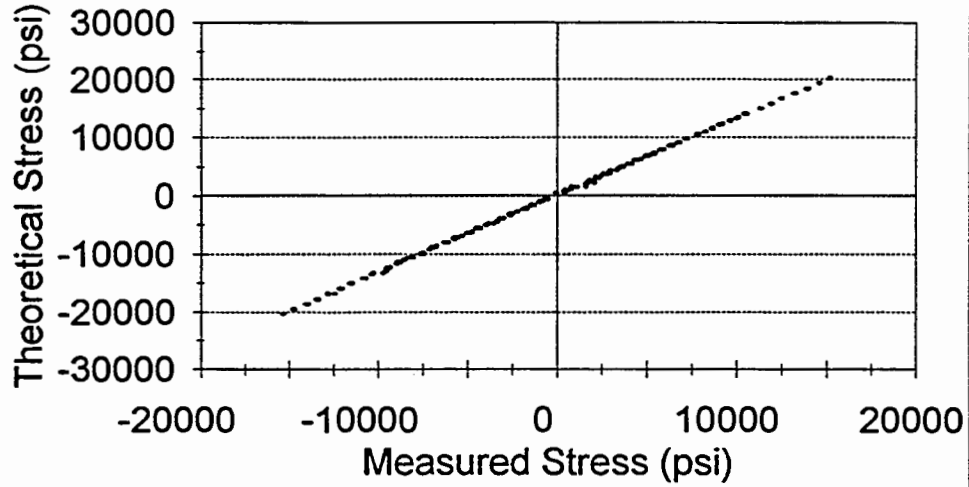
### Pile 4 Black Gage 4

Calibration Factor=1.371239



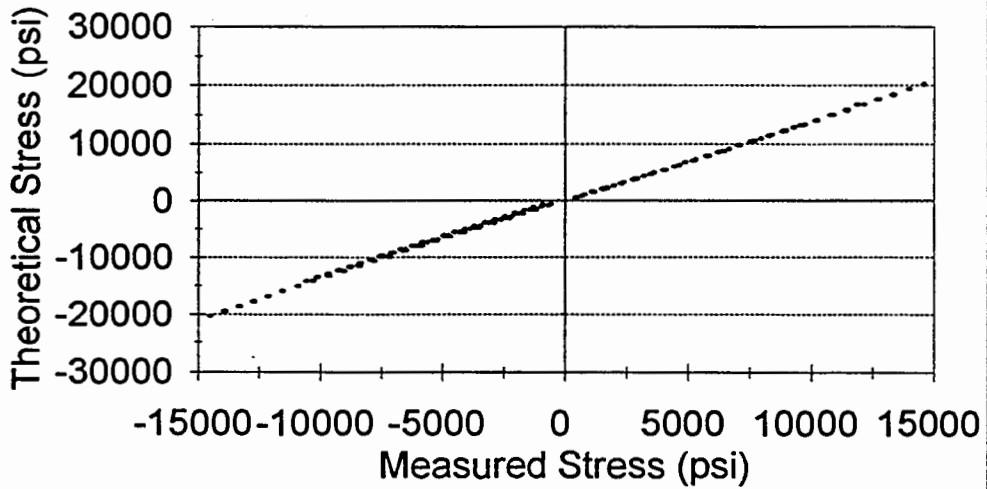
### Pile 4 Red Gage 5

Calibration Factor=1.326086



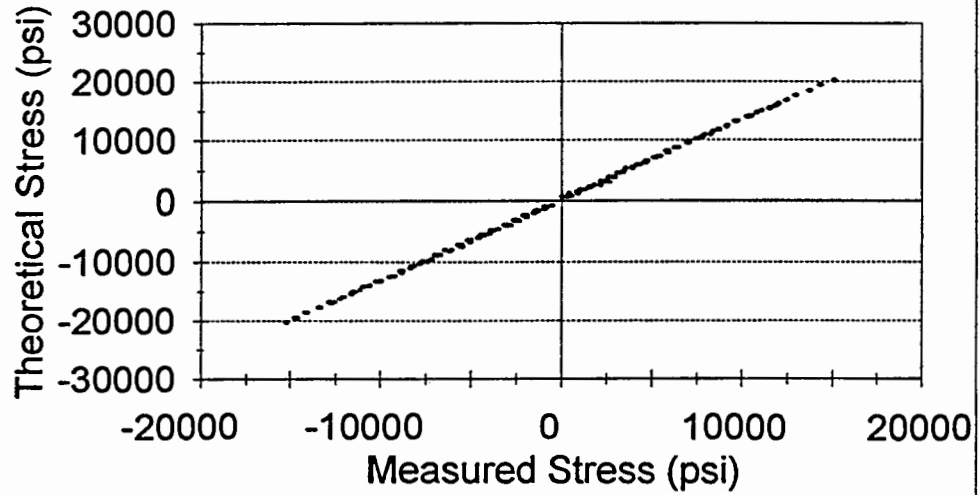
### Pile 4 Black Gage 5

Calibration Factor=1.371453



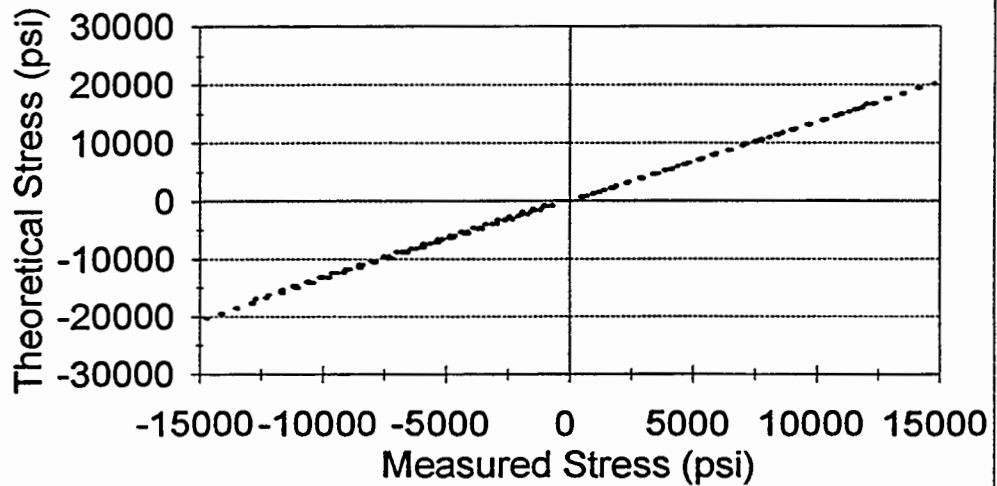
### Pile 4 Red Gage 6

Calibration Factor=1.338147



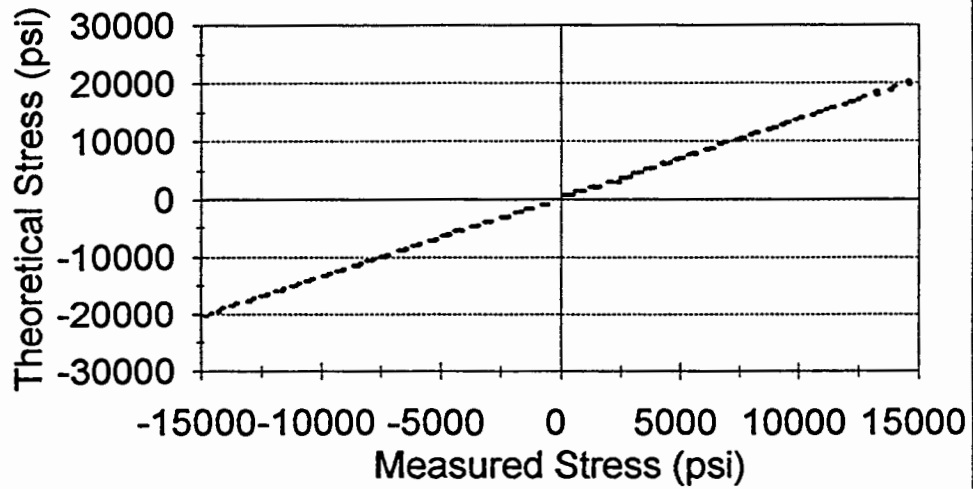
### Pile 4 Black Gage 6

Calibration Factor=1.355485



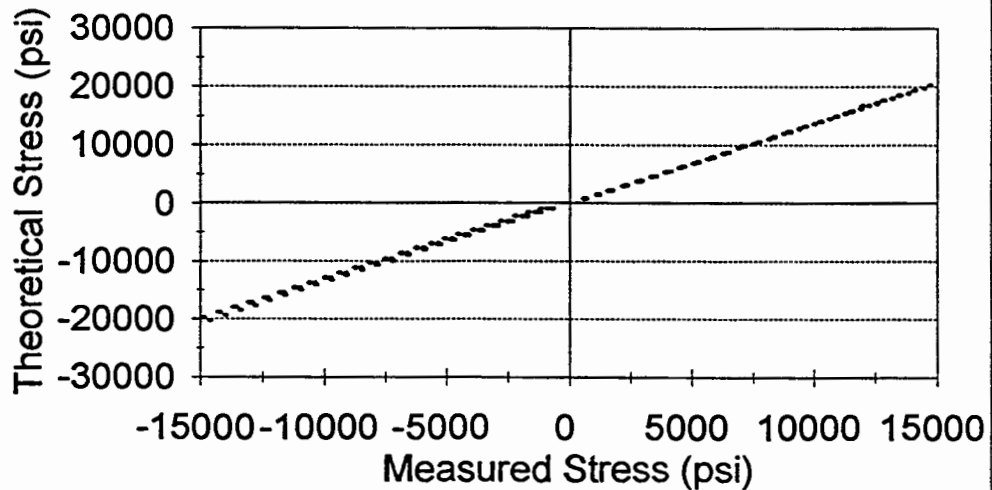
### Pile 4 Red Gage 7

Calibration Factor= 1.364325



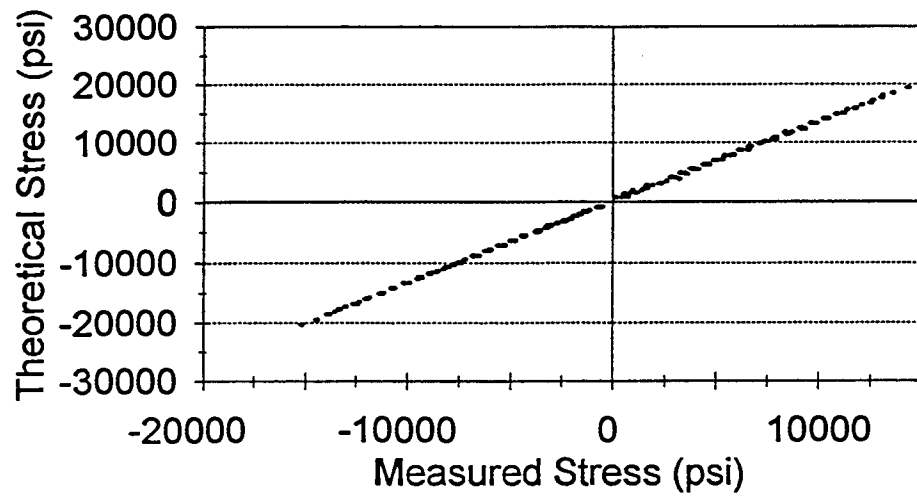
### Pile 4 Black Gage 7

Calibration Factor=1.357062



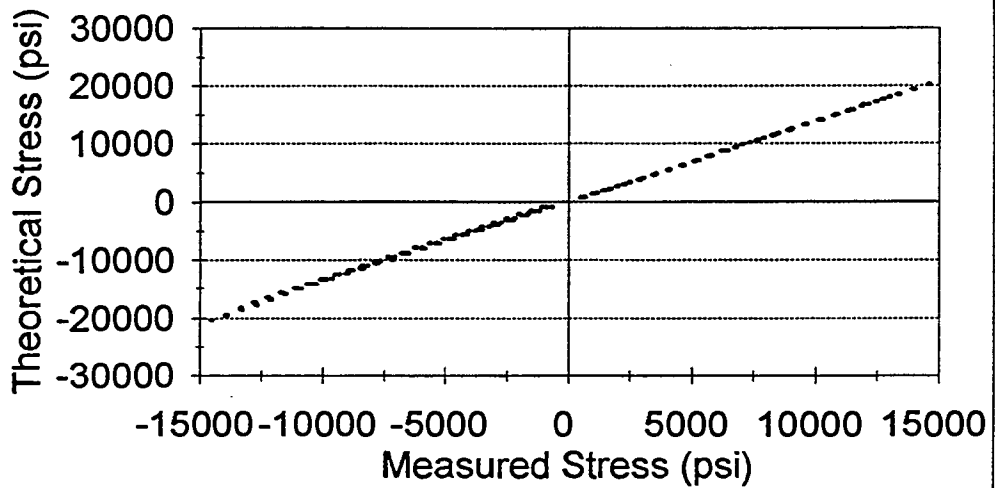
## Pile 4 Red Gage 8

Calibration Factor=1.349005



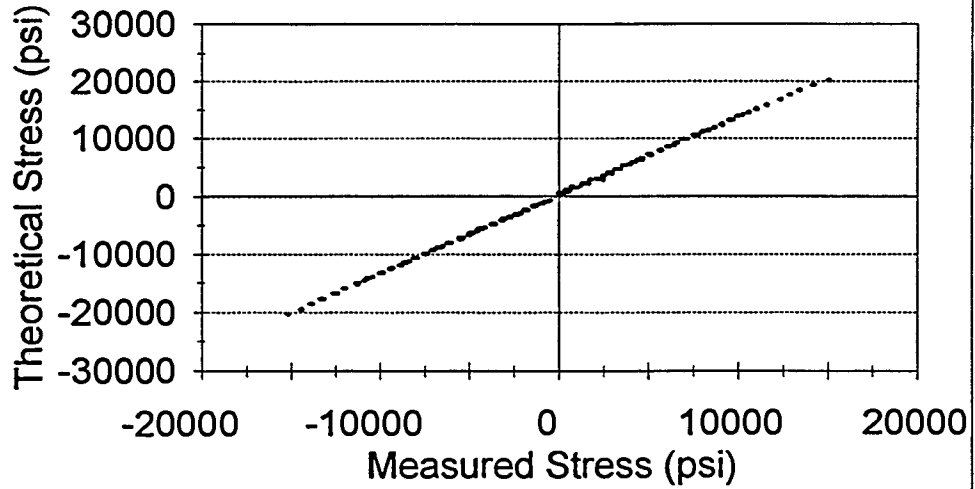
## Pile 4 Black Gage 8

Calibration Factor=1.373675



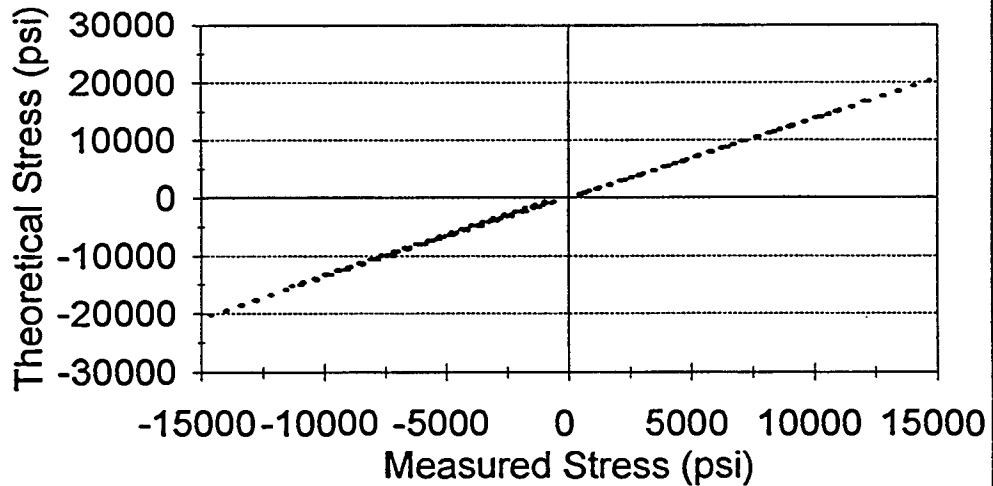
### Pile 4 Red Gage 9

Calibration Factor=1.357157



### Pile 4 Black Gage 9

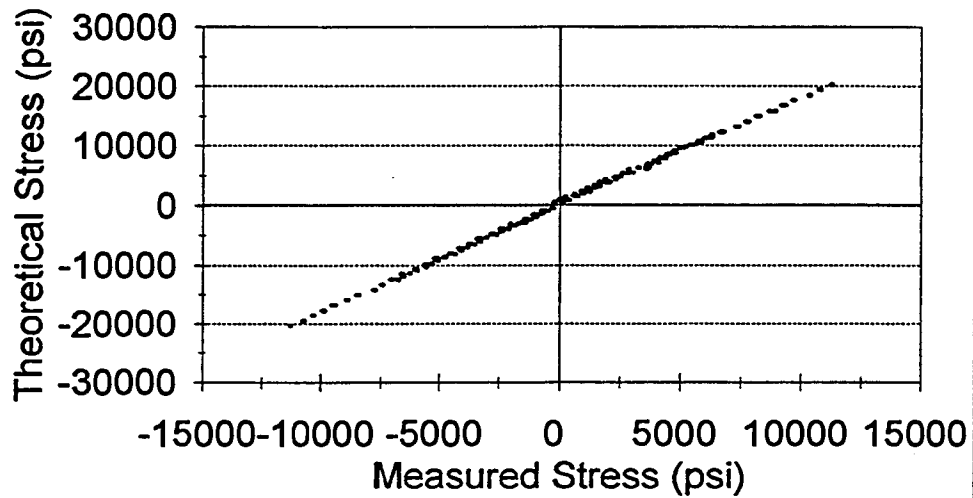
Calibration Factor=1.366966





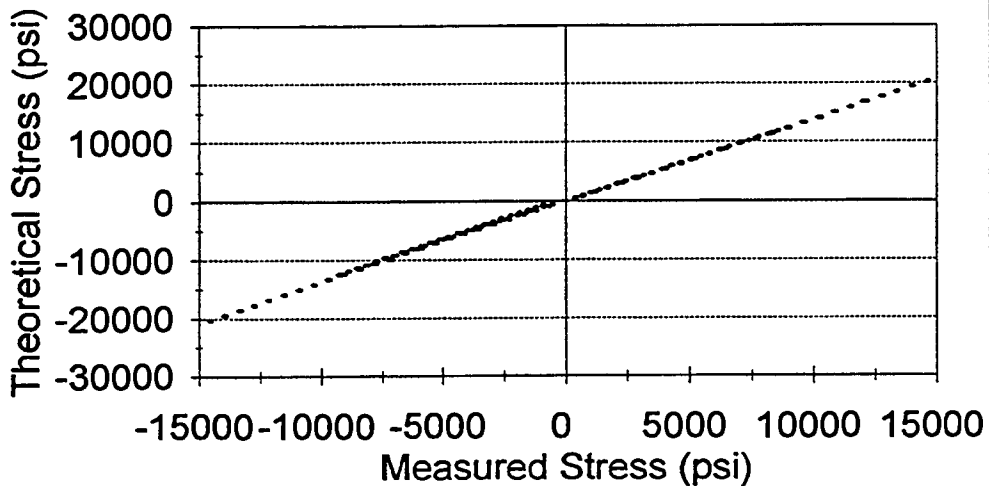
### Pile 4 Red Gage 10

Calibration Factor=1.816602



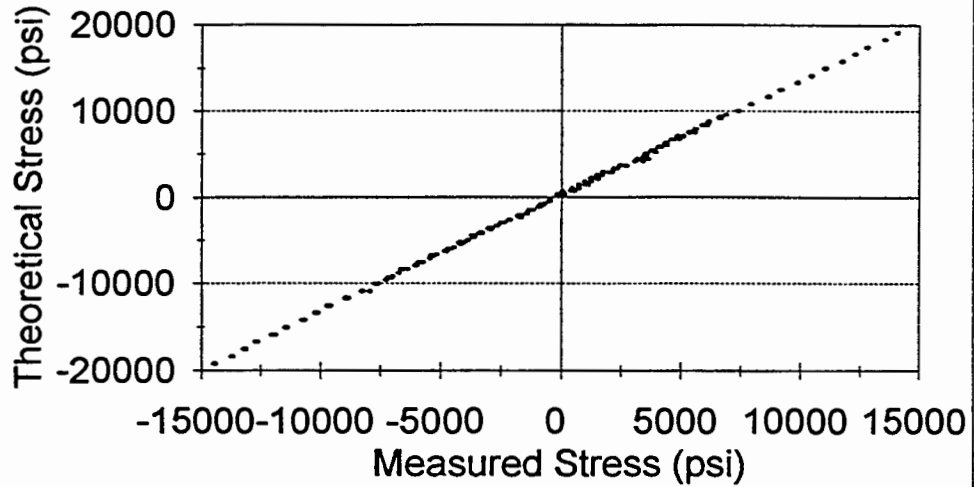
### Pile 4 Black Gage 10

Calibration Factor=1.370461



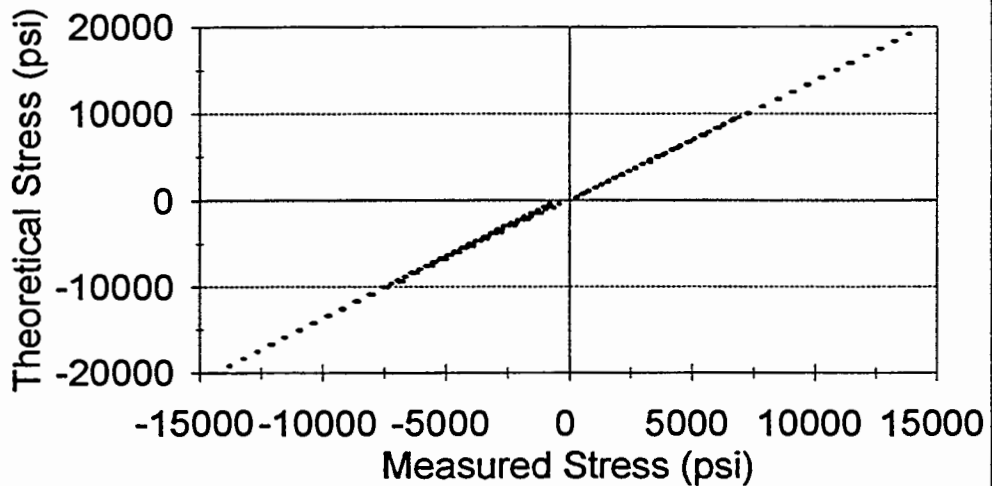
### Pile 4 Red Gage 11

Calibration Factor=1.341937



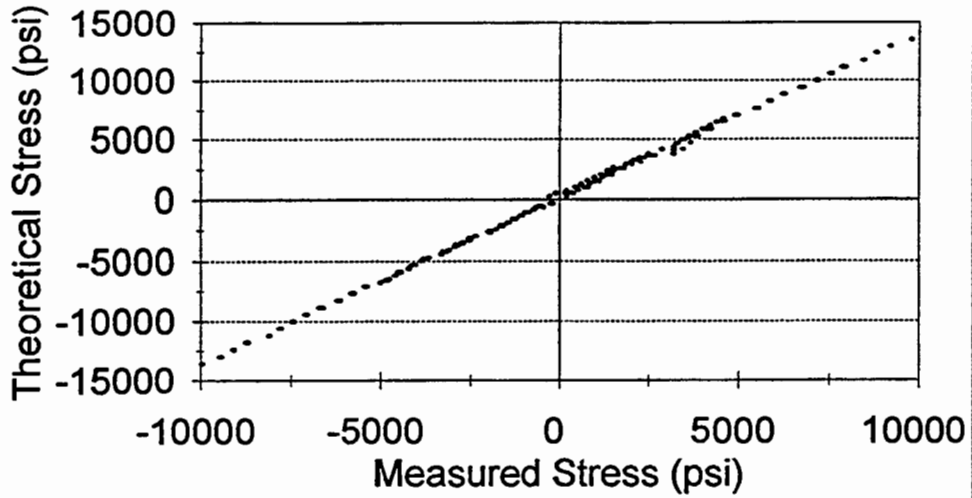
### Pile 4 Black Gage 11

Calibration Factor=1.368104



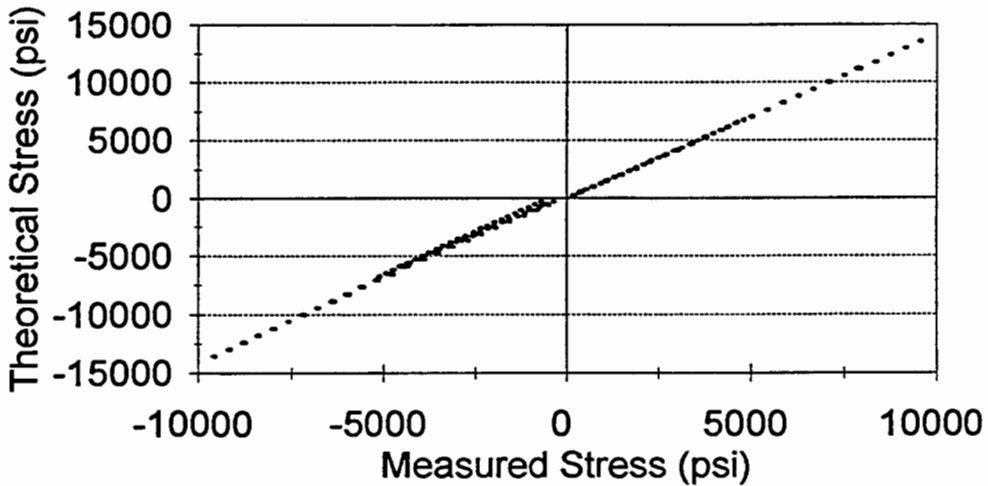
### Pile 4 Red Gage 12

Calibration Factor=1.375849



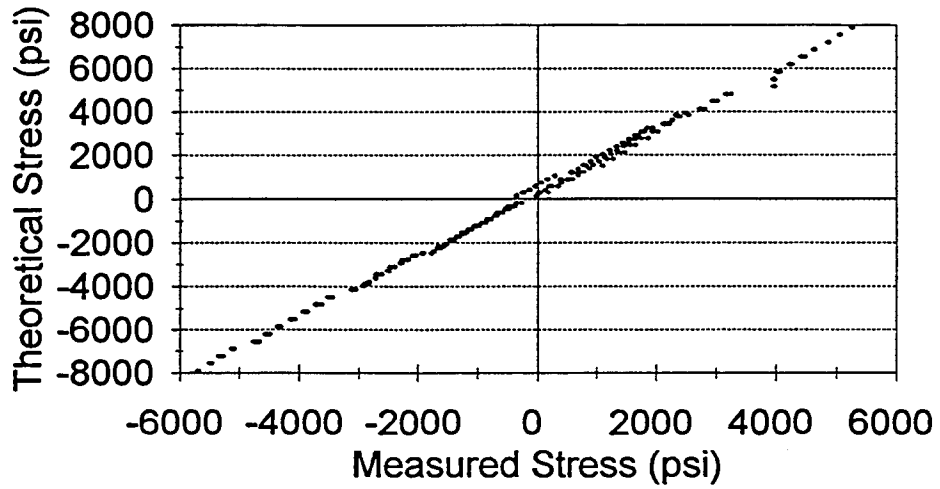
### Pile 4 Black Gage 12

Calibration Factor=1.386705



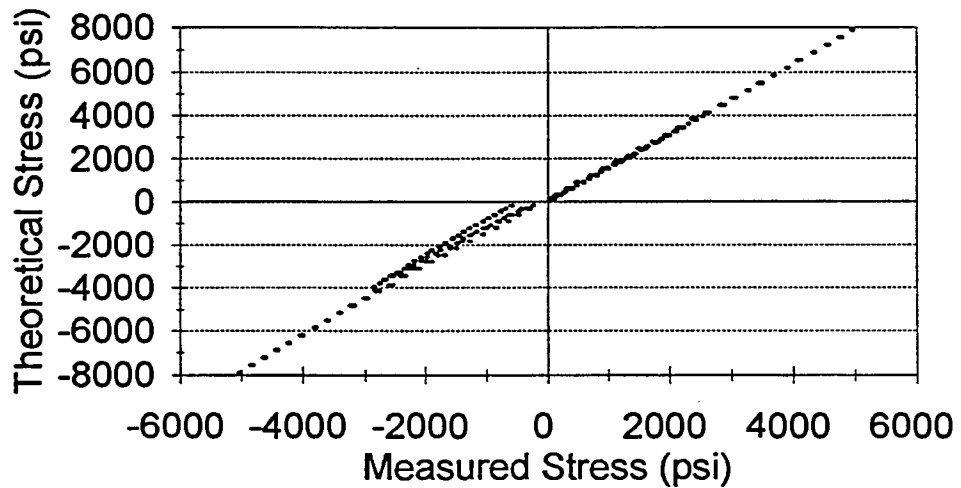
### Pile 4 Red Gage 13

Calibration Factor=1.40854



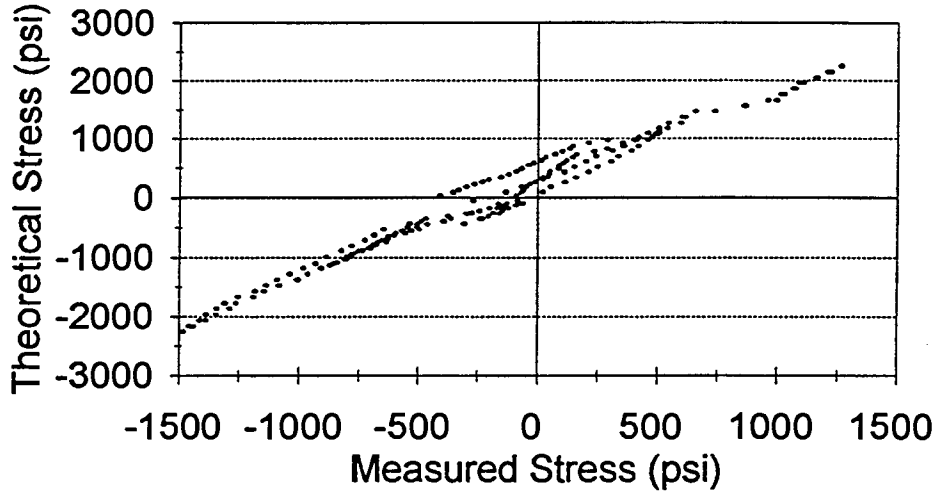
### Pile 4 Black Gage 13

Calibration Factor=1.514957



### Pile 4 Red Gage 14

Calibration Factor=1.459377



### Pile 4 Black Gage 14

Calibration Factor=1.316411

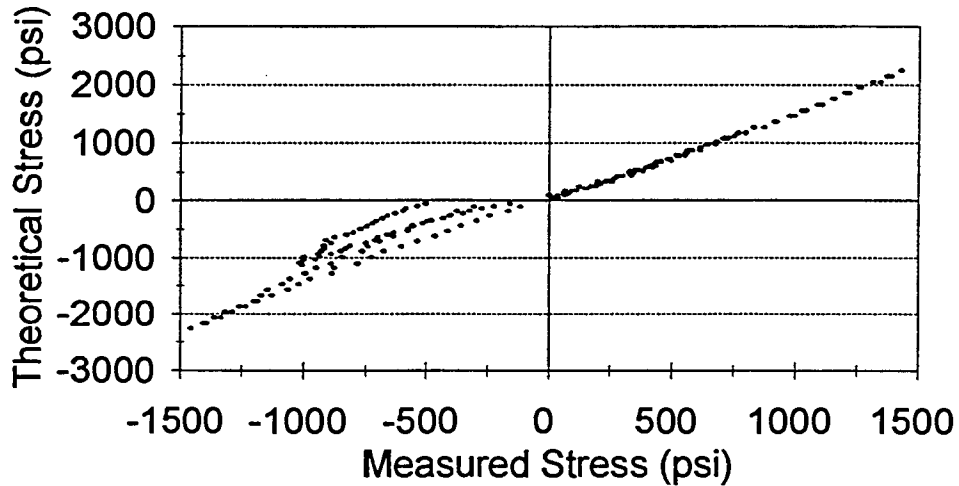
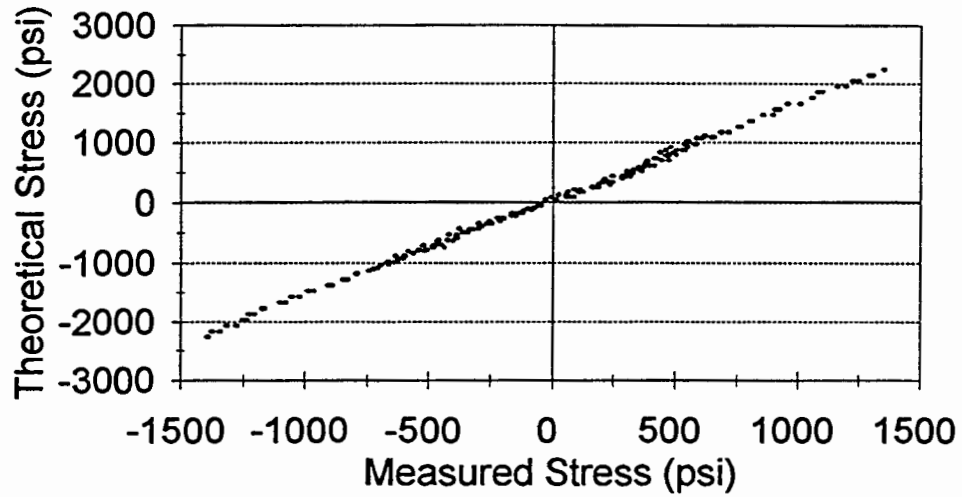


Figure C5. Pile 5 calibration (next 14 plots).

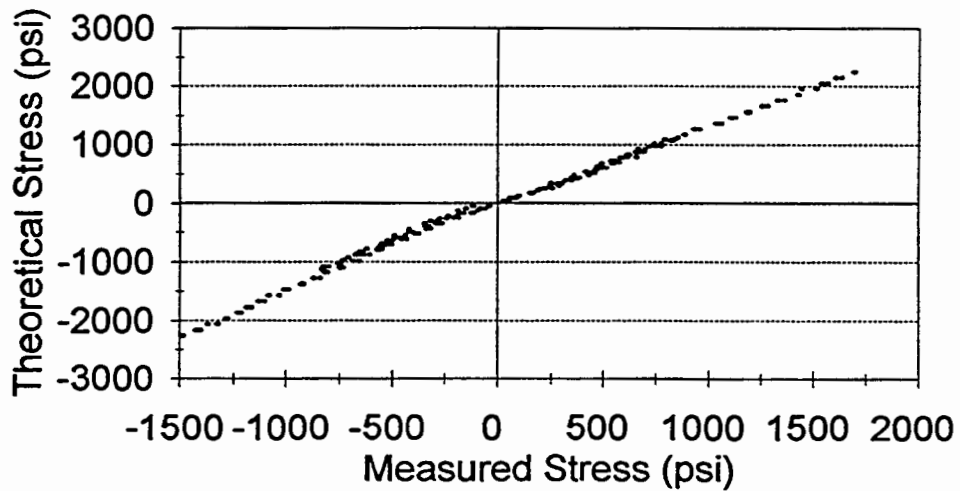
### Pile 5 Red Gage 1

Calibration Factor=1.598136



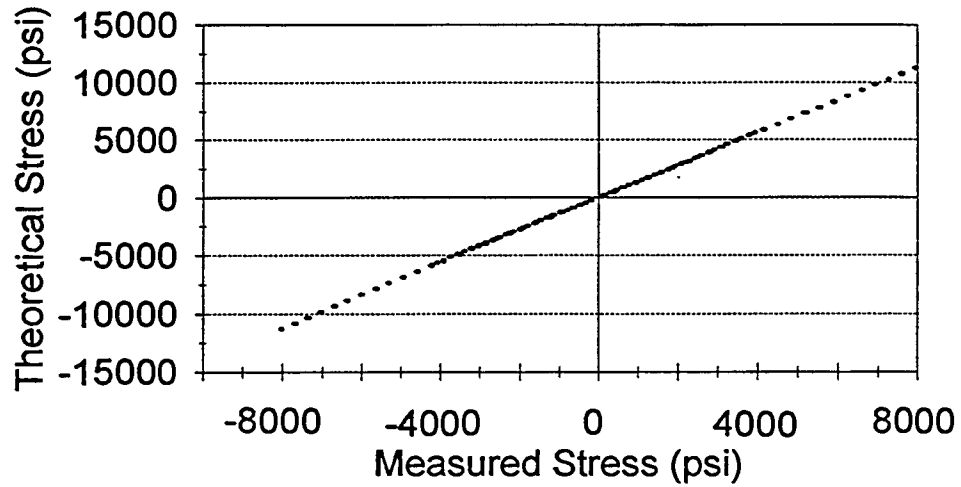
### Pile 5 Black Gage 1

Calibration Factor=1.374351



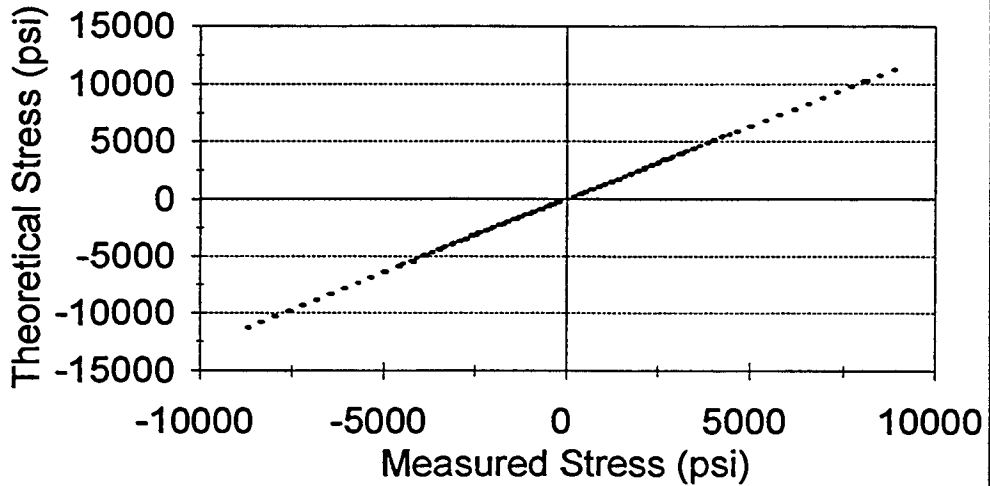
## Pile 5 Red Gage 2

Calibration Factor=1.406279



## Pile 5 Black Gage 2

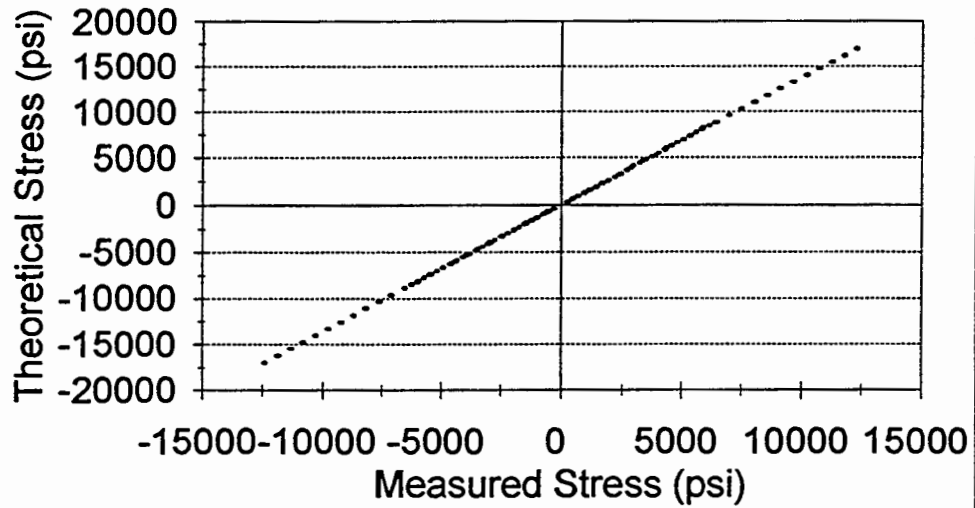
Calibration Factor=1.28021





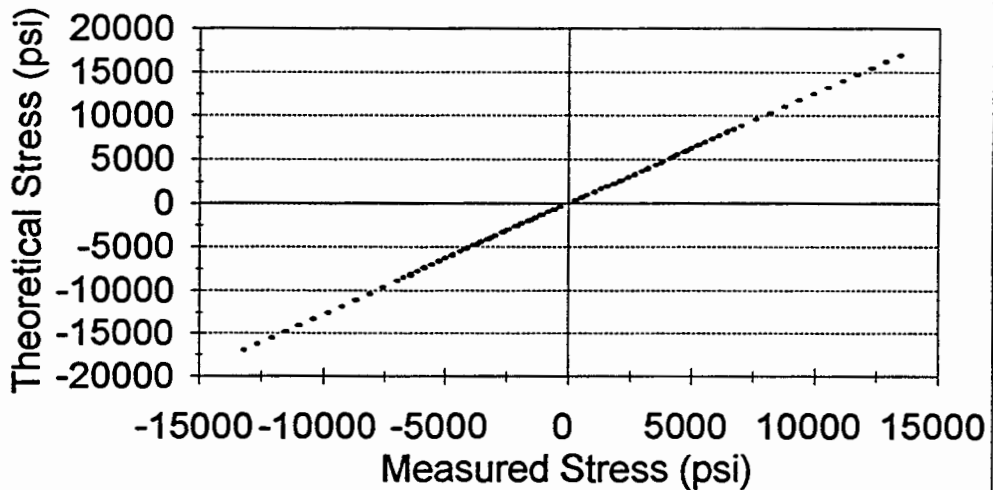
### Pile 5 Red Gage 3

Calibration Factor=1.366328



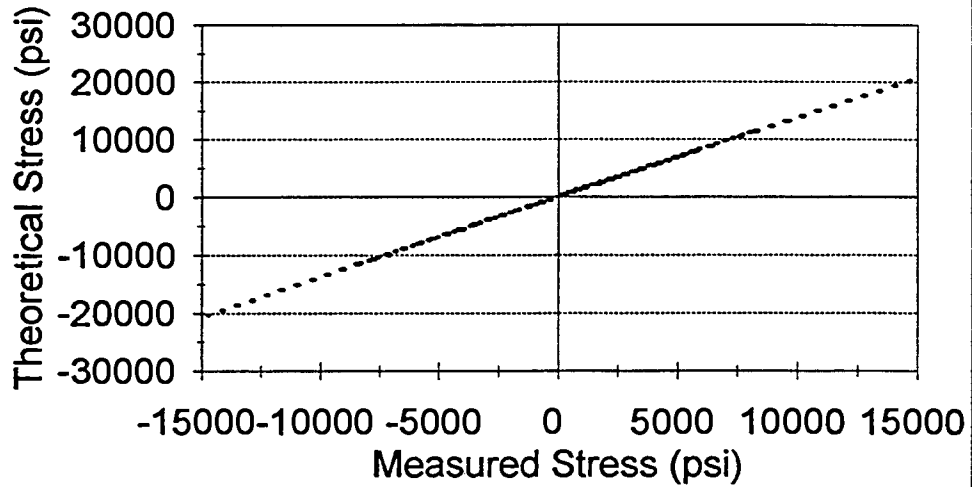
### Pile 5 Black Gage 3

Calibration Factor=1.266715



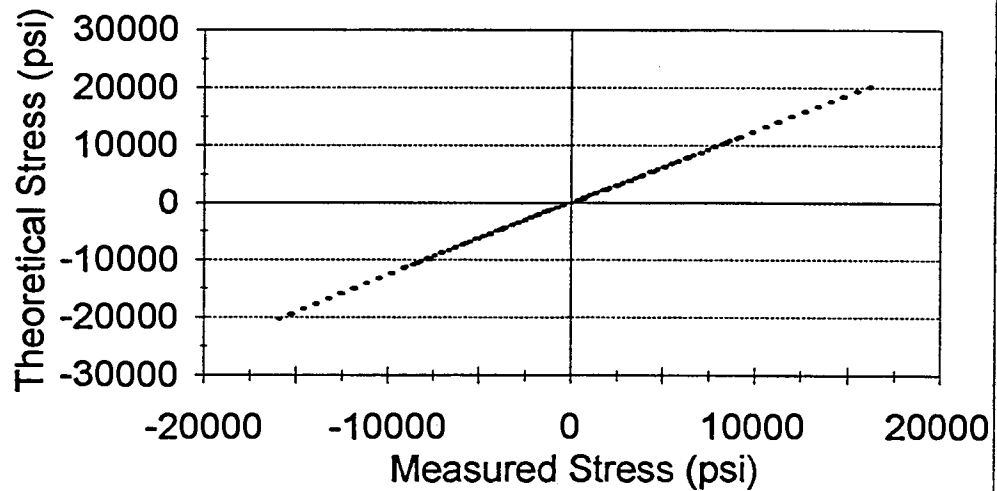
### Pile 5 Red Gage 4

Calibration Factor=1.379436



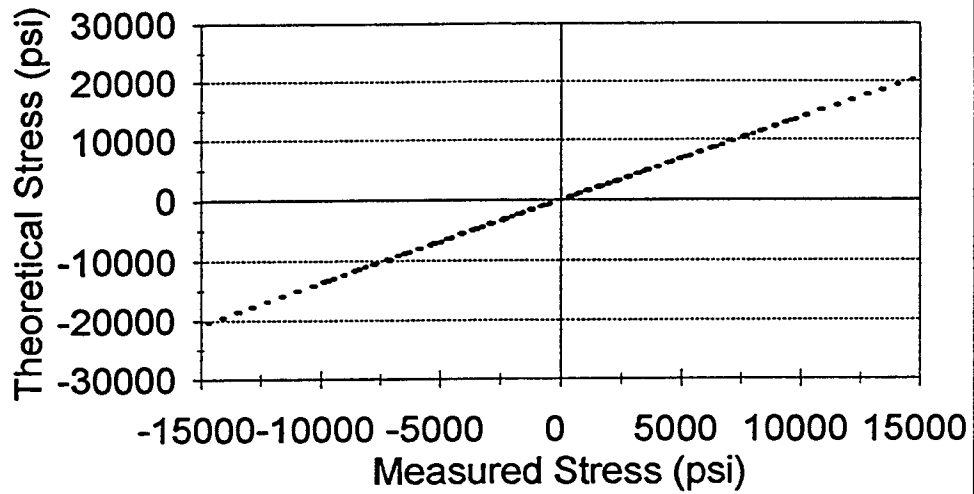
### Pile 5 Black Gage 4

Calibration Factor=1.2609



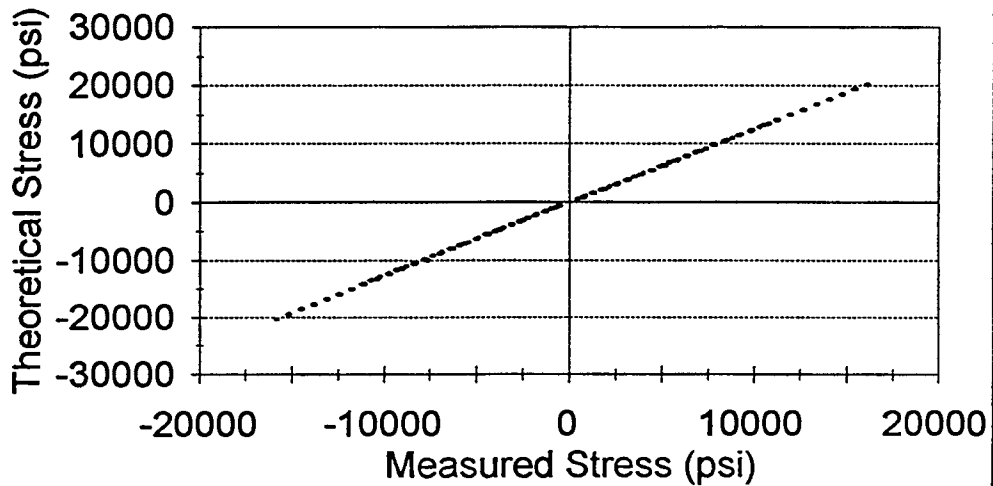
### Pile 5 Red Gage 5

Calibration Factor=1.376143



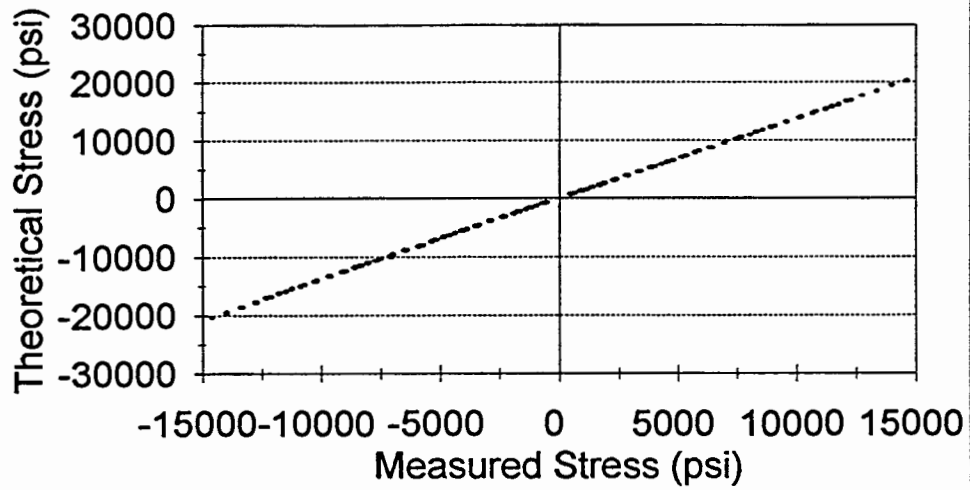
### Pile 5 Black Gage 5

Calibration Factor=1.263617



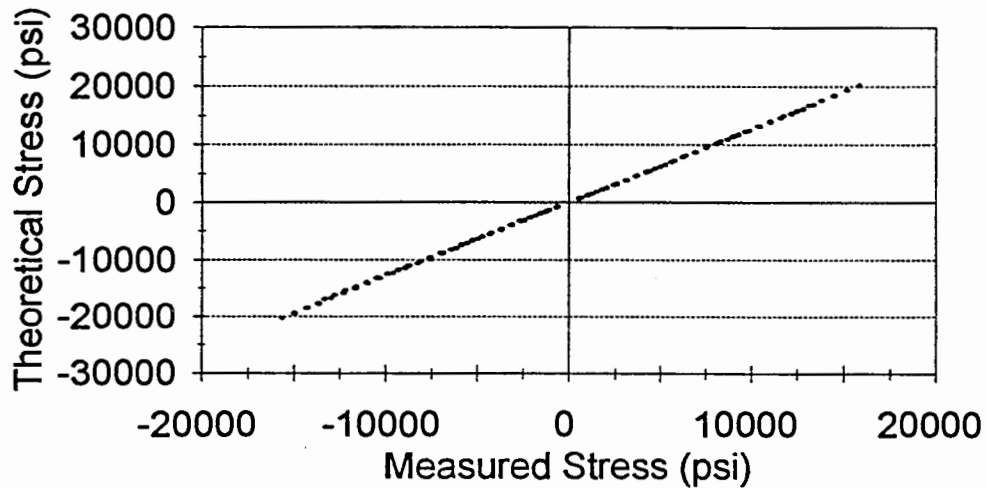
## Pile 5 Red Gage 6

Calibration Factor=1.382066



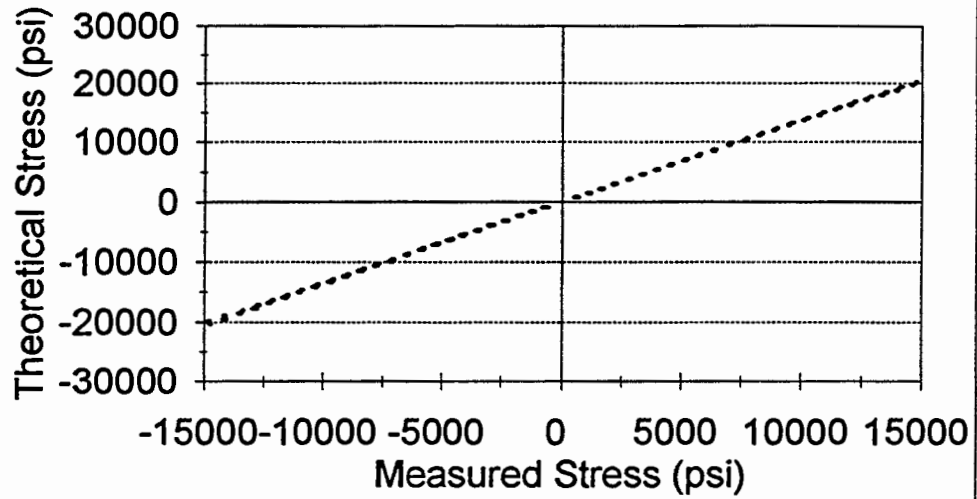
## Pile 5 Black Gage 6

Calibration Factor=1.279654



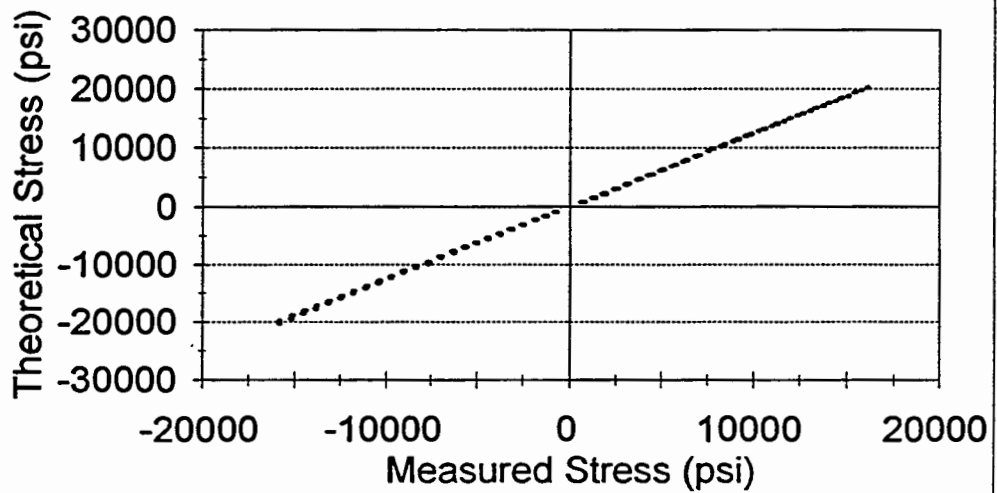
### Pile 5 Red Gage 7

Calibration Factor=1.36162



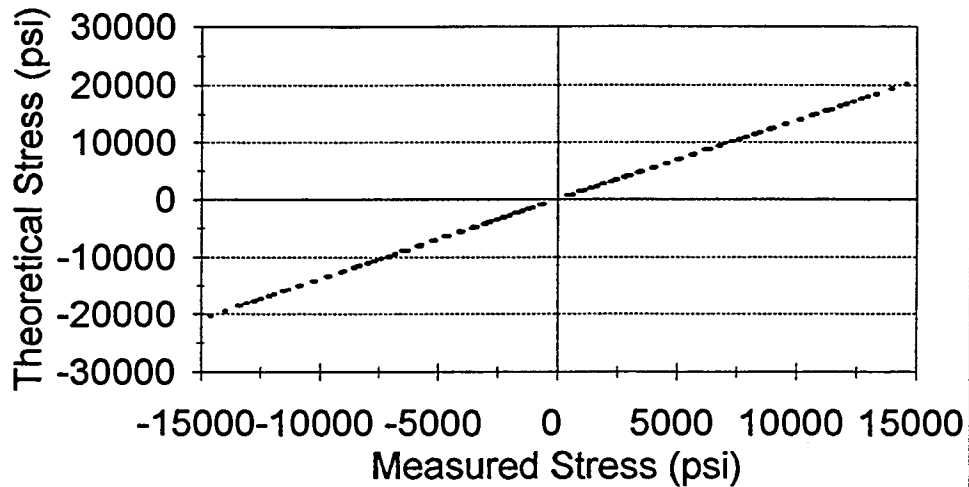
### Pile 5 Black Gage 7

Calibration Factor=1.258082



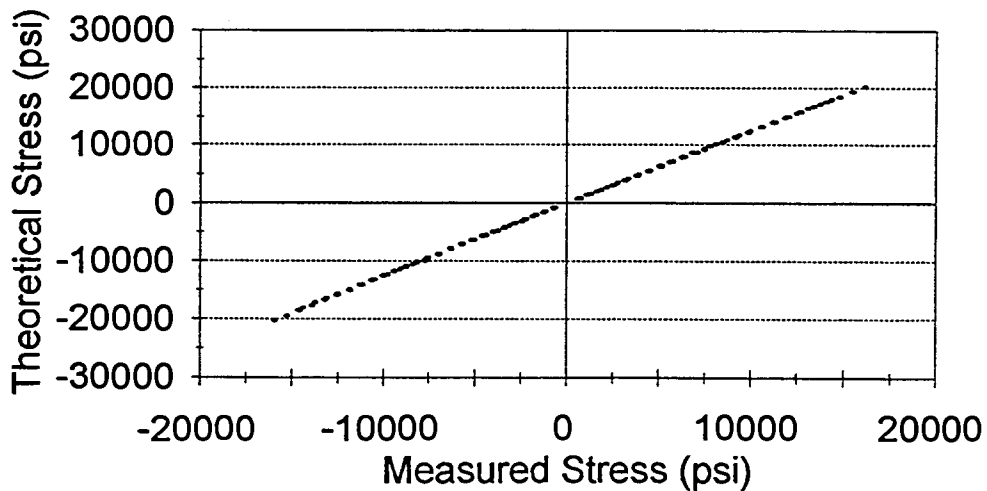
## Pile 5 Red Gage 8

Calibration Factor=1.389937



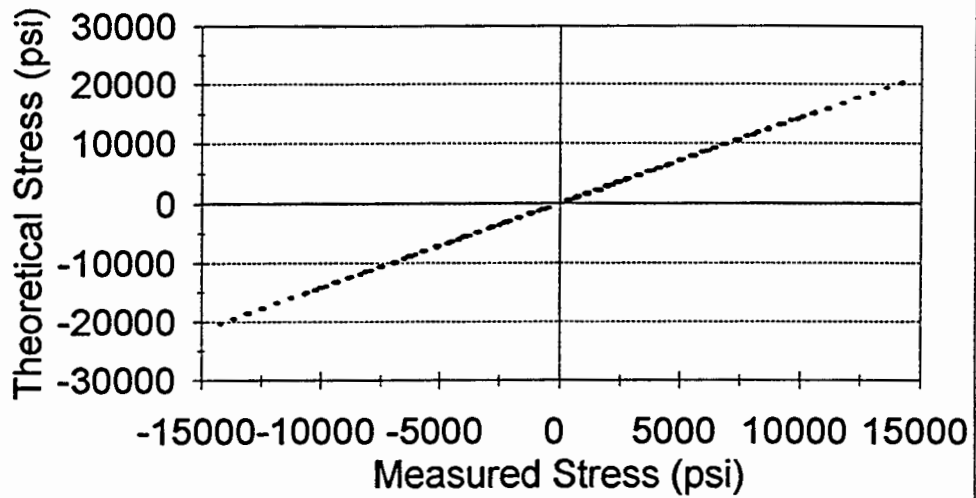
## Pile 5 Black Gage 8

Calibration Factor=1.260626



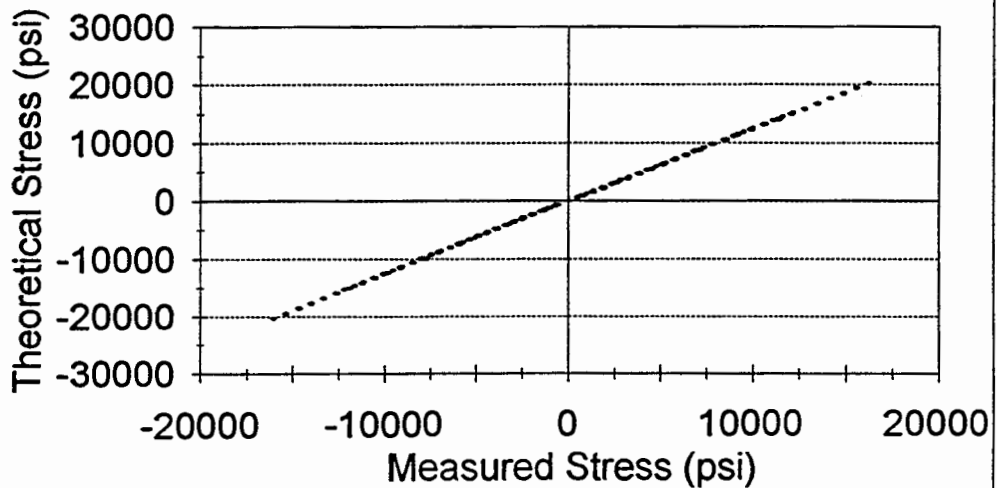
### Pile 5 Red Gage 9

Calibration Factor=1.429217



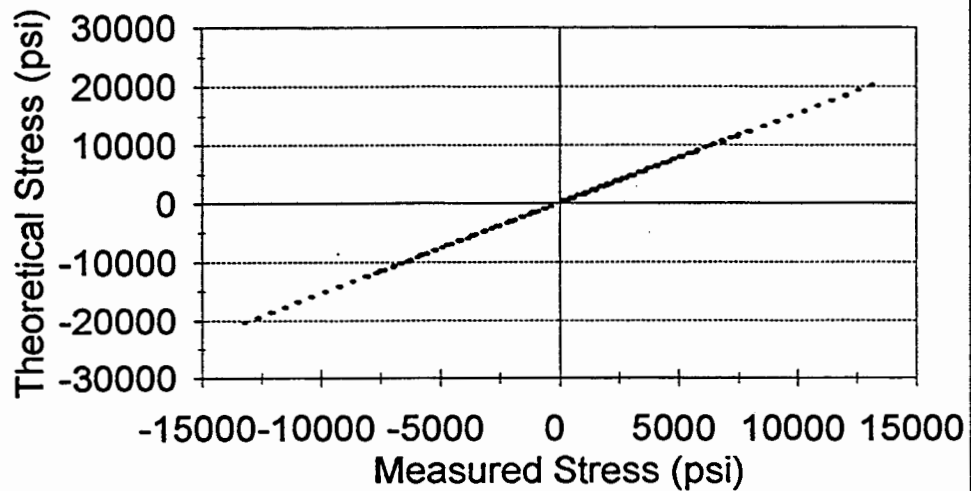
### Pile 5 Black Gage 9

Calibration Factor=1.254736



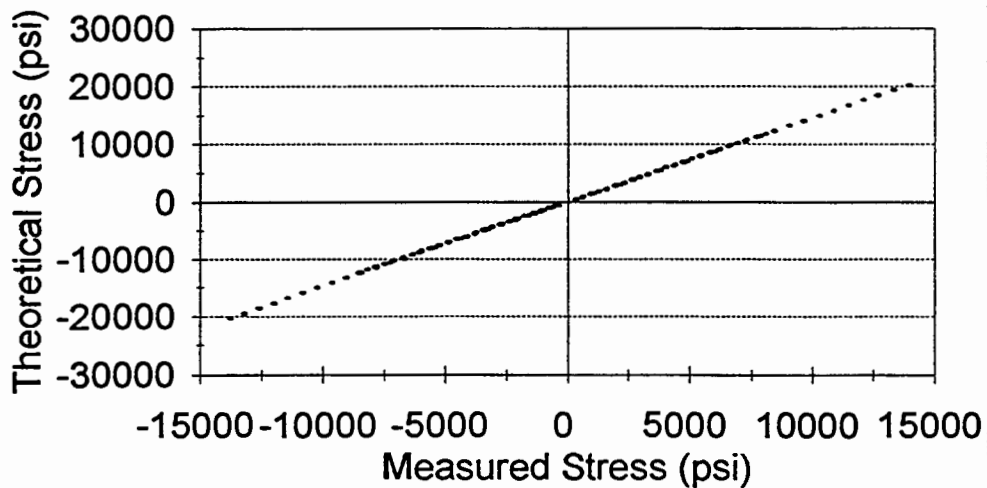
### Pile 5 Red Gage 10

Calibration Factor=1.546837



### Pile 5 Black Gage 10

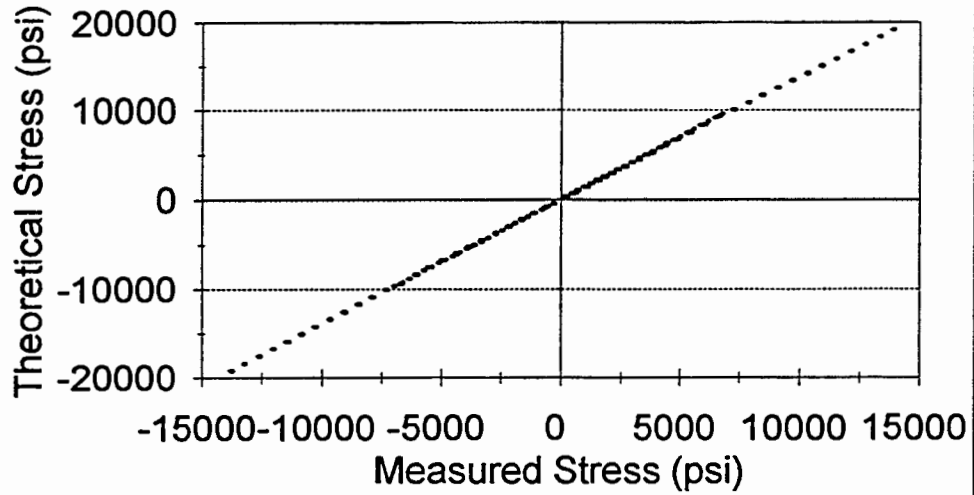
Calibration Factor=1.465135





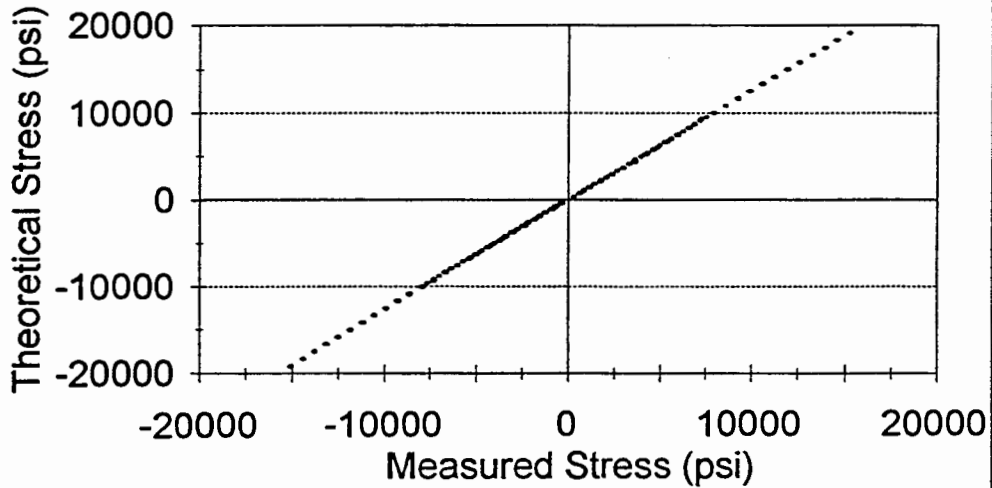
### Pile 5 Red Gage 11

Calibration Factor=1.385525



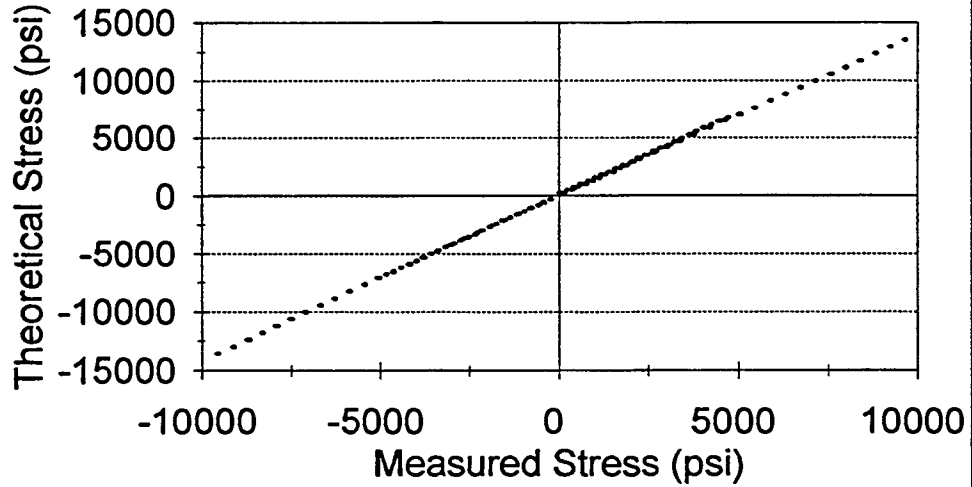
### Pile 5 Black Gage 11

Calibration Factor=1.264605



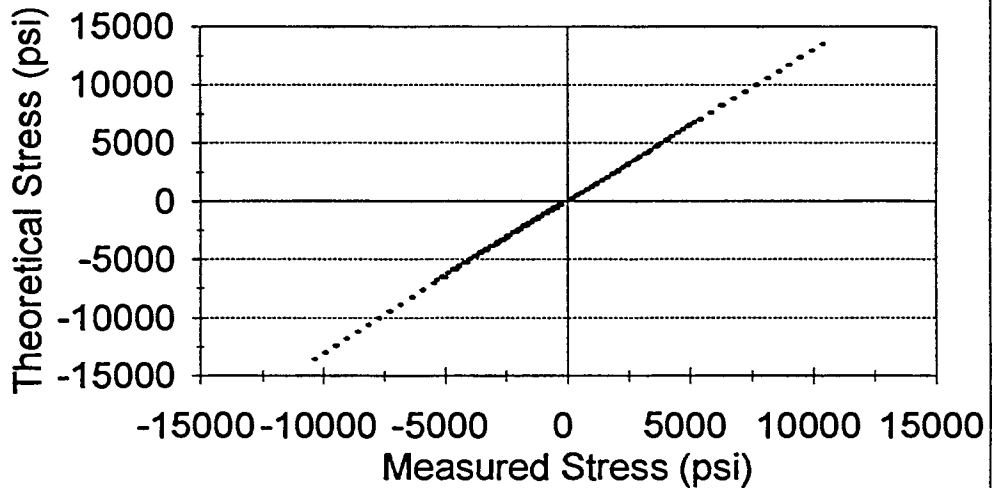
### Pile 5 Red Gage 12

Calibration Factor=1.410021



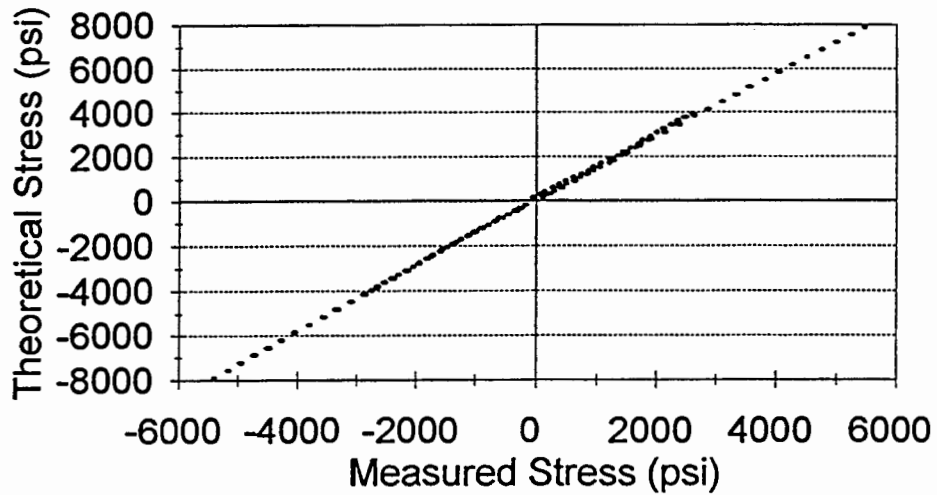
### Pile 5 Black Gage 12

Calibration Factor=1.2989



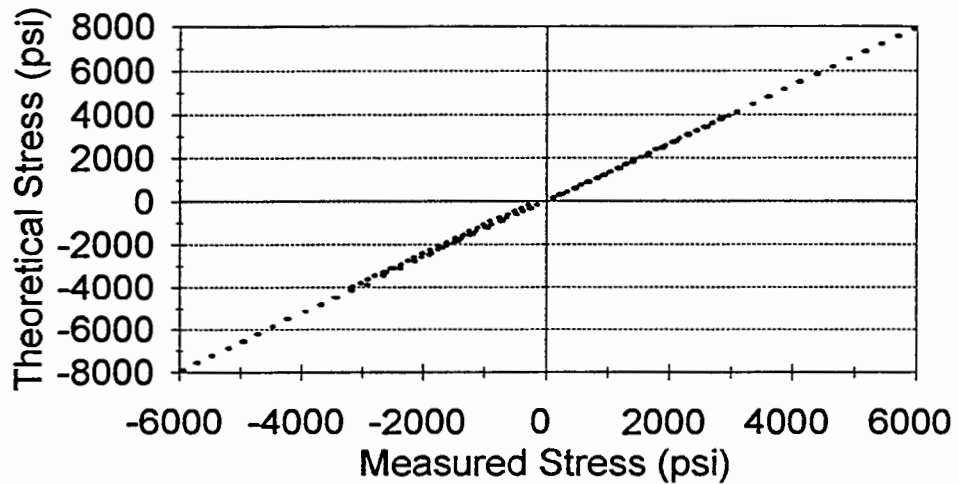
### Pile 5 Red Gage 13

Calibration Factor=1.451875

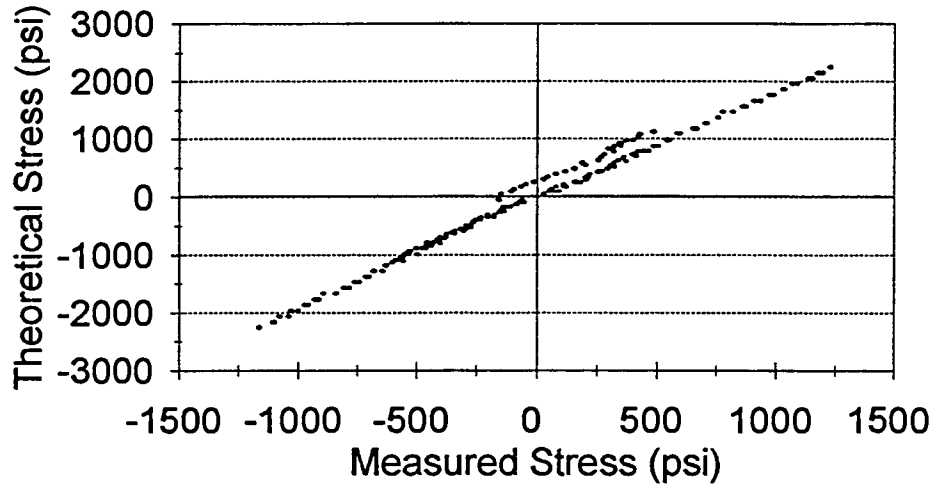


### Pile 5 Black Gage 13

Calibration Factor=1.314801



**Pile 5 Red Gage 14**  
Calibration Factor=1.881929



**Pile 5 Black Gage 14**  
Calibration Factor=1.413964

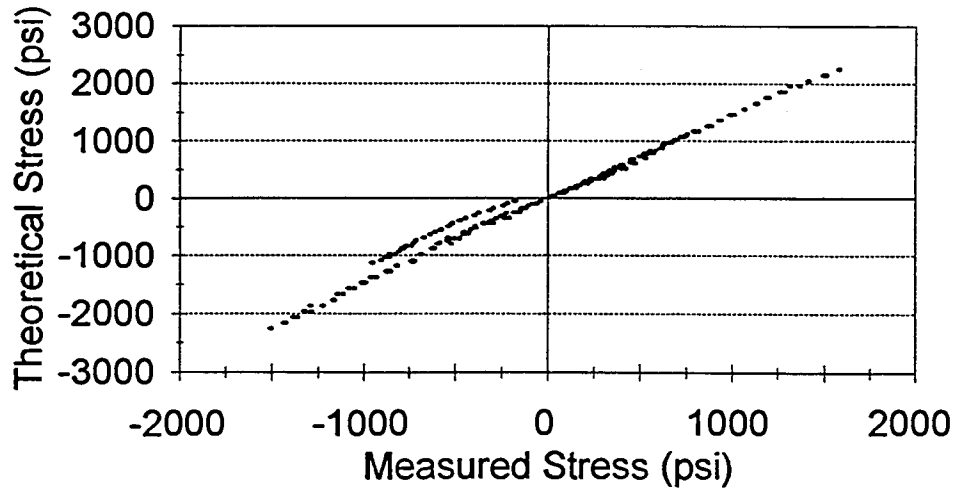
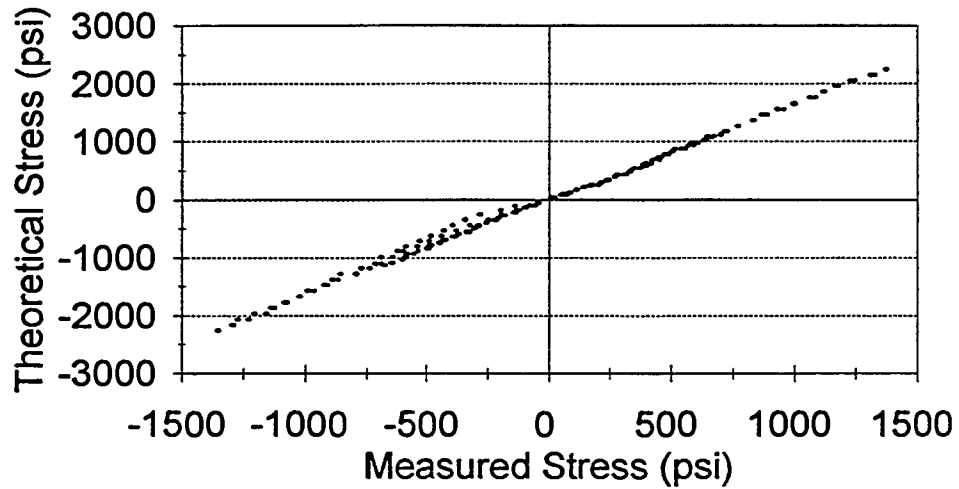


Figure C6. Pile 6 calibration (next 14 plots).

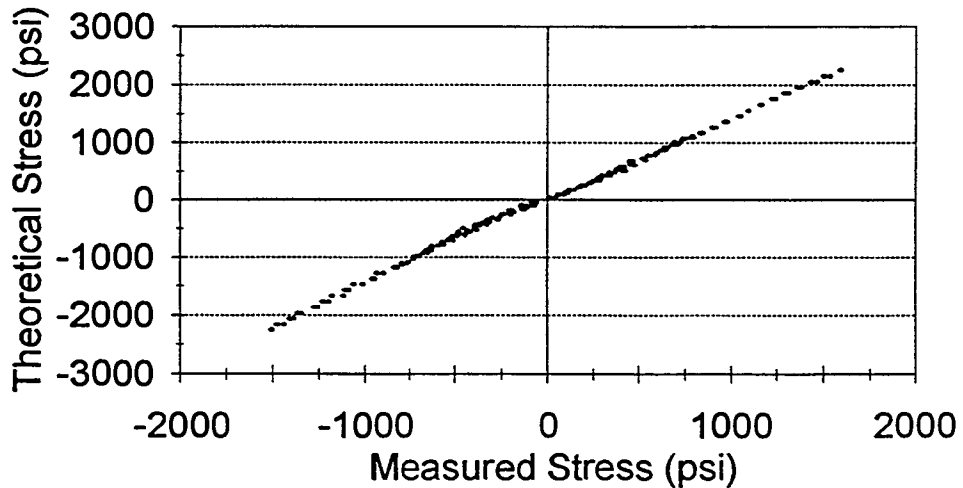
### Pile 6 Red Gage 1

Calibration Factor=1.623617



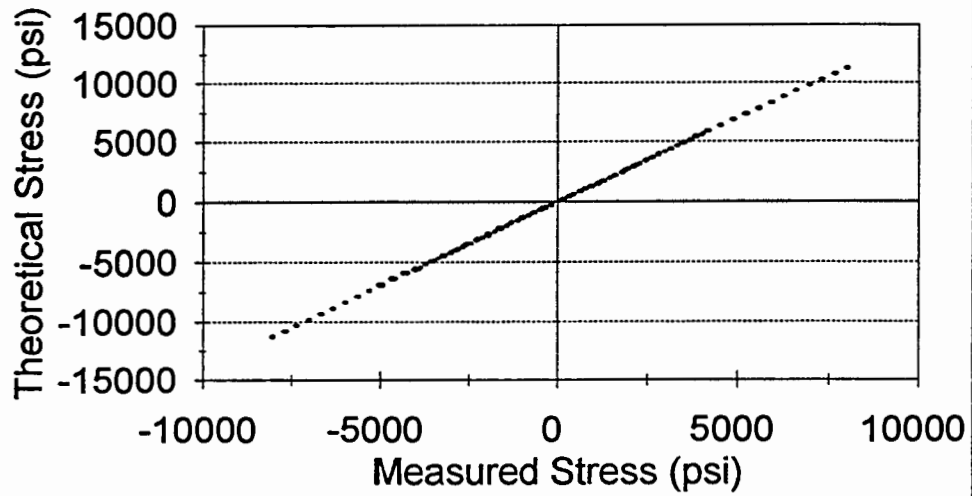
### Pile 6 Black Gage 1

Calibration Factor=1.416729



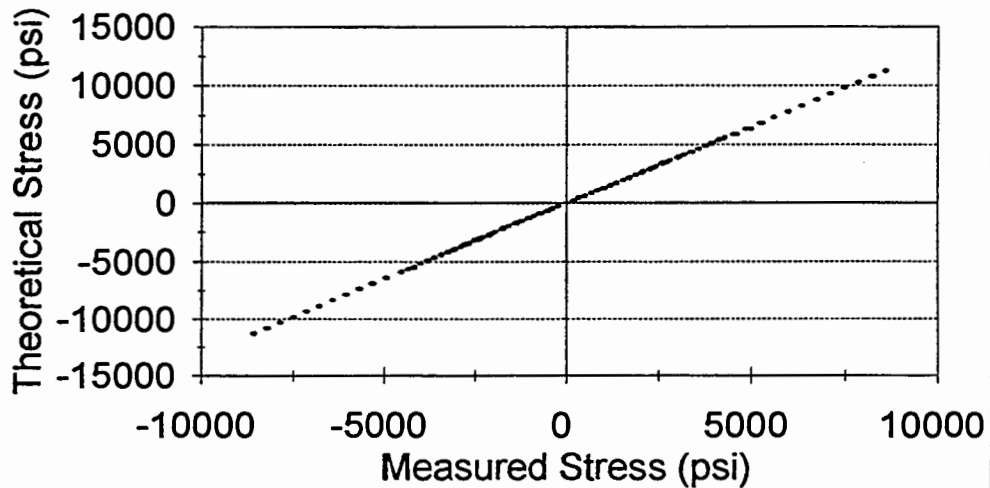
### Pile 6 Red Gage 2

Calibration Factor=1.401299



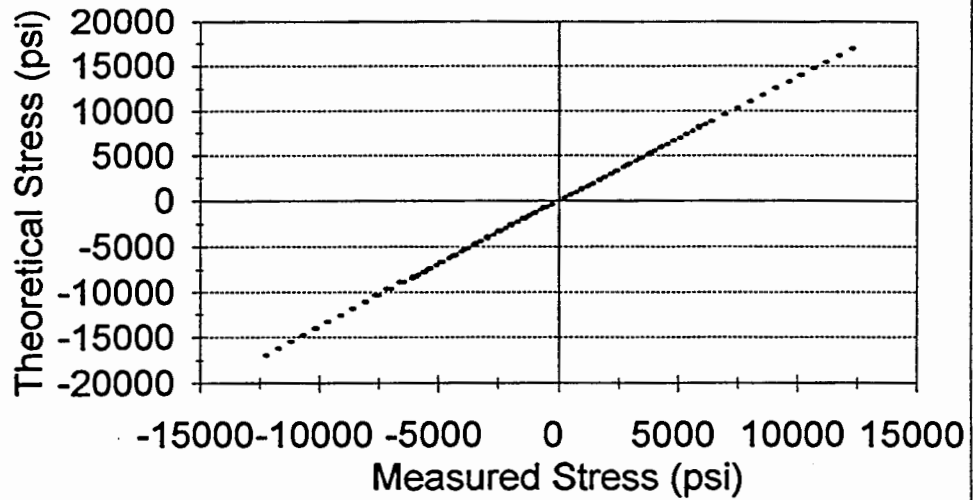
### Pile 6 Black Gage 2

Calibration Factor=1.305799



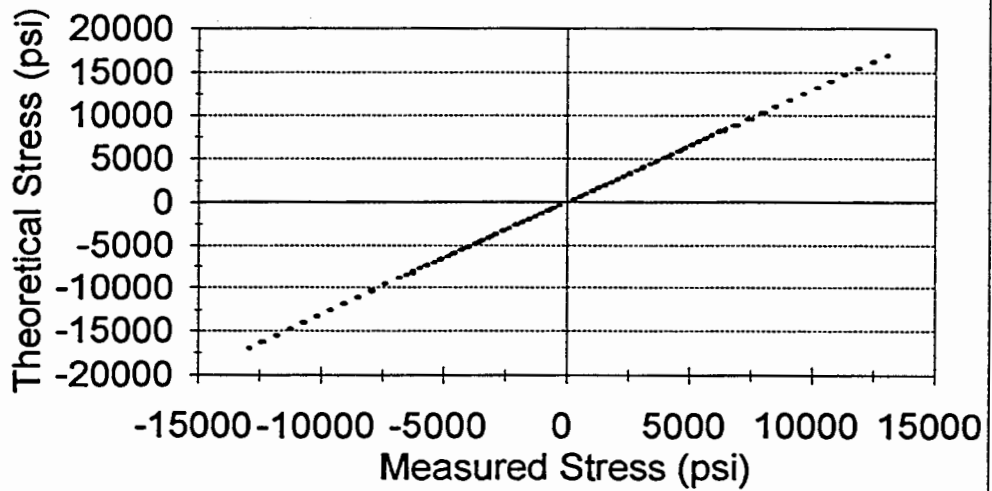
### Pile 6 Red Gage 3

Calibration Factor=1.376046



### Pile 6 Black Gage 3

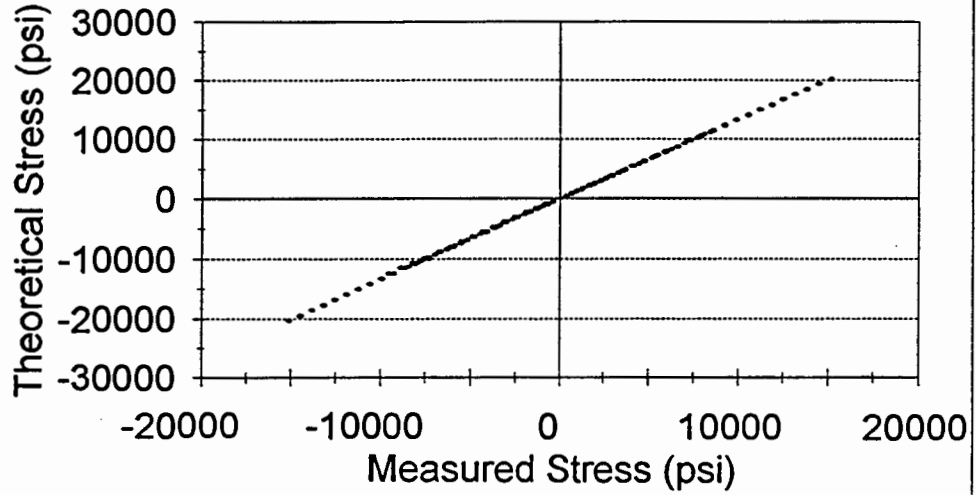
Calibration Factor=1.301758





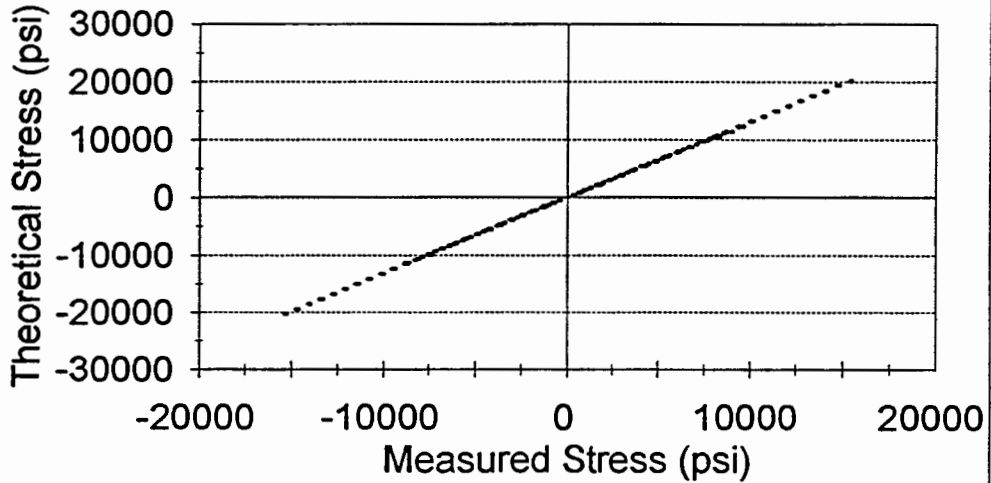
### Pile 6 Red Gage 4

Calibration Factor=1.337904



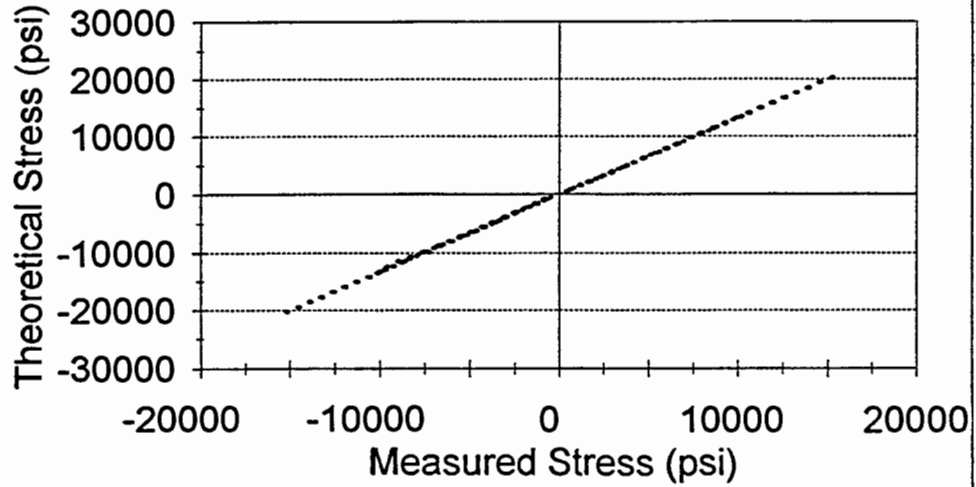
### Pile 6 Black Gage 4

Calibration Factor=1.31652



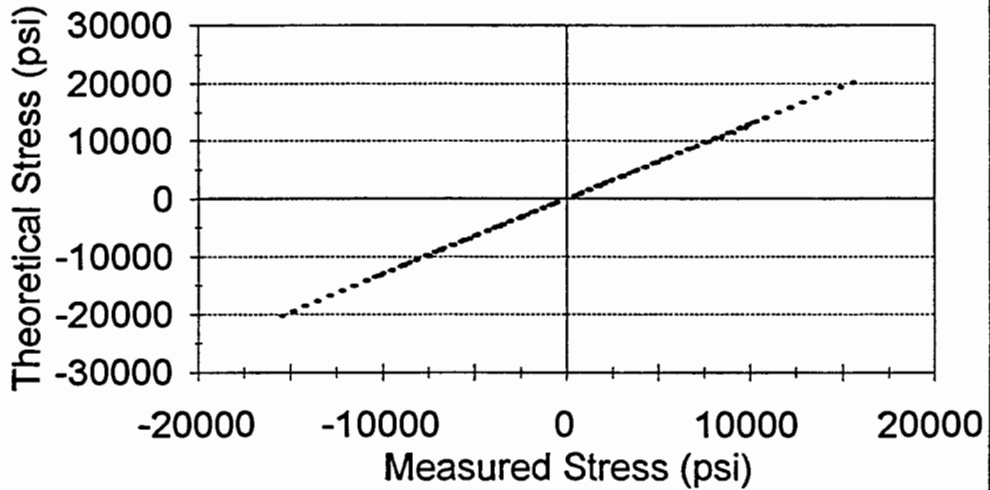
## Pile 6 Red Gage 5

Calibration Factor=1.329527

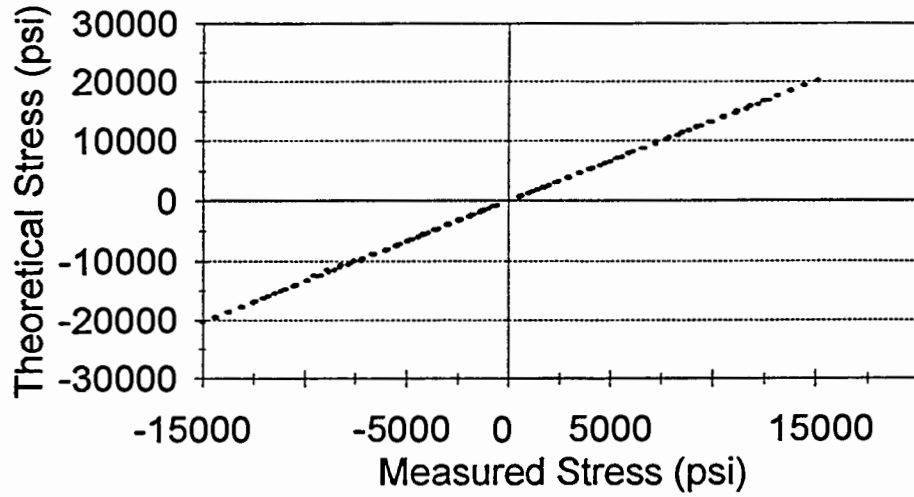


## Pile 6 Black Gage 5

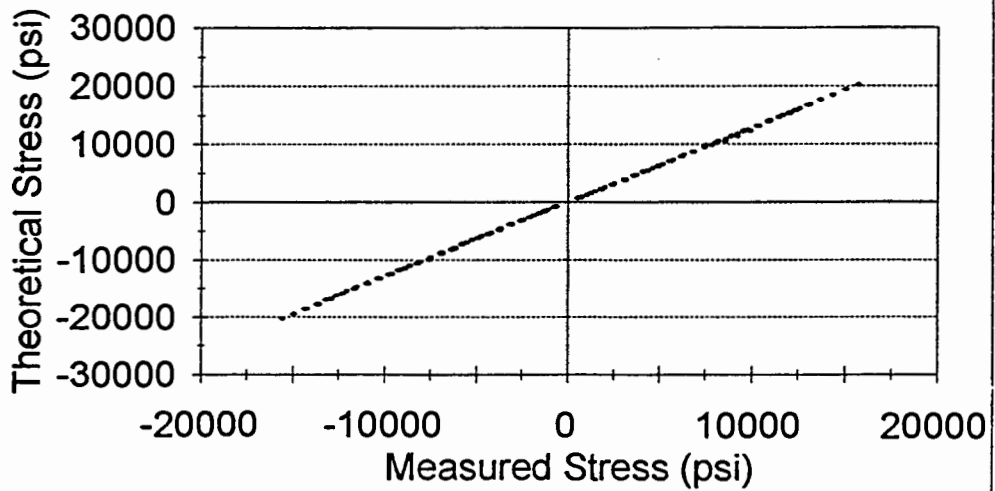
Calibration Factor=1.301035



**Pile 6 Red Gage 6**  
Calibration Factor=1.342282

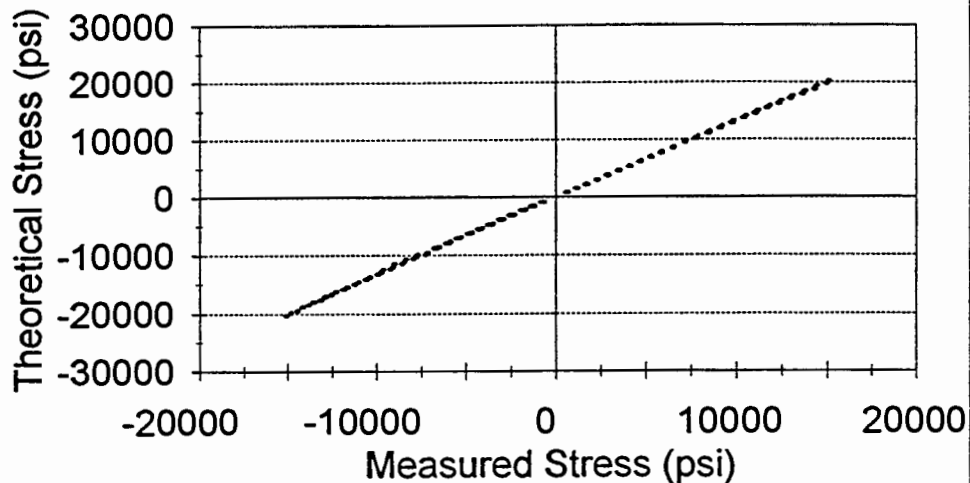


**Pile 6 Black Gage 6**  
Calibration Factor=1.288353



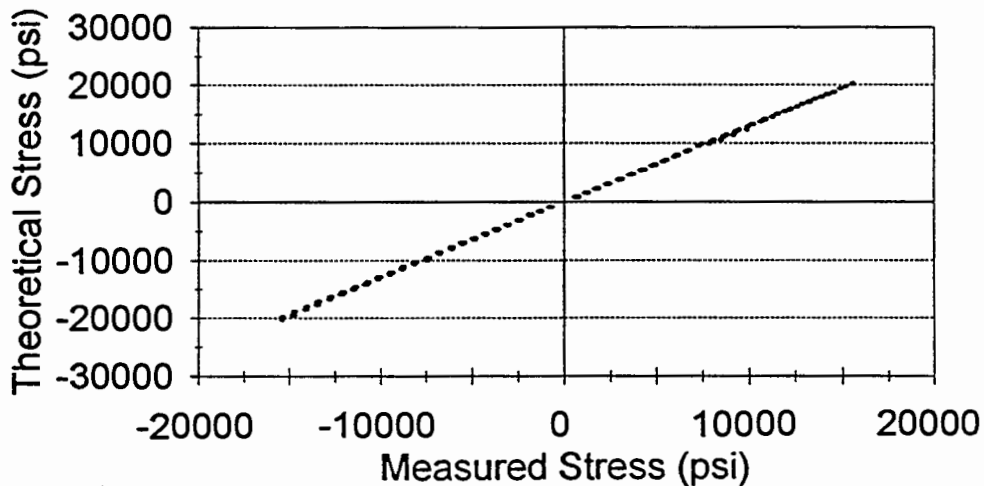
### Pile 6 Red Gage 7

Calibration Factor=1.333329

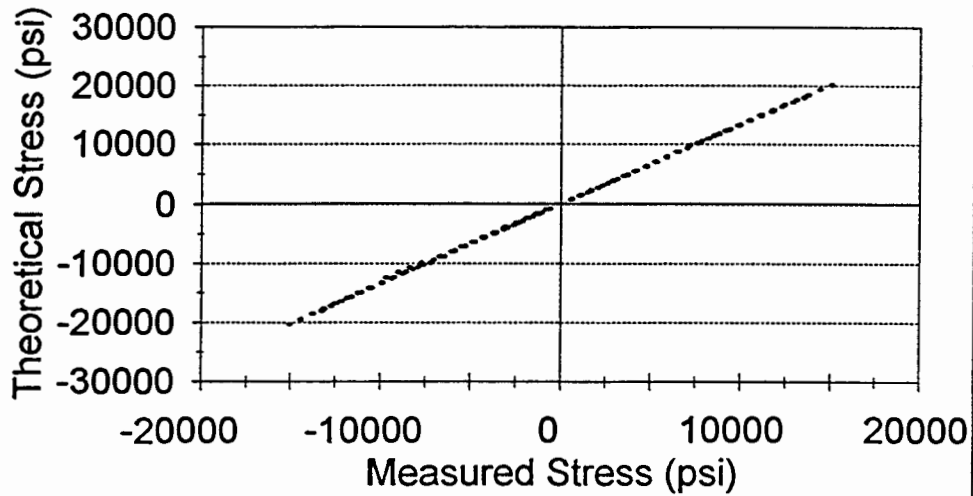


### Pile 6 Black Gage 7

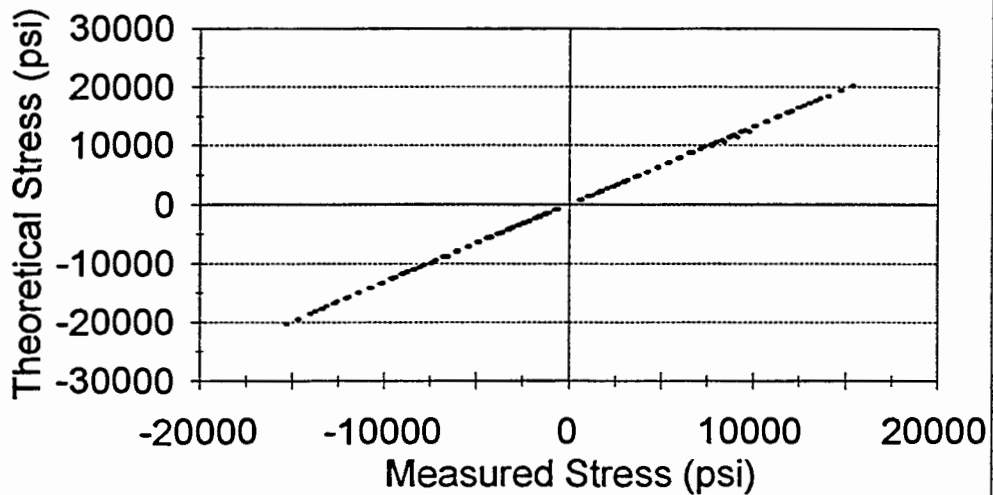
Calibration Factor=1.298401



**Pile 6 Red Gage 8**  
Calibration Factor=1.34487

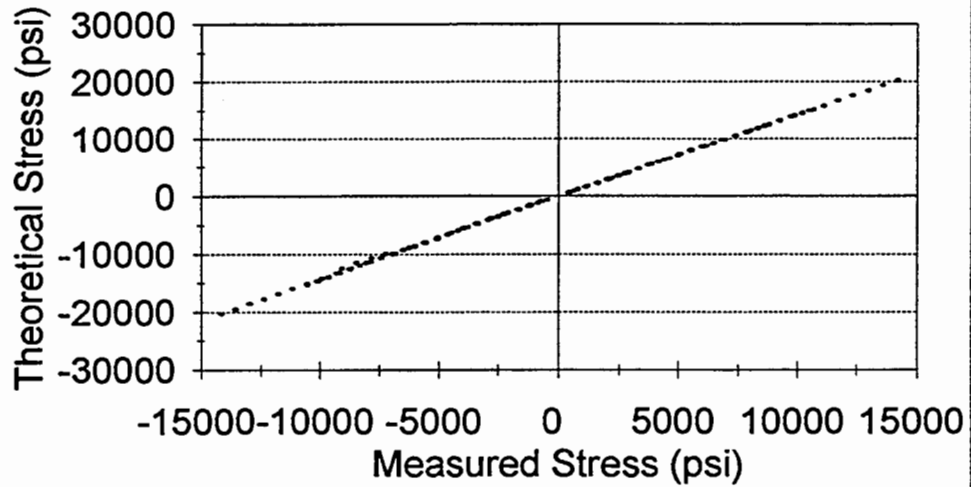


**Pile 6 Black Gage 8**  
Calibration Factor=1.319572



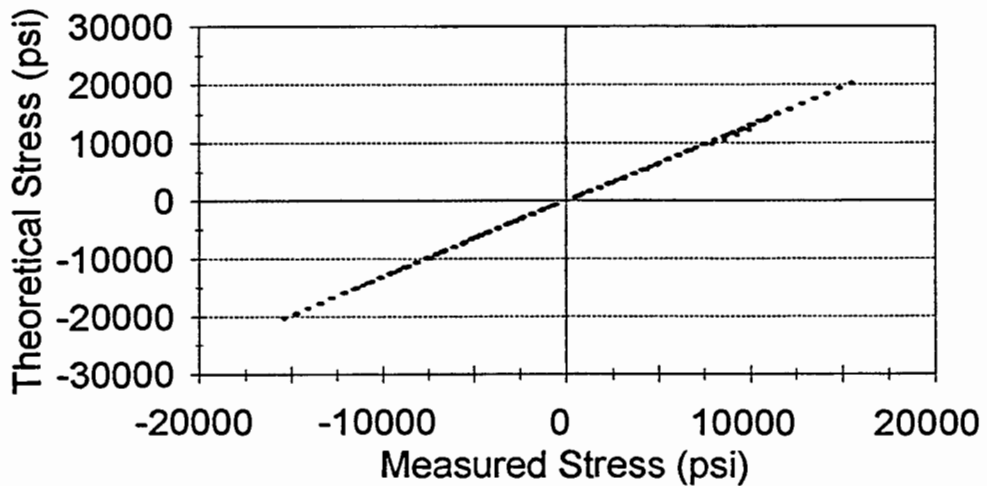
### Pile 6 Red Gage 9

Calibration Factor=1.311782



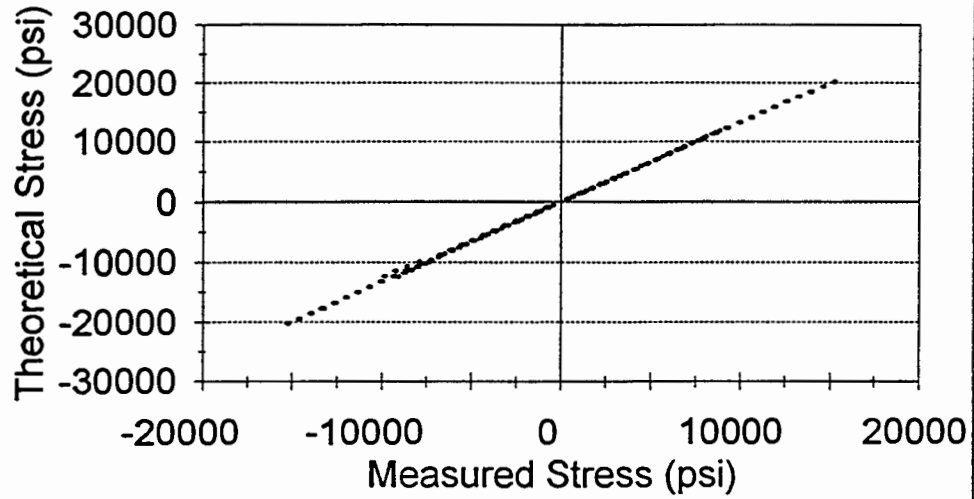
### Pile 6 Black Gage 9

Calibration Factor=1.311782



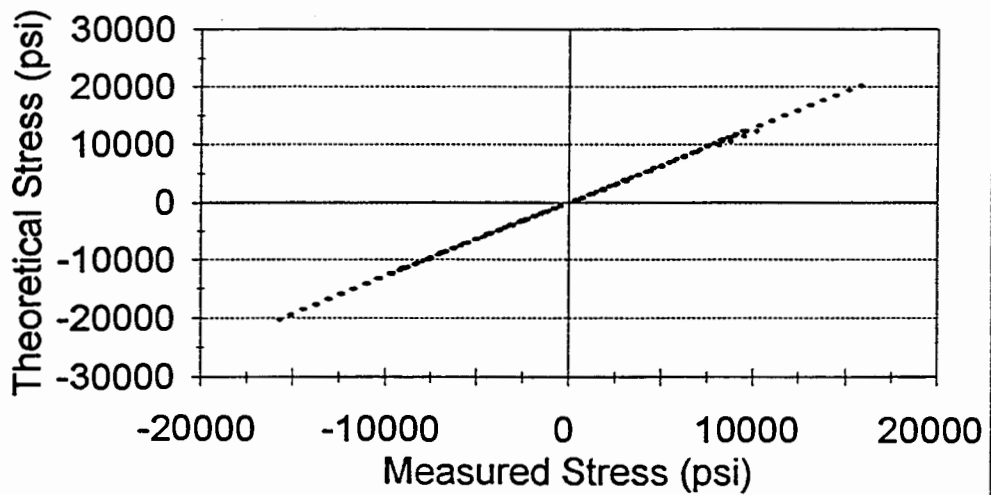
### Pile 6 Red Gage 10

Calibration Factor=1.33108



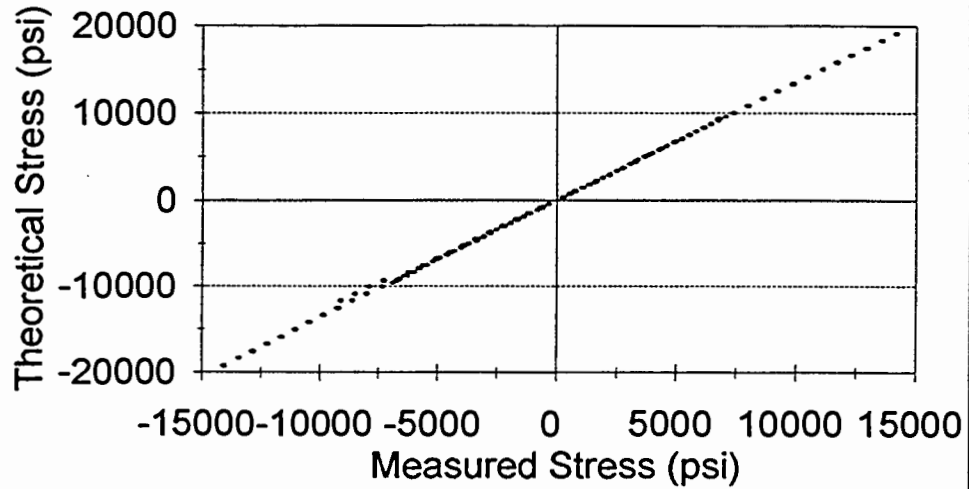
### Pile 6 Black Gage 10

Calibration Factor=1.286855



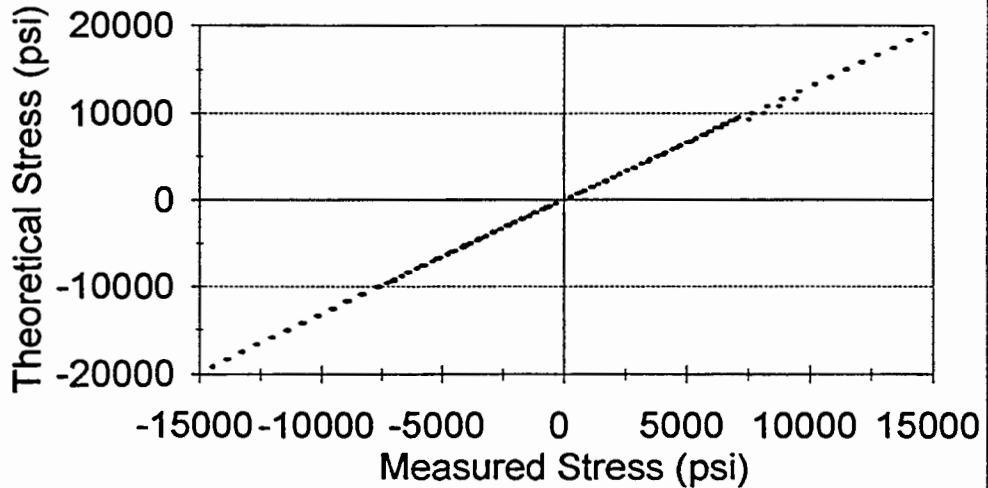
### Pile 6 Red Gage 11

Calibration Factor=1.357493



### Pile 6 Black Gage 11

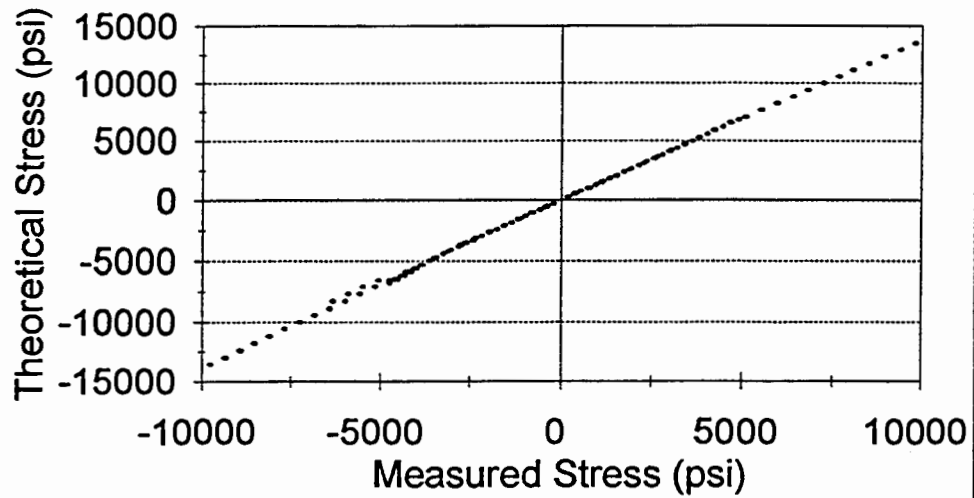
Calibration Factor=1.313282





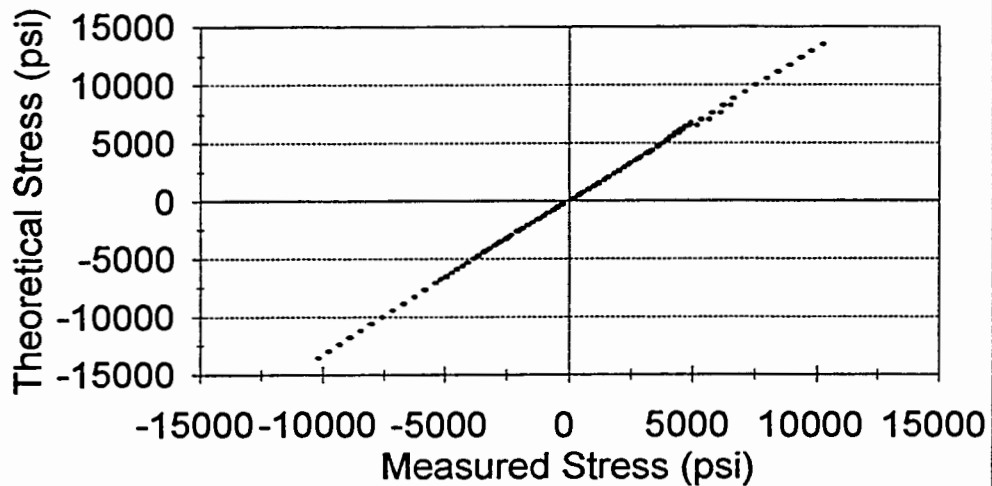
## Pile 6 Red Gage 12

Calibration Factor=1.381116



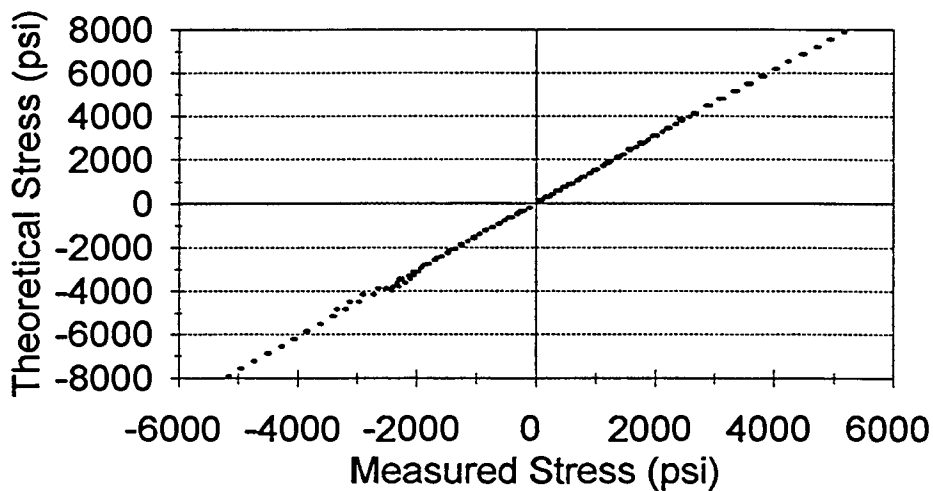
## Pile 6 Black Gage 12

Calibration Factor=1.323256



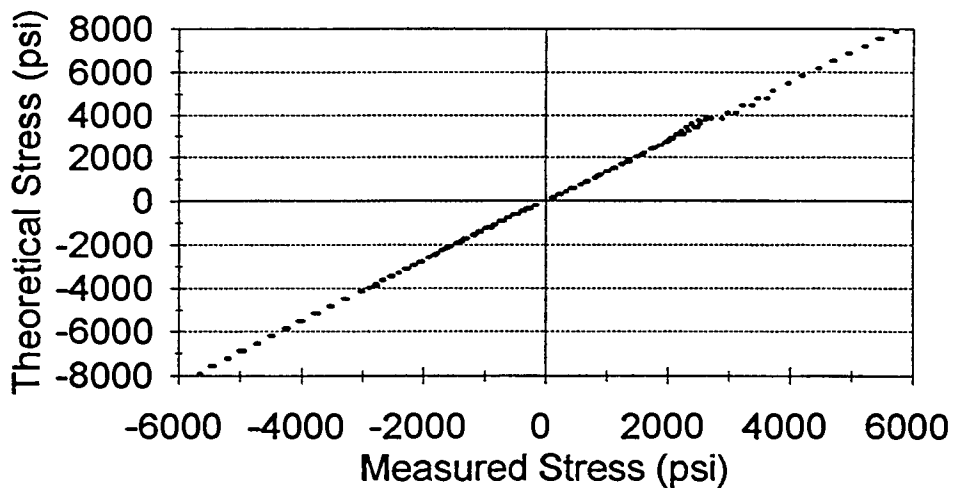
### Pile 6 Red Gage 13

Calibration Factor=1.529879



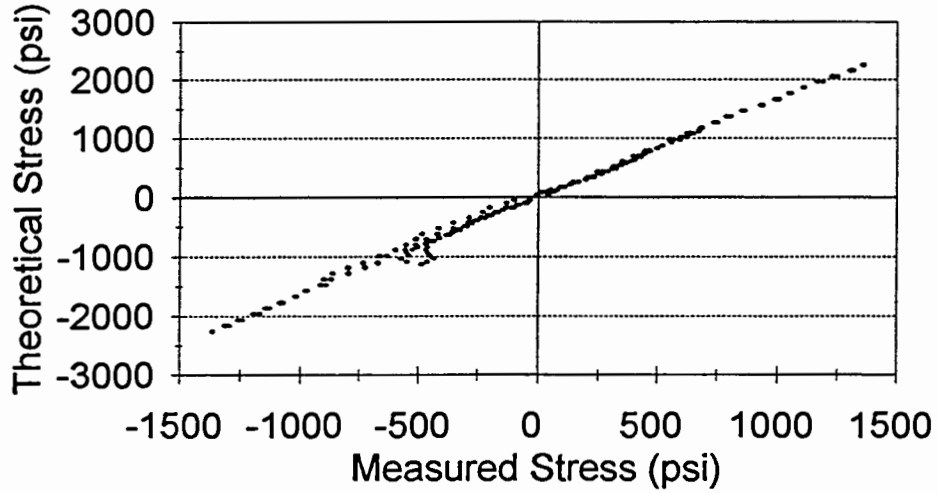
### Pile 6 Black Gage 13

Calibration Factor=1.381872



### Pile 6 Red Gage 14

Calibration Factor=1.658463



### Pile 6 Black Gage 14

Calibration Factor=1.600656

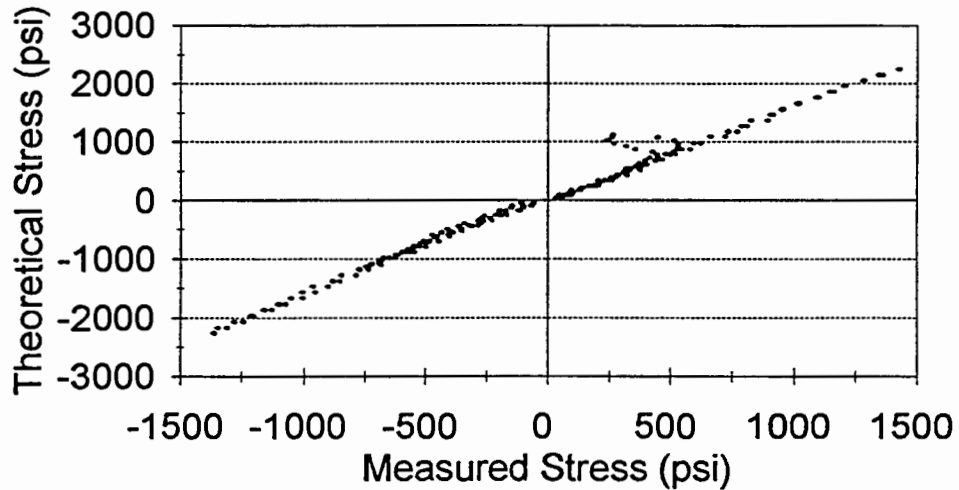
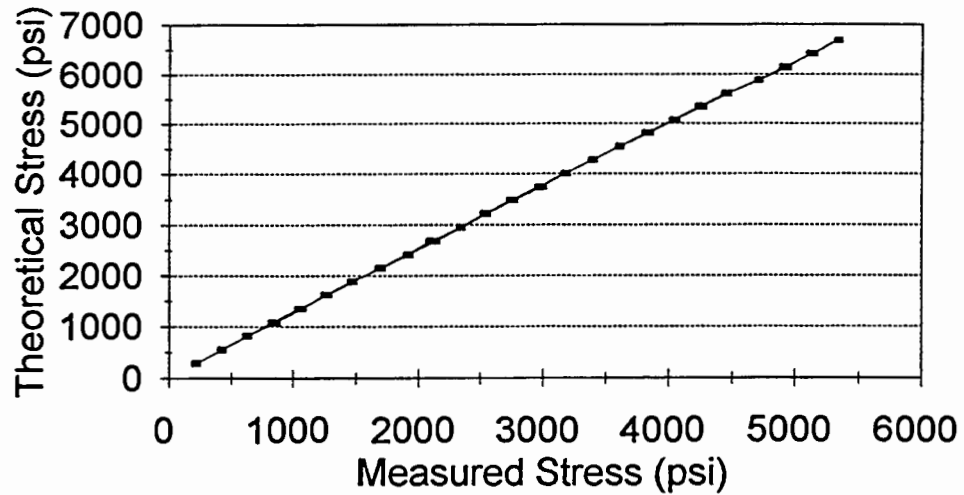


Figure C7. Load rod calibration (next 2 plots).

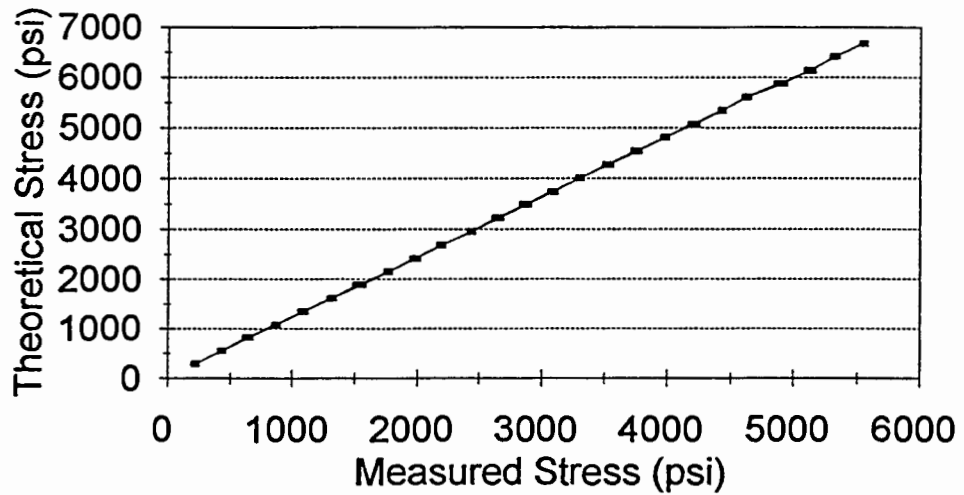
## Loadrod Red & Black 1

Calibration Factor = 1.256721



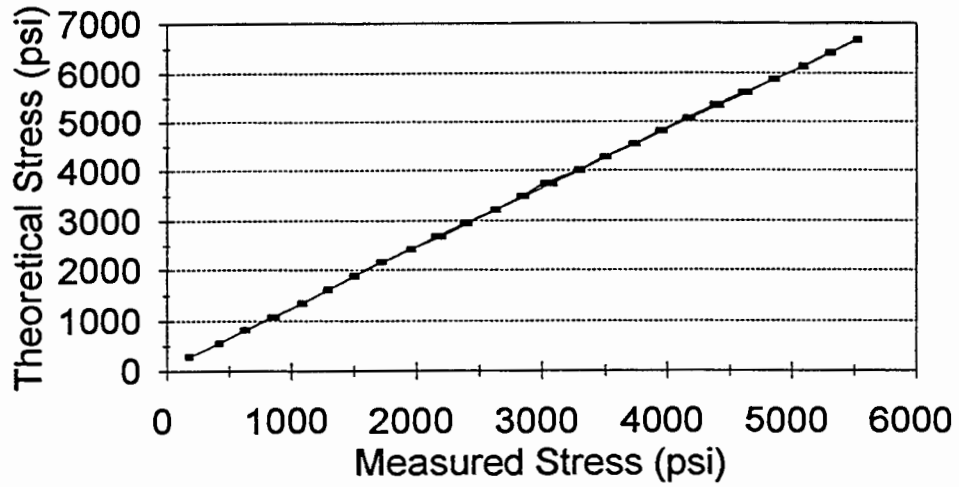
## Loadrod Red & Black 2

Calibration Factor = 1.209121



## Loadrod Red & Black 3

Calibration Factor = 1.217438



## Loadrod Red & Black 4

Calibration Factor = 1.2274

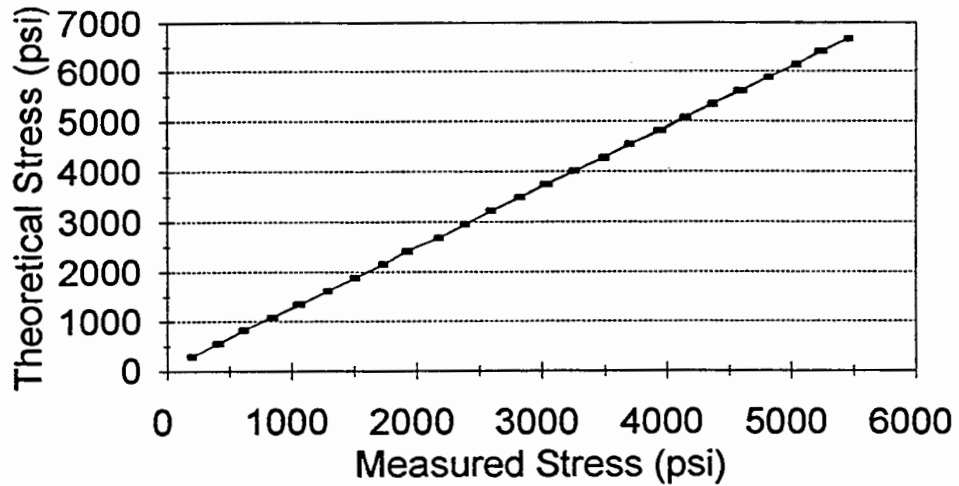
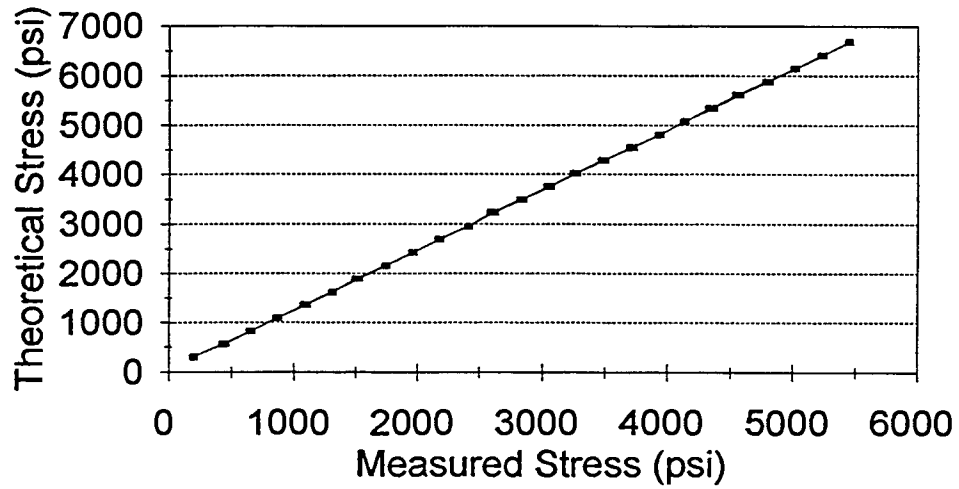


Figure C8. Load cell calibration.

## Load Cell A

Calibration Factor = 1.229666



## Load Cell B

Calibration Factor = 1.255374

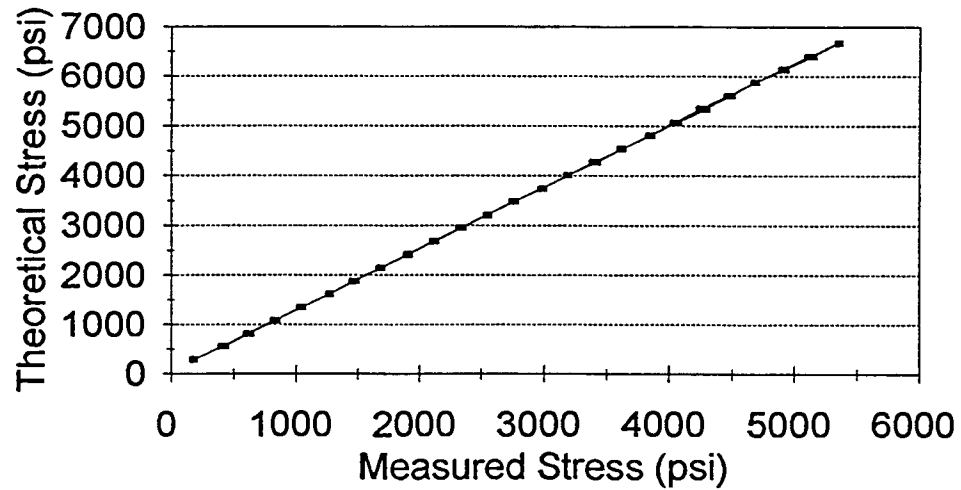
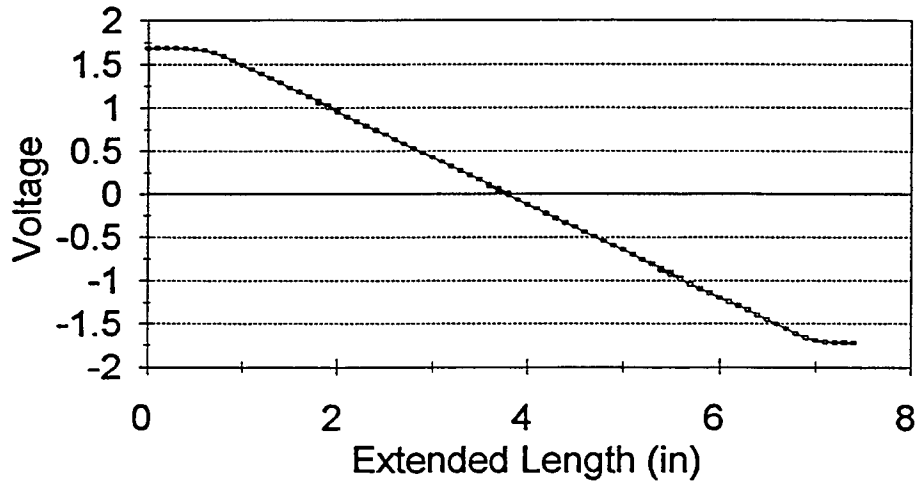




Figure C9. LVDT calibration.

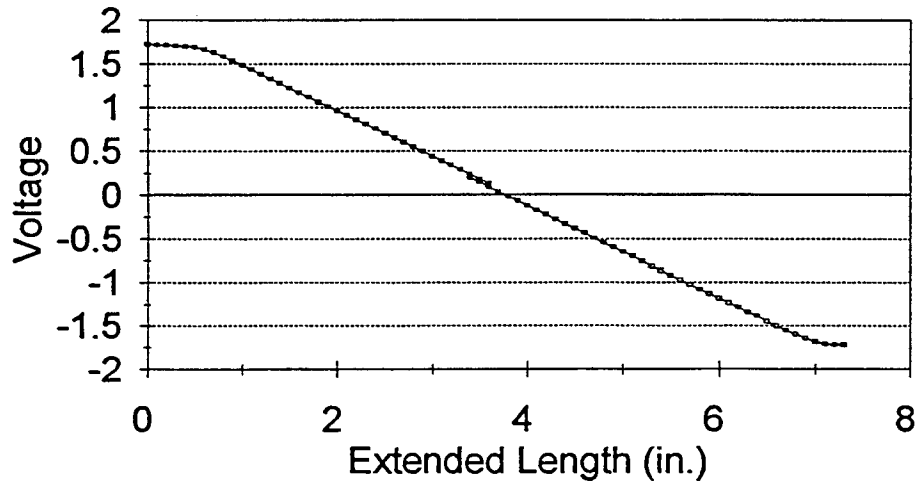
## Red LVDT Calibration

Linear Range Factor = 0.519 V/in.



## Blue LVDT Calibration

Linear Range Sensitivity = 0.519 V/in.





**APPENDIX D: LabVIEW TESTING SOFTWARE CODE**



Figure D1. LabVIEW testing software code (next 5 plots).

